R-13-18

Biosphere parameters used in radionuclide transport modelling and dose calculations in SR-PSU

Sara Grolander, Sara Grolander Miljökonsult AB

December 2013

Svensk Kärnbränslehantering AB
Swedish Nuclear Fuel
and Waste Management Co

Box 250, SE-101 24 Stockholm
Phone +46 8 459 84 00

ISSN 1402-3091
SKB R-13-18
ID 1425906

December 2013
Updated 2016-10

Biosphere parameters used in radionuclide transport modelling and dose calculations in SR-PSU

Sara Grolander, Sara Grolander Miljökonsult AB

This report concerns a study which was conducted for Svensk Kärnbränslehantering AB (SKB). The conclusions and viewpoints presented in the report are those of the author. SKB may draw modified conclusions, based on additional literature sources and/or expert opinions.

A pdf version of this document can be downloaded from www.skb.se.

Update notice

The original report, dated December 2013, was found to contain both factual and editorial errors which have been corrected in this updated version. The corrected factual errors are presented below.

Updated 2016-10

Location	Original text	Corrected text
Page 54, first paragraph, last sentence	"The water flows derived from the MIKE SHE simulation with a wetter and warmer climate are used to parameterise the water flows in the global warming climate case in the radionuclide model."	"The water flows derived from the MIKE SHE simulation with a wetter and warmer climate are used to parameterise the water flows in the extended global warming climate case in the radionuclide model."
Page 134, Table 12-1 and Table 12-2, first column, second row	Well id 12	Well id 29

Abstract

This report is produced within the biosphere part of the safety assessment SR-PSU and describes all biosphere parameters used in the radionuclide model for the biosphere. The report consists of several chapters where different parameter types are decribed (Chapter 3 – Radionuclide specific parameters, Chapter 4 – Landscape geometries, Chapter 5 – Regolith characteristics, Chapter 6 – Hydrological parameters, Chapter 7 – Element specific parameters, Chapter 8 – Aquatic ecosystem parameters, Chapter 9 – Terrestrial ecosystem parameters, Chapter 10 – Human characteristics, Chapter 11 – Non-human biota parameters, Chapter 12 – Parameters used in alternative calculation cases). Chapter 1 givs a general introduction to the SR-PSU safety assessment and Chapter 2 presents the conditions for parameterisation and the general assumption made in the parameterisation process.

Sammanfattning

Den här rapporten är en underlagsrapport till biosfärsdelen av säkerhetsanalysen SR-PSU och sammanställer alla parametrar som använts i radionuklidmodelleringen för biosfären. Rapporten består av kapitel där olika parametergrupper presenteras och beskrivs i detalj (kapitel 3 – radionuklid-specifika parametrar, kapitel 4 – landskapsparametrar, kapitel 5 – regolitparametrar, kapitel 6 – hydrologiska parametrar, kapitel 7 – ämnesspecifika parametrar, kapitel 8 – akvatiska ekosystemparametrar, kapitel 9 – terestra ekosystemparametrar, kapitel 10 – parametrar som beskriver människan, kapitel 11 – parametrar som beskriver biota (annan än människan), kapitel 12 – parametrar som används i alternativa beräkningsfall i SR-PSU). Kapitel 1 ger en introduktion till säkerhetsanalysen SR-PSU och beskriver den här rapportens roll i arbetet. I kapitel 2 finns en beskrivning av de förutsättningar och antaganden som ligger till grund för parameteriseringsarbetet.

Contents

1 Introduction

The final repository for short-lived low- and intermediate-level radioactive waste, SFR 1, is located in Forsmark in the Östhammar municipality (Figure 1-1), in the immediate vicinity of the Forsmark nuclear power plant (Figure 1-2). The SFR 1 repository consists of a set of disposal chambers situated in rock at ca 60 m depth beneath the sea floor, and is built to receive and after closure serve as a passive repository for low- and intermediate-level short-lived radioactive waste. The radioactive waste stored in SFR includes operational waste from Swedish nuclear power plants and from the interim storage facility for spent nuclear fuel, Clab, as well as radioactive waste from other industries, research institutions and medical care.

In order to be able to store also decommissioning waste from the Swedish nuclear power plants in SFR, an extension of the repository, referred to as SFR 3 is planned. An SFR repository extension called SFR 2 was included in earlier plans for disposal of reactor core components and internal parts. However, according to present plans a separate repository (SFL) will be built for disposal of these types of waste (SKB 2013a).

As a part of the license application for the extension of SFR, the Swedish Nuclear Fuel and Waste Management Company (SKB) has performed the SR-PSU project. The objective of SR-PSU is to assess the long-term radiological safety of the entire future SFR repository (the existing SFR 1 and the planned SFR 3). SR-PSU is reported in a series of SKB reports, which includes a main report, here referred to as SR-PSU Main report, and a set of primary references. These include, among others, the reports denoted as Biosphere synthesis report, Climate report, Radionuclide transport report, FEP report and FHA report throughout the SR-PSU reporting (see Section 1.1). In addition to these primary references, the safety assessment is based on a large number of background reports and other references (see Section 1.1).

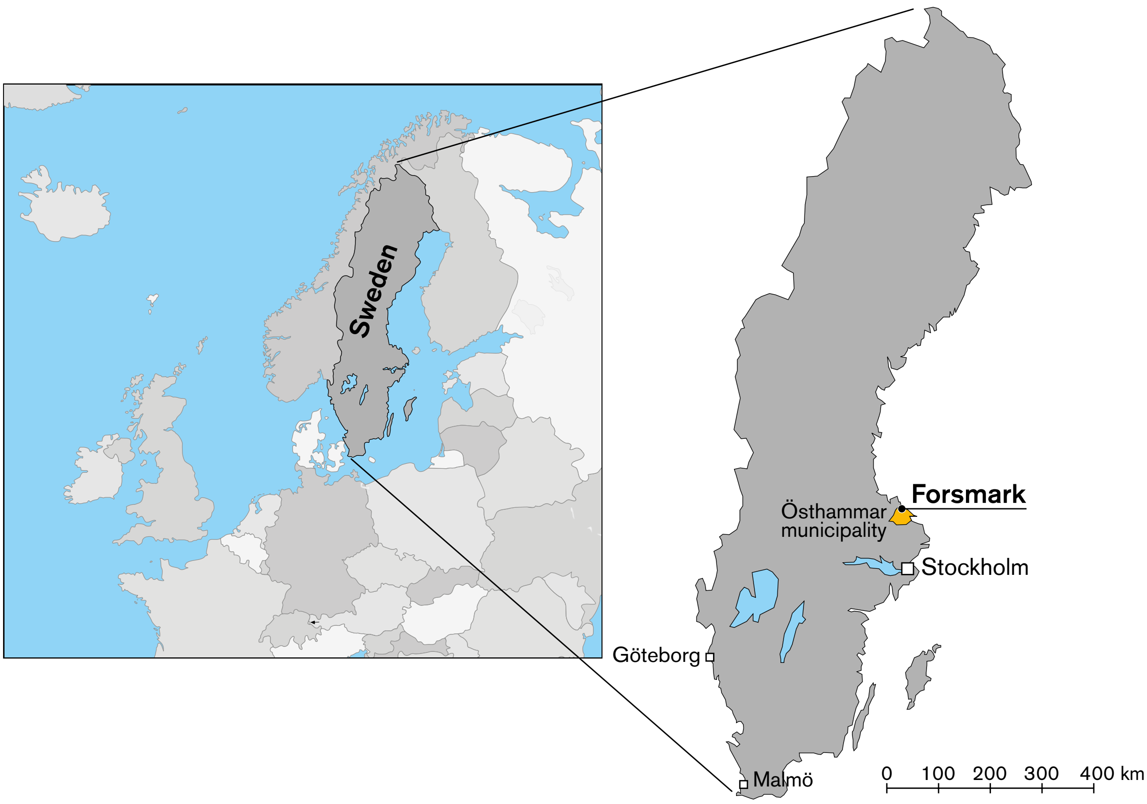

Figure 1-1. *Location of the Forsmark site in Sweden (right) and in context with the countries of Europe (left). The site is situated in the Östhammar municipality, which belongs to the County of Uppsala.*

Figure 1-2. *The surface part of the SFR facility in the harbour in Forsmark with the Forsmark nuclear power plant in the background.*

The biosphere is a key part of the system considered in a safety assessment of a nuclear waste repository. This is where the consequences of potential future radionuclide releases from the repository arise, and hence near-surface radionuclide transport and dose calculations are performed within the framework of the biosphere assessment. This report belongs to the sub-project of SR-PSU called SR-PSU Biosphere. SR-PSU Biosphere mainly describes the information needed to calculate impacts on humans and the environment in the event of a radionuclide release from SFR. The calculated impacts are then used to show compliance with regulations related to the future repository performance for time spans of up to 100,000 years after closure. Because of the uncertainties associated with the prediction of future development of the site over this time frame, a number of calculation cases are analysed to describe a range of possible site developments.

The SR-PSU Biosphere project is divided into a number of tasks.

1. Identification of features and processes of importance for modelling radionuclide dynamics in present and future ecosystems in Forsmark.
2. Description of the site and prediction of its future development with respect to the identified features and processes.
3. Identification and description of areas in the landscape that may be affected by releases of radionuclides from the existing repository and its planned extension.
4. Calculation of the radiological exposure to a representative individual of the most exposed group of humans in the future Forsmark landscape, and the radiological exposure of the other biota in the environment.

The SR-PSU biosphere assessment builds on previous safety assessments for the existing and planned nuclear waste repositories in Sweden. Between 2002 and 2008, SKB performed site investigations for a repository for spent nuclear fuel in Forsmark. Data from these site investigations were used to produce a comprehensive, multi-disciplinary site description (SKB 2008a). This description has been used as a basis for understanding and modelling of the site and site development.

The SFR repository has been operating since 1988 and a number of safety assessments have been performed for it since SKB received permission to start building SFR 1 in 1983, including the SAFE project (Lindgren et al. 2001, Kautsky 2001) and SAR-08 (SKB 2008b). In addition, safety assessments have been performed for a planned repository for spent nuclear fuel i.e. within the SR-Can (SKB 2006) and SR-Site (SKB 2011) projects, for which SKB handed in an application in 2011. This implies that the SR-PSU biosphere assessment is based on knowledge gathered from site data, site modelling and the previous safety assessments, together with modelling performed and data collected during the SR-PSU project.

The work done within the SR-PSU Biosphere project has been conducted by a number of people. Many of the project participants have been involved from the site investigation, via the site characterization and modelling tasks, through to the SR-PSU safety assessment; several members of the project group also have experience from previous safety assessments for SFR and for the planned repository for spent nuclear fuel. The project members in alphabetic order, their roles and affiliations are listed in Table 1-1.

Table 1-1. Project members of SR-PSU Biosphere in alphabetical order and their roles in the project.

Boris Alfonso, Facilia AB	Numerical modelling of impacts on non-human biota.
Eva Andersson	SKB Project manager SR-PSU Biosphere, process descriptions, limnic ecosystems.
Karin Aquilonius, Studsvik Nuclear AB	Marine ecosystems.
Rodolfo Avila, Facilia AB	Radionuclide modelling and dose assessment.
Sten Berglund, HydroResearch AB	Hydrology and near-surface radionuclide transport, editor of the biosphere synthesis report.
Lars Brydsten, Umeå University	GIS (geographical information system) analysis, regolith dynamics and lake development modelling.
Per-Anders Ekström, Facilia AB	Numerical modelling of radionuclide transport and doses.
Christin Eriksson, DHI Sverige AB	Oceanography.
Sara Grolander, Sara Grolander Miljökonsult AB	Distribution coefficient (K_d) and concentration ratio (CR) analysis, editor of present report.
Fredrik Hartz, Hartz Technology AB	GIS analysis and landscape development.
Thomas Hjerpe, Facilia AB	FEP handling.
Ben Jaeschke, SKB	Non-human biota.
Emma Johansson, SKB	Hydrology.
Ulrik Kautsky, SKB	Overall biosphere coordinator at SKB, scientific and method development.
Sven Keesmann, SKB	Radionuclide model report.
Tobias Lindborg, SKB	Site modelling and landscape development.
Anders Löfgren, EcoAnalytica	Terrestrial ecosystems.
Sara Nordén, SKB	Non-human biota, K_d and CR analysis.
Veronika Rensfeldt, Facilia AB	K_d and CR analysis.
Peter Saetre, SKB	Radionuclide model development, data evaluation, synthesis.
Mona Sassner, DHI Sverige AB	Hydrology.
Gustav Sohlenius, SGU	Regolith and future land use.
Viktor Smide, Hartz Technology AB	GIS analysis and illustrations.
Mårten Strömgren, Umeå University	GIS analysis, landscape development.
Mats Tröjbom, MTK AB	K_d and CR analysis, water chemistry.
Kent Werner, EmpTec Hydrology,	Wells, water resources management.
Per-Gustav Åstrand, Facilia AB	Numerical modelling of radionuclide transport and doses.

1.1 The SR-PSU report hierarchy

The SR-PSU project is reported in a series of SKB reports, which includes a main report and a set of primary references that are referred to by abbreviated names in the SR-PSU reporting. The primary references and the names used when referring to them in this and other SR-PSU reports are shown in Figure 1-3. In addition to the primary references, the safety assessment is based on a large number of background reports and other references.

Table 1-2 presents the background reports produced within SR-PSU Biosphere. The relationships between the background biosphere reports and the primary references are shown in Figure 1-4. The present report, the Parameter report (marked in orange in Figure 1-4) is one of the underlying references to the Biosphere synthesis report. As indicated in Figure 1-4, the Parameter report is based on input from a large number of background reports.

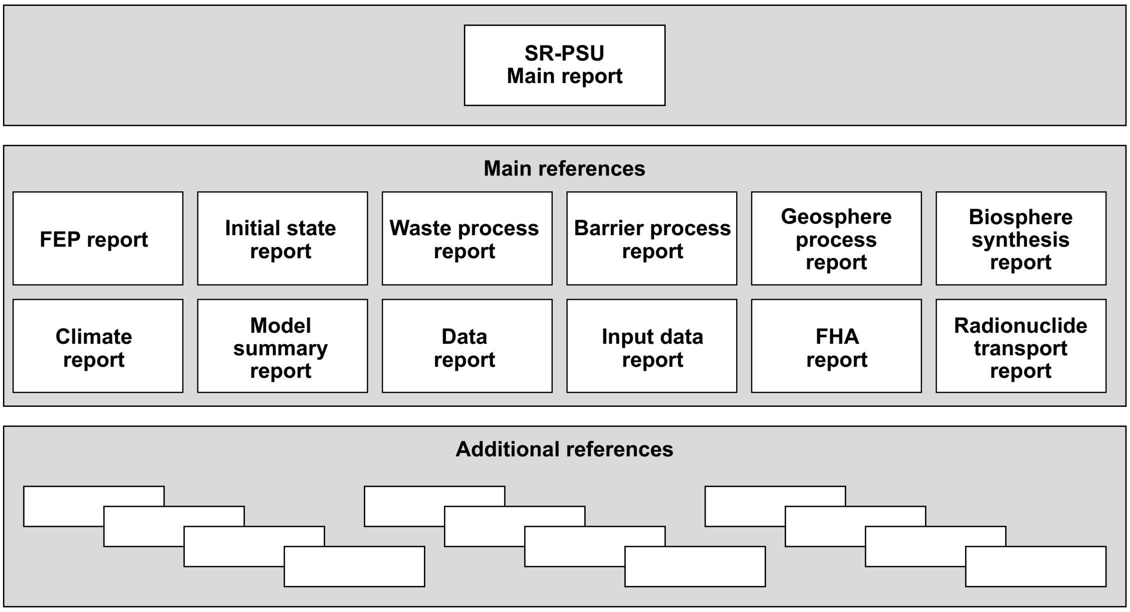

Figure 1-3. *Relationship between reports produced in the SR-PSU safety assesment.*

Table 1-2. Biosphere background reports produced within SR-PSU Biosphere; FEP stands for features, events and processes.

Report number	Short description and reference in text	Full title
R-12-03	DEM report, Strömgren and Brydsten (2013)	Digital elevation model (DEM) of Forsmark. SR-PSU Biosphere.
R-13-01	K_d and CR report, Tröjbom et al. (2013)	K_d and CR used for transport calculation in the biosphere in SR-PSU.
R-13-18	Biosphere parameter report, (This report)	Biosphere parameters used in radionuclide transport modelling and dose calculations in SR-PSU.
R-13-19	Surface hydrology report, Werner et al. (2013)	Hydrology and near-surface hydrogeology at Forsmark – synthesis for the SR-PSU project. SR-PSU Biosphere.
R-13-20	Hydrological data report, Werner et al. (2014)	Meteorological, hydrological and hydrogeological monitoring data from Forsmark – compilation and analysis for the SR-PSU project. SR-PSU Biosphere.
R-13-22	Regolith model report. Sohlenius et al. (2013)	Depth and stratigraphy of regolith at Forsmark. SR-PSU Biosphere.
R-13-27	Regolith lake development model, RLDM, Brydsten and Strömgren (2013)	Landscape development in the Forsmark area from the past into the future (8500 BC–40,000 AD).
R-13-43	Biosphere process definition report, SKB (2013c)	Components, features, processes and interactions in the SR-PSU biosphere modelling.
R-13-46	Biosphere radionuclide model report, Saetre et al. (2013a)	The biosphere model for radionuclide transport and dose assessment in SR-PSU.
R-14-02	Biosphere FEP handling report, SKB (2014a)	Handling of biosphere FEPs and recommendations for model development in SR-PSU.

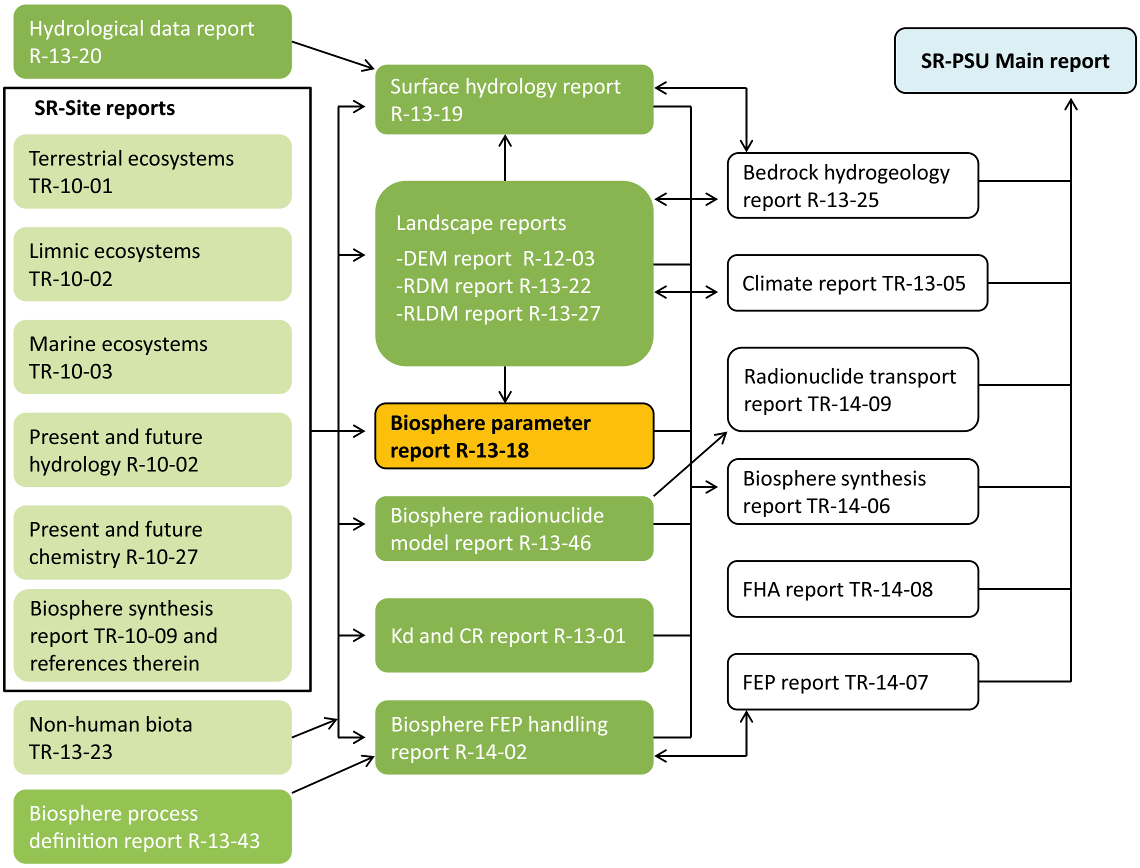

Figure 1-4. *Relationship between reports produced in the SR-PSU Biosphere project (dark green boxes). The present report is marked in orange and bold. Supporting documents produced within other biosphere projects at SKB are shown as light green boxes, whereas other reports in the SR-PSU project are shown in white except the SR-PSU Main report, which is shown in blue.*

1.2 This report

In this report, the parameters used for radionuclide transport modelling for the biosphere are presented. The report consists of nine sections describing different groups of parameters; Radionuclide specific parameters, Landscape geometries, Regolith characteristics, Hydrological flows, Element-specific parameters, Aquatic ecosystem parameters, Terrestrial ecosystem parameters, Human characteristics and parameters used for dose assessment for non-human biota (NHB).

This report has been written as a collaboration by several project members. The authors of the chapters of this report are listed below.

- Radionuclide Specific parameters – Per-Anders Ekström, Facilia AB.
- Landscape geometries – Anders Löfgren, EcoAnalytica
- Regolith characteristics – Gustav Sohlenius, SGU
- Hydrological flows – Mona Sasser, DHI
- Element-specific parameters – Sara Grolander, Sara Grolander Miljökonsult AB
- Aquatic ecosystem parameters – Eva Andersson, SKB
- Terrestrial ecosystem parameters – Anders Löfgren, EcoAnalytica
- Human characteristics – Peter Saetre, SKB
- Non-human biota parameters – Sara Nordén, SKB

Sara Grolander has been the editor of the report.

2 Conditions for parameterisation

This report present parameters used for the radionuclide transport model for the biosphere used to calculate radionuclide transport and doses to humans and wildlife in the Forsmark area for a time period of up to 100,000 years. In this chapter, an overview of the radionuclide transport model and the conditions for parameterisation set by alternative calculation cases (climate cases) and land-use variants is given. The methods used for selection of representative parameter values and distributions are also described in Section 2.6.

2.1 Radionuclide transport model

The radionuclide transport model for the biosphere calculates radionuclide transport and radiation doses and dose rates in the Forsmark area for a time period of 100,000 years. Two types of ecosystems are simulated in SR-PSU, namely aquatic ecosystems (sea, lake and river ecosystems), and terrestrial ecosystems (mire ecosystems and agricultural ecosystems). In these compartmental (or mass balance) models, each compartment represents a radionuclide inventory associated with a physical (or biological) component in the surface ecosystems. The dynamic change of the radionuclide content of each compartment is the result of one or more radionuclide fluxes (based on the processes that are operating) which are associated with the mass fluxes of water, solids (including organic matter) or gas, or with diffusion.

Figure 2-1 shows a graphical representation of the compartments and radionuclide fluxes identified for a coupled lake and mire ecosystem. The arrows in Figure 2-1 represent radionuclide fluxes between the compartments and fluxes into and out of the system. Radionuclide fluxes are linked to mass fluxes of gas (1, light blue), water (2, dark blue) and solid matter (3, black), to transitions between inorganic and organic forms of radionuclides (4, green), to diffusion in soil pore water (5, orange), and to ingrowth of wetland vegetation (6). The atmosphere serves as a source and sink of radionuclides.

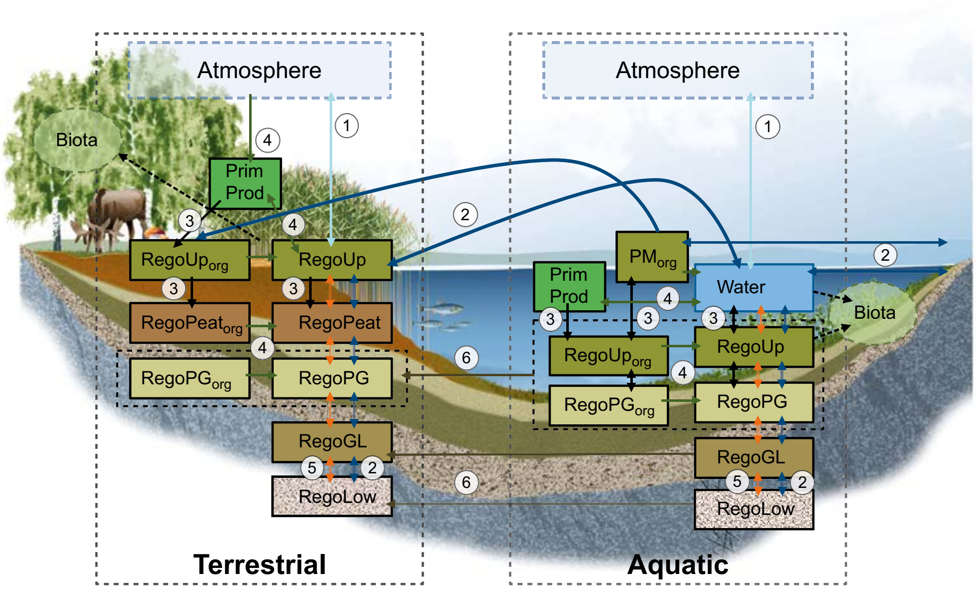

Figure 2-1. A graphical representation of the radionuclide transport model used to simulate transport and accumulation in a discharge area with two natural ecosystems (black dotted boxes). Each box corresponds to a radionuclide inventory associated with a physical compartment. Arrows represents radionuclide fluxes between compartments and fluxes into and out of the system. Radionuclide fluxes are linked to mass fluxes of gas (1, light blue), water (2, dark blue) and solid matter (3, black), to transitions between inorganic and organic forms of radionuclides (4, green), to diffusion in soil pore water (5, orange), and to ingrowth of wetland vegetation (6). The atmosphere serves as a source and sink of radionuclides.

Five regolith compartments are defined for the terrestrial ecosystem and four for the aquatic ecosystem. The RegoLow compartments represents till overlying the bedrock, the RegoGL compartment represents the glacial clay overlying the till. The RegoPG represents the postglacial gyttja clay layer. These lower layers (RegoLow, RegoGL and RegoPG) are identical in both terrestrial and aquatic ecosystems whereas the top layers differ between the ecosystems. In the terrestrial ecosystem, the peat is divided into one anoxic peat layer, RegoPeat, and one layer representing the oxidised top layer of the peat, RegoUp. In the aquatic ecosystem, the RegoUp layer represents the oxidised organic top sediment (5 cm for lakes and 10 cm for sea). The compartments marked with the suffixs _org in the figure represents the organic compartments, which are distinguished from the compartments representing inorganic solids and pore waters. Besides the regolith compartments, surface waters and primary producers are handled as separate compartments in the transport model. A detailed description of the radionuclide model and definitions of the model compartments are found in Saetre et al. (2013a).

2.2 Landscape development and biosphere objects

Seven biosphere objects have been identified as potential release areas in the Forsmark landscape. The identification of these biosphere objects is described in detail in the Biosphere synthesis report. The biosphere objects are shown in Figure 2-2, there are two types of biosphere objects, those with a lake stage in the succession and objects without a lake stage. The objects with a lake stage are marked in blue and the objects without a lake stage are marked in yellow (121_2 and 157_2). The objects are parts of larger areas here called basins (marked with grey). Several of the parameters presented in this report are object-specific, meaning that they describe properties that are dependent on which object they represent, for example the geometries of the object, the thickness of the regolith layers and water fluxes.

Due to landscape development (shoreline displacement) the landscape will go through successional changes during the modelled time period. At the start of the modelling time period all biosphere object are sea basins, but, due to land uplift, lakes will be formed, and then these lakes will be transformed into terrestrial areas. This means that several of the parameters presented in this report are time-dependent and alter during the modelled time period. The landscape development is illustrated in Figure 2-3.

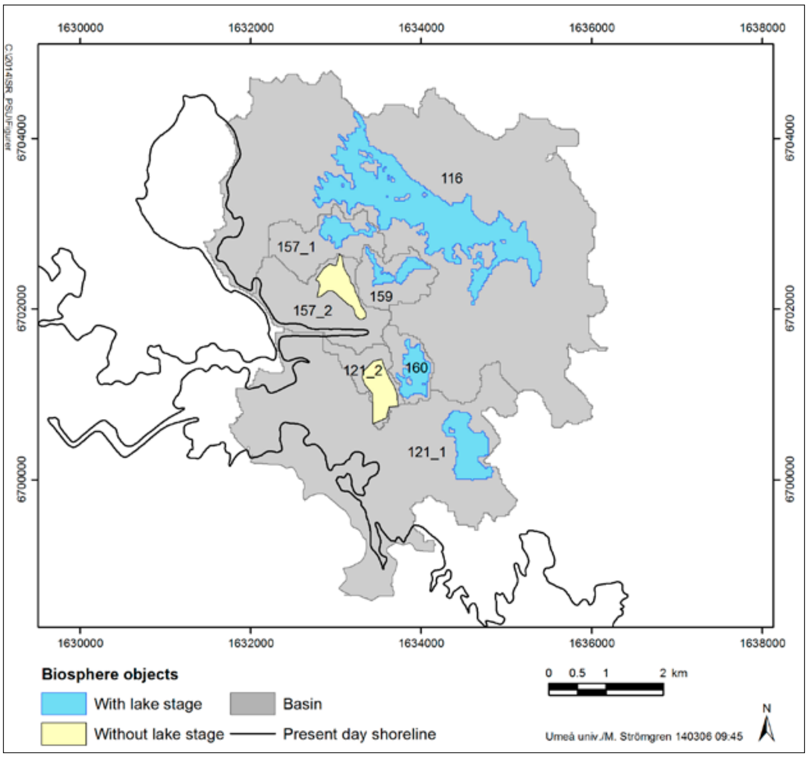

Figure 2-2. The seven biosphere objects (blue and yellow) and their associated basins (grey). The objects 121_2 and 157_2 have no lake stage in their succession (marked with yellow).

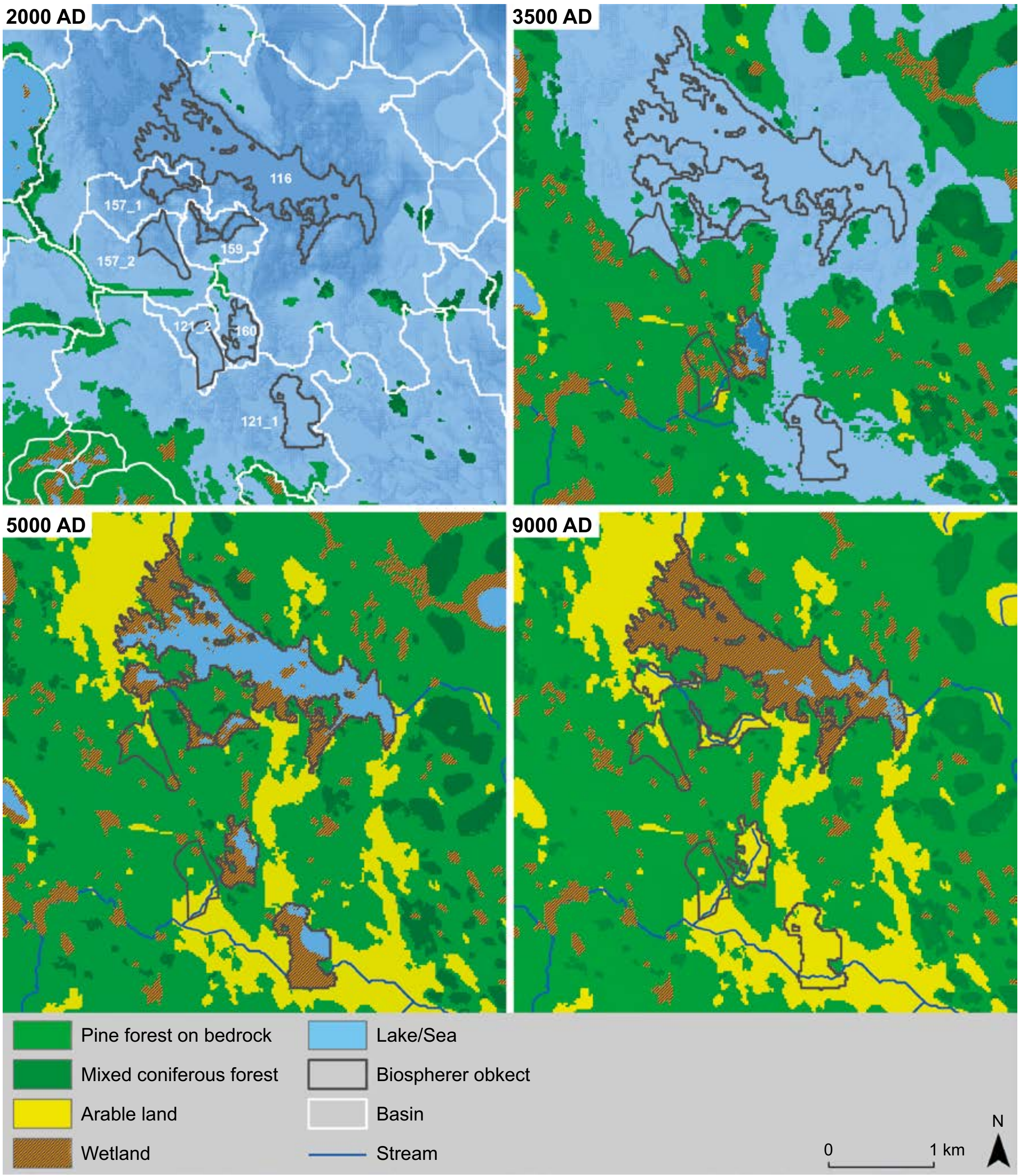

Figure 2-3. *The biosphere object succession and ecosystem development is shown for 2000, 3500, 5000 and 9000 AD using the landscape development model as background.*

2.3 Human inhabitants

In SR-PSU, a comprehensive range of potential exposure pathways for humans has been analysed (SKB 2014a). The possible exposure pathways to humans differ depending on the habits of the humans. It is impossible to predict the habits and diets of future humans. However, by assuming a range of human habits, a range of exposure pathways can be identified and used to define bounding cases to determine possible exposures of humans in the future. Four groups associated with different potential land-use variants were included in the analysis. These groups were considered credible to use as bounding cases for the most exposed groups with respect to exposure through all major exposure pathways (SKB 2014a). When characterising the most exposed groups, physical and biological characteristics of the biosphere objects, human requirements for energy and nutrients, and habits from historical and present societies were considered (Saetre et al. 2013a, b). The four land-use variants identified were the following.

Hunting and gathering (HG) – represents a community using natural ecosystems in the landscape for living space and food. The major exposure pathways are from foraging the landscape (fishing, hunting, and collecting berries and mushrooms), and from drinking surface water (from streams or lakes).

Infield–outland farming (IO) – represents self-sustained agriculture where infield farming of crops and livestock breeding are dependent on hay from wetlands (outland), used as fodder and organic fertilizer (manure). The major exposure pathways result from haymaking, from consumption of crops, meat and dairy products, and from drinking water from either a dug well or from surface water in the biosphere object.

Draining and cultivating a mire (DM) – represents self-sustained industrial agriculture in which wetlands are drained and used for agriculture (both crop and fodder production). The major exposure pathways are from growing food on land where radionuclides have accumulated for an extended period, and from drinking water from either a well (dug or drilled) or from surface water in the biosphere object.

Garden plot household (GP) – represents a household that is self-sustained with respect to vegetables and root crops produced through small-scale horticulture. The major exposure pathways result from fertilization and food production on the garden plot, and from using either a well (dug or drilled) or surface water for drinking and irrigation purposes.

Parameters describing these land-use varaints (the habits and characteristics of the population) are presented in Chapter 10 and properties of the agricultural soil types and of the crops that are cultivated are presented in Section 5.4 and Chapter 9.

2.4 Climate cases

Since the safety assessment covers thousands of years, climate conditions will vary. Climate affects the release and distribution of radionuclides, ecosystem functioning and exposure pathways. In SR-PSU, four climate cases are identified (SKB 2014d);

- the global warming climate case,
- the extended global warming climate case,
- the early periglacial climate case,
- the Weichselian glacial cycle climate case.

The climate cases cover both warmer and colder climate conditions which can have a large effect on the transport of radionuclides in the biosphere and possible exposure pathways for humans. Therefore, separate calculation cases have been identified for these climate conditions. For some of the parameters presented in this report, alternative parameter values are used for the different climate calculation cases. Here a short description is given of the calculation cases and of the parameter groups that are altered in the listed calculation cases. Detailed information on alternative parameter values is given in each of the following chapters (Chapters 3-11). A list of parameters altered in the climate calculation cases are presented in Appendix B.

The global warming calculation case is based on the reference evolution presented in the main report (SKB 2014b), which describes a reasonable evolution of the repository, the geosphere and the biosphere. This calculation case is used as a base case. The climate is assumed to be temperate for the first 50,000 years and the air temperature may increase by up to 3.7°C but will return to present conditions after c. 25,000 years (SKB 2014d). Although the temperature will increase, the degree of warming and the response in the biosphere is uncertain (see Andersson 2010, Aquilonius 2010 and Löfgren 2010 for further discussion on potential responses to warming of the ecosystems at Forsmark). Therefore, the most reliable data available for temperate conditions, i.e. site data under present conditions, are used for the entire time period of this calculation case. The parameter data used for this calculation case are considered to be the base case and these parameter data are used for all other calculation cases if no other values are stated.

The extended global warming calculation case is developed to evaluate the effect of warmer and wetter climate on repository safety. In the extended global warming climate case temperature may increase by c. 6°C and it may take 50,000 years before the temperature returns to its present-day value (SKB 2014d). Such a climate is similar to that of present day central and southern Europe. To fully investigate the effect of a warmer and wetter climate, the parameters for increased temperature are applied for the entire modelling period of 100,000 years. The hydrological parameters are affected by the warmer climate and therefore water balances for the biosphere objects were modelled using information on increases in temperature and the characteristics of wetter conditions taken from the climate report. Ecosystem parameters such as primary production concentration of carbon in the atmosphere are altered.

The early periglacial climate case is developed to evaluate the dose to humans and dose rates to wildlife in the early periglacial climate case (permafrost conditions). The term periglacial is today used for a range of cold but non-glacial environments. In the periglacial environment, permafrost is a central, but not defining, element. However, for the present work, the periglacial climate case is defined strictly as non-glacial regions that contain permafrost. Although true for most of the time, regions defined as periglacial are not necessarily the same as regions with a climate that supports permafrost growth. For example, at the end of a period with periglacial climate domain the climate may be relatively warm, not building or even supporting the presence of permafrost. Instead, permafrost may be diminishing. However, as long as permafrost is present, the region is defined as periglacial, regardless of the prevailing temperature at the ground surface. This way of defining the climate domain is used because the presence of the permafrost is more important for the safety function of the repository than the actual temperature at the ground surface. The definition of permafrost applies to the land ecosystem, i.e. the soil is at or below the freezing point of water (0°C) for two or more years. The uppermost permafrost in a terrestrial ecosystem is a thin active layer that seasonally thaws during the summer. The permafrost domain in limnic ecosystems means an environment with lower water temperature and only a relatively short ice-free season. The first periods of colder climate that can cause deep permafrost arise at around AD 17,000 and prevail for a few thousand years (SKB 2014d). At that time all of the model area is above shore line, and the regolith layers of the Forsmark landscape will be frozen. Therefore, discharge of deep groundwater will be restricted to unfrozen land areas, so-called discharge taliks. Taliks are typically formed below lakes with shallow permafrost depths but they might also form below other low points in the landscape as wetlands (Werner et al. 2013). A separate model for taliks was set up to investigate the potential doses from a lake talik and a wetland talik. Hydrological water fluxes are affected by permafrost conditions and therefore hydrological water fluxes were modelled for colder and dryer climate conditions (data from the SKB 2014d) at both wetland and lake taliks. Ecosystem parameters relating to vegetation production, and production of edible fish and crayfish, are altered to better reflect permafrost conditions. During periglacial climate conditions, cultivation is not possible on drained mires due to permafrost, and wells will not yield any water in the frozen ground. Thus, in the talik calculation case the exposed population is hunters and gatherers foraging in the Forsmark landscape. The taliks are located in object 157_1 (representing a talik under a wetland) and 114 (representing a talik under a lake). Therefore parameters for these two objects are used in this calculation case.

The Weichselian glacial cycle climate calculation case represents a repetition of conditions reconstructed for the last glacial cycle. This climate case is included to span the uncertainty in the onset of ice sheet growth in the Northern Hemisphere under fully natural climate variability, and for comparison with earlier safety assessments for the SFR repository. Current scientific knowledge on future climate evolution, reviewed in Section 3.3 in the SKB (2014d), suggests that the combination of human intervention and relatively small-amplitude variations in insolation will lead to a global climate evolution in the next 100,000 years which is significantly different from previous glacial cycles. Therefore, the Weichselian cycle case is not considered in the SR-PSU landscape development modelling. To assess the affect of this climate case a calculation case for submerged conditions is considered. In this calculation case the same parameter values as in the base case (global warming calculation case) are used. The biomass of the marine basin are dependent on depth and will therefore change over time.

2.5 Additional calculation cases

In addition to the four climate calculation cases, three alternative biosphere calculation cases have been developed in SR-PSU. For some of these cases, alternative or additional parameter values are used. These parameters are presented in Chapter 12 of this report.

- **Wells in discharge plume** or into repository or utilisation of water from the tunnel entrance of an abandoned repository. Addresses the dose contribution that results from drilling a geological well to secure drinking water resources either in the discharge plume or directly into the repository. All parameters are identical to the global warming calculation case. There is no agricultural land in the discharge plume or above the repository. Therefore, the only exposed population assumed to be able to drill a well into the geosphere is the garden plot household. Parameters describing the properties of the well are presented in Section 12.1.
- The calculation case **Distibuted release** is developed to examine uncertainties in the distribution of the radionuclide release in the landscape. All parameters are identical to the global warming calculation case. The only parameter that is altered is the release fraction, described in Section 12.2 and in detail in Odén et al. (2014).
- The calculation case **Alternative object delineation** is developed to investigate uncertainties in delineation of biosphere objects. The results arising with the initial delineation of biosphere object 157_2 in the global warming case is compared with the results arising with alternative delineation. Water balances for each alternative object delineation were modelled with MIKE SHE and model parameters were derived from these (Werner et al. 2013). Regolith depths were derived for the alternative object delineations, and deep peat mineralization rates were adjusted for the potential peat depth. The altered parameters are listed in Section 12.3. All other parameters were identical to the global warming case.

2.6 Selecting parameter values and probability density functions

The extensive site investigations performed by SKB at Forsmark have resulted in a detailed description of the site and its development (summarised in SKB 2014c). Site-specific data from the site description have as far as possible been utilised both for describing parameters and specifying parameter values. The parameters describe relevant properties of the ecosystems in the Forsmark area today and in the future. It is not possible to predict parameter values for a fully dynamic future ecosystem in detail, and instead data from the site and nearby ecosystems are used as natural analogues for the future ecosystems. This is based on the assumption that all relevant interactions among species and between organisms and the abiotic environment are contained in these analogue ecosystems.

Below is a brief description of the principles used to derive best estimate values of input parameters, and to describe the natural variation and measurement uncertainties in model parameter values.

For each parameter describing a property or process in biosphere objects, a best estimate was derived, and the parameter variation was described by a probability density function. Site data were utilised as far as possible, but in cases where the available site data were insufficient for reliable parameter estimation, data from the open literature were utilised. The biosphere objects develop in time, but for the purpose of the assessment the properties within an object are assessed to be homogenous and to represent a yearly average. Thus, the parameter values that were used in the simulations of transport, accumulation and exposure, should give representative descriptions (typical) of compartments or flows between compartments within a biosphere object, disregarding spatial variations *within* the compartments, and *temporal* variations during the year.

This means that when the variations in parameter values are quantified (e.g. in terms of standard deviation, or maximum and minimum values), the measures of variation should reflect the random variation of the typical value between years, or, if such data are not available, the random variation between compartments in similar landscape objects within the study area. Only the natural variation existing within one particular climate domain was used to characterise the probability distribution of a parameter.

The term “parameter uncertainty” is used in the context of assessing the precision of the estimated radionuclide doses. The parameter uncertainty refers to the combined effect of natural variation, comprising variation due to real and identifiable heterogeneity in nature, and measurement uncertainties (i.e. errors in measurements or limitations in the assessment).

Each parameter has been described by a best estimate (BE) and a probability density function (PDF), which includes both natural variation and measurement uncertainties. The shape of the PDF for each parameter was judged to be either log-normal or normal. For a lognormal distribution, the geometric mean and geometric standard deviation were used to describe the best estimate and the variation around the mean, whereas the arithmetic mean and standard deviation were used for parameters with a normal distribution. For each parameter, maximum and minimum values were also identified to set limits on the possible range of the parameter value. The possible range includes expected natural variation that is not observed at the site presently, but may historically have existed at the site or is expected in the future under similar climate conditions (e.g. due to the presence/characteristics of species/communities that are likely to develop on the site, but are not presently observed). The minimum and maximum values are used to truncate the distributions used in the radionuclide model.

When data were insufficient to estimate a parameter distribution, e.g. for properties of future site conditions estimated from literature data, the parameter was represented by a uniform distribution. For most of these parameters, the best estimate corresponded to the arithmetic mean of the minimum and maximum values. For some parameters for which data are scarce, the parameter uncertainty was handled by choice of cautious parameter values.

The best estimates and PDFs were used for deterministic and probabilistic calculations of human exposure and to assess potential radiological impacts on humans. The result of the probabilistic simulations were also used sensitivity analysis where the parameter variations were assessed. For the non-human dose assessment no probabilistic calculations were conducted. The parameters that were varied in the probabilistic simulations are listed in Appendix F.

3 Radionuclide-specific parameters

In the calculations of potential doses to humans, radionuclide-specific dose coefficients are used for converting the activity levels (Bq) of ingested or inhaled radionuclides as well as the activity concentrations in environmental media (Bq m^{-2} or Bq m^{-3}) to doses to humans (Sv). Humans can be exposed to radionuclides both externally and internally. External exposure comes from radiation emitted by radionuclides in surrounding environmental media such as air, water and soils. The internal exposure is always preceded by incorporation of radionuclides into the human body. Relevant pathways for internal exposure are mainly by inhalation of contaminated air, or ingestion of contaminated water and food (Avila and Bergström 2006). Other exposure pathways are discussed and dismissed as being of little significance for the long-term safety of a geological disposal facility at the Forsmark site in SKB (2014a).

Assessing the risk to the most exposed group is the motivation for the dose calculations and, for doing this, three different kinds of radionuclide-specific dose coefficients taking into account the above mentioned main exposure routes are used:

1. dose coefficients for external exposure from radionuclides in the ground, doseCoef_ext (Sv h^{-1} per Bq m^{-3}), and on the ground, doseCoef_ext_surf (Sv h^{-1} per Bq m^{-2}),
2. dose coefficients for ingestion, doseCoef_ing (Sv Bq^{-1}), and
3. dose coefficients for inhalation, doseCoef_inh (Sv Bq^{-1}).

Doses obtained with these coefficients are the committed effective doses to members of the public that are classified as adults. Any radioactive contamination of the biosphere due to releases from a geological disposal facility could be assumed to remain relatively constant over time periods spanning considerably longer than the human life span. Therefore, ICRP (2000) states that it is reasonable to calculate the annual dose averaged over the lifetime of the individuals, which means that it is not necessary to calculate doses to different age groups; this average can be adequately represented by the annual effective dose to an adult.

Previous safety assessments of planned geologic repositories in Sweden (Bergman et al. 1977, 1979, Bergström 1983) have shown that the only external exposure contributing significantly to the total dose is that from contaminated ground, this is also shown and discussed in SKB (2014a). Thus, the external exposure from air and water is negligible for all radionuclides of relevance, whereas for some radionuclides with high gamma-energy emissions and low bioavailability, such as Nb-94, the external exposure to radionuclides accumulated in the ground (soil) may give an important contribution to the total dose. Hence, exposure from radionuclides accumulated in the ground is included in SR-PSU.

In addition to this, an additional calculation case was studied in which peat and wood are combusted for heat generation. The exposure to radionuclides in the contaminated air was considered and therefore dose conversion factors (doseCoef_comb_peat, doseCoef_comb_wood) for the exposure by inhalation of contaminated air following the combustion of peat or wood with an assumed unit activity concentration (Sv $year^{-1}$ per Bq $kgdw^{-1}$) were used; these are presented in Section 3.4.1.

The radionuclide half-lifes and the decay chains used in the radionuclide transport model for the biosphere are not presented here; these can be found in the SKB (2014e) report. In this chapter the half-lifes used in calculation of dose coefficients are presented, these can in some cases differ from the half-lifes used in the radionuclide transport model. The potential differences on some of the long half-lives of modelled radionuclides (often several thousands of years) would give insignificant effect on the short time-span of exposure of the most exposed group (up to 50 years).

3.1 Experience from previous safety assessments

There is no difference between the modelling approaches used in SR-PSU and the approaches used in recent SKB safety assessments (SAR-08 (SKB 2008), SR-Site, (SKB 2011)).

In safety assessments performed before 2006, dose coefficients for external exposure were based on values in Svensson (1979). In safety assessments performed after 2006 (SAFE, SAR-08) external dose coefficients were based on values reported in Eckerman and Leggett (1996) and Eckerman and Ryman (1993).

One issue identified in previous safety assessment is the handling of the dose contribution of short-lived progeny. It is stated that the dose contribution from "short-lived" progeny is included in the dose coefficients of the parent radionuclide for external exposure, but the criterion for "short-lived" is not defined (Avila and Bergström 2006). This means that the handling of dose contribution of short-lived progeny has not been clarified in previous safety assessment.

In SR-PSU, the dose contributions of the progeny are accounted for in the dose calculations by either including the dose contribution of the short-lived progeny in the dose coefficient of the parent radionuclide or by modelling the progeny explicitly in the radionuclide transport calculations. These two approaches are described in Section 3.3.

3.2 Influence of climate on parameter values

Radionuclide dose coefficients are not affected by climate change. The same parameter values are used in all calculation cases.

3.3 Handling of the dose contribution of progeny in decay chains

The inventory of the SFR facility is identified in SKB (2013b). From the inventory a screening has been done based on two criteria;

1. half-life of the radionuclide is 10 years or longer,
2. radiotoxicity[1] of radionuclide at time of repository closure exceeds 0.01 Sv.

The radionuclides selected after the screening are included in the safety assessment. In addition, long-lived progeny of these selected radionuclides might be relevant for the safety assessment and are therefore included in the assessment and thus modelled explicitly. The selection of radionuclides is described in SKB (2014e). Table 3-1 lists the selected radionuclides (including progeny).

Table 3-1. Safety relevant radionuclides for the SR-PSU assessment.

Ac-227	Cm-243	Mo-93	Pu-239	Th-229
Ag-108m	Cm-244	Nb-93m	Pu-240	Th-230
Am-241	Cm-245	Nb-94	Pu-241	U-232
Am-242m	Cm-246	Ni-59	Pu-242	U-233
Am-243	Co-60	Ni-63	Ra-226	U-234
Ba-133	Cs-135	Np-237	Se-79	U-235
C-14	Cs-137	Pa-231	Sm-151	U-236
Ca-41	Eu-152	Pb-210	Sn-126	U-238
Cd-113m	H-3	Pd-107	Sr-90	Zr-93
Cl-36	Ho-166m	Po-210	Tc-99	
Cm-242	I-129	Pu-238	Th-228	

[1] Radiotoxicity is defined as the product of the inventory (Bq) and the dose coefficient for ingestion (doseCoeff_ing, Sv Bq^{-1}).

The dose calculations for most radionuclides are straightforward, the activity concentrations in environmental media are multiplied by the corresponding dose-coefficient. However, for some radionuclides radioactive progeny building up in the environmental media after radioactive decay have to be taken into account. Thus, it is appropriate to consider exposure from both the radionuclide and the progeny when assessing dose. The contribution of these radionuclide progeny are handled by assuming secular equilibrium and including the contribution of the progeny in the dose coefficient of the parent radionuclide.

A decay product is said to be in secular equilibrium when the ratio of its activity to that of the parent no longer changes with time. The reason for adopting this assumption is that the radionuclides in these chains have much shorter half-lives than those radionuclides explicitly modelled (many orders of magnitude). In the situation of secular equilibrium, the decay rate of parent radionuclide, and hence the production rate of progeny radionuclide, is approximately constant, because the half-life of the parent nuclide is very long compared to the timescale being considered. The quantity of the radionuclide progeny builds up until the number of progeny atoms decaying per unit time becomes equal to the number being produced per unit time; the quantity of radionuclide progeny then reaches a constant, equilibrium value. Assuming that the initial concentration of the progeny is zero, full equilibrium usually takes several half-lives of the progeny to establish. Thus, the equilibrium value for the activity in a progeny radionuclide is the same as the activity of parent radionuclide*,* adjusted by the branching ratio.

As an example, assume a unit activity of radionuclide Cs-137. The physical half-life is 30 years and in 94.6% of its transformations, the radioactive decay product Ba-137m is formed. Ba-137m has a half-life of 2.552 minutes and forms no radioactive decay products. Figure 3-1 illustrates the dynamic change of activity of Cs-137 and Ba-137m, assuming an initial unit activity of Cs-137. It shows that after about 20 minutes (~ 7 half-lives of Ba-137m), secular equilibrium has been established between Cs-137 and Ba-137m. Thus, when modeling Cs-137 there is no need to explicitly model Ba-137m. Instead, it is assumed that wherever there is any activity of Cs-137 there are the same activity corrected by 94.6% (the branching ratio) of Ba-137m. Accordingly, the dose coefficients for Cs-137 include the contribution of radiation from Ba-137m and thus Ba-137m is not modeled explicitly in the transport model.

In other cases, the contribution of progeny is small and can therefore be neglected in the dose calculations. As an example, for Gd-152 and Sm-147 which are a very long-lived (1.08×10^{14} and 1.06×10^{11} years, respectively) progenies of the relatively short-lived (13.33 and 2.6234 years, respectively) radionuclides Eu-152 and Pm-147. Thus, not much Gd-152 and Sm-147 will be built up before Eu-152 and Pm-147 have decayed. Figure 3-2 illustrates the amount of Gd-152 and Sm-147 that will build up from a unit initial activity of Eu-152 and Pm-147. Only 3.4×10^{-14} of the initial Eu-152 activity and 2.5×10^{-11} of the initial Pm-147 activity will build up as Gd-152 and Sm-147. Since the inhalation dose coefficient is only about 450 times and ingestion coefficient is only about 30 times larger for Gd-152 than for Eu-152 and corresponding values for Sm-147 and Pm-147 are 1920 and 188 (see Table 3-3) there is no need to take the dose contribution into account in the dose coefficients of the parent radionuclide or to explicitly model the radionuclides Gd-152 and Sm-147.

Out of the radionuclides identified in Table 3-1, 15 of them are part of decay chains for which the activity of the progeny radionuclide can be assessed by assuming secular equilibrium (as in the example with Cs-137 and Ba-137m). For these decay chains the contributions to dose from exposure of short-lived progeny present in the environment are included in the does coefficients of the parent radionuclide. These radionuclides are listed in Table 3-2.

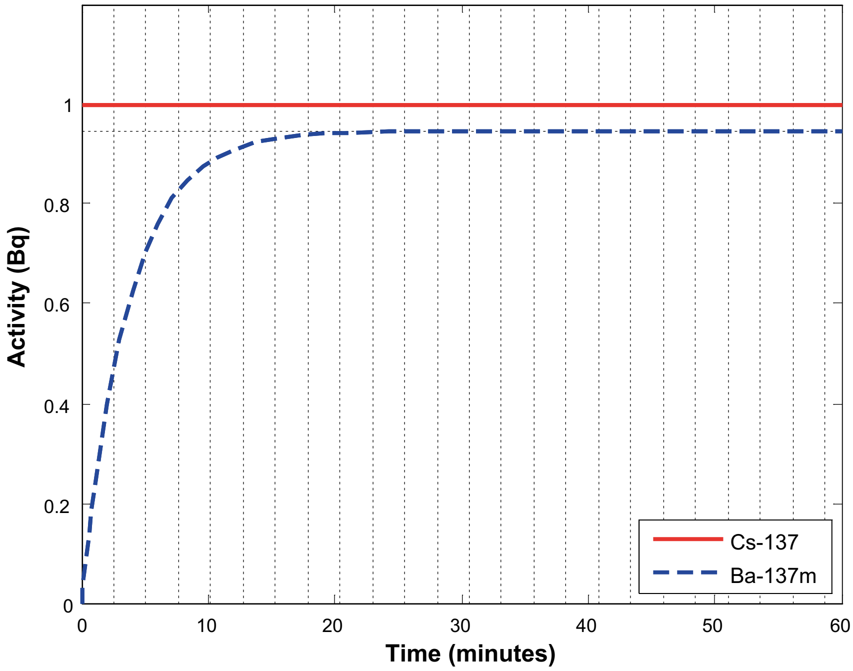

Figure 3-1. *Dynamic change of activity of Cs-137 and Ba-137m assuming an initial unit activity of Cs-137 and no initial activity of Ba-137m. Vertical dotted lines correspond to one half-life of Ba-137m (~ 2.5 minutes). Horizontal dotted line corresponds to the branching ratio Cs-137 – > Ba-137m (94.6%).*

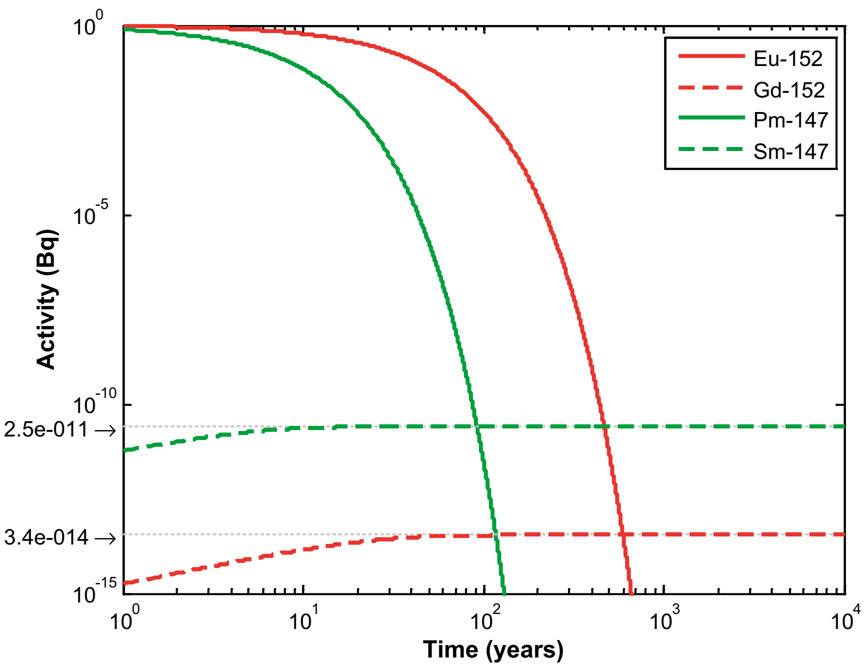

Figure 3-2. *Dynamic change of activity of Eu-152, Gd-152, Pm-147 and Sm-147 assuming an initial unit activity of Eu-152 and Pm-147 and no initial activity of Gd-152 and Sm-147. Horizontal dotted lines correspond to the activity levels that Gd-152 (3.4E–14Bq) and Sm-147 (2.5E–11Bq) will reach before Eu-152 and Pm-147 have decayed.*

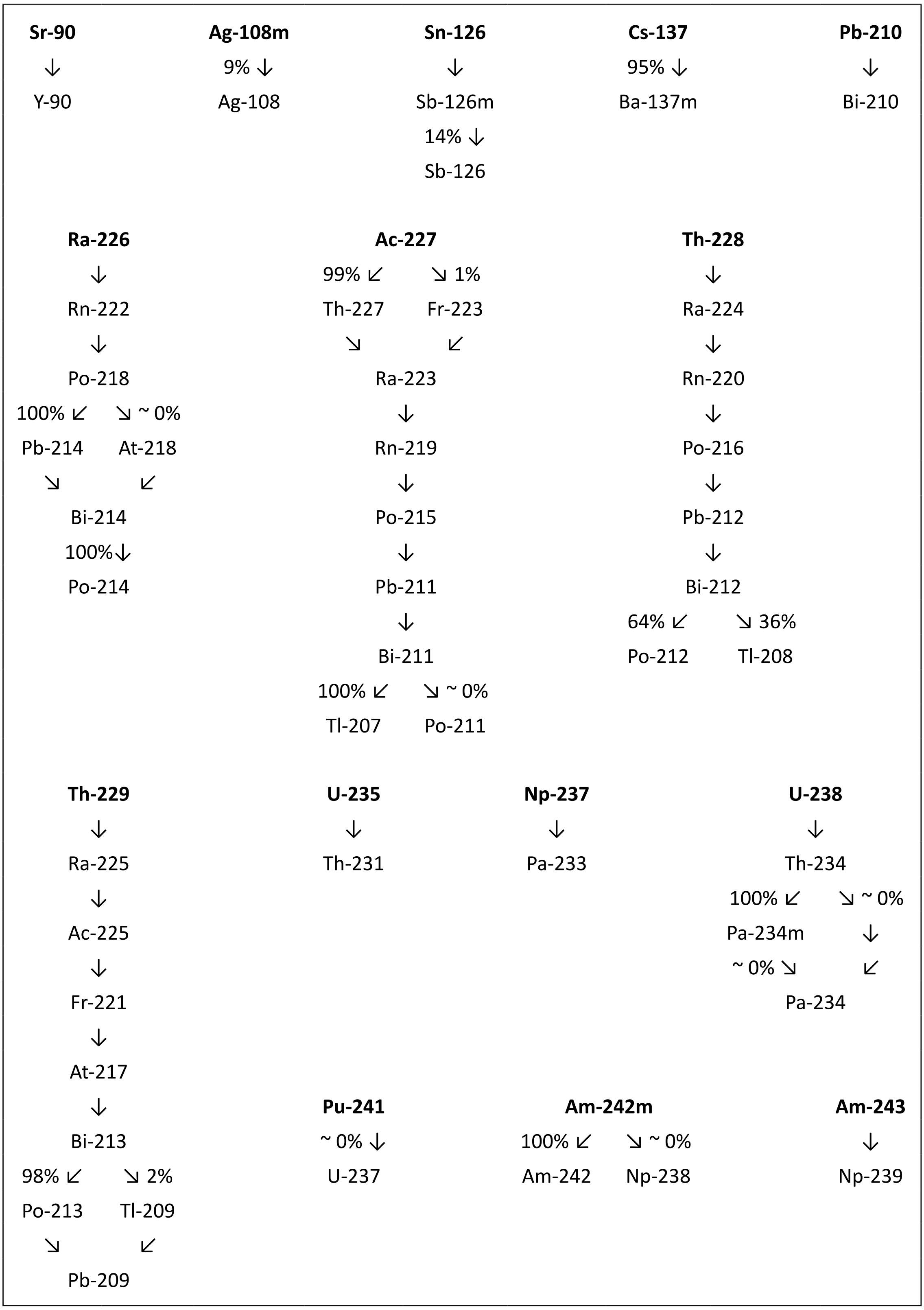

Figure 3-3. The decay chains for which the contribution of the progeny is included in the dose coefficient of the parent nuclide.

Table 3-2. Radionuclides implicitly taken account of in the biosphere assessment, their half-lives, decay modes, and radioactive progeny. Radiation decay data from ICRP (1983).

Radionuclide	Half-life	Decay modes[1]	Progeny (branching ratio)	
Y-90	64.0h	β–		
Ag-108	2.37m	EC,β+,β–		
Sb-126	12.4d	β–		
Sb-126m	19.0m	IT,β–	Sb-126 (14%)	
Ba-137m	2.552m	IT		
Tl-207	4.77m	β–		
Tl-208	3.07m	β–		
Pb-209	3.253h	β–		
Tl-209	2.20m	β–	Pb-209 (100%)	
Bi-210	5.012d	β–	Po-210 (100%)	
Bi-211	2.14m	α,β–	Tl-207 (99.72%)	Po-211 (0.28%)
Pb-211	36.1m	β–	Bi-211 (100%)	
Po-211	0.516s	α		
Bi-212	60.55m	β–,α	Po-212 (64.07%)	Tl-208 (35.93%)
Pb-212	10.64h	β–	Bi-212 (100%)	
Po-212	0.305us	α		
Bi-213	45.65m	β–,α	Po-213 (97.84%)	Tl-209 (2.16%)
Po-213	4.2us	α	Pb-209 (100%)	
Bi-214	19.9m	β–	Po-214 (99.98%)	
Pb-214	26.8m	β–	Bi-214 (100%)	
Po-214	164.3us	α	Pb-210 (100%)	
Po-215	0.001780s	α	Pb-211 (100%)	
Po-216	0.15s	α	Pb-212 (100%)	
At-217	0.0323s	α	Bi-213 (100%)	
At-218	2s	α	Bi-214 (100%)	
Po-218	3.05m	α,β–	Pb-214 (99.98%)	At-218 (0.02%)
Rn-219	3.96s	α	Po-215 (100%)	
Rn-220	55.6s	α	Po-216 (100%)	
Fr-221	4.8m	α	At-217 (100%)	
Rn-222	3.8235d	α	Po-218 (100%)	
Fr-223	21.8m	β–	Ra-223 (100%)	
Ra-223	11.434d	α	Rn-219 (100%)	
Ra-224	3.66d	α	Rn-220 (100%)	
Ac-225	10.0d	α	Fr-221 (100%)	
Ra-225	14.8d	β–	Ac-225 (100%)	
Th-227	18.718d	α	Ra-223 (100%)	
Th-231	25.52h	β–	Pa-231 (100%)	
Pa-233	27.0d	β–	U-233 (100%)	
Pa-234	6.70h	β–	U-234 (100%)	
Pa-234m	1.17m	β–,IT	U-234 (99.87%)	Pa-234 (0.13%)
Th-234	24.10d	β–	Pa-234m (99.8%)	Pa-234 (0.2%)
U-237	6.75d	β–	Np-237 (100%)	
Np-238	2.117d	β–	Pu-238 (100%)	
Np-239	2.355d	β–	Pu-239 (100%)	
Am-242	16.02h	EC,β–	Cm-242 (82.7%)	Pu-242 (17.3%)

[1] Decay modes: β– for beta minus decay, β+ for beta plus decay, EC for electron capture, α for alpha decay, IT for isometric and transition.

3.4 Radionuclide-specific dose coefficients

The dose coefficient for external exposure used in the assessment is defined as the dose rate to which an individual is exposed from a unit volumetric concentration in soil or from a unit surface concentration of the radionuclide. The values used for external exposure from a volumetric source are based on homogeneous distribution of the radionuclides in a soil layer of infinite depth and infinite lateral extent (Eckerman and Leggett 1996, Eckerman and Ryman 1993). The values were derived from calculations for a typical silt soil with a density of 1,600 kg m^{-3}, 0 ~ 2% air and 0 ~ 3% water content reported in Eckerman and Ryman (1993) taking into account the latest values of tissue weighting factors recommended by ICRP (1996). The very low water content, presumably based for an arid area, is cautious because the dose rates are expressed on a volumetric basis and would be decreased at higher densities corresponding to larger percentage water contents. In modelling of external exposure, the external coefficients could be converted to consider the actual density of the modelled soil (Eckerman and Leggett 1996, Eckerman and Ryman 1993), but this has not been taken into account in SR-PSU. This would not make a large difference for mineral soils. The effect would be larger for peat soils because of their low bulk density, but this would be partly compensated by high water content. Overall, for a density of 1,000 kg m^{-3}, the dose rates would increase by about 60%.

The internal dose coefficients presented in ICRP Publication 72 (ICRP 1996) take into account the dose due to ingrowth of radioactive progeny radionuclides within the body, following an intake of unit activity of the parent nuclide. The dose coefficient for internal exposure is defined as the committed effective dose to an individual from a unit intake of the radionuclide orally (ingested food/water or inhaled air). The dose is integrated over 50 years; hence the dose coefficients correspond to life-time committed effective doses for an adult. The dose coefficients defined in ICRP (1996) are used in this safety assessment.

As noted above, for intake of radionuclides, the dose coefficients take into account the radioactive progeny that are formed within the body (ICRP 1996). The extra contribution to dose from intake of short-lived progeny products present in the environment is very small, sometimes extremely small. However, for completeness, it is conservatively included in the final dose coefficients in the same way as for external exposure.

The dose coefficients for ingestion are independent of the ingestion pathway, i.e. via food or water. The only exception is carbon-14, for which different dose coefficients are used for ingestion via food and via water, because carbon is present in different chemical forms in water and food, and carbon-14 in food is more bioavailable (Leggett 2004). The coefficient for food is about 10 times higher than for water. The does coefficient for ingestion of water for carbon-14, doseCoef_ing_water_14C is 2.9E–11 Sv Bq^{-1}.

The inhalation dose coefficients are specified for different absorption rates from the respiratory tract: fast (F), moderate (M) and slow (S). Slow adsorption rates cause the highest exposure for most radionuclides, but there are exceptions; for example for isotopes of the actinides Np, Pu, Am and Cm the highest exposure is observed for fast absorption rates. The highest value for each isotope across different classes of absorption rates was pessimistically chosen. For carbon-14 the value for carbon-14 dioxide (CO_2) was used.

In Table 3-3 the dose coefficients due to exposure from each of the radionuclides that is explicitly modeled are listed and Table 3-4 lists corresponding dose coefficients for the short-lived progeny of the nuclides in Table 3-3 (these radionuclides are not explicitly modeled and are assumed to be in secular equilibrium with parent radionuclides). The dose coefficients are used to calculate the dose coefficients presented in Table 3-5 which includes both the contribution of the parent nuclide and those of the short-lived progeny. The dose coefficients listed in Table 3-5 are used in the dose calculations.

Table 3-3. Dose coefficients (Sv Bq^{-1}) for exposure from ingestion (doseCoef_ing) and inhalation (doseCoef_inh) (ICRP 1996). Dose coefficients (Sv h^{-1} per Bq m^{-3} and Sv h^{-1} per Bq m^{-2}) for external exposure (doseCoef_ext, doseCoef_ext_surf) (Eckerman and Leggett 1996, Eckerman and Ryman 1993) due to spatially uniformly distributed radionuclides to an infinite depth and surface exposure respectively. Values *include only* radiations emitted by the indicated radionuclide.

Radionuclide	Half-life	Decay modes[1]	Ingestion Sv Bq^{-1}	Inhalation Sv Bq^{-1}	Type –	External exposure Sv h^{-1} per Bq m^{-3}	Sv h^{-1} per Bq m^{-2}
H-3	12.35y	β–	1.8E–11	2.6E–10	S	–	–
C-14	5,730y	β–	5.8E–10	6.2E–12	CO_2	2.1E–19	4.6E–17
			2.9E–11*	–	–	–	–
Cl-36	3.01E5y	EC,β+,β–	9.3E–10	7.3E–09	M	4.8E–17	4.0E–14
Ca-41	1.4E5y	EC	1.9E–10	1.8E–10	S	–	–
Ni-59	7.5E4y	EC	6.3E–11	4.4E–10	S	–	–
Co-60	5.271y	β–	3.4E–09	3.1E–08	S	3.0E–13	8.3E–12
Ni-63	96y	β–	1.5E–10	1.3E–09	S	–	–
Se-79	65,000y	β–	2.9E–09	6.8E–09	S	2.9E–19	5.9E–17
Sr-90	29.12y	β–	2.8E–08	1.6E–07	S	1.2E–17	5.9E–15
Mo-93	3.5E3y	EC	3.1E–09	2.3E–09	S	8.0E–18	1.4E–14
Nb-93m	13.6y	IT	1.2E–10	1.8E–09	S	1.4E–18	2.5E–15
Zr-93	1.53E6y	β–	1.1E–09	2.5E–08	F	–	–
Nb-94	2.03E4y	β–	1.7E–09	4.9E–08	S	1.8E–13	5.4E–12
Tc-99	2.13E5y	β–	6.4E–10	1.3E–08	S	2.1E–18	2.3E–16
Pd-107	6.5E6y	β–	3.7E–11	5.9E–10	S	–	–
Ag-108m	127y	EC,IT	2.3E–09	3.7E–08	S	1.7E–13	5.6E–12
Cd-113m	13.6y	β–	2.3E–08	1.1E–07	F	1.2E–17	6.4E–15
Sn-126	1.0E5y	β–	4.7E–09	2.8E–08	M	2.5E–15	1.7E–13
I-129	1.57E7y	β–	1.1E–07	3.6E–08	F	1.8E–16	7.0E–14
Ba-133	10.74y	EC	1.5E–09	1.0E–08	S	3.5E–14	1.3E–12
Cs-135	2.3E6y	β–	2.0E–09	8.6E–09	S	6.2E–19	9.7E–17
Cs-137	30.0y	β–	1.3E–08	3.9E–08	S	1.6E–17	1.1E–14
Sm-151	90y	β–	9.8E–11	4.0E–09	M	1.3E–20	1.3E–17
Eu-152	13.33y	β–,EC,β+	1.4E–09	4.2E–08	M	1.3E–13	3.9E–12
Ho-166m	1.20E3y	β–	2.0E–09	1.2E–07	M	1.9E–13	5.9E–12
Pb-210	22.3y	β–	6.9E–07	5.6E–06	S	3.8E–17	7.7E–15
Po-210	138.38d	α	1.2E–06	4.3E–06	S	9.5E–19	2.9E–17
Ra-226	1,600y	α	2.8E–07	9.5E–06	S	5.6E–16	2.2E–14
Ac-227	21.773y	β–,α	1.1E–06	5.5E–04	F	8.6E–18	5.1E–16
Th-228	1.9131y	α	7.2E–08	4.0E–05	S	1.4E–16	7.7E–15
Th-229	7,340y	α	4.9E–07	2.4E–04	F	5.6E–15	2.8E–13
Th-230	7.7E4y	α	2.1E–07	1.0E–04	F	2.1E–17	2.3E–15
Pa-231	3.276E4y	α	7.1E–07	1.4E–04	M	3.4E–15	1.4E–13
U-232	72y	α	3.3E–07	3.7E–05	S	1.5E–17	2.9E–15
U-233	1.585E5y	α	5.1E–08	9.6E–06	S	2.4E–17	2.2E–15
U-234	2.445E5y	α	4.9E–08	9.4E–06	S	6.6E–18	2.1E–15
U-235	703.8E6y	α	4.7E–08	8.5E–06	S	1.3E–14	5.0E–13
U-236	2.3415E7y	α	4.7E–08	8.7E–06	S	3.4E–18	1.8E–15
Np-237	2.14E6y	α	1.1E–07	5.0E–05	F	1.3E–15	9.1E–14
Pu-238	87.74y	SF,α	2.3E–07	1.1E–04	F	2.2E–18	2.3E–15
U-238	4.468E9y	SF,α	4.5E–08	8.0E–06	S	1.5E–18	1.5E–15
Pu-239	24,065y	α	2.5E–07	1.2E–04	F	5.1E–18	1.0E–15
Pu-240	6,537y	SF,α	2.5E–07	1.2E–04	F	2.2E–18	2.2E–15
Am-241	432.2y	α	2.0E–07	9.6E–05	F	7.2E–16	8.4E–14
Pu-241	14.4y	α,β–	4.8E–09	2.3E–06	F	1.0E–19	6.2E–18
Am-242m	152y	α,IT	1.9E–07	9.2E–05	F	2.8E–17	8.1E–15
Pu-242	3.763E5y	SF,α	2.4E–07	1.1E–04	F	1.9E–18	1.8E–15
Cm-242	162.8d	SF,α	1.2E–08	5.9E–06	S	2.5E–18	2.5E–15
Am-243	7,380y	α	2.0E–07	9.6E–05	F	2.4E–15	1.7E–13
Cm-243	28.5y	α,EC	1.5E–07	6.9E–05	F	1.0E–14	4.2E–13
Cm-244	18.11y	SF,α	1.2E–07	5.7E–05	F	1.7E–18	2.3E–15
Cm-245	8,500y	α	2.1E–07	9.9E–05	F	5.9E–15	2.9E–13
Cm-246	4,730y	SF,α	2.1E–07	9.8E–05	F	1.6E–18	2.1E–15

* Dose coefficient used for ingestion of water (Leggett 2004).

[1] Decay modes: β– for beta minus decay, β+ for beta plus decay, EC for electron capture, α for alpha decay, IT for isometric transition, and SF for spontaneous fission.

Table 3-4. Dose coefficients (Sv Bq^{-1}) for exposure from ingestion (doseCoef_ing) and inhalation (doseCoef_inh) (ICRP 1996) for short-lived progeny not explicitly modelled. Dose coefficients (Sv h^{-1} per Bq m^{-3} and Sv h^{-1} per Bq m^{-2}) for external exposure (doseCoef_ext and doseCoef_ext_surf) (Eckerman and Leggett 1996, Eckerman and Ryman 1993) due to spatially uniformly distributed radionuclides to an infinite depth and surface exposure respectively. Values *include only* radiations emitted by the indicated radionuclide.

Radionuclide	Half-life –	Decay modes[3]	Ingestion Sv Bq^{-1}	Inhalation Sv Bq^{-1}	Type –	External exposure Sv h^{-1} per Bq m^{-3}	Sv h^{-1} per Bq m^{-2}
Y-90	64.0h	β–	2.7E–09	1.5E–09	S	7.7E–16	3.9E–13
Ag-108	2.37m	EC,β+,β–	–	–	–	2.2E–15	3.2E–13
Sb-126	12.4d	β–	2.4E–09	3.2E–09	S	3.1E–13	9.8E–12
Sb-126m	19.0m	IT,β–	3.6E–11	2.0E–11	S	1.7E–13	5.6E–12
Ba-137m	2.552m	IT	–	–	–	6.5E–14	2.1E–12
Tl-207	4.77m	β–	–	–	–	4.4E–16	2.0E–13
Tl-208	3.07m	β–	–	–	–	4.2E–13	1.1E–11
Pb-209	3.253h	β–	5.7E–11	6.1E–11	S	1.5E–17	1.1E–14
Tl-209	2.20m	β–	–	–	–	2.4E–13	6.9E–12
Bi-210	5.012d	β–	1.3E–09	9.3E–08	M	1.1E–16	1.3E–13
Bi-211	2.14m	α,β–	–	–	–	4.6E–15	1.6E–13
Pb-211	36.1m	β–	1.8E–10	1.2E–08	S	5.6E–15	3.4E–13
Po-211	0.516s	α	–	–	–	8.6E–16	2.7E–14
Bi-212	60.55m	β–,α	2.6E–10	3.1E–08	M	2.1E–14	8.1E–13
Pb-212	10.64h	β–	6.0E–09	1.9E–07	S	1.2E–14	4.9E–13
Po-212	0.305us	α	–	–	–	–	–
Bi-213	45.65m	β–,α	2.0E–10	3.0E–08	M	1.4E–14	6.0E–13
Po-213	4.2us	α	–	–	–	–	–
Bi-214	19.9m	β–	1.1E–10	1.4E–08	M	1.8E–13	5.2E–12
Pb-214	26.8m	β–	1.4E–10	1.5E–08	S	2.4E–14	8.6E–13
Po-214	164.3us	α	–	–	–	9.3E–18	2.9E–16
Po-215	0.001780s	α	–	–	–	1.8E–17	6.0E–16
Po-216	0.15s	α	–	–	–	1.9E–18	5.8E–17
At-217	0.0323s	α	–	–	–	3.2E–17	1.1E–15
At-218	2s	α	–	–	–	9.4E–17	1.3E–14
Po-218	3.05m	α,β–	–	–	–	1.0E–18	3.1E–17
Rn-219	3.96s	α	–	–	–	5.5E–15	1.9E–13
Rn-220	55.6s	α	3.5E–09[1]	2.1E–08[2]	–	4.1E–17	1.3E–15
Fr-221	4.8m	α	–	–	–	2.7E–15	1.0E–13
Rn-222	3.8235d	α	–	–	–	4.2E–17	1.4E–15
Fr-223	21.8m	β–	2.4E–09	8.9E–10	F	3.5E–15	2.8E–13
Ra-223	11.434d	α	1.0E–07	8.7E–06	S	1.1E–14	4.4E–13
Ra-224	3.66d	α	6.5E–08	3.4E–06	S	9.1E–16	3.3E–14
Ac-225	10.0d	α	2.4E–08	8.5E–06	S	1.1E–15	5.3E–14
Ra-225	14.8d	β–	9.9E–08	7.7E–06	S	1.7E–16	3.9E–14
Th-227	18.718d	α	8.8E–09	1.0E–05	S	9.3E–15	2.5E–13
Th-231	25.52h	β–	3.4E–10	3.3E–10	S	6.2E–16	5.6E–14
Pa-233	27.0d	β–	8.7E–10	3.9E–09	S	1.8E–14	6.7E–13
Pa-234	6.70h	β–	5.1E–10	4.0E–10	S	2.1E–13	6.5E–12
Pa-234m	1.17m	β–,IT	–	–	–	1.9E–15	3.9E–13
Th-234	24.10d	β–	3.4E–09	7.7E–09	S	4.1E–16	2.7E–14
U-237	6.75d	β–	7.6E–10	1.9E–09	S	9.3E–15	4.4E–13
Np-238	2.117d	β–	9.1E–10	3.5E–09	F	6.3E–14	1.9E–12
Np-239	2.355d	β–	8.0E–10	1.0E–09	S	1.3E–14	5.5E–13
Am-242	16.02h	EC,β–	3.0E–10	2.0E–08	S	8.6E–16	5.8E–14

[1] (NRC 1999).

[2] (ICRP 1993) recommended mean value.

[3] Decay modes: β– for beta minus decay, β+ for beta plus decay, EC for electron capture, α for alpha decay, IT for isometric transition, and SF for spontaneous fission.

Table 3-5. Dose coefficients (Sv Bq^{-1}) for exposure from ingestion (doseCoef_ing) and inhalation (dose_coef_inh) (ICRP 1996). Dose coefficients (Sv h^{-1} per Bq m^{-3} and Sv h^{-1} per Bq m^{-2}) for external exposure (doseCoef_ext and doseCoef_ext_surf) (Eckerman and Leggett 1996, Eckerman and Ryman 1993) due to spatially uniformly distributed radionuclides to an infinite depth and surface exposure respectively. Values *include* radiations emitted by the indicated radionuclide *as well as* the contribution from short-lived radioactive progeny.

Radionuclide	Ingestion Sv Bq^{-1}	Inhalation Sv Bq^{-1}	External exposure Sv h^{-1} per Bq m^{-3}	Sv h^{-1} per Bq m^{-2}
H-3	1.8E–11	2.6E–10	–	–
C-14	5.8E–10	6.2E–12	2.1E–19	4.6E–17
Cl-36	9.3E–10	7.3E–09	4.8E–17	4.0E–14
Ca-41	1.9E–10	1.8E–10	–	–
Ni-59	6.3E–11	4.4E–10	–	–
Co-60	3.4E–09	3.1E–08	3.0E–13	8.3E–12
Ni-63	1.5E–10	1.3E–09	–	–
Se-79	2.9E–09	6.8E–09	2.9E–19	5.9E–17
Sr-90⁺	3.1E–08	1.6E–07	7.9E–16	4.0E–13
Mo-93	3.1E–09	2.3E–09	8.0E–18	1.4E–14
Nb-93m	1.2E–10	1.8E–09	1.4E–18	2.5E–15
Zr-93	1.1E–09	2.5E–08	–	–
Nb-94	1.7E–09	4.9E–08	1.8E–13	5.4E–12
Tc-99	6.4E–10	1.3E–08	2.1E–18	2.3E–16
Pd-107	3.7E–11	5.9E–10	–	–
Ag-108m⁺	2.3E–09	3.7E–08	1.7E–13	5.6E–12
Cd-113m	2.3E–08	1.1E–07	1.2E–17	6.4E–15
Sn-126⁺	5.1E–09	2.8E–08	2.1E–13	7.1E–12
I-129	1.1E–07	3.6E–08	1.8E–16	7.0E–14
Ba-133	1.5E–09	1.0E–08	3.5E–14	1.3E–12
Cs-135	2.0E–09	8.6E–09	6.2E–19	9.7E–17
Cs-137⁺	1.3E–08	3.9E–08	6.2E–14	2.0E–12
Sm-151	9.8E–11	4.0E–09	1.3E–20	1.3E–17
Eu-152	1.4E–09	4.2E–08	1.3E–13	3.9E–12
Ho-166m	2.0E–09	1.2E–07	1.9E–13	5.9E–12
Pb-210⁺	6.9E–07	5.6E–06	1.4E–16	1.3E–13
Po-210	1.2E–06	4.3E–06	9.5E–19	2.9E–17
Ra-226⁺	2.8E–07	9.5E–06	2.0E–13	6.1E–12
Ac-227⁺	1.2E–06	5.5E–04	3.6E–14	1.7E–12
Th-228⁺	1.4E–07	4.4E–05	1.9E–13	5.2E–12
Th-229⁺	6.1E–07	2.4E–04	2.9E–14	1.2E–12
Th-230	2.1E–07	1.0E–04	2.1E–17	2.3E–15
Pa-231	7.1E–07	1.4E–04	3.4E–15	1.4E–13
U-232	3.3E–07	3.7E–05	1.5E–17	2.9E–15
U-233	5.1E–08	9.6E–06	2.4E–17	2.2E–15
U-234	4.9E–08	9.4E–06	6.6E–18	2.1E–15
U-235⁺	4.7E–08	8.5E–06	1.3E–14	5.6E–13
U-236	4.7E–08	8.7E–06	3.4E–18	1.8E–15
Np-237⁺	1.1E–07	5.0E–05	1.9E–14	7.6E–13
Pu-238	2.3E–07	1.1E–04	2.2E–18	2.3E–15
U-238⁺	4.8E–08	8.0E–06	3.0E–15	4.4E–13
Pu-239	2.5E–07	1.2E–04	5.1E–18	1.0E–15
Pu-240	2.5E–07	1.2E–04	2.2E–18	2.2E–15
Am-241	2.0E–07	9.6E–05	7.2E–16	8.4E–14
Pu-241⁺	4.8E–09	2.3E–06	3.3E–19	1.7E–17
Am-242m⁺	1.9E–07	9.2E–05	1.2E–15	7.5E–14
Pu-242	2.4E–07	1.1E–04	1.9E–18	1.8E–15
Cm-242	1.2E–08	5.9E–06	2.5E–18	2.5E–15
Am-243⁺	2.0E–07	9.6E–05	1.6E–14	7.3E–13
Cm-243	1.5E–07	6.9E–05	1.0E–14	4.2E–13
Cm-244	1.2E–07	5.7E–05	1.7E–18	2.3E–15
Cm-245	2.1E–07	9.9E–05	5.9E–15	2.9E–13
Cm-246	2.1E–07	9.8E–05	1.6E–18	2.1E–15

⁺ Dose coefficients include contribution from short-lived radioactive progeny assuming secular equilibrium.

3.4.1 Exposure to contaminated air following the combustion of peat or wood

The combustion of contaminated peat or wood may result in doses to humans by exposure to contaminated air (Stenberg and Rensfeldt 2014). In SR-PSU it has been assumed that peat or wood from each of the biosphere objects may be used for combustion in a household for heat production with exposure to an individual staying within 0–200 m of the release. It is assumed that the household combusts 3,440 kgdw peat per year or 4,000 kgdw wood per year (the fuel required to sustain an energy consumption of 20,000 kWh year^{-1}, assuming an energy content of 5.8 kWh kgdw^{-1} for peat and 5 kWh kgdw^{-1} for wood (Stenberg and Rensfeldt 2014)). Dose conversion factors ($DF_{combustion}$) for the exposure by inhalation of contaminated air following the combustion of peat or wood with an assumed unit activity concentration (Sv year^{-1} per Bq kgdw^{-1}) in a household are given in Table 3-6 (Stenberg and Rensfeldt 2014, Table 3-7).

The dose conversion factors include the dose contribution of the short-lived progeny by adding the dose contribution to the dose coefficient of the parent in the same way as for the other dose coefficients presented above.

Table 3-6. Dose conversion factors (Sv year^{-1} per Bq kgdw^{-1}) for the exposure by inhalation of contaminated air following the combustion of peat or wood (doseCoef_comb_wood, doseCoef_comb_peat) in a household with an energy consumption of 20,000 kWh year^{-1}. The dose conversion factors are calculated assuming exposure to an individual moving uniformly within 0–200 m from the release.

Radio-nuclide	Inhalation after combustion of peat Sv year^{-1} per Bq kgdw^{-1}	Inhalation after combustion of wood Sv year^{-1} per Bq kgdw^{-1}
Ac-227	1.04E–06	1.20E–06
Ag-108m	7.01E–11	8.06E–11
Am-241	1.82E–07	2.09E–07
Am-242m	1.74E–07	2.01E–07
Am-243	1.82E–07	2.09E–07
Ba-133	1.89E–11	2.18E–11
C-14	1.17E–14	1.35E–14
Ca-41	3.41E–13	3.92E–13
Cd-113m	2.08E–10	2.40E–10
Cl-36	1.38E–11	1.59E–11
Cm-242	1.12E–08	1.29E–08
Cm-243	1.31E–07	1.50E–07
Cm-244	1.08E–07	1.24E–07
Cm-245	1.87E–07	2.16E–07
Cm-246	1.86E–07	2.14E–07
Co-60	5.87E–11	6.76E–11
Cs-135	1.63E–11	1.87E–11
Cs-137	7.39E–11	8.50E–11
Eu-152	7.95E–11	9.15E–11
H-3	4.92E–13	5.67E–13
Ho-166m	2.27E–10	2.62E–10
I-129	6.82E–11	7.85E–11
Mo-93	4.36E–12	5.01E–12
Nb-93m	3.41E–12	3.92E–12
Nb-94	9.28E–11	1.07E–10
Ni-59	8.33E–13	9.59E–13
Ni-63	2.46E–12	2.83E–12
Np-237	9.47E–08	1.09E–07
Pa-231	2.65E–07	3.05E–07
Pb-210	1.06E–08	1.22E–08
Pd-107	1.12E–12	1.29E–12
Po-210	8.14E–09	9.37E–09
Pu-238	2.08E–07	2.40E–07
Pu-239	2.27E–07	2.62E–07
Pu-240	2.27E–07	2.62E–07
Pu-241	4.36E–09	5.01E–09
Pu-242	2.08E–07	2.40E–07
Ra-226	1.80E–08	2.07E–08
Se-79	1.29E–11	1.48E–11
Sm-151	7.57E–12	8.72E–12
Sn-126	5.38E–11	6.19E–11
Sr-90	3.06E–10	3.52E–10
Tc-99	2.46E–11	2.83E–11
Th-228	8.25E–08	9.50E–08
Th-229	4.56E–07	5.25E–07
Th-230	1.89E–07	2.18E–07
U-232	7.01E–08	8.06E–08
U-233	1.82E–08	2.09E–08
U-234	1.78E–08	2.05E–08
U-235	1.61E–08	1.85E–08
U-236	1.65E–08	1.90E–08
U-238	1.52E–08	1.75E–08
Zr-93	4.73E–11	5.45E–11

3.4.2 Exposure to progeny radionuclides in agricultural lands

The radionuclide transport model calculates analytically activity concentrations in agricultural soils depending on different source terms. These activity concentrations are either an average activity concentration during 50 years of agriculture or steady state solutions. As described in radionuclide transport model description, these activity concentrations do not take into account the potential exposure due to longer-lived radioactive progeny that may build up during this 50-year period.

To handle the potential contribution due to exposure from longer-lived radioactive progeny the scaling factors (dose_ingrowth_agri_ext/inh/ing, unitless) presented in Table 3-7 are used. These scaling factors are calculated by taking the quotient between the 50 years average of the exposure due to a unit concentration taking into account ingrowth and exposure to longer-lived progeny and the 50 year average of corresponding exposure not taking into account ingrowth of longer-lived progeny radionuclides.

Table 3-7. Scaling factors (dose_ingrowth_agri_ext/inh/ing, unitless) taking into account contribution of exposure from long-lived radioactive progeny in agricultural lands.

Radionuclide	External	Inhalation	Ingestion
Ac-227	1	1	1
Ag-108m	1	1	1
Am-241	1	1	1
Am-242m	1.002	1.2	1.2
Am-243	1	1.001	1.001
Ba-133	1	1	1
C-14	1	1	1
Ca-41	1	1	1
Cd-113m	1	1	1
Cl-36	1	1	1
Cm-242	1.1	4.1	4.2
Cm-243	1	1.001	1.001
Cm-244	1.004	1.007	1.007
Cm-245	1.002	1.033	1.032
Cm-246	1	1	1
Co-60	1	1	1
Cs-135	1	1	1
Cs-137	1	1	1
Eu-152	1	1	1
H-3	1	1	1
Ho-166m	1	1	1
I-129	1	1	1
Mo-93	1.1	1.5	1.023
Nb-93m	1	1	1
Nb-94	1	1	1
Ni-59	1	1	1
Ni-63	1	1	1
Np-237	1	1	1
Pa-231	6.3	3.0	1.8
Pb-210	1.006	1.7	2.7
Pd-107	1	1	1
Po-210	1	1	1
Pu-238	1	1	1
Pu-239	1	1	1
Pu-240	1	1	1
Pu-241	114.9	3.2	3.2
Pu-242	1	1	1
Ra-226	1	1.5	4.3
Se-79	1	1	1
Sm-151	1	1	1
Sn-126	1	1	1
Sr-90	1	1	1
Tc-99	1	1	1
Th-228	1	1	1
Th-229	1	1	1
Th-230	107.7	1.001	1.049
U-232	11,528	2.1	1.4
U-233	3.8	1.1	1.028
U-234	1.1	1.002	1.001
U-235	1.001	1.022	1.013
U-236	1	1	1
U-238	1	1	1
Zr-93	1	1.042	1.1

4 Landscape geometries

The safety assessment spans a long time scale; the largest changes in the landscape are seen before 20,000 AD. During this period, the coastal landscape will develop into an inland landscape, where most of the lakes develop into mires. Consequently the modelling time frame for the Landscape Developmental Model, LDM (SKB 2014c), is from the present to 40,000 AD. The LDM is based on data from a large number of different sources, e.g. the Digital Elevation Model, DEM (Strömgren and Brydsten 2013), the coupled Regolith-Lake Development Model, RLDM, (Brydsten and Strömgren 2013) and Regolith Depth Model, RDM (Sohlenius et al. 2013).

The LDM is used to describe geometric and time-dependent properties of the biosphere objects over time. By following the development of each biosphere object in the LDM, a large number of data have been extracted and used as input parameters in the radionuclide transport model for the biosphere. These parameters are areas of the biosphere objects, parameters describing transition stages, thicknesses of regolith layers and rates of sedimentation, resuspension and ingrowth of peat. These parameters are described in Sections 4.3 to 4.5.

The parameters that describe the landscape geometries have not been assigned probability density distribution functions. However, an alternative modelling approach was undertaken in order to study the effect of alternative delineations of the most affected biosphere object 157_2. In this approach, a number of parameters were assigned alternative values (area_obj, area_obj_ter, z_regoLow, z_regoGL, z_regoPG_ter and hydrological fluxes). This approach is presented in detail in the SKB (2014c) and the alternative parameters are described in Section 12.3 of this report.

4.1 Experience from previous safety assessments

The landscape modelling in SR-Site (Lindborg 2010, Lindborg et al. 2013) has been further developed and a number of improvements have been included in the LDM for SR-PSU (see also Brydsten and Strömgren 2013, SKB 2014c). Below are some of the improvements affecting the parameterisation in SR-PSU that were not included in the parameterisation in SR-Site.

- The new Digital Elevation Model, DEM, reported in Strömgren and Brydsten (2013) was used as input.
- An improved RDM based on new data showing stratigraphy, bathymetry (DEM) and distribution of Quaternary Deposits (QD) at the location of the present SFR was used (Sohlenius et al. 2013).
- Erodible material at the biosphere object threshold has been accounted for, when delineating the lake basin, which means that the extent of the object may differ in comparison with SR-Site biosphere objects (Brydsten and Strömgren 2013).
- The rate of ingrowth in shallow bays was adjusted in order to better fit the pattern of the recent past (Brydsten and Strömgren 2013).
- The sedimentation of glacial clay in the sea stage is included with the aim of introducing a more dynamic description of the glacial clay deposits in the landscape (Brydsten and Strömgren 2013).
- The wave model uses only a windspeed of 20 m s^{-1} as a result of a sensitivity analysis that suggested this limit (Brydsten and Strömgren 2013).

4.2 Influence of climate on parameter values

Climate changes have implications for some of the parameters presented in this chapter. The thickness of the peat layer is dependent on the balance between net primary production and mineralisation. This means that the ingrowth of peat may be faster during certain climate conditions and slower during permafrost conditions. The ingrowth during temperate conditions is considered to be a good estimate that will suitably represent somewhat colder and warmer conditions (see comparison with field estimates in Löfgren 2010). In the modelling of permafrost conditions, the peat ingrowth, sedimentation rate and resuspension rate are adjusted to a significantly lower level than for the base case (Brydsten and Strömgren 2013). However, the permafrost period occurs in the far future when all the relevant lakes already have been terrestrialised, meaning that the change in ingrowth will have no impact on the modelling results.

In the extended global warning case, the sea level will increase rather fast in the near future, this sea-level rise will be compensated by the isostatic uplift, giving no change in shore line location. This eustatic sea-level rise will then decrease and return to the levels estimated according to the base case shoreline regression predictions (SKB 2014d). In the calculation case of extended global warming, the landscape development (shore line displacement) is assumed to be delayed by 1,000 year (in comparison to the base case). Therefore the time dependent parameters presented below is shifted 1,000 years, meaning that the data presented for year 2000 is used for the year 1000 in this calculation case.

For the periglacial calculation case taliks are modelled in object 157_1 and 114. For object 114 geometric data for the year 17,500 AD are presented in Section 4.6. For object 157_1 the same data as for the base case are used for the period up to 17,500 AD (the year when the first permafrost occurs). For the permafrost period, 17,500 to 20,500 AD data for the year 17,500 AD are used.

For glacial condition, the simulations starts at year –9, 350 and ends at present (year 2000).

The other parameters are regarded to have robust values that are reasonable within the suggested ranges of potential temperatures and precipitation.

4.3 Parameters describing developmental stages of the biosphere object

The transitions of biosphere objects from marine basins to shallow sea bays, lakes and mires are driven by land-rise. These transitions are initiated when certain thresholds for the biosphere object are reached. The time at which a threshold is reached, for instance the year when the isolation of a lake starts, is used to specify the occurrence of a transition, in this case from a bay into a lake. These times of exceedance of thresholds are also used to determine when certain activities, e.g. draining of a mire, are possible. The thresholds are also used to interpolate other parameters between sea and lake stages, e.g. water fluxes and net primary production.

These parameter values are derived from the time series describing the development of the biosphere objects (Brydsten and Strömgren 2013).

4.3.1 Time at which lake isolation starts

Lakes are formed due to land-rise, which isolates marine basins from the adjacent marine areas. When the biosphere object has reached a certain height above sea level, the marine area will start to develop into a lake. The year when this threshold is reached is defined as the parameter, threshold_start. At this time, the marine basin becomes an isolated lake basin for short periods of the year. This time point is determined as the time when the lake threshold reach the sea level at periods of extreme low sea levels (1.2 m below the average sea level). For biosphere objects that develop into a wetland without having a lake stage, the parameter describes the year when land starts to appear within the biosphere object. The threshold_start values for each basin are presented in Table 4-1.

4.3.2 Time of complete isolation

The parameter, threshold_stop, represents the year when the isolation of a lake from a marine object is complete. Sea-level changes during a year make the transformation from marine to limnic conditions less clear. Therefore, in addition to a year describing the start of the isolation (see above) a stop year is also presented. The threshold_stop year represents the year where there is no longer any saltwater intrusion into the lake basin as the lake threshold is above the sea level even under periods of extreme high sea levels (1.0 m above the average sea level). For biosphere objects that develop into a wetland without having a lake stage this parameter describes the time when the complete biosphere object is above sea level at extreme high sea level. This also represents the time from when it is possible to drain and use the mire as agricultural land. The threshold_stop values for each basin are presented in Table 4-1.

4.3.3 Time when it is possible to use a well

For all objects except object 157_2 and 121_2 the time when it is possible to dig or drill a well is the same as the time when the isolation of a lake (threshold_stop above). That is when the object is 1 m above the sea level and salt water intrusions are unlikely to spoil the well water. For object 157_2 and object 121_2 the time when is it possible to dig or drill a well is time when the highest elevated part of the object is located 1 meter above sea level.

4.3.4 Time of isolation

The parameter, threshold_isolation, is the year when a lake is isolated from regular saltwater intrusions, and corresponds to the time point when the lake threshold reach the average sea level. However, for the two objects lacking a lake stage the corresponding time is when the object is considered to be completely above normal sea level. The threshold_isolation values for each basin are presented in Table 4-1.

4.3.5 Time when land areas start to appear in the object

The parameter, threshold_land, describes the time when the mire starts to appear in the biosphere object (shown in Table 4-1). This year occurs before the year threshold_start since reed ingrowth in shallow marine bays starts before the isolation of a lake.

4.3.6 Time when the whole biosphere object is turned into a wetland

The parameter, threshold_end, describes the time point when the lake basin has been filled with peat and the whole biosphere object has become a wetland (Table 4-1).

Table 4-1. Threshold_start and threshold_stop represent the start and stop of the isolation period for each basin in Forsmark. Threshold_isolation is the time point when the lake is isolated or when the mire object is above the sea level (when a lake stage is missing). Threshold_land is the time when land appears in the biosphere object and Threshold_end is the time point when the lake basin is filled with peat. Threshold_well is the year when it is possible to use a well in the object.

Biosphere object	threshold _start (year AD)	threshold_stop (year AD)	threshold_isolation (year AD)	threshold_land (year AD)	threshold_end (year AD)	threshold_well (year AD)
116	4307	4734	4540	4001	9900	4734
121_1	3592	4003	3818	3501	6400	4003
121_2	2613	3886	3683	2501	4000	2793
157_1	4261	4687	4493	4001	5700	4687
157_2	2984	4485	4276	2501	4500	3169
159	3856	4273	4084	3501	7600	4273
160	2990	3390	3210	2501	8800	3390

4.4 Parameters describing biosphere object geometries

The biosphere objects will develop over time due to land-rise. The geometries of the objects will therefore be altered in time (see Chapter 2). The regolith compartments are described in Chapter 2 and in Saetre et al. (2013a). The thicknesses of the compartments are object specific and derived from the RLDM (Brydsten and Strömgren 2013). The thicknesses of the postglacial sediments and the anoxic peat layer change with time whereas the thicknesses of the till, glacial clay and oxic peat/sediment layers are constant over time.

4.4.1 Total size of biosphere objects after isolation from the sea

The parameter, area_obj, describes the total size of the lake/terrestrial biosphere object at the time of isolation from the sea. The areas of the biosphere objects were derived using the locations of radionuclide discharge from the host rock and the RDLM model (SKB 2014c). The area of the object is not time-dependent.

Table 4-2. Size of the different biosphere objects after isolation from the sea (area_obj).

Biosphere object	area_obj (m^2)
116	1,491,600
121_1	270,000
121_2	176,524
157_1	103,600
157_2	146,704
159	103,200
160	158,400

4.4.2 Surface area of the aquatic part of each biosphere object

The parameter, area_obj_aqu, represents the surface area of the aquatic part of each biosphere object and is calculated for each time-step used in the radionuclide transport model for the biosphere. The aquatic area of the biosphere object is constant for most of the time during the marine stage. However, when the marine basins get shallower and closer to becoming lakes, the aquatic area of each object decreases, as part of the basin becomes land. Generally, the lake area is less than the total biosphere object area (area_obj) even in the first lake stage, due to reed ingrowth in the shallow bay stage. The data are object- and time-dependent, the data set used is presented in Appendix C.

4.4.3 Surface area of the terrestrial part of the biosphere objects

The parameter, area_obj_ter, represents the surface area covered with peat in a biosphere object and is calculated for each time-step used in the radionuclide transport model for the biosphere. This area starts to build up in the shallow bay stage, depending on how the water depth of the bay meets the criteria set for when reed may establish and expand. The maximum area of the mire is equal to the area_obj presented in Table 4-2. The data are object- and time-dependent, the data set used is presented in Appendix C.

4.4.4 Average depth of water

The parameter, z_water, represents the average water depth in a biosphere object (for the marine basin or the lake) and is calculated for each time-step used in the radionuclide model. The data are object- and time-dependent, the data set used is presented in Appendix C.

4.4.5 Thickness of glacial till layer

This parameter (z_regoLow) represents the total thickness of the glacial till covering the bedrock surface in the biosphere objects. The thickness and distribution of this layer is constant over time, from the deglaciation onwards. The distribution and thickness of clayey till with a low frequency of boulders originates from the RDM (Sohlenius et al. 2013).

Table 4-3. Mean thickness (m) of the lower regolith (z_regoLow) below the identified biosphere objects.

Biosphere object	Mean thickness (m)
116	2.99
121_1	6.26
121_2	3.97
157_1	3.14
157_2	2.34
159	2.46
160	2.21

4.4.6 Thickness of the glacial clay layer

The parameter z_regoGL represents the mean thickness of glacial clay covering the till and bedrock surface from the deglaciation onwards. The glacial clay accumulates during the marine stage, but the thickness and distribution of this layer is regarded as constant over time as soon as the biosphere object is above the Baltic Sea shoreline. The thickness of the glacial clay layer is based on the present distribution of glacial clay, as obtained from the regolith map in Sohlenius et al. (2013), on which a layer of clay was superimposed to represent the situation after the latest deglaciation. The erosion of glacial clay through time was thereafter modelled by Brydsten and Strömgren (2013) (See also discussion in Chapter 5 and in SKB 2014c). The values presented in Table 4-4 are means for each marine basin prior to isolation and also represent the glacial clay in the lakes and below the mires.

Table 4-4. Mean thickness (m) of the glacial clay (z_regoGL) below the identified biosphere objects when they are in a late sea stage (these values are expected to be valid also for later stages).

Biosphere object	Mean thickness (m)
116	2.35
121_1	2.62
121_2	0.61
157_1	1.39
157_2	0.184
159	0.37
160	0.43

4.4.7 Thickness of the postglacial gyttja clay in lakes

The parameter z_regoPG_aqu describes the thickness of post glacial clay gyttja that start to accumulate directly after deglaciation. These fine-grained sediments are rich in organic material, and are affected by both the rates of sedimentation and resuspension. In the RLDM clay gyttja accumulates in lakes, in shallow bays and in the deepest parts of the sea (Brydsten and Strömgren 2013). The thickness of this regolith layer is object- and time-dependent, and parameter values used are presented in Appendix C.

4.4.8 Thickness of post glacial gyttja in wetlands

The parameter z_regoPG_ter describes the thickness of post glacial gyttja clay found below the peat in the wetland. This thickness represents the accumulated gyttja-clay laid down during the sea and lake stages, which is covered by peat in the mire (Brydsten and Strömgren 2013). The data are object- and time-dependent, the data set used is presented in Appendix C.

4.4.9 Thickness of anoxic peat

The parameter z_regoPeat describes the thickness of the anoxic and biologically inactive peat layer below the oxic peat layer in the wetland. The peat thickness increases with time until the lake basin is filled with peat. The accumulation rate of peat is dependent on the balance between net primary production and mineralisation. The amount of the carbon stored in the anoxic deep peat layer (kgC) at time t is calculated by solving the differential equation, with initial conditions of zero peat carbon at the time of emergence:

$$\frac{dSOC_{regoPeat}}{dt} = Burial_C \times area_{obj\_ter} - SOC_{regoUp\_ter} \times minRate_{regoPeat}$$

Where;

$Burial_C$	is the yearly input of soil organic carbon to the anoxic peat layer from the surface peat layer (kgC m^{-2} $year^{-1}$), see Saetre et al. (2013a),
$area_{obj\_ter}$	is the surface area of covered by mire vegetation (m^2),
SOC_{regoUp_ter}	is the amount of refractory soil organic carbon in the deep peat layer (kgC),
$minRate_{regoPeat}$	is the mineralisation rate of refractory organic carbon in the anoxic environment of the peat (kgC kgC^{-1} $year^{-1}$) (see Section 9.9).

The thickness of the layer is then calculated by dividing the amount of soil organic carbon in the layer (kgC) with the area ($area_{obj\_ter}$, m^2), density ($dens_{regoPeat}$, kgdw m^{-3}) and peat carbon fraction (f_{C_peat}, kgC $kgdw^{-1}$):

$$z\_regoPeat = \frac{SOC_{regoPeat}}{area_{obj\_ter} \times dens_{regoPeat} \times f_{C\_peat}}$$

The parameter describing the depth of the deep peat layer is object- and time-dependent, and values used are presented in Appendix C.

The thickness of the oxic peat layer (z_regoUp_ter) is discussed in Section 9.7 in this report. Here it is simply noted that the thickness of z_regoUp is 0.3 m.

4.4.10 Illustration of time-dependent parameters

The Figure 4-1 illustrates the time-dependent landscape parameters area_obj_aqu, area_obj_ter, z_regoPG_ter, z_regoPG_aqu, and z_water over time. The area_obj_aqu and z_water are decreasing with time as the objects goes through the terristrialisation process. The area_obj_ter and the thickness of the regolith compartments (z_regoPG_aqu and z_regoPG_ter) starts to increase as *threshold_start* is reached.

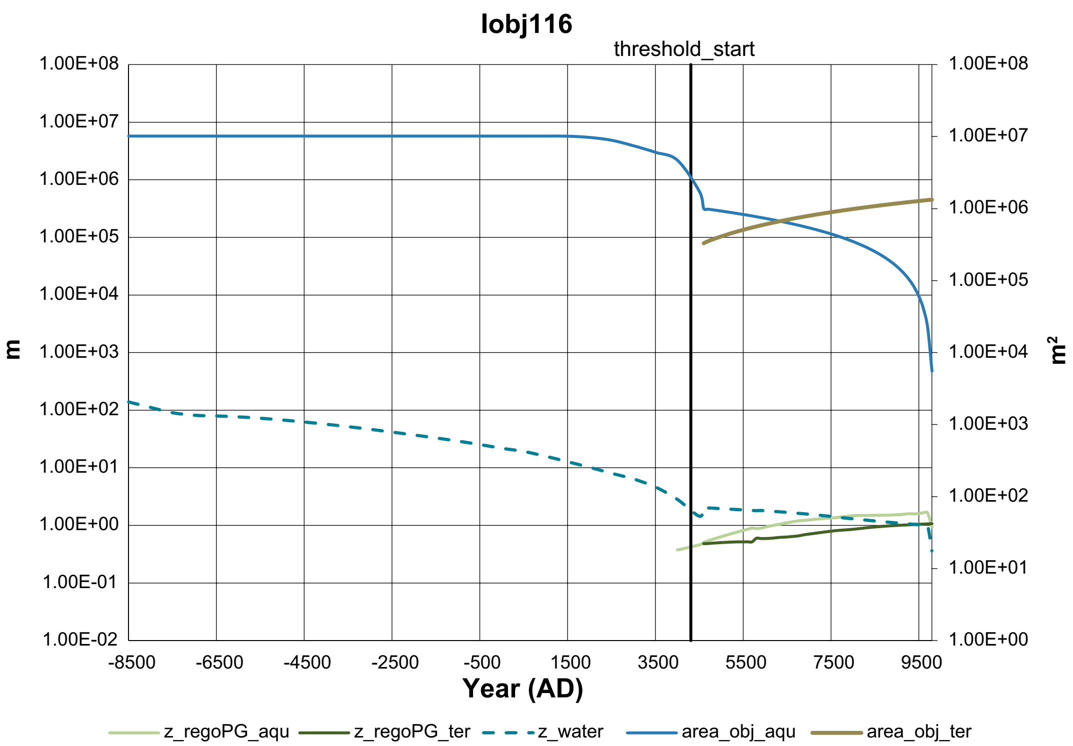

Figure 4-1. Illustration of the time-dependent parameters for object 116.

4.5 Parameters related to sedimentation, resuspension and lake infilling

The rates of sedimentation, resuspension and ingrowth of peat in the biosphere objects are derived in the RLDM (Brydsten and Strömgren 2013). The data are object and time-dependent and the data set used are presented in Appendix C.

4.5.1 Resuspension rate

The parameter, res_rate, represents an estimate of resuspension and is calculated for each time-step used in the radionuclide transport model for the biosphere. Resuspension is the process by which abiotic and biotic material that has been deposited on the bottom sediment is reconveyed into the overlaying water column. A resuspended particle may be resuspended c. 60 times per year in lakes (Valeur et al. 1995) and more than 100 times per year in sea basins until it is permanently buried in the sediment or transported out of the system by water currents or a stream. Here, resuspension is defined as the amount of material that is subject to resuspension in a year and is expressed as kgdw m^{-2} $year^{-1}$. In the model, a radionuclide is connected to a particle as soon as the particle reaches the sediment and therefore it is not of importance to measure the rate of resuspension, as the same particle may be counted many times. Instead it is of importance to estimate the amount of particles that are resuspended in a year. Resuspension is calculated for each time-step in the radionuclide transport model for the biosphere. It is set to zero for time-steps where the area for transport and erosion bottoms are zero and for remaining time-steps calculated as resuspension volume (vol_resusp) divided by the mean area for transport and erosion bottoms for the two time-steps t and t–1 ((area_transportBottom$_t$ + area_transportBottom $_{t-1}$ + area_erosionBottom $_t$ + area_erosionBottom $_{t-1}$)/2) and this quotient is divided by the time-step length to get the unit m $year^{-1}$.

The resuspension rate for periglacial conditions is based on the estimation of net sedimentation rate from SR-Site, (9.5×10^{-5} m^3 m^{-2} $year^{-1}$). The resuspension rate is assumed to be 65% of that rate. which is equivalent to the mean proportion of sedimentation and resuspension in 7 swedish lakes (Weyhenmeyer 1997).

4.5.2 Sedimentation rate

The parameter, sed_rate, represents the net amount of particulate that is deposited on lake and sea bottoms during a year and is expressed in kgdw m^{-2} $year^{-1}$. This is modelled using the RLDM (Brydsten and Strömgren 2013). Some of this material will permanently accumulate and some will be resuspended and return to the water column. Sedimentation is calculated for each time-step in the radionuclide model. It is calculated as a change in sediment volume divided by the mean water area for the two time-steps and this quotient is divided by the time-step length to get the unit m $year^{-1}$. For the limnic phase the gross and net sedimentation rates are equal.

The sedimentation rate for periglacial conditions is based on the estimation of net sedimentation rate from SR-Site, (9.5×10^{-5}), the sed_rate is the sum of the net sedimentation rate and the resuspended rate.

4.5.3 Ingrowth of peat

The parameter, Ter_growth, represents the horizontal ingrowth of peat covering the lake and sea surface. It is calculated as the difference in terrestrial area per time unit.

$$Ter_{growth} = \frac{\partial area\_obj\_ter}{\partial time}$$

4.6 Parameters for object 114

Object 114 is used in the periglacial calculation case since a Talik is located in the object. The parameters describing the geometries of this object is presented here. The thickness of the regolith layers are presented in Werner et al. (2013) (based on modelling in Bosson et al. 2010). The layers representing marine sediment, lake sediment, surface layers and post glacial clay has been summed up and represent the thickness of z_regoPG_aqu. The terrestrial and aquatic area of the object is defined in Werner et al. (2013).

The depth of the surface water, z_water, is the mean depth whitin the lake of object 114 in.

Table 4-5. Geometries of object 114.

Parameter	Unit	Value
area_obj	m^2	3.0 E+06
area_obj_ter	m^2	1.3E+06
area_obj_aqu	m^2	1.7E+06
z_water	m	3.5
z_regoGL	m	3.8
z_regoPG_aqu	m	8.4
z_regoLow	m	5.3

4.7 Parameters for object 1 and 10

Object 1 is defined as the Baltic sea. The area and average depth of the object 1 is defined in the SR-Site, see Table 4-6.

The basin of the Grepen, the sea basin inside of the island Gräsö, is defined as Object 10. The volume of object 10 changes over time, this volume is defined as the volume water of the basin Grepen (the basin between the main land and the island Gräso) excluding the ten biosphere objects, see Table 4-7. The parameter threshold_stream för object 10, defines the point in time when this object is no longer assumed to be marine, this year is set to year 10,000 AD, and is defined as the year when the water volume of the basin is no longer changing.

Table 4-6. Parameter defining object 1, the Baltic sea.

Parameter	Value	Unit
Aqu_area_obj	3.7E+11	m^2
depth_aver	56	m
wat_ret	22	year

Table 4-7. Volume of water of object 10 over time.

Year (AD)	vol_water (m^3)
–6500	3.E+10
–3000	2.E+10
–1000	1.E+10
0	7.E+09
1000	5.E+09
2000	3.E+09
3000	2.E+09
4000	1.E+09
5000	5.E+08
6000	2.E+08
7000	1.E+08
8000	7.E+07
9000	3.E+07
10,000	2.E+05

5 Regolith characteristics

In this section, properties of the modelled natural regolith and cultivated soils are presented. The regolith layers used in the radionuclide model are described in Saetre et al. (2013a). The lowermost regolith layer is the RegoLow layer characterised by water saturated (anoxic) till. The till layer is overlaid by a layer of glacial clay, RegoGL. On top of the glacial clay layer is a layer of post glacial clay, RegoPG, characterised by gyttja clay. This layer is also water saturated and anoxic. The peat layer overlying the post glacial clay is divided into two compartments; the lower is the water saturated, anoxic part of the peat column, RegoPeat, whereas the uppermost is unsaturated and oxic, RegoUp.

Agriculture is assumed to be possible on glacial clay both in the infield-outland agricultural land-use variant and in the small-scale garden plot land-use variant. In the drained-mire agricultural land-use variant, agriculture is assumed to occur when a mire/lake ecosystem is drained and the underlying peat and gyttja is cultivated. Parameters describing the properties of agricultural soils are therefore presented for glacial clay, peat and gyttja in Section 5.4.

Porosities and densities are expected to be normally distributed, for many regolith layers. Some regolith layers, such as peat, surficial aquatic sediments and drained cultivated peaty soils are regarded as representing different stages of development that are dependent on the age of the mire, lake or the drained mire and they are therefore assigned uniform distributions of properties, i.e. the different porosity and density values are taken to represent different successional stages. Similarly, the pore water content of agricultural soils was given a uniform distribution. Soil diffusivity is assumed to be log-normal distributed. Minimum and maximum values as well as standard deviations are presented where data are available. Data for some parameters was taken from the literature and lack, in some cases, information concerning the statistical distributions of the observations.

5.1 Experience from previous safety assessments

Data used for regolith parameters in the previous safety assessment, SR-Site, were re-evaluated and some data were excluded and some new data were included. SR-PSU also includes some regolith parameters that were not used in SR-Site. The main differences between SR-Site and SR-PSU are:

- In SR-Site, the properties of agricultural soils (Löfgren 2010) were mainly obtained from the literature, whereas new data from the surroundings of Forsmark were used for SR-PSU.
- In SR-PSU, the properties of cultivated soils used in garden plots and in early agricultural societies were determined. These land-use variants were not represented in SR-Site. Furthermore, the water content (S_w_regoUp) in soils used for agriculture was estimated for SR-PSU.
- In SR-PSU, different regolith parameter values were used for accumulation bottoms (regoUp) in aquatic and marine environments. In SR-Site the same parameter value was used for both these environments.
- Data representing postglacial clays (RegoPG) were re-evaluated for SR-PSU and some of the data used in SR-Site were excluded, due to a too high uncertainty of the estimations.
- In SR-PSU, a larger data set was used for calculating regolith parameters representing peat and till.

5.2 Influence of climate on parameter values

The regolith parameters are not expected to be significantly affected by a warmer climate. Peat properties may, however, change slightly over time, since peat accumulation and peat properties are sensitive to climate variations (Charman 2002). A colder climate with periglacial conditions can be expected to change the regolith properties. Deeper horizons will be constantly frozen, whereas the topsoil (active layer) may become water logged, causing increased porosity and lower dry bulk density. A colder climate may change properties of the accumulating sediments (regoPG), and a lower organic carbon content may cause higher density and lower porosity of these sediments. However, in this safety assessment, no alternative porosities and densities for periglacial conditions have been assigned, since the possible differences between the regolith parameters reflecting the present climatic conditions and the parameters in a periglacial environment were regarded as relatively small. Land-use will also change in a periglacial environment, since cultivation of soils and artificial lowering of the groundwater table are not likely to occur. The parameterisation of drained wetlands is therefore not needed for the periglacial environment.

5.3 Density and porosity of non-cultivated soils

Densities and porosities for different regolith layers are presented in this section. Porosity is expressed as the volume of pores divided by the total volume of the sample. The calculation of porosity is based on results from analyses of water content and the content of organic material. For these calculations, it was assumed that the pore volume is water saturated, and that the organic and minerogenic materials have densities of 1 and 2.65 g cm^{-3}, respectively. The dry bulk density is based on calculations from analyses of water content and the content of organic material in the same samples. Again for these calculations it was assumed that the organic material and minerogenic material have densities of 1 and 2.65 g cm^{-3}, respectively.

5.3.1 Density and porosity of till

The lower most regolith layer is till. Dry bulk density and porosity of till is represented by the parameter dens_regoLow and poro_regoLow, see Table 5-1. The values presented here were obtained from till sampled in machine-dug trenches by Lundin et al. (2005). The data represent the different types of till in the Forsmark area (gravelly till-boulder clay). Samples from the uppermost 0.8 m were not used since the physical properties in this region may be affected by roots and soil-forming processes. Samples were taken using steel cylinders with a height of 5 cm and a radius of 3.6 cm. Two replicates were taken at each sampling site.

Table 5-1. Density and porosity of till, dens_regoLow and poro_regoLow (Lundin et al. 2005).

	N	Average	Stdev	Min	Max	Distribution
Porosity (m^{-3} m^{-3})	26	0.21	0.05	0.14	0.32	Normal
Dry bulk density (kg m^{-3})	26	2,115	138	1,800	2,300	Normal

5.3.2 Density and porosity of glacial clay

The parameters poro_regoGL and dens_regoGL represents the porosity and dry bulk density of glacial clay, see Table 5-2. All analysed samples are from Lake Eckarfjärden (Nordén 2007). Glacial clay is a heterogeneous deposit with respect to physical properties. Layers of sand and silt, with a relatively high hydraulic conductivity, may occur in the deepest part of this deposit. These coarse-grained units have a higher density and lower porosity compared with the surrounding glacial clay. Accordingly, properties of glacial clay in the Forsmark area may have a higher variability than reflected by the samples studied here. A comparison with the properties of glacial clay obtained during SKB's site investigation at Laxemar-Simpevarp (Löfgren 2010) shows that the glacial clay at that site has a porosity and dry bulk density that are very close to the values from Forsmark. The average porosity of glacial clay at Laxemar-Simpevarp is 0.74 m^{-3} m^{-3} and the average dry bulk density is 696 kgdw m^{-3} (11 samples were analysed).

Table 5-2. Density and porosity of glacial clay, dens_regoGL and poro_regoGL (Nordén 2007).

	N	Average	Stdev	Min	Max	Distribution
Porosity (m^{-3} m^{-3})	6	0.75	0.03	0.69	0.78	Normal
Dry bulk density (kgdw m^{-3})	6	673	79	582	818	Normal

5.3.3 Density and porosity of postglacial clay gyttja

The parameters poro_regoPG and dens_regoPG represent the porosity and dry bulk density of post-glacial clay gyttja see Table 5-3. In the Forsmark area the postglacial clay contains organic material and is therefore characterised as clay gyttja (clay with an organic content between 6 and 20%). Some of the lake sediments attributed to regoPG have an even higher organic content and are in fact characterised as gyttja (organic content > 20%).

All data were obtained from sediments sampled in seabays (Sternbeck et al. 2006). The organic carbon content is, however, higher in corresponding lake sediments (Hedenström and Sohlenius 2008). The dry bulk densities are therefore likely to be lower in corresponding lake sediments compared with the values presented here. On the other hand, all data presented here are from the uppermost metre of sediments. Density and porosity can be expected to be higher and lower, respectively, in deeper-lying sediments due to compaction by overlying deposits. It is consequently uncertain if the parameter values presented in Table 5-3 are representative for all regoPG and it can be suspected that the porosity and dry bulk densities of regoPG generally are lower and higher, respectively. The difference would be expected to be included in the given distribution.

Table 5-3. Density and porosity of postglacial clays, mainly clay gyttja dens_regoPG and poro_regoPG (Sternbeck et al. 2006).

	N	Average	Stdev	Min	Max	Distribution
Porosity (m^{-3} m^{-3})	6	0.92	0.01	0.90	0.93	Normal
Dry bulk density (kg m^{-3})	6	182	29	156	222	Normal

5.3.4 Density and porosity of anoxic peat

The parameters poro_regoPeat and dens_regoPeat represent the porosity and dry bulk density of the anoxic layer of peat (Table 5-4 and Table 5-5), which is the lower regolith layer in wetlands. The anoxic layer consists of the peat below 30 cm depth. Peat above that level is assumed to be oxic and is attributed to the terrestrial RegoUp compartment.

The values presented here reflect the properties of fen peat in the Forsmark region. Samples with *Sphagnum* peat were omitted, since these samples are considered to reflect the properties of bog peat, which is characterised by rain-fed production on the bog plane and has restricted connection to the groundwater. Bogs are consequently of less interest in a safety assessment, since radionuclides discharging in groundwater are not expected to enter that ecosystem.

Data from four studies were used for calculating parameter values for porosity and dry bulk density. The peat properties vary widely between and within the studied mires partly as an effect of the age of the mire. Mires situated higher above present sea level have been uplifted for a longer period of time and are therefore older. In the youngest wetlands, peat with a very low bulk density is often overlain by peat with a higher density. The peat has probably started to form along the shores of shallow lakes which successively have been covered by a mat of vegetation. That has recently occurred in the young wetlands and the mat of vegetation is still underlain by material with a high water content. Altitudes (Table 5-4) were used to calculate the ages of the mires, by using a shore-line displacement model (SKB 2014c). The ages range between approximately 500 and 4,800 years.

Two of the studies were conducted at the Rönningarna mire (Sternbeck et al. 2006, Sheppard et al. 2009) and Löfgren (2011) studied peat from Stenrösmossen and Labboträsk, all situated at the Forsmark site. Additional data from Stenrösmossen, Backbotten and Hjortronmossen were also used (data collected by Swedish Geological Survey in an ongoing project, Schoning (2014)). The two latter wetlands are situated outside the Forsmark area, but in a similar environment (wetlands in recently uplifted areas). Data in Sheppard et al. (2009) and Löfgren (2011) did not allow calculations of porosity, since there were no data on water content or wet density.

In Table 5-4 and Table 5-5, the average values for each of the investigated mires are presented. These average values were thereafter used to calculate the average value for the studied mires. That was done since the mires represent a span of ages, and peat accumulation has occurred considerably longer in the old mires compared with the young. In the parameterisation, a uniform distribution was assumed because both density and porosity of peat is believed to be related to the successional stage of the mire (age or m.a.s.l. Table 5-4 and Table 5-5) and consequently the peat in a mire may follow a gradient from minimum to maximum. The max and min values represent the entire modelled mire and since the studied mires represent a span of ages with different properties the average max and min values from the studied mires were used.

Table 5-4. Density (kg m^{-3}) of the anoxic layer of peat, dens_regoPeat. The same values are used to characterise regoUp_ter (Sternbeck et al. 2006, Sheppard et al. 2009, Löfgren 2011, Schoning 2014).

	N	Average	Stdev	Min	Max	M.a.s.l.	Distribution
Rönningarna	7	102	26	70	152	11.5	
Backbotten	4	119	25	94	148	29	
L Hjortronmossen	1	136				13	
Stenrösmossen	12	97	31	40	154	8.5	
Labboträsk II	4	65	35	34	111	3–5	
Labboträsk I	4	82	33	54	120	2.7	
Average of the studied mires	6	100		65	136		Uniform

Table 5-5. Porosity (m^{-3} m^{-3}) of the anoxic layer of peat, poro_regoPeat. The same values are used to characterise regoUp_ter (Sternbeck et al. 2006, Schoning 2014).

	N	Average	Stdev	Min	Max	M.a.s.l.	Distribution
Rönningarna	4	0.92	0.02	0.90	0.94	11.5	
Backbotten	4	0.90	0.02	0.88	0.93	29	
L Hjortronmossen	1	0.90				13	
Stenrösmossen	4	0.90	0.01	0.88	0.90	8.5	
Average of the studied mires	4	0.90		0.88	0.94		Uniform

5.3.5 Density and porosity of oxic peat

The parameters poro_regoUp_ter and dens_regoUp_ter represents the porosity and dry bulk density of the uppermost oxic peat layer, which corresponds to the uppermost 30 cm of peat. Initially it was assumed that the uppermost peat should be characterised by a higher density and lower porosity compared with the underlying peat. Compaction from overlying peat should cause lower porosity and higher dry bulk density in the lower peat layers. However, the peat studied showed no significant difference in porosity and density between the uppermost 30 cm and the deeper-lying peat. Indeed, in some of the young peatlands, the deep-lying peat is characterised by a higher porosity and lower density than the overlying peat. The same parameter values were therefore used for the compartment RegoUp as for RegoPeat (Table 5-4 and Table 5-5).

There may be several reasons for the lack of difference between the uppermost and lower-lying peat. In general, the degree of humification is low in the uppermost peat, giving rise to low dry bulk density and high porosity. However, in the wetlands studied here the degree of humification in the upper peat is not lower than the humification in lower-lying peat. All samples studied here are from young wetlands with relatively thin layers of peat (up to 2 m) and the effect of compaction may consequently be low.

5.3.6 Porosity and density of aquatic sediments

The parameters poro_regoUp_sea, poro_regoUp_lake, dens_regoUp_sea and dens_regoUp_lake represents the porosity and dry bulk density of the upper layer of aquatic sediments, which currently are deposited at accumulation bottoms. The parameters refer to the uppermost 5 cm and 10 cm layer of regolith in lakes and sea, respectively.

Two of the samples used for calculating the values presented here were obtained from bays along the coast of the Forsmark area (Sternbeck et al. 2006). Data from three additional samples were obtained from SGU's database for marine geology and represent sediments sampled at the floor of Öregrundsgrepen during SGU's regular marine geological surveys.

It should be noted that the porosity and density for the accumulation bottoms are very similar to corresponding data from RegoPG (compare Table 5-3 and Table 5-6). This probably reflects the low degree of consolidation of the samples used for calculating RegoPG. Furthermore, there are no data available from accumulation bottoms situated at the floor of lakes. Sediments from lakes are expected to have higher porosities and lower densities compared with corresponding deposits from bays, due to the generally higher organic content of lake sediments (Hedenström and Sohlenius 2008). This is confirmed by data from 14 sites in a bay of Lake Mälaren, c. 80 km south of the Forsmark area, presented by Håkansson and Jansson (2002), showing a significantly higher porosity (0.97 m^{-3} m^{-3}) and lower dry bulk density (61 kg m^{-3}) compared with the data presented for the sea bays (Table 5-6). The data from Håkansson and Jansson (2002) are thought to be representative for the lakes in Forsmark and are therefore used here. The uppermost sediments in lakes from the Forsmark area have organic contents (Hedenström 2004) close to corresponding sediments from Lake Mälaren (Håkansson and Jansson 2002), and it is therefore assumed that the density and porosity of sediments from Lake Mälaren are close to the values in lakes in the Forsmark area. In the parameterisation, a uniform distribution was assumed, because both density and porosity of aquatic sediments are believed to be related to the successional stage of the lake (age) and consequently therefore follow a gradient from minimum to maximum.

Table 5-6. Porosity and density of the uppermost sediment at accumulation bottoms sampled at sea (Sternbeck et al. 2006, SGU database) and in lakes (Håkansson and Jansson 2002). The Lake data comes from Lake Mälaren and the min and max values for these data are unfortunately not presented in Håkansson and Jansson (2002).

	N	Average	Stdev	Min	Max	Distribution
poro_regoUp_lake (m^{-3} m^{-3})	14	0.97	0.0044			Normal
dens_regoUp_lake (kg m^{-3})	14	61	24.4			Normal
poro_regoUp_sea (m–3 m^{-3})	5	0.92		0.90	0.94	Uniform
dens_regoUp_sea (kg m^{-3})	5	179		133	236	Uniform

5.4 Properties of cultivated soils

Three agricultural land-use variants are included in the safety assessment SR-PSU; modern agricultural practices with draining of wetland, early agriculture with infield-outland practices, and a modern garden plot utilised by a household. In the modern agricultural land-use variant, drained mire with peat and/or clay gyttja is cultivated. Glacial clay is assumed to be cultivated in the infield-outland land-use variant, since areas with glacial clay are common in the Forsmark area and could be cultivated without lowering the groundwater table. Glacial clay is also assumed to be utilised in the garden plot land-use variant. Properties for these agricultural soil types (peat, clay gyttja and glacial clay) are presented in this section.

5.4.1 Density and porosity of peat and clay gyttja in a cultivated wetland

The parameters dens_regoUp_peat, dens_regoUp_clay, poro_regoUp_peat and poro_regoUp_clay represents the dry bulk densities and porosities of the upper 0.3 m of regolith in areas used as arable land, where modern cultivation techniques, e.g. draining of wetlands, are used. The parameter values represent drained wetlands, i.e. discharge areas, where peat (Table 5-7) and clay gyttja (Table 5-8) are the dominating regolith types. Two alternative sets of parameters (peat and clay gyttja) are therefore presented here. Cultivated clay gyttja and peat are not present in the Forsmark area of today. The data used here are from a study by Sheppard et al. (2011), where samples from arable land in the surroundings of Forsmark were studied.

The values presented here are similar to those from cultivated peat at Bälinge Mosse, situated in the same part of Sweden as Forsmark (McAfee 1985, Table 14). Also, cultivated peat at Majnegården in southern Sweden shows similar values (Berglund 1996). Berglund et al. (1989) have studied the properties of gyttja soils and have obtained similar bulk densities and porosities as reported here. In the parameterisation a uniform distribution was assumed because both density and porosity of drained peat and clay gyttja are believed to be related to the age since drainage and would consequently follow a gradient from minimum to maximum.

Table 5-7. Density and porosity of peat in areas used for cultivation (dens_regoUp_peat and poro_regoUp_peat). These two parameters represent one type of soil (peat) used for agriculture in discharge areas for groundwater. The samples were taken 0.2 m below ground surface (Sheppard et al. 2011).

	N	Average	Stdev	Min	Max	Distribution
Porosity (m^{-3} m^{-3})	5	0.75		0.71	0.80	Uniform
Density (kg m^{-3})	5	274		220	320	Uniform

Table 5-8. Density and porosity of clay gyttja in areas used for cultivation (dens_regoUp_clay and poro_regoUp_clay). These two parameters represent one type of soil (clay gyttja) used for agriculture in discharge areas for groundwater. The samples were taken 0.2 m below ground surface (Sheppard et al. 2011).

	N	Average	Stdev	Min	Max	Distribution
Porosity (m^{-3} m^{-3})	4	0.63		0.57	0.67	Uniform
Dry bulk density (kg m^{-3})	4	771		704	886	Uniform

5.4.2 Density and porosity of cultivated glacial clay

The parameters dens_regoUp and poro_regoUp represent the density and porosity of glacial clay soils assumed to be utilised in the early agriculture land-use variant with infield-outland practises and in the garden plot land-use variant see Table 5-9. These soils can be used for cultivation without lowering the groundwater table and without the use of machines. The data presented here are suggested to represent soils that were cultivated in pre-industrial times, but it is also suggested that the same type of soil can be used for gardening vegetables. Glacial clay is common in the Forsmark area and is suitable for cultivation. Layers of glacial clay are often situated at the transition between water-deposited clays and till layers, and at many sites glacial clay can be cultivated without lowering the groundwater table. This assumption is supported by data from the village of Valö, close to Forsmark, showing that, at the beginning of the 18th century (1709 AD), a large proportion of the arable land was situated in areas with glacial clay (Lindborg 2010).

The samples used for calculation of these parameters were taken from arable land in the surroundings of Forsmark (Sheppard et al. 2011). The samples were taken 0.2–0.3 m below the ground surface.

Table 5-9. Porosity and dry bulk density for glacial clay, dens_regoUp and poro_regoUp, in the upper soil horizons sampled at sites used as arable land. The samples were taken 0.2–0.3 m below the ground surface (Sheppard et al. 2011).

	N	Average	Stdev	Min	Max	Distribution
Porosity (m^{-3} m^{-3})	3	0.38	0.07	0.30	0.44	Normal
Dry bulk density (kg m^{-3})	4	1,564	225	1,329	1,778	Normal

5.4.3 Degree of compaction of clay gyttja and peat in a drained mire

The parameters compact_gyttja and compact_peat represent the degree of compaction of the soil when a wetland is transformed from its natural state into arable land. The lowering of the groundwater table causes compaction of the uppermost soil layers, which in turn causes higher dry bulk densities and lower porosities.

As mentioned above (Section 5.4.1), clay gyttja and peat in former wetlands are commonly used as arable land. The un-drained and drained dry bulk densities of these deposits were therefore used to calculate the compaction. The compaction of peat was calculated as the ratio between dry bulk density of un-drained peat in wetlands (see Table 5-4) and the dry density of cultivated wetlands (period of cultivation unknown). The ratios between dry bulk density of un-drained peat (Table 5-4) and cultivated peat (Table 5-7) for the six mires ranged between 0.44 and 0.24. The minimum value represents compaction of peat in a mire with relatively consolidated peat, whereas the maximum value represents compaction of peat in a young mire with relatively unconsolidated peat. The average of these was chosen as a best estimate. The dry bulk densities used for calculation of peat compaction are similar to values reported by Berglund (1996). The corresponding ratio for clay gyttja was calculated as the ratio between the density of RegoPG (Table 5-3) and the density of cultivated clay gyttja (Table 5-8), and the average value is 0.25 (ranging between 0.20 and 0.29). It may be surprising that clay gyttja has a smaller compaction ratio than peat (i.e. it becomes more compacted), since peat is characterised by higher water content than minerogenic deposits such as clay gyttja. Peat should consequently be more sensitive to compaction than clay gyttja. However, this smaller compaction ratio is an effect of the low density and high porosity of the clay gyttja in lakes and sea bays. It is likely that these sediments will consolidate when uplifted or overlain by layers of sediment and peat.

Table 5-10. The ratios between the densities of unconsolidated peat and clay gyttja and the densities of corresponding cultivated deposits, compact_peat and compact_gyttja. The ratios were used to estimate the degree of compaction due to cultivation (data used for the calculations is described above).

	N	Average	Min	Max	Distribution
Compactation ratio of peat	5	0.34	0.24	0.44	Uniform
Compactation ratio of clay gyttja	6	0.25	0.20	0.29	Uniform

5.4.4 Pore water content of agricultural soils

The parameter S_w_regoUp reflects the amount of water contained in the pores of soils that can be used for cultivation. In the Forsmark area, there are no direct measurements of this parameter.

S_w_regoUp for drained mires (representing soils cultivated by an industrial agricultural society where modern cultivation techniques, e.g. draining of wetlands, are used) where peat and clay gyttja are the dominating regolith types is presented in Table 5-11. Two alternative sets of parameters (peat and clay gyttja) are presented here.

The cultivated glacial clay in the Forsmark area (used for the early agricultural and garden plot land-use variants) has an average clay content of more than 40% (cf. Sheppard et al. 2011) and can therefore be classified as stiff clay (“styv lera”). The values presented here (Table 5-11) represent the values from stiff clay.

The highest value (max in Table 5-11) represents saturated conditions at field capacity, and the lowest value (min in Table 5-11) represent the wilting point, i. e. the water content in soils where no water is accessable for plants. The parameter is expressed as the proportion of the pores that are filled with water. The values presented in Table 5-11 are assumed to have a uniform distribution between what is regarded as a wet year and a dry year. The values presented here should be regarded as rough estimates, as the degree of water saturation is highly dependent on local climate, but may also change from one year to another. Furthermore, the values presented in Grip and Rodhe (1985) represent conditions in soils unaffected by soil-forming processes.

Water saturation data (volume of water/total soil volume) for peat and clay gyttja were taken from the literature (Berglund 1996), since information from the Forsmark area is lacking. For determining the proportion of pores filled with water, data on soil porosity is needed. That value was taken from results (average value) of porosity determinations of the uppermost horizon in peat and clay gyttja from the surroundings of the Forsmark area (Sheppard et al. 2011).

Table 5-11. The proportion of pores filled with water, S_w_regoUp, in peat, clay gyttja and glacial clay. Min represents the wilting point and max the field capacity.

	Average	Min	Max	Distribution
Peat (drained mire)	0.63	0.40	0.86	Uniform
Clay gyttja (drained mire)	0.60	0.32	0.87	Uniform
Glacial clay (inland outfield and garden plot)	0.60	0.4	0.8	Uniform

5.4.5 Diffusivity of CO_2 in soil

Field and laboratory experiments show that the loss of inorganic carbon by degassing is driven primarily by gaseous diffusion in unsaturated soils (Sheppard et al. 1994).

The molecular diffusivity, or diffusion coefficient, (D_CO2_soil_peat, D_CO2_soil_clay, D_CO2_soil), is a proportionality constant between the molar flux due to molecular diffusion and the gradient in the concentration of the molecules of interest. A compound's diffusion coefficient is typically four orders of magnitude greater in air than in water (Haynes 2012). However the molecular diffusivity of carbon dioxide in soil also depends on temperature, the amounts of water and air in the soil, and the soil porosity.

Figure 5-1 shows the relationship between the relative diffusivity of CO_2 in soil and the fraction of air-filled porosity.

Here we used a linear relationship to describe the effect of temperature on CO_2 diffusivity in air (Lerman 1979). To account for the effects of soil porosity and soil water saturation we used the Millington-Quirk model (Millington and Quirk 1961), which has been shown to provide reliable results in organic soils (Iiyama and Hasegawa 2005). Thus, the overall diffusivity of CO_2 in unsaturated soil (D_CO2_soil, 10^{-4} m^2 s^{-1}) is described by:

$$D_{CO2\_soil} = \frac{{\theta_{air}}^{10/3}}{\theta^2} D_{CO2\_air}$$

$$D_{CO2\_air} = 0.1325 + \mathrm{T} \cdot \beta_T$$

$$\theta_{air} = \theta\,(1 - S_w)$$

Where

θ_{air} is the air-filled porosity (m^3 m^{-3}),

θ is the total soil porosity termed (m^3 m^{-3}),

D_{CO2_air} is the diffusivity in air (10^{-4} m^2 s^{-1}),

T is the temperature (°C),

β_T is a coefficient for temperature dependence (10^{-4} m^2 s^{-1} per°C),

S_W is the degree of water saturation of the pore volume (m^3 m^{-3}).

The coefficient for temperature response was taken from Lerman (1979) (β_T = 0.0009 10^{-4} m^2 s^{-1} per°C). We calculated the soil diffusivity of CO_2 for three types of agricultural soil at a temperature of 10°C, which is the approximate mean soil temperature during the period that lacks ground frost in Forsmark (Heneryd 2007). The response of diffusivity to temperature is relatively small (approximately a 4% change in the diffusivity of CO_2 in air for a change of 6°C). Best estimates for soil diffusivity were first calculated for typical values of soil saturation and soil porosity (mean values) for each soil. Then randomly drawn parameter values from the distributions of soil saturation (uniform between low and high) and porosity (normal) were used to recalculate the soil diffusivity for each soil (n=100). The resulting distributions were positively skewed and approximately log-normal distributed. From these simulations the geometric mean and the geometric standard deviation were estimated. The 2.5 and 97.5 percentiles from the empirical distributions were used as lower and upper boundaries for the derived probability density functions.

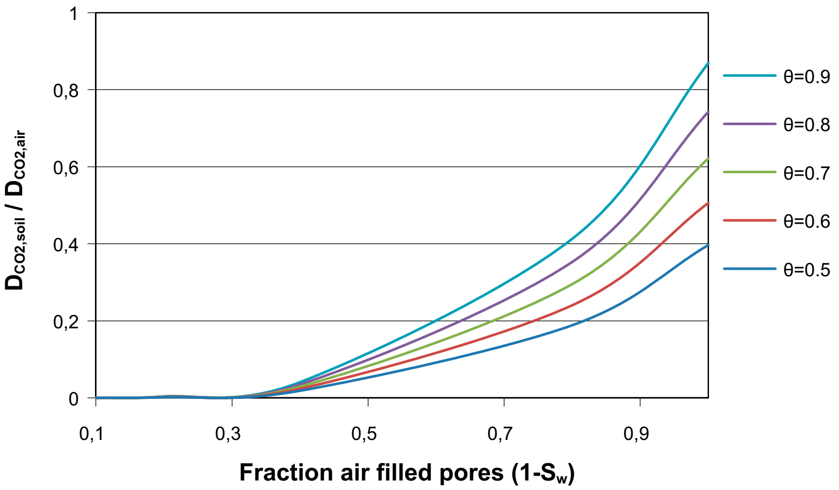

Figure 5-1. *Relative diffusivity as a function of soil porosity and water saturation of soil.*

Table 5-12. Soil diffusivity for three agricultural soils. The first two soil are organic and result from draining a mire or lowering a lake. The third soil has a primarily inorganic parent material, namely glacial clay. Soil properties affecting the diffusivity (i.e. soil water saturation and soil porosity) are listed for each soil type.

Land-use variant	Parent soil	Saturation (S_w)			Porosity		Soil diffusivity (D_{CO2_soil} m^2 $year^{-1}$)					Distribution
		Low	**High**	**Reference**	**Mean**	**Stdev**	**$Mean_{deter}$**	**Geomean**	**GeoStdev**	**Min**	**Max**	
Drained mire	Peat	0.40	0.86	Berglund 1996	0.75	0.03	11.1	7.9	4.4	0.5	54.1	lognormal
	Clay gyttja	0.32	0.87	Berglund 1996	0.63	0.04	11.7	10.8	4.5	0.5	69.5	lognormal
Infield-outland Garden plot	Glacial clay	0.40	0.80	This report	0.38	0.07	5.8	4.7	3.2	0.6	24.1	lognormal

6 Hydrological parameters

The hydrological fluxes used in the safety assessment SR-SPU represents water exchanges between marine basins of the radionuclide model described in Section 6.3, and water fluxes between compartments of the radionuclide model for terrestrial and limnic ecosystems described in Section 6.4. The water fluxes between the marine basins were derived from a 3-dimensional hydrological model implemented with the tool MIKE 3 FM for the period with marine basins. The parameters representing fluxes of water between compartments of the radionuclide model for marine, limnic and terrestrial ecosystems were derived from a 3-dimensional hydrogeological model, including groundwater in bedrock, groundwater in regolith and surface water, implemented with the tool MIKE SHE. The modelling and results are described in detail in Werner et al. (2013).

The hydrological parameters are time dependent. Due to landscape development, objects transform from a marine stage into a limnic and/or terrestrial stage during the course of time. For each stage of a biosphere object (marine, limnic or terrestrial) considered in the biosphere radionuclide modelling, a set of parameters describing water fluxes for the particular stage is provided from MIKE 3 FM (fluxes between marine basins) or MIKE SHE (fluxes between compartments of marine, limnic or terrestrial ecosystems).

6.1 Experience from previous safety assessments

The current hydrological modelling approach dates back to the previous SFR safety assessment SAFE (Lindgren et al. 2001) and has been further developed in the follow-up project SAR-08 (SKB 2008) and the projects for the assessment of the repository for spent nuclear fuel at the Forsmark site, SDM-Site (Bosson et al. 2008) and SR-Site (Bosson et al. 2010). The hydrological modelling for SAR-08 was also based on the SDM-Site project. Concepts and tools, as in the application of various modules of the MIKE SHE software (DHI 2012), for the near-surface hydrology modelling have been continuously developed. Compared with SDM-Site and SR-Site, updates to the hydrological modelling in the SR-PSU project mainly concern enhancements to the underlying geometrical models of present and future landscapes, and further development of models of future land- and water-resource management (drainage and water supply by wells).

6.2 Influence of climate on parameter values

The climate affects the hydrology of the site. A simulation case based on present-day climate conditions and an additional simulation case for warmer and wetter climate conditions were modelled with MIKE SHE (modelling fluxes between compartments of marine, limnic or terrestrial ecosystems) for the SR-PSU assessment (Werner et al. 2013). Moreover, permafrost conditions were analysed using MIKE SHE modelling results from the SR-Site assessment. The fluxes between marine basins, modelled using MIKE 3 FM, were not altered in the different climate cases.

The present-day climate case is represented by locally measured meteorological data during a selected period (October 1, 2003–September 30, 2004; average of the Högmasten and Storskäret meteorological stations). The selected one-year period has an accumulated precipitation that is close to that of the reference normal period 1961–1990, both on a monthly and annually basis (Bosson et al. 2010). Specifically, the selected one-year period, which in the following is referred to as the normal year, has an annual average air temperature of 6.4°C (minimum –13.2°C and maximum 23.4°C) and an accumulated precipitation of 583 mm. The annual average air temperature for the normal year is almost identical to the annual average for the period 2004–2010 (6.7°C). Moreover, the accumulated precipitation during the normal year (583 mm) is slightly above the estimated annual average (569 mm) for the reference normal period (Johansson 2008) and close to the annual average precipitation (589 mm) for the period 2004–2010. The water flows derived from the MIKE SHE simulations with the present-day climate are used to parameterise the water flows in the global warming climate case in the radionuclide model.

The wetter and warmer climate is defined by meteorological data available in Kjellström et al. (2009). Specifically, Kjellström et al. (2009) present meteorological data for a wet period of 50 years, having an annual average precipitation of c. 1,280 mm. In this data set, Bosson et al. (2010) found a three-year period that includes both a very wet year and a year with an accumulated precipitation that is close to the 50-year average. The chosen period, which in the following is referred to as the wet and warm climate case, has an annual average air temperature of 7.7°C (minimum –16.1°C and maximum 24.2°C). The annual average precipitation is c. 1,500 mm, i.e. almost three times the accumulated precipitation during the normal year. For further details on data-selection processes and meteorological data for the normal year and the wetter and warmer period, see Bosson et al. (2010). The water flows derived from the MIKE SHE simulation with a wetter and warmer climate are used to parameterise the water flows in the extended global warming climate case in the radionuclide model.

A periglacial climate with permafrost conditions and taliks dramatically reduce the hydrologic connectivity in the landscape. Based on DarcyTools-calculated exit locations for periglacial conditions within SR-PSU, separate water balances were extracted for two potential taliks based on SR-Site MIKE SHE modelling results representing periglacial conditions (Bosson et al. 2010). One of the chosen taliks is at the location of biosphere object 157_1 (i.e. exit locations north of SFR), whereas the other talik is object 114 of Bosson et al. (2010), coinciding with exit-location areas at the north-eastern DarcyTools model boundary. When the model stage is switched from "global warming" to "permafrost" at AD 17,500 the release of radionuclides is redirected from object 157_2 to object 157_1 and the hydrological parameterisation for taliks is adopted in objects 157_1 and 114. Conceptual details of the hydrological modelling cases are provided in Werner et al. (2013) and in SKB (2014c) in relation to the handling of these cases in the radionuclide transport model.

6.3 Inter-basin water exchange in marine areas

For the marine stage, a parameter quantifying inter-basin water exchanges (WF_lobjxx), i.e. annual average water flows between neighbouring marine basins, was calculated by the flexible-mesh modelling tool MIKE 3 FM using site data from Forsmark. The modelling conducted within the SR-site project by Karlsson et al. (2010) was updated, since a new updated DEM was made available. The updated modelling is briefly described in Werner et al. (2013).

The inter-basin water exchange was calculated for 38 delineated marine basins. Among the 38 marine basins are the basins for the seven SR-PSU biosphere objects (116, 121_1, 121_2, 157_1, 157_2, 159 and 160). Their spatial configuration and connectivity in the marine stage is illustrated in Figure 6-1.

Specifically, gross in- and outflows were used to calculate net flows and their directions across basin boundaries. The major factors influencing long-term changes of inter-basin water exchanges are the long-term developments of the interchange between Öregrundsgrepen and the Baltic Sea and the bathymetry of Öregrundsgrepen, which were determined from the DEM (Strömgren and Brydsten 2013) and long-term landscape development (Brydsten and Strömgren 2013).

The parameter WF_lobjxx was calculated by the FM 3 tool for the years 6500, 3000 and 1000 BC, and for 1,000-year intervals from 0 until the year of isolation or up to 9000 AD (Werner et al. 2013). The basin isolation year, which is represented by the parameter threshold_isolation (see Section 4.3), is defined as the year when the lake threshold or the whole basin is located above sea level. For the basin isolation year, WF_lobjxx was calculated using the surface-water flux out of the object (q_downstream_iso derived from MIKE SHE simulations) multiplied by the area of the object, whereas all other water flows were set to zero at the basin-isolation year.

The water exchange between Öregrundsgrepen and the Baltic Sea, parameterised by WF_Baltic, was calculated as the water volume of Öregrundsgrepen (excluding basins defined as biosphere objects) divided by the residence time of the water in Öregrundgrepen.

The WF_lobjxx parameter values for the seven objects are presented in Appendix D.

The WF_lobjxx parameter values are not altered in the different climate calculation cases during the marine phase.But for the terrestrial phase the flow differs between the climate cases since the surface-water flux to downstream object was calculated by multiplying q_dowmstream_iso with the area of the object.

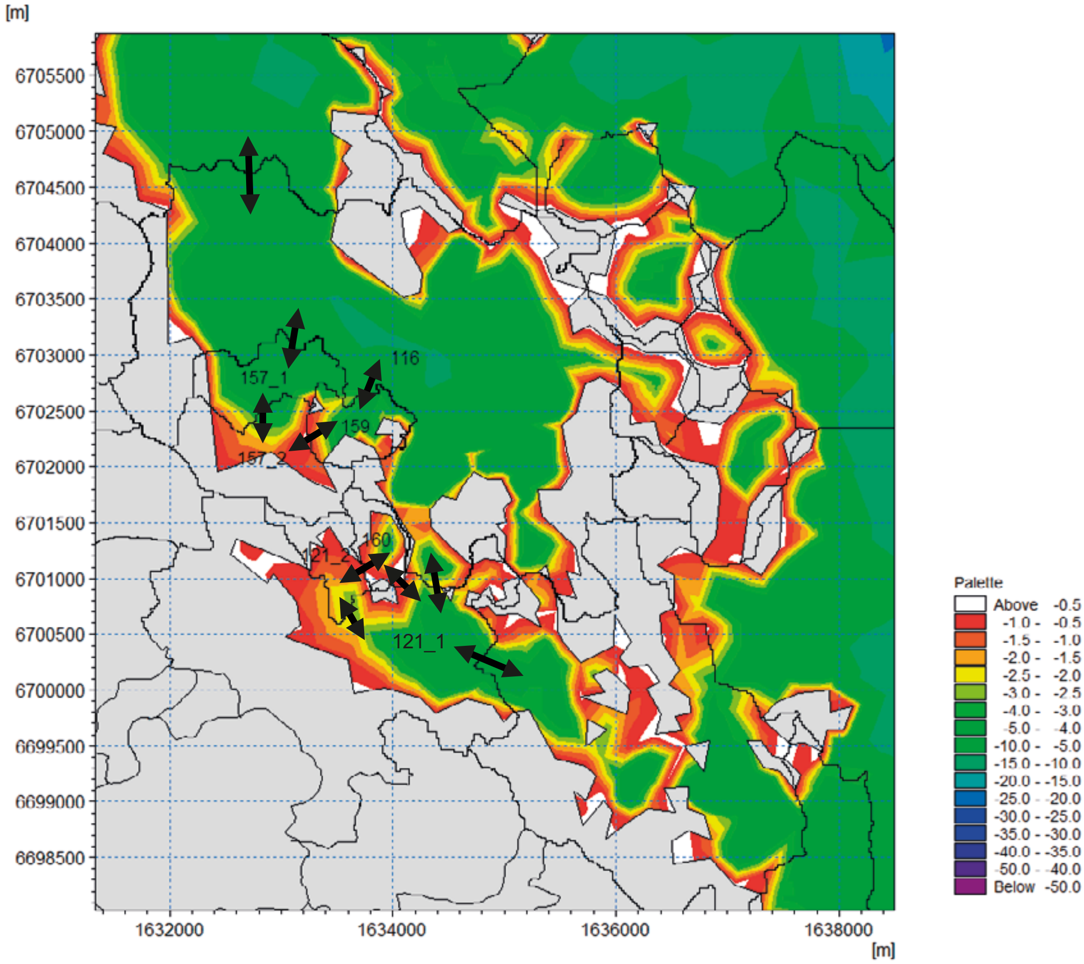

Figure 6-1. *Illustration of the hydrological connectivity between adjacent marine basins on a bathymetric map for the year 3000 AD. The two basins beyond objects 116 and 121_1, although not spatially connected, are pooled as a single object 10 (Öregrundsgrepen) which, in turn, exchanges water with the outer Baltic Sea (object 1).*

6.4 Inter-compartment water fluxes in marine, limnic and terrestrial ecosystems

Parameters quantifying water fluxes between compartments of the radionuclide model for marine, terrestrial and limnic systems were calculated with the MIKE SHE water flow modelling tool (DHI 2012) using site data from Forsmark (Werner et al. 2013). For the marine system, only parameters between different compartments of the model in the regolith below the sea were calculated with the MIKE SHE modelling tool, whereas the fluxes between different sea basins were quantified with the MIKE 3 FM modelling tool (see Section 6.3)

The MIKE SHE model was set up and calibrated for today's conditions. Based on this so called 2000 AD model, models were subsequently set up taking into account landscape development up to the years 3000, 5000, and 11,000 AD (Brydsten and Strömgren 2013). Figure 6-2 shows the land and water areas for the biosphere objects at present and at the three future times for which MIKE SHE simulations, and thus the parameterisations of water fluxes, were made. The figure also shows flow directions between the biosphere objects at future times. At 3000 AD, all biosphere objects are still submerged, whereas the land surface has risen above the shoreline due to shoreline displacement between 3000 and 5000 AD for all objects. Subsequent to the marine stage of an object, for most objects a lake is formed and eventually mire areas are formed around the lake. At 5000 AD, 5 of the 7 biosphere objects partially consist of limnic systems and partially terrestrial systems.

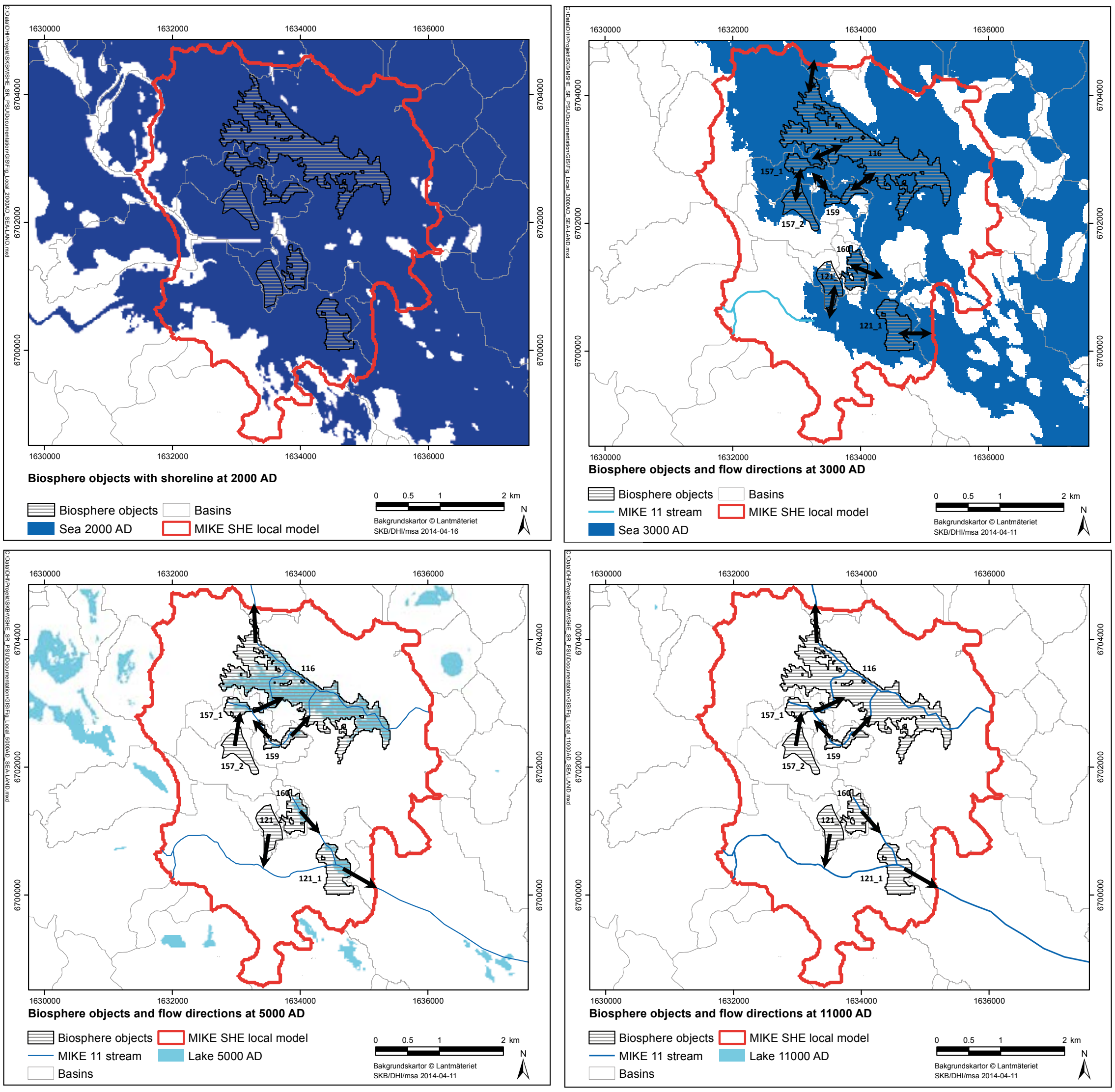

***Figure 6-2.** Maps showing present land and water areas and at the three future times for which MIKE SHE simulations were made. In the upper figures, the sea is still present within the model area, whereas in the lower two figures the sea is displaced further away from the model area. The figures also show flow directions between objects at the future times.*

However, two of the objects (157_2 and 121_2) do not form a lake, as they are transformed to terrestrial systems directly after the marine stage. At 11,000 AD, all limnic systems within the regional MIKE SHE area have been transformed into terrestrial systems (Brydsten and Strömgren 2013). No models were setup for times after 11,000 AD. At 11,000 AD, the sea is displaced far away from the model area and no further impact on hydrological flows from the bedrock due to sea displacement is expected.

In total, parameters representing 27 inter-compartment water fluxes were calculated for the future times described above, using the water-balance utility in MIKE SHE. For each time slice, parameter values were calculated using locally measured meteorological data (described in Section 6.2), representing a normal year for present, temperate climate conditions.

The delivered flux values from the MIKE SHE model are mapped to relevant regolith compartments of the radionuclide transport model. Upwards and downwards vertical fluxes regolith layer boundaries are estimated under the assumption that fluxes at intermediate depths between calculation layer boundaries, at which MIKE SHE calculates fluxes, change linearly with depth in each MIKE SHE calculation layer. For each biosphere object and time, the calculation of across-boundary fluxes is based on the average regolith thickness for the aquatic (lake) and the terrestrial (mire) parts, respectively, for associated times in the dynamic regolith depth and stratigraphy model (Brydsten and Strömgren 2013). Hence, for each biosphere object upward and downward fluxes are calculated to obtain corresponding net fluxes at each regolith layer boundary at the times 3000, 5000 and 11,000 AD. For more details on how the mapping is made, see Werner et al. (2013) and Saetre et al. (2013a).

Table 6-1 lists the delivered parameters, divided into the four categories marine, limnic and terrestrial systems and surface-water flows. The illustration of radionuclide transport compartments of biosphere objects in Figure 2-1 includes both limnic and terrestrial systems, but this figure also clarifies parameters for the marine stage. Blue arrows represent advective fluxes derived from the MIKE SHE model. During the marine stage, i.e. at 3000 AD among the future times considered in the MIKE SHE modelling, only fluxes represented by the blue vertical arrows in the aquatic part (right side) of Figure 2-1 are calculated (cf. first column of Table 6-1), and no surface-flow parameters are delivered for the marine stage.

The parameter names follow inter-compartment fluxes. For example, the *q_low_gl_sea* parameter is the water flux (*q_*) from the RegoLow (*low_*) to the RegoGL (*gl_*) for the marine period (*sea*). In the same way, *q_gl_low_sea* is the corresponding water flux from the RegoGL to the RegoLow for the marine stage (3000 AD).

For objects that contain both limnic and terrestrial systems at 5000 AD, parameters representing all inter-compartment fluxes (blue arrows denoted as "2" in Figure 2-1) are delivered to the radionuclide transport model. The blue arrows are represented by the parameters in columns 2 (limnic), 3 (terrestrial) and 4 (surface flow) in Table 6-1.The parameter names for the vertical fluxes follow the same system as for the marine phase. The only difference between marine and limnic parameter names is the suffix, *sea* vs. *lake*. For terrestrial systems, there is a difference in the layer description above the RegoPG compared with aquatic systems. Specifically, terrestrial systems have a peat compartment between the RegoGL and the RegoUp compartments, whereas aquatic systems have a surface-water compartment above the RegoUp compartment. The parameter names for terrestrial systems are given in the same way as for marine and limnic systems, with the suffix *ter*. The surface-water parameters describe fluxes between limnic and terrestrial systems within one object (*q_up_wat_ter* and *q_wat_up_ter*) as well as fluxes going out from the biosphere object to a biosphere object located downstream (*q_downstream*).

For biosphere objects that are terrestrial at all times after the marine stage, i.e. objects 157_2 and 121_2, the only vertical fluxes considered are those in the terrestrial part (left side) of Figure 2-1, with parameter names according to column 3 in Table 6-1. However, the surface-water flux parameter *q_downstream* (in column 4) is also used for describing the outflow from the biosphere object to its associated downstream object.

For the terrestrial stage (11,000 AD) the vertical fluxes in terrestrial systems (left side) of Figure 2-1 are delivered, with parameter names according to column 3 in Table 6-1. For biosphere objects with former limnic systems, in the radionuclide transport model a stream remains in the terrestrial systems of those biosphere objects at 11,000 AD. The 5 objects following this evolution are 157_1, 159, 116, 160 and 121_2. For these objects, the surface-water flow parameters from column 4 in Table 6-1 are also delivered. The parameters *q_up_wat_ter* and *q_wat_up_ter* then represent surface-water fluxes between the terrestrial system and the stream. The *q_downstream* still represents the water flux leaving the biosphere object.

It has to be considered that fluxes for different object stages refer to different periods in time and that the threshold values described in Section 4.3 control when the parameter values take effect in simulated time. For the transition periods between the marine, limnic and terrestrial stages the water fluxes were linearly interpolated. This is described further in Saetre et al. (2013a). The terrestrial fluxes are defined for two years, 5000 AD and 11,000 AD, these are used to interpolate between the year of threshold isolation and threshold end.

Table 6-1. Parameters representing inter-compartment water fluxes in marine, limnic and terrestrial systems, surface-water fluxes between terrestrial and limnic compartments (q_up_wat_ter, q_wat_up_ter) and fluxes out from biosphere objects (q_downstream).

Marine (sea)	Limnic (lakes)	Terrestrial	Surface-water flow
q_low_gl_sea	q_low_gl_lake	q_low_gl_ter_(iso,end)	q_up_wat_ter
q_gl_low_sea	q_gl_low_lake	q_gl_low_ter_(iso,end)	q_wat_up_ter
q_gl_pg_sea	q_gl_pg_lake	q_gl_pg_ter_(iso,end)	q_downstream
q_pg_gl_sea	q_pg_gl_lake	q_pg_gl_ter_(iso,end)	
q_pg_up_sea	q_pg_up_lake	q_pg_peat_ter_(iso,end)	
q_up_pg_sea	q_up_pg_lake	q_peat_pg_ter_(iso,end)	
q_up_wat_sea	q_up_wat_lake	q_peat_up_ter_(iso,end)	
q_wat_up_sea	q_wat_up_lake	q_up_peat_ter_(iso,end)	

All parameter values delivered represent annual averages and are area-normalised fluxes. For more details about how the parameters were derived from the MIKE SHE model, and information about the flow models from which water balance data were extracted, see Werner et al. (2013).

Parameter values according to Table 6-1 were delivered for simulations based on present-day climate conditions. Parameter values were also delivered for the 5000 AD model, using climate data representing a warmer and wetter climate (see Werner et al. 2013 for details). Moreover, parameter values were also delivered for a periglacial climate with groundwater discharge at taliks for objects 157_2 and 114 (Bosson et al. 2010).

Parameter values were delivered for all biosphere objects and the delivered data are listed in Appendix D. Not all of the objects appear in every biosphere calculation case. For most calculation cases of the biosphere transport modelling, the total release of radionuclides is assumed to take place in object 157_2. The system is in this case reduced to the set of objects 116, 157_1 and 157_2. After the marine stage, object 159 is located upstream of objects 157_1 and 116, and it is thus not included. The consideration of further objects would only dilute radionuclide concentrations and reduce the maximum calculated dose. Additionally to the three mentioned objects, the object 114 is considered when assessing early periglacial conditions but without being hydrologically connected to any other object. For more information about the different calculation cases and how the parameters were implemented in the radionuclide transport model, see SKB (2014c).

7 Element-specific parameters

In this section, soil/liquid partitioning coefficients, K_d, used to assess sorption of elements to regolith and particulate matter are described. Concentration ratio, CR and transfer coefficient, TC, values used to calculate uptake of radionuclides in biota are also presented. The K_d, CR and TC parameters are element-specific and are compiled for each of the 31 elements included in the safety assessment. K_d values are derived for 9 soil types and for particulate matter in lake and sea water. CR values are used both to calculate concentrations in biota utilised as human foods, to assess dose rates to wildlife and to assess radionuclide concentrations in the environment. In total, CR values are derived for 61 biota types for each of the 31 elements included in the safety assessment. TC values are presented for cow meat and cow milk. A detailed basis for the derivation of the K_d, CR and TC values can be found in Tröjbom et al. (2013).

Diffusivity in free solution (D_water), was used to calculate the diffusive flow of radionuclides in the regolith compartments, the data used are also element-specific and are presented in Section 7.5.

7.1 Experience from previous safety assessments

In the previous safety assessment, SR-Site, K_d and CR values were derived by combining site data with literature data using Bayesian statistical methods (Nordén et al. 2010). The Bayesian statistical methods could, in some cases where data were scarce, give unexpected results, as for example unrealistically large ranges. In this safety assessment, data from different sources were not combined using statistical methods. Instead a systematic and transparent method was used to derive the K_d, CR and TC parameter values, the method is described in detail in Tröjbom et al. (2013). In short, data from different sources were compared in order to select the most representative data. Site-specific data were given highest priority since K_d and CR are highly affected by the local biogeochemical environment. The method used in described in detail in Tröjbom et al. (2013).

Even where site-specific data were available in the previous safety assessment, data were still scarce. Additional site investigations have been conducted and a new set of site-specific data have been made available (Sheppard et al. 2011). K_d values were measured in soils in low-lying areas of the landscape, these areas may be used for agricultural purposes, and are therefore of special interest in the safety assessment. This study resulted in 50 estimates of K_d values from five different soil types. In addition to these, samples of cereals were collected and CR values were reported. These new site-specific data were used for parameterisation in this safety assessment.

Another difference in this safety assessment compared with previous safety assessments is the use of elemental or parameteric analogues to fill data gaps, the use of analogue has been applied in a systematic way and rely more on site-specific data. In cases when the variability in the the variability in the underlying distribution from which the data are drawn.is not satisfactorily determined (for instance where few samples are avaliable), the parameter ranges are adjusted based on information from a larger data set representing several elements. This method ensures that the selected data ranges are not underestimated due to scarce data. The method used is described in detail in Tröjbom et al. (2013).

Diffusivity for free solution is handled in the same way as in previous safety assessment since no new data have become available.

7.2 Influence of climate on parameter values

Element-specific parameters are assumed to not be affected significantly by climate variations. The selected solis and biota are assumed to be representive also for warmer and colder climate Accordingly, the same parameter values are used in all calculation cases.

7.3 Soil/liquid partitioning coefficient, K_d

Distribution coefficients, K_d, were used to calculated the sorption of elements onto soils and particulate matter. The K_d model assumes a linear relationship between the concentration of an element sorbed to a solid phase and the elemental concentration in the dissolved phase. The K_d values are both element-specific and site-specific since they depend on both the properties of the elements and the biogeochemical environment in the regolith or water compartment. In this safety assessment, K_d values have been derived for 31 elements in 9 regolith compartments, and for particulate matter in limnic and marine systems. The K_d parameters are listed and described in Table 7-1. The parameterisation methods used and the data selected are presented in Tröjbom et al. (2013).

The selection of K_d values was based on a large set of site data collected both in Laxemar-Simpevarp and Forsmark (Sheppard et al. 2009, 2011, Engdahl et al. 2008, Kumblad and Bradshaw 2008). Despite the large site dataset, data were missing or not sufficient for parameterisation in some cases. In these cases, data gaps were filled by assigning values for elemental or parameteric analogues. In some cases, literature data were used to assign parameter values, but in most cases literature data were used as supporting information.

Table 7-1. K_d parameters used for estimation of sorption in the radionuclide transport model.

Parameter	Description
kD_PM_lake	Distribution coefficient for particulate matter in lake water
kD_PM_sea	Distribution coefficient for particulate matter in sea water
kD_regoGL	Distribution coefficient in glacial clay
kD_regoLow	Distribution coefficient in lower regolith (till)
kD_regoPeat	Distribution coefficient anoxic layer of terrestrial regolith (peat)
kD_regoPG	Distribution coefficient in post-glacial sediments
kD_regoUp_aqu	Distribution coefficient in upper layer of aquatic regolith
kD_regoUp – Drained_mire	Distribution coefficient in cultivated peat soils in industrial agricultural lands
kD_regoUp – Garden plot	Distribution coefficient in soils of a modern kitchen garden
kD_regoUp – Inland_outfield	Distribution coefficient in sandy soils in early agricultural lands
kD_regoUp_ter	Distribution coefficient of upper oxic layer of terrestrial regolith (peat)

7.4 Concentration ratios

Concentration ratios, CR, were used to calculate uptake of radionuclides in biota. CR assumes a linear relationship between concentrations in biota and in surrounding media (soil or water). The CR values are element-specific, site-specific and biota-type-specific, since the uptake in biota depends on the properties of the element, the properties of the biota type and also on the biogeochemical environment of the surrounding medium (soil or water). CR values were assigned to 16 biota types for the calculation of environmental concentrations in biota and doses to humans. In addition, CR values were assigned to 41 biota types for calculation of dose rates to the biota in the dose assessment for non-human biota. The CR parameters used for calculation of dose to humans are listed and described in Table 7-2. The CR values used for calculation of dose rates to non-human biota are listed in Table 7-3. Four representative species other than the standard reference organisms included in the ERICA Tool have also been considered in this assessment; a freshwater benthic primary producer (microphytobenthos), a freshwater bird (Black tern), a marine bird (Ruddy turnstone) and a marine mammal (European otter). The approach has been to use the same CR values as for corresponding reference organisms since those are primarily based on site chemistry data. For microphytobenthos the CR values for limnic phytoplankton (cR_Lake_pp_plank_NHB) have been used. The birds and otter are assumed to feed in the aquatic ecosystems and CR values for limnic or marine birds (cR_Lake_bird_NHB, cR_Sea_bird_NHB) or marine mammals (cR_Sea_mammal_NHB) were used for simulating radionuclide uptake in those organisms.

CR values were assigned to the 31 elements included in the safety assessment, using a large site and literature data set. The parameterisation methods used and the data selected are presented in detail in Tröjbom et al. (2013). Site data were used when possible, but, in many cases, site data were not available. In these cases, parameteric and/or elemental analogues were used for parameterisation. In cases where no site data or suitable analogues were available, literature data were used for the parameterisation. Literature data were complied and used as supporting data to evaluate uncertainties in the selected site data.

Table 7-2. CR parameters used for estimation of uptake in biota in the radionuclide transport model.

Parameter	Description
cR_agri_cereal	Concentration ratio between soil and cereal
cR_agri_fodder	Concentration ratio between soil and fodder
cR_agri_tuber	Concentration ratio between soil and potatoes
cR_agri_veg	Concentration ratio between soil and vegetables
cR_food_herbiv	Concentration ratio with respect to herbivores and their diet
cR_lake_cray	Concentration ratio for crayfish in lake water
cR_lake_fish	Concentration ratio for fish in lake water
cR_lake_pp_macro	Concentration ratio for macrophytes in lake water
cR_lake_pp_micro	Concentration ratio for microphytobenthos in lake water
cR_lake_pp_plank	Concentration ratio for plankton in lake water
cR_ter_mush	Concentration ratio between edible mushrooms and soil
cR_ter_pp	Concentration ratio for terrestrial primary producers and soil
cR_sea_fish	Concentration ratio for fish in sea water
cR_sea_pp_macro	Concentration ratio for macrophytes in sea water
cR_sea_pp_micro	Concentration ratio for microphytobenthos in sea water
cR_sea_pp_plank	Concentration ratio for plankton in sea water
TC_meat	Transfer coefficient from intake of radionuclides in fodder and water to meat from cows
TC_milk	Transfer coefficient from intake of radionuclides in fodder and water to milk from cows

Table 7-3. Parameters used for estimation of dose rates to non-human biota (NHB).

Parameter	Description
cR_Lake_amph_NHB	Concentration ratio between lake water and amphibians
cR_Lake_bent_fish_NHB	Concentration ratio between lake water and benthic fish
cR_Lake_bird_NHB	Concentration ratio between lake water and birds
cR_Lake_bivalve_NHB	Concentration ratio between lake water and bivalves
cR_Lake_crust_NHB	Concentration ratio between lake water and crustaceans
cR_Lake_Fish_NHB	Concentration ratio between lake water and fish
cR_Lake_gastr_NHB	Concentration ratio between lake water and gastropods
cR_Lake_ins_larvae_NHB	Concentration ratio between lake water and insect larvae
cR_Lake_mammal_NHB	Concentration ratio between lake water and mammals
cR_Lake_pel_fish_NHB	Concentration ratio between lake water and pelagic fish
cR_Lake_pp_plank_NHB	Concentration ratio between lake water and phytoplankton
cR_Lake_pp_vasc_NHB	Concentration ratio between lake water and vascular plants
cR_Lake_zoopl_NHB	Concentration ratio between lake water and zooplankton
cR_Sea_bent_fish_NHB	Concentration ratio between sea water and benthic fish
cR_Sea_bent_moll_NHB	Concentration ratio between sea water and benthic molluscs
cR_Sea_bird_NHB	Concentration ratio between sea water and birds
cR_Sea_crust_NHB	Concentration ratio between sea water and crustaceans
cR_Sea_Fish_NHB	Concentration ratio between sea water and fish
cR_Sea_mammal_NHB	Concentration ratio between sea water and mammals
cR_Sea_pel_fish_NHB	Concentration ratio between sea water and pelagic fish
cR_Sea_polych_NHB	Concentration ratio between sea water and polychaete worms
cR_Sea_pp_macro_NHB	Concentration ratio between sea water and macrophytes
cR_Sea_pp_plank_NHB	Concentration ratio between sea water and phytoplankton
cR_Sea_pp_vasc_NHB	Concentration ratio between sea water and vascular plants
cR_Sea_zoopl_NHB	Concentration ratio between sea water and zooplankton
cR_Ter_amph_NHB	Concentration ratio between soil and amphibians
cR_Ter_bird_egg_NHB	Concentration ratio between soil and bird eggs
cR_Ter_bird_NHB	Concentration ratio between soil and birds
cR_Ter_detr_inv_NHB	Concentration ratio between soil and detrivorous invertebrates
cR_Ter_fl_ins_NHB	Concentration ratio between soil and flying insects
cR_Ter_gastr_NHB	Concentration ratio between soil and gastropods
cR_Ter_mammal_large_NHB	Concentration ratio between soil and large mammals
cR_Ter_mammal_small_NHB	Concentration ratio between soil and small mammals
cR_Ter_pp_grass_NHB	Concentration ratio between soil and grass and herbs
cR_Ter_pp_lich_NHB	Concentration ratio between soil and lichens and bryophytes
cR_Ter_pp_NHB	Concentration ratio between soil and primary producers
cR_Ter_pp_shrub_NHB	Concentration ratio between soil and shrubs
cR_Ter_pp_tree_NHB	Concentration ratio between soil and trees
cR_Ter_rept_NHB	Concentration ratio between soil and reptiles
cR_Ter_soil_inv_NHB	Concentration ratio between soil and soil invertebrates

7.5 Diffusivity in free solution

Diffusivity (D_water), is a proportionality constant between the mass flux due to molecular diffusion and the gradient in the concentration of the element. The diffusivity values were used in the radionuclide transport model for calculation of the diffusion fluxes between different regolith compartments. The values used are the recommended values for diffusivities in free solution, presented in Olsson and Neretnieks (1997, cited in Liu et al. 2006). For most of the elements included in the safety assessment, the diffusivity is assumed to be 1×10^{9} m^2 s^{-1}. The values used are shown in Table 7-4. This coefficient has an SI unit of m^2 s^{-1}, but in the radionuclide transport model the unit m^2 $year^{-1}$ was used.

Table 7-4. Diffusivity of different element in free solution presented in m^2 $year^{-1}$.

Element	D_water (m^2 $year^{-1}$)
Ac	3.2E–02
Ag	5.3E–02
Am	3.2E–02
Ba	3.2E–02
C	3.8E–02
Ca	3.2E–02
Cd	2.3E–02
Cl	6.3E–02
Cm	3.2E–02
Co	3.7E–02[1]
Cs	6.6E–02
Eu	3.2E–02
Ho	3.2E–02
H	3.8E–02
I	6.3E–02
Mo	3.2E–02
Nb	3.2E–02
Ni	2.1E–02
Np	3.2E–02
Pa	3.2E–02
Pb	3.2E–02
Pd	3.2E–02
Po	3.2E–02
Pu	3.2E–02
Ra	2.8E–02
Se	3.2E–02
Sm	3.2E–02
Sn	3.2E–02
Sr	2.5E–02
Tc	3.2E–02
Th	4.7E–03
U	3.2E–02
Zr	3.2E–02

[1] The value for Co should be 2.2E–02. The value of 3.7E–02 was used in the safety assessment. This was discovered late in the work process and since the effect on the results is insignificant no corrections were made in the analysis.

8 Aquatic ecosystem parameters

This chapter describes parameters for the limnic and marine ecosystems. For a detailed description of these aquatic ecosystems see Andersson (2010) and Aquilonius (2010). The parameter values are, as far as possible, based on site-specific data, and otherwise on literature data. The landscape changes with time due to shore-line displacement, resulting in the transformation of marine basins into lakes, which, in time, are transformed to wetlands. Often a small stream remains that passes through the wetland. The geometry of the marine basins and lakes changes with time and therefore some aquatic parameters are time dependent and change with each time step in the model (i.e. 500 years for the marine stage and 100 years for the limnic stage). Other parameters are more related to the type of ecosystem and then one parameter value is valid for the entire marine stage and one for the entire limnic stage (lake and stream).

Some assumptions as to the development of lakes and marine basins in the future and under different climates that are relevant for the choice of parameter values are also discussed in this chapter. Although photic depth is not used in the radionuclide transport model, the calculation of photic depth in lakes is described as it is used in the calculations of biological parameters, i.e. primary production only occurs in the photic zone (e.g. Wetzel 2001).

8.1 Experience from previous safety assessments

Transport of radionuclides in aquatic ecosystems has been modelled in previous safety assessments at SKB for SAFE, SAR-08 and SR-Site. Experience from these assessments, site investigations and research has led to continual development of the radionuclide transport model and updating of the parameters. Below is a comparison of aquatic parameters in SR-PSU with those used in previous safety assessments.

Ecosystem models were basically the same for SAFE and SAR-08, although some parameter values were updated between the assessments (Karlsson et al. 2001, Bergström et al. 2008). Since SAR-08, the biosphere radionuclide transport model has been extended and continuous development of the landscape is now modelled. Consequently, the majority of aquatic parameters are new. Also, many parameters that were used in SAR-08 (e.g. relating to edible food, particulate matter, DIC) have also been updated due to new site data and updated models.

The SR-PSU radionuclide transport model closely resembles the SR-Site model, although some updates have been made (Saetre et al. 2013a). Consequently, many of the aquatic parameters are identical to parameters used in SR-Site (aquatic SR-Site parameters are presented in Andersson (2010) and Aquilonius (2010)). However, since the model has been updated, some new parameters have been added and some parameters have been altered. In SR-Site, parameters for primary production in aquatic systems reflected net ecosystem production, i.e. primary production minus community respiration. In SR-PSU, the gross primary production is used and parameters relating to mineralisation rate are added. In this way, the aquatic part of the system more closely resembles the terrestrial part of the model, and it is easier to evaluate the effects of parameteric uncertainties related to the incorporation of elements from organic matter into sediments. Also, the handling of degassing of carbon across the water-air interface has been further developed in SR-PSU and modelling of gas uptake and degassing have been updated with a number of new parameters (see below).

8.2 Influence of climate on parameter values

For aquatic ecosystems, altered climatic conditions are expected to have some effects on the parameter values used in the associated calculation cases. Even though several studies indicate rapid and observable changes in aquatic ecosystems following climate changes, the response is often difficult to predict (e.g. Smith et al. 2008, George 2010, Adrian et al. 2009). Ecosystems are complex and the vast number of interactions leads to varying effects of temperature changes, e.g. the same temperature increase may lead to completely opposite responses in two different aquatic ecosystems (for detailed descriptions of expected responses of the aquatic ecosystems in Forsmark to altered climate conditions see Chapter 8 in Andersson (2010) and Chapter 7 in Aquilonius (2010)). For most parameters, site data of today at ambient climate conditions have been used to parameterise the global warming case, extended global warming case, periglacial climate case and talik case. This is justified by the fact that many parameters to a great degree, are dependent on factors other than temperature, such as catchment characteristics, lake morphometry, and nutrient status. Moreover, ranges in the estimates are assumed to cover also variations in the parameter values for future changes in climate. There are some exceptions to this. Although primary production may remain similar in both warmer and colder climates, fish production is often lower in colder climates and crayfish are dependent on longer vegetation periods than are encountered in periglacial conditions. Therefore, the production of edible food parameters are altered (see Section 8.10 below).

8.3 Assumptions for limnic ecosystems

The present lakes in the Forsmark area are oligotrophic hardwater lakes, thoroughly described in the limnic ecosystem report (Andersson 2010). This type is very special, with low amounts of biota in the water column and high amounts of primary producers in the benthic habitat. Other lake types in the region are dystrophic lakes and larger eutrophic lakes. New lakes will form in the model area in the time frame of the safety analysis. It is likely that the lakes will have oligotrophic hard water characteristics. Moreover, the oligotrophic hardwater lakes are assumed to be autochthonous (i.e. the food web is mainly dependent on in-lake primary produced organic matter) and thus have a higher potential to incorporate radionuclides into the food web than lakes that are more dependent on allochthonous organic matter. Radionuclides from a geological repository tend to discharge at low points in the landscape such as lakes, streams and sometimes wetlands (SKB 2014c). A larger proportion of carbon-14 discharge from a repository can be incorporated in the aquatic food web if the aquatic ecosystem is autochthonous than if it depends on carbon from outside the lake, which is likely to be uncontaminated. Thus, all present and future lakes in the area are treated as oligotrophic hardwater lakes for two reasons, 1) it is assumed to be the most likely evolution, and 2) it is assumed to be the most cautious assumption. In order to ensure that the potential significance of other lake types in radionuclide modelling is taken into account, these other lake types are considered in the estimation of minimum and maximum parameter values.

The biomasses and production of benthic macrobiota, microbiota, and pelagic biota in the stream stage of the objects are assumed to be similar on an areal basis to those of the lake stage and no separate parameter values are calculated for streams. Below follows a short description of the measurements in streams that justify this assumption.

For streams in the area, data on macrophytes and biomass are rather scarce. The estimated biomass of macrophytes in streams (mean 35 gC m^{-2}, median 12 gC m^{-2}) (further described in Section 3.10.2 in Andersson (2010)) is close to the median biomass in lakes.

The biomass of the microphytobenthos in streams is probably smaller than that in lakes, since there are no thick microbial mats. However, the benthic bacterial biomass may still be high. The biomass of microbiota depends on many factors: flow rates, nutrients, temperatures and catchment characteristics. In arid regions where streams have little riparian vegetation, autotrophic production may be the major energy input to aquatic ecosystems, but in temperate regions with catchments dominated by coniferous vegetation (as in Forsmark), energy comes mainly from allochthonous inputs (Lamberti 1996). In the latter areas, year-round shading by conifers probably limits autotrophic production. However, in the present Forsmark streams there are examples of dense vegetation (see Andersson 2010) indicating that production may be high. In order not to underestimate the potential uptake by primary producers, the same biomass and production as in lakes has been assumed for microphytobenthos in streams. Biomass has therefore also been set to the same value as in lakes.

Planktonic biomass varies along the stream section. Immediately downstream of a lake outlet, the phytoplankton biomass is usually very similar to that of the lake (further discussed in Section 3.10.2 in Andersson (2010) and in Wetzel (2001)). Further downstream from a lake outlet, the phytoplankton biomass decreases. In larger streams, there may be a productive phytoplankton community. Assuming the same phytoplankton biomass as in lakes probably is an overestimation (see Section 3.10.2 and Chapter 6 in Andersson 2010), but this has a minor influence on the results of the assessment calculations due to the shallow depth of most streams in the model. Also the biomasses per unit area of edible fish and crayfish are assumed to be the same in lakes and streams. For shallow lakes (maximum depth less than 1 m), a permanent fish population is assumed not to exist (Andersson 2010). Migrating fish can occur in much shallower streams occasionally. Thus, for permanent fish populations, the same assumptions as for the lakes are assumed to be applicable.

Even if production in one primary producer community (macrophytes, microphytobenthos and phytoplankton) is lower, it is possible that this is compensated for by higher production in another. Thus, as data from the streams are scarce it is reasonable to use the same data as for lakes as nutrient and light conditions are similar.

8.4 Assumptions for marine ecosystem

The marine basins in the model area in Forsmark are represented both by near-shore, shallow, secluded areas with high primary production (autotrophic) dominated by benthic macrophyte production, as well as deeper heterotrophic areas dominated by the influx of carbon from more productive areas (see further Aquilonius 2010). The main focus in the safety assessment is the coastal area, since the most likely radionuclide discharge points from the repository are located in the coastal basins, hence, where parameters differ between coastal and off shore locations, the value representative of coastal basins is generally used (e.g. piston_vel).

8.5 Particulate matter and dissolved inorganic carbon

The chemical properties of surface water affect the transport and accumulation of radionuclides. This section describes the concentrations of particulate matter (conc_PM_lake, conc_PM_sea) which are important for sorption/desorption of radionuclides (i.e. determine the available surface for sorption), and the concentrations of dissolved inorganic carbon, DIC, (conc_DIC_lake, conc_DIC_sea) which are important for the distribution of carbon-14. Several other chemical properties may also affect the transport of radionuclides, e.g. pH, salinity and temperature (described in Section 8.8).

8.5.1 Particulate matter

The concentrations of particulate matter (described below) are used together with K_d values (see Section 7.3) to model the transport of radionuclides associated to particulate matter.

Concentration of particulate matter in lake

The parameter conc_PM_lake represents the concentration of particulate matter in lake water. This parameter was estimated based on site data on suspended particles in three Forsmark lakes in 2007 and 2008 (n=63) (Data from Sicada[2], March 2009). Many measurements were below the detection limit (< 2 mg L^{-1}), in which case half the detection limit was used in the calculations. This approach is strengthened by a study of suspended particles at one occasion in April 2008 where measurements were performed with lower detection limit than usual (Engdahl et al. 2008). On that occasion, mean concentration from three lakes in the Forsmark area were about 1 mg L^{-1}, i.e. half detection limit. Monthly averages were calculated from the standard site investigations for each lake (i.e. not including Engdahl et al. 2008) and the annual mean concentration was calculated for the three lakes from these monthly means and used as the parameter value).

[2] SKB's database Sicada, access might be given on request.

The minimum value was taken from the one sampling occasion in April 2008 (Engdahl et al. 2008) and was assumed to represent an annual minimum. This is because many of the measurements in the site investigations were below detection limit and may very well have been as small, or smaller, than the measurement in April 2008. The maximum value was set to the maximum observed value during the site investigations (i.e. a single observation). Thus, a single estimate was used to represent an upper bound annual mean value for lakes in a temperate region. This results in a somewhat higher annual estimate than expected to occur in the present oligotrophic hardwater lakes of Forsmark but might be appropriate to use as an annual mean for other lake types forming in Forsmark in the future, i.e. the range is over estimated for present conditions in order to not underestimate the range for possible future lake types in the area.

The concentration of particulate matter in streams was also measured during site investigations in Forsmark (see Andersson 2010). However, almost all values were below the detection limit, and any observed differences between the concentrations in streams and lakes were too small to indicate any real difference. The lake value of conc_PM_lake was therefore used for both lakes and streams.

Concentration of particulate matter in sea

This parameter (conc_PM_sea) represents the concentration of particulate matter in the water column. The particulate matter in sea water was measured at four sites during 2007 and 2008 (N=15) in Forsmark (Data from Sicada[3] , March 2009). Minimum and maximum are the measured minimum and maximum values over all sites and sampling events. Some measurements were below the detection limit (< 2 mg L^{-1}), in which case the value was not used. Monthly averages were calculated from the standard site investigations for each sampling site and the annual mean concentration was calculated from these monthly means and used as the parameter value (Table 8-1).

Table 8-1. Parameter values of particulate matter for lakes and sea (conc_PM_lake, conc_PM_sea). Mean and stdev are for the marine values based on 15 sampling occasions distributed over 4 sites and for the limnic values on annual mean from 3 lakes (see text)

	Mean	Stdev	Minimum	Maximum	Distribution
conc_PM_lake (kgdw m^{-3})	0.0011	0.00004	0.0003	0.0025	Normal
conc_PM_sea (kgdw m^{-3})	0.0029	0.0012	0.0015	0.0054	Normal

8.5.2 Dissolved inorganic carbon

The concentration of dissolved inorganic carbon, DIC, is used to model the concentration of carbon-14 transferred upwards in the food chain, i.e. any carbon-14 released into the water is assumed to be incorporated into biota in relation to its proportion to carbon-12 already present in the water volume.

Concentration of DIC in lake water

This parameter (conc_DIC_lake) represents the concentration of dissolved inorganic carbon, which was sampled and analysed during the site investigations in Forsmark. The mean values from 6 lakes (Tröjbom and Söderbäck 2006) were used to calculate the parameter value, Table 8-2.

The high concentration of DIC in the Forsmark lakes is due to the calcareous soils in the area. With time, the calcite will be depleted and the soil contribution of DIC to lakes will become small (Tröjbom and Grolander 2010). Therefore, the median value for lakes in the Laxemar-Simpevarp area was used as a minimum value of this parameter. This is one order of magnitude lower than the mean value, but some individual observations during the year are even lower in the Forsmark area (see Section 3.9 in Andersson 2010). The maximum value was set to the highest mean value of the 6 observed lakes in the Forsmark area (Tröjbom and Söderbäck 2006). The median, mean, minimum and maximum values of DIC are presented in Table 8-2. The measured concentration of dissolved inorganic carbon in streams is similar to that in lakes, so the values for lakes were used for steams.

[3] SKB's database Sicada, access can be given on request.

Concentration of DIC in sea water

This parameter (conc_DIC_sea) represents the concentration of DIC in the marine water column. Mean, minimum and maximum represent the range of measurements. The concentrations of DIC were sampled and analysed during the site investigations in Forsmark. The annual average value at five sites during the years 2002 to 2006 (n=5, 267 subsamples) have been used in the radionuclide model calculations. The parameter values (conc_DIC_sea) are presented in Table 8-2.

Table 8-2. Mean, minimum and maximum of conc_DIC in lakes and sea in Forsmark. The measured concentrations of DIC in streams are presented as a comparison to the lake values that were used in the model.

	Mean	Stdev	Minimum	Maximum	Distribution
conc_DIC_sea (kgC m^{-3})	0.011	0.005	0.0003	0.027	Normal
conc_DIC_lake (kgC m^{-3})	0.022	0.010	0.0023	0.029	Normal
Measured concentration of DIC in Forsmark streams (kgC m^{-3})	0.026	0.010	0.0009	0.059	

8.6 Biomass and production of primary producers

Production of biota is important for uptake of radionuclides into organisms. Uptake is calculated using concentration factors, CRs, which are further described in Section 7.4. The production of biota is important not only for estimating radionuclide uptake in biota, but also for estimating the flux of radionuclides to sediments in lakes and sea. The biota incorporate radionuclides and the production excess (i.e. the net ecosystem production) settles on the lake or sea floor as sediment or is transported to downstream objects. It is therefore important to estimate biomass (biom_pp) and net primary productivity of biota (NPP), as well as the fraction of production that is not decomposed but contributes to sedimentation (f_refrac, described in Section 8.7). After sedimentation, organic matter it is further mineralised and only a small fraction is permanently buried. This fraction is estimated by calculating the mineralisation rate (min_rate) for the different sediment layers (upper regolith and post glacial deposits) as described in Section 8.7. To be able to calculate the biomass, production and fraction of primary producers not decomposed, the aquatic ecosystems are divided into three communities according to habitat: 1) phytoplankton (biom_pp_plank, NPP_plank), 2) macrophytes including macro-algae (biom_pp_macro, NPP_macro) and 3) microphytobenthos (biom_pp_micro, NPP_micro).

8.6.1 Parameters affecting biomass and production of primary producers

Biomass and production of primary producers are dependent on many factors of which nutrient and light availability are often the most important. Nutrient concentrations in future aquatic ecosystems are assumed to be similar to those occurring at present. Light availability on the other hand may differ due to the different geometry of future marine and lake basins. Therefore the photic depth (the depth to which photosynthesis is possible) and basin depth of aquatic objects have been calculated, as described below, although they are not directly incorporated into the radionuclide transport model. Instead, the depth parameters are used in calculation of biomass and production described below.

Photic depth

The photic depth, i.e. where there is enough light for photosynthesis to occur, corresponds to the depth at which 1% of the incoming light remains. The present-day lakes in Forsmark are all shallow and the entire lake bottoms are situated within the photic zone. Some of the future lakes will be deeper and probably contain aphotic bottoms, i.e. where the light climate is too poor to allow photosynthesis. Although the entire depth of the present-day Forsmark lakes is photic, a theoretical photic depth in the lakes has been calculated with the aid of light extinction curves from present lakes.

Light measurements in two lakes in Forsmark, Bolundsfjärden and Eckarfjärden, were performed biweekly from 2003 to 2008 in the SKB site investigations (Sicada[4], March 2009). For each date, a regression of light extinction was used to extrapolate the curve until only 1% of the incoming light remained (Figure 8-1). For weeks lacking measurements, a mean for the photic zone was calculated from the weeks before and after. Production in the lakes occurs mainly during the summer (Andersson and Brunberg 2006), so the mean annual photic depth was calculated from the beginning of April to the end of September. A calculation for Eckarfjärden and Bolundsfjärden resulted in a mean photic depth of 4.3 m. This photic depth has been assumed to be valid for future lakes and streams. Other factors may influence photic depth, such as water chemistry and the biomass of plankton. In two large Uppland lakes, Limmaren and Erken, the Secchi depth (approximately half the photic depth) is c. 2 and 5 m, respectively (Weyhenmeyer 1999, Weyhenmeyer et al. 1999) thus indicating photic depths of 4 and 10 metres, respectively. Thus, although photic depth may vary it is clear that our estimate is within the range of values derived from present-day Secchi depths in deep lakes in the region.

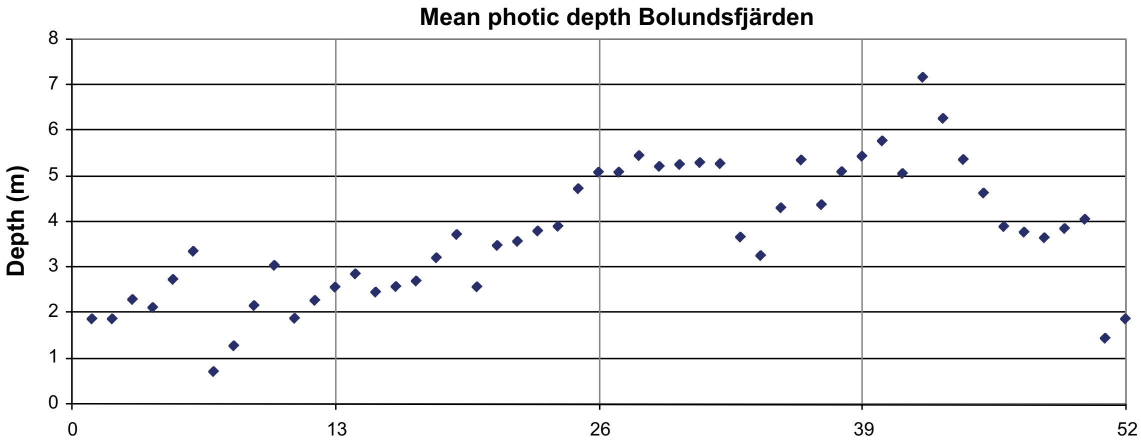

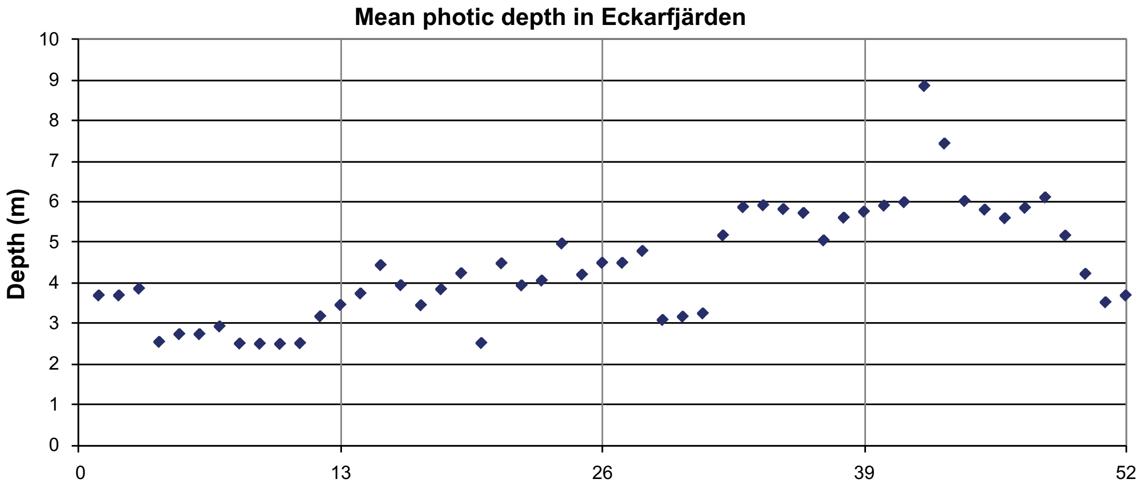

Figure 8-1. *Theoretical photic depth in lakes Bolundsfjärden and Eckarfjärden, calculated by extrapolating light extinction curves in the lakes.*

[4] SKB's database Sicada, access might be given on request.

8.6.2 Biomass

The biomass parameters represent the biomass of primary producers of the three communities in the aquatic ecosystem; the benthic macrophyte community (biom_pp_macro), the benthic microphyte community (biom_pp_micro) and the pelagic plankton community (biom_pp_plank).

For lakes, the biomasses of these primary producers were based on site data, literature and assumptions regarding relationships between biomass, production and light (further explained below and discussed in Andersson (2010).

For the sea, the biomasses of the different primary producer communities were interpolated with a GIS model. The GIS model used site data, literature values and assumptions described in detail in Chapter 4 in Aquilonius (2010) to estimate biomasses for each grid cell (20×20 m) in the marine model area.

In order to generate parameter values for the various time steps in the radionuclide model, the annual mean values in the separate basins were correlated with depth, and the parameter values versus depth are presented in Figure 8-2, Figure 8-3 and Figure 8-4. Primary producers occur down to depths at which 1% of incoming light remains (photic depth). The measured abundances of primary producers indicate a small difference in photic depth between the communities (19 versus 20 m), and accordingly the same depth was used for all communities. The geometric parameters of the basins (mean depth, maximum depth, photic area) are modelled in the dynamic landscape model (Brydsten and Strömgren 2013).

The times series with the object-specific biomasses are presented in Appendix C.

Biomass for macrophytes in lakes

The parameter biom_pp_macro represents the biomass of macro-algae described as mean biomass per m^2 lake area. For calculation of this parameter, the biomass in the photic zone is multiplied by the photic area and divided by the lake area.

In the Forsmark lakes, the biomass of macro-algae in the photic zone is estimated as the median biomass of *Chara* sp. from site investigations in Lake Bolundsfjärden (22 gC m^{-2}, further described in Andersson (2010)). This biomass was used for the entire photic zone, although measurements in present-day lakes only reach depths of c. 2 m, i.e. the maximum depths of the present-day lakes. However, *Chara* has been found to depths of c 40 m in other lakes (Kufel and Kufel 2002 and references therein) and therefore *Chara* was assumed to occur at the entire photic depth (down to 4.3 m) in the future larger and deeper lakes.

The median value of the macro-algae biomass in Forsmark (22 gC m^{-2}) is in the lower part of the range (recalculated to 11–134 gC m^{-2}) found in a literature review by Kufel and Kufel (2002 and references therein). The minimum and maximum values for macro-algae were set to the minimum and maximum values found in the literature (i.e. 11 and 134 gC m^{-2}, respectively) although the higher values most probably represent more nutrient-rich lakes than the Forsmark lakes.

Biomass for microphytobenthos in lakes

The parameter biom_pp_micro represents the biomass of microphytobenthos described as a mean biomass per m^2 lake area. For calculations of this parameter the mean biomass in the photic zone is multiplied by the photic area and divided by the lake area.

Most Forsmark lakes contain a "microbial mat", i.e. a thick microbial matrix consisting of microphytobenthos and benthic bacteria. The microbial mats in Forsmark are several centimetres thick, which is remarkable in comparison with most other lakes in Sweden and Europe (Andersson 2005). In general, light is assumed to penetrate benthic matrixes down to depths of millimetres (Hill 1996 and references therein), and the algal matrix in lakes in Sweden and Europe is usually only millimetres thick (e.g. Hargrave 1969, Wiltshire 2000). The microbial mats of the Forsmark lakes are further described in the limnic ecosystem report (Andersson 2010). Th mean value of microphytobenthos biomass (3.8 g C m^{-2}) from site-specific measurements at 1.5 m depth in Lake Eckarfjärden was assumed to be valid for the entire photic zone in future Forsmark lakes. A few of the Forsmark lakes in the area lack a thick microbial mat, and in those kinds of lakes the biomass is undoubtedly lower.

No correlations have been found between the occurrence of microbial mats and depth or height above sea level. Therefore, it is not possible to predict which of the future lakes will contain the microbial mats. Since most lakes contain these thick microbial mats, the same biomass is assumed for all future lakes.

The annual mean biomass of the microphytobenthos in Lake Eckarfjärden during the period 2000 to 2002 ranged from 2.8 to 5.8 g C m^{-2} (Andersson et al. 2003, Blomqvist et al. 2002). The geometric and arithmetic means for microphytobenthos biomass are similar, 3.6 and 3.8 g C m^{-2}. The dataset is small (n=3 years) and it is difficult to draw any conclusion regarding ranges in annual means. However, the range assuming a lognormal distribution (1.6–8.1 g C m^{-2}) is somewhat larger, and in order to avoid underestimating maximum values, the larger value of a 95% confidence interval (8.1 g C m^{-2}) has been used in calculating the maximum benthic community biomass. Some lakes in Forsmark lack a microbial mat, typical of the majority of the lakes. A minimum biomass of microphytobenthos was calculated by assuming a few millimetres thick microbial mat corresponding to more normal occurrence of benthic microalgae, and the biomass in the photic area was set to one order of magnitude lower (0.38 gC m^{-2}) than in lakes with microbial mats.

Biomass of phytoplankton in lakes

The parameter biom_pp_plank represents the biomass of phytoplankton, described as a mean biomass per m^2 lake area.

The phytoplankton biomass has been investigated for 3 years in the existing Lake Eckarfjärden in Forsmark and the annual mean biomass ranged from 0.022 to 0.057 gC m^{-3}. The annual mean biomass was used for the parameter calculations (biomass and species composition of phytoplankton in Forsmark lakes are further described in Andersson (2010)), i.e. the average biomass per m^3 of phytoplankton (mean 0.04 gC m^{-3}, n=3 years) was multiplied by the average depth to obtain the biomass per m^2.

Both the geometric and the arithmetic mean phytoplankton biomass density were 0.04 g C m^{-3}. The dataset is small (n=3 years) and it is difficult to draw any conclusion regarding distribution. Calculating a range using 95% confidence interval using a lognormal distribution gives a somewhat higher range than using normal distribution (minimum 0.015 gC m^{-3} and a maximum of 0.097 gC m^{-3}). This range is very similar to the phytoplankton range in oligotrophic lakes obtained from the literature (0.02 to 0.10 gC m^{-3} (Wetzel 2001 and references therein). Minimum and maximum values were set to the literature range for oligotrophic lakes i.e. 0.02 and 0.10 gC m^{-3}, respectively.

Biomass of macrophytes in sea

biom_pp_macro represents the biomass of the macro-benthic producer community (macrophytes). In areas shallower than 19 m (the photic area), biomass was calculated according to the macrobenthic biomass correlation with depth based on site data. The macrobenthic biomasses were calculated with the depth function from (Olenin 1997):

Biomass (kgC m^{-2}) = 0.0387 $e^{-0.17x}$, where x is m depth)

This equation result in biomasses that are in accordance with reported biomasses of benthic macrophytes and their depth distribution (Figure 8-2).

Biomass of microphytobenthos in sea

This parameter represents the biomass of the microbenthic producer community, i.e. the microphytobenthos. For the microbenthic community, the biomass for the various time steps in the radionuclide transport model were calculated according to the microphytobenthic biomass correlation with depth down to 19 m. The micro-benthic biomass was calculated according to:

Biomass (kgC m^{-2}) = 0.0002x + 0.0038

where x is depth in m

The biomass equation is based on site-specific GIS model of the area, (see Section 6 in Aquilonius (2010)). In Figure 8-3 the mean parameter values versus mean depth in the separate marine basins are plotted together with the depth function of the parameter.

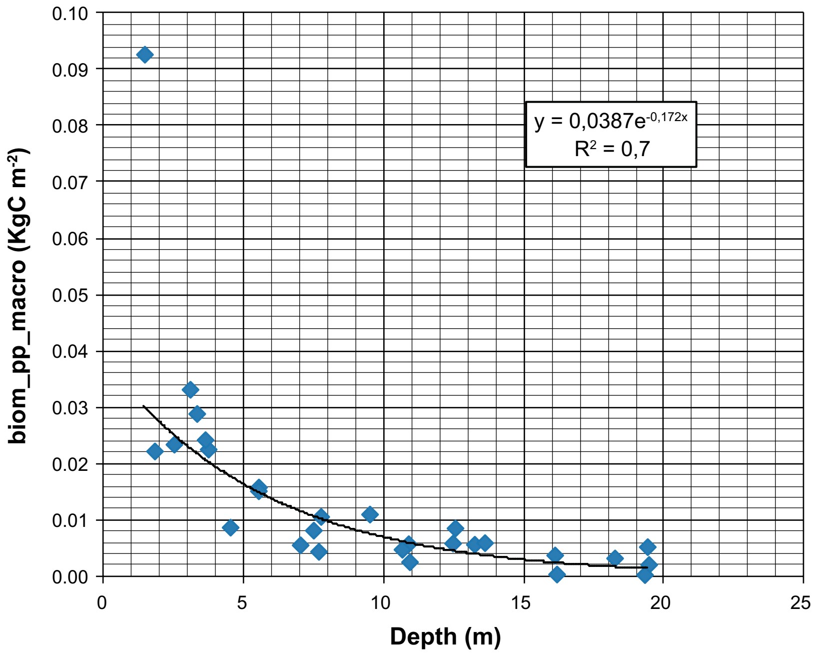

Figure 8-2. *Macro-benthic biomass (biom_pp_macro) vs. depth in the marine model area in Forsmark based on GIS modelling of present marine basins in Forsmark together with the equation used to derive mean values of microphytobenthos biomass in future marine basins.*

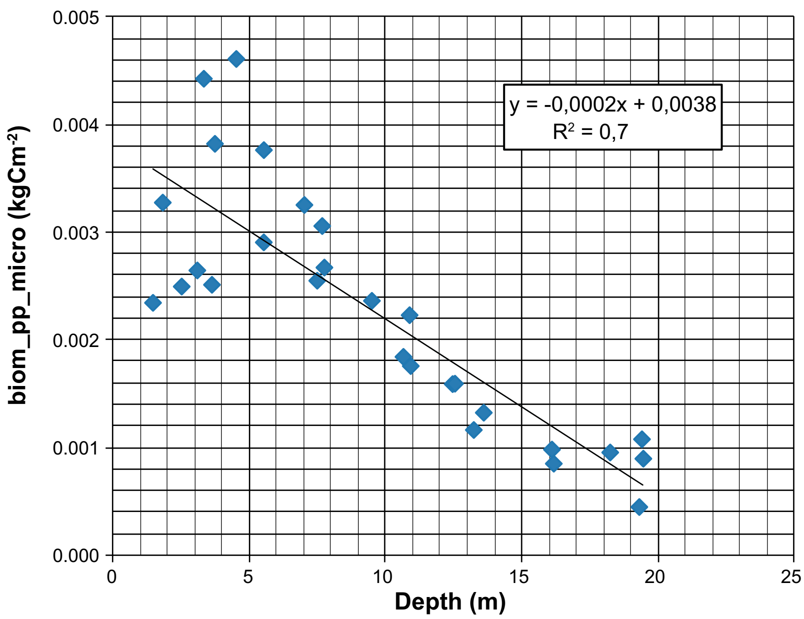

Figure 8-3. *Microbenthic biomass (biom_pp_micro) versus depth in the marine model area in Forsmark based on GIS modelling of present marine basins in Forsmark together with the equation used to derive mean parameter values of microphytobenthos biomass in future marine basins.*

Biomass of phytoplankton in the sea

This parameter (biom_pp_plank) represents the biomass of the pelagic plankton community (phytoplankton) per area of the sea basin. The biomass was calculated according to the pelagic biomass in samples from site investigation in Forsmark (Aquilonius 2010) and the correlation of these data with depth. In Figure 8-4 the mean parameter value versus mean depth in the separate marine basins (from the site-specific GIS model of the area, see Section 6 in Aquilonius (2010)) is plotted together with the depth function of the parameter.

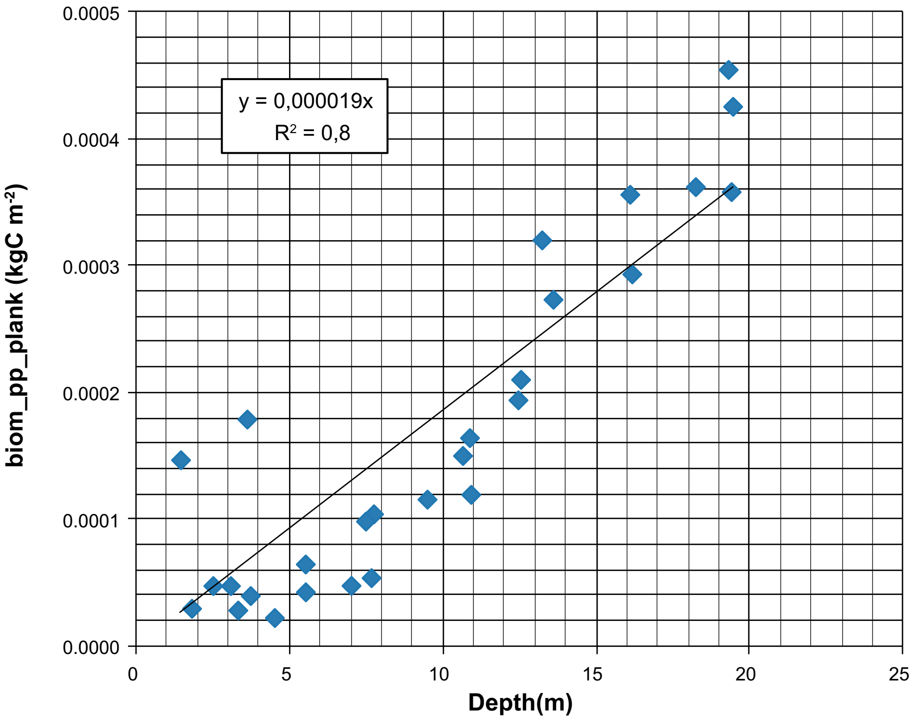

Figure 8-4. *Pelagic biomass (biom_pp_plank) vs. depth in the marine model area in Forsmark based on GIS modelling of present marine basins in Forsmark together with the equation used to derive mean parameter values of phytoplankton biomass in future marine basins.*

8.6.3 Net primary production

This parameter represents the net primary production (NPP) for each aquatic primary producer community, i.e. the benthic macrophyte community (NPP_macro), the benthic microphytic community (NPP_micro) and the pelagic community (NPP_plank).

The times series with the object-specific NPP values are presented in Appendix C.

NPP of macro-algae and macrophytes in lakes

The parameter NPP_macro represents the net productivity of macro-algae and macrophytes. The annual production of macro-algae (8.7×10^{-2} kgC $m^{-2}year^{-1}$) was measured at Forsmark (Karlsson and Andersson 2006) and this production was applied to the entire photic area in all lakes. The productivity in streams is assumed to be identical to the productivity in lakes, although species composition may differ.

The estimated primary production by macro-algae is within the range of values reported in the literature. Also the relation between maximum biomass and production of macro-algae is in accord with the literature, e.g. Wetzel (2001, p 554) suggested that the maximum biomass of *Chara* corresponds to 10–80% of net primary production, whereas Blindow et al. (2006) assumed that a small proportion of biomass production was lost and considered a reasonable value of production of *Chara* to be 1.2 to 1.4 times maximum biomass. Measurements of the production in Lake Bolundsfjärden in Forsmark suggest an annual production of 4 times the maximum biomass of *Chara*. Minimum and maximum production rates from the literature may be higher than appropriate for this lake type, but minimum production was set to 1.4 times maximum biomass (as suggested by Rich et al. (1971) and also cited by Blindow et al. (2006)) whereas maximum production was set to 10 times the maximum biomass (as suggested for maximum production by Wetzel (2001)), i.e. minimum 3.1×10^{-2} kgC $m^{-2}year^{-1}$ and maximum 2.2×10^{-1} kgC $m^{-2}year^{-1}$.

NPP of microphytobenthos in lakes

The parameter NPP_micro represents the net primary productivity of the microphytobenthos. The annual production of the microphytobenthos (5.6×10^{-2} kgC m^{-2} $year^{-1}$) measured at 1.5 m depth (further described in Andersson 2010) in one of the Forsmark lakes was applied to the entire photic area in both present and future lakes. Primary production by microphytobenthos may increase at shallower depths and decrease at larger depths than 1.5 metres, but in a whole ecosystem perspective this is compensated for by decreased and increased production of phytoplankton (NPP_plank). No corrections for depth have been made for either microphytobenthos or phytoplankton, since the responses are assumed to offset each other. The productivity in streams is assumed to be identical to the productivity in lakes.

The annual production of microphytobenthos has been measured in Lake Eckarfjärden in Forsmark for 2 years (mean 5.6×10^{-2}, min 3.4×10^{-2}, max 7.7×10^{-2} kgC m^{-2} $year^{-1}$). Some lakes in the area lack microbial mats and for these, the production is probably much smaller. Minimum biomass was assumed to be one magnitude lower than the mean value, i.e. the same assumption as used for production by microphytobenthos. Since measurements only cover 2 years, the range in production may be higher than captured in the site-specific measurements. The production in the lakes is already estimated to be high but a somewhat larger maximum was chosen than seen in the 2 years measurement, i.e. double the mean production, i.e. 1.12×10^{-1} kgC m^{-2} $year^{-1}$.

NPP of phytoplankton in lakes

The parameter NPP_plank represents the net primary productivity of phytoplankton. The integrated primary production of phytoplankton to 1.5 m depth (2.4×10^{-2} kgC m^{-2} $year^{-1}$) was used as a measure of primary production for all future lakes (further described in Section 3.10 in Andersson (2010)). Although some future lakes will be shallower and others deeper, no correction has been made for depth, but the estimate is assumed to be reasonable for the entire photic zone. Most primary production occurs in the upper part of the pelagic habitat and primary production of phytoplankton has been shown to be directly proportional to light (Wetzel and Likens 1991). The median light extinction equation from site measurements during the period 2003 to 2008 resulting in a photic depth of 4.3 m showed that 80% of total primary production occurs in the upper 1.5 metres (Figure 8-5) (see Andersson 2010). Thus, in lakes that are deeper than 1.5 metres, primary production may be underestimated by at most 20%. Likewise, in 1 metre deep lakes which occur in a few time steps, the primary production is overestimated by up to at most 40%. In addition, as primary production decreases in the pelagic community it may increase in the benthic community (NPP_micro and NPP_macro) due to increased light conditions when water depths decreases. No changes are made for production in the benthic community when water depth decreases and thus it is realistic to assume the same production value as at present. The productivity in streams is assumed to be identical to the productivity in lakes

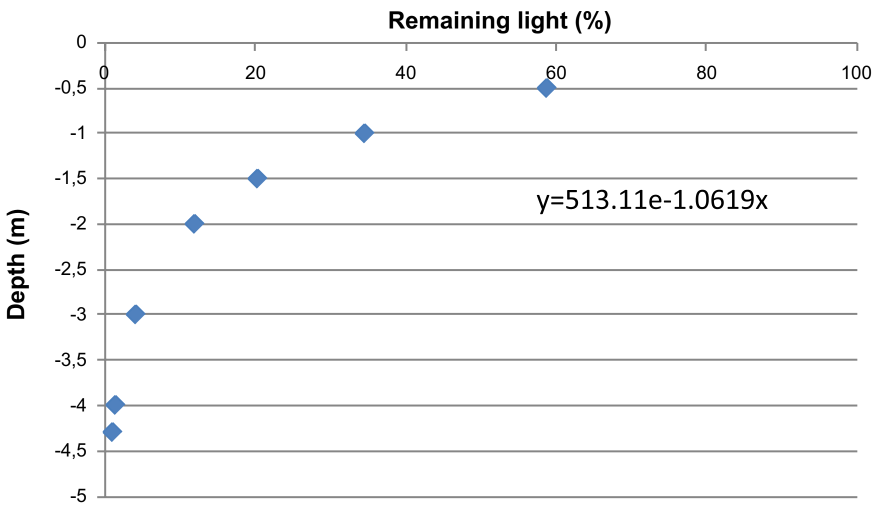

Figure 8-5. *Light extinction curve from May 2005 in Eckarfjärden. This equation results in a photic depth of 4.3 m (photic depth is the depth at which 1% of the incoming light remains).*

Primary production has been measured for 2 years in the Forsmark lakes with small differences between years ($2.3–2.5\times10^{-2}$ kgC m^{-2} $year^{-1}$ (Andersson 2010). In the literature, on the other hand, phytoplankton production spans a wide range, but measured production is well within the range for oligotrophic lakes reviewed in Wetzel (2001) (range 6×10^{-4} to 0.18 kgC m^{-2} $year^{-1}$). However, the range given by Wetzel (2001) includes very deep lakes and permanently ice covered lakes. Thus, the literature range is probably much larger than what can be expected for the Forsmark site. Future lakes in Forsmark may be deeper and have a somewhat altered nutrient status, but are assumed to largely resemble the present-day lakes regarding flora. Thus, the range of phytoplankton production is not assumed to differ greatly from today. If phytoplankton production is altered greatly, this change is probably compensated for by altered benthic production. A realistic change in productivity is thus set to a factor 2, i.e. minimum 1.2×10^{-2} kgC m^{-2} $year^{-1}$ and maximum 4.8×10^{-2} kgC m^{-2} $year^{-1}$.

NPP of macrophytes in sea

The net primary production of macrophytes (NPP_macro) has been modelled in GIS as dependent on irradiance and possible substrates in the model area (see Sections 4 and 6 in Aquilonius 2010). The parameter NPP_macro was calculated for the marine time steps for various basin depths using the depth function for NPP:

$$NPP_{macro}\ (kgC\ m^{-2}) = 0.197\ e^{-0.163x}$$

where x is depth in m.

NPP of microphytobenthos in sea

The net primary production of microphytes (NPP_micro) has been modelled in GIS as dependent on irradiance and possible substrates in the model area (see Sections 4 and 6 in Aquilonius 2010). NPP_micro was calculated using the resulting depth function:

$$NPP_{micro}\ (kgC\ m^{-2}) = 0.0021x + 0.0496$$

where x is depth in m.

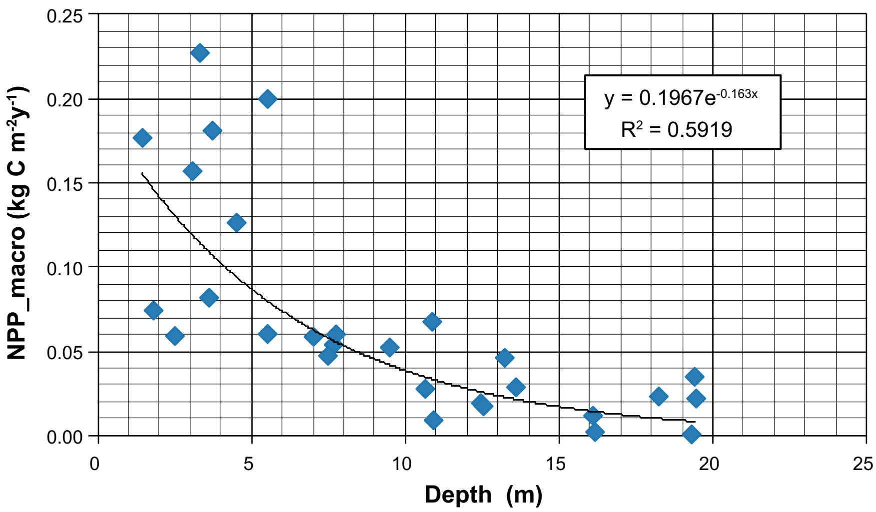

Figure 8-6. *The mean macrophyte NPP value versus mean depth in the separate marine basins based on GIS modelling in the present Forsmark area (see Aquilonius 2010) and the equation used to calculate macrophyte NPP in future marine basins.*

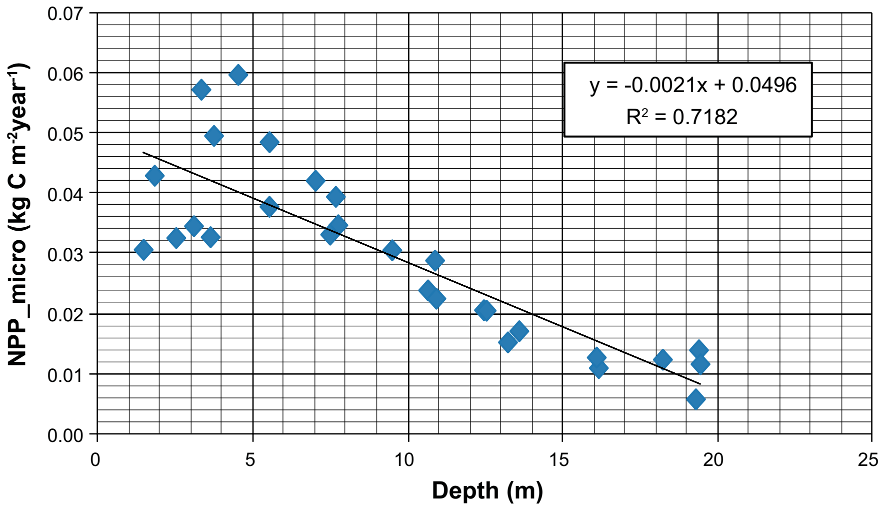

Figure 8-7. *The mean microphytobentos NPP value versus mean depth in the separate marine basins based on GIS modelling in the present Forsmark area (see Aquilonius 2010) and the equation used to calculate microphytobenthos NPP in future marine basins.*

NPP of phytoplankton in sea

Based on the phytoplankton biomass interpolated over the marine model area in a GIS model, the annual average phytoplankton production (NPP_plank) was obtained by multiplying the areal biomass by an overall production-biomass (P/B) ratio set to 101 year^{-1} in Forsmark (Aquilonius 2010, Chapter 4 and 6, Harvey et al. 2003, Sandberg et al. 2000, Elmgren 1984, Wulff and Ulanowicz 1989). The mean values of NPP per basin were correlated to the mean depth of the basins (r=0.8).

Based on the GIS model of biomasses and assumptions of P/B relationship, the parameter, NPP_plank, was calculated for the various basin depths using the depth functions for NPP:

$$NPP_{plank}\ (kgC\ m^{-2}) = 0.0019x$$

where x is depth in m.

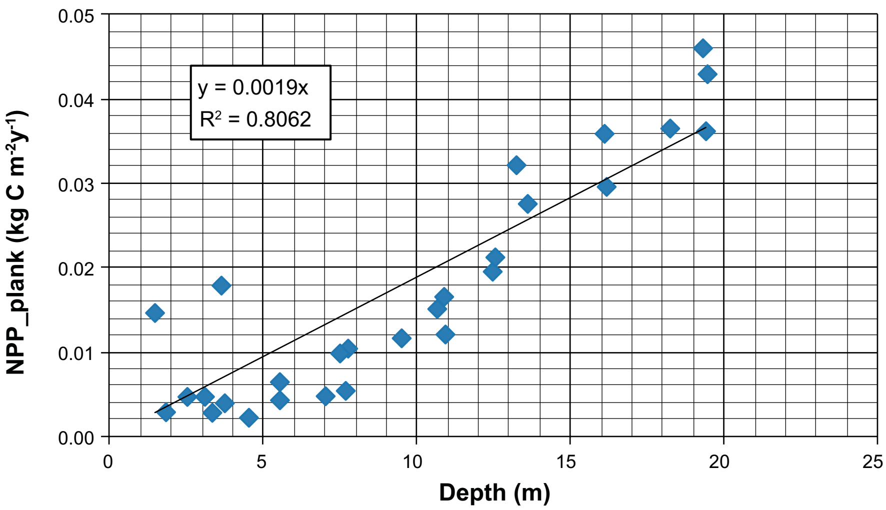

Figure 8-8. *The mean phytoplankton NPP value versus mean depth in the separate marine basins based on GIS modelling in the present Forsmark area (see Aquilonius 2010) and the equation used to calculate phytoplankton NPP in future marine basins.*

8.7 Decomposition and mineralisation

Elements incorporated into primary producers can be released upon decomposition and only a fraction will settle on sediments in aquatic ecosystems. In the sediments further decomposition (i.e. mineralisation) occurs, decreasing the amount of organic matter that is permanently stored in the sediments. To calculate the amount of carbon that accumulate in sediments, the fraction of primary production that contributes to sedimentation (refractory organic carbon) and the mineralisation rate in the sediments are calculated.

8.7.1 Thickness of oxidising upper regolith layer

z_regoUp_lake

Lake_z_regoUp represents the depth of the upper oxygenated regolith layer in lakes and streams. Most of the lake sediments in the Forsmark area are covered by a loose layer of algae and cyanobacteria (microbial mat) that can be very thick. This layer is easily mixed and the thickness of the oxygenated zone is estimated to equal that of the microbial mat. In lakes lacking a microbial mat, the thickness of the oxygenated zone is estimated to be 1 cm. There is no correlation between lake bathymetry and the occurrence or absence of microbial mats (Andersson 2010, Table 3.17). Lake_z_regoUp was calculated as the mean thickness of the oxygenated zone investigated lakes of today: mean 0.053 m, (min 0.01 m, max 0.30 m, n=9 lakes, 149 subsamples). In streams, the redox zone may be thinner than in the lakes (0.053 m) as no thick microbial mat is found in the streams. On the other hand, stream currents stir up the sediments, and benthic fauna in streams may create a deeper oxygenated zone than in lakes lacking a microbial mat. As no measurements of Lake_z_regoUp are available for the streams today, the value for the lakes is also used for the streams.

z_regoUp_sea

The mean depth of the parameter was set to 0.1 m according to Håkansson et al. (2004) (minimum 0 and maximum 0.2 m) based on an average of data from the Baltic Sea.

8.7.2 Refractory organic carbon

Refractory organic carbon is the part of the primary production NPP that is not decomposed or exported, but contributes to the sediment accumulation of organic carbon, i.e. the refractory organic matter left after initial mineralisation.

On the time scale of a year, the primary producer biomass is assumed to be in equilibrium, which means that the net primary production (NPP) is balanced by an equal loss of biomass through grazing and litter production. Most of the biomass lost is easily metabolized by grazers and decomposers (see minRate below), but a part of the lost biomass is made up of refractory carbon (f_refrac) which decomposes much more slowly and thus will contribute to the build-up of organic matter in the surface sediments.

The flow of radionuclides associated with the flow of dead organic matter from primary producers to the upper sediments is assumed to be directly related to the fraction of the primary producer biomass that is not easily decomposed (f_refrac_i). To get the total flux of radionuclides associated with litter production a sum is taken across all primary producer communities (i = {plank, micro, macro}). The parameters for refractionary carbon for the different communities are described below and summarised in Table 8-3.

Fraction of macrophyte production that contribute to sediment accumulation in lakes

The parameter f_refrac_macro_lake is the fraction of primary production of macrophytes in lakes that is not degraded but instead contributes to sediment accumulation of organic carbon. For macrophytes, especially macro-algae, a larger part of the production may remain in the sediments without decomposition than for phytoplankton. In the sediments of Forsmark lakes, parts of *Chara* are sometimes found at great depths. Many experiments focusing on decomposition rates go on for a couple of weeks whereas here the interest is in one year decomposition rates to derive an annual mean. Literature suggests that 20–100% of the initial dry weight of submerged macrophytes is decomposed (Wetzel 2001, p 653, Belova 1993, Chimney and Pietro 2006). Values in the higher range are for easily degradable macrophytes and values in the lower range are usually for relatively short time periods. *Chara* is sometimes mentioned as more slowly degraded than other macrophytes. Different studies suggest that between 20 and 40% of nutrients assimilated by Chara during growing season remains in the plant tissues (Kufel and Kufel 2002, Rodrigo et al. 2007). Based on these studies, minimum and maximum amount remaining after initial decomposition were set to 0.2 and 0.4 respectively and the parameter value was set to 0.3.

Fraction of phytoplankton production that contribute to sediment accumulation in lakes

The parameter f_refrac_plank_lake is the fraction of primary production of phytoplankton in lakes that is not degraded but instead contributes to sediment accumulation of organic carbon. Phytoplankton are small and easily degradable and large amounts of phytoplankton production are decomposed by bacteria in lakes. For example, Wetzel (2001, pp 516–517) states that between 75 and 99% of phytoplankton production in lakes is decomposed by the time it reaches the sediment surface. The phytoplankton community in the Forsmark lakes is largely made up of *chrysophytes* and *cryptophytes* which should be relatively easily degradable. However, although f_refrac_plank_lake could be set to correspond to the highest decomposition rate, the parameter value is instead set to 0.1 (90% are assumed to be decomposed and 10% remain undegraded) in order not to underestimate the transport of carbon to the sediment. The minimum and maximum values are set to 0.01 and 0.25, respectively (i.e. corresponding 99 and 75% decomposition).

Fraction of microphytobenthos production that contribute to sediment accumulation in lakes and sea

The parameters f_refrac_micro_lake and f_refrac_mico_sea are the fractions of primary production of microphytobenthos that are not degraded on an annual basis, but instead contribute to sediment accumulation of organic carbon. For microphytobenthos, fewer studies on decomposition are available than for phytoplankton. Since both phytoplankton and microphytobenthos are microbiota and can be assumed to resemble each other, the same parameter values as for phytoplankton have been applied, i.e. 0.1 (min 0.01, max 0.25).

Fraction of macrophytes that contribute to sediment accumulation in seas

The parameter f_refrac_macro_sea is the fraction of primary production of macrophytes in marine basins that is not degraded but instead contributes to sediment accumulation of organic carbon. A large fraction of the photosynthetic carbon in marine ecosystems is decomposed within the system. The high content of structural carbon in perennial macrophytes makes them less useful for herbivory, consumption and microbial decomposition than phytoplankton.

Accumulation rates of organic carbon in different basins of the open Baltic Sea (not coasts) range from c 0.0035 to 0.050 kgC m^{-2} $year^{-1}$ during the past c 60 years (Emeis et al. 2000, Algesten et al. 2006, Jonsson et al. 2000, Leipe et al. 2011). In coastal basins on the other hand, accumulation is often higher than in offshore areas and e.g. in the Bothnian Bay is on average 0.024 kgC m^{-2} $year^{-1}$ (range: 0.020–0.028 kgC m^{-2} $year^{-1}$) (Algesten et al. 2006). The average long-term accumulation rate of organic carbon in coastal sites in Forsmark is 0.014 kgC m^{-2} $year^{-1}$ according to Sternbeck et al. (2006).

More studies are available on the amount of NPP that contributes to sediment accumulation for phytoplankton than for macrophytes (see f_refrac_plank). However, if the sediment accumulation is known and by assuming that 10% of annual NPP from phytoplankton and microphytobenthos remain undegraded (see f_frefrac_plank and f_refrac_micro) and contributes to the accumulation, the contribution from macrophytes to accumulation can be calculated.

If the estimate from Sternbeck et al. (2006) of 0.014 kgC m^{-2} $year^{-1}$ is used together with mean production for future marine basins, an estimate for marine basins in Forsmark of c. 13% of NPP by macrophytes remains undegraded and contribute to accumulation This is somewhat low compared with literature and e.g. Duarte and Cebrián (1996) report that macrophytes on average contribute 24–43% of their NPP to the sediments, and Hesikanen and Leppänen (1995) reported that for the Baltic sea 39% of carbon from net primary production during the vegetation period is transferred to the sediments.

If the value of sediment accumulation estimated as 0.24 kgC m^{-2} $year^{-1}$ from the Bothnian Bay (Algesten et al. 2006) is used instead of the value from Forsmark (Sternbeck et al. 2006), 28% of NPP by macrophytes remains undegraded. However, it is likely that more is degraded in the warmer Forsmark coastal areas than in the Bothnian Bay and carbon accumulation in coastal areas most probably also includes allochtonous material from terrestrial areas. Thus, by using the value of 28% of macrophytes remaining undegraded might result in an overestimation of the auotochtonous carbon fraction transferred to the sediment. Nevertheless, since it is a cautious assumption to have more carbon remaining (more carbon and elements are bound into sediments than transported out of the model area) data from Algesten et al. (2006) were applied and the parameter value was set to 0.3, the minimum was set to 0.1 (based on Sternbeck et al. 2006) and the maximum to 0.4 (based on Duarte and Cebrián 1996).

Fraction of phytoplankton production that contribute to sediment accumulation in seas

The parameter f_refrac_plank_sea, is the fraction of primary production of phytoplankton in marine basins that is not degraded on an annual basis, but instead contributes to sediment accumulation of organic carbon. These primary producers are more easily degradable and are probably more rapidly consumed/mineralized than macrophytes. Duarte and Cebrián (1996) stated that less than 1% of oceanic phytoplankton is transferred to the sediments due to the high fraction rapidly used for herbivory and decomposition, whereas James (2005) stated that up to 10% of the phytoplankton production is transferred to the sediment in the sea. The value from James (2005) of 0.1 is chosen in order to not underestimate the transport of carbon to the sediment. The minimum value was set to 0.01 as in Duarte and Cebrián whereas the maximum value was set to 0.025 (identical to the lake value).

Table 8-3. Mean, minimum and maximum of f_refrac in Forsmark, used in the radionuclide modelling.

	Mean	Minimum	Max	Distribution
f_refrac_macro_lake (kgC kgC^{-1})	0.30	0.20	0.40	Uniform
f_refrac_micro_lake (kgC kgC^{-1})	0.10	0.01	0.25	Uniform
f_refrac_plank_lake (kgC kgC^{-1})	0.10	0.01	0.25	Uniform
f_refrac_macro_sea (kgC kgC^{-1})	0.30	0.10	0.40	Uniform
f_refrac_micro_sea (kgC kgC^{-1})	0.10	0.01	0.25	Uniform
f_refrac_plank_sea (kgC kgC^{-1})	0.10	0.01	0.25	Uniform

8.7.3 Mineralisation rate

When organic matter is metabolised by decomposers as an energy source, organic carbon is transformed to inorganic carbon (CO_2 under aerobic conditions, and CO_2/CH_4 under anaerobic conditions). This process is referred to as mineralisation and is dependent on the bacterial biomass, temperature, concentration of organic carbon, and quality of the organic carbon as food source for the bacteria (e.g. Tranvik 1988, Schallenberg and Kalff 1993, Gudasz 2010, Gudasz et al. 2010). The flow of carbon-14 from an organic carbon pool (OC/POC) to the corresponding inorganic carbon pool, is, in the radionuclide transport modelling, expressed using the mineralisation rate, minRate (kgC kgC^{-1} $year^{-1}$). The parameter values for mineralisation rates in aquatic systems are described below and summarised in Table 8-4.

Mineralisation rate of organic carbon in the upper oxygenated sediment layer in lakes

This parameter minRate_regoUp describes the mineralisation rate of organic carbon in the upper oxygenated sediment layer (regoUP) in lakes. Carbon burial in sediments, i.e. the amount of organic carbon in the sediments that is permanently buried and not mineralised, shows a large variations worldwide (Burdige 2007, Algesten et al. 2003, Sobek et al. 2009). Sobek et al. (2009) showed that the mean burial efficiency in 27 lakes worldwide was 48%, indicating that about half of the organic carbon in sediments is mineralised. However, both Sobek et al. (2009) and Gudasz et al. (2010) showed that there is an increased sediment bacterial metabolism with increasing autochthonous carbon sources (i.e. organic carbon produced within the aquatic system). The Forsmark lakes have a large autochtonous production compared with the input of terrestrial organic carbon (Andersson 2010). A large fraction of the organic carbon produced in lakes is quickly mineralised and it is sometimes difficult to differentiate between f_refrac and mineralisation rate, i.e. the amount of carbon burial is affected by both f_refrac and mineralisation rate. Mineralisation rate can be estimated by comparing primary production, estimated fraction that remains after initial mineralisation (f_refrac) and carbon content of the upper regolith. This was done in SR-PSU with a C-12 model (see SKB 2014a) where f_refrac was set to 0.3 (see reasoning above) and the carbon content of upper regolith in the present-day lakes was used as a reference to see what mineralisation rate was needed to achieve the present carbon content. The resulting mineralisation rate of 0.03 was used as a parameter value for future lakes. Minimum and maximum rates were set to 0.02 and 0.04, respectively.

Mineralisation rate of organic carbon in the upper oxygenated sediment layer in seas

This parameter minRate_regoUp_sea describes the mineralisation rate of organic carbon in the upper oxygenated sediment layer (regoUP) in marine basins. For lakes the organic carbon burial efficiency varies over a large range, from less than 1% to nearly 100% (Burdige 2007). Organic carbon burial efficiency in marine sediments is in general somewhat lower than in lakes (mean 29%, Burdige 2007). As for lakes, the organic carbon burial efficiency is assumed to be higher for sediments with high terrestrial organic carbon inputs. Marine basins often have low inputs of terrestrial carbon, which can explain a lower carbon burial than in lakes. However, the lakes in Forsmark are to a large degree dependent on autochthonous production and the marine basins and lakes in Forsmark can be assumed to be similar in terms of mineralisation rates. As stated for lakes above, a large fraction of the produced organic carbon is mineralised before the organic matter reaches the sediment and it is sometimes difficult to differentiate between f_refrac and mineralisation rate, i.e. the amount of carbon burial is affected by both f_refrac and mineralisation rate. The same parameter value as for lakes has been applied for the marine basins, i.e. mean 0.03, min 0.02, max 0.04.

Mineralisation rate of organic carbon in anoxic post glacial sediments in lakes and seas

The parameters minRate_regoPG_lake and minRate_regoPG_sea describe the mineralisation rates of organic carbon in anoxic post glacial sediments in lakes and marine basins, respectively. Mineralisation in deeper layers is less studied than mineralisation in upper sediment layers, but it is known that mineralisation is much lower in anoxic than in oxic conditions (e.g. Burdige 2007). Decomposition in deep catotelm has been studied and for parameterisation of decomposition in the post-glacial clay layer below peat it is assumed to be similar to the decomposition in catotelm (Clymo and Bryant 2008). It is also assumed that the mineralisation rate in post-glacial deposits should be similar regardless of whether the area is situated below peat or lakes and the representative value used in the terrestrial part (based on Clymo and Bryant 2008), representing catotelm peat dominated by Sphagnum, was used also for the lake and marine stage of the biosphere objects. Thus, the mean value was set to 6.5×10^{-5} kgC kgC^{-1} year^{-1}. The range was assumed to be small and minimum and maximum values was achieved by assuming a 20% range around the mean (i.e. min 5.2×10^{-5}, max 7.8×10^{-5} kgC kgC^{-1} year^{-1}).

Mineralisation rate of organic carbon in particulate matter in lakes and seas

The parameters, minRate_water_PM_lake and minRate_water_PM_sea describe the mineralisation rates of organic carbon in particulate matter in the water column in lakes and marine basins, respectively. The particulate matter in water is assumed to be of similar composition to the organic carbon in the surface sediments and the same parameter value as for minRate_regoUP_lake and minRate_regoUp_sea was applied (mean 0.03 kgC kgC^{-1} year^{-1}, minimum 0.02, maximum 0.04).

Table 8-4. Parameter value and minimum and maximum values of minRate in Forsmark, used in the radionuclide transport model.

	Mean	Min	Max	Distrubution
minRate_PM_lake/sea (kgC kgC^{-1} year^{-1})	0.03	0.02	0.04	Uniform
minRate_regoUp_lake/sea (kgC kgC^{-1} year^{-1})	0.03	0.02	0.04	Uniform
minRate_regoPG_lake/sea (kgC kgC^{-1} year^{-1})	6.5 E–5	5.2E–5	7.8E–5	Uniform

8.8 Gas exchange across the air-water interface

There is a gas exchange of carbon dioxide, CO_2 across the air-water interface. The exchange is a physical process driven by the differences in partial pressure of CO_2, between water and air. In the radionuclide model, the CO_2 flux involving the isotopes carbon-14 and carbon-12, are of interest, in order to estimate the influx of uncontaminated carbon-12 from atmosphere to the water and the release of carbon-14 to the atmosphere.

The flux of radionuclides between the atmosphere and water is dependent on height of the atmospheric layers where the exchange occur, roughness length of water surfaces, solubility of the gas in water and biotic processes (see e.g. Cole and Caraco 1998). During periods with high primary production (and thereby uptake of CO_2) there is an inflow of CO_2 from the atmosphere to the water, whereas during periods with high decomposition there is an outflow of CO_2 from water to the atmosphere. Due to large fluxes of CO_2 between water and air this can be an important flux for the isotope carbon-14, but also other volatile radionuclides may be exchanged across the air-water interface. The gas flux across the air-water interface can be described by chemical equilibrium and a gas exchange coefficient, often called the piston velocity (piston_vel). Parameters describing the fraction of CO_2 that is dissolved in the water (f_H2CO3), the solubility of CO_2 in the water (solubilityCoef_lake/sea), dissociation constants K1 and K2, Schmidt number, pH, height of atmospheric layers (height_L1_aqu and height_L2_aqu) and roughness length of water (z0_Aqu) are other parameters needed for calculating the transfer of carbon-14 between atmosphere and water.

The net flux of gas between the water and the overlying air layer, i.e. the Degassing and GasUptake parameters, can be described mathematically (Cole and Caraco 1998). In the radionuclide model (Saetre et al. 2013a), the flux of CO_2 is calculated by using a mathematical expression of gas flux from Cole and Caraco (1998).

$$J = \Psi\,(Conc_{surface} - Conc_{eqwater}) = Degassing - GasUptake$$

Where:

Ψ is the piston velocity (gas transfer velocity), which is the height of the water that is equilibrated with the atmosphere per unit time for a given gas at a given temperature (m year^{-1}) (see Section 8.10).

$Conc_{surface}$ is the concentration of gas in the surface water (mol m^{-3}). In the radionuclide model this concentration of gas in the surface water is calculated as the fraction of DIC in the form of CO_2/H_2CO_3 (described below) of the total DIC pool in water (conc_DIC described above).

$Conc_{eqwater}$ is the concentration of gas in water if in equilibrium with the atmosphere (mol m^{-3}). In the radionuclide model, the solubility coefficient for CO_2 (in lake and marine water) is used to calculate the solubility of CO_2 in water at equilibrium with the atmosphere.

8.8.1 Piston velocity

Piston velocity is the height of the water that is equilibrated with the atmosphere per unit time. Several processes influence the piston velocity, such as surface films, bubble entrainment, rain and boundary layer stability, kinetic viscosity of the water and wind speed. The dominant effect is caused by wind speed which is the reason why parameterisation of piston velocity is often related to wind speed (e.g. Wanninkhof et al. 2009, Wesslander 2011).

There are several expressions for piston velocity where wind speed has been treated in different ways and attributed different degrees of significance e.g. (Cole and Caraco 1998, Wanninkhof 1992, Wanninkhof and McGillis 1999, Algesten et al. 2006). Calculating the piston velocity according to Wanninkhof (1992) gives about half the value in comparison with calculating it according to Cole and Caraco (1998), and about a six times larger value than calculations according to Wanninkhof and McGillis (1999). An inter-comparison between different expressions for piston velocity showed that differences between expressions are largest at wind speeds above 10 m s^{-1} (Kuss et al. 2004). In Figure 8-9, piston velocity using various expressions and the monthly average wind speed at Örskär in Forsmark are presented.

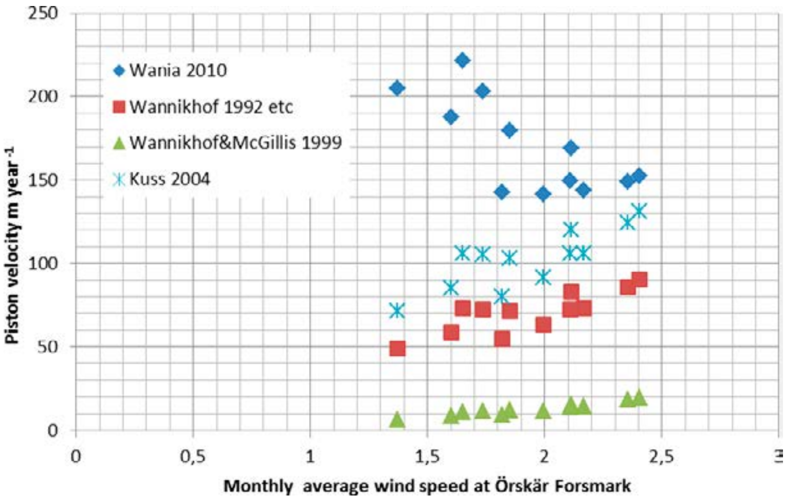

***Figure 8-9.** Monthly average wind speed at Örskär in Forsmark and piston velocity calculated according to various expressions (Wania et al. 2010, Wannikhof 1992, Wannikhof and McGillis 1999, Kuss et al. 2004).*

Piston velocity for lakes

The parameter Piston_vel_lake is the piston velocity for lakes. As stated above, there are a number of expressions for piston velocity. The study by Cole and Caraco (1998) is developed especially for low-wind oligothropic lakes, whereas Wannikhof´s expressions are developed for marine environments and often used in the Baltic Sea. Cole and Caraco (1998) define low-wind environment as wind speed below 5 or 6 m s^{-1}. The wind speed measurements in Forsmark (see below), measured at 10 m height at Örskär should according to Cole and Caraco (1998) be considered as a low-wind environment and their expression have been used for the calculation of piston velocity in the Forsmark lakes:

$$\psi 600 = 2.07 \; + 0.21 u^{1.7} \sqrt{660/Sc}$$

Where ψ600, the piston velocity, describes the gas transfer dependence on u (wind velocity at 10 m height, in m s^{-1}), and the kinetic viscosity of the water as described by a constant and the Schmidt number (Sc). The Schmidt number is dimensionless and depends on temperature and salinity. In the calculations of piston velocity in aquatic ecosystems in Forsmark, the Schmidt number has been calculated based on monthly mean temperatures in the surface water (see Section 8.8.4 for description of Schmidt numbers).

Piston velocity in the aquatic ecosystems was calculated for the period April to November, i.e. the ice-free season in lakes (Andersson 2010). This may mean that the outburst of CO_2 at ice break is not included in the calculation of CO_2 in the atmosphere. However, as ice break occurs early in the season, production is relatively low, and thus any CO_2 released to the atmosphere would be effectively diluted at the time when it was taken up by primary producers in the terrestrial area.

Piston velocity was calculated on a monthly basis for the vegetation period based on Schmidt number (depending on site specific temperature), and wind speed. From these monthly piston velocities a mean piston velocity was calculated and assumed to be a representative parameter value for the entire vegetation period (mean = 201 m $year^{-1}$, stdev = 26).

Piston velocity for sea

The parameter Piston_vel_sea is the piston velocity for marine basins. As stated above, there are a number of expressions for calculation of piston velocities. For sea the expression according to Wanninkhof (1992) is the most frequently used and using that would make comparison with other studies easier. However, the marine basins in Forsmark are situated near-shore and thus the expression by Cole and Caraco (1998) might be more accurate. In addition, the expression by Cole and Caraco (1998) is used both for the lakes and the terrestrial ecosystem in SR-PSU, i.e. making comparison between ecosystems in Forsmark easier.

Accordingly, in the radionuclide modelling of the marine ecosystem in Forsmark, the piston velocity (m $year^{-1}$) was calculated according to Cole and Caraco (1998) (see description above for piston velocity lake). As for lakes, piston velocity was calculated for the period April to November, i.e. the vegetation period and ice-free season in lakes (Andersson 2010).

Piston velocity was calculated on a monthly basis for the vegetation period based on Schmidt number (based on temperature) and wind speed. From these monthly piston velocities, a mean piston velocity was calculated and assumed to be a representative parameter value for the entire vegetation period (mean = 187 m $year^{-1}$, stddev = 26).

8.8.2 Fraction of total DIC present as CO_2

The fraction of the total DIC pool that is contributed by CO_2 in water can be described by considering equilibrium of the carbonate system. The fraction of total DIC that occur as CO_2 affects the flux of CO_2 across the water-air interface at high pH and low wind velocities (Wanninkhof and Knox 1996).

The concentration of CO_2 in the water, based on the fraction of inorganic carbon in the form of CO_2/H_2CO_3, is described by the parameter f_H2CO3. This parameter is sometimes also denoted a0 or "chemical enhancement factor for CO_2". The other constituents of the carbonate system are HCO_3^- and CO_3^{2-}. The equilibrium fraction of total DIC present as CO_2 can for a closed system be described by two temperature-dependent dissociation constants (K1 and K2) and pH according to the following expression:

$$\text{f\_H2CO3} = \frac{1}{(1 + (\text{K1}/[H^+]) + (\text{K1 x K2}/[H^+]^2)}$$

where:

K1 and K2 represents the dissociation constants and (H+) is the hydrogen concentration. Temperature has generally only a minor effect on the dissociation constants whereas pH determines most of the variation of f_H2CO3. At low pH H_2CO_3 dominates. When pH increases the dominance will switch to HCO_3^- and when pH is above 10.5 CO_3^{2-} dominates. As pH increases above 6 the reaction rate of CO_2 dissolved in the water to form HCO_3^- increases and this reaction rate of CO_2 becomes faster than the diffusion process through the water film, and the pH will thereby restrict the potential degassing (Stumm and Morgan 1996, Wetzel 2001).

Fraction of dissolved CO_2 of total DIC in lakes

The parameter f_H2CO3_lake is the fraction of dissolved CO_2 of total DIC in lakes and is calculated according to the expression above. The dissociation constants for freshwater (T=25°C) systems K1 = 4.47×10^{-7} and K2 = 4.68×10^{-11} (Weiss 1974) were used.

As described above, f_H2CO3 is pH dependent and changes over the year (Figure 8-10). However, although the fraction may be high during winter there is a low flow of CO_2 at that period due to ice coverage and thus f_H2CO3 is calculated for the ice-free season. Monthly mean pH values for April to November from three lakes in Forsmark were used (SR-PSU Chemistry database[5]) to calculate monthly f_H2CO3. A mean value for the ice-free season was calculated from the monthly means and used as the parameter value (0.035, stdev = 0.065).

Fraction of dissolved CO_2 of total DIC in seas

The parameter f_H2CO3_ sea is the fraction of CO_2 of total DIC in marine basins and was calculated according to the expression above. The dissociation constants K1 and K2 according to Prieto and Millero (2002) (T=25) K1 = 1.15×10^{-6} and K2 = 7.41×10^{-10} were used.

As described above, f_H2CO3 is pH-dependent and varies over the year (Figure 8-11). Although the amount of CO_2 is high during winter the exchange of CO_2 across the air water interface is often limited at this part of the year due to ice coverage and the mean pH value for the vegetation period (April to November) was used in the calculation of the parameter value (pH described in Section 8.8.4 below). Monthly mean values of f_H2CO3_sea were calculated and a mean of these monthly values for the ice free season was used as the parameter value (0.009, stdev = 0.003).

[5] SR-PSU chemistry database are stored at svn/Indata/Chemsitry. Data may be made available upon request.

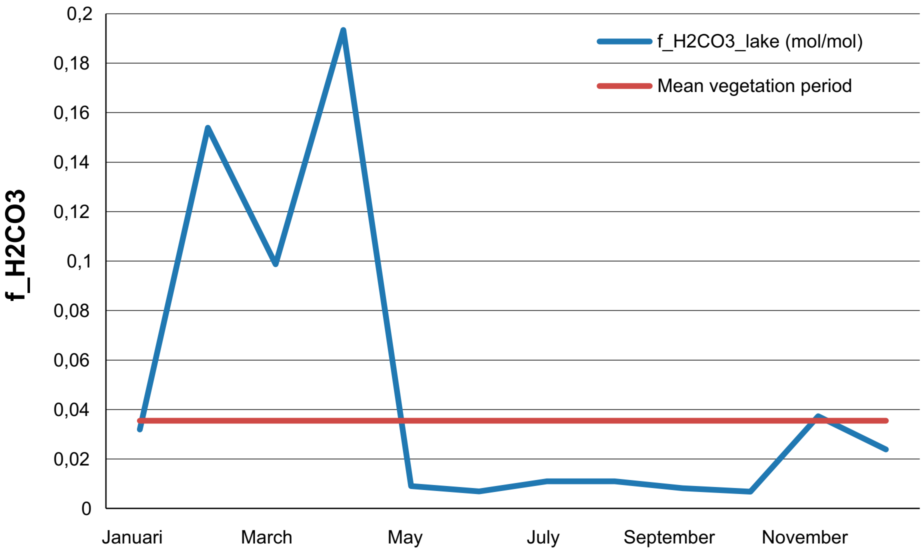

Figure 8-10. *Monthly mean values compared to mean value of f_H2CO3 in lakes compared to the mean value of mean f_H2CO3 for the vegetation period in Forsmark.*

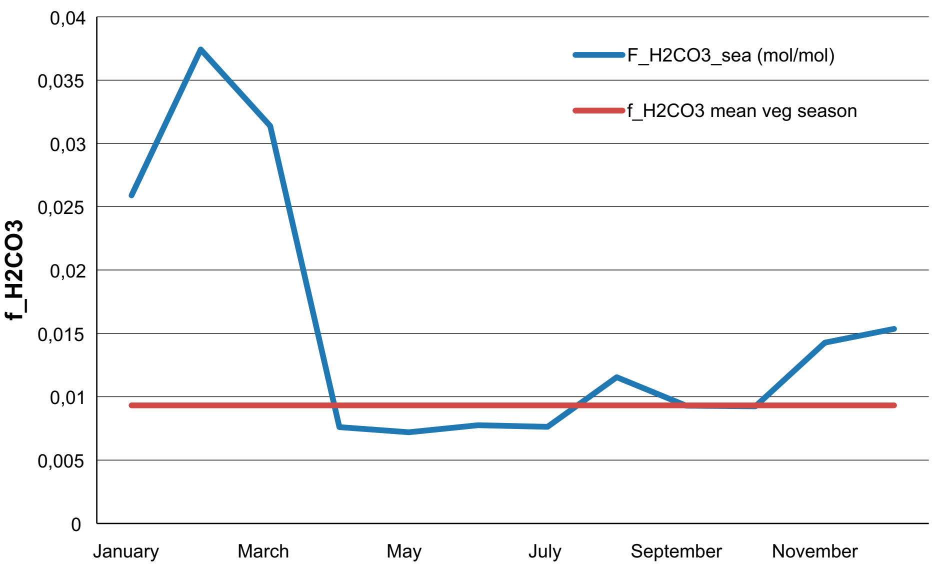

Figure 8-11. *Seasonal variation and mean for the vegetation period of the parameter f_H2CO3 in the marine ecosystem in Forsmark.*

8.8.3 Solubility of CO_2 at equilibrium

The solubility of CO_2 in water at equilibrium with atmosphere can be expressed as a function of the atmospheric concentration of the gas and a solubility constant, KH_{cc} (mole l^{-1} atm^{-1}), by an expression from Weiss (1974):

$$KH_{CC} = exp^{(A1+A2\left(\frac{100}{T}\right)} + \mathrm{A3ln}^{\left(\frac{T}{100}\right)} + \mathrm{S‰[B1} + B2^{\left(\frac{T}{100}\right)} + B3^{\left(\left(\frac{T}{100}\right)\hat{}2\right)}$$

$$KH_{CC} = \mathrm{EXP(A1 + A2(100/t) + A3ln(t/100) + S‰[B1 + B2(t/100) + B3(t/100)2)}$$

Where the As and Bs are constants, T (K) is the absolute temperature, and S‰ is salinity (used for sea water).

KH_{cc} is used in the radionuclide model to calculate Conc_eqwater, i.e. the concentration of gas in water in equilibrium with the atmosphere (mol m^{-3}). In the radionuclide transport model, the solubility coefficient is dimensionless and KH_{cc} is therefore converted by using a conversion factor for Henry´s law, and thereafter denoted the SolubilityCoef_lake and SolubilityCoef_sea, representing the solubility of CO_2 in water.

A higher solubility is found at low temperatures, i.e. the parameters SolubilityCoef_lake and SolubilityCoef_sea are higher during winter. However, the solubility will be restricted by an ice sheet (at least in lakes) during the winter such that there is no exchange between the air and water. The mean values for SolubilityCoef_lake and SolubilityCoef_sea are therefore based on the monthly mean temperature during ice-free season April–November (Andersson 2010).

SolubilityCoef_lake

SolubilityCoef_lake describes the solubility of CO_2 in water at equilibrium for lakes. The mean water temperature was based on site data for lakes in Forsmark (described below). Monthly solubility coefficients were calculated with the equation above for the ice free season April–November. A mean value of these monthly means was used as parameter value (mean = 1.1, stdev = 0.2, minimum = 0 and maximum = 1.5). The minimum was set to zero can be seen to represent the annual minimum during winter.

SolubilityCoef_sea

SolubilityCoef_sea describes the solubility of CO_2 in water at equilibrium for the marine basins. The mean water temperature and salinity was based on site data for the marine ecosystem in Forsmark (described below). Monthly solubility coefficients were calculated with the equation above for the ice free season April–November. A mean value of these monthly means was used as parameter value (mean = 1.4, stdev = 0.3, minimum = 1.1, maximum = 1.8).

8.8.4 Wind speed, pH, salinity, temperature, and Schmidt number

There are a number of site-specific parameters used in the calculation of piston velocity, concentration of CO_2 and the concentration of gas in water at equilibrium. These are; wind speed, temperature, pH, salinity and Schmidt number. Thus, although they are not directly used in the radionuclide transport model they are used in the calculation of parameters. Therefore, the assumptions and calculations of these parameters are described below and summarised in Table 8-5.

Wind speed

Wind speed was used in the calculations of piston_vel, and has been measured in Forsmark at 10 m height at Örskär (Table 8-5).

pH and salinity

Monthly mean pH and salinity values for the period April–November were used in the calculations of f_H2CO3 in aquatic ecosystems.

For lakes, pH was calculated from surface-water measurements in 13 lakes included in the water chemistry data base[6]. Monthly mean pH values were calculated and used in the parameter calculation and ranged from 7.0–8.5 for the period April–November (mean = 7.9).

For the sea ecosystem, pH was calculated based on data from the site investigations from 2002 to 2006 and monthly mean pH values for the ice-free season were used in the parameter calculation. For this period, pH ranged from 7.8–8.0 (mean = 7.9).

The monthly mean salinity measured during site investigations was used for the calculations of SolubilityCoef_sea (Table 8-5).

[6] SR-PSU chemistry database, stored at svn/indata/Chemistry. Data may be made available upon request.

Table 8-5. Monthly mean temperature, salinity, pH and wind speed for marine and lake sites in Forsmark during 2002–2006. Marine sampling sites PFM000062, PFM000063, PFM000064, PFM000065, PFM000082, PFM000083, PFM000084, PFM000153, and PFM102269 were used.

Month	Wind speed at Örskär on 10 m height (m s^{-1})	pH Sea	pH Lake	Salinity (psu)
Jan	2.36	7.5	7.8	4.33
Feb	2.17	7.4	7.1	4.10
Mar	2.00	7.5	7.3	3.53
Apr	2.11	7.8	7.0	4.75
Maj	1.85	8.0	8.0	4.88
Jun	1.74	7.9	8.0	4.81
Jul	1.37	8.0	8.3	4.82
Aug	1.65	8.0	8.3	4.85
Sep	1.60	7.8	7.9	4.66
Nov	1.82	7.8	8.5	4.18
Dec	2.11	7.8	7.8	4.31

Schmidt number and temperature

Water temperature is used for the calculation of SolubilityCoef and the Schmidt number. The Schmidt number is used in the calculations of Piston velocity and describes the kinetic viscosity of water divided by the diffusion coefficient of the gas. It is dimensionless and depends on temperature. The Schmidt number in the aquatics ecosystems in Forsmark is calculated according to the polynomial fit for CO_2 in fresh and sea water presented by Wanninkhof (1992), were the Schmidt number (Sc) is defined as:

$$Sc = A - BT + CT^2 - DT^3$$

Where A, B, C and D are constants for CO_2 in fresh respectively sea water in a temperature range between 0 and 30 degrees Celsius, and T is the water temperature in degree Celsius.

The Schmidt number is temperature dependent and the monthly Schmidt numbers was calculated based on monthly average water temperature during vegetation period April–November (Table 8-6). Monthly mean Schmidt numbers for lake and sea were then used in the calculations of Piston velocity.

Table 8-6. Calculated (according to Wanninkhof 1992) Schmidt number for lake and sea, based on monthly average temperature.

Month	Mean monthly temperature sea water (°C)	Mean monthly temperature lake water (°C)	Schmidt number in seawater at	Schmidt number in lake water at
January	0.24		2043	
February	0.47		2015	
Mars	1.09		1940	
April	6.19	6.8	1424	1258
May	10.04	13.4	1134	851
June	15.39	18.5	841	645
July	18.51	22.0	717	545
August	19.49	21.2	683	564
September	13.45	14.2	934	813
October	2.72	8.0	1758	1169
November	2.12		1823	1575
December			1988	

8.9 Aquatic atmosphere parameters

The atmosphere of the aquatic system is divided into two layers (Layers 1 and 2) as defined in Saetre et al. (2013a). The parameters defining the height of these layers are presented here together with parameters describing the roughness length of the water surface and the wind speed.

Height of Layer 1

This parameter (height_L1_aqu) is the layer where concentrations are calculated for estimation of inhalation doses and the layer for which exchange between the atmosphere and water is calculated. This layer is assumed to be 1 m.

Height of Layer 2

The parameter height_L2_aqu is the height, from the water surface, of the second atmospheric layer (See radionuclide model description Saetre et al. 2013a). This value is set to equal to the reference height where wind speed is measured, i.e. 10 m.

Roughness length

The roughness length (z0_aqu) is the height of the extrapolated logarithmic wind profile where U(z0)=0. Thus, z0 is an integration constant. Because this parameter is dependent on the state of the surface it is called roughness parameter or roughness length.

Many field experiments above water surfaces have been carried out during extensive sea measurement programs that investigated the roughness length parameterisation (Edson et al. 2007, Sun et al. 2001, Vickers and Mahrt 2010, Vercauteren 2011). However, fewer field experiments have collected comparable data to investigate these parameterisations over lakes. An example of a few of the available studies is the one that has been performed by Vercauteren (2011), who carried out a detailed study for parameterisation of z0 for several lakes.

According to Foken (2008) the values of z0 given by various authors for different types of surfaces differ only very slightly. An exception is observed for the case of low roughness (ice and water), where a larger variation is observed. A possible explanation lies in the way z0 values are estimated. The most common method for estimation of z0 is the direct determination using the vertical profile equation under neutral conditions using wind velocity measurements at different levels. However, in the case of low roughness, as it is commonly the case above water surfaces, this method is very inaccurate, because small errors in the measurements of the wind velocity can cause large changes in the estimated roughness length. For this reason for water surfaces, z0 is generally parameterised as a function of the wind velocity. Foken (2008) highly recommends using the relation by Zilitinkevich (1969).

For this study, the same parameter value is applied for lakes and marine areas and the parameter value is set to the middle of the interval (0.0001–0.001) given in Foken (2008, Table 3.1, p 62) for water surfaces. Minimum and maximum values are set to the minimum and maximum in Foken (2008).

Wind speed

Wind speed (vel_wind_height_ref_aqu) is used in the calculations of fluxes in the atmosphere. Mean wind speed measured at the meteorological station Örskär at Forsmark 2002–2006 for the ice-free season (April to December) was used as the parameter value. The mean value was 1.7 m s^{-1} (stdev 0.25).

Height of measured wind spped

This parameter (height_ref_aqu) is used in the calculation of atmospheric flux. This parameter is the height of the measured wind speed which is 10 m.

8.10 Human food parameters

Human utilise aquatic ecosystems for food. This may be an important pathway for human exposure, and thus the amounts of edible products that can be harvested from aquatic ecosystems are used in the calculation of how the biosphere objects are utilised when calculating dose.

The food production can be categorized as food normally consumed and edible products. Food from aquatic ecosystems normally consumed is e.g. fish, whereas edible products are everything that has some potential to be consumed by humans. Potentially it is possible to eat almost any organism above a certain size that can be handled. However, the effort to collect the food in comparison with the energy it supplies is often too large to be efficient. The benthic meiofauna (organisms < 1 mm) in Forsmark are small and not easily caught. The macrophytes in the Baltic and oligotrophic hard-water lakes are generally not very tasty and not used as food today. Benthic fauna and algae may potentially serve as fertilizers in farming. Seals can potentially serve as food, but are not used at present. Moreover, seals are not stationary in small basins such as the biosphere objects and from a radionuclide perspective any seal present in the Forsmark area in the future would have very diluted concentrations of radionuclides compared with fish, since the seals feed from large areas.

Freshwater mussels are not eaten in Sweden today as they are considered to taste bad. The mussel *Anodonta anatina* is abundant in the lakes today, although it is not likely that it will be eaten. Firstly, it does not taste good, and secondly, the effort required to collect the mussels is considered greater than that required to collect mussels from the nearby coastal areas. Even in other parts of the world where other species of freshwater mussels have been consumed, in the past, the contribution of freshwater mussels to total diet has been small due to low energy input from the mussels (Parmalee and Klippel 1974). Combining the facts that present species do not taste good, the effort to collect them is rather high, and that mussels have contributed only in a minor way to total diet even in other parts of the world hosting more tasty species, leads to the assumption that mussels in the Forsmark lakes will not be utilised as a food source.

Crayfish is a potential food source from lakes. Crayfish are not present in the lakes today. However, there are several examples of successful introduction of crayfish to lakes and it is possible that future lakes in the area will contain crayfish that can be utilised as food.

The production by nesting birds in the marine model area (Löfgren 2010) is insignificant in comparison with fish production and is therefore not included in the radionuclide model. The filter feeder *Macoma baltica* is present in the marine ecosystem in Forsmark today. However, this is not caught today and is not likely to be in the future either since the individuals are small, not very tasty and not easily collected. In addition, due to the low salinity, it is not likely that the area will be inhabited by other filter feeders in the future. Likewise, no larger crustaceans (e.g. Shrimps, Crabs, and Lobsters) exist in the marine model area today and they are not likely to be present in the future, mainly due to the low salinity in the Baltic Sea.

Summarizing, today only fish, crayfish, filter feeders, seals and sea birds can be assumed to be considered as normally eaten. Of these, only fish and crayfish are assumed to make a significant contribution to the diets of future human populations in the Forsmark area.

8.10.1 Fish production

Fish is a common food source and is presently caught both in lakes and in marine basins. However, no large-scale fishing occur in the lakes and coastal basins today and therefore no information on how much fish could be harvested are found in the literature. Instead, the amount of fish that could theoretically be harvested is calculated based on an estimation of fish stocks in the area and the amount of fish that can be sustainably harvested is described by the parameters prod_edib_fish_lake and prod_edib_fish_sea. A minimum depth is required to allow fish and crayfish populations in lakes and streams, as these animals do not inhabit systems with poor oxygen conditions which may occur in shallow lakes and streams during winter. This depth requirement is described in the parameters z_min_prod_edib_fish_lake for fish. As fish populations are assumed to be affected by colder temperatures, different parameter values are given for a periglacial climate domain.

Production of edible fish in lakes

The parameter prod_edib_fish_lake represents the productivity of edible fish in lakes. Today, fishing in the Forsmark lakes is considered minimal. Some fishing may occur, but to the authors' knowledge the local inhabitants do not use the lakes much for fishing. However, fish is widely used as a food source today, and in the future fish from the lakes may be utilised to a higher degree than at present.

Fish production was calculated from production/biomass (P/B) ratios. P/B ratios are dependent on fish size (weight and length), and an allometric relationship has been established from studies of 79 freshwater species in Canada (Randall and Minns 2000). Several of the fish species are similar to the Scandinavian species, and the P/B ratio is well correlated to size for most animals (Banse and Mosher 1980, Downing and Plante 1993, Randall and Minns 2000). The maximum lengths of the fish species caught in surveying gillnets were taken from the site study at Forsmark (Borgiel 2004). These fish lengths from Forsmark were compared with the data from Randall and Minns (2000), and for each species a mean P/B was estimated for this range (Andersson 2010, Section 3.10). This P/B ratio was multiplied by the estimated biomass per m^2 to obtain the area-specific fish production for each tabulated species in each of the studied lakes: Eckarfjärden, Fiskarfjärden, Bolundsfjärden and Gunnarsbo-Lillfjärden. The total sum of fish production for each lake was used to obtain an estimate of average fish production for the area; of 5.3×10^{-4} kgC m^{-2} $year^{-1}$. This corresponds to 60 kg ww ha^{-1} $year^{-1}$ which is 2.4 times higher than the highest production values reported for Swedish lakes for which the suggested range is 3–25 kg ww ha^{-1} $year^{-1}$ (Alanärä and Näslund 1995). However, the Swedish estimates of fish production include only fish species that are normally consumed and do not, as in our estimate, include e.g. Crucian carp. Different fish species are preferred in the diet in different areas of the world due to cultural differences as well as the amount of other available food sources. All fish species are therefore considered in our estimate, as future populations in Forsmark may utilize other species than at present. However, it is an unreasonable assumption that the entire fish production can be harvested from lake ecosystems. Different sources suggest that between 10 and 75% of the fish production can be sustainably harvested (Alanärä and Näslund 1995, Degerman et al. 1998, Näslund et al. 2000, Waters 1992). However, it seems that the higher figure 75% is an overestimate, since severe effects on fish populations have been noted at much lower catches. Näslund et al. (2000) and Waters (1992) state that 50% is the highest possible yield for a long-term sustainable fish population. Since over-fishing leads to reduced catches for a long time afterwards, we have chosen a 50% catch of fish population to estimate the maximum annual yield. This corresponds to a sustainable yield of 2.7×10^{-4} kgC m^{-2} $year^{-1}$ (stdev 7.3×10^{-5}).

Production of edible fish in seas

The parameter prod_edib_fish_sea represents the productivity of fish normally consumed. The production of fish is estimated by using a size-dependent ratio for fish production from a study of Canadian freshwater fish (Randall and Minns 2000) together with fish abundance from Forsmark. The site-specific proportion of each size range of marine fish species in the marine area in Forsmark (Heibo and Karås 2005), was compared with the data from Randall and Minns (2000) and for each species a mean P/B was estimated for this range. Fish biomasses modelled in GIS for each of the 28 basins (Aquilonius 2010) were multiplied by the P/B ratios to calculate the production of edible fish. The mean production of the different basins was chosen as the parameter value (mean 8.4×10^{-5} kgC m^{-2}, stdev 6.6×10^{-5} kgC m^{-2}). All fish production in the marine basins is assumed to be available for human catch.

Fish production in lakes is assumed to be lower during permafrost conditions than at present. Our estimate of present-day fish productivity was 2.4 times higher than the highest value reported by Alanärä and Näslund (1995). Fish production in the lower range reported by Alanärä and Näslund (1995) (3–25 kg ww $ha^{-1}year^{1}$) corresponds to the production in the northern part of Sweden, i.e. with a colder climate, and could be a good estimate for the permafrost domain. However, the estimate by Alanärä and Näslund (2005) includes only species that are normally consumed at present. We therefore multiply the production value of 3 kg ww ha^{-1} year by 2.4 (corresponding to the ratio between estimated production in Forsmark and the highest production values given by Alanärä and Näslund (1995). It is assumed that 50% of the production can be sustainably harvested, resulting in an edible fish productivity of 3.2×10^{-5} kgC m^{-2}. The standard deviation for the parameter value is calculated by assuming that the lower value from Alanärä and Näslund (2005) (1.3×10^{-5} kgC m^{-2}) is the lower 95^{th} percentile resulting in a standard deviation of 1.2×10^{-5} kgC m^{-2}.

In the sea, high production of fish can occur also at cold climates and no alternative parameter sets were applied for fish production in the sea.

Water depth required for a permanent fish population in lakes

The parameter z_min_prod_edib_fish_lake represents the threshold at which there can no longer be a permanent fish population in lakes. In shallow lakes, fish catches decrease with decreasing maximum depth and approach zero at a maximum depth of 1 m (Andersson 2010, Section 3.10.1). We have therefore imposed the constraint that there are no fish in future aquatic objects if the maximum depth is less than 1 m.

Since the lakes in the Forsmark area have ice coverage in winter, the theoretical minimum depth that will allow for a permanent fish population must be at least as deep as the ice cover. In addition, oxygen is consumed in the water below the ice so there must be sufficient additional unfrozen water depth to ensure that there is not total anoxia. The maximum ice cover of the Forsmark lakes is c. 40 cm (Borgiel and Andersson, personal observation) and it is reasonable to assume that the water depth below the ice must be at least 3 dm in the deepest parts to allow for a permanent fish population. Therefore we set the minimum to 0.7 m and the maximum is set to 1.3 m in order to vary the parameter symmetrically around the best estimate of the parameter (1 m).

Water depth required for a permanent fish population in sea

The parameter z_min_prod_edib_fish_sea represents the threshold at which there can no longer be a permanent fish population in marine basins. Most marine basins are transformed to lakes before the depth of the basin sets any constraints on availability as a habitat for fish. Nevertheless, theoretically, marine basins may be too shallow to contain a permanent fish population if they have shallow depths and are covered with ice. The same minimum depths as for lakes have been applied, i.e. parameter value 1 m, minimum 0.7 and maximum 1.3.

Conversion factors for fish

In order to model the transfer of carbon-14 in water into fish knowledge of the amount of carbon per wet weight and dry weight is needed. The parameter f_DW _FW_fish_lake/sea represents the ratio of dry weight to fresh weight in fish and f_C_fish represents the ratio of carbon to dry weight in fish. The parameters were calculated based on site-specific measurements from fish in Forsmark (SR-PSU chemistry database, Hannu and Karlsson 2006, Roos et al. 2007). Mean values from these studies were used as parameter values (Table 8-7).

Table 8-7. Fraction of dry weight too fresh weight and fraction of carbon to dry weight for fish.

Parameter	Best estimate	Description	Unit
f_DW_FW_fish_lake	0.21	Ratio of dry weight to fresh weight for fish in lake	kgdw $kgfw^{-1}$
f_DW_FW_fish_sea	0.21	Ratio of dry weight to fresh weight in marine fish	kgdw $kgfw^{-1}$
f_C_fish	0.44	Ratio of carbon to dry weight in fish	kgC $kgdw^{-1}$

8.10.2 Production of crayfish

The parameter prod_edib_cray_lake represents the productivity of crayfish that may be consumed by humans. There are no crayfish in the present-day shallow lakes in Forsmark, but some of the future lakes in the area will be considerably deeper. In these deeper lakes, significant areas will consist of aphotic bottoms lacking microbial mats, and they can be assumed to more closely resemble other deep lakes in the region, such as Lake Erken, where crayfish are abundant. Therefore, in order to avoid underestimating potential food production in the Forsmark lakes, it has been assumed that crayfish occur and contribute to human food in lakes with a mean depth over 2 metres (further discussed in z_min_prod_edib_crayfish_lake below). Although the Swedish Board of Fisheries reports crayfish yields of 5–50 kg ha^{-1} in productive crayfish lakes (Fiskeriverket 2003), the higher values in this range are seldom reported. In Lake Erken, which is considered to be a very good crayfish location in Uppland, 5–10 tonnes of signal crayfish (equivalent to 2–4 kg ha^{-1} or 0.015–3×10^{-5} kgC m^{-2} were caught in 2008). This is the highest catch in the lake since the crayfish plague wiped out the native noble crayfish in the 1930s (Naturvatten 2014). Thus, a high crayfish yield in deep future Forsmark lakes is assumed to be similar to that in Lake Erken. Although 3×10^{-5} kgC m^{-2} is the maximum yield in Lake Erken over the last 40 years, it is chosen as a conservative value in order to avoid under-estimating the importance of this food source.

The minimum crayfish yield is set to 0 as it is assumed that many of the future lakes will not contain crayfish. The maximum crayfish yield could be higher than the highest recent catch in Lake Erken. Estimated maximum catches in Lake Erken before the crayfish plague wiped out the noble crayfish population in the 1930s could have been as high as 75 tonnes per year (Naturvatten 2014). However, such large catches were most probably not sustainable in the long-term. Moreover, there are rumours that the lake was almost empty of crayfish in the late 19th century, probably due to other diseases than the plague that came in the 1930s. Thus, although the yield in future Forsmark lakes could be very high for some years, a sustainable yield is assumed to be at most twice the present yield in Lake Erken, i.e. maximum crayfish yield is set to 6×10^{-5} kgC m^{-2}.

It is assumed that no crayfish are present in the lakes during permafrost periods as crayfish needs longer ice-free periods than those experienced in a cold periglacial climate.

Water depth required for a permanent crayfish population in lakes

z_min_prod_edib_cray_lake represents the minimum depth of lakes to enable a crayfish population. Crayfish do not occur in the present-day lakes in the Forsmark regional model area. There are two main factors which prevent crayfish from establishing in the oligotrophic hardwater lakes which are typical of the Forsmark area. Firstly, crayfish prefer stony or hard bottom substrates with a rich abundance of shelters. The thick and fluffy microbial mat and the rich *Chara* vegetation that dominate the shallow Forsmark lakes provide unsuitable substrates for crayfish, and areas with more suitable crayfish habitats in the present-day lakes are very restricted (Eva Andersson, personal observation). Secondly, crayfish are sensitive to low oxygen conditions. The Forsmark lakes show strongly reduced oxygen concentrations during periods with ice cover (see Section 3.9.1 in Andersson 2010), and this is reflected in the fish community which is dominated by species tolerant to low oxygen conditions (see Section 3.10 in Andersson 2010). Even if it is not possible to totally rule out a future establishment of crayfish in shallow lakes in the area, these two factors mean that there will never be more than a sparse crayfish population that will only marginally contribute to human food supply. It is likely that any future shallow lake (mean depth < 2 m) in the area will develop into an oligotrophic hardwater lake, which means that crayfish production in these lakes will be insignificant. Consequently, crayfish are assumed not to occur in future shallow lakes (mean depth < 2 m) and this parameter is set to 2 m.

The minimum depth of 2 m for crayfish population to be able to inhabit the Forsmark lakes is derived from discussion and is not measured at the site since no crayfish occur today. Therefore, it is difficult to give an absolute variation of the parameter. To evaluate the effect on dose to humans, minimum and maximum values for this parameter were set to 1.5 and 2.5 metres in the probabilistic simulations of the model, although this span is probably somewhat large.

9 Terrestrial ecosystem parameters

During the modelled time period, all the biosphere objects will reach a terrestrial stage that is represented by a mire. Such wetlands may be further used for forestry or agricultural production after drainage, and radionuclides may be transferred in proportion to concentrations in environmental media to the vegetation. The parameters presented below are those describing biota and, to some extent, human utilisation associated with wetlands, agricultural use of drained wetlands and garden plots in the dose modelling.

All parameters given a central value were assumed to be drawn from normal distributions except, 1) parameter values describing the successional development of the mire were assumed to be derived from a uniform distribution, 2) parameter values for which data were lacking to give an appropriate description of the distribution were assumed to be derived from a uniform distribution.

For each parameter for which the central value was assumed to be derived from a normal distribution, the variation was assigned following the guidelines; 1) if the data set from which the central value was calculated contained information on the variation, these data were used, 2) if such information was missing, the variation was estimated based on information from a "closely related" parameter using the coefficient of variation, 3) if it was difficult to identify such a "closely related" parameter the standard variation/deviation was derived from the assumption that the (available) minimum value represents the 2.5% percentile. Furthermore, a minimum and a maximum value were estimated for each parameter and these were used to truncate the distributions in the probabilistic modelling. In some cases, the distributions are minimum truncated to avoid negative values.

9.1 Experience from previous safety assessments

Transport of radionuclides in terrestrial ecosystems has been modelled in previous safety assessments at SKB for SAFE (Lindgren et al. 2001, Kautsky 2001), SAR-08 (SKB 2008b) and SR-Site (Avila et al. 2010). Experience from these assessments, site investigations and research has led to a continual development of the radionuclide transport model for the biosphere and updating of parameters. Below is a comparison of terrestrial parameters in SR-PU with previous used parameters in SAFE, SAR-08 and SR-Site.

Ecosystem models were basically the same for the projects SAFE and SAR-08 although some parameter values were updated between the assessments (Karlsson et al. 2001, Bergström et al. 2008). Since SAR-08, the biosphere radionuclide transport model has been extended and a continuous development of the landscape is now modelled and as a result the majority of the terrestrial parameters are new. Also, many parameters that were used previously in SAR-08, (e.g. production of berries and mushrooms) have been updated due to improved or new data and updated models.

The SR-PSU model closely resembles the SR-Site model, although some updates have been made (Saetre et al. 2013a). Consequently, many of the parameters are identical to parameters used in SR-Site (terrestrial SR-Site parameters are presented in Löfgren 2010). As a consequence of the update, some new parameters have been added and some parameters have been altered, e.g. the handling of carbon degassing across the water-air interface has been further developed in SR-PSU and parameters relating to gas uptake and degassing have been updated, with the introduction also of a number of new parameters (see below).

9.2 Influence of climate on parameter values

In the global warming climate calculation case, the estimated maximum temperature increase is an increase of the yearly average temperature from +4.7°C to +8.4°C in the Forsmark region (SKB 2014d). This increase approximates the difference between the region of Skåne in southern Sweden (7–8°C) compared with Forsmark, therefore production estimates from Skåne were used as an analogue for such a climate change. The increase in production is also a function of other properties such as soil type, but the climate is here assumed to be the dominating factor determining the increased production in southern Sweden.

In the extended global warming climate calculation case, an even larger increase in the yearly average temperature (+6°C) was assumed, suggesting an approximate maximal increase to +10.7°C in the Forsmark region (SKB 2014d). Such a climate is similar to central and southern Europe and this area can therefore be used as an analogue for estimation of parameter values. Global warming is an issue of increasing concern, and reports of potential effects on different properties have been published for different purposes (e.g. Ministry of Environment 2007). An alternative parameterisation has been provided for properties associated with agricultural production and human food production for an extended global warming climate.

A periglacial estimate describes the properties of a treeless tundra environment. In the case of certain parameters, the same estimate is used for both the temperate domain and the periglacial domain since little change is expected to occur. For some parameters (e.g. fungi production) it was difficult to find data that matches the periglacial case and estimates as close as possible to periglacial conditions were derived.

Under glacial or submerged conditions, the terrestrial environment is considered to be covered with ice or water all year round and consequently, no terrestrial exposure routes would be present during these conditions.

Alternative parameterisations of parameters that are affected by climate are presented under each of the following parameter descriptions and listed in Appendix B.

9.3 Biomass and net primary production for a mire

The vegetation on the mire is described both in regard to the standing biomass and the yearly net primary production, NPP, including both above- and below-ground production from all functional layers, such as bryophytes, herbs, dwarf shrubs and trees, if present. This parameter (NPP_ter) is used to estimate the uptake of atmospheric CO_2 and the uptake of carbon by roots. At a coastal location such as Forsmark, mire formation and the following succession will span a number of different mire types, with different vegetation communities. The different successional stages of the wetland will differ in properties such as vegetation, biomass, NPP and peat accumulation. The infilling of a lake in the Forsmark region is characterised by reed expansion, which generally is followed by stages characterised by *Bryales* peat, *Carex* peat, fen wood peat and *Sphagnum* peat (Bergström 2001, Fredriksson 2004, Sohlenius et al. 2014). The peat layer generally thickens with time, with thin layers in wetlands close to the coast and thicker layers further inland (Hedenström and Sohlenius 2008). Most wetlands are considered to be discharge areas for groundwater. Also, raised bogs, with rain-fed production on the bog plane and a restricted or non-existent connection to the groundwater table, are of limited interest to a safety assessment where the radionuclides enter the ecosystem from below. Moreover, the bog peat has been regarded to be less suitable for agricultural purposes, due to the low pH (SKB 2014a).

Figure 9-1 shows estimated biomass and NPP for a number of different mire communities that may be used to illustrate the successional development in Forsmark. Reed starts to expand in the lake basin, which then is followed by *Bryales* and *Carex* communities forming rich fens. In the long term, these are replaced by poor fen communities dominated by *Sphagnum* as the influence of mineral-enriched groundwater diminishes over time. Stages with trees are regularly found in the peat cores, often in the marginal parts of the fens (e.g. Bergström 2001), but may also cover most of the mire surface for shorter periods (e.g. von Post and Granlund 1926). Generally, it has been suggested that the presence of woody peat indicates drier conditions and a lowered groundwater table rather than a distinct successional stage in the mire ontogeny. Based on the historical peat archives, this stage is regarded to be less frequent than wetter conditions (von Post and Granlund 1926). Therefore the central value describing the biomass represents a mean of the three successional stages without trees (Figure 9-1), but the minimum and maximum values also includes the treed fen, e.g. an alder swamp and a Norway spruce swamp (Figure 9-1). The range in production is assumed to include increased production caused by global warming, because of inclusion of data from the more southerly located Laxemar-Simpevarp area (Figure 9-1). A uniform distribution was used to describe the directional character of the successional development for both parameters in the probabilistic simulation (Table 9-1).

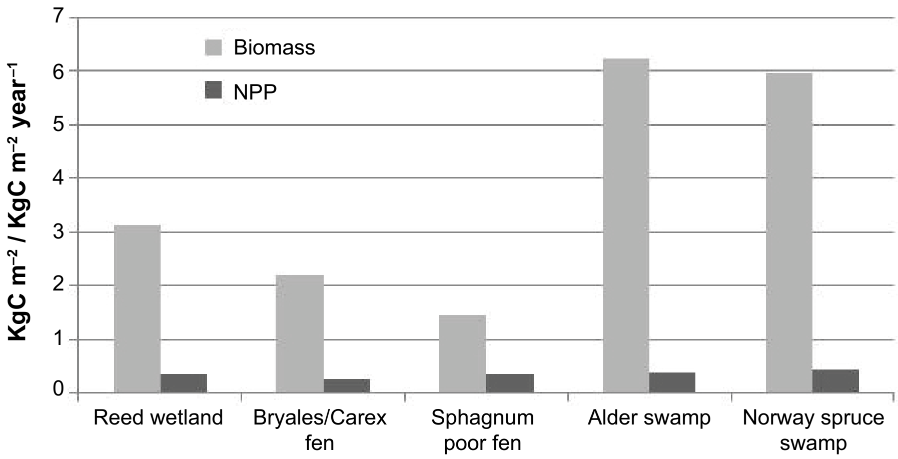

Figure 9-1. *Above- and below-ground biomass (kgC m^{-2}) and net primary production (kgC m^{-2} year^{-1}) for a number of different mire communities that can be used to illustrate potential successional stages in mire development. Fen communities dominated by trees may occur in different stages during development. The bog has been left out of this description. The large increase in biomass is an effect of the presence of trees. Data describing the reed wetland are means from five Scandinavian localities (Andersson et al. 2003 (from Forsmark), Brix et al. 2001, Löfgren 2005), where below-ground NPP is assumed to be 77% of the above-ground NPP (Asaeda and Karunaratne 2000). Data for the other four wetlands are from Löfgren (2005, 2010, Chapter 6). The third and fifth vegetation types are mires from Laxemar-Simpevarp, and the second and fourth are from Forsmark.*

Table 9-1. Parameter values for mire biomass and NPP used in the global warming base case.

Parameter	Unit	Central value	Minimum	Maximum	Distribution
NPP_ter	kgC m^{-2} year^{-1}	0.32	0.25	0.43	Uniform
biom_pp_ter	kgC m^{-2}	2.26	1.45	5.97	Uniform

These estimates of biomass and NPP in periglacial conditions are based on nine different studies from arctic and alpine tundra communities classified as wet sedge-moss communities presented in a review by Wielgolaski et al. (1981) (Table 9-2).

Table 9-2. Parameter values for mire biomass and NPP during periglacial conditions.

Parameter	Unit	Central value	Minimum	Maximum	Distribution
NPP_ter_perm	kgC m^{-2} year^{-1}	0.09	0.04	0.42	Uniform
biom_pp_ter_perm	kgC m^{-2}	0.82	0.48	1.88	Uniform

Modelling approaches investigating a smaller temperature increase than assumed in the extended global warming climate case suggest that the NPP in forest ecosystems will increase in the short perspective (< 100 years) (e.g. Wolf et al. 2008, Kjellström et al. 2009). Here, an increase of 50% is assumed for mean, minimum and maximum values for both NPP and biomass in mire ecosystems (Table 9-3).

Table 9-3. Parameter values for mire biomass and NPP during an extended global warming climate.

Parameter	Unit	Central value	Minimum	Maximum	Distribution
NPP_ter	kgC m^{-2} year^{-1}	0.47	0.38	0.65	Uniform
biom_pp_ter	kgC m^{-2}	3.26	2.18	8.96	Uniform

9.4 Carbon in the mire ecosystem

Parameters that are specifically used to model fluxes of carbon-14 in the terrestrial ecosystems are listed in this section.

9.4.1 Dissolved inorganic carbon in pore water

This parameter (conc_DIC_regoUp) describes the concentration of dissolved inorganic carbon, DIC, in the peat pore water that is present in regoUp (the oxic peat layer) and potentially available for root uptake. The parameter values represent the concentration during the vegetation period and were sampled during one occasion in late summer in the Forsmark area at three different mires representing a successional gradient, spanning approximately from 450 to 1,500 years of age (Löfgren 2011). The samples represent the depth 0.35–0.45 m and are therefore somewhat deeper than the defined root zone interval (z_regoUp_ter = 0.30 m). Typically, this concentration does increase with depth and is a function of incoming calcite-enriched ground water, decomposition (CO_2 production) and degassing at the water-atmosphere boundary layer (e.g. Webster and McLaughlin 2010). The values might therefore be a slight overestimate of an integrated estimate of the root zone concentration. However, the range that is used is expected to include the potential values. For the three successional stages sampled it is expected that the later stage would be more dominating over time, suggesting that this stage should be more heavily weighted in the average estimate and therefore the average would be lowered. Moreover, a lower value is regarded as more cautious, because the activity concentration of carbon-14 is calculated based on the concentration of carbon-12. Consequently, a central value was chosen that represents a latter successional stage, whereas the range is built upon the individual samples from all three successional stages (Löfgren 2011). The central value is also close to the mean of surface samples from 12 mires in northern Sweden (Nilsson and Bohlin 1993).

Today there are no measurements available describing the DIC concentration in the peat pore water just above the water table in a drained mire. The general pattern during the mire succession is that pH decreases and also the DIC concentration. In Forsmark, the stage at which drainage would be suitable could be when a sufficient part or the whole lake basin is filled with peat. The DIC concentration could be approximated by the measured concentrations in Stenrösmossen that is approximately 1,400 years old based on time since isolation and is located within the Forsmark area. However, for mires found in low-lying areas with large catchments the decrease in pH and DIC concentrations (and Ca^{2+}) would be slower due to a larger total pool of carbonates in the soil (of the total catchment) and estimates from the younger Labboträsk II that is approximately 600 years old and also located within the Forsmark area could be used as maximum values for the DIC concentrations (Löfgren 2011). To what extent the concentration of DIC in peat pore water from the mire would be suitable to describe the same property in the drained peat above the water table is difficult to evaluate. As the peat is located above the water table the important influence from the groundwater disappears and solid $CaCO_3$ earlier adsorbed to the peat would leach. However, CO_2 from oxidation processes will also be available and dissolve in pore water reaching maximum values during the peak temperature in summer, suggesting that somewhat higher values might be found than measured in Stenrösmossen. The mean from the youngest investigated mire Labboträsk I is therefore chosen to describe maximum DIC concentration in the peat pore water potentially found in a drained mire.

The soil in the garden plot and in the infield-outland is glacial clay. There are no estimates of DIC concentrations in near-surface pore water that exactly matches this soil type. Instead a mean was used for the DIC concentration from a soil pipe in till below peat at a depth of approximately 3.5 m in the Forsmark area. This mean was built upon 25 measurements between 2003 and 2009 (soil pipe SFM0032). Minimum and maximum values were based on over 400 measurements from 30 different soil pipes between 2003 and 2009 representing several different soil types. A uniform distribution was assumed in the probabilistic simulation.

Table 9-4. The parameter values chosen to represent the concentration of dissolved inorganic carbon in the soil water of different soils

Land-use type	Parameter	Unit	Central value	Minimum	Maximum	Distribution
Drained mire	conc_DIC_regoUp	kgC m^{-3}	0.032	0.006	0.046	Uniform
Garden plot	conc_DIC_regoUp	kgC m^{-3}	0.062	0.005	0.165	Uniform
Infield-outland	conc_DIC_regoUp	kgC m^{-3}	0.062	0.005	0.165	Uniform
Mire	conc_DIC_regoUp_ter	kgC m^{-3}	0.014	0.006	0.071	Uniform

9.4.2 Fraction of total DIC present as CO_2 in peat pore water

This parameter (f_H2CO3_ter) describes the fraction of H_2CO_3 to the total pool of dissolved inorganic carbon (DIC) in peat pore water. H_2CO_3 represents the dissolved CO_2 that is available for degassing from the peat pore water surface. The other constituents are HCO_3^- and CO_3^{2-}, all of which are in equilibrium described by two temperature-dependent dissociation constants. The relative proportions between the three constituents are pH-dependent (Figure 9-2). At low pH, H_2CO_3 dominates but as pH increases the dominance will switch to HCO_3^- and then CO_3^{2-} as pH rises above 10.5. As pH increases above 6, the reaction rate of CO_2 dissolved in the pore water to form HCO_3^- increases and this reaction rate of CO_2 becomes faster than the diffusion process through the water film and the pH will thereby restrict the potential degassing (Stumm and Morgan 1996, Wetzel 2001). The relationship between the fraction of H_2CO_3 to the total pool of DIC (f_H2CO3_ter), pH and the dissociation constants may be approximated by the following expression for a closed system.

$$f\_H2CO3 = \frac{1}{(1 + (K1/[H+]) + (K1 * K2/[H+]^2))}$$

where K1 and K2 represent the dissociation constants of the two equilibria

$H_2CO_3 \leftrightarrow HCO_3 \leftrightarrow CO_3^{-2}$ and (H^+) is the hydrogen concentration.

Generally, the temperature has a small effect on this parameter (Figure 9-2), whereas pH alone determines most of the variation in f_H2CO3.

The central value of f_H2CO3_ter is calculated for a mire with a pH of 6.5, representing an early successional fen in connection with a lake (Labboträsk I in Löfgren 2011), at a mean temperature (during the ice-free season) of 15°C. Minimum and maximum describes the pH range during fen succession. Minimum is calculated for pH 8 representing the very young mire (estimated from small young lakes by Qvarfordt et al. (2011)). Maximum is calculated for a pH of 5 representing a late successional *Sphagnum*-dominated poor fen. The parameter value is not regarded as sensitive to climate change, due to the insignificant dependence on temperature (Figure 9-2).

Table 9-5. Fraction of H_2CO_3 to the total pool of dissolved inorganic carbon (DIC) in peat pore water.

Land-use type	Parameter	Unit	Central value	Minmum	Maximum	Distribution
Mire	f_H2CO3_ter	Bq Bq^{-1}	0.46	0.03	0.96	Uniform

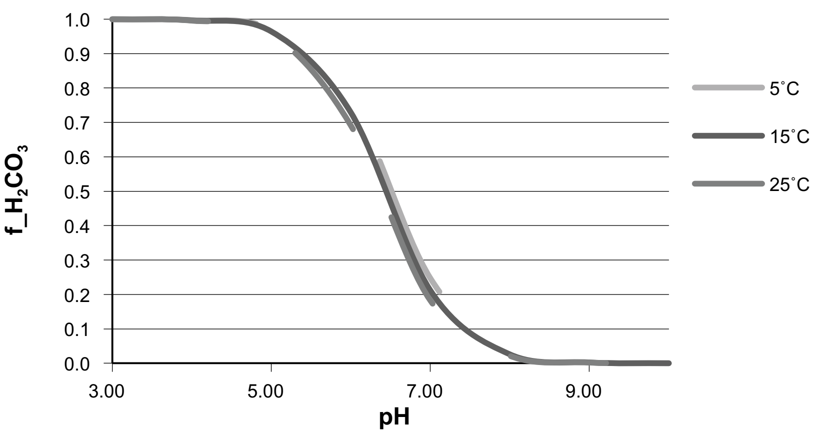

***Figure 9-2.** The fraction of dissolved CO_2 to the total DIC pool (f_H2CO3) plotted against pH and its dependence on the temperature-dependent dissociation constants.*

9.4.3 Carbon content of peat

This parameter (f_C_peat) describes the carbon content as a fraction of the dry weight of the whole peat column and the value is based on a mean estimate from 73 mires in Finland spanning both coastal and inland localities and *Carex* and *Sphagnum* dominated peat (Mäkilä and Goslar 2008).

Table 9-6. Carbon content of peat, described as a fraction carbon of dry weight.

Parameter	Unit	Central value	Stdev	Minimum	Maximum	Distribution
f_C_peat	kgC kgdw^{-1}	0.46	0.03	0.4	0.55	Normal

9.4.4 Carbon root uptake by vascular plants

Carbon uptake from the atmosphere is the most important pathway for the vegetation, but roots can also incorporate inorganic carbon from the soil by root uptake. This parameter (f_rootUptake) is the fraction of the total carbon uptake that is taken up by roots. Several studies suggest that the amount of incorporated carbon via roots is small in comparison to the carbon assimilated from atmospheric CO_2 across many different functional types. Estimates for *Salix* by Vuorinen et al. (1989) show that direct root uptake of carbon may be 1 to 2% of the carbon assimilated by leaves. In a study on *Phragmites australis* where carbon-14-labelled DIC was added to the rhizosphere interstitial water the uptake was less than 1% of the amount of carbon fixed from the atmosphere by aerial plant tissue (Brix 1990). Ford et al. (2007) demonstrated that carbon-13-labelled CO_2 dissolved in soil water can be absorbed and fixed in the tree *Pinus taeda* seedlings, but also in this study DIC supplied from the soil contributed less than 1% to total seedling carbon gain. Sheppard et al. (1991) estimated that about 1.7% of the plant carbon may be derived directly from root uptake in a carbonated soil, but also showed that the values were much lower in a non-carbonated soil. A study by Amiro and Ewing (1992) on the uptake of inorganic carbon-14 by bean plant roots showed that carbon-14 uptake via the roots was independent of the photosynthetic rate and, in most cases, could be predicted by knowing the transpiration rate and the nutrient solution concentration. Hwang and Morris (1992) calculated the uptake of non-atmospheric carbon to be 10% of the total uptake of the large perennial grass *Spartina alterniflora* found in intertidal wetlands, but did not account for respiration losses for the internal turnover of carbon dioxide suggesting a somewhat lower figure.

In wetlands and especially in fens, characterised by a high- and low-fluctuating water level, bryophytes are partially submerged in wet habitats. Diffusion of CO_2 is approximately 100 times lower in water than in air and water therefore acts as barrier to CO_2 assimilation. Therefore, submerged conditions cause high resistance to CO_2 uptake with consequences for NPP. Results from carbon-13/carbon-12 ratios presented by Proctor et al. (1992) suggested that partially submerged bryophytes mainly used CO_2 originating from the atmosphere. Complete submerged conditions will occur mainly during peak water level e.g. the spring flood. Completely submerged bryophytes will not be able to use atmospheric CO_2. Bryophytes are known to be almost obligate CO_2 users and are therefore not able to use bicarbonates as for example submerged vascular plants (Bain and Proctor 1980). High concentrations of CO_2, due to respiration, so-called substrate-derived CO_2 in the water-inundated surface peat layer may partly compensate for low diffusion (e.g. Rydin and Clymo 1989). In conclusion, the CO_2 derived directly from the fen water by bryophytes is regarded to be of less importance as compared to atmospheric CO_2 for NPP for most bryophytes during the vegetation period. This pattern is even more pronounced as compared with the total NPP where vascular plants contribute with the major part of the total NPP on the fens in Forsmark. This parameter value is not regarded to be sensitive to climate change.

Table 9-7. Fraction of the total carbon uptake that is taken up by roots.

Parameter	Unit	Central value	Minimum	Maximum	Distribution
f_rootUptake	kgC kgC^{-1}	0.02	0.01	0.1	Uniform

9.4.5 Piston velocity

In a biosphere object volatile radionuclides may be exchanged across the atmosphere-surface water interface. Such a gas flux may be described by the equation,

$$J = -\psi(C_{surf} - C_{eq})$$

where

J is the gas exchange between surface water and atmosphere,

C_{surf} is the concentration of the gas in the surface water,

C_{eq} is the concentration of gas in the atmosphere and

ψ is the gas exchange coefficient. It has the dimension of a velocity (m s^{-1}) and is referred here to as the piston velocity. This velocity is estimated from experiments using a tracer gas and is normalised to the gas of interest (Cole and Caraco 1998, McGillis et al. 2000). In the radionuclide model it is at present time the CO_2 flux of the isotope carbon-14 that is of primary interest for this gas exchange. The piston velocity for CO_2 is calculated as

$$\psi_{CO2} = \psi 600(Sc_{CO2}/600)^{-1/2}$$

where

$$\psi_{600} = (2.07 + 0.215 \times U_{10}{}^{1.7}/365{,}000$$

is an empirically derived best-fit power function for the piston velocity (piston_vel_ter in m s^{-1}) of the tracer gas SF_6 normalised to a dimensionless Schmidt number of 600, which is dependent on wind speed at 10 m height (U_{10}, in m s^{-1}) and SC_{CO2} is the Schmidt number of CO_2 (Cole and Caraco 1998). This expression includes the constant 365,000 to transform the piston velocity from cm h^{-1} into m s^{-1}. The exchange over a lake or sea water surface is affected by the wind speed. However, in a mire the water surface is commonly found just below the peat surface and is often covered with dense vegetation. It is therefore assumed that the effect of wind speed is negligible and is consequently set to zero. The Schmidt number for CO_2 is temperature dependent and is described by:

$$Sc_{CO2} = 1{,}911 - 113.7 \times T + 2.967 \times T^2 - 0.02943 \times T^3$$

where T is the temperature in °C. The Schmidt number was calculated based on the monthly temperature of four small shallow lakes close to the coast (Qvarfordt et al. 2011), which are assumed to represent the peat pore water in the z_regoUp_ter (0.3 m) of the mire. The piston velocity was averaged across months to describe the yearly exchange (m $year^{-1}$), which is expected to occur during the ice-free season. This period is assumed to be similar to the ice-free season in the lakes (~ 240 days during April–November, Andersson 2010).

A comparison of the impact of temperature and the effect of ice-free conditions on the yearly average piston velocity showed that the latter had the largest impact on the result (Figure 9-3). Minimum and maximum values were therefore calculated based on variations in number of ice-free days alone (227–267 days during 2002–2007, Andersson 2010), where the minimum represented 7 ice-free months and the maximum 9 ice-free months (Table 9-8). It is therefore a slight overestimation of the actual exchange as the effect of the temperature is neglected. In the periglacial climate case, it is assumed that there are four ice-free months of the year and a lower water temperature is used corresponding to April, May and September for 2011 (Table 9-8).

In the extended global warming calculation case, it is assumed that there are 11 ice-free months of the year, but the same water temperatures as for 2011 (Table 9-8).

A modelling approach, where the radionuclide transport model for the biosphere was used to study the performance of carbon-12 in the model and the result was compared with empirical estimates, suggested that the degassing of CO_2 was too effective in the model (SKB 2014a, Chapter 9). The calculated piston velocity (Table 9-7) returned a too low concentration of dissolved CO_2 in the pore water of the upper peat layer. The measured concentrations were three times larger than the value that the model returned. Therefore, the piston velocity was reduced by a factor of three, based on the linear relationship between the piston velocity and the CO_2 concentration in the pore water. This was done for all three climate cases (Table 9-8).

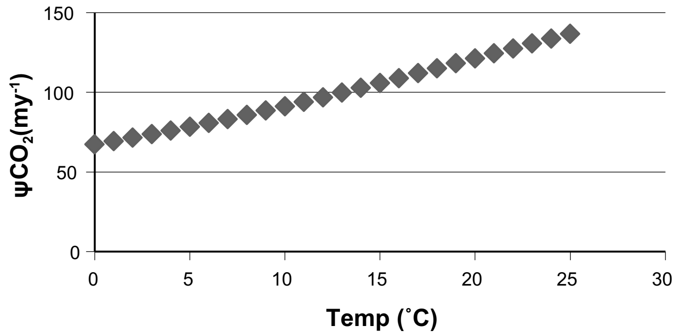

__Figure 9-3.__ Description of the temperature dependency of the piston velocity expressed as m year^{-1}.

Table 9-8. Piston velocities for the three climate cases (m year^{-1}). The values within parentheses are the values that were calculated, whereas the adjusted values (based on model calibration) were used in the radionuclide transport modelling (see text for further information).

	Central value	Minimum	Maximum	Distribution
Piston velocity (piston_vel_ter) for global warming base case (m year^{-1})	50 (151)	45 (145)	55 (157)	Uniform
Piston velocity (piston_vel_ter_perm) for periglacial climate case (m year^{-1})	47 (141)	42 (133)	52 (152)	Uniform
Piston velocity (piston_vel_ter) for extended global warming climate case (m year^{-1})	46 (137)	41 (134)	51 (145)	Uniform

9.4.6 Solubility of CO_2 at equilibrium

The equilibrium concentration of a volatile element in pore water can be expressed as a function of the atmospheric concentration of the volatile element and a solubility constant (k_solubility), the so called Henry´s coefficient, using Henry´s law. This equilibrium concentration is further used to calculate the gross flux of the volatile element from the atmosphere into the surface peat pore water. This solubility constant (solubilityCoef_ter) is dimensionless (mol m^{-3} per mol m^{-3} or kM kM^{-1}, $k_{H.cc}$) and describes the relationship between the concentration in the peat pore water of the compartment z_regoUp_ter (0.3 m) and the concentration in the atmosphere. This constant is temperature dependent and the relationship may be approximated by

$$k_{H.cp}(T) = k_{H.cp}(T^{\ominus}) \exp\left[C\left(\frac{1}{T} - \frac{1}{T^{\ominus}}\right)\right]$$

where $k_{H.cp}$ is the Henry´s law constant expressed as the relationship between the concentration in the fluid and the partial pressure of the gas in the atmosphere (converted to $k_{H.cc}$ by multiplying with 24.46).

T is the temperature in the fluid in Kelvin.

$T^{\ominus}$ refers to the standard temperature (298 K) and

C is an element-specific constant (2,400 K for CO_2). In the current assessment, it is the gas transport of carbon-14 that is modelled.

Figure 9-4 shows the variation in the solubility constant for CO_2 as the function of the intra annual mean temperature pattern of four small shallow lakes (Qvarfordt et al. 2010, 2011) that is used to approximate the peat pore water of the upper 0.3 m of the mire. A higher solubility is found at low temperatures, but the solubility will be restricted by an ice sheet during the winter. Therefore, the mean value is based on the monthly mean temperatures during the ice-free season (April-November, Andersson 2010).

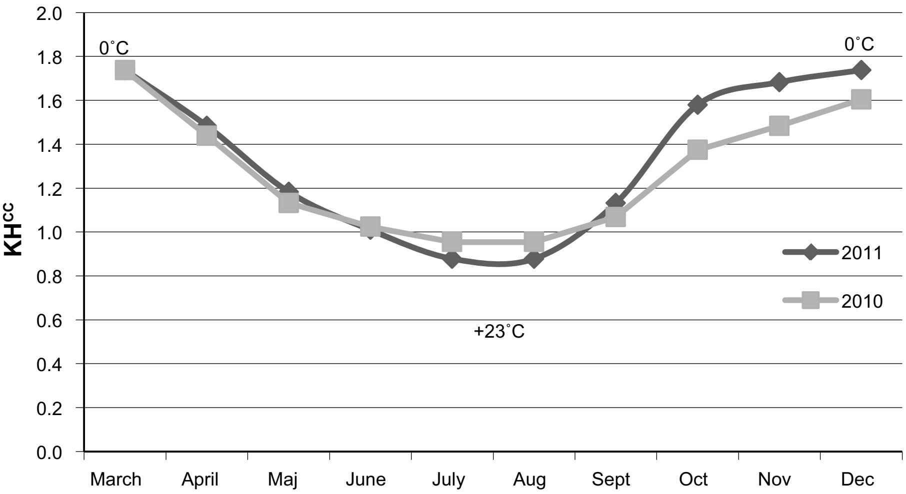

Figure 9-4. *Monthly estimates of Henry´s coefficient describing the intra-annual variation in solubility of CO_2 over two years based on the mean temperature of four small shallow lakes that are used to approximate the temperature of the surface peat pore water in a mire. The temperatures in the figure refer to lowest and highest values in 2011. The mean value of the coefficient during the ice-free season (April–November) was 1.23 for 2011 and 1.18 for 2010.*

A central value of the solubility of CO_2 in the peat pore water was estimated based on the mean temperature of four lakes from the year 2011 (Qvarfordt et al. 2011, Figure 9-4). An estimate of the variation was based on the coefficient of variation for the yearly mean solubility constant between 2003 and 2009 from Lake Labboträsk in Forsmark (see Table 9-9).

For periglacial conditions, this parameter was calculated for a case with only four months of ice-free conditions and where the water temperatures were based on the early season (April–May) and the late season (September– October) temperatures of today (5°C, 12.5°C, 14°C and 3°C). A standard deviation was estimated using the same coefficient of variation as for the temperate case. For an extended global warming climate, the number of ice-free days during the year would increase and also the temperature. However, the same value is used as for the temperate case (see Table 9-9).

Table 9-9. Solubility coefficients for the different climate conditions (mol m^{-3} per mol m^{-3}). The min value was set to zero to avoid negative parameter values in the probabilistic modelling.

	Central value	Stdev	Minimum	Maximum	Distribution
Solubility coefficient, global warming climate, extended global warming (solubilityCoef_ter)	1.23	0.05	0		Normal
Solubility coefficient, Periglacial climate (solubilityCoef_ter_perm)	1.34	0.05	0		Normal

9.5 Terrestrial atmosphere parameters

The atmosphere compartment of the terrestrial ecosystem is divided into two layers overlying the canopy layer (Saetre et al. 2013a). The heights of these layers are presented here together with the drag coefficient and Kármán constant.

9.5.1 Drag coefficient

The drag coefficient (dragCoef) is a dimensionless quantity that is used to quantify the drag or resistance of the vegetation in the canopy atmosphere. It is used in the equation of the extinction (attenuation) coefficient of the vegetation, used to model the wind profile in the canopy layer. The value (0.2 unitless) used in the simulations for all types of vegetation is taken from Goudriaan (1977), where this value is recommended for grasses, maize and coniferous forest.

9.5.2 Height of the terrestrial Layer 1

The height of the first above-canopy atmospheric layer (height_L1_ter) is assumed to be 2.5 m. This value defines the thickness of the air layer directly above the canopy, where air concentrations are representative for estimation of inhalation doses of exposed individuals.

9.5.3 Height of the terrestrial Layer 2

Height of the second above-canopy atmospheric layer (height_L2_ter), assumed for convenience to be 10 m, which is the height at which measured values of wind velocities are available. As showed in Saetre et al. (2013a) this parameter has a weak influence on the dose estimates.

9.5.4 Kármán constant

The von Kármán constant (or Kármán constant) is a dimensionless constant (karman_const) describing the logarithmic velocity profile of a turbulent fluid flow near a boundary with a no-slip condition, i.e. when viscous fluids at a solid boundary will have zero velocity relative to the boundary. The von Kármán constant is used in the equations that are used to model the vertical profiles of wind speed and resistances. It is considered to be a universal constant equal to 0.41 (Arya 2001).

9.5.5 Leaf width

This parameter (leaf_width_ter) describes the width of the plant leaves for different types of vegetation. Generally, there may be a large plasticity in this type of character that is dependent on environmental factors such as soil type, nutrient supply, exposure and water availability. The central value is chosen to represent a typical and/or well-managed and productive habitat/crop. The parameter Leaf_ width _ter represents the vegetation on the mire, which is characterised by different *Carex* species. This represents a set of different potential vascular plant species during succession from narrow-leaved *Carex lasiocarpa* (min) to broad-leaved *Phragmites australis* (max). Estimates for fodder are based on potential grass species and some herbaceous species. Estimates for cereals, potato and cabbage are all built upon expert judgement, whereas the other estimates are taken from Mossberg and Stenberg (2003). The standard deviations were derived by using the coefficient of variation from the biomass estimates above (CV=0.16). The mean value for the mire would also be applicable to the periglacial and extended global warming climate cases (see Table 9-10).

Table 9-10. Width of leaves of different crops and mire vegetation (m).

Parameter	Unit	Central value	Stdev	Minimum	Maximum	Distribution	Genus/species
leaf_width_ter	m	0.005		0.001	0.03	uniform	*Carex sp.*
leaf_width_cereal	m	0.015	0.002	0.005	0.03	normal	*Barley*
leaf_width_fodder	m	0.02	0.003	0.005	0.04	normal	*Poaceae*
leaf_width_tuber	m	0.06	0.01	0.03	0.1	normal	*Potatoe*
leaf_width_veg	m	0.15	0.024	0.1	0.25	normal	*Cabbage*

9.5.6 Leaf area index

Leaf area index, LAI, is used in two different approaches; 1) to describe the density of the canopy in the atmospheric modelling of carbon-14. 2) to describe the potential adherence of radionuclides to the plant leaf surface when using irrigation in agricultural systems. The leaf area index describes the density of the vegetation and is expressed as the one-sided area of the green leaves in relation to the ground area. Generally, there is an increase in LAI from the beginning of the vegetation period reaching a peak during mid-summer and then a decrease towards the end of the vegetation period. For agricultural systems where crops are sown and grown during a single vegetation period, there is a steady increase in LAI until harvest. Consequently, the peak estimate will be higher than the average value during the vegetation period for most ecosystems in northern latitudes. For agricultural systems there are also periods during the vegetation period that are devoid of vegetation (e.g. after harvest or prior to sowing). Such periods have not been accounted for and the presented average estimates may therefore be slightly overestimated on an annual basis. However, in most cases, edible parts are produced in the mid-season when the LAI is at its peak (cereals and berries). On the other hand vegetables are steadily growing until harvest and the LAI could then roughly be described by the peak value divided by 2. Here, values represent peak values over all crops/ecosystems in order to have consistent approach, but which is somewhat cautious in some aspects.

The LAI representing the mire (LAI_ter) is based on the mean peak values from four boreal mires covering both rich and poor fens and one treed poor fen (Riutta et al. 2007, Glenn et al. 2006, Syed et al. 2006). The maximum value is taken from a reed wetland (Hardej and Ozimek 2002).

The LAI for cereals is represented by barley (LAI_cereal) and in grass crops the peak LAI is typically 3-6 (Williams 1980). The best estimate is from a study in south-central Sweden (Persson 1997) and the maximum value was from Petterson (1987).

Fodder (LAI_fodder) may to a large extent be dominated by different grass species and the same range is used for fodder as for barley. Fodder also to some extent contain other leguminous forage crops and the best estimate was chosen from Persson (1997).

A LAI range for potatoes (LAI_tuber) was suggested by Bergström and Barkefors (2004). Gordon et al. (1997) showed that Atlantic and Nordic varieties had a maximum LAI between 3 and 4, which was similar to their best estimate.

The leaf area index for vegetables (LAI_vegetables) is represented by cabbage (see also separate description of yield). Bergström and Barkefors (2004) suggested a best estimate and a range for leafy vegetables that was used. Lotz et al. (1997) showed a similar range for cabbage in a study on interspecific competition.

Standard deviations were based on a coefficient of variation from data describing LAI for the mire. The parameter values used are listed in Table 9-11.

Table 9-11. Parameter values describing the peak LAI (leaf area index) for four crops and mire vegetation (ter).

Crop	Unit	Central value	Stdev	Minimum	Maximum	Distribution
LAI_cereal	$m^2\ m^{-2}$	4	0.6	3	6.3	Normal
LAI_fodder	$m^2\ m^{-2}$	6	–	3	6.3	Uniform
LAI_ter	$m^2\ m^{-2}$	1.2		1	6	Uniform
LAI_tuber	$m^2\ m^{-2}$	4	0.6	3	5	Normal
LAI_veg	$m^2\ m^{-2}$	5	0.6	4	6	Normal

A comparison of LAI between three boreal and three arctic (Soegaard et al. 2000, Oechel et al. 2000) and one subarctic mire (Aurela et al. 2007) suggested small differences and the boreal value presented above could also represent periglacial conditions.

For the extended global warming case the LAI is expected to increase. The LAI on three temperate mires (Guo and Sun 2011, Moore et al. 2002, Chojnicki et al. 2007) were higher than the boreal estimate. The maximum was the same as for the boreal case. The increase in LAI for mire vegetation (50%) was assumed to also be representative for cereals. The standard deviation for cereals was assumed to be the same as for the temperate climate. Fodder LAI was assumed to be approximately the same as for the temperate climate (Table 9-12).

Table 9-12. Parameter values describing the peak LAI (leaf area index) for four crops and mire vegetation (ter) used in the extended global warming case.

Crop	Unit	Central value	Stdev	Minimum	Maximum	Distribution
LAI_cereal	$m^2\ m^{-2}$	6	0.6			Normal
LAI_ter	$m^2\ m^{-2}$	2.4		2.1	6	Uniform

9.5.7 Concentration of carbon in the atmosphere

The behaviour of carbon-14 in the biosphere is modelled using a specific activity approach, which is motivated by the strong influence that the carbon cycle has on the environmental behaviour of this radionuclide. The specific activity of carbon-14 in air is calculated using the total carbon concentration (all isotopes) in the atmosphere (conc_C_atmos). The Global Monitoring Division of the Earth System Research Laboratory has measured CO_2 and other greenhouse gases for several decades at a globally distributed network of air sampling sites (Tans 2009). The data were reported as the dry air mole fraction and were converted into mol CO_2 at +5°C using the ideal gas law. This estimate was then converted to kgC m^{-3}. The annual average of 2008 was used to represent a central value of the carbon concentration (representing 385 ppm of CO_2). The minimum value represents the value at the start of the measurements in 1959 and the maximum represents the maximum concentration used in the IPCC emission scenario A1B (717 ppm, SKB 2014d). A uniform distribution is assumed in the probabilistic estimates (Table 9-13).

The periglacial climate case is associated with low CO_2 concentration in the atmosphere and the estimate was taken from Kjellström et al. (2009), where it was based on ice-core records spanning the last 800,000 years (Kjellström et al. 2009 and references within) (Table 9-13). The standard deviation is based on the calculated coefficient of variation from the measurements at the Earth System Research Laboratory (Tans 2009)

The extended global warming climate case is associated with a high carbon emission rate and the value is taken from the IPCC climate scenario A2 (856 ppm, IPCC SRES 2000) and the standard deviation is based on the calculated coefficient of variation from the measurements at the Earth System Research Laboratory (Tans 2009). A normal distribution is assumed for the periglacial and the extended global warming distributions (Table 9-13).

Table 9-13. Carbon content of the atmosphere in different climate cases (kgC m^{-3}).

	Central value	Minimum	Maximum	Stdev	Distribution
Global warming climate case conc_C_atmos (kgC m^{-3})	2.0E–4	1.7E–4	3.8E–4		Uniform
Periglacial climate case conc_C_atmos (kgC m^{-3})	1.1E–4	0		1.4E–2	Normal
Extended global warming climate case conc_C_atmos (kgC m^{-3})	4.5E–4	0		1E–6	Normal

9.5.8 Wind velocity

The parameter wind velocity at 10 m height (vel_wind_height_ref_ter) was determined with data from the local meteorological station Högmasten at the Forsmark site. The data set was obtained from the SKB database Sicada (the Sicada delivery ID is Sicada_09_054_windspeed). The wind speed is registered at a height of 10 m (height_ref_ter) every 30 minutes and calculations are based on data for the period May 2003 to July 2007. Monthly means were calculated for the whole period, and the monthly means were used for the missing months in 2003 and 2007 so the data set would represent five years (Löfgren 2010, p 345).

Table 9-11. The wind velocity at 10 meters height (m s^{-1}).

Parameter	Unit	Central value	Stdev	Minimum	Maximum	Distribution
vel_wind_height_ref_ter	m s^{-1}	1.9	0.1	1.8	2.0	Normal
height_ref_ter	m	10	–	–	–	–

9.5.9 Vegetation height

This parameter (height_CA_cereal, height_CA_fodder, height_CA_tuber, height_CA_ter, height_CA_veg) describes the above-ground height of the canopy layer. Table 9-12 shows the different vegetation types or crops for which canopy heights were estimated. For monocultures, such as crops, estimates cover the variation within the species, whereas for "natural" ecosystems estimates have to cover different dominating species, e.g. due to succession. The height of the canopy layer of the mire is described by a mean that represents a *Carex*/herb dominated fen, minimum is a bryophyte dominated fen and maximum represents a reed dominated fen. The mean value for the mire would also be applicable to a periglacial and an extended global warming climate. The standard deviations were derived by using the coefficient of variation (CV) from the biomass estimates above (CV=0.16).

Table 9-12. The canopy heights of different agricultural and wetland vegetation communities.

Vegetation	Unit	Central value	Stdev	Minimum	Maximum	Distribution	Genus/species
height_CA_cereal	m	0.9	0.14	0.4	1.2	normal	*Hordeum, Avena*
height_CA_fodder	m	0.4	0.06	0.25	0.6	normal	*Poaceae,herbs*
height_CA_tuber	m	0.4	0.06	0.25	0.7	normal	*Potatoe*
height_CA_ter	m	0.3		0.05	2.0	uniform	*Carex, Phragmites*
height_CA_veg	m	0.25	0.04	0.15	0.4	normal	*Cabbage*

9.6 Fluxes of chlorine in ecosystems

These parameters describe natural concentration of stable chlorine in mire ecosystems.

9.6.1 Concentration of chlorine in mire vegetation

This parameter (conc_Cl_PP_ter) describes the naturally occuring combined organic and inorganic chlorine concentration in the vegetation of the treeless mire (see Section 9.3). It is based on measurements from one alder swamp forest, a drained peatland with forest regrowth and one oak forest in Laxemar in south of Sweden (Löfgren 2010). The seven samples represents three green tissue samples from trees and four samples from the field layer and are presented as gCl kgC^{-1}. No values were found for mire vegetation in the literature, but Van den Hoof and Thiry (2012) presented a figure for pine tree needles corresponding to 1.2 gCl kgC^{-1}. Similarly, Lovett et al. (2005) reported two values for sugar maple leaves of 0.7 and 0.8 gCl kgC^{-1}. Lobert et al. (1999) reviewed the chlorine content for a broad spectrum of functional groups covering both tropical as well as temperate vegetation and reported a range between 0.02 and 18.8 gCl kgC^{-1} based on 531 observations. For plant growth, a general Cl^- requirement of 2 g kgC^{-1} has been suggested (assuming a carbon content of 0.5 kg kg^{-1} dw), but deficiency symptoms have been observed at 0.2–11.4 gCl kgC^{-1}, whereas toxic levels between 8–100 gCl kgC^{-1} have been reported for agricultural crops (White and Broadley 2001). The geometric mean was chosen to represent the central value of the seven observations from Laxemar. The minimum was also taken from the seven samples whereas maximum was set to the upper range of where toxic levels were observed. (GM = 2.1, GSD = 3.5, minimum = 0.2, maximum = 100 gCl kgC^{-1}).

9.6.2 Concentration of dissolved chlorine in the mire pore water

This parameter describes the concentration of dissolved chlorine in mire pore water of the upper oxidised part of the peat layer that is available for root uptake (conc_Cl_regoUp_ter_D). It is based on measurements from five mires in Forsmark, where each mire is represented by 5 pooled samples covering an area of 300 m^2 taken at a depth of 20–25 cm below the ground surface (Sheppard et al. 2011). A geometric mean of the five samples was chosen to represent the best estimate. (GM = 13.9, GSD = 4.9. minimum = 3.1, maximum = 242.1 gCl m^{-3}).

9.6.3 Discrimination factor during decomposition for chlorine

The parameter df_decomp_Cl describes the rate of chlorine released through fast mineralisation of litter (mire vegetation or lake vegetation) relative the rate of organic matter decomposition. For all other elements we assume that radionuclides in plant and litter are incorporated into organic matter and released in proportion to the mineralisation of organic matter (df_decomp_ter and df_decomp_aqu = 1). However, approximately 60% of chlorine in living plant tissue is found in inorganic form (Redon et al. 2011), and this fraction can be expected to be readily released when the leaves senesce and cell membranes are disrupted. If it is assumed that all inorganic radionuclides in litter are released within a year, then df_decomp can be calculated from the partitioning of radionuclides in the organic and inorganic fractions:

df_decomp= f_org + f_inorg /(1-f_refrac),

where f_org and f_inorg is fractions of a radionuclide in organic matter and inorganic form respectively, and f_refrac is the fraction of refractory organic material in litter (which is left after initial mineralisation). The central value of df_decomp_Cl was calculated by adopting the value by Redon et al. (2011) for f_org and the f_refrac described earlier (see 9.9). A minimum value was calculated by assuming a somewhat more effective mineralisation (f_refrac = 0.2). A maximum value was calculated by assuming that only 20% of the chlorine is found in the organic fraction (Bastviken pers. Com.)

Table 9-13. Parameter value describing the fraction of chlorine that is available through mineralisation. Values are unitless.

Parameter	Central value	Minimum	Maximum	Distribution
df_decomp_Cl	1.26	1.15	1.34	Uniform

9.7 Depth of biological active layer of peat and cultivated peat

The parameter z_regoUp_ter represents the depth (m) of the more or less unsaturated peat layer where the highest biological activity is found e.g. the largest part of the heterotrophic respiration and all autotrophic root respiration occurs in this zone if vascular plants are present. This zone represents the volume from which root uptake occurs. The below-ground biomass is typically found in the uppermost 30 cm. As an example Saarinen (1996) showed that the roots of *Carex rostrata* were found to a depth of 23 cm in a Finnish mire. The distinction between this layer and the permanently anoxic layer beneath may be more or less sharp and vary as a consequence of the plant community and the variation in groundwater depth. *Sphagnum*-dominated poor fens and bogs have a sharper boarder between the acrotelm and the permanently anoxic catotelm layer, whereas fens with a more dominating vascular plant community will have a somewhat more diffuse zone between these zones called mesotelm. This is due to the aerenchyma that many wetland vascular plants have that is able to transport oxygen (and carbon dioxide and methane) from the atmosphere down to the roots and to the root exudates provided by the plants in this oxygen-enriched zone. The depth of this zone also changes during the year due to temperature but mainly due to variation in water table depth and NPP. The variation in water table depth is generally less in fens fed by minerogenic water, as compared with rain-fed bogs (e.g. Kettunen et al. 1999, Webster and McLaughlin 2010) and the water table is usually found close to the vegetation surface in the fens in Forsmark (Löfgren 2011). Fens in Forsmark are characterised by a high abundance of vascular plants and a dominating *Sphagnum* community is only present in late successional bog-like stages further inland (> 2,000 years old). Overall, a lowered water table decreases methane emissions and increases oxidation processes as the unsaturated zone increases, whereas a high water table will increase methane emissions and decrease mineralisation processes as a consequence of a change in the aerobic/anaerobic environments. One way of assessing the depth to which there are aerobic conditions is to use data describing the methane oxidation that occurs in presence of oxygen. Sund et al. (1994) found the maximum oxidation rate to be close to the water table depth and diminished between 0.1 to 0.4 m below the average water table depth. Similar intervals were also found by Kettunen et al. (1999). Mäkilä and Goslar (2008) estimated the age of the acrotelm to between 300 and 500 years, which was found less than 0.4 m below the peat surface, based on a large sample from Finnish mires. The depth of this zone was set to 0.30 m below the peat surface and is an approximated depth during the vegetation period. The minimum is set to 0.1 m and the maximum to 0.40 m below the peat surface. The distribution was defined as uniform, due to the potential for all values within the range to occur during successional development.

In the drained mire, z_drain_agri defines the unsaturated regolith layer, which also approximates the effective drainage depth of the mire. This is the depth in which all roots are contained. Mueller et al. (2005) showed that the water table depth is the best measure for controlling both production and water use efficiency at comparable climatic and soil conditions. Too shallow a water table depth will lower the production and it is therefore a trade-off when investing time making the drainage channel system deep enough. Mueller et al. (2005) showed that different grass species suitable for hay production could reach high production at a water table depth of around 0.5. Here, this figure is used to represent a suitable water table depth for all crops that are cultivated on the drained mire. This parameter is assumed to be a fixed value and was not varied in the probabilistic simulations. The z_drain_agri depth is applied on the consolidated peat or gyttja. This approximates close to 1.5 m of unconsolidated peat in an newly drained fen. The consolidation starts immediately as the draining begins and is a function of subsidence and oxidation rates. The time varies, but is here assumed to be representative of at least 50 years of agricultural use. In the modelling the process of consolidation is also assumed to take place instantaneously, which means that the crop will be exposed to the radionuclide inventory of, in this case, 1.5 m undrained and unconsolidated peat immediately instead of a successive increase of the peat depth (see also description of compaction in Section 5.4.3).

For the garden plot and the infield-outland calculation cases z_regoUp represents the thickness of the layer in arable land that is regularly ploughed (Karlsson et al. 2001) and is also the layer in which most of the roots are found.

Table 9-14. The depth of the upper biological active layer in mires, drained mires and cultivated soils (m).

Land-use type	Parameter	Unit	Central value	Minimum	Maximum	Distribution
Mire	z_regoUp_ter	m	0.3	0.1	0.4	Uniform
Drained_mire	z_drain_agri	m	0.5			Uniform
Garden_plot	z_regoUp	m	0.25	0.2	0.3	Uniform
Infield_outland	z_regoUp	m	0.25	0.2	0.3	Uniform

9.8 Hydrological fluxes in agricultural soil

This section describes the downward and upward fluxes of water in a drained mire used for agricultural purposes.

9.8.1 Percolation in areas used for cultivation

This parameter (percolation_agri) is used to calculate the leaching of radionuclides previously incorporated into the organic soil layer. Percolation is the net downward flow (precipitation-interception-evaporation-transpiration) to the saturated zone causing leaching in the upper aerated and biologically active layer (z_regoUp). The evapotranspiration is expected to be higher on agricultural land during the vegetation period (=less runoff), but is on the other hand lower during other periods due to lack of vegetation and lower potential evaporation rates. A general figure based on the landscape area therefore may be a good enough best estimate of the actual amount of water passing the upper peaty soil layer of the agricultural land causing leaching of radionuclides.

The percolation is derived from hydrological modelling using MIKE-SHE simulations describing the landscape of Forsmark at 2000 AD, 5000 AD and 10,000 AD (Bosson et al. 2010). Based on these three simulations with a similar climate as today the mean percolation was 0.198 $m^3 m^{-2} year^{-1}$ (0.183, 0.183, 0.227 $m^3 m^{-2} year^{-1}$).

The percolation was of similar magnitude to the runoff (the runoff/percolation ratio was 0.96, 1.01 and 0.81 for the three simulations), which made it possible to use statistics describing runoff to infer statistics for the percolation. The modelled runoff is similar to the long-term data set from Vattholma (Larsson-McCann et al. 2002). Minimum, maximum and standard deviation values for runoff were based on this time serie of monthly mean discharge from year 1917 to 2000 (SMHI station 50110). Data are presented in Table 9-15.

According to an earlier calculation, a global warming case would both include a higher temperature as well as more precipitation. Simulating wetter and warmer conditions inferred from global warming, hydrological modelling (Bosson et al. 2010) suggested that both the runoff and the percolation will increase (mean from three simulations was 0.262 $m^3 m^{-2} year^{-1}$). This value is within the range given for the probabilistic simulation below and is therefore considered to be included in the probabilistic approach.

In an extended global warming calculation case, the percolation has been shown to be affected by a variety of different factors and can therefore present a range of different values (e.g. BACC (2008) presented data for the change in volume of discharge into the Bothnian Sea). It was concluded that the range presented in the main temperate case would also include this case.

In the periglacial calculation case, no draining of mires for agricultural use is considered, and therefore no alternative data for percolation are needed.

Table 9-15. Percolation in agricultural soils.

Parameter	Unit	Central value	Stdev	Minimum	Maximum	Distribution
percolation_agri	$m^3 m^{-2} year^{-1}$	0.20	0.08	0.07	0.45	Normal

9.8.2 Upward flux of groundwater into the unsaturated zone of the agricultural land

This parameter (flux_water_satSoil_agri) describes the upward flux of groundwater into the unsaturated zone of the agricultural land, where the roots are found. This groundwater flux is driven by evapotranspiration and is affected by the amount of water originating from precipitation that is available in the root zone. The potential use of groundwater mainly depends on water table depth, crop type and biomass (Mueller et al. 2005). The upward transport of radionuclides in the agricultural land is proportional to the upward flux of groundwater and the concentration of radionuclides in the solute phase.

Johansson and Klingspor (1977) modelled the daily balance between precipitation and evapotranspiration during the vegetation period for a number of different regional areas in Sweden during a normal year (1976) and a dry year, taking the soil type into account (detailed description of methods in Johansson (1973)). A need for additional water is defined as when the water content in the root zone comes close to the wilting point. At that point, additional water is needed to support plant maintenance and growth. The modelled need for additional water input could be provided either by irrigation or by capillary rise from deeper soil layers and the groundwater table. The results of the modelling suggest that potatoes and fodder generally need more water than barley. The range of the additional need for water was 20 mm during a normal year and 65 mm during a dry year for barley in central Sweden. For potatoes and hay the range was between 80 and 115 mm. Both these studies represent agricultural land dominated by a low organic content and fine grained soil, such as clay, whereas the agricultural soils considered in the biosphere objects are dominated by peat soils. Peat soils have a high water-holding capacity and may therefore be regarded similar to fine-grained agricultural soils in that respect. Another consideration is the relatively shallow groundwater table in the drained peatland compared with the investigated agricultural lands.

Generally, the evapotranspiration during the vegetation period is dominated by water originating from precipitation, but Mueller et al. (2005) found that this dominance decreased as the water table depth decreased and water originating from groundwater became dominant for e.g. grasslands with a shallow groundwater depth and wetlands (see also Johansson 1973). Mueller et al. (2005)

estimated the groundwater recharge during the vegetation period to be 10–60 mm for spring barley and 80–300 mm for pasture grasses for various soils and groundwater depth levels. The higher end represents conditions with shallower groundwater depths, which would be similar to conditions in a drained peatland. The larger span for grass is explained by the larger span in groundwater table (GWT) depth with 0.4–1.2 m for grasses and 0.8–1.0 m for spring barley. This also illustrates a higher tolerance for a more shallow GWT depth for hay. Moreover, because of the higher annual mean temperature (but similar annual precipitation) and higher production on the fields in central Germany investigated by Mueller et al. (2005) the values are expected to be higher than those from central Sweden.

In the earlier safety assessment of SFR the upward transport from the GWT to the unsaturated zone below an upper soil layer (ploughing depth, same as here) was estimated to be 200 mm (range 100 to 300 mm), where the GWT depth was approximately one metre. The upward transport to the top soil was set to 100 mm (range 50 to 200 mm) (Karlsson et al. 2001). The first figure was based on lysimeter experiments (BIOMOVS II 1996) and the second was set to 100 mm as "the influence of capillary rise will decrease when the distance to the groundwater table increases".

These studies present estimates of similar magnitude and may vary due to factors such as crop, biomass, water table depth and climate. Based on the two previous studies it is suggested that the upward flux of groundwater from a drained mire with shallow groundwater table, would be within the range of 20 to 65 mm for barley as a long-term annual average, while the flux would be between 80 and 300 mm for hay. These ranges would also include warmer conditions. A central value was chosen within the range presented above and standard deviation was calculated by assuming that the minimum value represented the 2.5% percentile.

Table 9-16. Parameter values describing the upward transport of groundwater into the root zone for cereals grown on a drained mire. All values are in $m^3\ m^{-2}\ year^{-1}$.

Parameter	Mean	Stdev	Minimum.	Maximum.	Distribution
Flux_water_satSoil_agri	0.04	0.012	0.02	0.07	Normal

9.9 Mineralisation

Organic matter is continuously produced within the ecosystem and is found as biomass and as organic matter in the soil. The mineralisation of organic matter is dependent on several factors, such as temperature, oxygen availability and quality of the organic material. Below, the mineralisation rates for different parts of the terrestrial ecosystem are described.

9.9.1 Mineralisation rate in different layers and ecosystems

In wetlands the mineralisation is constrained by the variation in oxygen availability temperature and accumulation of refractory organic matter and metabolic end products down the peat profile (Limpens et al. 2008). Wetlands exhibit anaerobic conditions throughout most of the peat profile and most of the decomposition occurs in the uppermost layer (the acrotelm) that is periodically enriched with oxygen (Malmer and Wallén 2004). In vascular-plant-dominated mires, this zone goes deeper due to their potential of transporting oxygen through aerenchyma down to the root zone creating a periodically and spatially variable oxic/anoxic zone (mesotelm). Decomposition in this zone therefore is temporally and spatially variable due to variation in oxygen availability. This zone is generally absent in bryophyte dominatedmires such as bog-like wetlands dominated by *Sphagnum* species. The water table fluctuation is the main determinant of the border between the acrotelm and the deeper peat. Below the acrotelm (and the mesotelm) there is the zone described as having permanent anoxic conditions (catotelm) characterised by a low decomposition rate (i.e. 50 to 100 times lower than the decomposition in the acrotelm).

Decomposition of above-ground recently shed litter is characterised by a relatively fast mineralisation rate, although there are differences in regard to quality of the litter. Generally, vascular plant litter has a higher relative mass loss than for example *Sphagnum* litter during the first few years

(Thormann et al. 2001). In the peat bog profile most of the decomposition occurs in the upper 10 cm and decrease fast with depth. For fens this depth gradient is less steep as the mesotelm provides periodically oxic conditions increasing the decay potential. Wetland plant species generally have a large root biomass in comparison with the above-ground biomass (e.g. Backéus 1990), suggesting that the input of litter to the mesotelm is large.

The initial mass loss is described by the parameter f_refrac_ter and is here defined as the litter remaining after 10 years, which represents the years of relatively fast decay under predominately oxic conditions. Few experimental estimates are available for a ten year period in wetlands. An alternative way of estimating the decay is to use a modelling approach. A single-exponential linear regression model has been used to describe the decay process (e.g. Heal et al. 1978, Moore et al. 2007). However, estimates from this type of model tend to underestimate the remaining mass in the later stages (Yu 2006). Nevertheless, Figure 9-5 shows the mass loss after 10 years based on a litter bag experiment in a temperate poor fen in North America over 4.5 years. Similar experiments show a broad span of decay constants, with the mass loss for underground parts spanning between 5 and 77% (Thormann et al. 2001). Reader and Stewart (1972) related the NPP to the long-term accumulation and showed that less than 10% of the NPP ended up as peat deep in the profile. Based on these patterns, the parameter value describes the initial mass loss of the litter in a fen, where it was assumed that 30% was left after initial decay and that this then entered the somewhat deeper semi-oxic compartment. A span was assumed where the minimum was set to 5% and maximum to 50% (Table 9-18). This span is assumed to cover a range of different temperature conditions, including the temperature increase associated with the base climate case.

The parameter minRate_regoUp_ter represents the mineralisation in the acrotelm and mesotelm layer after the initial mass loss and is the mineralisation of more refractory organic material in a zone with more or less oxic conditions. Mäkilä and Goslar (2008) made detailed descriptions of the carbon accumulation rate in a large number of peat profiles in southern and central Finland. The general pattern was that the carbon loss became close to zero between the age of 300 and 500 years reflecting the zone where partly oxic conditions becomes permanently anoxic (i.e. mesotelm turns to catotelm). The sampled mire could be divided according to different geographical zones, coastal mires and ombrotrophic mires dominated by *Sphagnum* and Aapa mires with *Carex* sp. These figures were relatively similar, and the lowest decomposition rate was found in the region where the largest accumulation was found (Table 9-17). A similar value was found by Beer and Blodau (2007) in the upper zone of a peat bog in Canada based on measurements of decomposition products and modelling (0.003 $year^{-1}$). Similarly, Clymo and Bryant (2008) used a figure of 0.0034 $year^{-1}$ to describe mesotelm decay. Based on these figures and the basis of representing a fen in a coastal area of central Sweden, the central value was set to 0.0029 $year^{-1}$ approximated by the *Carex*-dominating aapa mires (Table 9-18).

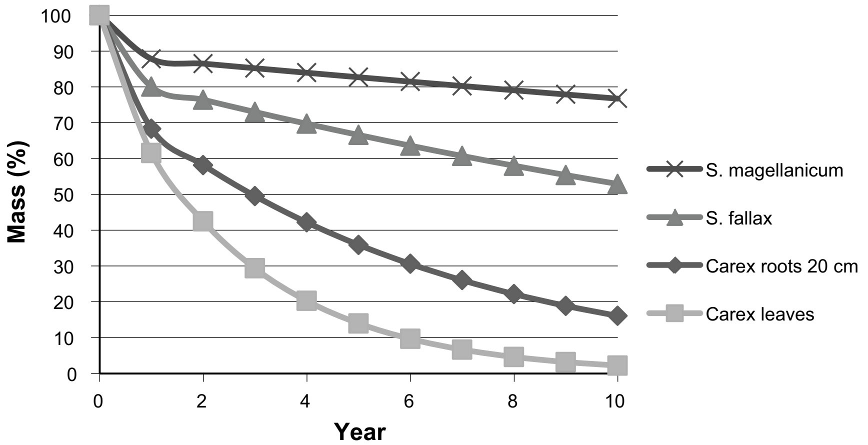

Figure 9-5. *Modelled mass loss for Sphagnum fallax, S. magellanicum and Carex rostrata using a single-exponential linear regression model: i.e. ln y=a–kt where a is the intercept, t the time and k the decay constant taken from Moore et al. (2007).*

Table 9-17. Estimates of mass loss in the upper part of the peat column recalculated after Mäkilä and Goslar (2008).

	Geographical region in Finland		
	Coastal mire	Raised bog	Aapa mire
10 year (gDW)	116	78	96
300 year (gDW)	40	20	16
Remaining mass	0.34	0.26	0.17
Decomp per year	0.0023	0.0026	0.0029

minRate_regoPG_ter represents the mineralisation in the post glacial (PG) gyttja clay deposited below the peat during the preceding marine and lake stages. Deeper peat is less susceptible to environmental fluctuations and the decomposition rate is expected to be similar to deep-lying peat and fairly constant over time. It is therefore assumed that decomposition in the post-glacial gyttja clay layer is similar as the decomposition in deep catotelm. The representative value was taken from Clymo and Bryant (2008) representing catotelm peat dominated by *Sphagnum* and the range is assumed to be 20% around the mean for the minimum and maximum mineralisation rates.

When the mire is drained with the purpose of growing crops the peat will be subjected to compaction (see separate parameter for regolith, Section 5.4.3) and to increased mineralisation due to the oxidised conditions above the new groundwater level. Numerous studies have been performed on agricultural land with organic soil in order to estimate greenhouse-gas emission (e.g. review in Maljanen et al. 2010, Kasimir-Klemedtsson et al. 1997). Maljanen et al. (2010) concluded that the CO_2 emissions from peatlands used for agriculture differ in magnitude resulting from differences in cultivation methods, crops and weather conditions. Moreover, factors such as draining depth and soil properties are factors that also influence the mineralisation rate (e.g. Berglund and Berglund 2011). A mean estimate from 19 studies of the CO_2-C gas emissions gave an average of 0.64 kgC $m^{-2}year^{-1}$ (Oleszczuk et al. (2008), only including data based on CO_2 flux measurements). Assuming a groundwater level below 1 m and a bulk density similar to a degraded organic soil in Forsmark suggested a mean mineralisation rate of 0.005 $year^{-1}$. A closer examination of CO_2 flux data from Maljanen et al. (2007), where data were available for carbon content, bulk density, water table depth and crops (barley, grass, ley and without vegetation), suggested a range between 0.005 and 0.009 $year^{-1}$ for areas that had been drained between 40 to 100 years ago. Similarly, data from Berglund (2008) from two drained mires suggested that the rate of mineralisation in the early phase (26 and 41 years after drainage) was 0.004 and 0.007 $year^{-1}$ for a drained bog and fen, respectively, after discarding the first 6 to 14 years of initial compaction. Based on these figures, the best estimate is chosen from the fen in accordance with the assumption that the fen generally is regarded more suitable for agricultural purposes. A standard deviation was derived for the mineralisation rate of postglacial deposits by assuming that the minimum value was equal to the 5% percentile.

Generally, the variation in mineralisation may be large due to differences in temperature and precipitation on a year- to-year basis (e.g. Waddington and Roulet 2000). A long-term temperature or precipitation change will also affect the long-term mineralisation rate e.g. Lund et al. (2010) showed a positive correlation between ecosystem respiration and air temperature for mire ecosystems. The parameters f_refrac_ter and minRate_regoUp_ter would be sensitive to an increased temperature, whereas minRate_regoPG_ter is expected to be less sensitive to changes in the assumed future temperature, due to its fairly deep deposition under anoxic conditions. The parameter f_refrac_ter is here assumed to be constant meaning that the actual amount of organic material incorporated into rego_Up_ter is less under colder conditions and larger under warmer conditions due to the lower and higher NPP, respectively. It is also suggested that the large span describing the potential distribution of f_refrac_ter in the probabilistic calculations will include the effects of both colder and warmer conditions. The minRate_regoUp_ter is expected to be much less under a periglacial climate and was scaled down by the same value as the empirically derived NPP values (28% of the global warming values describing the central value, minimum and maximum).

Table 9-18. The parameters and their estimated values that describe the mineralisation within the peat column. The unit can be expressed as kgC kgC^{-1} year^{-1} or as year^{-1}.

Land-use type	Parameter	Unit	Central value	Stdev	Minimum	Maximum	Distribution
Mire	f_refrac_ter	kgC kgC	0.3		0.05	0.5	Uniform
Drained mire	minRate	kgC kgC year^{-1}	0.007		0.004	0.009	Uniform
Garden plot	minRate	kgC kgC year^{-1}	0.0029		0.0023	0.0034	Uniform
Infield outland	minRate	kgC kgC year^{-1}	0.0029		0.0023	0.0034	Uniform
Mire	minRate_regoUp_ter	kgC kgC year^{-1}	0.0029		0.0023	0.0034	Uniform
Mire	minRate_regoPG_ter	kgC kgC year^{-1}	6.5E–5	8.0E–6	5.2E–5	7.8E–5	Normal

9.9.2 Mineralisation rate in the anoxic peat layer at equilibrium

Peat accumulation in anoxic, water saturated, environments is primarily limited by oxygen depletion (Limpens et al. 2008), and organic matter accumulation will reach a steady state when the depth of the anoxic peat layer is approaching the groundwater level. For wetlands that develop in lakes, this depth is assumed to be sufficiently well approximated by the average depth of the lake basin (i.e. organic matter accumulation in the model reflects filling the original lake basin with peat). Thus, for modelling purposes, the mineralisation rate in the anoxic peat layer is set to the rate that will balance the input of organic matter at a peat depth corresponding to the groundwater level. In mathematical terms this mineralisation rate (kgC kgC^{-1} year^{-1}) can be expressed as the area-specific carbon burial rate (kgC m^{-2} year^{-1}) divided by the area specific mass of a peat layer at equilibrium depth (kgC m^{-2}).

$$minRate_{regoPeat} = \frac{Burial_C}{z_{regoPeat\_equlib} \times dens \times_{regoPeat\_ter} f_{C\_peat}}$$

where

$Burial_C$ is the yearly input of soil organic carbon to the anoxic peat layer from the partly oxygenated peat layer (kgC m^{-2} year^{-1}),

$z_{regoPeat\_equlib}$ is equilibrium depth of the anoxic peat layer at the end stage of terrestrialisation (m),

f_{C_peat} is the fraction of carbon in peat (kgC kgdw^{-1}), and

$dens_{regoUp\_ter}$ is the density of the upper terrestrial layer (kgdw m^{-3}).

From mass balance it follows that the area-specific rate of carbon burial ($Burial_C$, kgC year^{-1} m^{-2}) equals the input of refractory carbon from litter less the loss of carbon from mineralisation in the uppermost peat layer. Mathematically, this can be expressed (Saetre et al. 2013a):

$$Burial_C = NPP_{ter} \times f_{refrac\_ter} - SOC_{regoUp\_ter} \times minRate_{regoUp\_ter} / area_{obj\_ter}$$

where

NPP_{ter} is the net primary productivity per unit area (kgC m^{-2} year^{-1}),

$area_{obj\_ter}$ is the area of the terrestrial ecosystem (m^2),

f_{refrac_ter} is the refractory material left after mineralisation (kgC kgC^{-1}),

SOC_{regoUp_ter} is the amount of soil organic carbon in the upper peat layer (kgC), and

$minRate_{regoUp\_ter}$ is the mineralisation rate of refractory organic carbon in oxic environment (kgC kgC^{-1} year^{-1}).

At the end stage also the upper peat layer will be in equilibrium, and the area-specific amount of soil carbon of this compartment will simply be the depth of the layer multiplied by the density of peat and its carbon fraction.

$$SOC_{regoUp\_ter}/area_{obj\_ter} = z_{regoUp} \times dens_{regoUp\_ter} \times f_{c\_peat}$$

Thus the mineralisation rate in the peat layer

$$minRate_{regoPeat} = \frac{NPP_{ter} \times f_{refrac\_ter} - z_{regoUp} \times dens_{regoUp\_ter} \times f_{C\_peat} \times minRate_{regoUp\_ter}}{z_{regoPeat\_equlib} \times dens_{regoPeat\_ter} \times f_{C\_peat}}$$

The mineralisation rate is expected to be lower in the anoxic compared with the oxic layer (the parameter minRate_regoUp_ter = 0.0029), but is higher for two objects (Table 9-19). This is explained by the fact that the average peat layer thicknesses of these objects are rather thin and this layer will be dominated by oxidised conditions.

For the calculation case alternative object delineation, the mineralisation rate is altered. This is described in Section 12.3.

Table 9-19. The mineralisation rate in the anoxic peat layer at equilibrium, which is reached in the specified year.

Biosphere object	Year (AD)	$minRate_{regoPeat}$ (kgC^{-1} $year^{-1}$)
116	9900	0.0011
160	8800	0.0008
121_1	6300	0.0016
121_2	4000	0.0053
157_1	5700	0.0009
157_2	4500	0.0064
159	7600	0.0008

9.10 Dust concentration

This parameter (conc_Dust) describes the dust concentration in the air above mires and drained mires. No site-specific data on dust concentrations are available from the Forsmark area. The estimate for the pristine mire is instead built upon measurements made during 7 years at two costal locations (IVL 2009). The largest part of the dust is represented by small particles (< 10µm) and larger particles (soot). The larger particles are of minor importance for the total dust concentration. It was not possible to get longer time series of both fractions from the same site and two relatively closely situated sites at the southeast coast of Sweden were therefore used to make aggregated estimates (Aspvreten and Hoburgen). As a central value, a value recommended for use in assessments of doses to the public (UNSCEAR 2000) was used (0.05 mg m^{-3}). The value is of the same order of magnitude as dust concentrations recommended for outdoor environments in risk assessments for contaminated ground by the Swedish Environmental Protection Agency (Liljelind and Barregård 2008, Naturvårdsverket 2009) and is approximately three times higher than the estimates from the two coastal locations. It is therefore considered as a cautious estimate.

In the probabilistic calculations for a drained mire, a maximum value 10% higher than the best estimate was used, whereas half of the best estimate is used as a minimum value. For the cases of garden plot and infield-outland, the same values were used as for the drained mire. In the probabilistic calculations a uniform distribution was used for all four sets of values.

Table 9-20. The parameter values describing the dust concentration for different environments (kgdw m^{-3}).

Land-use type	Parameter	Central value	Minimum	Maximum	Distribution
Drained mire	conc_Dust	5.00E–08	2.50E–08	5.50E–08	Uniform
Garden plot	conc_Dust	5.00E–08	2.50E–08	5.50E–08	Uniform
Infield outland	conc_Dust	5.00E–08	2.50E–08	5.50E–08	Uniform
Mire	conc_Dust_ter	1.4E–08	1.2E–08	5.0 E–08	Uniform

9.11 Crop yields

These parameters represent the total yield at harvest of four different representative crops that have been grown and still are grown in the region today. The production estimates represents an industrial community at the beginning of the 20th century (Saetre et al. 2013b). The representative for a cultivated cereal is barley, which is the most productive of the most commonly grown cereals in regard to absolute yield during the 19th century and today (Jordbruksverket 2012). Barley is also the cereal species that is most appropriate to cultivate on organic soil (Berglund 2008). Moreover, barley is today the most commonly grown cereal in the Forsmark area. Harvest of hay for storage is necessary to sustain livestock during winter conditions. Hay has historically been harvested from several different ecosystems, such as sea and lake shores, mires and from agricultural land (Löfgren 2010). Potatoes are a highly productive commonly grown crop, which represents a crop with edible roots. Also cabbage is commonly grown and has been chosen to represent a highly productive vegetable that is also suitable for consideration in a case in which the effects of irrigation are investigated.

The statistics in Table 9-21 have been derived from agricultural statistics available from the Swedish Board of Agriculture (Jordbruksverket 2012). For barley, hay and potatoes, the mean values only represents the national mean estimated yield between 1913 and 1917, because of the increasing yields during the rest of the century (Figure 9-6). The standard deviation, minimum and maximum are based on the period 1913 to 1962. Uppsala County generally has a lower yield than the national average for potatoes and barley, but has a slightly higher hay production per unit area. Moreover, there is a gradient with lower yields when approaching the coast and the Forsmark yield area, which reflects different soils and climate (Löfgren 2010, Table 4-11). By using the maximum value for Sweden (which reflects the yield in the southernmost Sweden) a reasonable estimate for global warming conditions has been included.

Statistics representing the garden plot describe the potential production of today and for vegetables the statistics are based on national figures for the period 1971 to 2008 (Figure 9-7). Statistics describing potato production are based on the period 1963 to 2007. The same source was used as for the agricultural statistics above.

The carbon content was calculated using data from the National Food Agency´s database (Livsmedelsverket 2001) for cereals and potatoes, 0.35 kgC kgdw^{-1} and 0.08 kgC kgdw^{-1} respectively. For fodder, the carbon content was assumed to be 0.46 kgC kgdw^{-1} (Löfgren 2010).

Table 9-21. Parameter values describing the yield for four crops with different properties representing an industrial agricultural society at the beginning of the 20th century.

Land-use type	Parameter	Unit	Central value	Stdev	Minimum	Maximum	Distribution
Drained mire	biom_cereal	kgC m^{-2}	0.06	0.011	0.048	0.097	Normal
Drained mire	biom_fodder	kgC m^{-2}	0.160	0.029	0.081	0.216	Normal
Drained mire	biom_tuber	kgC m^{-2}	0.096	0.015	0.056	0.136	Normal
Infield outland	biom_cereal	kgC m^{-2}	0.05	0.010	0.03	0.07	Normal
Garden plot	biom_tuber	kgC m^{-2}	0.219	0.036	0.137	0.295	Normal
Garden plot	biom_veg	kgC m^{-2}	1.03	0.12	0.84	1.22	Normal

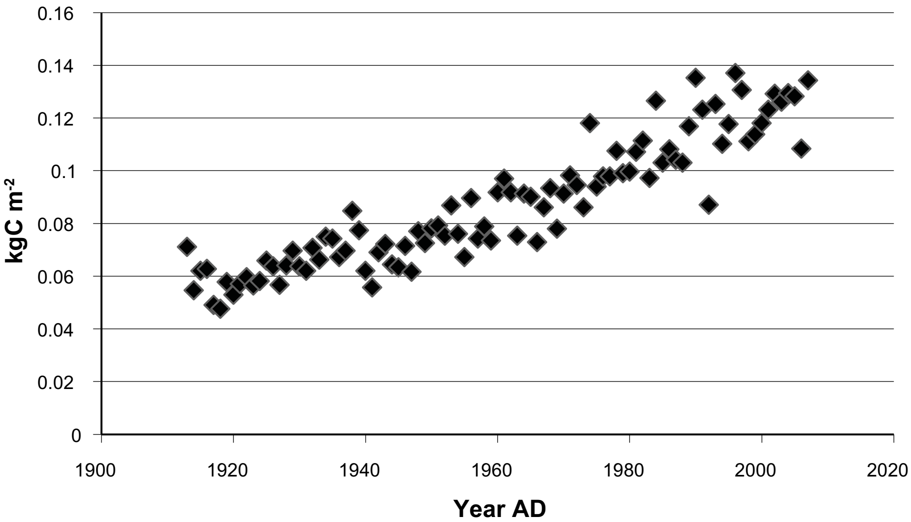

Figure 9-6. *National average of barley yield between 1913 and 2007 in Sweden (Jordbruksverket 2012, see text).*

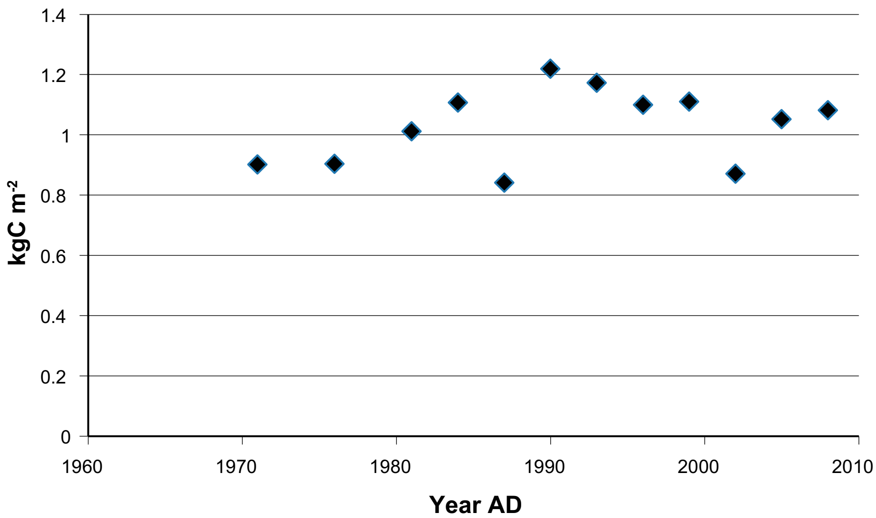

Figure 9-7. *National average of cabbage yield between 1971 and 2008 in Sweden (Jordbruksverket 2012, see text).*

The production of cereals on arable land during the time of an infield-outland farming system is based on a food and energy budget for 6 adult individuals (Widgren 1979). Then the production on 1 ha of arable land was estimated to 500 kgC ha^{-1}. The standard deviation was deduced from the coefficient of variation for barley in an industrial agricultural system. Minimum and maximum values were estimated by applying a factor of ±40%, which was the mean range for production estimates of barley, hay and potatoes in an industrial agricultural system.

This parameter describes the above-ground biomass at harvest for cabbage. It is used for estimating the retention of radionuclides in the case where effects of irrigation are investigated on the garden plot. The values are based on national statistics between 1971 and 2008 available from the Swedish Board of Agriculture (Jordbruksverket 2012). A normal distribution was assumed. (Mean = 1.03, Stdev = 0.12, minimum = 0.84, maximum = 1.22 kgC m^{-2} $year^{-1}$).

In the modelling of the atmospheric concentrations of volatile radionuclides it is necessary to take into account uptake by the vegetation. In the case of carbon-14, the carbon net assimilation is estimated for the different crops by applying biomass conversion factors on the yield estimates presented in Table 9-22. To the cereal estimate a generic value of threshing loss (5%) and straw yield (40%) was added to the above-ground production. The below-ground production was assumed to be 33%

of the above-ground production for cereals and fodder. The above-ground production for tuber was assumed to be 154% of the below-ground production (Bray 1963). A standard deviation was derived for the NPP of cereal representing a preindustrial community by assuming the same coefficient of variation as for the industrial agricultural community NPP.

In northern Europe, crop yield is limited by low temperature and in southern Europe by high temperature and low rainfall. Somewhere in between these geographical locations, the maximum crop yields are expected. The extended global warming climate implies a maximum annual mean temperature of above 10 degrees, which is similar to the annual mean temperatures of southern Europe. We assume that a maximum yield approximated by central European yields is reached somewhere during an extended global warming climate. A comparison of grain yields between Sweden and central Europe suggests a potential increase of 70% (e.g. Olesen et al. 2011). Accordingly, this factor was applied to the yield estimates of all agricultural products for the extended global warming calculation case.

Table 9-22. Parameter values describing the total NPP for four crops with different properties representing an industrial agricultural society at the beginning of the 20th century.

Land-use type	Parameter	Unit	Central value	Stdev	Min	Max	Distribution
Drained mire	NPP_cereal	kgC m^{-2} $year^{-1}$	0.117	0.022	0.094	0.19	Normal
Drained mire	NPP_fodder	kgC m^{-2} $year^{-1}$	0.213	0.039	0.108	0.287	Normal
Drained mire	NPP_tuber	kgC m^{-2} $year^{-1}$	0.158	0.025	0.092	0.224	Normal
Garden plot	NPP_tuber	kgC m^{-2} $year^{-1}$	0.361	0.059	0.226	0.487	Normal
Garden plot	NPP_veg	kgC m^{-2} $year^{-1}$	1.37	0.16	1.117	1.623	Normal
Infield-outland	NPP_cereal	kgC m^{-2} $year^{-1}$	0.1	0.02	0.06	0.14	Normal.

9.12 Production of berries, mushroom and game

As berries, mushrooms and game are assumed to be consumed by humans (Saetre et al. 2013b), the production of these food sources is described in this section.

9.12.1 Production of berries

The parameter production of berries (prod_edib_berry) is an estimate of the berry yield on mires around Forsmark. Cranberry and cloudberry represents the most productive edible berries on the mires, but also bilberry and lingonberry have been included because of their occurrence in wetland forests. Cranberry and cloudberry production estimates were taken from Kardell and Carlsson (1982), whereas bilberry and lingonberry estimates were taken from investigated wetlands, as described in Kardell (1993). These estimates represent the area south of the Norrland border and the estimate on the mire is close to, but somewhat lower than, the average production per unit area in the forest (Löfgren 2010. Landscape type Peatland. Table 4-56). Minimum, maximum and standard deviation were based on figures for cranberry and cloudberry (Kardell and Carlsson 1982), but also a maximum estimate for cranberry from Ruuhijarvi (1974) was included. Moreover, the collected amount is generally around 5% of the actual yield (modern estimate, Kardell 1980), see Table 9-23.

For the periglacial climate calculation case an estimate was found from a "foothill tundra" locality in northern Canada (Murray et al. 2005). Here, cranberry dominated together with crowberry, but cloudberry and some bilberry were also present. They estimated both an "actual" and a maximum yield (1.2E–04 and 2.3E–04 kgC m^{-2} $year^{-1}$). This estimate was close to the estimate for boreal conditions (see above) and the boreal estimate can therefore also be used to represent the periglacial case.

For the extended global warming climate calculation case, the total berry yield would be expected to be lower from a south-central European perspective, but it is difficult to estimate. The higher value from the main climate case is therefore used.

9.12.2 Production of game

This parameter (prod_edib_game) represents the production of wild game that is hunted in the area or the region. The production estimates are based on the population sizes and their energy budgets in terms of consumption, respiration and digestion. The production was assumed to represent the long-term potential harvest that would keep the game populations near the sizes that are found today. No distinction was made between wetland and forest during the inventories of wild game and the production estimates have not been proportioned according to consumption from forest and wetland ecosystems. In the forest, roe deer and moose represent over 90% of the production of hunted game. Roe deer and moose population figures were adjusted, as the densities were estimated after the hunting season, by increasing the density figures by a value corresponding to the loss from hunting in the area based on local hunting statistics. The production values represent the parts of the animal that is normally eaten. A minimum and a maximum value were calculated for the production of game meat based on hunting statistics describing the number of moose felled in Uppsala County (see Löfgren 2010, Section 13.3.5 for details). The estimate is assumed to be the same for both colder and warmer climate conditions. (Mean = 7.8E–06, minimum = 5.3E–06, maximum = 9.1E–06 kgC m^{-2} $year^{-1}$).

9.12.3 Production of mushrooms

This estimate describes the yield of edible mushrooms in wetlands (prod_edib_mush). Few studies have estimated the production of fungi in wetlands, but Salo (1979) investigated fungi yield on drained and fertilized bog ecosystems in Finland and reported a maximum value on a drained and fertilized mire of 0.11 $gCm^{-2}year^{-1}$. The edible fraction was, however not presented. Kardell (1994) investigated the production of edible fungi in nine Swedish swamp forests during 4 to 5 years. He found the highest figures in southernmost Sweden and the lowest figures in the northernmost localities. The yield is generally expected to be lower in large treeless peatlands with deep peat and most species that are edible are found on more minerogenic wetlands with trees, such as Norwegian spruce swamp forests or around streams and mire edges. However, it is assumed here that the edible fungi yield presented by Kardell (1994) also is representative for treeless peatlands with deeper peat. Furthermore, it is assumed that all the production is utilised, when normally a part of the edible production is removed before eating (Kardell 1994). The carbon content was assumed to be 1.5% of the fresh weight (Löfgren 2010). (Mean = 3.0E–05, stdev = 2.0E–05, minimum = 1.0E–05 maximum = 7.0 E–05 kgC m^{-2} $year^{-1}$).

For the periglacial climate calculation case no estimates of edible fungi yields in tundra environments have been found. The temperate estimate is therefore used. This is probably an overestimate because the yield in Sweden becomes lower in the northern part than in the southern part of the country (Kardell 1994, Kardell and Eriksson 1987), which suggests a declining fungal yield with increasing latitude in boreal areas.

For the extended global warming climate case no south-central European estimates of fungi yield have been found, but it is expected to be lower than in the northern part of Europe. The temperate estimate is used.

Table 9-23. Production of edible berries, game and mushrooms (kgC m^{-2} $year^{-1}$).

Parameter	Central value	Stdev	Minimum	Maximum	Distribution
Production berries (prod_edib_berry)	1.10E–04	2.00E–05	7.00E–05	1.20E–03	Normal
Production of game (prod_edib_game)	7.8E–06		5.3E–06	9.1E–06	Uniform
Production of mushrooms (prod_edib_mush)	3.00E–05	2.00E–05	1.00E–05	7.00E–05	Normal

9.13 Characteristics of cattle and herbivores in general

To calculate dose contributions from domestic animals, in this case cattle, characteristics such as ingestion rates, concentrations of carbon and the density of milk are needed.

9.13.1 Ingestion of carbon by cattle

This parameter (ingRate_C_cattle) describes the fodder consumption, in terms of carbon intake per unit time, of cattle in a self-sustainable farm in the beginning of the 20th century. Today there is a large difference between meat-producing and milk-producing cattle (Nordén et al. 2010, approximately a factor 2). Analogous to the case of water consumption (below), values for the fodder consumption of beef cattle of today (Nordén et al. 2010) were used to represent the fodder consumption of cattle producing both milk and meat at a small self-sustainable farm at the beginning of the 20th century. (Mean = 4, minimum = 3, maximum = 5 kgC day^{-1}, uniform distribution.)

9.13.2 Ingestion of soil by cattle

Soil adheres to vegetation consumed by cattle (ingRate_soil_cattle) and the amount of soil unconsciously consumed was calculated by Davis et al. (1993) and the value was extracted from that study in Karlsson et al. (2001) and Nordén et al. (2010). A relatively wide parameter range was set because of the difficulties in verifying such data. (Mean = 0.3. minimum = 0.15. maximum = 0.5. kgdw day^{-1}. uniform distribution.)

9.13.3 Ingestion of water by cattle

This parameter (ingRate_water_cattle) describes the water consumption of cattle in a self-sustainable farm in the beginning of the 20th century. No data have been found describing the approximate water consumption at that time. Today there is a large difference between meat-producing and milk-producing cattle (Nordén et al. 2010, approximately a factor 2). At that time this differentiated management, where milk production was optimised by a narrower window for production of milk from each animal, was not practiced and will probably not be rational for a small self-sustainable farm. An estimate of the water consumption in the beginning of the 20th century based on a scaling using the milk and meat production of today and then, resulted in a too low a water consumption. Therefore, values for the water consumption of beef cattle of today (Nordén et al. 2010) were used to represent the water consumption of cattle producing both milk and meat at a small self-sustainable farm at the beginning of the 20th century (mean = 0.04, minimum = 0.02, maximum = 0.06, m^3 day^{-1}, uniform distribution).

9.13.4 Density of milk

The value describing the density of milk (dens_milk) was obtained from the Swedish National Food Administration (Nordén et al. 2010). The milk density varies somewhat between milk with different fat contents, but the difference is very small (1.03–1.04 kg L^{-1}). A 5% variation is assumed to cover the minimum and maximum interval and a normal distribution is assumed. (Central value = 1.03, minimum = 0.98, maximum = 1.08, kgfw L^{-1}.)

9.13.5 Concentration of carbon in milk

The carbon content of milk (conc_C_milk) was used to calculate the concentration of radionuclides in milk from domestic cattle. In the absence of site-specific data on the carbon content of milk (conc_C_milk), the value for this parameter was taken from Avila and Bergström (2006) (see also Nordén et al. 2010, Section 6.3.1). The parameter value was calculated using an equation relating the protein, carbohydrate and fat contents with the C content in food (Altman and Ditmer 1964, Dyson 1978, Rouwenhorst et al. 1991). The values of the carbon content of proteins, carbohydrates and lipids in milk used in the calculations were taken from the database of the National Food Agency (Livsmedelsverket 2001). A 5% variation is assumed to cover the minimum and maximum interval and a normal distribution is assumed. The standard deviation was assigned by assuming that the minimum value represented the 5% confidence value. (Mean = 0.064, stdev = 0.001, minimum = 0.061, maximum = 0.067, kgC $kgfw^{-1}$.)

9.13.6 Concentration of carbon in meat

This parameter describes (conc_C_meat) the carbon concentration in animals that is of potential relevance to human consumption. Estimates from Forsmark and Laxemar-Simpevarp suggest a carbon content of 12% based on the fresh weight of muscle tissue from moose, roe deer, red fox and rodents (Tröjbom and Nordén 2010, Hannu and Karlsson 2006, Engdahl et al. 2006). A minimum value was set at 9% describing the carbon content from a roe deer in Forsmark (Hannu and Karlsson 2006). Additionally, different meat products were examined in the National Food Agency´s database (Livsmedelsverket 2001), where the carbon content was calculated based on protein, carbohydrate and fat contents (Altman and Ditmer 1964, Dyson 1978, Rouwenhorst et al. 1991). This approach suggested a similar mean and an upper limit of 20% (Livsmedelsverket 2001). A normal distribution was assumed (mean = 0.12, stdev = 0.02, minimum = 0.09, maximum = 0.20, kgC $kgfw^{-1}$).

9.13.7 Herbivore diet

When estimating uptake of radionuclides in terrestrial herbivores in the mire ecosystem the parameter "fraction of mushrooms in the diet of terrestrial herbivores" (f_mush_herbiv) is used. The parameter is dimensionless. The value is based on dietary data and abundance data as biomass per square metre (Avila 1998, Avila and Moberg 1999). A value was calculated for both moose and roe deer, which are the two dominating species in the region. The mean value was assumed to be the value weighted for the relative abundance of the two species. The value describing the fraction of mushrooms in the diet of moose, which is the less abundant species, was used as the minimum value. The estimate for roe deer was assigned as the maximum fraction in the diet. The sensitivity of this parameter value to climate change would be dependent on how fungi production correlates with temperature, which seems to be slightly negative with increasing temperature (within Sweden, see prod_edib_mush below), it is therefore assumed to be within the suggested range. The parameter was given a uniform distribution, (mean = 0.06, minimum = 0.01, maximum = 0.14, kgC kgC^{-1}).

9.13.8 Fraction of radionuclides remaining in manure after fodder has passed the digestive system of cattle

This parameter (f_loss_orgFert) was used to describe the fraction of radionuclides remaining in manure after fodder has passed through the digestive system of cattle. Manure has historically been an important source for soil improvement of infields. No loss is assumed as the best estimate, meaning that this fraction includes radionuclides that are re-excreted following uptake from the gastrointestinal tract. A minimum value of 0.8 is assumed to be possible. (Mean = 1, minimum = 0.8, maximum = 1, Bq Bq^{-1}, uniform distribution.)

9.14 Parameters specific to garden-plot calculations

There are several possible exposure pathways that are likely to affect a small group of future permanent residents, who are not necessarily self-sustained with respect to food production. These exposure pathways include irrigation, soil improvement with ash from burning peat and wood, and fertilisation with seaweeds. Large-scale irrigation is considered unlikely in relation to the location of the biosphere objects (drained mires) and the present and future climate, but scoping calculations have been done in order to evaluate the outcome of irrigation on small-scale production of potatoes and vegetables under temperate conditions (see SKB 2014a, Chapter 4). Moreover, further cases have been identified where fertilisation of a garden plot using marine macrophytes and ash from burning wood or peat are investigated (SKB 2014a). Below parameters are presented that have been used in the simulation of irrigation, fertilisation with algae, and fertilisation with wood and peat ash.

9.14.1 Area of garden plot

The area of the garden plot (area) that is used to support one individual´s need for vegetables and tubers is based on modern estimates of food intake (represents 3% and 5% of the total food intake, respectively; Saetre et al. 2013b) and modern national production estimates of vegetables and tubers (1.03 and 0.22 kgC m^{-2} $year^{-1}$, Jordbruksverket 2012)). The total need of food is assumed to be

110 kgC year^{-1} (see Section 10.4) correspondingly, the relative fraction of the area used for production of each crop was calculated based on their production to sustain one individual with vegetables and potatoes. These values are assumed to be constant over time.

Table 9-24. The size of the garden plot and the relative fractions of occupied area for the two crops in the garden plot.

Parameter	Unit	Central value
area	m^2 ind^{-1}	28
f_area_veg	m^2 m^{-2}	0.1
f_area_tuber	m^2 m^{-2}	0.9

9.14.2 Amount of water used for irrigation

This parameter describes the total amount of water per unit area (amount_irrig) that is used to irrigate the garden plot. The crop use in this case is dominated by potatoes and therefore the amount of water needed is taken from calculations based on the water need for potatoes presented in Johansson and Klingspor (1977). They calculated the daily balance between precipitation and evapotranspiration during the vegetation period for a number of different regional areas in Sweden during a normal year (1976) and a dry year (detailed description of methods in Johansson (1973)). The deficit could either be supplied from capillary rise or by irrigation. Their results suggested that potatoes and fodder generally need more water than e.g. barley. The minimum value represented a normal year in northern Sweden, while the maximum value represented a dry year in southern Sweden. This range would include an increase in temperature and drier conditions that could be compared with conditions in the south of Sweden (> +4°C difference). A standard deviation was derived by assuming that the minimum value represented the 5% percentile. (Mean = 0.09, stdev = 0.015, minimum = 0.065, maximum = 0.125 m^3 m^{-2}.)

9.14.3 Leaf storage capacity

In earlier safety assessments by SKB (SR 97 (SKB 1999), SAFE (Lindgren et al. 2001, Kautsky 2001)) interception of radionuclides from irrigation water was described by a lumped parameter that was independent of element-specific behaviour. Bergström and Barkefors (2004) identified a need to split this factor into three parameters, one of which (coefRetent, see Section 9.3 in Nordén et al. 2010) is element-specific (described below as the wash-off coefficient). The other parameters used to simulate retention of radionuclides on crops after irrigation are the leaf area index (LAI, see Section 9.5) and the leaf storage capacity (LeafStoreCapacy_tuber, LeafStoreCapacy_veg). The leaf storage capacity describes the thickness of the water layer from which the radionuclide has been removed by sorption and other processes to the leaf surface and is expressed in m^3 m^{-2}. The values used in SR-PSU and SR-Site were taken from Bergström and Barkefors (2004) who recommended using a value of 0.3 mm per LAI based on Pröhl (1990). The minimum and maximum values are also given in Bergström and Barkefors (2004) but without references. The same data were used for vegetables (LeafStoreCapacy_veg) and tubers (LeafStoreCapacy_tuber). A uniform distribution was assumed, (central value value = 3.0E–04, minimum = 2.0E–04, maximum = 4.0E–04 m^3 m^{-2}).

9.14.4 Wash off coefficient

This coefficient (washOffCoef) describes the decrease in activity on vegetation with time after an irrigation event and is the result of rain, wind and growth. This decrease in activity is described by a first-order rate constant,

$$\lambda_w = \frac{\ln(2)}{T_w}$$

where T_w is the half-life for a certain element and plant type (IAEA 2010). The half-life is dependent on a number of different factors, but has been shown to be reasonably similar among elements.

Therefore one value is used to represent all elements. The value is chosen to represent cereals, grass and rice from eight studies and is based on a compilation by IAEA (2010). A normal (truncated) distribution was assigned, central value = 15.3, stdev = 6.6, minimum = 7.2, maximum = 25.3 $year^{-1}$).

9.14.5 Number of irrigation occasions

Irrigation mainly occurs during the latter part of the growing season and may be performed at a number of occasions (N_irrig). Potatoes represent the main crop in the irrigation case and the values are from Bergström and Barkefors (2004). (Mean = 4, minimum = 3, maximum = 5, number $year^{-1}$.)

9.14.6 Length of growing season

The length of the growing season is here defined as the number of days with > +5°C (time_vegPeriod). Forsmark is located in a region having between 180 to 210 days (SLU 2014). This range was used to estimate the mean length of the vegetation period (195 days). The minimum value was taken from the northern Sweden (120–150 days) and the maximum was from the very south of Sweden (240 days). Estimates of temperature from a local meteorological station at Forsmark between 2004 and 2006 resulted in a mean of 204 days, which was similar to the mean of central Sweden. (Mean = 0.53, minimum = 0.37, maximum = 0.66, year $year^{-1}$.)

9.14.7 Demand for algae as fertilizer

In the archipelago and in other coastal regions, it was earlier common to use wind-driven macrophytes as a fertiliser on smaller areas of arable land (SKB 2014a, Chapter 2). This parameter (demand_algFertil) describes the potential load of fertilisers per square metre of garden plot per year. The figure is based on cultivation experiments from the south of Sweden, where 40 tons of algae (wet weight) ha^{-1} was used (Ohlsson 1991). This amount was recalculated to dry weight based on the nitrogen content in the algae (192 kg ha^{-1}) that constitutes approximately 3% of the dry weight. The calculation to carbon content is based on estimates from algae in marine basins from Forsmark (34% carbon, Hannu and Karlsson 2006). This parameter was regarded as a constant (central value = 0.22 kgC m^{-2} $year^{-1}$).

9.14.8 Wood as fuel for a household

This parameter (area_support_wood) describes the necessary area that is needed to supply a household (5 persons) with wood for heating the house assuming an energy consumption of 20,000 kWh per household (the average energy used for heating in one- and two dwelling buildings, excluding household electricity, in Sweden 2012 was 16,800 kWh, (Statens energimyndighet 2013). It is assumed that the wood extraction is sustainable in the long-term, meaning that the amount extracted equals the net primary production of the forest. It is also assumed that the forest that is used for wood extraction is found on a wetland, which is a potential discharge area for deep groundwater. As an example, the production estimates for wood and branches were taken from a wetland forest in Forsmark (108±30 gC m^{-2} $year^{-1}$ (mean and stdev), denoted as SS1 in Löfgren 2010). However, this forest is not situated on a deep peat layer and the production would be expected to be lower under such conditions. The wood is suggested to be dominated by Norway spruce with a high density (equals a high energy content) and a water content of 29.4%, which suggest an energy content of 3.56 kWh kg^{-1} wood (Liss 2005). The amount of wood that is required to provide a household with energy is calculated based on the energy consumption (above). The standard deviation for the area was calculated by assuming that the 95% confidence interval for the NPP represented minimum and maximum NPP values. These were used to calculate the minimum and maximum area of forest necessary to use to provide enough wood for a household and thus for each individual in the household by dividing by five. The minimum and maximum were then used to calculate a standard deviation by assuming they represented the 2.5% and 97.5% percentiles of the necessary area. The parameter f_C_wood describes the carbon content in the stem wood and is based on estimates from Norway spruce (Löfgren 2010, Table 6-5).

Table 9-25. Parameters used for the calculations of dose from wood used as fuel in a house-hold.

Parameter	Unit	Central value	Stdev	Minimum	Maximum	Distribution
area_support_wood	m^2 ind^{-1}	3,520	630	2,290	7,640	Normal
fuel_cons_wood	kgdw $year^{-1}$	3,970				Constant
f_C_wood	kgC $kgdw^{-1}$	0.48				Constant

9.14.9 Peat as fuel for a household

Peat has been used for heating houses (Liljegren 2010). The mass of peat needed to heat a household over a 50-year period (an approximate life-time), corresponding to a yearly need of 20,000 kWh $year^{-1}$ (the average energy used for heating in one- and two dwelling buildings, excluding household electricity, in Sweden 2012 was 16,800 kWh, Statens energimyndighet, 2013) is described by the parameter demand_peat. The energy content is 5.8 kWh $kgdw^{-1}$ (Statens energiverk 1985). This is expressed on the individual basis where a household is assumed to include 5 individuals. The amount of peat that is needed to produce 20,000 kWh $year^{-1}$ is described by the parameter fuel_cons_peat. Both these parameters are assumed to be constant. The fraction of carbon in peat is described earlier in this chapter (f_C_peat) see Section 9.4.3.

Table 9-26. Two parameters describing the area of the mire of peat needed for generating heat

Parameter	Unit	Value	Comment
demand_peat	kgdw ind^{-1}	34,000	Constant
fuel_cons_peat	kgdw $year^{-1}$	3,450	Constant

10 Human characteristics

In order to assess the potential exposure to a representative person of the most exposed group, assumptions on the habits and characteristics of future humans inhabiting the area are needed. Due to the long time-scales, SKB deem it impossible to assign characteristics and habits that are likely to provide realistic estimates of the actual features and behaviour of humans in the far future. Instead, SKB has performed an exposure-pathway analysis to identify relevant pathways of exposure. Following international recommendations (ICRP 2006, IAEA 2003), most exposed groups were constructed based on the pathway analysis. Each groups reflects a combination of exposure pathways resulting from reasonable and sustainable land use and habits, with respect to the Forsmark area and human physiological requirements. SKB argues that these groups are credible bounding cases for future exposure (SKB 2014a).

The four exposed goups/land use variants used in SR-PSU are: hunter and gatherers, infield-outland agriculture, modern agriculture, and small-scale horticulture. The hunter-gather community forage multiple forest, mire, lake and sea ecosystems in the landscape. In the infield-outland farming system, hay from one biosphere object is used to feed animals and fertilize infield arable land. An industrial-age agricultural system was used to assess maximum exposure from draining and cultivating the lake/mire system in a biosphere object. Finally, a garden plot was used to calculate the combined exposure from irrigation, combustion and fertilization at the household scale. In this section, parameters used to represent human characteristics (common to all exposed groups) and habits (specific to land-use variants) are presented.

10.1 Experience from previous safety assessment

The International Commission on Radiological Protection (ICRP) has published basic anatomical and physiological data that serve as a common reference in assessments of radiological protection (ICRP 1975, 2002). These data serve as the starting point when SKB selects parameter values describing intake of energy and water, and the rate of inhalation. The ICRP data is scaled to units relevant for the biosphere assessment and contrasted against other sources of relevant data (Table 10-1). From such a comparison the consumption rates of water was updated in SR-PSU (Section 10.3).

There is presently no consensus or recommendations on what human habits should be used in prospective safety assessments. Instead the guidelines of the ICRP states that the habits of the most exposed individuals need to reflect all relevant pathways of exposure, and should be subject to *reasonableness* and *sustainability* with respect to the location or situation under consideration (ICPR 2006). The relative importance of exposure pathways may vary between the properties of radionuclides, and between the time and location of a release in a developing landscape. Thus several plausible sets of habits with different vulnerability to relevant exposure pathways were considered in the SR-PSU safety assessment (SKB 2014a).

Similar to the previous SKB safety assessment SR-Site, the habits of the most exposed group was set to meet the physical and biological constraints of the biosphere objects, and the physiological and nutritional needs of the inhabitants. That is, if the demand of energy of the most exposed group was not met by the productivity of land affected by radionuclides from the repository, then individuals were assumed to consume food from unaffected areas. In addition, intake of fish was constrained by the upper safe intake of proteins in SR-PSU (Section 10.11).

To make sure the land use associated with the most exposed group was sustainable and reasonable, historical records were used to support constructs representing the self-sustained communities, hunter-gatherers, infield-outland farmers and drained mire farmers (Saetre et al. 2013b). Present day productivity rates (conditioned on the input of commercial fertilisers) were only used to characterise cultivation of a garden plot supporting a local household with potatoes and vegetables. Consequently, most parameters associated with use of arable land were updated in SR-PSU.

Table 10-1. Anatomical and physiological reference properties of adults for use in previous SKB safety assessments.

Property	Reference Value Male	Female	Reference
Height (cm)	176	163	ICRP (2002)
Mass (kg)	73	60	ICRP (2002)
Body surface (m^2)	1.9	1.66	ICRP (2002)
Energy demand (kgC $year^{-1}$)[a]	110	76	Avila and Bergström (2006)
Protein intake (kgdw day^{-1})	0.095	0.066	ICRP (1993)
Carbohydrate intake (kgdw day^{-1})	0.39	0.27	ICRP (1993)
Fat intake (kgdw day^{-1})	0.12	0.085	ICRP (1993)
Intake of water[b] (m^3 $year^{-1}$)	0.6*	0.44	Avila and Bergström (2006)
Inhalation rate (m^3 day^{-1})	22.9	18.5	ICRP (2002)

a = Derived from listed dietary intake of protein, carbohydrates and fat.

b = Calculated from reference values in ICRP 23, excluding water in food and milk.

* = Updated to 0.74 m^3 day^{-1} in this report (see below).

10.2 Influence of climate on parameter values

The characteristics of the reference man, and parameter's derived from him, are deemed to be adequate also for periglacial conditions and a warmer climate than today. This is because, the response of energy expenditure and respiratory rate to temperature change is expected to be limited (~ 5% to a 10°C change) and shielding by e.g. clothes dampens temperature variations (ICPR 1975). Moreover, the water consumption rate for temperate conditions is applicable also to the climate in central southern Europe.

Diet fractions and group size are primarily driven by land use and unaffected by climate variation. However, under permafrost conditions cultivation of land is strongly limited and it is not possible to extract water from wells. Thus a hunter-gatherer band was the only exposed group assessed during periods of periglacial conditions. As the productivity of terrestrial food items was not significantly altered during simulations of periglacial conditions (Section 9.11), there was no rational for adjusting the group size of the most exposed group.

The productivity of wetland ecosystems is expected to increase by approximately 50% in a warmer climate with a significantly elevated atmospheric concentration of CO_2 (Section 9.3). The corresponding increase in productivity of crops and fodder plants is expected to be 70% (Section 9.11). Thus the area needed to support the most exposed group with hay or agricultural food items may decrease during periods of the extended global warming climate case. However, as estimates of hay and food production are high (Section 10.8), the support areas under temperate conditions are already well below the area of the smallest biosphere object, and therefore there is no need to adjust these parameter values for a warmer climate.

10.3 Water ingestion rate of future humans

The parameter ingRate_water, describes the water ingestion rate per individual member of a self-sustainable community. The following parameter description is taken from Werner et al. (2013).

In principle, there are two ways to estimate the drinking-water needs for an individual, either based on the needs set by the human physiology (and associated fluid-intake recommendations) or based on statistics on actual fluid intakes. Both demonstrate large variability depending on factors such as climate, activity level and diet, and such factors need to be taken into account for the present purposes.

The daily water losses from a human body (urine, insensible losses, faeces and sweat) must be balanced by water gains through direct intake of water or other fluids, water contained in food and water generated by metabolism (oxidation of food). Based on physiological data, ICRP (1975,

2002) presents the daily fluid balance for a "reference man" for the purposes of radiological risk analyses. According to the water balance for an adult male (with a weight of 73 kg), the total daily water losses are 2.9 L day^{-1} (the corresponding sum for an adult female is c. 2.2 L day^{-1}). These losses must then be balanced by direct intake of water or other fluids (2.6 L day^{-1}) and metabolism (0.3 L day^{-1}). For a reference intake of 0.7 L day^{-1} of water contained in food (ICRP 1975), the need of an adult male for direct intake of water or other fluids is hence 1.9 L day^{-1}. Avila and Bergström (2006) assumed daily water losses of 2.95 L day^{-1} and that the sum of intake of water contained in food plus water generated by metabolism equals 1 L day^{-1}, which hence yields a need for direct intake of water or other fluids of 1.95 L day^{-1}.

Gleick (1996) reports results of various physiological studies of human water requirements, suggesting a minimum requirement for fluid replacement of 3 L day^{-1} under average temperate conditions. WHO (2011) recommends a direct fluid intake of 2 L day^{-1}, as an average for both males/females and for all ages. Moreover, the recommended minimum fluid intake was 2.9 L day^{-1} during NASA's early space flights, and the National Academy of Sciences (1977) recommends a water intake of 2–4.5 L day^{-1} depending on energy intake in food. Members of self-sustaining communities are likely involved in hard and prolonged physical activities, which, in combination with a warmer climate, puts their fluid needs above present-day averages. For instance, US Army (2008) recommends a daily water intake of 6–11 L day^{-1} for field personnel active in temperate climates. A direct fluid intake of 2 L day^{-1} for adults is recommended by US EPA (2000) to be used in risk analyses related to drinking water in the USA, which is also recommended for corresponding risk analyses in Sweden (Westrell et al. 2006).

There are few surveys of present-day drinking habits that are relevant for the present purposes and/or for a reference man defined for the purposes of radiological risk analyses. Most such surveys are focused on risks associated to intakes of tap water, whereas a large part of current fluid intakes are fluids other than tap water. Moreover, current average physical activities are likely less hard and less prolonged compared with those of members of self-sustaining communities, who also likely loose more water during work in a warmer climate than today (cf. above).

For instance, French survey data presented in Antoine et al. (1986), which are referred to by ICRP (2002) and Avila and Bergström (2006), show an average intake of tap water and other fluids of c. 1.3 L day^{-1} (0.5 m^3 $year^{-1}$). However, the average intake of water contained in food in that study was 1 L day^{-1}, which corresponds to an average direct intake of water and other fluids of 1.6 L day^{-1} if the reference value of 0.7 L day^{-1} (cf. above) is used. The total average water intake in the study was 2.7 L day^{-1}, which is within the interval for daily water losses for a mixed male/female group according to ICRP (1975, 2002). Moreover, US survey data presented in Ershow and Cantor (1989), also referred to in ICRP (2002) and Avila and Bergström (2006), show an average water intake of 1–1.6 L day^{-1} (0.4–0.6 m^3 $year^{-1}$), including direct intake of water, water added to other beverages and water added to food during preparation. However, the survey data do not take into account the intake of water contained in food or other fluid intakes (e.g. milk or soft drinks). In fact, in the Ershow and Cantor (1989) study the average tap-water intake (c. 1 L day^{-1}) was just 55% of the total average water intake, which was 2 L day^{-1} (US EPA 2011). In a recent Swedish survey (Westrell et al. 2006), the average water intake was c. 1.9 L day^{-1}. This average includes tap water and bottled water, but not other fluid intakes (e.g. milk or soft drinks).

Assuming that water is the only source for direct fluid intake, 2 L day^{-1} (0.73 m^3 $year^{-1}$) per person is used here as one of the inputs to estimate total water demands for different types of self-sustaining communities. This drinking-water need is supported by, for instance, the needs set by human physiology (e.g. ICRP 1975, 2002) and fluid-intake recommendations in terms of human health (WHO 2011) and for risk-analysis purposes in Sweden and USA (US EPA 2000, Westrell et al. 2006).

10.4 Ingestion rate of food

The human food ingestion rate (ingRate_C) is expressed in kg carbon per year. The total intake of carbon by an individual is related to the food energy intake, 10 kcal is approximately equivalent to 1 g C. Total energy expenditure is age- and gender-dependent (see Avila and Bergström 2006, Table A-1) and varies widely due to individual differences in activity, body size and body composition. The reference value of energy expenditure by an adult male given in ICRP (2002) is 2,800 kcal day^{-1} (Avila and Bergström 2006, Table A-1) and since usage of metabolic fuel is normally balanced by variations in food intake (ICRP 2002), we can estimate that the yearly carbon intake is around 102 kg. The same calculation for adult females gives a value of 66 kgC $year^{-1}$. Carbon intake by male adults can also be estimated from the values of protein intake (0.095 kg day^{-1}), carbohydrate intake (0.39 kg day^{-1}) and fat intake (0.12 kg day^{-1}) given in ICRP (1975) and the carbon content in proteins, carbohydrates and fats: 0.53, 0.44 and 0.66 $kg_C\ kg^{-1}$, respectively (Altman and Ditmer 1964, Dyson 1978, Rouwenhorst et al. 1991). This gives a value of around 110 kgC $year^{-1}$ for adult males, which is the value used in previous safety assessments and in the current safety assessment, SR-PSU. (The same calculation for adult females gives a value of around 76 kgC $year^{-1}$).

10.5 Inhalation rate

To calculate exposure through inhalation, the inhalation rate (inhRate, expressed in $m^3\ h^{-1}$) is used. The inhalation rate of an individual varies during the day depending on the activities and time spent outdoors and indoors. In ICRP (2002), reference values of total ventilation during a day are provided for members of the public at various ages (see Avila and Bergström 2006, Table A-1). The highest value, 22 $m^3\ day^{-1}$, is for adult males, which is close to the value used in previous assessments, i.e. 1 $m^3\ h^{-1}$ or 24 $m^3\ day^{-1}$, accordingly the value of 1 $m^3\ h^{-1}$ is used also in SR-PSU.

10.6 Diet fractions from cultivation of land

These parameters (f_diet_cereal, f_diet_meat, f_diet_milk, f_diet_tuber, f_diet_veg) describe the fractions of the yearly energy demand covered by consumption of different food items assuming a self-sustained agrarian community or a household cultivating vegetables and potatoes on a garden plot. For the infield-outland agriculture land-use variant the diet fractions were derived from an Iron-Age family (Table 10-2), whereas fractions for the drained mire variant was derived from industrial-age, small-scale farming (Table 10-3). A detailed historical background to these two land-use variants is presented in Saetre et al. (2013b).The diet fraction for the garden plot variant were derived from present day food statistcs.

The infield-outland diet fractions were derived from land use and consumption of a self-sustained family farm with a mixed herd of livestock (Widgren 1979; Table 10-2). This agricultural system is based on the principle that the production of fodder supporting the livestock herd through the winter period balances the need for manure to fertilise the infield cropland. To scale diet fractions in carbon units, carbon contents for meat and milk were used from previous SKB safety assessments (Avila 2006, Tröjbom and Nordén 2010, respectively). The carbon content of cereals was calculated from the nutrient content of whole grain meal from barley, wheat, rye and oats, and the carbon content of protein (0.53), carbohydrates (0.44) and fat (0.66) (Altman et al. 1989, Dyson 1978, Rouwenhorst et al. 1991).

Table 10-2. The contribution of different food items (f_diet) to the total carbon intake for a self-sustained farmer community, according to an Iron-Age infield-outland agricultural system. Updated from Widgren (1979).

Land-use	Area (ha)	Food item	Production (kg $year^{-1}$)	Calorie content (kcal kg^{-1})	Carbon content (gC kg^{-1})	Daily Consumption (kcal $indv^{-1}$)	Daily Consumption (gC $indv^{-1}$)	f_diet (kgC kgC^{-1})
Arable	3	Cereal	1,500	3,200	0.35	2,192	239	0.71
Meadow	30	Milk	2,800	400	0.06	511	82	0.24
Pasture[a]	30	Meat	300	2,000	0.12	274	16	0.05
					Total:	2,977	337	1

a = Minimum area of pasture assuming primary productivity as meadow (500 kg hay ha^{-1}, Wennberg 1947).

For the land-use variant representing cultivation of a drained wetland or lake, diet fractions were calculated for a self–sustained small-scale farm at the turn of the 19th century. The typical consumption pattern of food was assumed to be proportional to agricultural yield of cereal, potato, meat and milk (kg year^{-1}) at the time, and production values were derived from official national statistics provided by the Swedish board of agriculture (Jordbruksverket 2012) (Table 10-3). Diet fractions were scaled in carbon units using the nutrient content of whole grain meal from barley, wheat, rye and oats, and the carbon content of protein, carbohydrates and fat (see above). The carbon content of potato was calculated from the average nutrient content of raw and cooked potatoes, and the carbon content of protein, carbohydrates and fat (see above).

The fraction of potatoes and vegetables for the garden-plot land use variant were derived from a recent summary of Swedish consumption statistics, published by the Swedish Board of Agriculture (Wikberger and Johansson 2006). The relative contributions of major food types were scaled in terms of yearly carbon consumption, using the listed nutrient contents and the carbon content of protein, carbohydrates and fat (Saetre et al. 2013b, Table S2). The resulting fractions for potatoes (f_diet_tuber) and vegetables (f_diet_veg) were 0.05 and 0.03 kgC kgC^{-1}, respectively.

10.7 Diet fractions for drained mire agriculture

These parameters (f_area_cereal, f_area_potato, f_area_fodder) describe the fraction of arable land-used for cultivation of cereals, potato and fodder respectively (Table 10-3). The fractions were derived from national statistics on production (kg year^{-1}) and productivity (kg year^{-1} ha^{-1}) at the turn of the 19th century (Jordbruksverkets 2012).

Table 10-3. Land-use (f_area) and corresponding contribution of different food items (f_diet) to the total carbon intake for a self-sustained farmer according to an industrial-age agricultural system.

Land-use	f_area (%)[a]	Food item	Productivity (kg m^{-2} year^{-1})[a]	Carbon content (g_C kg^{-1})	Yearly consumption (kgC indv^{-1})[c]	f_diet (kgC kgC^{-1})
Cereal	48%	Wheat	0.22	0.35	66	0.60
		Rye	0.16			
		Barley	0.20			
		Oats	0.18			
Root crop	5.8%	Potato	1.29	0.08	12	0.11
Green fodder & pasture	33%	Pig[b]	0.003	0.12	4	0.04
		Cattle[b]	0.005			
		Milk[b]	0.10	0.06	27	0.25
Fallow	12%		–			
Other	1.6%		–			
				Total:	110	1

a = Based on national statistics from the turn of the 19th century.

b = Productivity of meat and milk refers to area of green fodder production and pasture, and 2/3 of area used for crop production (Morell 1998).

c = Consumption is assumed to be proportional to food production.

10.8 Support areas for infield-outland and industrial-agriculture

The support area (area_support) in the infield-outland variant describe the size of the mire (m^2) required to supply winter fodder for the livestock associated with one adult individual (area_support for infield-outland). In the industrial-age agricultural scenario, the support area is the size of the drained mire (m^2) required to support the energy demand of one adult individual (area_support for industrial-age).

By combining the ecological basis of production and the physical features of the landscape (including distance), the land-use pattern of Iron-Age farming has been surprisingly well predicted for family-sized groups (Widgren 1979). In these simulations, Widgren (1979) estimated that 15,000 kg winter fodder (hay on dry weight basis) is needed to support a livestock herd corresponding an Iron-Age infield-outland farm of six adult individuals. Assuming that the productivity of grass and sedges in the future wetlands in the Forsmark area can be estimated from highly productive mires in central Sweden (up to 2,400 kgdw per hectare), the support area for one adult individual will corresponds to 10,000 m^2.

The theoretical support area for industrial-age agriculture was calculated from land-use patterns and productivity from the turn of the 19th century (Table 10-3). That is, by assuming that the annual energy demand of an adult individual equals 110 kgC (Avila and Bergström 2006), and that consumption is directly proportional to production, the support area for one individual equals 6,200 m^2. Though this support area is a theoretical construct, which does not account for losses due to food handling and storage, it matches fairly well the typically required area of 5 to 10 ha of arable land needed to support a small-scale family farm during the early industrial-age (Morell 1998).

10.9 Area of cultivated land, demand of hay and pasture.

The area (area) of arable land needed to support one adult individual in the infield-outland agricultural land-use scenario was set to be 5,000 m^2, following Widgren's (1979) calculations for a self-sufficient Iron-Age farm. The corresponding yearly demand of winter fodder for fertilising this land (demand_hay) is 0.23 kgC per m^{-2} of arable land. This value corresponds to a yearly hay demand of 15,000 kgdw per 3 ha of arable land (Widgren 1979), and a carbon content of 0.46 kgC $kgdw^{-1}$ for hay (Löfgren 2010). Hay covers approximately half of the yearly fodder consumption of the livestock (f_meadow = 0.5), and livestock is assumed to cover the remaining part by grazing uncontaminated outland pastures.

For the drained mire scenario the all drained land (6,200 m^2 per individual, cited from above) was used to represent cultivated land in calculations for the near surface atmosphere above the three types of cultivated crops (cereals, potatoes and fodder). This is an upper boundary as no one crop alone occupies this area, and a proportion of the drained land is left as a fallow. However, this area was used to not overestimate dilution by advection, accounting for the fact that arable land of different crops may be located adjacent to each other.

The total area of the garden plot (area) was set to 28 m^2 per individual. This area corresponds to the areas needed to cultivate the yearly consumption of potatoes (5.5 kgC) and vegetables (3.3 kgC) for one individual, based on present day productivity of potatoes and cabbage in (0.22 and 1.0 kgC m^{-2} $year^{-1}$).

10.10 Number of individuals in the most exposed group

The number of individuals (N_group) for the two agricultural scenarios (infield-outland and industrial-age) was set to 10 adult individuals. This group size was considered to be the smallest sustainable and reasonable group size that could be supported by historical records (Saetre et al. 2013b).

For example, archaeological records suggest that the typical size of an Iron-Age farm (representing the principles behind the infield-outland agricultural system), spanned from a core family to that of an extended three generations family (Lindquist 1974). Similarly, at the turn of the nineteenth century (a period when draining and cultivation of lake and mires was common), the majority of the farming population was found on self-sufficient small-scale family farms (Morell 1998).

The number of individuals in a hunting and gathering community was set to 30 individuals. This number corresponds to the median group size from an historic ethnographic review of 300 hunter and gatherer communities (Marlow 2005), and it also matches the expected value when group size is described as a function of habitat characteristics of undisturbed forest ecosystems in Central Sweden and at the site (biomass of primary producers 15–20 kgdw m^{-2}, Nilsson and Cory 2011, Löfgren 2010).

The number of individuals in the garden plot variant was set to one family of five individuals. This size was chosen to avoid dilution in this land use variant, as the sources of radionuclides in the included exposure pathways (well water and seaweeds or biofuel ash for fertilization) is limited (SKB 2014a). Moreover, this small group size is in line with recommendations in the Swedish regulations with respect to exposure from a well (SSM 2008).

10.11 Upper boundary for safe consumption of fish

From analysis of stable isotopes, it can be inferred that marine proteins frequently made up all of dietary protein intake for hunting and gathering communities living on the Baltic coast. However, as the fish of the Baltic coast typically has a very low fat content (e.g. perch, pike, and cod), there is an upper boundary as to how much contaminated fish could possibly be consumed (f_diet_fish_max). Excessive protein consumption may lead to toxic effects due to elevated levels of amino acids, ammonia, and insulin (causing nausea and diarrhea), and thus the upper level for healthy consumption of protein is 25% of the total energy intake (Bilsborough and Mann 2006). Given a total energy demand of 3,000 kcal day^{-1}, and an energy content of protein of 4 kcal g^{-1}, the maximum safe yearly consumption is 68 kg of proteins. With a protein to carbon ratio of 1.8 g gC^{-1} (perch, pike, and cod), this corresponds to a maximum yearly fish consumption of 38 kgC, or 35% of a yearly carbon consumption of 110 kg (cited from Saetre et al. 2013b).

10.12 External exposure time

These variables describe the potential yearly exposure time for future human inhabitants with respect to external exposure (time_exposure) and exposure through inhalation. As exposure from aquatic habitats is expected to be small compared to exposure from land (SKB 2014a), the parameter values reflect the maximum time that future inhabitants will be in direct contact with contaminated wetlands, foraging or collecting hay, or the time spent working contaminated arable land.

In the agricultural land-use variant, historical records on work time (per unit area, Myrdal 1996) were combined with estimates of the area needed to support one adult individual (Table 10-4) to calculate the parameter values. Records from the 1700s were used for infield-outland variant, whereas records from end of the 1800s (industrial age) were used for cultivation of a drained mire. The support area of cropland and meadows were taken from Iron-Age farming (infield-outland, Widgren 1979) and estimated from official Swedish statistics on land-use and productivity at the end of the 1800s (industrial-age, 3), respectively. Thus, the potential yearly time spent on cultivated land (time_exposure) is 54 hours for farmers draining a mire. This time was also used as an upper boundary for the time spent cultivating vegetables and potatoes on the garden plot. The corresponding times for the infield-outland variant are 120 hours spent on arable land (time_exposure × f_time_agri = 220×0.55), and 100 hours spent mowing hay from wet meadows (time_exposure × f_time_hay = 220×0.45).

For hunter and gatherers an upper boundary for the time spent in the biosphere object was set to 8,760 hours a year (24 h day^{-1}), assuming that the band set up camp in the drier areas of the biosphere object.

Table 10-4. Time spent on arable land and meadows for two different self-sustained agricultural communities.

Work time and associated land	Infield-outland	Industrial-age
Time spent in 10 h units per ½ ha[a]		
Haymaking	1	1
Plowing	1	1.5
Sowing	0.15	0.1
Harvesting	11	6
Agricultural land per adult indv (ha)[b]		
Cropland	0.5	0.3
Meadow/ green fodder	5	0.2
Total time per adult (h $year^{-1}$)		
Cultivated area	120	54
Meadow	100	

[a] Myrdal 1996.

[b] From Widgren 1979 (Table 1 and Table 2).

11 Non-human biota parameters

In this safety assessment exposure to non-human biota is estimated through calculation of dose rates to the reference organisms from the ERICA Tool (Beresford et al. 2007, Brown et al. 2008). An earlier study (Jaeschke et al. 2013) showed that some adjustments of this organism set should be made in order to fully represent current conditions in the Forsmark area. These modifications are described below, in Section 11.1, and in more detail in SKB (2014a). In total, 41 organism types have been used as target organisms in this safety assessment.

The calculation of exposure to non-human biota is described in detail in Saetre et al. (2013a). Organism-, nuclide- and radiation type-specific dose conversion coefficients (DCC) are calculated, and these are, together with environmental radionuclide concentrations, organism habitat preferences and radiation weighting factors, used to estimate internal and external exposures.

When estimating internal exposure, uptake of radionuclides in organisms is estimated using concentration ratios, CR (further described in Section 7.4). The uptake of carbon-14 and tritium is modelled differently (see Saetre et al. 2013a) and for this the carbon and dry weight fractions of organisms have been used.

11.1 Experience from previous safety assessments

The only comparable former assessment is the supplementary dose assessment performed for non-human biota within SR-Site (Jaeschke et al. 2013). That study also investigated the effects of organism size, habitat and CR values on the estimated dose rates. The main conclusions have been utilised in this study, i.e. site-specific CR values have been utilised. In line with the recommendations in Jaeschke et al. (2013), occupancy of a few organisms has been altered (from on soil/sediment to in soil/sediment) and a few representative species for the Forsmark site have been added to include the impact of occupancy in both aquatic and terrestrial ecosystems (for details, see SKB 2014a).

11.2 Influence of climate on parameter values

None of these parameters are assumed to be affected by climate factors in any significant way and therefore the parameters are not altered in the various climate calculation cases. What has been slightly altered (for the periglacial climate case) is the set of organisms for which exposure is estimated. This is further discussed in SKB (2014c).

11.3 Dose conversion coefficients, DCCs

Dose estimates to non-human biota are calculated using organism-, radionuclide- and radiation type-specific dose conversion coefficients (DCC) according to the methods described in Ulanovsky and Pröhl (2006) and Ulanovsky et al. (2008). Eight different kinds of coefficients are used (coefficients are valid for aquatic as well as terrestrial ecosystems if not otherwise stated, values are tabulated in Appendix E):

- DCC for internal exposure from alpha radiation, DCC_int_alpha, ((μGy h^{-1}) per (Bq $kgfw^{-1}$)).
- DCC for internal exposure from beta/gamma radiation, DCC_int_beta_gamma ((μGy h^{-1}) per (Bq $kgfw^{-1}$)).
- DCC for internal exposure from low beta radiation, DCC_int_low_beta ((μGy h^{-1}) per (Bq $kgfw^{-1}$)).

- DCC for external exposure from beta/gamma radiation in aquatic ecosystems, DCC_ext_beta_gamma, ((µGy h^{-1}) per (Bq l^{-1})).
- DCC for external exposure from low beta radiation in aquatic ecosystems, DCC_ext_low_beta, ((µGy h^{-1}) per (Bq l^{-1})).
- DCC for external exposure from beta/gamma radiation in soil in terrestrial ecosystems, DCC_ext_in_soil_beta_gamma, ((µGy h^{-1}) per (Bq $kgdw^{-1}$)).
- DCC for external exposure from beta/gamma radiation on soil in terrestrial ecosystems, DCC_ext_on_soil_beta_gamma, ((µGy h^{-1}) per (Bq $kgdw^{-1}$)).
- DCC for external exposure from beta/gamma radiation in air in terrestrial ecosystems, DCC_ext_in_air_beta_gamma, ((µGy h^{-1}) per (Bq m^{-3})).

11.4 Occupancy factors

When estimating external exposure to non-human biota the parameter occupancy factor is used to describe which habitat each considered organism is utilising. The possible occupancies in aquatic ecosystems are in or on sediment and in or on water, whereas occupancy in terrestrial ecosystems includes in or on soil, and in air.

In this assessment, the default values in the ERICA Tool have generally been used, assuming that each organism type predominally utilises one habitat. A change of occupancy from *on* to *in* sediment was performed for marine benthic molluscs, limnic bivalve molluscs and crustaceans as recommended in Jaeschke et al. (2013). All occupancy factors are presented in Table 11-1.

Table 11-1. Assumed habitat use and occupancy factors used in the safety assessment for non-human biota in SR-PSU.

Organisms	Habitat	Occupation factor
Terrestrial ecosystem		
Soil Invertebrate	In soil	1
Detritivorous invertebrate	In soil	1
Gastropod	On soil	1
Amphibian	On soil	1
Reptile	On soil	1
Flying insects	On soil	1
Lichen and bryophytes	On soil	1
Grasses and Herbs	On soil	1
Tree	On soil	1
Mammal (small)	In soil	1
Mammal (large)	On soil	1
Bird	On soil	1
Bird egg	On soil	1
Marine ecosystem		
Phytoplankton	In water	1
Macroalgae	On sediment	1
Vascular plant	On sediment	1
Zooplankton	In water	1
Polychaete worm	In sediment	1
Benthic mollusc	In sediment[2]	1
Crustacean	On sediment	1
Benthic fish	On sediment	1
Pelagic fish	In water	1
(Wading) bird	In water	1
Mammal	In water	1
European otter[1]	On soil (TE)/in water	0.6/0.4
Ruddy Turnstone[1]	On soil (TE)	1
Limnic ecosystem		
Phytoplankton	In water	1
Vascular plant	On sediment	1
Zooplankton	In water	1
Insect larvae	In sediment	1
Bivalve mollusc	In sediment[2]	1
Gastropod	On sediment	1
Crustacean	In sediment[2]	1
Benthic fish	On sediment	1
Pelagic fish	In water	1
Amphibian	In water	1
Bird	In water	1
Mammal	In water	1
Black Tern[1]	On soil (TE)/in water	0.6/0.4
Microphytobenthos[1]	On sediment	1

[1] Representative species for the Forsmark area (discussed in SKB 2014a).
[2] Habitat differing from that of the ERICA Reference organism, changed in accordance with recommendations in Jaeschke et al. (2013).

11.5 Radiation weighting factors

Radiation weighting factors are used to take account of the relative biological effectiveness of different radiations (α, low-energy β and high energy β+γ), giving weighted biota dose rates. The discussion on the appropriate choice of radiation weighting factors is still on-going and no definitive recommendation has been made in the ERICA methodology. However, it has been suggested that biota-specific radiation weighting factors of 3 for low-energy electrons ($E < 10$ keV), 1 for all other β particles and electrons (as well as for γ and x-rays, the "reference radiations") and 10 for α-radiation can be used. The value of 3 for low-energy electrons reflects the experimental relative biological effectiveness, RBE values for tritium (Straume and Carsten 1993), and the value of 10 for α-particles (lower than the value of 20 used in human protection) is used because the latter was intended to represent relative biological effectiveness (RBE) for stochastic effects (primarily the induction of cancers), whereas in non-human biota it is the deterministic effects that are of importance (Vives i Batlle et al. 2004). Throughout this assessment, these default weighting factors (β+γ radiation, w_beta_gamma, 1; low β radiation, w_low_beta, 3; and α radiation, w_alpha, 10) have been applied.

11.6 Fraction of carbon in organisms

Estimations of radionuclide uptake in biota are, for most radionuclides, performed using Concentration Ratios. The exception is uptake of carbon-14 and tritium for which uptake is modelled differently due to the nature of these two elements for which stable isotopes are very abundant in the environment. The modelling is described in detail in Saetre et al. (2013a).

For uptake of carbon-14, a parameter named fraction carbon in organism (f_C_org) is used (unit kgC $kgfw^{-1}$). Literature values (from IAEA 2010) have been utilised for this parameter, see Table 11-2.

Table 11-2. Carbon content of different organisms used in the assessment.

Organism	Carbon content (f_C_org) kgC $kgfw^{-1}$
Freshwater	
Amphibian	7.0E–02
Benthic fish	1.2E–01
Bird	2.4E–01
Bivalve mollusc	7.2E–02
Black tern	2.4E–01
Crustacean	1.2E–01
Gastropod	7.2E–02
Insect larvae	1.2E–01
Mammal	1.5E–01
Microphytobenthos	8.9E–02
Pelagic fish	1.2E–01
Phytoplankton	7.6E–02
Vascular plant	4.0E–02
Zooplankton	1.2E–01
Marine	
Benthic fish	1.2E–01
Benthic mollusc	7.2E–02
Bird (Wading)	2.4E–01
Crustacean	1.2E–01
European otter	1.5E–01
Macroalgae	7.6E–02
Mammal	1.5E–01
Pelagic fish	1.2E–01
Phytoplankton	7.6E–02
Polychaete worm	1.2E–01
Ruddy Turnstone	2.4E–01
Vascular plant	4.0E–02
Zooplankton	1.2E–01
Terrestrial	
Amphibian	7.0E–02
Bird	2.4E–01
Bird egg	2.4E–01
Detritivorous invertebrate	1.2E–01
European otter	1.5E–01
Flying insects	1.2E–01
Gastropod	7.2E–02
Grasses & Herbs	1.0E–01
Lichen & bryophytes	1.0E–01
Mammal (Deer)	1.5E–01
Mammal (Rat)	1.5E–01
Reptile	7.0E–02
Ruddy Turnstone	2.4E–01
Shrub	1.0E–01
Soil Invertebrate	1.2E–01
Tree	1.0E–01

11.7 Fraction dry weight of organisms

The parameter fraction dry weight in organism, f_DW_org (in the unit kgdw kgfw^{-1}) is used when estimating uptake of tritium. For this parameter, a conservative value of 0 (assuming 100% water content) is used for terrestrial organisms. For aquatic organisms, literature values (from IAEA 2010) have been used, see Table 11-3.

Table 11-3. Fraction dry weight of organisms (kgdw kgfw^{-1})

Organisms	Fraction dry weight of organisms (f_DW_org) kgdw kgfw^{-1}
Freshwater	
Amphibian	1.50E–01
Benthic fish	2.50E–01
Bird	3.20E–01
Bivalve mollusc	1.80E–01
Black tern	3.20E–01
Crustacean	2.45E–01
Gastropod	1.80E–01
Insect larvae	2.45E–01
Mammal	3.20E–01
Microphytobenthos	2.35E–01
Pelagic fish	2.50E–01
Phytoplankton	1.60E–01
Vascular plant	1.30E–01
Zooplankton	2.45E–01
Marine	
Benthic fish	2.50E–01
Benthic mollusc	1.80E–01
Bird (Wading)	3.20E–01
Crustacean	2.45E–01
European otter	3.20E–01
Macroalgae	1.60E–01
Mammal	3.20E–01
Pelagic fish	2.50E–01
Phytoplankton	1.60E–01
Polychaete worm	2.45E–01
Ruddy turnstone	3.20E–01
Vascular plant	1.30E–01
Zooplankton	2.45E–01

12 Alternative calculation cases

In addition to the four climate calculation cases, three alternative biosphere calculation cases have been developed in SR-PSU, *Wells in discharge plume, Distributed release* and *Alternative object delineation*. For some of these cases, alternative or additional parameter values are used, in this section these parameters are presented.

12.1 Wells in discharge plume

These parameters are used in the calculation case with a well in the discharge plume in the radionuclide transport modelling.

12.1.1 Water extraction rate of a drilled well

The parameter q_well defines the water extraction rate from a drilled well. For simplicity 700 L day^{-1} (or 255 m^3 year^{-1}) was used for all drilled wells in the area biosphere objects (i.e. in or in the well interaction area). This parameter value corresponds to the water demand (humans and livestock) associated with a group of industrial age farmers that drain and cultivate a mire (Werner et al. 2013). The rate is higher than the minimum water use associated a rural family cultivating a garden plot (200 L day^{-1}) and somewhat lower than the present-day water use of 5 individuals (900 L day^{-1}) connected to a public water works (either of these could correspond to a garden-plot household). A sensitivity analysis showed that the amount of particles trapped in extracted well water increase approximately linearly with the well discharge in the range of 700 to 2,800 L day^{-1} (Werner et al. 2013), and thus particle (and presumably radionuclide) concentration in extracted water is insensitive to the well discharge in this range. However, it should be note that the value of q_well need to be matched with the value of the release fraction reaching into a well (f_well_agri, f_well_interaction). With the selected parameter value this match is ensured, as the well discharge was set to 700 L day^{-1} in the simulations used to derive release fractions reaching a drilled well (Werner et al. 2013).

12.1.2 Probability of well to be drilled within the interaction area

The parameter, p_well_interaction, defines the probability for a water-supply well to be drilled in rock within the well interaction area, i.e. the area (or rather, volume) in which such wells may have the highest concentrations of radionuclides originating from SFR. According to a regional analysis of well density (including both wells in regolith and wells in rock), the current well density is c. 0.5 wells per km^2 in areas where the shoreline passed up to approximately 1,000 years ago in Forsmark, i.e. corresponding to approximately 4000 AD in the SR-PSU case (Werner et al. 2013). There is a peak (c. 0.9 wells per km^2) at a shoreline passage c. 1,800 years ago (approximately 5000 AD in the SR-PSU case). Moreover, the well density is below 0.5 wells per km^2 in areas where the shoreline passed more than 2,000 years ago (i.e. beyond 5000 AD in the SR-PSU case). Hence, an average well density of 0.5 wells per km^2 seems appropriate for calculations of the probability for a well to be drilled at random within a given area. The well interaction area, delineated based on DarcyTools particle-tracking results, has a size of 0.26 km^2. For a well density of 0.5 wells per km^2 this size corresponds to a probability of 0.13 for a well to be drilled in rock at random within this area. In comparison, the delineated risk area for SFR 1 and SFR 2 is slightly larger than the risk area delineated by Holmén and Stigson (2001) for SFR 1.

12.1.3 The fraction of a potential release that may interact with a water-supply

This parameter, f_well_interaction, describes the fraction of a potential release from the repository that may interact with a water-supply drilled in rock in the well interaction area. As shown in Table 12-1 and Table 12-2, a number of well locations within this area were analysed using DarcyTools. Table 12-1 and Table 12-2 show that the average particle-capture ratio for the analysed wells is rather constant among SFR facility parts (c. 2–8% of released particles). Therefore, 10% can be used as a conservative, upper boundary for the fraction from any repository part that is captured by a generic well drilled in rock at random within the well interaction area.

Table 12-1. Results of SFR 1 forward particle tracking in terms of particle-caption ratios. Well discharge Q_{well} = 700 L day^{-1} (from Appendix 3 in Werner et al. 2013).

Well id	1BTF	2BTF	1BLA	1BMA	Silo	Average
29	$2.30\cdot10^{-1}$	$3.18\cdot10^{-1}$	$3.13\cdot10^{-1}$	$1.67\cdot10^{-1}$	$1.43\cdot10^{-2}$	**$2.08\cdot10^{-1}$**
21	0	0	0	0	0	**0**
22	0	0	0	0	0	**0**
23	$5.43\cdot10^{-2}$	$1.43\cdot10^{-2}$	$4.78\cdot10^{-3}$	$1.51\cdot10^{-4}$	$1.71\cdot10^{-1}$	**$4.88\cdot10^{-2}$**
24	0	$3.02\cdot10^{-4}$	$8.54\cdot10^{-3}$	$4.92\cdot10^{-2}$	0	**$1.94\cdot10^{-2}$**
25	$4.81\cdot10^{-2}$	$5.77\cdot10^{-2}$	$6.18\cdot10^{-2}$	$4.65\cdot10^{-2}$	$1.01\cdot10^{-1}$	**$6.30\cdot10^{-2}$**
26	$1.99\cdot10^{-2}$	$2.29\cdot10^{-2}$	$2.42\cdot10^{-2}$	$1.81\cdot10^{-2}$	$5.36\cdot10^{-2}$	**$2.77\cdot10^{-2}$**
27	$7.28\cdot10^{-3}$	$8.40\cdot10^{-5}$	0	0	$6.64\cdot10^{-2}$	**$2.46\cdot10^{-2}$**
28	0	0	$6.30\cdot10^{-5}$	$1.06\cdot10^{-3}$	0	**$5.60\cdot10^{-4}$**
Average	**$7.19\cdot10^{-2}$**	**$6.89\cdot10^{-2}$**	**$6.87\cdot10^{-2}$**	**$4.70\cdot10^{-2}$**	**$8.12\cdot10^{-2}$**	

Table 12-2. Results of SFR 3 forward particle tracking in terms of particle-caption ratios. Well discharge Q_{well} = 700 L day^{-1} (Appendix 3 in Werner et al. 2013).

Well id	2BLA	3BLA	4BLA	5BLA	2BMA	1BRT	Average
29	$1.69\cdot10^{-2}$	$4.20\cdot10^{-3}$	$1.10\cdot10^{-3}$	$4.30\cdot10^{-4}$	$3.6\cdot10^{-4}$	$5.57\cdot10^{-2}$	**$1.31\cdot10^{-2}$**
21	$9.00\cdot10^{-6}$	$2.36\cdot10^{-4}$	$9.05\cdot10^{-4}$	$1.21\cdot10^{-2}$	$4.24\cdot10^{-2}$	$4.00\cdot10^{-6}$	**$9.29\cdot10^{-3}$**
22	$1.04\cdot10^{-2}$	$1.36\cdot10^{-2}$	$1.96\cdot10^{-2}$	$2.14\cdot10^{-2}$	$1.28\cdot10^{-2}$	$1.02\cdot10^{-3}$	**$1.31\cdot10^{-2}$**
23	$1.15\cdot10^{-1}$	$9.83\cdot10^{-2}$	$6.29\cdot10^{-2}$	$3.78\cdot10^{-2}$	$3.34\cdot10^{-2}$	$1.22\cdot10^{-1}$	**$7.82\cdot10^{-2}$**
24	0	0	0	0	0	$1.00\cdot10^{-6}$	**$1.67\cdot10^{-7}$**
25	$9.34\cdot10^{-2}$	$4.42\cdot10^{-2}$	$2.46\cdot10^{-2}$	$1.85\cdot10^{-2}$	$1.99\cdot10^{-2}$	$1.30\cdot10^{-1}$	**$5.51\cdot10^{-2}$**
26	$6.24\cdot10^{-2}$	$3.15\cdot10^{-2}$	$2.00\cdot10^{-2}$	$1.63\cdot10^{-2}$	$1.87\cdot10^{-2}$	$8.48\cdot10^{-2}$	**$3.90\cdot10^{-2}$**
27	$6.48\cdot10^{-2}$	$4.52\cdot10^{-2}$	$4.41\cdot10^{-2}$	$3.88\cdot10^{-2}$	$2.09\cdot10^{-2}$	$3.36\cdot10^{-2}$	**$4.12\cdot10^{-2}$**
28	0	0	0	0	0	0	**0**
Average	**$5.18\cdot10^{-2}$**	**$3.39\cdot10^{-2}$**	**$2.47\cdot10^{-2}$**	**$2.08\cdot10^{-2}$**	**$2.12\cdot10^{-2}$**	**$5.34\cdot10^{-2}$**	

12.1.4 Fraction of particles that reaches a well associated to future, potential agricultural settlements

This parameter, f_well_agri, is the ratio between the number of particles that reaches a certain well drilled in rock, associated to future, potential agricultural settlements, and the number of particles released from a certain SFR facility part (Table 12-4). Using DarcyTools, particles released at SFR 1 and SFR 3 were only captured in a few of the examined wells and particle-capture ratios were small (see Figure 6-13 and Appendix 3 in Werner et al. 2013). The parameter values for f_well_agri were derived by using the maximum particle-capture ratio for each repository part (over all wells) as a best estimate, and uncertainty in this parameter was cautiously handled by multiplying the particle-capture ratio with an uncertainty factor of two. Hence, f_well_agri has different values for different combinations of SFR facility parts and drilled wells.

Table 12-3. Results of forward particle tracking in terms of particle-capture ratios for wells drilled in rock, associated to future, potential agricultural settlements. Well discharge q-well = 700 L day^{-1} (Appendix 3 in Werner et al. 2013).

SFR 1						
Well id	**1BTF**	**2BTF**	**1BLA**	**1BMA**	**Silo**	
11	$2.00\cdot10^{-5}$	$1.00\cdot10^{-5}$	0	0	$9.00\cdot10^{-5}$	
SFR 3						
Well id	**2BLA**	**3BLA**	**4BLA**	**5BLA**	**2BMA**	**1BRT**
3	0	$4.00\cdot10^{-5}$	$3.00\cdot10^{-5}$	$2.00\cdot10^{-5}$	$2.00\cdot10^{-5}$	$2.00\cdot10^{-5}$
5	0	$1.00\cdot10^{-5}$	$2.00\cdot10^{-5}$	$2.10\cdot10^{-4}$	$9.1\cdot10^{-4}$	0
11	$1.19\cdot10^{-3}$	$1.72\cdot10^{-3}$	$1.01\cdot10^{-3}$	$5.60\cdot10^{-4}$	$4.3\cdot10^{-4}$	$8.70\cdot10^{-4}$

Table 12-4. The parameter values of f_well_agri, which describes the ratio between the number of particles that reaches a certain well and the number of particles released from a certain SFR facility part for different parts of the SFR facility (Bq year^{-1}) per (Bq year^{-1}).

SFR facility	f_well_agri	SFR facility	f_well_agri
BLA1	0	BMA2	2.00E–03
BLA2	2.00E–03	BTF1	4.00E–05
BLA3	3.00E–03	BTF2	2.00E–05
BLA4	2.00E–03	BRT	2.00E–03
BLA5	1.00E–03	Silo	2.00E–04
BMA1	0.00E+00		

12.2 Distributed release

The parameter f_release is used in the calculation case *Distributed release* to estimate the proportion of the release that reaches the different biosphere objects. Hydrogeological modelling indicates that the major fraction of a potential release from the present repository (SFR1) and its planned extension (SFR3) will be discharged into a limited area in the future Forsmark landscape, i.e. into biosphere object 157_2. Consequently, dose and dose rate estimates in the base case were based on the assumption that all radionuclides will be discharged into object 157_2, and that radionuclides reach other biosphere objects only through horizontal fluxes of groundwater and surface water.

However, for a few repository parts, a fraction of the release is expected to be directly discharged to other biosphere objects. To quantify the effects of the simplified handling of the large-scale spatial distribution of the release in the base case, the alternative calculation case *Distibuted release* was set up. The 2BMA part of the repository had the largest fraction of exit points located outside of object 157_2. Thus for this simulation the release fractions from 2BMA to each of the biosphere objects were used. Release fractions were determined for 17 hydrogeological simulations (Odén et al. 2014), and in calculation case Distributed release the maximum release fraction, over the 17 simulations, was cautiously used for each biosphere object and time (Table 12-5).

Table 12-5. Distribution of maximum proportions of radionuclide releases (in % of total potential release from 2BMA) between the different biosphere objects in the 17 performed hydrological simulations.

Time (AD)	157_2	159	157_1	116	121_2	160	121_1
2000	100	0	0	0.1	0.3	0	0
2500	97.4	0	0	0	22.4	0	0.1
3000	97.7	0.2	0.6	0	12.8	1.8	23.7
3500	99.1	2.7	6.6	1.4	10	3.3	0
5000	94.6	15.5	9.4	3.5	7.2	1.8	0
9000	95.8	13.2	10.2	1.7	8.4	0.4	0

12.3 Alternative object delineation

This section presents the parameters that is altered in the calculation case alternative object delineation. Alternative methods for delineating biosphere objects can be applied in order to examine how the object delineation may affect object properties and the environmental concentrations that result from a constant release of radionuclides. Therefore, four alternative delineations of biosphere object 157_2 have been performed in SR-PSU, see SKB (2014c) for more information. The four alternative object delineations are described here:

Area with upward hydraulic gradients (Upward). The original biosphere object 157_2 was outlined based on particle discharge at the bedrock-regolith interface. For this alternative delineation, it is assumed that all radionuclides are released to areas that are defined as discharge areas all the way from the bedrock to the surface.

Wetland areas (Wetl). In this delineation it was assumed that all radionuclides are released to the area of the object that has wetland properties.

Areas with a high density of discharge-location at the interface between rock and regolith (HD-Disch). In the delineation based on discharge points from DarcyTools the area with a high density of discharge points was selected as an alternative delineation of biosphere object 157_2.

Potential future arable land (Arable). In the LDM, a future landscape is described in which most of the potential arable land is used. For this delineation it was assumed that the combined thickness of peat postglacial clay and glacial clay was at least 0.5 m after drainage, accounting for the compaction and oxidation of peat and postglacial clay associated with drainage. When these criteria are applied on biosphere object 157_2, only a small area is regarded suitable for long-term agricultural practices.

In addition to these cases the base case delineation of object 157_1 (here called the reference) where used to assess the effects of the alternative object delineations.

Parameters defining the geometries of the alternative object delineations were used. The thickness of the regolith layers (till, glacial clay and post glacial sediments), the area of the object and the area of the terrestrial part of the object were altered in the object delineations. The ingrowth of peat and the mineralization rate of peat were also altered.

Water balances were extracted for the identified subareas of object 157_1. The water balances were derived using the MIKE SHE 5000 AD local model setup (Werner et al. 2013). As expected, the largest net vertical groundwater fluxes from rock to regolith are obtained for subareas with upward hydraulic gradients (*Upward*) and high discharge-location density (*HD-disch*). The smallest net flux is obtained for arable land (*Arable*), which is characterised by thick layers of low-permeable regolith. In subareas with shallow depth to the groundwater table (*Wetl*), net vertical groundwater fluxes are similar to those obtained for the entire biosphere object.

The parameters are listen in Table 12-6 and Table 12-7.

Table 12-6. Parameters altered in the alternative object delineation case.

Parameter	Unit	Arable	UpwGrad	Reference	HD_disch	Wetl
area_obj	m	2.92E+04	1.32E+05	1.68E+05	4.72E+04	8.40E+04
minRate_regoPeat	kgC kgC^{-1} year^{-1}	2.10E–03	7.16E–03	7.16E–03	5.29E–03	3.04E–03
z_regoGL	m	1.04E+00	2.30E–01	1.70E–01	1.10E–01	3.50E–01
z_regoLow	m	1.82E+00	2.23E+00	2.40E+00	2.66E+00	1.89E+00
q_downstream_end	m^3 m^{-2} year^{-1}	6.68E+00	1.47E+00	1.16E+00	1.69E+00	2.32E+00
q_downstream_iso	m^3 m^{-2} year^{-1}	6.68E+00	1.47E+00	1.16E+00	1.69E+00	2.32E+00
q_gl_low_ter_end	m^3 m^{-2} year^{-1}	1.50E–02	1.51E–02	8.09E–03	3.24E–02	8.98E–02
q_gl_low_ter_iso	m^3 m^{-2} year^{-1}	1.50E–02	1.51E–02	8.09E–03	3.24E–02	8.98E–02
q_gl_pg_ter_end	m^3 m^{-2} year^{-1}	1.47E–01	2.98E–01	2.03E–01	2.55E–01	2.14E–01
q_gl_pg_ter_iso	m^3 m^{-2} year^{-1}	1.47E–01	2.98E–01	2.03E–01	2.55E–01	2.14E–01
q_low_gl_ter_end	m^3 m^{-2} year^{-1}	1.16E–01	2.86E–01	1.51E–01	2.53E–01	1.98E–01
q_low_gl_ter_iso	m^3 m^{-2} year^{-1}	1.16E–01	2.86E–01	1.51E–01	2.53E–01	1.98E–01
q_peat_pg_ter_end	m^3 m^{-2} year^{-1}	3.18E–03	2.44E–01	2.85E–01	2.56E–01	1.93E–01
q_peat_pg_ter_iso	m^3 m^{-2} year^{-1}	3.18E–03	2.44E–01	2.85E–01	2.56E–01	1.93E–01
q_peat_up_ter_end	m^3 m^{-2} year^{-1}	4.40E–01	6.25E–01	6.19E–01	1.04E+00	1.43E+00
q_peat_up_ter_iso	m^3 m^{-2} year^{-1}	4.40E–01	6.25E–01	6.19E–01	1.04E+00	1.43E+00
q_pg_gl_ter_end	m^3 m^{-2} year^{-1}	1.54E–02	1.65E–02	5.59E–02	3.25E–02	1.04E–01
q_pg_gl_ter_iso	m^3 m^{-2} year^{-1}	1.54E–02	1.65E–02	5.59E–02	3.25E–02	1.04E–01
q_pg_peat_ter_end	m^3 m^{-2} year^{-1}	1.47E–01	5.14E–01	4.71E–01	6.81E–01	4.57E–01
q_pg_peat_ter_iso	m^3 m^{-2} year^{-1}	1.47E–01	5.14E–01	4.71E–01	6.81E–01	4.57E–01
q_up_peat_ter_end	m^3 m^{-2} year^{-1}	1.79E–01	3.61E–01	4.11E–01	4.48E–01	5.48E–01
q_up_peat_ter_iso	m^3 m^{-2} year^{-1}	1.79E–01	3.61E–01	4.11E–01	4.48E–01	5.48E–01
q_up_wat_ter_end	m^3 m^{-2} year^{-1}	6.68E+00	1.47E+00	1.16E+00	1.69E+00	2.32E+00
q_up_wat_ter_iso	m^3 m^{-2} year^{-1}	6.68E+00	1.47E+00	1.16E+00	1.69E+00	2.32E+00
q_wat_up_ter_end	m^3 m^{-2} year^{-1}	0.00E+00	0.00E+00	0.00E+00	0.00E+00	0.00E+00
q_wat_up_ter_iso	m^3 m^{-2} year^{-1}	0.00E+00	0.00E+00	0.00E+00	0.00E+00	0.00E+00

Table 12-7. Time dependent parameters altered in the alternative object delineation case.

Parameter	Unit	Year (AD)	Reference	Arable	UpwGrad	HD_disch	Wetl
area_obj_ter	m^2	2500	0.00E+00	0.00E+00	0.00E+00	0.00E+00	0.00E+00
area_obj_ter	m^2	3000	2.71E+02	2.71E+02	2.71E+02	2.71E+02	2.71E+02
area_obj_ter	m^2	3500	2.73E+04	2.73E+04	2.73E+04	2.73E+04	2.73E+04
area_obj_ter	m^2	4000	1.32E+05		1.32E+05		
area_obj_ter	m^2	4276	1.68E+05	2.92E+04	1.32E+05	4.72E+04	8.40E+04
z_regoPG_ter	m	2500	0.00E+00	0.00E+00	0.00E+00	0.00E+00	0.00E+00
z_regoPG_ter	m	3000	1.16E–01	1.16E–01	1.16E–01	1.16E–01	1.16E–01
z_regoPG_ter	m	3500	2.65E–01	2.65E–01	2.65E–01	2.65E–01	2.65E–01
z_regoPG_ter	m	4000	2.88E–01	2.88E–01	2.88E–01	2.88E–01	2.88E–01
z_regoPG_ter	m	4276	3.10E–01	4.10E–01	3.30E–01	3.10E–01	3.60E–01
Ter_growth	m^3 $year^{-1}$	0	0.00E+00	0.00E+00	0.00E+00	0.00E+00	0.00E+00
Ter_growth	m^2 $year^{-1}$	2500	5.42E–01	5.42E–01	5.42E–01	5.42E–01	5.42E–01
Ter_growth	m^2 $year^{-1}$	3000	5.41E+01	5.41E+01	5.41E+01	5.41E+01	5.41E+01
Ter_growth	m^2 $year^{-1}$	3500	2.09E+02	2.41E+00	2.09E+02	2.56E+01	7.31E+01
Ter_growth	m^2 $year^{-1}$	4000	1.30E+02		2.64E+00		
Ter_growth	m^2 $year^{-1}$	4276	0.00E+00	0.00E+00	0.00E+00	0.00E+00	0.00E+00
WF_lobj157_1	m^3 $year^{-1}$	2000	7.48E+08	7.48E+08	7.48E+08	7.48E+08	7.48E+08
WF_lobj157_1	m^3 $year^{-1}$	3000	4.01E+08	4.01E+08	4.01E+08	4.01E+08	4.01E+08
WF_lobj157_1	m^3 $year^{-1}$	4275	1.95E+05	1.95E+05	1.95E+05	7.98E+04	1.95E+05

References

SKB's (Svensk Kärnbränslehantering AB) publications can be found at www.skb.se/publications.

Adrian R, O'Reilly C M, Zagarese H, Baines S B, Hessen D O, Keller W, Livingstone D M, Sommaruga R, Straile D, Van Donk E, Weyhenmeyer G A, Winder M, 2009. Lakes as sentinels of climate change. Limnology and Oceanography 54, 2283–2297.

Alanärä A, Näslund I, 1995. Modern fiskevård: steg för steg. Umeå: Sveriges lantbruksuniversitet. (Kompendium 8). (In Swedish.)

Algesten G, Sobek S, Bergström A-K, Ågren A, Tranvik L J, Jansson M, 2003. Role of lakes for organic carbon cycling in the boreal zone. Global Change Biology 10, 141–147.

Algesten G, Brydsten L, Jonsson P, Kortelainen P, Löfgren S, Rahm L, Raike A, Sobek S, Tranvik L, Wikner J, Jansson M, 2006. Organic carbon budget for the Gulf of Bothnia. Journal of Marine Systems 63, 155–161.

Altman P L, Ditmer D S (eds), 1964. Biology data book. Washington, DC: Federation of American Societies for Experimental Biology.

Amiro B D, Ewing L L, 1992. Physiological conditions and uptake of inorganic carbon-14 by plant roots. Environmental and Experimental Botany 32, 203–211.

Andersson E (ed), 2010. The limnic ecosystems at Forsmark and Laxemar-Simpevarp. SR-Site Biosphere. SKB TR-10-02, Svensk Kärnbränslehantering AB.

Andersson E, 2005. Benthic-pelagic microbial interactions and carbon cycling in clearwater lakes. PhD thesis. Uppsala University, Sweden. (Digital comprehensive summaries of Uppsala dissertations from the Faculty of Science and Technology 52)

Andersson E, Brunberg A-K, 2006. Net autotrophy in an oligotrophic lake rich in dissolved organic carbon and with high benthic primary production. Aquatic Microbial Ecology 43, 1–10.

Andersson E, Tudorancea M-M, Tudorancea C, Brunberg A-K, Blomqvist P, 2003. Water chemistry, biomass and production of biota in Lake Eckarfjärden during 2002. SKB R-03-27, Svensk Kärnbränslehantering AB.

Antoine J M, Magliola C, Counzy F, Darret G, Mareshi J P, 1986. Estimation of the share of each water source for adults in France. Water intake provided to French adults. Annals of Nutrition & Metabolism 30, 407–414.

Aquilonius K, 2010. The marine ecosystems at Forsmark and Laxemar-Simpevarp. SR-Site Biosphere. SKB TR-10-03, Svensk Kärnbränslehantering AB.

Arya S P, 2001. Introduction to micrometeorology. 2nd ed. Burlington: Elsevier Science.

Asaeda T, Karunaratne S, 2000. Dynamic modeling of the growth of *Phragmites australis*: model description. Aquatic Botany 67, 301–318.

Aurela M, Riutta T, Laurila T, Tuovinen J-P, Vesala T, Tuittila E-S, Rinne J, Haapanala S, Laine J, 2007. CO_2 exchange of a sedge fen in southern Finland – the impact of a drought period. Tellus 59B, 826–837.

Avila R, 1998. Radiocaesium transfer to roe deer and moose: modelling and experimental studies. Uppsala: Swedish University of Agricultural Sciences. (Agraria 136)

Avila R, 2006. The ecosystem models used for dose assessments in SR-Can. SKB R-06-81, Svensk Kärnbränslehantering AB.

Avila R, Bergström U, 2006. Methodology for calculation of doses to man and implementation in Pandora. SKB R-06-68, Svensk Kärnbränslehantering AB.

Avila R, Moberg L, 1999. A systematic approach to the migration of ^{137}Cs in forest ecosystems using interaction matrices. Journal of Environmental Radioactivity 45, 271–282.

Avila R, Ekström P-A, Åstrand P-G, 2010. Landscape dose conversion factors used in the safety assessment SR-Site. SKB TR-10-06, Svensk Kärnbränslehantering AB.

BACC, 2008. Assessment of climate change for the Baltic Sea basin. The BACC (BALTEX Assessment of Climate Change for the Baltic Sea basins) author team. Berlin: Springer.

Backéus I, 1990. Production and depth distribution of fine roots in a boreal open bog. Annales Botanici Fennici 27, 261–265.

Bain J T, Proctor M C F, 1980. The requirement of aquatic bryophytes for free CO_2 as an inorganic carbon source: some experimental evidence. New Phytologist 86, 393–400.

Banse K, Mosher S, 1980. Adult body mass and annual production/biomass relationships of field populations. Ecological Monographs 50, 355–379.

Beer J, Blodau C, 2007. Transport and thermodynamics constrain below-ground carbon turnover in a northern peatland. Geochimca et Cosmochimica Acta 71, 2989–3002.

Belova M, 1993. Microbial decomposition of freshwater macrophytes in the littoral zone of lakes. Hydrobiologia 251, 59–64.

Beresford N, Brown J, Copplestone D, Garnier-Laplace J, Howard B J, Larsson C-M, Oughton O, Pröhl G, Zinger I (eds), 2007. D-ERICA: An integrated approach to the assessment and management of environmental risks from ionising radiation. Description of purpose, methodology and application. Contract number: FI6R-CT-2004-508847. European Commission.

Berglund K, 1996. Cultivated organic soils in Sweden: properties and amelioration. PhD thesis. Swedish University of Agricultural Sciences, Department of Soil Sciences.

Berglund K, 2008. Torvmarken: en resurs i jordbruket igår, idag och även i morgon? In Runefelt L (ed). Svensk mosskultur: odling, torvanvändning och landskapets förändring 1750–2000. Stockholm: Kungl. Skogs- och lantbruksakademien, 483–498. (In Swedish.)

Berglund K, Miller U, Persson J, 1989. Gyttjejordar, deras sammansättning och egenskaper. Uppsala: Swedish University of Agricultural Sciences, Department of Soil Sciences. (Hydrotechnics Report 160) (In Swedish.)

Berglund Ö, Berglund K, 2011. Influence of water table level and soil properties on emissions of greenhouse gases from cultivated peat soil. Soil Biology and Biochemistry 43, 923–931.

Bergman R, Bergström U, Evans S, 1977. Ecologic transport and radiation doses from groundwaterborne radioactive substances. KBS TR 40, Svensk Kärnbränsleförsörjning AB.

Bergman R, Bergström U, Evans S, 1979. Dose and dose commitment from groundwaterborne radioactive elements in the final storage of spent nuclear fuel. KBS TR 100, Svensk Kärnbränsleförsörjning AB.

Bergström E, 2001. Late Holocene distribution of lake sediment and peat in NE Uppland, Sweden. SKB R-01-12, Svensk Kärnbränslehantering AB.

Bergström U, 1983. Dose and dose commitment calculations from groundwater borne radioactive elements released from a repository for spent nuclear fuel. SKBF/KBS TR 83-49, Svensk Kärnbränsleförsörjning AB.

Bergström U, Barkefors C, 2004. Irrigation in dose assessments models. SKB R-04-26, Svensk Kärnbränslehantering AB.

Bergström U, Avila R, Ekström P-A, de la Cruz I, 2008. Dose assessments for SFR 1. SKB R-08-15, Svensk Kärnbränslehantering AB.

Bilsborough S, Mann N, 2006. A review of issues of dietary protein intake in humans. International Journal of Sport Nutrition and Exercise Metabolism 16, 129–152.

BIOMOVS II, 1996. Model validation studies of water flow and radionuclide transport in vegetated soils using lysimeter data. Technical Report 15. Available at: http://www.iaea.org/inis/collection/NCLCollectionStore/_Public/31/047/31047296.pdf

Blindow I, Hargeby A, Meyercordt J, Schubert H, 2006. Primary production in two shallow lakes with contrasting plant form dominance: a paradox of enrichment? Limnology and Oceanography 51, 2711–2721.

Blomqvist P, Nilsson E, Brunberg A-K, 2002. Habitat distribution, water chemistry, and biomass and production of pelagic and benthic microbiota in Lake Eckarfjärden, Forsmark. SKB R-02-41, Svensk Kärnbränslehantering AB.

Borgiel M, 2004. Forsmark site investigation. Sampling of freshwater fish. SKB P-04-06, Svensk Kärnbränslehantering AB.

Bosson E, Gustafsson L-G, Sassner M, 2008. Numerical modelling of surface hydrology and near-surface hydrogeology at Forsmark. Site descriptive modelling, SDM-Site Forsmark. SKB R-08-09, Svensk Kärnbränslehantering AB.

Bosson E, Sassner M, Sabel U, Gustafsson, L-G, 2010. Modelling of present and future hydrology and solute transport at Forsmark. SR-Site Biosphere. SKB R-10-02, Svensk Kärnbränslehantering AB.

Bray J R, 1963. Root production and the estimation of the net productivity. Canadian Journal of Botany 41, 65–72.

Brix H, 1990. Uptake and photosynthetic utilization of sediment-dervied carbon by *Phragmites australis* (Cav.) Trin. ex Steudel. Aquatic Botany 38, 377–389.

Brix H, Sorrell B K, Lorenzen B, 2001. Are *Phragmites*-dominated wetlands a net source or net sink of greenhouse gases? Aquatic Botany 69, 313–324.

Brown J E, Alfonso B, Avila R, Beresford N A, Copplestrone D, Pröhl G, Ulanovsky A, 2008. The ERICA Tool, Journal of Environmental Radioactivity 99, 1371–1383.

Brydsten L, Strömgren M, 2013. Landscape development in the Forsmark area from the past into the future (8500 BC – 40,000 AD). SKB R-13-27, Svensk Kärnbränslehantering AB.

Burdige D J, 2007. Preservation of organic matter in marine sediments: controls, mechanisms, and an imbalance in sediment organic carbon budgets? Chemical Reviews 107, 467–485.

Charman D, 2002. Peatlands and environmental change. Chichester: Wiley.

Chimney M J, Pietro K C, 2006. Decomposition of macrophyte litter in a subtropica constructed wetland in south Florida (USA). Ecological Engineering 27, 301–321.

Chojnicki B H, Urbaniak M, Jozefczyk D, Augustin J, Olejnik J, 2007. Measurements of gas and heat fluxes at Rzecin wetland. In Okruszko T, Maltby E, Szatylowicz J, Swiatek D, Kotowski W (eds). Wetlands: monitoring, modeling and management. London: Taylor & Francis, 125–131.

Clymo R S, Bryant C L, 2008. Diffusion and mass flow of dissolved carbon dioxide, methane, and dissolved organic carbon in a 7-m deep raised peat bog. Geochimca et Cosmochimica Acta 72, 2048–2066.

Cole J J, Caraco N F, 1998. Atmospheric exchange of carbon dioxide in a low-wind oligotrophic lake measured by the addition of SF_6. Limnology and Oceanography 43, 647–656.

Davis P A, Zach R, Stephens M E, Amiro B D, Bird G A, Reid J A K, Sheppard M I, Sheppard S C, Stephenson M, 1993. The disposal of Canada's nuclear fuel waste: the biosphere model, BIOTRAC, for postclosure assessment. Report AECL 10720, COG-93-10, Atomic Energy of Canada Limited.

Degerman E, Nyberg P, Näslund I, Jonasson D, 1998. Ekologisk fiskevård. Jönköping: Sportfiskarna, Sveriges sportfiske- och Fiskevårdsförbund. (In Swedish.)

DHI, 2012. MIKE SHE – user manual. Hørsholm, Denmark: DHI Water & Environment.

Downing I A, Plante C, 1993. Production of fish populations in lakes. Canadian Journal of Fisheries and Aquatic Sciences 50, 110–120.

Duarte C M, Cebrián J, 1996. The fate of marine autotrophic production. Limnology and oceanography 41, 1758–1766.

Dyson R D, 1978. Cell biology: a molecular approach. 2nd ed. Boston: Allyn and Bacon.

Eckerman K F, Leggett R W, 1996. DCFPAK: Dose coefficient data file package for Sandia National Laboratory. ORNL/TM-13347, Oak Ridge National Laboratory, Oak Ridge, TN.

Eckerman K F, Ryman J C, 1993. External exposure to radionuclides in air, water, and soil. Federal Guidance Report 12. EPA-402-R-93-081, U.S. Environmental Protection Agency, Washington, DC.

Edson J, Crawford T, Crescenti J, Farrar T, Frew N, Gerbi G, Helmis C, Hristov T, Khelif D, Jessup A, Jonsson H, Li M, Mahrt L, McGillis W, Plueddemann A, Shen L, Skyllingstad E, Stanton T, Sullivan P, Sun J, Trowbridge J, Vickers D, Wang S, Wang Q, Weller R, Wilkin J, Williams A J, Yue D K P, Zappa C, 2007. The coupled boundary layers and air-sea transfer experiment in low winds. Bulletin of the American Meteorological Society 88, 341–356.

Elmgren R, 1984. Trophic dynamics in the enclosed, brackish Baltic Sea. Rapports et Procès-verbaux des Réunions du Conseil International pour l'Exploration de la Mer 183, 152–169.

Emeis K-C, Struck U, Leipe T, Pollehne F, Kunzendorf H, Christiansen C, 2000. Changes in the C, N, P burial rates in some Baltic Sea sediments over the last 150 years – relevance to P regeneration rates and the phosphorus cycle. Marine Geology 167, 43–59.

Engdahl A, Ternsell A, Hannu S, 2006. Oskarshamn site investigation. Chemical characterisation of deposits and biota. SKB P-06-320, Svensk Kärnbränslehantering AB.

Engdahl A, Rådén R, Borgiel M, Omberg L-G, 2008. Oskarshamn and Forsmark site investigation. Chemical composition of suspended material, sediment and pore water in lakes and sea bays. SKB P-08-81, Svensk Kärnbränslehantering AB.

Ershow A G, Cantor K P, 1989. Total water and tap water intake in the United States: population-based estimates of quantities and sources. Life Sciences Research Office, Federation of American Societies for Experimental Biology.

Fiskeriverket, 2003. Kräftfiskevård: hot, möjligheter och bestämmelser. Göteborg: Fiskeriverket. (F-fakta 15) (In Swedish.)

Foken T, 2008. Micrometeorology. Berlin: Springer.

Ford C R, Wurzburger N, Hendrick R L, Teskey R O, 2007. Soil DIC uptake and fixation in *Pinus taeda* seedlings and its C contribution to plant tissues and ectomycorrhizal fungi. Tree Physiology 27, 375–383.

Fredriksson D, 2004. Forsmark site investigation. Peatland investigation Forsmark. SKB P-04-127, Svensk Kärnbränslehantering AB.

George G, 2010. The impact of climate change on European lakes. New York: Springer. (Aquatic Ecology Series 4)

Gleick P H, 1996. Basic water requirements for human activities: meeting basic needs. Water International 21, 83–92.

Glenn A J, Flanagan L B, Syed K H, Carlson P J, 2006. Comparison of net ecosystem CO_2 exchange in two peatlands in western Canada with contrasting dominant vegetation, *Sphagnum* and *Carex*. Agricultural and Forest Meteorology 140, 115–135.

Gordon R, Brown D M, Dixon M A, 1997. Estimating potato leaf area index for specific cultivars. Potato Research 40, 251–256.

Goudriaan J, 1977. Crop micrometeorology: a simulation study. Wageningen, The Netherlands: Centre for Agricultural Publishing and Documentation.

Grip H, Rodhe A, 1985. Vattnets väg från regn till bäck. Stockholm : Forskningsrådens förlagstjänst. (In Swedish.)

Gudasz C, 2010. Boreal lake sediments as sources and sinks of carbon. PhD thesis. Uppsala University. Uppsala: Acta Universitatis Upsaliensis.

Gudasz C, Bastviken D, Steger K, Premke K, Sobek S, Tranvik L, 2010. Temperature-controlled organic carbon mineralization in lake sediments. Nature 466, 478–482.

Guo Y, Sun L, 2011. Surface energy fluxes and control of evapotranspiration from a *Carex lasiocarpa* mire in the Sanjiang Plain, Northeast China. International Journal of Biometeorology 56, 221–232.

Hannu S, Karlsson S, 2006. Forsmark site investigation. Chemical characterisation of deposits and biota. SKB P-06-220, Svensk Kärnbränslehantering AB.

Hardej M, Ozimek T, 2002. The effect of sewage sludge flooding on growth and morphometric parameters of *Phragmites australis* (Cav.) Trin. ex Steudel. Ecological Engineering 18, 343–350.

Hargrave B T, 1969. Epibenthic algal production and community respiration in the sediments of Marion Lake. Journal of Fisheries Research Board of Canada 26, 2003–2026.

Harvey C J, Cox S P, Essington T E, Hansson S, Kitchell J F, 2003. An ecosystem model of food web and fisheries interactions in the Baltic Sea. ICES Journal of Marine Science 60, 939–950.

Haynes W H (ed), 2012. CRC handbook of chemistry and physics: a ready-reference book of chemical and physical data. 93rd ed. Boca Raton, FL: CRC Press.

Heal O W, Latter P M, Howson J, 1978. A study of the rates of decomposition of organic matter. In Heal O W, Perkins D F (eds). Production ecology of British moors and montane grassland. Berlin: Springer-Verlag, 136–159.

Hedenström A, 2004. Forsmark site investigation. Investigation of marine and lacustrine sediment in lakes. Stratigraphical and analytical data. SKB P-04-86, Svensk Kärnbränslehantering AB.

Hedenström A, Sohlenius G, 2008. Description of the regolith at Forsmark. Site descriptive modelling SDM-Site Forsmark. SKB R-08-04, Svensk Kärnbränslehantering AB.

Heibo E, Karås P, 2005. Forsmark site investigation. The coastal fish community in the Forsmark area SW Bothnian Sea. SKB P-05-148, Svensk Kärnbränslehantering AB.

Heneryd N, 2007. Forsmark site investigation. Measurements of ground respiration, primary production and NEE in terrestrial habitats. SKB P-07-23, Svensk Kärnbränslehantering AB.

Hesikanen A-S, Leppänen J-M, 1995. Estimation of export production in the coastal Baltic Sea: effect of resuspension and microbial decomposition on sediment measurements. Hydrobiologia 316, 211–224.

Hill W R, 1996. Effects of light. In Stevenson R J, Bothwell M L, Lowe R L (eds). Algal ecology: freshwater benthic ecosystems. San Diego, CA: Academic Press, 121–148.

Holmén J G, Stigsson M, 2001. Future hydrogeological conditions at SFR. SKB R-01-02, Svensk Kärnbränslehantering AB.

Hwang Y-H, Morris J T, 1992. Fixation of inorganic carbon from different sources and its translocation in *Spartina alterniflora* Loisel. Aquatic Botany 43, 137–147.

Håkansson L, Jansson M, 2002. Principles of lake sedimentology. Caldwell, NJ: The Blackburn Press.

Håkanson L, Gyllenhammar A, Brolin A, 2004. A dynamic compartmental model to predict sedimentation and suspended particulate matter in coastal areas. Ecological Modelling 175, 353–384.

IAEA, 2003. "Reference Biospheres" for solid radioactive waste disposal. Report of BIOMASS Theme 1 of the BIOsphere Modelling and ASSessment (BIOMASS) Programme. Part of the IAEA Co-ordinated Research Project on Biosphere Modelling and Assessment (BIOMASS). IAEABIOMASS-6, International Atomic Energy Agency.

IAEA, 2010. Handbook of parameter values for the prediction of radionuclide transfer in terrestrial and freshwater environments. Vienna: International Atomic Energy Agency. (Technical Reports Series 472)

ICRP, 1975. Reference man: anatomical, physiological and metabolic characteristics. Oxford: Pergamon. (ICRP Publication 23)

ICRP, 1983. Radionuclide transformations: energy and intensity of emissions. New York: Pergamon. (ICRP Publication 38; Annals of the ICRP 11–13)

ICRP, 1993. Protection against radon-222 at home and at work. Oxford: Pergamon. (ICRP Publication 65; Annals of the ICRP 23(2))

ICRP, 1996. Age-dependent doses to members of the public from intake of radionuclides: Part 5, Compilation of ingestion and inhalation dose coefficients. Oxford: Pergamon. (ICRP Publication 72, Annals of the ICRP 26 (1))

ICRP, 2000. Radiation protection recommendations as applied to the disposal of long-lived solid radioactive waste. Oxford: Pergamon. (ICRP Publication 81; Annals of the ICRP 28 (4))

ICRP, 2002. Basic anatomical and physiological data for use in radiological protection: reference values. Oxford: Pergamon. (ICRP Publication 89; Annual of the ICRP 32 (3–4))

ICRP, 2006. Assessing dose of the representative person for the purpose of the radiation protection of the public. The optimisation of radiological protection: broadening the process. Oxford: Pergamon. (ICRP Publication 101; Annals of the ICRP 36 (3))

Iiyama I, Hasegawa S, 2005. Gas diffusion coefficient of undisturbed peat soils. Soil Science and Plant Nutrition 51, 431–435.

IPCC SRES, 2000. Special report on emissions scenarios: a special report of Working Group III of the Intergovernmental Panel on Climate Change. Cambridge: Cambridge University Press.

IVL, 2009. Data describing dust concentration in air is available from the Swedish Environmental Research Institute, http://www.ivl.se/tjanster/datavardskap/luftkvalitet.4.7df4c4e812d2da6a41680004804.html, accessed 2009-04-05.

Jaeschke B, Smith K, Nordén S, Alfonso B, 2013. Assessment of risk to non-human biota from a repository for the disposal of spent nuclear fuel at Forsmark, Sweden. Supplementary information. SKB TR-13-23, Svensk Kärnbränslehantering AB.

James R (ed), 2005. Marine biogeochemical cycles. 2nd ed. Oxford: Butterworth-Heinemann.

Johansson P-O, 2008. Description of surface hydrology and near-surface hydrogeology at Forsmark. Site descriptive modelling, SDM-Site Forsmark. SKB R-08-08, Svensk Kärnbränslehantering AB.

Johansson W, 1973. Method using meteorological data for estimation of soil moisture content and soil moisture changes in cultivated land. Grundförbättring 26, 57–153. (In Swedish with summary in English)

Johansson W, Klingspor P, 1977. Bevattning inom lantbruket 1976 : bevattnad areal, vattenåtgång och vattentäkter. Uppsala: Institutionen för markvetenskap, avdelningen för lantbrukets hydroteknik. (Stenciltryck 100) (In Swedish.)

Jonsson P, Eckhéll J, Larsson P, 2000. PCB and DDT in laminated sediments from offshore and archipelago areas of the NW Baltic Sea. Ambio 29, 268–276.

Jordbruksverkets statistikdatabas, 2012. Data describing production of different agricultural products in Sweden. The data base is accessible from http://statistik.sjv.se/PXWeb/pxweb/sv/Jordbruksverkets%20statistikdatabas/?rxid=5adf4929-f548-4f27-9bc9-78e127837625, accessed 2012-11-21.

Kardell L, 1980. Occurrence and production of billberry, lingonberry and raspberry in Sweden's forests. Forest Ecology and Management 2, 285–298.

Kardell L, 1993. Produktion av skogsbär och matsvampar på Ekenäs gård i Södermanland. Rapport 56, Swedish University of Agricultural Sciences, Uppsala, Sweden. (In Swedish.)

Kardell L, 1994. Produktion av matsvamp i sumpskog. Jordstjärnan 15, 12–28. (In Swedish.)

Kardell L, Carlsson E, 1982. Hjortron, tranbär, lingon: förekomst och bärproduktion i Sverige 1978–1980 (Cloudberry, cranberry, lingonberry: occurrence and production in Sweden (1978–1980). Rapport 25, Swedish University of Agricultural Sciences, Uppsala, Sweden. (In Swedish.)

Kardell L, Eriksson L, 1987. The effect of forest operations on the production of edible mushrooms. Sveriges skogsvårdsförbunds tidskrift 85, 3–23.

Karlsson A, Eriksson C, Borell Lövstedt C, Liungman O, Engqvist A, 2010. High-resolution hydrodynamic modelling of the marine environment at Forsmark between 6500 BC and 9000 AD. SKB R-10-09, Svensk Kärnbränslehantering AB.

Karlsson S, Andersson E, 2006. Forsmark site investigation. Distribution, production and respiration of submerged vegetation in Lake Bolundsfjärden. SKB P-06-221, Svensk Kärnbränslehantering AB.

Karlsson S, Bergström U, Meili M, 2001. Models for dose assessments. Models adapted to the SFR area, Sweden. SKB TR-01-04, Svensk Kärnbränslehantering AB.

Kasimir-Klemedtsson Å, Klemedtsson L, Berglund K, Martikainen P, Silvola J, Oenema O, 1997. Greenhouse gas emission from farmed organic soils: a review. Soil Use and Management 13, 245–250.

Kautsky U (ed), 2001. The biosphere today and tomorrow in the SFR area. SKB R-01-27, Svensk Kärnbränslehantering AB.

Kettunen A, Kaitala V, Lehtinen A, Lohila A, Alm J, Silvola J, Martikainen P J, 1999. Methane production and oxidation potentials in relation to water table fluctuations in two boreal mires. Soil Biology and Biochemistry 31, 1741–1749.

Kjellström E, Strandberg G, Brandefelt J, Näslund J-O, Smith B, Wohlfart B, 2009. Climate conditions in Sweden in a 100,000-year time perspective. SKB TR-09-04, Svensk Kärnbränslehantering AB.

Kufel L, Kufel I, 2002. *Chara* beds acting as nutrient sinks in shallow lakes – a review. Aquatic Botany 72, 249–260.

Kumblad L, Bradshaw C, 2008. Element composition of biota, water and sediment in the Forsmark area, Baltic Sea. Concentrations, bioconcentration factors and partitioning coefficients (K_d) of 48 elements. SKB TR-08-09, Svensk Kärnbränslehantering AB.

Kuss J, Nagel K, Schneider B, 2004. Evidence from the Baltic Sea for an enhanced CO_2 air–sea transfer velocity. Tellus B 56, 175–182.

Lamberti G A, 1996. The role of periphyton in benthic food webs. In Stevenson R J, Bothwell M L, Lowe R L (eds). Algal ecology: freshwater benthic ecosystems. San Diego, CA: Academic Press, 533–572.

Larsson-McCann S, Karlsson A, Nord M, Sjögren J, Johansson L, Ivarsson M, Kindell S, 2002. Meteorological, hydrological and oceanographical information and data for the site investigation program in the communities of Östhammar and Tierp in the northern part of Uppland. SKB TR-02-02, Svensk Kärnbränslehantering AB.

Leggett R W, 2004. A biokinetic model for carbon dioxide and bicarbonate. Radiation Protection Dosimetry 108, 203–213.

Leipe, T, Tauber, F, Vallius, H, Virtasalo, J, Uścinowicz, S, Kowalski, N, Lindgren, S, Myllivarta, T 2011. Particulate organic carbon (POC) in surface sediments of the Baltic Sea. Geo-Marine Letters 31, 175–188.

Lerman A, 1979. Geochemical processes: Water and sediment environments. New York: Wiley.

Liljegren R, 2010. Pluddertorv, tramptorv och maskintorv. Om torvtäkt och torvanvändning i Sverige 1800–1950. In Runefelt L (ed). Svensk mosskultur: odling, torvanvändning och landskapets förändring 1750–2000. 2nd ed. Stockholm: Kungl. Skogs- och lantbruksakademien.

Liljelind I, Barregård L, 2008. Hälsoriskbedömning vid utredning av förorenade områden. Rapport 5859, Naturvårdsverket. (In Swedish.)

Limpens J, Berendse1 F, Blodau C, Canadell J G, Freeman C, Holden J, Roulet N, Rydin H, Schaepman-Strub G, 2008. Peatlands and the carbon cycle: from local processes to global implications – a synthesis. Biogeosciences 5, 1475–1491.

Lindborg T (ed), 2010. Landscape Forsmark – data, methodology and results for SR-Site. SKB TR-10-05, Svensk Kärnbränslehantering AB.

Lindborg T, Brydsten L, Sohlenius G, Strömgren M, Andersson E, Löfgren A, 2013. Landscape development during a glacial cycle: modeling ecosystems from the past into the future. Ambio 42, 402–413.

Lindgren M, Pettersson M, Karlsson S, Moreno L, 2001. Project SAFE. Radionuclide release and dose from the SFR repository. SKB R-01-18, Svensk Kärnbränslehantering AB.

Lindquist S-O, 1974. The development of the agrarian landscape on Gotland during early Iron Age. Norwegian Archaeological Review 7, 6–32.

Liss J-E, 2005. Brännved: energiinnehåll i några olika trädslag. Arbetsdokument 1, Högskolan Dalarna. (In Swedish.)

Liu J, Löfgren M, Neretnieks I, 2006. SR-Can. Data and uncertainty assessment. Matrix diffusivity and porosity in situ. SKB R-06-111, Svensk Kärnbränslehantering AB.

Livsmedelsverket, 2001. Data from the National Food Agency's database (http://www7.slv.se/SokNaringsinnehall) was used to describe the carbon content of proteins, carbohydrates and lipids for different food items. [accessed 2009-05-11].

Lobert J M, Keene W C, Logan J A, Yevich R, 1999. Global chlorine emissions from biomass burning: reactive chlorine emissions inventory. Journal of Geophysical Research Atmospheres 104, 8373–8389.

Lotz L A P, Groeneveld J, Theunissen J, van den Broek R C F M, 1997. Yield loss of white cabbage by competition with clovers grown as cover crop. Netherlands Journal of Agricultural Science 45, 393–405.

Lovett G M, Likens G E, Buso D C, Driscoll C T, Bailey S W, 2005. The biogeochemistry of chlorine at Hubbard Brook, New Hampshire, USA. Biogeochemistry 72, 191–232.

Lund M, Lafleur, P M, Roulet N T, Lindroth A, Christensen T R, Aurela M, Chojnicki B H, Flanagan L B, Humphreys E R, Laurila T, Oechel W C, Olejnik J, Rinne J, Schubert P, Nilsson M B, 2010. Variability in exchange of CO_2 across 12 northern peatland and tundra sites. Global Change Biology 16, 2436–2448.

Lundin L, Stendahl J, Lode E, 2005. Forsmark site investigation. Soils in two large trenches. SKB P-05-166, Svensk Kärnbränslehantering AB.

Löfgren A, 2005. Oskarshamn/Forsmark site investigation. Estimation of biomass and net primary production in field and ground layer, and biomass in litter layer in different vegetation types in Forsmark and Oskarshamn. SKP P-05-80, Svensk Kärnbränslehantering AB.

Löfgren A (ed), 2010. The terrestrial ecosystems at Forsmark and Laxemar-Simpevarp. SR-Site Biosphere. SKB TR-10-01, Svensk Kärnbränslehantering AB.

Löfgren A, 2011. Dissolved inorganic carbon and organic carbon in mires in the Forsmark area. A pilot study. SKB P-11-23, Svensk kärnbränslehantering AB.

Maljanen M, Hytönen J, Mäkiranta P, Alm J, Minkkinen K, Laine J, Martikainen P J, 2007. Greenhouse gas emissions from cultivated and abandoned organic croplands in Finland. Boreal Environment Research 12, 133–140.

Maljanen M, Sigurdsson B D, Guðmundsson J, Óskarsson H, Huttunen J T, Martikainen P J, 2010. Greenhouse gas balances of managed peatlands in the Nordic countries – present knowledge and gaps. Biogeosciences 7, 2711–2738.

Malmer N, Wallén B, 2004. Input rates, decay losses and accumulation rates of carbon in bogs during the last millennium: internal processes and environmental change. The Holocene 14, 111–117.

Marlow F W, 2005. Hunter–gatherers and human evolution. Evolutionary Antropology 14, 54–67.

McAfee M, 1985. The rise and fall of Bälinge mossar. Uppsala: Swedish University of Agricultural Sciences, Department of Soil Sciences. (Hydrotechnics Report 147.)

McGillis W R, Dacey J W H, Frew N M, Bock E J, Nelson R K, 2000. Water–air flux of dimethylsulfide. Journal of Geophysical Research 105, 1187–1193.

Millington R J, Quirk J P, 1961. Permeability of porous solids. Transactions of the Faraday Society 57, 1200–1207.

Ministry of Environment, 2007. Sverige inför klimatförändringarna: hot och möjligheter (in Swedish). Stockholm: Fritzes. (Statens offentliga utredningar 2007:60) (In Swedish.)

Moore T R, Bubier J L, Frolking S E, Lafleur P M, Roulet N T, 2002. Plant biomass and production and CO_2 exchange in an ombrotrophic bog. Journal of Ecology 90, 25–36.

Moore T R, Bubier J L, Bledzki L, 2007. Litter decomposition in temperate peatland ecosystems: The effect of substrate and site. Ecosystems 10, 949–963.

Morell M, 1998. Det svenska jordbrukets historia. Bd 4, Jordbruket i industrisamhället 1870–1945. Stockholm: Natur och Kultur. (In Swedish.)

Mossberg B, Stenberg L, 2003. Den nya nordiska floran. Stockholm: Wahlström & Widstrand. (In Swedish.)

Mueller L, Behrendt A, Schalitz G, Schindler U, 2005. Above ground biomass and water use efficiency of crops at shallow water tables in a temperate climate. Agricultural Water Management 75, 117–136.

Murray G, Boxall P C, Wein R W, 2005. Distribution, abundance, and utilization of wild berries by the Gwich'in people in the Mackenzie River delta region. Economic Botany 59, 174–184.

Myrdal J, 1996. Betingsläror och arbetsåtgång i lantbruket. In Perlinge A (ed). Landbon, ladan och lagen och hägnaderna, arbetstiden och bygdelaget samt ytterligare 20 agrarhistoriska artiklar. Stockholm: Kungliga Skogs- och lantbruksakademien. (In Swedish.)

Mäkilä M, Goslar T, 2008. The carbon dynamics of surface peat layers in southern and central boreal mires of Finland and Russian Karelia. Suo 59, 49–69.

National Academy of Sciences, 1977. Drinking water and health. Washington, DC: National Academy Press.

Naturvatten, 2014. Erkenkräftan. Norrtälje: Naturvatten i Roslagen AB. Available at: http://www.naturvatten.se/k-erkenk.htm. [September 2014].

Naturvårdsverket, 2009. Riktvärden för förorenad mark. Modellbeskrivning och vägledning. Rapport 5976, Naturvårdsverket. (In Swedish.)

Nilsson M, Bohlin E, 1993. Methane and carbon dioxide concentrations in bogs and fens – with special reference to the effects of the botanical composition of the peat. Journal of Ecology 81, 615–625.

Nilsson P, Cory N, 2011. Skogsdata: aktuella uppgifter om de svenska skogarna från Riksskogstaxeringen. 2011. Umeå : Institutionen för skoglig resurshushållning, SLU. (In Swedish.)

Nordén S, 2007. Forsmark site investigation. Collection of archive samples. SKB P-07-196, Svensk Kärnbränslehantering AB.

Nordén S, Avila R, de la Cruz I, Stenberg K, Grolander S, 2010. Element-specific and constant parameters used for dose calculations in SR-Site. SKB TR-10-07, Svensk Kärnbränslehantering AB.

NRC, 1999. Risk assessment of radon in drinking water. Committee on the Risk Assessment of Exposure to Radon in Drinking Water, Board on Radiation Effects Research, Commission on Life Sciences, National Research Council. Washington, DC: National Academy Press, 1999.

Näslund I, Bergwall L, Jacobsson G, 2000. Nyttjande av fiskebestånd – optimering av biologisk och ekonomisk synvinkel. Lägesrapport April 2000. Länsstyrelsen Jämtlands län. (In Swedish.)

Odén M, Follin S, Öhman J, Vidstrand P, 2014. SR-PSU Bedrock hydrogeology. Groundwater flow modelling methodology, setup and results. SKB R-13-25, Svensk Kärnbränslehantering AB.

Oechel W C, Vourlitis G L, Hastings S J, Zulueta R C, Hinzman L, Kane D, 2000. Acclimation of ecosystem CO_2 exchange in the Alaskan Arctic in response to decadal climate warming. Nature 406, 978–981.

Ohlsson F, 1991. Vattenväxter – i kampen mot övergödningen. Odlaren nr 5, Förbundet organisk biologisk odling. Available at: http://www.vaxteko.nu/html/sll/forb_org_biol_odl/odlaren/ODN91-5/ODN91-5A.HTM. [7 February 2014]. (In Swedish.)

Olenin S, 1997. Benthic zonation of the Eastern Gotland Basin, Baltic Sea. Netherlands Journal of Aquatic Ecology 30, 265–282.

Olesen J E, Trnka M, Kersebaum K C, Skjelvåg A O, Seguin B, Peltonen-Sainio P, Rossi F, Kozyra J, Micale F, 2011. Impacts and adaptation of European crop production systems to climate change. European Journal of Agronomy 34, 96–112.

Oleszczuk R, Regina K, Szajdak L, Höper H, Maryganova V, 2008. Impacts of agricultural utilization of peat soils on the greenhouse gas balance. In Strack M (ed). Peatlands and climate change. Jyväskylä, Finland: International Peat Society, 70–97.

Parmalee P W, Klippel W E, 1974. Freshwater mussels as a prehistoric food resource. American Antiquity 39, 421–434.

Persson G, 1997. Comparison of simulated water balance for willow, spruce, grass ley and barley. Nordic Hydrology 28, 85–98.

Pettersson R, 1987. Primary production in arable crops: above-ground growth dynamics, net production and nitrogen uptake. PhD thesis. Department of Ecology and Environmental Research SLU, Uppsala.

Prieto F J M, Millero F J, 2002. The values of $pK_1 + pK_2$ for the dissociation of carbonic acid in seawater. Geochimica et Cosmochimica Acta. 66, 2529–2540.

Proctor M C F, Raven J A, Rice S K, 1992. Stable carbon isotope discrimination measurements in Sphagnum and other bryophytes: physiological and ecological implications. Journal of Bryology 17, 193–202.

Pröhl G, 1990. Modellierung der Radionuklidausbreitung in Nahringsketten nach Deposition von Strontium-90, Cäsium-137 ind Jod-131 auf landwirtschaftlich genutzte. GSF-Bericht 29/90, GSF-Forschungszentrum für Umvelt und Gesundheit, Neuherberg. (In German.)

Qvarfordt S, Borgiel M, Berg C, 2010. Monitoring Forsmark. Hydrochemical investigations in four calciferous lakes in the Forsmark area. Results from complementary investigations in the Forsmark area, 2008–2009. SKB P-10-25, Svensk Kärnbränslehantering AB.

Qvarfordt S, Borgiel M, Berg C, 2011. Forsmark site investigation. Hydrochemical investigations in four caciferous lakes in the Forsmark area. Results from the second year of a complementary investigations in the Forsmark area. SKB P-11-47, Svensk Kärnbränslehantering AB.

Randall R G, Minns C K, 2000. Use of fish production per unit biomass ratios for measuring the productive capacity of fish habitats. Canadian Journal of Fisheries and Aquatic Sciences 57, 1657–1667.

Reader R J, Stewart J M, 1972. The relationship between net primary production and accumulation for a peatland in southeastern Manitoba. Ecology 53, 1024–1037.

Redon P-O, Abdelouas A, Bastviken D, Cecchini S, Nicolas M, Thiry Y, 2011. Chloride and organic chlorine in forest soils: storage, residence times, and influence of ecological conditions. Environmental Science & Technology 45, 7202–7208.

Rich P H, Wetzel R G, Thuy N V, 1971. Distribution, production and role of aquatic macrophytes in a southern Michigan marl lake. Freshwater Biology 1, 3–21.

Riutta T, Laine J, Aurela M, Rinne J, Vesala T, Laurila T, Haapanala S, Pihlatie M, Tuittila E-S, 2007. Spatial variation in plant community functions regulates carbon gas dynamics in a boreal fen ecosystem. Tellus B 59, 838–852.

Rodrigo M A, Rojo C, Álvarez-Cobelas M, Cirujano S, 2007. *Chara hispida* beds as a sink of nitrogen: evidence from growth, nitrogen uptake and decomposition. Aquatic Botany 87, 7–14.

Roos P, Engdahl A, Karlsson S, 2007. Oskarshamn and Forsmark site investigations. Analysis of radioisotopes in environmental samples. SKB P-07-32, Svensk Kärnbränslehantering AB.

Rouwenhorst R J, Jzn F J, Scheffers W A, van Dijken J P, 1991. Determination of protein concentration by total organic carbon analysis. Journal of Biochemical Methods 22, 119–128.

Ruuhijärvi R, 1974. Soiden karpalosadoista [On the cranberry yields on peatlands]. Suo 25, 25–30. (In Finnish.)

Rydin H, Clymo R S, 1989. Transport of carbon and phosphorus compounds about *Sphagnum*. Proceedings of the Royal Society of London B 237, 63–84.

Saarinen T, 1996. Biomass and production of two vascular plants in a boreal mesotrophic fen. Canadian Journal of Botany 74, 934–938.

Saetre P, Nordén S, Keesmann S, Ekström P-A, 2013a. The biosphere model for radionuclide transport and dose assessment in SR-PSU. SKB R-13-46, Svensk Kärnbränslehantering AB.

Saetre P, Valentin J, Lagerås P, Avila R, Kautsky U, 2013b. Land-use and food intake of future inhabitants: outlining a representative individual of the most exposed group for dose assessment. Ambio 42, 488–496.

Salo K, 1979. Mushrooms and mushroom yield on transitional peatlands in central Finland. Annales Botanici Fennici 16, 181–192.

Sandberg J, Elmgren R, Wulff F, 2000. Carbon flows in Baltic Sea food webs – a re-evaluation using a mass balance approach. Journal of Marine Systems 25, 249–260.

Schallenberg B, Kalff J, 1993. The ecology of sediment bacteria in lakes and comparison with other aquatic ecosystems. Ecology 74, 919–934.

Schoning K, 2014. Torvtillväxt och kolackumulation hos unga torvmarker i Uppland. SGU-rapport 2014:35, Sveriges geologiska undersökning. (In Swedish.)

Sheppard M I, Sheppard S C, Amiro B D, 1991. Mobility and plant uptake of inorganic ^{14}C and ^{14}C-labelled PCB in soils of high and low retention. Health Physics 61, 481–492.

Sheppard M I, Ewing L L, Hawkins J L, 1994. Soil degassing of carbon-14 dioxide: rates and factors. Journal of Environmental Quality 23, 461–468.

Sheppard S C, Long J, Sanipelli B, Sohlenius G, 2009. Solid/liquid partition coefficients (K_d) for selected soils and sediments at Forsmark and Laxemar–Simpevarp. SKB R-09-27, Svensk Kärnbränslehantering AB.

Sheppard S C, Sohlenius G, Omberg L-G, Borgiel M, Grolander S, Nordén S, 2011. Solid/liquid partition coefficients (K_d) and plant/soil concentration ratios (CR) for selected soils, tills and sediments at Forsmark. SKB R-11-24, Svensk Kärnbränslehantering AB.

SKB, 1999. Deep repository for spent nuclear fuel. SR 97 – Post-closure safety. Main report – Vol. I, Vol. II and Summary. SKB TR-99-06, Svensk Kärnbränslehantering AB.

SKB, 2006. Long-term safety for KBS-3 repositories at Forsmark and Laxemar – a first evaluation. Main report of the SR-Can project. SKB TR-06-09, Svensk Kärnbränslehantering AB.

SKB, 2008a. Site description of Forsmark at completion of the site investigation phase. SDM-Site Forsmark. SKB TR-08-05, Svensk Kärnbränslehantering AB.

SKB, 2008b. Safety analysis SFR 1. Long-term safety. SKB R-08-130, Svensk Kärnbränslehantering AB.

SKB, 2011. Long-term safety for the final repository for spent nuclear fuel at Forsmark. Main report of the SR-Site project, Volume I–III. SKB TR-11-01, Svensk Kärnbränslehantering AB.

SKB, 2013a. RD&D Programme 2013. Programme for research, development and demonstration of methods for the management and disposal of nuclear waste. SKB TR-13-18, Svensk Kärnbränslehantering AB.

SKB, 2013b. Låg- och medelaktivt avfall i SFR. Referensinventarium för avfall 2013. SKB R-13-37, Svensk Kärnbränslehantering AB. (In Swedish.)

SKB, 2013c. Components, features, processes and interactions in the biosphere. SKB R-13-43, Svensk Kärnbränslehantering AB.

SKB, 2014a. Handling of biosphere FEPs and recommendations for model development in SR-PSU. SKB R-14-02, Svensk Kärnbränslehantering AB.

SKB, 2014b. Safety analysis for SFR. Long-term safety. Main report for the safety assessment SR-PSU. SKB TR-14-01, Svensk Kärnbränslehantering AB.

SKB, 2014c. Biosphere synthesis report for the safety assessment SR-PSU. SKB TR-14-06, Svensk Kärnbränslehantering AB.

SKB, 2014d. Climate and climate related issues for the safety assessment SR-PSU. SKB TR-13-05, Svensk Kärnbränslehantering AB.

SKB, 2014e. Radionuclide transport and dose calculations for the safety assessment SR-PSU. TR-14-09, Svensk Kärnbränslehantering AB.

SLU, 2014. Markinfo. Available at: http://www-markinfo.slu.se/eng/climate/vegper.html. Uppsala: Department of Soil and Environment SLU. [13 August 2014].

Smith B, Aasa A, Ahas R, Blenckner T, Callaghan T V, de Chazal J, Humborg C, Jönsson A M, Kellomäki S, Kull A, Lehikoinen E, Mander Ü, Nõges P, Nõges T, Rounsevell M, Sofiev M, Tryjanowski P, Wolf A, 2008. Climate-related change in terrestrial and freshwater ecosystems. In Assessment of climate change for the Baltic Sea Basin. Berlin: Springer, 221–308.

Sobek S, Durisch-Kaiser E, Zurbrügg R, Wongfun N, Wessels M, Pasche N, Wehrli B, 2009. Organic carbon burial efficiency in lake sediments controlled by oxygen exposure time and sediment source. Limnology and Oceanography 54, 2243–2254.

Soegaard H, Nordstroem C, Friborg T, Hansen B U, 2000. Trace gas exchange in a high arctic valley 3. Integrating and scaling CO_2 fluxes from canopy to landscape using flux data, footprint modeling, and remote sensing. Global Biogeochemical Cycles 14, 725–744.

Sohlenius G, Strömgren M, Hartz F, 2013. Depth and stratigraphy of regolith at Forsmark. SR-PSU Biosphere. SKB R-13-22, Svensk Kärnbränslehantering AB

Sohlenius G, Schoning K, Baumgartner A, 2014. Development, carbon balance and agricultural use of peatlands – overview and examples from Uppland, Sweden. SKB TR-13-20, Svensk Kärnbränslehantering AB.

SSM, 2008. The Swedish Radiation Safety Authority's regulations and general advice concerning the protection of human health and the environment in connection with the final management of spent nuclear fuel and nuclear waste. Stockholm: Swedish Radiation Safety Authority. (SSMFS 2008:37).

Statens energimyndighet, 2013. Energistatistik för småhus 2012 (Energy Statistics for one- and two-dwelling buildings in 2012). Eskilstuna: Statens energimyndighet. (In Swedish.)

Statens energiverk, 1985. Förbränning av torvbränslen: hur kan miljökraven tillgodoses? Stockholm: Liber. (Statens energiverk 1985:2) (In Swedish.)

Stenberg K, Rensfeldt V, 2015. Estimating doses from exposure to contaminated air when burning peat or wood. SKB R-14-33, Svensk Kärnbränslehantering AB.

Sternbeck J, Land M, Nilsson Ö, 2006. Oskarshamn and Forsmark site investigations. ^{210}Pb and ^{14}C dating of sediments and peat. Accumulation rates of carbon, nitrogen and phosphorus. SKB P-06-301, Svensk Kärnbränslehantering AB.

Straume T, Carsten A L, 1993. Tritium radiobiology and relative biological effectiveness. Health Physics 65, 657–672.

Strömgren M, Brydsten L, 2013. Digital elevation model of Forsmark. Site-descriptive modelling. SR-PSU Biosphere. SKB R-12-03, Svensk Kärnbränslehantering AB.

Stumm W, Morgan J J, 1996. Aquatic chemistry: chemical equilibria and rates in natural waters. New York: Wiley.

Sun J, Vandemark D, Mahrt L, Vickers D, Crawford T, Vogel C, 2001. Momentum transfer over the coastal zone. Journal of Geophysical Research 106, 12437– 12448.

Sund I, Nilsson M, Granberg G, Svensson B H, 1994. Depth distribution of microbial production and oxidation of methane in northern boreal peatlands. Microbial Ecology 27, 253–265.

Svensson L, 1979. Dose conversion factors for external photon radiation. FOA C 40060-A3, Swedish Defence Research Agency, Stockholm. (In Swedish.)

Syed K H, Flanagan L B, Carlson P J, Glenn A J, van Gaalen K E, 2006. Environmental control of net ecosystem CO_2 exchange in a treed, moderately rich fen in northern Alberta. Agricultural and Forest Meteorology 140, 97–114.

Tans P, 2009. Trends in carbon dioxide. National Oceanic & Atmospheric Administration/Earth System Research Laboratoty, U.S. Department of Commerce. Available at: http://www.cmdl.noaa.gov/ccgg/ trends/. [16 April 2009].

Thormann M N, Bayley S E, Currah R S, 2001. Comparison of decomposition of below ground and above ground plant litters in peatlands of boreal Alberta, Canada. Canadian Journal of Botany 79, 9–22.

Tranvik L J, 1988. Availability of dissolved organic carbon for plantonic bacteria in oligotrophic lakes of different humic content. Microbial Ecology 16, 311–322.

Tröjbom M, Grolander S, 2010. Chemical conditions in present and future ecosystems in Forsmark. Implications for selected radionuclides in the safety assessment SR-Site. SKB R-10-27, Svensk Kärnbränslehantering AB.

Tröjbom M, Nordén S, 2010. Chemistry data from surface ecosystems in Forsmark and Laxemar–Simpevarp. Site specific data used for estimation of CR and K_d values in SR-Site. SKB R-10-28, Svensk Kärnbränslehantering AB.

Tröjbom M, Söderbäck B, 2006. Chemical characteristics of surface systems in the Forsmark area. Visualisation and statistical evaluation of data from shallow groundwater, precipitation, and regolith. SKB R-06-19, Svensk Kärnbränslehantering AB.

Tröjbom M, Grolander S, Rensfeldt V, Nordén S, 2013. K_d and CR used for transport calculation in the biosphere in SR-PSU. SKB R-13-01, Svensk Kärnbränslehantering AB.

Ulanovsky A, Pröhl G, 2006. A practical method for assessment of dose conversion coefficients for aquatic biota. Radiation and Environmental Biophysics 45, 203–214.

Ulanovsky A, Pröhl G, Gómez-Ros J M, 2008. Methods for calculating dose conversion coefficients for terrestrial and aquatic biota. Journal of Environmental Radioactivity 99, 1440–1448.

UNSCEAR, 2000. Sources and effects of ionizing radiation: UNSCEAR 2000 report to the General Assembly with scientific annexes. Vol. I. New York: United Nations Scientific Committee on the Effects of Atomic Radiation.

US Army, 2008. Water planning guide. Potable water consumption planning factors by environmental region and command level. Force Development Directorate, United States Army Combined Arms Command, Ft. Lee, VA.

US EPA, 2000. Methodology for deriving ambient water quality criteria for the protection of human health. EPA822-B-00-004, U.S. Environmental Protection Agency, Washington, D.C.

US EPA, 2011. Exposure factors handbook. EPA/600/R-09/052F, U.S. Environmental Protection Agency, Washington, D.C.

Valeur J R, Jensen A, Pejrup M, 1995. Turbidity, particle fluxes and mineralization of C and N in a shallow coastal area. Marine and Freshwater Research 46, 409–418.

Van den Hoof C, Thiry Y, 2012. Modelling of the natural chlorine cycling in a coniferous stand: implications for chlorine-36 behaviour in a contaminated forest environment. Journal of Environmental Radioactivity 107, 56–67.

Vercauteren N, 2011. Water vapor and heat exchange over lakes. PhD thesis. École Polytechnique Fédérale de Lausanne.

Vickers D, Mahrt L, 2010. Sea-surface roughness lengths in the midlatitude coastal zone. Quarterly Journal of the Royal Meteorological Society 136, 1089–1093

Vives i Batlle J, Jones S R, Gómez-Ros J M, 2004. A method for calculation of dose per unit concentration values for aquatic biota. Journal of Radiological Protection 24, A13–A34.

von Post L, Granlund E, 1926. Södra Sveriges torvtillgångar. Stockholm. (Sveriges geologiska undersökning. Ser. C 335). (In Swedish.)

Vourinen A H, Vapaavuori E M, Lapinjoki S, 1989. Time-course of uptake of dissolved inorganic carbon through willow roots in light and darkness. Physiologia Plantarum 77, 33–38.

Waddington J M, Roulet N T, 2000. Carbon balance of a boreal patterned peatland. Global Change Biology 6, 87–97.

Wania R, Ross I, Prentice I C, 2010. Implementation and evaluation of a new methane model within a dynamic global vegetation model: LPJ-WHyMe v1. 3.1. Geoscientific Model Development 3, 565–584.

Wanninkhof R, 1992. Relationship between wind speed and gas exchange over the ocean. Journal of Geophysical Research 97, 7373–7382.

Wanninkhof R, Knox M, 1996. Chemical enhancement of CO_2 exchange in natural waters. Limnology and Oceanography 41, 689–697.

Wanninkhof R, McGillis W R, 1999. A cubic relationship between air-sea CO_2 exchange and wind speed. Geophysical Research Letters 26, 1189–1892.

Wanninkhof R, Asher W E, Ho D T, Sweeney C, McGillis W R, 2009. Advances in quantifying air-sea gas exchange and environmental forcing. Annual Review of Marine Science 1, 213–244.

Waters T F, 1992. Annual production, production/biomass ratio, and the ecotrophic coefficient for management of trout in streams. North American Journal of Fisheries Management 12, 34–39.

Webster K L, McLaughlin J W, 2010. Importance of the water table in controlling dissolved carbon along a fen nutrient gradient. Soil Science Society of America Journal 74, 2254–2266.

Weiss R F, 1974. Carbon dioxide in water and seawater: the solubility of a non-ideal gas. Marine Chemistry 2, 203–215.

Wennberg A, 1947. Lantbebyggelsen i nordöstra Östergötland 1600–1875. Lund: Gleerups. (In Swedish.)

Werner K, Sassner M, Johansson E, 2013. Hydrology and near-surface hydrogeology at Forsmark – synthesis for the SR-PSU project. SR-PSU Biosphere. SKB R-13-19, Svensk Kärnbränslehantering AB.

Werner K, Norville J, Öhman J, 2014. Meteorological, hydrological and hydrogeological monitoring data from Forsmark – compilation and analysis for the SR-PSU Project. SR-PSU Biosphere. SKB R-13-20, Svensk Kärnbränslehantering AB.

Wesslander K, 2011.The carbon dioxide system in the Baltic Sea surface waters. PhD thesis. University of Gothenburg, Department of Earth Sciences.

Westrell T, Andersson Y, Stenström T A, 2006. Drinking water consumption patterns in Sweden. Journal of Water and Health 4, 511–522.

Wetzel R G, 2001. Limnology: lake and river ecosystems. 3rd ed. San Diego: Academic Press.

Wetzel R G, Likens G E, 1991. Limnological analysis. 2nd ed. New York: Springer.

Weyhenmeyer G, 1997. Quatification of resuspended particles in sedimentation traps. Verhandlungen des Internationalen Vereinigung für theoretische und angewandte Limnologie 26, 271–277.

Weyhenmeyer G, 1999. Lake Erken: meteorological, physical, chemical and biological data and a list of publications from 1933 to 1998. Uppsala: Department of Limnology, University of Uppsala. (Scripta Limnologica Upsaliensia 1999 B:16)

Weyhenmeyer G A, Blenckner T, Petersson K, 1999. Changes of the plankton spring outburst related to the North Atlantic Oscillation. Limnology and Oceanography 44, 1788–1792.

White P J, Broadley M R, 2001. Chloride in soils and its uptake and movement within the plant: a review. Annals of Botany 88, 967–988.

WHO, 2011. Guidelines for drinking-water quality. 4th ed. Geneva: World Health Organisation.

Widgren M, 1979. A simulation model of farming systems and land use in Sweden during the early Iron Age, c. 500 B.C. – A.D. 550. Journal of Historical Geography 5, 21–32.

Wielgolaski F E, Bliss L C, Svoboda J, Doyle G, 1981. Primary production of tundra. In Bliss L C, Heal O W, Moore J J (eds). Tundra ecosystems: a comparative analysis. Cambridge: Cambridge University Press, 187–226.

Williams T E, 1980. Herbage production: grasses and leguminous forage crops. In Holmes W (ed.) Grass, its production and utilization. Oxford, Alden Press: 6–69.

Wiltshire K H, 2000. Algae and associated pigments of intertidal sediments, new observations and methods. Limnologica 30, 205–214.

Wikberger C, Johansson M, 2006. Konsumtion av livsmedel och dess näringsinnehåll. Statistikrapport 2006:2, Swedish Board of Agriculture, Stockholm, Sweden. (In Swedish, with summary in English).

Wolf A, Callaghan T V, Larson K, 2008. Future changes in vegetation and ecosystem function of the Barents region. Climatic Change 87, 51–73.

Wulff F, Ulanowicz R E, 1989. A comparative anatomy of the Baltic Sea and Chesapeake Bay ecosystems. In Wulff F, Field J G, Mann K H (eds). Network analysis in marine ecology. Berlin: Springer-Verlag. (Coastal and Estuarine Studies 32), 232–256.

Yu Z, 2006. Modeling ecosystem processes and peat accumulation in boreal peatlands. In Wieder R K, Vitt D H (eds) Boreal peatland ecosystems. Berlin: Springer-Verlag. (Ecological Studies 188), 313–329.

Zilitinkevich S S, 1969. On the computation of the basic parameters of the interaction between the atmosphere and the ocean. Tellus 21, 17–24.

Appendix A

List of parameters

Table A-1. Radionuclide-specific parameters.

Parameter name	Description	Unit	Chapter in parameterreport	Additional PSU reference	Delivered in file
doseCoef_ext	Dose coefficent for external exposure	$(\text{Sv h}^{-1})\ (\text{Bq m}^{-3})^{-1}$	3.4		RadionuclideSpecific.xlms
doseCoef_ing	Dose coefficent for ingestion	Sv Bq^{-1}	3.4		RadionuclideSpecific.xlms
doseCoef_inh	Dose coefficient for inhalation	Sv Bq^{-1}	3.4		RadionuclideSpecific.xlms
doseCoef_combPeat	Dose coefficient for combustion of peat	$(\text{Sv year}^{-1})\ (\text{Bq kgdw}^{-1})^{-1}$	3.4.1	Stenberg and Rensfeldt 2015	RadionuclideSpecific.xlms
doseCoef_combWood	Dose coefficient for combustion of wood	$((\text{Sv year}^{-1})\ (\text{Bq kgdw}^{-1})^{-1}$	3.4.1	Stenberg and Rensfeldt 2015	RadionuclideSpecific.xlms
doseCoef_ext_surf	Dose coefficent for external exposure	$(\text{Sv h}^{-1})\ (\text{Bq m}^{-2})^{-1}$	3.4		RadionuclideSpecific.xlms
dose_ingrowth_agri_ext	Average relative contribution including daughter radionuclides in agricultural lands	unitless	3.4.2		RadionuclideSpecific.xlms
dose_ingrowth_agri_inh	Average relative contribution including daughter radionuclides in agricultural lands	unitless	3.4.2		RadionuclideSpecific.xlms
dose_ingrowth_agri_ing	Average relative contribution including daughter radionuclides in agricultural lands	unitless	3.4.2		RadionuclideSpecific.xlms
doseCoef_ing_water_14C	Dose coefficient from ingestion of carbon-14 in water	Sv Bq^{-1}	3.4		SiteGeneric.xlsm

Table A-2. Landscape geometries. Time dependent parameters are presented in Appendix C.

Parameter	Description	Unit	Chapter in parameterreport	Additional PSU reference	Delivered in file
Time dependent					
area_obj_aqu	Surface area of aquatic object	m^2	4.4.2	Brydsten and Strömgren 2013	TimeSeries_converted.xlms
area_obj_ter	Surface area of terrestrial object	m^2	4.4.3	Brydsten and Strömgren 2013	TimeSeries_converted.xlms
res_rate	Gross resuspension rate per unit surface area	$m^3\ m^{-2}\ year^{-1}$	4.5.1	Brydsten and Strömgren 2013	TimeSeries_converted.xlms
sed_rate	Gross sedimentation rate per unit surface area	$m^3\ m^{-2}\ year^{-1}$	4.5.2	Brydsten and Strömgren 2013	TimeSeries_converted.xlms
z_water	Average depth of water	m	4.4.4	Brydsten and Strömgren 2013	TimeSeries_converted.xlms
z_regoPG_aqu	Depth of aquatic post-glacial sediments	m	4.4.7	Brydsten and Strömgren 2013	TimeSeries_converted.xlms
z_regoPG_ter	Depth of terrestrial post-glacial sediments	m	4.4.8	Brydsten and Strömgren 2013	TimeSeries_converted.xlms
Ter_growth	is the horizontal rate of mire vegetation ingrowth	$m^2\ year^{-1}$	4.5.3		Ter_growth.xlsx
Constant over time					
area_obj	Area of the lake object	m^2	4.4.1	Brydsten and Strömgren 2013	ObjectSpecific.xlsm
z_regoLow	Average depth of regolow (till)	m	4.4.5		ObjectSpecific.xlsm
z_RegoGL	Depth of glacial clay	m	4.4.6		ObjectSpecific.xlsm
threshold_start	The year a threshold starts isolating a baythat will become a lake	year	4.3.1	Brydsten and Strömgren 2013	ObjectSpecific.xlsm
threshold_stop	The final year a threshold has isolated a bay	year	4.3.2	Brydsten and Strömgren 2013	ObjectSpecific.xlsm
threshold_isolation	The year a threshold has isolated a bay	year	4.3.4	Brydsten and Strömgren 2013	ObjectSpecific.xlsm
threshold_land	The year reed areas starts to appear in objekt	year	4.3.5	Brydsten and Strömgren 2013	ObjectSpecific.xlsm
threshold_end	The last year of terrestrial ingrowth	year	4.3.6	Brydsten and Strömgren 2013	ObjectSpecific.xlsm
threshold_well	is the point in time after which it is feasible to construct a well	year	4.3.3		ObjectSpecific.xlsm

Table A-3. Regolith characteristics.

Parameter	Description	Unit	Chapter in parameterreport	Additional PSU reference	Delivered in file
Non-cultivated soils					
dens_regoLow	Density of the lower regolith layer (till)	kgdw m^{-3}	5.3.1		SiteGeneric.xlms
dens_regoGL	Density of glacial clay	kgdw m^{-3}	5.3.2		SiteGeneric.xlms
dens_regoPG	Density of post-glacial sediments	kgdw m^{-3}	5.3.3		SiteGeneric.xlms
dens_regoPeat	Density of anoxic layer of terrestrial regolith (peat)	kgdw m^{-3}	5.3.4		SiteGeneric.xlms
dens_regoUp_lake	Density of upper 5 cm layer of aquatic regolith (lake)	kgdw m^{-3}	5.3.6		SiteGeneric.xlms
dens_regoUp_sea	Density of upper 10 cm layer of aquatic regolith (sea)	kgdw m^{-3}	5.3.6		SiteGeneric.xlms
dens_regoUp_ter	Density of upper oxic layer of terrestrial regolith (peat)	kgdw m^{-3}	5.3.5		SiteGeneric.xlms
poro_regoLow	Porosity of lower regolith layer (Till)	m^3 m^{-3}	5.3.1		SiteGeneric.xlms
poro_regoGL	Porosity of glacial clay	m^3 m^{-3}	5.3.2		SiteGeneric.xlms
poro_regoPG	Porosity of post-glacial sediments	m^3 m^{-3}	5.3.3		SiteGeneric.xlms
poro_regoPeat	Porosity of anoxic layer of terrestrial regolith (peat)	m^3 m^{-3}	5.3.4		SiteGeneric.xlms
poro_regoUp_lake	Porosity of upper 5 cm layer of aquatic regolith (lake)	m^3 m^{-3}	5.3.6		SiteGeneric.xlms
poro_regoUp_sea	Porosity of upper 10 cm layer of aquatic regolith (sea)	m^3 m^{-3}	5.3.6		SiteGeneric.xlms
poro_regoUp_ter	Porosity of upper oxic layer of terrestrial regolith (peat)	m^3 m^{-3}	5.3.5		SiteGeneric.xlms
Infield-outland					
dens_regoUp	Density of glacial clay in early agricultural societies	kgdw m^{-3}	5.4.2		SiteGeneric.xlms
poro_regoUp	Porosity of glacial clay in early agricultural society	m^3 m^{-3}	5.4.2		SiteGeneric.xlms
S_w_regoUp	Degree of saturation in upper layer of sand soils in early agricultural society	m^3 m^{-3}	5.4.4		SiteGeneric.xlms
D_CO2_soil	is the diffusivity of CO2 in soil, based on the porosity and water content of the soil	m^2 $year^{-1}$	5.4.5		SiteGeneric.xlms
Drained mire					
poro_regoUp_clay	Porosity of agricultural soil from claygyttja	m^3 m^{-3}	5.4.1		SiteGeneric.xlms
poro_regoUp_peat	Porosity of agricultural soil from peat	m^3 m^{-3}	5.4.1		SiteGeneric.xlms
dens_regoUp_clay	Density of agricultural soil from claygyttja	kgdw m^{-3}	5.4.1		SiteGeneric.xlms
dens_regoUp_peat	Density of agricultural soil from peat	kgdw m^{-3}	5.4.1		SiteGeneric.xlms
S_w_regoUp_peat	Degree of saturation in upper soil layer in industrial agricultural society	m^3 m^{-3}	5.4.4		SiteGeneric.xlms
compact_gyttja	Initial immediate compactation of agricultural soils and reduction due to oxidation	m m^{-1}	5.4.3		SiteGeneric.xlms
compact_peat	Initial immediate compactation of agricultural soils and reduction due to oxidation	m m^{-1}	5.4.3		SiteGeneric.xlms
D_CO2_soil_clay	is the diffusivity of CO_2 in soil, based on the porosity and water content of the soil	m^2 $year^{-1}$	5.4.5		SiteGeneric.xlms
D_CO2_soil_peat	is the diffusivity of CO_2 in soil, based on the porosity and water content of the soil	m^2 $year^{-1}$	5.4.5		SiteGeneric.xlms
Garden plot					
poro_regoUp	Porosity of soils in a modern kitchen garden plot	m^3 m^{-3}	5.4.2		SiteGeneric.xlms
dens_regoUp	Density of soil in modern kitchen garden plot	kgdw m^{-3}	5.4.2		SiteGeneric.xlms
S_w_regoUp	Degree of saturation in soils in a modern kitchen garden	m^3 m^{-3}	5.4.4		SiteGeneric.xlms
D_CO2_soil	is the diffusivity of CO2 in soil, based on the porosity and water content of the soil	m^2 $year^{-1}$	5.4.5		SiteGeneric.xlms

Table A-4. Hydrological parameters. (The hydrological data are presented in Appendix D.)

Parameter	Description	Unit	Chapter in parameterreport	Additional PSU reference	Delivered in file
q_low_gl_sea	Water flux from lower regolith to glacial clay layer in marine phase	$m^3\ m^{-2}\ year^{-1}$	6.4	Werner et al. 2013	q_flux.xlms
q_gl_low_sea	Water flux from glacial clay layer to lower regolith in marine phase	$m^3\ m^{-2}\ year^{-1}$	6.4	Werner et al. 2013	q_flux.xlms
q_gl_pg_sea	Water flux from glacial clay to post glacial clay layer in marine phase	$m^3\ m^{-2}\ year^{-1}$	6.4	Werner et al. 2013	q_flux.xlms
q_pg_gl_sea	Water flux from post glacial clay to glacial clay layer in marine phase	$m^3\ m^{-2}\ year^{-1}$	6.4	Werner et al. 2013	q_flux.xlms
q_pg_up_sea	Water flux from post glacial clay to upper sediment layer in marine phase	$m^3\ m^{-2}\ year^{-1}$	6.4	Werner et al. 2013	q_flux.xlms
q_up_pg_sea	Water flux from upper sediment to post glacial clay layer in marine phase	$m^3\ m^{-2}\ year^{-1}$	6.4	Werner et al. 2013	q_flux.xlms
q_up_wat_sea	Water flux from upper sediment layer to water column in marine phase	$m^3\ m^{-2}\ year^{-1}$	6.4	Werner et al. 2013	q_flux.xlms
q_wat_up_sea	Water flux from water column to upper sediment layer in marine phase	$m^3\ m^{-2}\ year^{-1}$	6.4	Werner et al. 2013	q_flux.xlms
q_low_gl_lake	Water flux from lower regolith to glacial clay layer for aquatic part in limnic phase	$m^3\ m^{-2}\ year^{-1}$	6.4	Werner et al. 2013	q_flux.xlms
q_gl_low_lake	Water flux from glacial clay layer to lower regolith for aquatic part in limnic phase	$m^3\ m^{-2}\ year^{-1}$	6.4	Werner et al. 2013	q_flux.xlms
q_gl_pg_lake	Water flux from glacial clay to post glacial clay layer for aquatic part in limnic phase	$m^3\ m^{-2}\ year^{-1}$	6.4	Werner et al. 2013	q_flux.xlms
q_pg_gl_lake	Water flux from post glacial clay to glacial clay layer for aquatic part in limnic phase	$m^3\ m^{-2}\ year^{-1}$	6.4	Werner et al. 2013	q_flux.xlms
q_pg_up_lake	Water flux from post glacial clay to upper sediment layer for aquatic part in limnic phase	$m^3\ m^{-2}\ year^{-1}$	6.4	Werner et al. 2013	q_flux.xlms
q_up_pg_lake	Water flux from upper sediment to post glacial clay layer for aquatic part in limnic phase	$m^3\ m^{-2}\ year^{-1}$	6.4	Werner et al. 2013	q_flux.xlms
q_up_wat_lake	Water flux from upper sediment layer to water column for aquatic part in limnic phase	$m^3\ m^{-2}\ year^{-1}$	6.4	Werner et al. 2013	q_flux.xlms
q_wat_up_lake	Water flux from water column to upper sediment layer for aquatic part in limnic phase	$m^3\ m^{-2}\ year^{-1}$	6.4	Werner et al. 2013	q_flux.xlms
q_downstream_iso	Water flux from water column downstream in lake phase	$m^3\ m^{-2}\ year^{-1}$	6.4	Werner et al. 2013	q_flux.xlms
q_low_gl_ter_iso	Water flux from lower regolith to glacial clay layer for terrestrial part in limnic phase	$m^3\ m^{-2}\ year^{-1}$	6.4	Werner et al. 2013	q_flux.xlms
q_gl_low_ter_iso	Water flux from glacial clay layer to lower regolith for terrestrial part in limnic phase	$m^3\ m^{-2}\ year^{-1}$	6.4	Werner et al. 2013	q_flux.xlms
q_gl_pg_ter_iso	Water flux from glacial clay to post glacial clay layer for terrestrial part in limnic phase	$m^3\ m^{-2}\ year^{-1}$	6.4	Werner et al. 2013	q_flux.xlms
q_pg_gl_ter_iso	Water flux from post glacial clay to glacial clay layer for terrestrial part in limnic phase	$m^3\ m^{-2}\ year^{-1}$	6.4	Werner et al. 2013	q_flux.xlms
q_up_wat_ter_iso	Water flux from upper peat layer to water column for terrestrial part in limnic phase	$m^3\ m^{-2}\ year^{-1}$	6.4	Werner et al. 2013	q_flux.xlms
q_wat_up_ter_iso	Water flux from water column to upper peat layer for terrestrial part in limnic phase	$m^3\ m^{-2}\ year^{-1}$	6.4	Werner et al. 2013	q_flux.xlms
q_pg_peat_ter_iso	Water flux from post glacial clay to peat layer for terrestrial part in limnic phase	$m^3\ m^{-2}\ year^{-1}$	6.4	Werner et al. 2013	q_flux.xlms
q_peat_pg_ter_iso	Water flux from peat to post glacial clay layer for terrestrial part in limnic phase	$m^3\ m^{-2}\ year^{-1}$	6.4	Werner et al. 2013	q_flux.xlms
q_peat_up_ter_iso	Water flux from peat to upper peat layer for terrestrial part in limnic phase	$m^3\ m^{-2}\ year^{-1}$	6.4	Werner et al. 2013	q_flux.xlms
q_up_peat_ter_iso	Water flux from upper peat to peat layer for terrestrial part in limnic phase	$m^3\ m^{-2}\ year^{-1}$	6.4	Werner et al. 2013	q_flux.xlms
q_downstream_end	Water flux from water column downstream in stream phase	$m^3\ m^{-2}\ year^{-1}$	6.4	Werner et al. 2013	q_flux.xlms
q_low_gl_ter_end	Water flux from lower regolith to glacial clay layer for terrestrial part in mire phase	$m^3\ m^{-2}\ year^{-1}$	6.4	Werner et al. 2013	q_flux.xlms
q_gl_low_ter_end	Water flux from glacial clay layer to lower regolith for terrestrial part in mire phase	$m^3\ m^{-2}\ year^{-1}$	6.4	Werner et al. 2013	q_flux.xlms
q_gl_pg_ter_end	Water flux from glacial clay to post glacial clay layer for terrestrial part in mire phase	$m^3\ m^{-2}\ year^{-1}$	6.4	Werner et al. 2013	q_flux.xlms
q_pg_gl_ter_end	Water flux from post glacial clay to glacial clay layer for terrestrial part in mire phase	$m^3\ m^{-2}\ year^{-1}$	6.4	Werner et al. 2013	q_flux.xlms
q_up_wat_ter_end	Water flux from upper peat layer to water column for terrestrial part in mire phase	$m^3\ m^{-2}\ year^{-1}$	6.4	Werner et al. 2013	q_flux.xlms
q_wat_up_ter_end	Water flux from water column to upper peat layer for terrestrial part in mire phase	$m^3\ m^{-2}\ year^{-1}$	6.4	Werner et al. 2013	q_flux.xlms
q_pg_peat_ter_end	Water flux from post glacial clay to peat layer for terrestrial part in mire phase	$m^3\ m^{-2}\ year^{-1}$	6.4	Werner et al. 2013	q_flux.xlms
q_peat_pg_ter_end	Water flux from peat to post glacial clay layer for terrestrial part in mire phase	$m^3\ m^{-2}\ year^{-1}$	6.4	Werner et al. 2013	q_flux.xlms
q_peat_up_ter_end	Water flux from peat to upper peat layer for terrestrial part in mire phase	$m^3\ m^{-2}\ year^{-1}$	6.4	Werner et al. 2013	q_flux.xlms
q_up_peat_ter_end	Water flux from upper peat to peat layer for terrestrial part in mire phase	$m^3\ m^{-2}\ year^{-1}$	6.4	Werner et al. 2013	q_flux.xlms
WF_lobjXX	Water flow from lobjxx to lobjyy	$m^3\ year^{-1}$	6.3	Werner et al. 2013	WF_landscape.xlsm

Table A-5. Element-specific parameters.

Parameter	Description	Unit	Chapter in parameterreport	Additional PSU reference	Delivered in file
Concentration ratios					
cR_agri_cereal	Concentration ratio between soil and cereal	kgdw kgC^{-1}	7.4	Tröjbom et al. 2013	ElementSpecific.xlsm
cR_agri_fodder	Concentration ratio between soil and fodder	kgdw kgC^{-1}	7.4	Tröjbom et al. 2013	ElementSpecific.xlsm
cR_agri_tuber	Concentration ratio between soil and potatoes	kgdw kgC^{-1}	7.4	Tröjbom et al. 2013	ElementSpecific.xlsm
cR_agri_veg	Concentration ratio between soil and vegetables	kgdw kgC^{-1}	7.4	Tröjbom et al. 2013	ElementSpecific.xlsm
cR_food_herbiv	Concentration ratio with respect to herbivores and their diet	kgdw kgC^{-1}	7.4	Tröjbom et al. 2013	ElementSpecific.xlsm
cR_lake_cray	Concentration ratio for crayfish in lake water	m^3 kgC^{-1}	7.4	Tröjbom et al. 2013	ElementSpecific.xlsm
cR_lake_fish	Concentration ratio for fish in lake water	m^3 kgC^{-1}	7.4	Tröjbom et al. 2013	ElementSpecific.xlsm
cR_lake_pp_macro	Concentration ratio for macrophytes in lake water	m^3 kgC^{-1}	7.4	Tröjbom et al. 2013	ElementSpecific.xlsm
cR_lake_pp_micro	Concentration ratio for microphytobenthos in lake water	m^3 kgC^{-1}	7.4	Tröjbom et al. 2013	ElementSpecific.xlsm
cR_lake_pp_plank	Concentration ratio for plankton in lake water	m^3 kgC^{-1}	7.4	Tröjbom et al. 2013	ElementSpecific.xlsm
cR_sea_fish	Concentration ratio for fish in sea water	m^3 kgC^{-1}	7.4	Tröjbom et al. 2013	ElementSpecific.xlsm
cR_sea_pp_macro	Concentration ratio for macrophytes in sea water	m^3 kgC^{-1}	7.4	Tröjbom et al. 2013	ElementSpecific.xlsm
cR_sea_pp_micro	Concentration ratio for microphytobenthos in sea water	m^3 kgC^{-1}	7.4	Tröjbom et al. 2013	ElementSpecific.xlsm
cR_sea_pp_plank	Concentration ratio for plankton in sea water	m^3 kgC^{-1}	7.4	Tröjbom et al. 2013	ElementSpecific.xlsm
cR_ter_mush	Concentration ratio between edible mushrooms and soil	kgdw kgC^{-1}	7.4	Tröjbom et al. 2013	ElementSpecific.xlsm
Transfer coefficents					
cR_ter_pp	Concentration ratio for terrestrial primary producers and soil	kgdw kgC^{-1}	7.4	Tröjbom et al. 2013	ElementSpecific.xlsm
TC_meat	Transfer coefficient from intake of radionuclides in fodder and water to cow meat	d $kgfw^{-1}$	7.4	Tröjbom et al. 2013	ElementSpecific.xlsm
TC_milk	Transfer coefficient from intake of radionuclides in fodder and water to cow milk	day L^{-1}	7.4	Tröjbom et al. 2013	ElementSpecific.xlsm
Kd (soil/liquid distribution coefficents					
kD_PM_lake	Distribution coefficient for particulate matter in lake water	m^3 $kgdw^{-1}$	7.3	Tröjbom et al. 2013	ElementSpecific.xlsm
kD_PM_sea	Distribution coefficient for particulate matter in sea water	m^3 $kgdw^{-1}$	7.3	Tröjbom et al. 2013	ElementSpecific.xlsm
kD_regoGL	Distribution coefficient in glacial clay	m^3 $kgdw^{-1}$	7.3	Tröjbom et al. 2013	ElementSpecific.xlsm
kD_regoLow	Distribution coefficient in lower regolith (till)	m^3 $kgdw^{-1}$	7.3	Tröjbom et al. 2013	ElementSpecific.xlsm
kD_regoPeat	Distribution coefficient anoxic layer of terrestrial regolith (peat)	m^3 $kgdw^{-1}$	7.3	Tröjbom et al. 2013	ElementSpecific.xlsm
kD_regoPG	Distribution coefficient in post-glacial sediments	m^3 $kgdw^{-1}$	7.3	Tröjbom et al. 2013	ElementSpecific.xlsm
kD_regoUp_aqu	Distribution coefficient in upper layer of aquatic regolith	m^3 $kgdw^{-1}$	7.3	Tröjbom et al. 2013	ElementSpecific.xlsm
kD_regoUp_ter	Distribution coefficient of upper oxic layer of terrestrial regolith (peat)	m^3 $kgdw^{-1}$	7.3	Tröjbom et al. 2013	ElementSpecific.xlsm
kD_regoUp, Drained mire	Distribution coefficient in cultivated peat soils in industrial agricultural lands	m^3 $kgdw^{-1}$	7.3	Tröjbom et al. 2013	ElementSpecific.xlsm
kD_regoUp, Garden plot	Distribution coefficient in soils of a modern kitchen garden plot	m^3 $kgdw^{-1}$	7.3	Tröjbom et al. 2013	ElementSpecific.xlsm
kD_regoUp, infield-outland	Distribution coefficient in sandy soils in early agricultural lands	m^3 $kgdw^{-1}$	7.3	Tröjbom et al. 2013	ElementSpecific.xlsm
Diffusivity					
D_water	Diffusivity	m^2 $year^{-1}$	7.5		ElementSpecific2.xlsm

Parameter	Description	Unit	Chapter in parameterreport	Additional PSU reference	Delivered in file
Concentration rations for non-human biota calculations					
cR_Lake_amph_NHB	Concentration ratio between lake water and amphibians	kgdw kgfw^{-1}	7.4	Tröjbom et al. 2013	ElementSpecific_NHB.xlsm
cR_Lake_bent_fish_NHB	Concentration ratio between lake water and benthic fish	kgdw kgfw^{-1}	7.4	Tröjbom et al. 2013	ElementSpecific_NHB.xlsm
cR_Lake_bird_NHB	Concentration ratio between lake water and birds	kgdw kgfw^{-1}	7.4	Tröjbom et al. 2013	ElementSpecific_NHB.xlsm
cR_Lake_bivalve_NHB	Concentration ratio between lake water and bivalves	kgdw kgfw^{-1}	7.4	Tröjbom et al. 2013	ElementSpecific_NHB.xlsm
cR_Lake_crust_NHB	Concentration ratio between lake water and crustaceans	kgdw kgfw^{-1}	7.4	Tröjbom et al. 2013	ElementSpecific_NHB.xlsm
cR_Lake_Fish_NHB	Concentration ratio between lake water and fish	kgdw kgfw^{-1}	7.4	Tröjbom et al. 2013	ElementSpecific_NHB.xlsm
cR_Lake_gastr_NHB	Concentration ratio between lake water and gastropods	kgdw kgfw^{-1}	7.4	Tröjbom et al. 2013	ElementSpecific_NHB.xlsm
cR_Lake_ins_larvae_NHB	Concentration ratio between lake water and insect larvae	kgdw kgfw^{-1}	7.4	Tröjbom et al. 2013	ElementSpecific_NHB.xlsm
cR_Lake_mammal_NHB	Concentration ratio between lake water and mammals	kgdw kgfw^{-1}	7.4	Tröjbom et al. 2013	ElementSpecific_NHB.xlsm
cR_Lake_pel_fish_NHB	Concentration ratio between lake water and pelagic fish	kgdw kgfw^{-1}	7.4	Tröjbom et al. 2013	ElementSpecific_NHB.xlsm
cR_Lake_pp_plank_NHB	Concentration ratio between lake water and phytoplankton	kgdw kgfw^{-1}	7.4	Tröjbom et al. 2013	ElementSpecific_NHB.xlsm
cR_Lake_pp_vasc_NHB	Concentration ratio between lake water and vascular plants	kgdw kgfw^{-1}	7.4	Tröjbom et al. 2013	ElementSpecific_NHB.xlsm
cR_Lake_zoopl_NHB	Concentration ratio between lake water and zooplankton	kgdw kgfw^{-1}	7.4	Tröjbom et al. 2013	ElementSpecific_NHB.xlsm
cR_Sea_bent_fish_NHB	Concentration ratio between sea water and benthic fish	kgdw kgfw^{-1}	7.4	Tröjbom et al. 2013	ElementSpecific_NHB.xlsm
cR_Sea_bent_moll_NHB	Concentration ratio between sea water and benthic molluscs	kgdw kgfw^{-1}	7.4	Tröjbom et al. 2013	ElementSpecific_NHB.xlsm
cR_Sea_bird_NHB	Concentration ratio between sea water and birds	kgdw kgfw^{-1}	7.4	Tröjbom et al. 2013	ElementSpecific_NHB.xlsm
cR_Sea_crust_NHB	Concentration ratio between sea water and crustaceans	kgdw kgfw^{-1}	7.4	Tröjbom et al. 2013	ElementSpecific_NHB.xlsm
cR_Sea_Fish_NHB	Concentration ratio between sea water and fish	kgdw kgfw^{-1}	7.4	Tröjbom et al. 2013	ElementSpecific_NHB.xlsm
cR_Sea_mammal_NHB	Concentration ratio between sea water and mammals	kgdw kgfw^{-1}	7.4	Tröjbom et al. 2013	ElementSpecific_NHB.xlsm
cR_Sea_pel_fish_NHB	Concentration ratio between sea water and pelagic fish	kgdw kgfw^{-1}	7.4	Tröjbom et al. 2013	ElementSpecific_NHB.xlsm
cR_Sea_polych_NHB	Concentration ratio between sea water and polychaete worms	kgdw kgfw^{-1}	7.4	Tröjbom et al. 2013	ElementSpecific_NHB.xlsm
cR_Sea_pp_macro_NHB	Concentration ratio between sea water and macrophytes	kgdw kgfw^{-1}	7.4	Tröjbom et al. 2013	ElementSpecific_NHB.xlsm
cR_Sea_pp_plank_NHB	Concentration ratio between sea water and phytoplankton	kgdw kgfw^{-1}	7.4	Tröjbom et al. 2013	ElementSpecific_NHB.xlsm
cR_Sea_pp_vasc_NHB	Concentration ratio between sea water and vascular plants	kgdw kgfw^{-1}	7.4	Tröjbom et al. 2013	ElementSpecific_NHB.xlsm
cR_Sea_zoopl_NHB	Concentration ratio between sea water and zooplankton	kgdw kgfw^{-1}	7.4	Tröjbom et al. 2013	ElementSpecific_NHB.xlsm
cR_Ter_amph_NHB	Concentration ratio between soil and amphibians	kgdw kgfw^{-1}	7.4	Tröjbom et al. 2013	ElementSpecific_NHB.xlsm
cR_Ter_bird_egg_NHB	Concentration ratio between soil and bird eggs	kgdw kgfw^{-1}	7.4	Tröjbom et al. 2013	ElementSpecific_NHB.xlsm
cR_Ter_bird_NHB	Concentration ratio between soil and birds	kgdw kgfw^{-1}	7.4	Tröjbom et al. 2013	ElementSpecific_NHB.xlsm
cR_Ter_detr_inv_NHB	Concentration ratio between soil and detrivorous invertebrates	kgdw kgfw^{-1}	7.4	Tröjbom et al. 2013	ElementSpecific_NHB.xlsm
cR_Ter_fl_ins_NHB	Concentration ratio between soil and flying insects	kgdw kgfw^{-1}	7.4	Tröjbom et al. 2013	ElementSpecific_NHB.xlsm
cR_Ter_gastr_NHB	Concentration ratio between soil and gastropods	kgdw kgfw^{-1}	7.4	Tröjbom et al. 2013	ElementSpecific_NHB.xlsm
cR_Ter_mammal_large_NHB	Concentration ratio between soil and large mammals	kgdw kgfw^{-1}	7.4	Tröjbom et al. 2013	ElementSpecific_NHB.xlsm
cR_Ter_mammal_small_NHB	Concentration ratio between soil and small mammals	kgdw kgfw^{-1}	7.4	Tröjbom et al. 2013	ElementSpecific_NHB.xlsm
cR_Ter_pp_grass_NHB	Concentration ratio between soil, grass and herbs	kgdw kgfw^{-1}	7.4	Tröjbom et al. 2013	ElementSpecific_NHB.xlsm
cR_Ter_pp_lich_NHB	Concentration ratio between soil, lichens and bryophytes	kgdw kgfw^{-1}	7.4	Tröjbom et al. 2013	ElementSpecific_NHB.xlsm
cR_Ter_pp_NHB	Concentration ratio between soil and primary producers	kgdw kgfw^{-1}	7.4	Tröjbom et al. 2013	ElementSpecific_NHB.xlsm
cR_Ter_pp_shrub_NHB	Concentration ratio between soil and shrubs	kgdw kgfw^{-1}	7.4	Tröjbom et al. 2013	ElementSpecific_NHB.xlsm
cR_Ter_pp_tree_NHB	Concentration ratio between soil and trees	kgdw kgfw^{-1}	7.4	Tröjbom et al. 2013	ElementSpecific_NHB.xlsm
cR_Ter_rept_NHB	Concentration ratio between soil and reptiles	kgdw kgfw^{-1}	7.4	Tröjbom et al. 2013	ElementSpecific_NHB.xlsm
cR_Ter_soil_inv_NHB	Concentration ratio between soil and soil invertebrates	kgdw kgfw^{-1}	7.4	Tröjbom et al. 2013	ElementSpecific_NHB.xlsm

Table A-6. Parameters for aquatic ecosystems. (Time dependent data are presented in Appendix C.)

Parameter	Description	Unit	Chapter in parameterreport	Additional PSU reference	Delivered in file
biom_pp_macro	Biomass of macrobentic community in water per unit surface area	kgC m^{-2}	8.6		TimeSeries_converted.xlsm
biom_pp_micro	Biomass of microbenthic community in water per unit surface area	kgC m^{-2}	8.6		TimeSeries_converted.xlsm
biom_pp_plank	Biomass of pelagic community in water per unit surface area	kgC m^{-2}	8.6		TimeSeries_converted.xlsm
NPP_macro	Net primary production of macrobenthic community in water per unit surface area	kgC m^{-2} $year^{-1}$	8.6		TimeSeries_converted.xlsm
NPP_micro	Net primary production of microbenthic community in water per unit surface area	kgC m^{-2} $year^{-1}$	8.6		TimeSeries_converted.xlsm
NPP_plank	Net primary production of pelagic community in water per unit surface area	kgC m^{-2} $year^{-1}$	8.6		TimeSeries_converted.xlsm
conc_DIC_lake	Concentration of dissolved inorganic carbon in lake water	kgC m^{-3}	8.5.2		SiteGeneric_aquatic.xlsm
conc_DIC_sea	Concentration of dissolved inorganic carbon in sea water	kgC m^{-3}	8.5.2		SiteGeneric_aquatic.xlsm
conc_PM_lake	Concentration of suspended matter in lake	kgdw m^{-3}	8.5.1		SiteGeneric_aquatic.xlsm
conc_PM_sea	Concentration of suspended matter in sea	kgdw m^{-3}	8.5.1		SiteGeneric_aquatic.xlsm
f_C_fish	Fraction of carbon to dry weight in fish	kgC $kgdw^{-1}$	8.10.1		SiteGeneric_aquatic.xlsm
f_DW_FW_fish_lake	Fraction of dry weight to fresh weight for fish in lake	kgdw $kgfw^{-1}$	8.10.1		SiteGeneric_aquatic.xlsm
f_DW_FW_fish_sea	Fraction of dry weight to fresh weight in marine fish	kgdw $kgfw^{-1}$	8.10.1		SiteGeneric_aquatic.xlsm
f_H2CO3_lake	Fraction of dissolved inorganic carbon in lake water in the form of CO_2/ H_2CO_3	Bq Bq^{-1}	8.8.3		SiteGeneric_aquatic.xlsm
f_H2CO3_sea	Fraction of dissolved inorganic carbon in sea water in the form of CO2/ H2CO3	Bq Bq^{-1}	8.8.3		SiteGeneric_aquatic.xlsm
f_refrac_macro_lake	Fraction of refractory organic matter of macrobenthic primary producers in lake water left after initial mineralization	kgC kgC^{-1}	8.7.2		SiteGeneric_aquatic.xlsm
f_refrac_macro_sea	Fraction of refractory organic matter of macrobenthic primary producers in sea water left after initial mineralization	kgC kgC^{-1}	8.7.2		SiteGeneric_aquatic.xlsm
f_refrac_micro_lake	Fraction of refractory organic matter of microbenthic primary producers in lake water left after initial mineralization	kgC kgC^{-1}	8.7.2		SiteGeneric_aquatic.xlsm
f_refrac_micro_sea	Fraction of refractory organic matter of microbenthic primary producers in sea water left after initial mineralization	kgC kgC^{-1}	8.7.2		SiteGeneric_aquatic.xlsm
f_refrac_plank_lake	Fraction of refractory organic matter of pelagic primary producers in lake water left after initial mineralization	kgC kgC^{-1}	8.7.2		SiteGeneric_aquatic.xlsm
f_refrac_plank_sea	Fraction of refractory organic matter of pelagic primary producers in sea water left after initial mineralization	kgC kgC^{-1}	8.7.2		SiteGeneric_aquatic.xlsm
height_ref_aqu	Reference height used for defining wind velocity	m	8.9		SiteGeneric_aquatic.xlsm
minRate_regoPG_lake	Mineralization rate in post-glacial sediments in lake	kgC kgC^{-1} $year^{-1}$	8.7.3		SiteGeneric_aquatic.xlsm
minRate_regoPG_sea	Mineralization rate in post-glacial sediments in sea	kgC kgC^{-1} $year^{-1}$	8.7.3		SiteGeneric_aquatic.xlsm
minRate_regoUp_lake	Mineralization rate in upper regolith in lake	kgC kgC^{-1} $year^{-1}$	8.7.3		SiteGeneric_aquatic.xlsm

Parameter	Description	Unit	Chapter in parameterreport	Additional PSU reference	Delivered in file
minRate_regoUp_sea	Mineralization rate in upper regolith in sea	kgC kgC^{-1} year^{-1}	8.7.3		SiteGeneric_aquatic.xlsm
minRate_water_PM_lake	Mineralization rate in particular matter in lake water	kgC kgC^{-1} year^{-1}	8.7.3		SiteGeneric_aquatic.xlsm
minRate_water_PM_sea	Mineralization rate in particular matter in sea water	kgC kgC^{-1} year^{-1}	8.7.3		SiteGeneric_aquatic.xlsm
piston_vel_lake	Gas exchange coefficient for lake water in contact with the atmosphere	m year^{-1}	8.8.2		SiteGeneric_aquatic.xlsm
piston_vel_sea	Gas exchange coefficient for sea water in contact with the atmosphere	m year^{-1}	8.8.2		SiteGeneric_aquatic.xlsm
prod_edib_cray_lake	Sustainable yield with respect to edible crayfish per unit area in the lake	kgC m^{-2} year^{-1}	8.10.2		SiteGeneric_aquatic.xlsm
prod_edib_fish_lake	Sustainable yield with respect to edible fish per unit area in the lake	kgC m^{-2} year^{-1}	8.10.1		SiteGeneric_aquatic.xlsm
prod_edib_fish_sea	Sustainable yield with respect to edible fish per unit area in the sea	kgC m^{-2} year^{-1}	8.10.1		SiteGeneric_aquatic.xlsm
solubilityCoef_lake	Solubility coefficient for carbon dioxide in lake water (function of temperature, salinity etc)	(mol m^{-3}) (mol m^{-3})$^{-1}$	8.8.4		SiteGeneric_aquatic.xlsm
solubilityCoef_sea	Solubility coefficient for carbon dioxide in sea water (function of temperature, salinity etc)	((mol m^{-3}) (mol m^{-3})$^{-1}$	8.8.4		SiteGeneric_aquatic.xlsm
vel_wind_height_ref_aqu	Wind velocity at reference height	m s^{-1}	8.9		SiteGeneric_aquatic.xlsm
z_min_prod_edib_cray_lake	Smallest water depth for production of crayfish in lake	m	8.10.2		SiteGeneric_aquatic.xlsm
z_min_prod_edib_fish_lake	Smallest water depth for production of fish in lake	m	8.10.1		SiteGeneric_aquatic.xlsm
z_min_prod_edib_fish_sea	Smallest water depth for production of fish in sea	m	8.10.1		SiteGeneric_aquatic.xlsm
z_regoUp_lake	Depth of the upper oxygenated regolith layer in lake	m	8.7.1		SiteGeneric_aquatic.xlsm
z_regoUp_sea	Depth of the upper oxygenated regolith layer in sea	m	8.7.1		SiteGeneric_aquatic.xlsm

Table A-7. Parameters for mire and agricultural ecosystems.

Parameter	Description	Unit	Chapter in parameterreport	Additional PSU reference	Delivered in file
Mire ecosystem					
biom_pp_ter	Total biomass of terrestrial primary producers per unit area	kgC m^{-2}	9.3		SiteGeneric.xlsm
conc_C_atmos	Concentration of carbon in the atmosphere (above the ground)	kgC m^{-3}	9.4.1		SiteGeneric.xlsm
conc_Cl_PP_ter	Concentration of chlorine in vegetation	gCl kgC^{-1}	9.5.1		SiteGeneric.xlsm
conc_Cl_regoUp_ter_D	Concentration of dissolved chlorine in the mire	gCl m^{-3}	9.5.2		SiteGeneric.xlsm
conc_DIC_regoUp_ter	Concentration of dissolved inorganic carbon in oxygenated peat layer of the mire	kgC m^{-3}	9.4.2		SiteGeneric.xlsm
conc_Dust_ter	Concentration of fine soil particles in air above wetland vegetation	kgdw m^{-3}	9.9		SiteGeneric.xlsm
dragCoef	Drag coefficient of the canopy	Unitless	9.4.10		SiteGeneric.xlsm
f_C_peat	Fraction of carbon to dry weight ratio of peat	kgC $kgdw^{-1}$	9.4.4		SiteGeneric.xlsm
f_H2CO3_ter	Fraction of dissolved inorganic carbon in peat in the form of CO2/H2CO3	Bq Bq^{-1}	9.4.3		SiteGeneric.xlsm
f_mush_herbiv	Fraction of mushrooms in the diet of terrestrial herbivores	kgC kgC^{-1}	9.11.7		SiteGeneric.xlsm
f_refrac_ter	Fraction of refractory organic material of mire primary producers left after initial mineralization	kgC kgC^{-1}	9.7.1		SiteGeneric.xlsm
f_rootUptake	Fraction of carbon in newly synthesized biomass assimilated via root uptake	kgC kgC^{-1}	9.4.5		SiteGeneric.xlsm
height_CA_ter	Height from the ground of the canopy layer in a mire	m	9.4.9		SiteGeneric.xlsm
height_L1_ter	Height from the ground of the first above-canopy layer	m	9.4.10		SiteGeneric.xlsm
height_L2_ter	Height from the ground of the second above-canopy layer	m	9.4.10		SiteGeneric.xlsm
height_ref_ter	Reference height used for defining wind velocity	m	9.4.8		SiteGeneric.xlsm
karman_const	Von Karman constant	Unitless	9.4.10		SiteGeneric.xlsm
LAI_ter	Ratio of total upper leaf surface of vegetation divided by the surface area of the mire on which the vegetation grows (Leaf Area Index)	m^2 m^{-2}	9.4.10		SiteGeneric.xlsm
leaf_width_ter	Leaf width of terrestrial vegetation	m	9.4.10		SiteGeneric.xlsm
minRate_regoPeat	Mineralization rate in peat	$year^{-1}$	9.7.1		ObejcSpecific.xlsm
minRate_regoPG_ter	Mineralization rate in terrestrial post-glacial sediments	kgC kgC^{-1} $year^{-1}$	9.7.1		SiteGeneric.xlsm
minRate_regoUp_ter	Mineralization rate in upper terrestrial regolith	kgC kgC^{-1} $year^{-1}$	9.7.1		SiteGeneric.xlsm
NPP_ter	Total net primary production (above and below ground) in terrestrial ecosystem	kgC m^{-2} $year^{-1}$	9.3		SiteGeneric.xlsm
piston_vel_ter	Gas exchange coefficient for peat pore water in contact with the atmosphere	m $year^{-1}$	9.4.6		SiteGeneric.xlsm
prod_edib_berry	Sustainable yield with respect to edible berries per unit area	kgC m^{-2} $year^{-1}$	9.10.1		SiteGeneric.xlsm
prod_edib_game	Sustainable yield with respect to edible game per unit area	kgC m^{-2} $year^{-1}$	9.10.2		SiteGeneric.xlsm
prod_edib_mush	Sustainable yield with respect to edible mushrooms per unit area	kgC m^{-2} $year^{-1}$	9.10.3		SiteGeneric.xlsm
solubilityCoef_ter	Solubility coefficient for carbon dioxide in pore water	(mol m^{-3}) (mol m^{-3})$^{-1}$	9.4.7		SiteGeneric.xlsm
vel_wind_height_ref_ter	Wind velocity at reference height	m s^{-1}	9.4.8		SiteGeneric.xlsm
z_regoUp_ter	Depth of oxygenated and biologically active peat layer	m	9.5		SiteGeneric.xlsm
df_decomp	is the fraction of the radionuclide that is available for release through mineralisation of labile organic matter		9.6.3		ElementSpecific2.xlsx
Agricultural ecosystem (common parameters for all agricultural societies					
height_CA_cereal	Height from the ground of the canopy layer for cereal	m	9.4.9		SiteGeneric.xlsm
height_CA_fodder	Height from the ground of the canopy layer for fodder	m	9.4.9		SiteGeneric.xlsm

Parameter	Description	Unit	Chapter in parameterreport	Additional PSU reference	Delivered in file
height_CA_tuber	Height from the ground of the canopy layer for tuber	m	9.4.9		SiteGeneric.xlsm
LAI_cereal	Ratio of total upper leaf surface of vegetation divided by the surface area of the agricultural lands on which the vegetation grows (Leaf Area Index)	$m^2\ m^{-2}$	9.4.10		SiteGeneric.xlsm
LAI_fodder	Ratio of total upper leaf surface of vegetation divided by the surface area of the agricultural lands on which the vegetation grows (Leaf Area Index)	$m^2\ m^{-2}$	9.4.10		SiteGeneric.xlsm
LAI_tuber	Ratio of total upper leaf surface of vegetation divided by the surface area of the agricultural lands on which the vegetation grows (Leaf Area Index)	$m^2\ m^{-2}$	9.4.10		SiteGeneric.xlsm
leaf_width_cereal	Leaf width of cereal	m	9.4.10		SiteGeneric.xlsm
leaf_width_fodder	Leaf width of fodder	m	9.4.10		SiteGeneric.xlsm
leaf_width_tuber	Leaf width of tubers	m	9.4.10		SiteGeneric.xlsm
ingRate_C_cattle	Daily energy demand for cattle expressed in units of carbon	$kgC\ day^{-1}$	9.11.1		SiteGeneric.xlsm
ingRate_soil_cattle	Daily ingestion rate for a cow of soil	$kgdw\ day^{-1}$	9.11.2		SiteGeneric.xlsm
ingRate_water_cattle	Daily ingestion rate of water by cattle	$m^3\ day^{-1}$	9.11.3		SiteGeneric.xlsm
conc_C_meat	Concentration of carbon in meat	$kgC\ kgfw^{-1}$	9.11.6		SiteGeneric.xlsm
conc_C_milk	Concentration of carbon in milk	$kgC\ kgfw^{-1}$	9.11.5		SiteGeneric.xlsm
dens_milk	Density of milk	$kgfw\ L^{-1}$	9.11.4		SiteGeneric.xlsm
dens_water	Density of water	$kg\ m^{-3}$			SiteGeneric.xlsm
Drained mire					
biom_cereal	Yield as biomass of cereal per unit area at end of vegetation period (drained mire)	$kgC\ m^{-2}$	9.9		SiteGeneric.xlsm
biom_fodder	Yield as biomass of fodder per unit area at end of vegetation period (drained mire)	$kgC\ m^{-2}$	9.9		SiteGeneric.xlsm
biom_tuber	Yield as biomass of tuber per unit area at end of vegetation period (drained mire)	$kgC\ m^{-2}$	9.9		SiteGeneric.xlsm
conc_DIC_regoUp	Concentration of dissolved inorganic carbon in cultivated peat layer	$kgC\ m^{-3}$	9.4.2		SiteGeneric.xlsm
conc_Dust	Concentration of fine soil particles in air above agricultural land	$kgdw\ m^{-3}$	9.8		SiteGeneric.xlsm
Flux_water_satSoil_agri	Water flux from saturated to unsaturated zone growing cereals	$m^3\ m^{-2}\ year^{-1}$	9.6.2		SiteGeneric.xlsm
minRate	Mineralization rate for cultivated peat	$kgC\ kgC^{-1}\ year^{-1}$	9.7.1		SiteGeneric.xlsm
NPP_cereal	Total net primary production (above and below ground) of cereal in cultivated peat	$kgC\ m^{-2}\ year^{-1}$	9.9		SiteGeneric.xlsm
NPP_fodder	Total net primary production (above and below ground) of fodder in cultivated peat	$kgC\ m^{-2}\ year^{-1}$	9.9		SiteGeneric.xlsm
NPP_tuber	Total net primary production (above and below ground) of tuber in cultivated peat	$kgC\ m^{-2}\ year^{-1}$	9.9		SiteGeneric.xlsm
percolation_agri	Downward flux of water from peaty soil under industrial agricultural practices	$m^3\ m^{-2}\ year^{-1}$	9.6.1		SiteGeneric.xlsm
z_drain_agri	Trenching depth after compactation	m	9.5		SiteGeneric.xlsm
Garden plot					
amount_irrig	Total amount of water used for all irrigation events during the vegetation period	$m^3\ m^{-2}\ year^{-1}$	9.12.2		SiteGeneric.xlsm
biom_tuber	Yield as biomass of tuber per unit area at end of vegetation period (Garden plot)	$kgC\ m^{-2}$	9.9		SiteGeneric.xlsm
biom_veg	Yield as biomass of vegetables per unit area at end of vegetation period (modern kitchen garden)	$kgC\ m^{-2}$	9.9		SiteGeneric.xlsm
conc_DIC_regoUp	Concentration of dissolved inorganic carbon in modern kitchen garden	$kgC\ m^{-3}$	9.4.2		SiteGeneric.xlsm
conc_Dust	Concentration of fine soil particles in air above modern kitchen garden	$kgdw\ m^{-3}$	9.8		SiteGeneric.xlsm
f_area_tuber	Fraction of area used for tuber	$m^2\ m^{-2}$	11.7		SiteGeneric.xlsm

Parameter	Description	Unit	Chapter in parameterreport	Additional PSU reference	Delivered in file
f_area_veg	Fraction of area used for vegetables	$m^2\ m^{-2}$	11.7		SiteGeneric.xlsm
height_CA_veg	Height from the ground of the canopy layer for vegetables	m	9.4.9		SiteGeneric.xlsm
LAI_veg	Leaf area index for leafy vegetables	$m^2\ m^{-2}$	9.4.10		SiteGeneric.xlsm
leaf_width_veg	Leaf width of vegetables	m	9.4.10		SiteGeneric.xlsm
LeafStoreCapacy_tuber	Leaf storage capacity for tubers	$m^3\ m^{-2}$	9.12.3		SiteGeneric.xlsm
LeafStoreCapacy_veg	Leaf storage capacity for leafy vegetables	$m^3\ m^{-2}$	9.12.3		SiteGeneric.xlsm
minRate	Mineralization rate for agricultural soils (modern kitchen garden)	$kgC\ kgC^{-1}\ year^{-1}$	9.7.1		SiteGeneric.xlsm
N_irrig	Number of irrigation events	$year^{-1}$	9.12.5		SiteGeneric.xlsm
NPP_ag_veg	The above-ground net primary production for vegetables in the garden plot	$kgC\ m^{-2}\ year^{-1}$	9.11		SiteGeneric.xlsm
NPP_tuber	Total net primary production (above and below ground) of tuber in garden plot	$kgC\ m^{-2}\ year^{-1}$	9.9		SiteGeneric.xlsm
NPP_veg	Total net primary production (above and below ground) of vegetables	$kgC\ m^{-2}\ year^{-1}$	9.9		SiteGeneric.xlsm
percolation_agri	Downward flux of water from light soil under early agricultural practices	$m^3\ m^{-2}\ year^{-1}$	9.6.1		SiteGeneric.xlsm
time_vegPeriod	Time of vegetation period	$year\ year^{-1}$	9.12.6		SiteGeneric.xlsm
washoffCoef	Removal of deposited radionuclides from the plant leaf surface	$year^{-1}$	9.12.4		SiteGeneric.xlsm
z_regoUp	Depth of agricultural soils in a modern kitchen garden	m	9.5		SiteGeneric.xlsm
Infield-outland					
biom_cereal	Yield as biomass of cereal per unit area at end of vegetation period (inland-outfield)	$kgC\ m^{-2}$	9.9		SiteGeneric.xlsm
conc_DIC_regoUp	Concentration of dissolved inorganic carbon in the biologically active peat layer	$kgC\ m^{-3}$	9.4.2		SiteGeneric.xlsm
conc_Dust	Concentration of fine soil particles in air above sandy soils of agricultural land	$kgdw\ m^{-3}$	9.8		SiteGeneric.xlsm
demand_hay	Demand of winter fodder for organic fertilization in the infield-outland system	$kgC\ m^{-2}\ year^{-1}$	11.9		SiteGeneric.xlsm
f_loss_orgFert	Fraction of the original activity concentration in hay remaining when manure is applied to arable land	$Bq\ Bq^{-1}$	9.11.8		SiteGeneric.xlsm
minRate	Mineralization rate associated with organic fertilizer	$kgC\ kgC^{-1}\ year^{-1}$	9.7.1		SiteGeneric.xlsm
NPP_cereal	Total net primary production (above and below ground) of cereal in sandy soils	$kgC\ m^{-2}\ year^{-1}$	9.9		SiteGeneric.xlsm
percolation_agri	Downward flux of water from soil under modern practice	$m^3\ m^{-2}\ year^{-1}$	9.6.1		SiteGeneric.xlsm
z_regoUp	Depth of agricultural soils in early agricultural societies	m	9.5		SiteGeneric.xlsm
Combustion parameters					
f_C_wood	Fraction Carbon to dry weight of fire wood producing terrestrial primary producers, e.g. stem wood of Norway spruce	$kgC\ kgdw^{-1}$	9.13.8		SiteGeneric.xlsm
fuel_cons_peat	the yearly consumption of peat fuel to produce 20 000 kWh	$kgdw\ year^{-1}$	9.13.9		SiteGeneric.xlsm
fuel_cons_wood	the yearly consumption of wood fuel in dry weight to produce 20 000 kWh	$kgdw\ year^{-1}$	9.13.8		SiteGeneric.xlsm
area_support_wood	the area supporting a house-holds need of fire wood for heating (corresponding to 20,000 kWh year-1) per individual	$m^2\ ind^{-1}$	9.13.8		SiteGeneric.xlsm
demand_peat	the mass of peat needed to heat a house-hold over a 50-year period (corresponding to 20,000 kWh year-1) per individual	$kgdw\ ind^{-1}$	9.13.9		SiteGeneric.xlsm
demand_AlgFertil	Demand algea for organic fertilization in the infield-outland system	$kgC\ m^{-2}\ year^{-1}$	9.13.7		SiteGeneric.xlsm
f_combust	is the fraction of the fuel inventory that ends up in fly ash and gas after combustion of wood or peat				

Table A-8. Human characteristics

Parameter	Description	Unit	Chapter in parameterreport	Additional PSU reference	Delivered in file
ingRate_C	Yearly energy demand for an adult individual in units of carbon	kgC year^{-1}	10.4		SiteGeneric.xlsm
ingRate_water	Human ingestion rate of water per year	m^3 year^{-1}	10.3		SiteGeneric.xlsm
inhRate	Human inhalation rate of volume air	m^3 h^{-1}	10.5		SiteGeneric.xlsm
Drained mire					
time_exposure	Time spent outdoor in contact with contaminated ground (arable land) in an industrial age agricultural system	h year^{-1}	10.12		SiteGeneric.xlsm
N_group	Number of individuals in the most exposed industrial agricultural group	unitless	10.10		SiteGeneric.xlsm
f_diet_tuber	Fraction of the yearly energy demand that is covered by consumption of tuber	kgC kgC^{-1}	10.7		SiteGeneric.xlsm
f_diet_milk	Fraction of the yearly energy demand that is covered by consumption of milk	kgC kgC^{-1}	10.7		SiteGeneric.xlsm
f_diet_meat	Fraction of the yearly energy demand that is covered by consumption of meat	kgC kgC^{-1}	10.7		SiteGeneric.xlsm
f_diet_cereal	Fraction of the yearly energy demand that is covered by consumption of cereal	kgC kgC^{-1}	10.7		SiteGeneric.xlsm
f_area_tuber	Fraction of area used for tuber	m^2 m^{-2}	10.7		SiteGeneric.xlsm
f_area_fodder	Fraction of area used for fodder	m^2 m^{-2}	10.7		SiteGeneric.xlsm
f_area_cereal	Fraction of area used for cereal	m^2 m^{-2}	10.7		SiteGeneric.xlsm
area_support	Drained wetland area required to support the energy demand of an individual of the most exposed group (drained mire)	m^2	10.8		SiteGeneric.xlsm
Hunter gatherer					
time_exposure	Time spent in contact with contaminated ground (camp ground) in a hunting gathering community	h year^{-1}	10.12		SiteGeneric.xlsm
N_group	Number of individuals in the most exposed hunter and gatherer group	unitless	10.10		SiteGeneric.xlsm
f_diet_fish_max	Fraction of fish in diet corresponding to the maximum healthy protein consumption	kgC kgC^{-1}	10.11		SiteGeneric.xlsm
Garden plot					
time_exposure	Time spent outdoor in contact with garden plot contaminated by irrigation water	h year^{-1}	10.12		SiteGeneric.xlsm
N_group	Number of individuals in the most exposed group using a garden plot	unitless	10.10		SiteGeneric.xlsm
f_diet_veg	Fraction of the yearly energy demand that is covered by consumption of vegetables	kgC kgC^{-1}	10.6		SiteGeneric.xlsm
f_diet_tuber	Fraction of the yearly energy demand that is covered by consumption of tuber	kgC kgC^{-1}	10.6		SiteGeneric.xlsm
area	Area of agricultural land used to support one individuals need for vegetables	m^2	9.14.1		SiteGeneric.xlsm
Infield-outland					
time_exposure	Time spent outdoor in contact with contaminated ground (mire and arabale) in an infield outland agricultural system	h year^{-1}	10.12		SiteGeneric.xlsm
N_group	Number of individuals in the most exposed early agricultural group	unitless	10.10		SiteGeneric.xlsm
f_time_hay	Fraction of time spent working on collecting hay in contaminated wetland in an infield outland agricultural system	year year^{-1}	10.12		SiteGeneric.xlsm
f_time_agri	Fraction of time spent working on arable land in an infield outland agricultural system	year year^{-1}	10.12		SiteGeneric.xlsm

Parameter	Description	Unit	Chapter in parameterreport	Additional PSU reference	Delivered in file
f_meadow	Contribution of hay (winter fodder) to the yearly fodder demand	unitless	10.9		SiteGeneric.xlsm
f_diet_milk	Fraction of the yearly energy demand that is covered by consumption of milk	kgC kgC^{-1}	10.6		SiteGeneric.xlsm
f_diet_meat	Fraction of the yearly energy demand that is covered by consumption of meat	kgC kgC^{-1}	10.6		SiteGeneric.xlsm
f_diet_cereal	Fraction of the yearly energy demand that is covered by consumption of cereal	kgC kgC^{-1}	10.6		SiteGeneric.xlsm
area_support	Mire area required to support winter fodder for the livestock associated with an individual of the most exposed group	m^2	10.8		SiteGeneric.xlsm
area	Area of agricultural land used to support one individual of the most exposed group (infield-outland)	m^2	10.9		SiteGeneric.xlsm
demand_hay	Demand of winter fodder for organic fertilization in the infield-outland system	kgC m^{-2} $year^{-1}$	10.9		SiteGeneric.xlsm

Table A-9. Parameter used for non-human biota.

Parameter	Description	Unit	Chapter in parameterreport	Additional PSU reference	Delivered in file
f_DW_org	Fraction dry weight (kgdw) in organism (kgfw)	kgdw $kgfw^{-1}$	11.7		OrganismSrecific_NHB.xlsm
f_C_org	Fraction carbon (kgC) in organism (kgfw)	kgdw $kgfw^{-1}$	11.6		OrganismSrecific_NHB.xlsm
OCC	Occupancy factor for organism in habitat	unitless	11.4		OrganismSrecific_NHB.xlsm
w_alpha	Weighting factor of internal alpha for the radionuclide i.	unitless	11.5		RadionuclideSpecific_NHB..xlsm
w_beta_gamma	Weighting factor of internal beta gamma for the radionuclide i.	unitless	11.5		RadionuclideSpecific_NHB..xlsm
w_low_beta	Weighting factor of internal low energy beta for the radionuclide i.	unitless	11.5		RadionuclideSpecific_NHB..xlsm

Table A-10. Dose coefficient for non-human biota assessment. (The dose coefficients are presented in Appendix E.)

Parameter	Description	Unit	Chapter in parameterreport	Additional PSU reference	Delivered in file
All organisms					
DCC_int_alpha	DCC for internal exposure from alpha radiation	(μGy h^{-1})/(Bq $kgfw^{-1}$)	11.3		RadionuclideSpecific_NHB.xlsx
DCC_int_beta_gamma	DCC for internal exposure from beta/gamma radiation	(μGy h^{-1})/(Bq $kgfw^{-1}$)	11.3		RadionuclideSpecific_NHB.xlsx
DCC_int_low_beta	DCC for internal exposure from low beta radiation	(μGy h^{-1})/(Bq $kgfw^{-1}$)	11.3		RadionuclideSpecific_NHB.xlsx
Terrestrial organisms					
DCC_ext_in_air_beta_gamma	DCC for external exposure from beta/gamma radiation in air in terrestrial ecosystems	(μGy h^{-1})/(Bq m^{-3})	11.3		RadionuclideSpecific_NHB.xlsx
DCC_ext_in_soil_beta_gamma	DCC for external exposure from beta/gamma radiation in soil in terrestrial ecosystems	(μGy h^{-1})/(Bq $kgdw^{-1}$)	11.3		RadionuclideSpecific_NHB.xlsx
DCC_ext_on_soil_beta_gamma	DCC for external exposure from beta/gamma radiation on soil in terrestrial ecosystems	(μGy h^{-1})/(Bq $kgdw^{-1}$)	11.3		RadionuclideSpecific_NHB.xlsx
Aquatic organisms					
DCC_ext_low_beta	DCC for external exposure from low beta radiation in aquatic ecosystems	(μGy h^{-1})/(Bq L^{-1})	11.3		RadionuclideSpecific_NHB.xlsx
DCC_ext_beta_gamma	DCC for external exposure from beta/gamma radiation in aquatic ecosystems	(μGy h^{-1})/(Bq L^{-1})	11.3		RadionuclideSpecific_NHB.xlsx

Table A-11. Alternative calculation cases.

Parameter	Description	Unit	Chapter in parameterreport	Additional PSU reference	Delivered in file
Well in discharge plum					
q_well	Drilled well water extraction rate	$m^3\ year^{-1}$	12.1.1	Werner et al. (2013)	SiteGeneric.xlsm
well_interaction_area		m	12.1.2	Werner et al. (2013)	RepositoryBiosphereInterface.xlsx
p_well_interaction_area		unitless	12.1.2	Werner et al. (2013)	RepositoryBiosphereInterface.xlsx
f_well_agri	is the fraction of the release going to the well	unitless	12.1.4	Werner et al. (2013)	RepositoryBiosphereInterface.xlsx
f_well_interaction		unitless	12.1.3	Werner et al. (2013)	RepositoryBiosphereInterface.xlsx
Distibute release					
f_release	Fraction of release object	$(Bq\ year^{-1})\ (Bq\ year^{-1})^{-1}$	12.2		f_release.xlsx
Alternative object delineation					
area_obj		m	12.3		AreaSensitivity/params.xlsx
minRate_regoPeat		$kgC\ kgC^{-1}\ year^{-1}$	12.3		AreaSensitivity/params.xlsx
z_regoGL		m	12.3		AreaSensitivity/params.xlsx
z_regoLow		m	12.3		AreaSensitivity/params.xlsx
q_downstream_end		$m^3\ m^{-2}\ year^{-1}$	12.3	Werner et al. (2013)	AreaSensitivity/params.xlsx
q_downstream_iso		$m^3\ m^{-2}\ year^{-1}$	12.3	Werner et al. (2013)	AreaSensitivity/params.xlsx
q_gl_low_ter_end		$m^3\ m^{-2}\ year^{-1}$	12.3	Werner et al. (2013)	AreaSensitivity/params.xlsx
q_gl_low_ter_iso		$m^3\ m^{-2}\ year^{-1}$	12.3	Werner et al. (2013)	AreaSensitivity/params.xlsx
q_gl_pg_ter_end		$m^3\ m^{-2}\ year^{-1}$	12.3	Werner et al. (2013)	AreaSensitivity/params.xlsx
q_gl_pg_ter_iso		$m^3\ m^{-2}\ year^{-1}$	12.3	Werner et al. (2013)	AreaSensitivity/params.xlsx
q_low_gl_ter_end		$m^3\ m^{-2}\ year^{-1}$	12.3	Werner et al. (2013)	AreaSensitivity/params.xlsx
q_low_gl_ter_iso		$m^3\ m^{-2}\ year^{-1}$	12.3	Werner et al. (2013)	AreaSensitivity/params.xlsx
q_peat_pg_ter_end		$m^3\ m^{-2}\ year^{-1}$	12.3	Werner et al. (2013)	AreaSensitivity/params.xlsx
q_peat_pg_ter_iso		$m^3\ m^{-2}\ year^{-1}$	12.3	Werner et al. (2013)	AreaSensitivity/params.xlsx
q_peat_up_ter_end		$m^3\ m^{-2}\ year^{-1}$	12.3	Werner et al. (2013)	AreaSensitivity/params.xlsx
q_peat_up_ter_iso		$m^3\ m^{-2}\ year^{-1}$	12.3	Werner et al. (2013)	AreaSensitivity/params.xlsx
q_pg_gl_ter_end		$m^3\ m^{-2}\ year^{-1}$	12.3	Werner et al. (2013)	AreaSensitivity/params.xlsx
q_pg_gl_ter_iso		$m^3\ m^{-2}\ year^{-1}$	12.3	Werner et al. (2013)	AreaSensitivity/params.xlsx
q_pg_peat_ter_end		$m^3\ m^{-2}\ year^{-1}$	12.3	Werner et al. (2013)	AreaSensitivity/params.xlsx
q_pg_peat_ter_iso		$m^3\ m^{-2}\ year^{-1}$	12.3	Werner et al. (2013)	AreaSensitivity/params.xlsx
q_up_peat_ter_end		$m^3\ m^{-2}\ year^{-1}$	12.3	Werner et al. (2013)	AreaSensitivity/params.xlsx
q_up_peat_ter_iso		$m^3\ m^{-2}\ year^{-1}$	12.3	Werner et al. (2013)	AreaSensitivity/params.xlsx

Parameter	Description	Unit	Chapter in parameterreport	Additional PSU reference	Delivered in file
q_up_wat_ter_end		$m^3\ m^{-2}\ year^{-1}$	12.3	Werner et al. (2013)	AreaSensitivity/params.xlsx
q_up_wat_ter_iso		$m^3\ m^{-2}\ year^{-1}$	12.3	Werner et al. (2013)	AreaSensitivity/params.xlsx
q_wat_up_ter_end		$m^3\ m^{-2}\ year^{-1}$	12.3	Werner et al. (2013)	AreaSensitivity/params.xlsx
q_wat_up_ter_iso		$m^3\ m^{-2}\ year^{-1}$	12.3	Werner et al. (2013)	AreaSensitivity/params.xlsx
Timedependent					**AreaSensitivity/params.xlsx**
area_obj_ter		m^2	12.3		AreaSensitivity/params.xlsx
z_regoPG_ter		m	12.3		AreaSensitivity/params.xlsx
WF_lobj157_1		$m^3\ year^{-1}$			AreaSensitivity/params.xlsx
Ter_growth		$m^2\ year^{-1}$	12.3		AreaSensitivity/params.xlsx

Appendix B

Parameters altered in climate calculation cases

Table B-1. Parameters in this table are altered in the climate calculation case extended global warming.

Parameter	Description	Unit	Chapter in parameterreport	Appendix in parameterreport	Additional PSU reference	Delivered in file
Mire and agricultural parameters						
biom_cereal (Drained_mire)	Yield as biomass of cereal per unit area at end of vegetation period (drained mire)	kgC m^{-2}	9.9			WarmerClimate/SiteGeneric.xlsm
biom_fodder (Drained_mire)	Yield as biomass of fodder per unit area at end of vegetation period (drained mire)	kgC m^{-2}	9.9			WarmerClimate/SiteGeneric.xlsm
biom_tuber (Drained_mire)	Yield as biomass of tuber per unit area at end of vegetation period (drained mire)	kgC m^{-2}	9.9			WarmerClimate/SiteGeneric.xlsm
NPP_cereal (Drained_mire)	Total net primary production (above and below ground) of cerial in cultivated peat	kgC m^{-2} $year^{-1}$	9.10			WarmerClimate/SiteGeneric.xlsm
NPP_fodder (Drained_mire)	Total net primary production (above and below ground) of fodder in cultivated peat	kgC m^{-2} $year^{-1}$	9.10			WarmerClimate/SiteGeneric.xlsm
NPP_tuber (Drained_mire)	Total net primary production (above and below ground) of tuber in cultivated peat	kgC m^{-2} $year^{-1}$	9.10			WarmerClimate/SiteGeneric.xlsm
biom_pp_ter	Total biomass of terrestrial primary producers per unit area	kgC m^{-2}	9.3			WarmerClimate/SiteGeneric.xlsm
conc_C_atmos	Concentration of carbon in the atmosphere (above the ground)	kgC m^{-3}	9.4			WarmerClimate/SiteGeneric.xlsm
LAI_cereal	Ratio of total upper leaf surface of vegetation divided by the surface area of the agricultural lands on which the vegetation grows (Leaf Area Index)	m^2 m^{-2}	9.4.10			WarmerClimate/SiteGeneric.xlsm
LAI_ter	Ratio of total upper leaf surface of vegetation divided by the surface area of the mire on which the vegetation grows (Leaf Area Index)	m^2 m^{-2}	9.4.10			WarmerClimate/SiteGeneric.xlsm
NPP_ter	Total net primary production (above and below ground) in terrestrial ecosystem	kgC m^{-2} $year^{-1}$	9.3			WarmerClimate/SiteGeneric.xlsm
piston_vel_ter	Gas exchange coefficient for peat pore water in contact with the atmosphere	m $year^{-1}$	9.4.6			WarmerClimate/SiteGeneric.xlsm
Hydrological flows						
q_downstream_end	Water flux from water column downstream in stream phase	m^3 m^{-2} $year^{-1}$	6.4	Appendix D	Werner et al. 2013	WarmerClimate/q_flux.xlsm

Parameter	Description	Unit	Chapter in parameterreport	Appendix in parameterreport	Additional PSU reference	Delivered in file
q_downstream_iso	Water flux from water column downstream in lake phase	$m^3\ m^{-2}\ year^{-1}$	6.4	Appendix D	Werner et al. 2013	WarmerClimate/q_flux.xlsm
q_gl_low_lake	Water flux from glacial clay layer to lower regolith for aquatic part in limnic phase	$m^3\ m^{-2}\ year^{-1}$	6.4	Appendix D	Werner et al. 2013	WarmerClimate/q_flux.xlsm
q_gl_low_sea	Water flux from glacial clay layer to lower regolith in marine phase	$m^3\ m^{-2}\ year^{-1}$	6.4	Appendix D	Werner et al. 2013	WarmerClimate/q_flux.xlsm
q_gl_low_ter_end	Water flux from glacial clay layer to lower regolith for terrestrial part in mire phase	$m^3\ m^{-2}\ year^{-1}$	6.4	Appendix D	Werner et al. 2013	WarmerClimate/q_flux.xlsm
q_gl_low_ter_iso	Water flux from glacial clay layer to lower regolith for terrestrial part in limnic phase	$m^3\ m^{-2}\ year^{-1}$	6.4	Appendix D	Werner et al. 2013	WarmerClimate/q_flux.xlsm
q_gl_pg_lake	Water flux from glacial clay to post glacial clay layer for aquatic part in limnic phase	$m^3\ m^{-2}\ year^{-1}$	6.4	Appendix D	Werner et al. 2013	WarmerClimate/q_flux.xlsm
q_gl_pg_sea	Water flux from glacial clay to post glacial clay layer in marine phase	$m^3\ m^{-2}\ year^{-1}$	6.4	Appendix D	Werner et al. 2013	WarmerClimate/q_flux.xlsm
q_gl_pg_ter_end	Water flux from glacial clay to post glacial clay layer for terrestrial part in mire phase	$m^3\ m^{-2}\ year^{-1}$	6.4	Appendix D	Werner et al. 2013	WarmerClimate/q_flux.xlsm
q_gl_pg_ter_iso	Water flux from glacial clay to post glacial clay layer for terrestrial part in limnic phase	$m^3\ m^{-2}\ year^{-1}$	6.4	Appendix D	Werner et al. 2013	WarmerClimate/q_flux.xlsm
q_low_gl_lake	Water flux from lower regolith to glacial clay layer for aquatic part in limnic phase	$m^3\ m^{-2}\ year^{-1}$	6.4	Appendix D	Werner et al. 2013	WarmerClimate/q_flux.xlsm
q_low_gl_sea	Water flux from lower regolith to glacial clay layer in marine phase	$m^3\ m^{-2}\ year^{-1}$	6.4	Appendix D	Werner et al. 2013	WarmerClimate/q_flux.xlsm
q_low_gl_ter_end	Water flux from lower regolith to glacial clay layer for terrestrial part in mire phase	$m^3\ m^{-2}\ year^{-1}$	6.4	Appendix D	Werner et al. 2013	WarmerClimate/q_flux.xlsm
q_low_gl_ter_iso	Water flux from lower regolith to glacial clay layer for terrestrial part in limnic phase	$m^3\ m^{-2}\ year^{-1}$	6.4	Appendix D	Werner et al. 2013	WarmerClimate/q_flux.xlsm
q_peat_pg_ter_end	Water flux from peat to post glacial clay layer for terrestrial part in mire phase	$m^3\ m^{-2}\ year^{-1}$1	6.4	Appendix D	Werner et al. 2013	WarmerClimate/q_flux.xlsm
q_peat_pg_ter_iso	Water flux from peat to post glacial clay layer for terrestrial part in limnic phase	$m^3\ m^{-2}\ year^{-1}$	6.4	Appendix D	Werner et al. 2013	WarmerClimate/q_flux.xlsm
q_peat_up_ter_end	Water flux from peat to upper peat layer for terrestrial part in mire phase	$m^3\ m^{-2}\ year^{-1}$	6.4	Appendix D	Werner et al. 2013	WarmerClimate/q_flux.xlsm
q_peat_up_ter_iso	Water flux from peat to upper peat layer for terrestrial part in limnic phase	$m^3\ m^{-2}\ year^{-1}$	6.4	Appendix D	Werner et al. 2013	WarmerClimate/q_flux.xlsm
q_pg_gl_lake	Water flux from post glacial clay to glacial clay layer for aquatic part in limnic phase	$m^3\ m^{-2}\ year^{-1}$	6.4	Appendix D	Werner et al. 2013	WarmerClimate/q_flux.xlsm
q_pg_gl_sea	Water flux from post glacial clay to glacial clay layer in marine phase	$m^3\ m^{-2}\ year^{-1}$	6.4	Appendix D	Werner et al. 2013	WarmerClimate/q_flux.xlsm

Parameter	Description	Unit	Chapter in parameterreport	Appendix in parameterreport	Additional PSU reference	Delivered in file
q_pg_gl_ter_end	Water flux from post glacial clay to glacial clay layer for terrestrial part in mire phase	$m^3\ m^{-2}\ year^{-1}$	6.4	Appendix D	Werner et al. 2013	WarmerClimate/q_flux.xlsm
q_pg_gl_ter_iso	Water flux from post glacial clay to glacial clay layer for terrestrial part in limnic phase	$m^3\ m^{-2}\ year^{-1}$	6.4	Appendix D	Werner et al. 2013	WarmerClimate/q_flux.xlsm
q_pg_peat_ter_end	Water flux from post glacial clay to peat layer for terrestrial part in mire phase	$m^3\ m^{-2}\ year^{-1}$	6.4	Appendix D	Werner et al. 2013	WarmerClimate/q_flux.xlsm
q_pg_peat_ter_iso	Water flux from post glacial clay to peat layer for terrestrial part in limnic phase	$m^3\ m^{-2}\ year^{-1}$	6.4	Appendix D	Werner et al. 2013	WarmerClimate/q_flux.xlsm
q_pg_up_lake	Water flux from post glacial clay to upper sediment layer for aquatic part in limnic phase	$m^3\ m^{-2}\ year^{-1}$	6.4	Appendix D	Werner et al. 2013	WarmerClimate/q_flux.xlsm
q_pg_up_sea	Water flux from post glacial clay to upper sediment layer in marine phase	$m^3\ m^{-2}\ year^{-1}$	6.4	Appendix D	Werner et al. 2013	WarmerClimate/q_flux.xlsm
q_up_peat_ter_end	Water flux from upper peat to peat layer for terrestrial part in mire phase	$m^3\ m^{-2}\ year^{-1}$	6.4	Appendix D	Werner et al. 2013	WarmerClimate/q_flux.xlsm
q_up_peat_ter_iso	Water flux from upper peat to peat layer for terrestrial part in limnic phase	$m^3\ m^{-2}\ year^{-1}$	6.4	Appendix D	Werner et al. 2013	WarmerClimate/q_flux.xlsm
q_up_pg_lake	Water flux from upper sediment to post glacial clay layer for aquatic part in limnic phase	$m^3\ m^{-2}\ year^{-1}$	6.4	Appendix D	Werner et al. 2013	WarmerClimate/q_flux.xlsm
q_up_pg_sea	Water flux from upper sediment to post glacial clay layer in marine phase	$m^3\ m^{-2}\ year^{-1}$	6.4	Appendix D	Werner et al. 2013	WarmerClimate/q_flux.xlsm
q_up_wat_lake	Water flux from upper sediment layer to water column for aquatic part in limnic phase	$m^3\ m^{-2}\ year^{-1}$	6.4	Appendix D	Werner et al. 2013	WarmerClimate/q_flux.xlsm
q_up_wat_sea	Water flux from upper sediment layer to water column in marine phase	$m^3\ m^{-2}\ year^{-1}$	6.4	Appendix D	Werner et al. 2013	WarmerClimate/q_flux.xlsm
q_up_wat_ter_end	Water flux from upper peat layer to water column for terrestrial part in mire phase	$m^3\ m^{-2}\ year^{-1}$	6.4	Appendix D	Werner et al. 2013	WarmerClimate/q_flux.xlsm
q_up_wat_ter_iso	Water flux from upper peat layer to water column for terrestrial part in limnic phase	$m^3\ m^{-2}\ year^{-1}$	6.4	Appendix D	Werner et al. 2013	WarmerClimate/q_flux.xlsm
q_wat_up_lake	Water flux from water column to upper sediment layer for aquatic part in limnic phase	$m^3\ m^{-2}\ year^{-1}$	6.4	Appendix D	Werner et al. 2013	WarmerClimate/q_flux.xlsm
q_wat_up_sea	Water flux from water column to upper sediment layer in marine phase	$m^3\ m^{-2}\ year^{-1}$	6.4	Appendix D	Werner et al. 2013	WarmerClimate/q_flux.xlsm
q_wat_up_ter_end	Water flux from water column to upper peat layer for terrestrial part in mire phase	$m^3\ m^{-2}\ year^{-1}$	6.4	Appendix D	Werner et al. 2013	WarmerClimate/q_flux.xlsm
q_wat_up_ter_iso	Water flux from water column to upper peat layer for terrestrial part in limnic phase	$m^3\ m^{-2}\ year^{-1}$	6.4	Appendix D	Werner et al. 2013	WarmerClimate/q_flux.xlsm

Table B-2. Parameters in this table are altered in the climate calculation early periglacial climate case.

Parameter	Description	Unit	Chapter in parameterreport	Appendix in parameterreport	Additional PSU reference	Delivered in file
Aquatic ecosystem						
prod_edib_cray_lake	Sustainable yield with respect to edible crayfish per unit area in the lake	kgC m^{-2} $year^{-1}$	8.9.2			ColderClimate/SiteGeneric_aquatic.xlsm
prod_edib_fish_lake	Sustainable yield with respect to edible fish per unit area in the lake	kgC m^{-2} $year^{-1}$	8.9.1			ColderClimate/SiteGeneric_aquatic.xlsm
Mire ecosystem						
biom_pp_ter	Total biomass of terrestrial primary producers per unit area	kgC m^{-2}	9.3			ColderClimate/SiteGeneric.xlsm
conc_C_atmos	Concentration of carbon in the atmosphere (above the ground)	kgC m^{-3}	9.4.1			ColderClimate/SiteGeneric.xlsm
NPP_ter	Total net primary production (above and below ground) in terrestrial ecosystem	kgC m^{-2} $year^{-1}$	9.3			ColderClimate/SiteGeneric.xlsm
piston_vel_ter	Gas exchange coefficient for peat pore water in contact with the atmosphere	m $year^{-1}$	9.4.6			ColderClimate/SiteGeneric.xlsm
solubilityCoef_ter	Solubility coefficient for carbon dioxide in pore water of the upper peat layer	(mol m^{-3}) (mol m^{-3})$^{-1}$	9.4.7			ColderClimate/SiteGeneric.xlsm
minRate_regoUp_ter	Mineralization rate of refractory organic carbon in oxic terrestrial regolith	kgC kgC^{-1} $year^{-1}$	9.7.1			ColderClimate/SiteGeneric.xlsm
Parameters for object 157_1						
q_downstream_end	Water flux from object downstream in perglacial phase	m^3 m^{-2} $year^{-1}$	6.4	Appendix D	Werner et al. 2013	ColderClimate/lobj157_1.xlsx
q_low_gl_ter_end	Water flux from lower regolith to glacial clay layer for terrestrial part in perglacial phase	m^3 m^{-2} $year^{-1}$	6.4	Appendix D	Werner et al. 2013	ColderClimate/lobj157_1.xlsx
q_gl_low_ter_end	Water flux from glacial clay layer to lower regolith for terrestrial part in perglacial phase	m^3 m^{-2} $year^{-1}$	6.4	Appendix D	Werner et al. 2013	ColderClimate/lobj157_1.xlsx
q_gl_pg_ter_end	Water flux from glacial clay to post glacial clay layer for terrestrial part in perglacial phase	m^3 m^{-2} $year^{-1}$	6.4	Appendix D	Werner et al. 2013	ColderClimate/lobj157_1.xlsx
q_pg_gl_ter_end	Water flux from post glacial clay to glacial clay layer for terrestrial part in perglacial phase	m^3 m^{-2} $year^{-1}$	6.4	Appendix D	Werner et al. 2013	ColderClimate/lobj157_1.xlsx
q_up_wat_ter_end	Water flux from upper peat layer to water column for terrestrial part in perglacial phase	m^3 m^{-2} $year^{-1}$	6.4	Appendix D	Werner et al. 2013	ColderClimate/lobj157_1.xlsx
q_wat_up_ter_end	Water flux from water column to upper peat layer for terrestrial part in perglacial phase	m^3 m^{-2} $year^{-1}$	6.4	Appendix D	Werner et al. 2013	ColderClimate/lobj157_1.xlsx
q_pg_peat_ter_end	Water flux from post glacial clay to peat layer for terrestrial part in perglacial phase	m^3 m^{-2} $year^{-1}$	6.4	Appendix D	Werner et al. 2013	ColderClimate/lobj157_1.xlsx

Parameter	Description	Unit	Chapter in parameterreport	Appendix in parameterreport	Additional PSU reference	Delivered in file
q_peat_pg_ter_end	Water flux from peat to post glacial clay layer for terrestrial part in perglacial phase	$m^3\ m^{-2}\ year^{-1}$	6.4	Appendix D	Werner et al. 2013	ColderClimate/lobj157_1.xlsx
q_peat_up_ter_end	Water flux from peat to upper peat layer for terrestrial part in perglacial phase	$m^3\ m^{-2}\ year^{-1}$	6.4	Appendix D	Werner et al. 2013	ColderClimate/lobj157_1.xlsx
q_up_peat_ter_end	Water flux from upper peat to peat layer for terrestrial part in perglacial phase	$m^3\ m^{-2}\ year^{-1}$	6.4	Appendix D	Werner et al. 2013	ColderClimate/lobj157_1.xlsx
q_low_gl_lake	Water flux from lower regolith to glacial clay layer for aquatic part in periglacial phase	$m^3\ m^{-2}\ year^{-1}$	6.4	Appendix D	Werner et al. 2013	ColderClimate/lobj157_1.xlsx
q_gl_low_lake	Water flux from glacial clay layer to lower regolith for aquatic part in periglacial phase	$m^3\ m^{-2}\ year^{-1}$	6.4	Appendix D	Werner et al. 2013	ColderClimate/lobj157_1.xlsx
q_gl_pg_lake	Water flux from glacial clay to post glacial clay layer for aquatic part in periglacial phase	$m^3\ m^{-2}\ year^{-1}$	6.4	Appendix D	Werner et al. 2013	ColderClimate/lobj157_1.xlsx
q_pg_gl_lake	Water flux from post glacial clay to glacial clay layer for aquatic part in periglacial phase	$m^3\ m^{-2}\ year^{-1}$	6.4	Appendix D	Werner et al. 2013	ColderClimate/lobj157_1.xlsx
q_pg_up_lake	Water flux from post glacial clay to upper sediment layer for aquatic part in periglacial phase	$m^3\ m^{-2}\ year^{-1}$	6.4	Appendix D	Werner et al. 2013	ColderClimate/lobj157_1.xlsx
q_up_pg_lake	Water flux from upper sediment to post glacial clay layer for aquatic part in periglacial phase	$m^3\ m^{-2}\ year^{-1}$	6.4	Appendix D	Werner et al. 2013	ColderClimate/lobj157_1.xlsx
q_up_wat_lake	Water flux from upper sediment layer to water column for aquatic part in periglacial phase	$m^3\ m^{-2}\ year^{-1}$	6.4	Appendix D	Werner et al. 2013	ColderClimate/lobj157_1.xlsx
q_wat_up_lake	Water flux from water column to upper sediment layer for aquatic part in periglacial phase	$m^3\ m^{-2}\ year^{-1}$	6.4	Appendix D	Werner et al. 2013	ColderClimate/lobj157_1.xlsx
sed_rate	Gross sedimentation rate per unit surface area	$m\ year^{-1}$	4.5.3			ColderClimate/lobj157_1.xlsx
res_rate	Gross resuspension rate per unit surface area	$m\ year^{-1}$	4.5.2			ColderClimate/lobj157_1.xlsx
Parameters for object 114						
z_regoLow	Average depth of regolow (till and filling)	m	4.6			ColderClimate/lobj114.xlsm
z_regoGL	Depth of glacial clay	m	4.6			ColderClimate/lobj114.xlsm
z_regoPG_aqu	Depth of terrestrial post-glacial sediments	m	4.6			ColderClimate/lobj114.xlsm
z_water	Average depth of water	m	4.6			ColderClimate/lobj114.xlsm
area_obj	Area of the lake object	m^2	4.6			ColderClimate/lobj114.xlsm
area_obj_aqu	Surface area of aquatic object	m^2	4.6			ColderClimate/lobj114.xlsm
area_obj_ter	Surface area of terrestrial object	m^2	4.6			ColderClimate/lobj114.xlsm
q_low_gl_lake	Water flux from lower regolith to glacial clay layer for aquatic part in limnic phase	$m^3\ m^{-2}\ year^{-1}$	6.4	Appendix D	Werner et al. 2013	ColderClimate/lobj114.xlsm
q_gl_low_lake	Water flux from glacial clay layer to lower regolith for aquatic part in limnic phase	$m^3\ m^{-2}\ year^{-1}$	6.4	Appendix D	Werner et al. 2013	ColderClimate/lobj114.xlsm

Parameter	Description	Unit	Chapter in parameterreport	Appendix in parameterreport	Additional PSU reference	Delivered in file
q_gl_pg_lake	Water flux from glacial clay to post glacial clay layer for aquatic part in limnic phase	m^3 m^{-2} $year^{-1}$	6.4	Appendix D	Werner et al. 2013	ColderClimate/lobj114.xlsm
q_pg_gl_lake	Water flux from post glacial clay to glacial clay layer for aquatic part in limnic phase	m^3 m^{-2} $year^{-1}$	6.4	Appendix D	Werner et al. 2013	ColderClimate/lobj114.xlsm
q_pg_up_lake	Water flux from post glacial clay to upper sediment layer for aquatic part in limnic phase	m^3 m^{-2} $year^{-1}$	6.4	Appendix D	Werner et al. 2013	ColderClimate/lobj114.xlsm
q_up_pg_lake	Water flux from upper sediment to post glacial clay layer for aquatic part in limnic phase	m^3 m^{-2} $year^{-1}$	6.4	Appendix D	Werner et al. 2013	ColderClimate/lobj114.xlsm
q_up_wat_lake	Water flux from upper sediment layer to water column for aquatic part in limnic phase	m^3 m^{-2} $year^{-1}$	6.4	Appendix D	Werner et al. 2013	ColderClimate/lobj114.xlsm
q_wat_up_lake	Water flux from water column to upper sediment layer for aquatic part in limnic phase	m^3 m^{-2} $year^{-1}$	6.4	Appendix D	Werner et al. 2013	ColderClimate/lobj114.xlsm
q_downstream_end	Water flux from water column downstream in stream phase	m^3 m^{-2} $year^{-1}$	6.4	Appendix D	Werner et al. 2013	ColderClimate/lobj114.xlsm
biom_pp_macro	Biomass of macrobentic community in water per unit surface area	kgC m^{-2}	8.6			ColderClimate/lobj114.xlsm
biom_pp_micro	Biomass of microbenthic community in water per unit surface area	kgC m^{-2}	8.6			ColderClimate/lobj114.xlsm
biom_pp_plank	Biomass of pelagic community in water per unit surface area	kgC m^{-2}	8.6			ColderClimate/lobj114.xlsm
NPP_macro	Net primary production of macrobenthic community in water per unit surface area	kgC m^{-2} $year^{-1}$	8.6			ColderClimate/lobj114.xlsm
NPP_micro	Net primary production of microbenthic community in water per unit surface area	kgC m^{-2} $year^{-1}$	8.6			ColderClimate/lobj114.xlsm
NPP_plank	Net primary production of pelagic community in water per unit surface area	kgC m^{-2} year–^{1}	8.6			ColderClimate/lobj114.xlsm
res_rate	Gross resuspension rate per unit surface area	m $year^{-1}$	4.5			ColderClimate/lobj114.xlsm
sed_rate	Gross sedimentation rate per unit surface area	m $year^{-1}$	4.5			ColderClimate/lobj114.xlsm

Appendix C

Time-dependent parameters

Table C-1. Time-dependent parameters for object 116.

Year (AD)	area_obj_aqu (m^2)	area_obj_ter (m^2)	z_regoPG_aqu (m)	z_regoPG_ter (m)	z_water (m)	res_rate (m^3 m^{-2} $year^{-1}$)	sed_rate (m^3 m^{-2} $year^{-1}$)	Ter_growth (($m^2 year^{-1}$)	biom_pp_macro (kgC m^{-2})	biom_pp_micro (kgC m^{-2})	biom_pp_plank (kgC m^{-2})	NPP_macro (kgC m^{-2} $year^{-1}$)	NPP_micro (kgC m^{-2} $year^{-1}$)	NPP_plank (kgC m^{-2} $year^{-1}$)
–8500	1.02E+07	0		0	1.39E+02	0	1.23E–04	0	0	0	3.80E–04	0	0	3.61E–02
–8000	1.02E+07	0		0	1.12E+02	0	1.23E–04	0	0	0	3.80E–04	0	0	3.61E–02
–7500	1.02E+07	0		0	9.05E+01	1.95E–04	1.23E–04	0	0	0	3.80E–04	0	0	3.61E–02
–7000	1.02E+07	0		0	8.17E+01	2.97E–04	1.23E–04	0	0	0	3.80E–04	0	0	3.61E–02
–6500	1.02E+07	0		0	7.95E+01	1.22E–04	1.23E–04	0	0	0	3.80E–04	0	0	3.61E–02
–6000	1.02E+07	0		0	7.66E+01	1.25E–04	1.23E–04	0	0	0	3.80E–04	0	0	3.61E–02
–5500	1.02E+07	0		0	7.25E+01	1.23E–04	1.23E–04	0	0	0	3.80E–04	0	0	3.61E–02
–5000	1.02E+07	0		0	6.77E+01	1.23E–04	1.23E–04	0	0	0	3.80E–04	0	0	3.61E–02
–4500	1.02E+07	0		0	6.24E+01	1.23E–04	1.23E–04	0	0	0	3.80E–04	0	0	3.61E–02
–4000	1.02E+07	0		0	5.71E+01	1.23E–04	1.23E–04	0	0	0	3.80E–04	0	0	3.61E–02
–3500	1.02E+07	0		0	5.18E+01	1.23E–04	1.23E–04	0	0	0	3.80E–04	0	0	3.61E–02
–3000	1.02E+07	0		0	4.67E+01	1.23E–04	1.23E–04	0	0	0	3.80E–04	0	0	3.61E–02
–2500	1.02E+07	0		0	4.17E+01	1.26E–04	1.26E–04	0	0	0	3.80E–04	0	0	3.61E–02
–2000	1.02E+07	0		0	3.72E+01	1.82E–04	1.82E–04	0	0	0	3.80E–04	0	0	3.61E–02
–1500	1.02E+07	0		0	3.30E+01	3.28E–04	3.28E–04	0	0	0	3.80E–04	0	0	3.61E–02
–1000	1.02E+07	0		0	2.91E+01	4.60E–04	4.60E–04	0	0	0	3.80E–04	0	0	3.61E–02
–500	1.02E+07	0		0	2.54E+01	5.07E–04	5.07E–04	0	0	0	3.80E–04	0	0	3.61E–02
0	1.02E+07	0		0	2.19E+01	7.37E–04	7.37E–04	0	0	0	3.80E–04	0	0	3.61E–02
500	1.02E+07	0		0	1.92E+01	7.86E–04	7.86E–04	0	0	0	3.65E–04	0	0	3.65E–02
1000	1.02E+07	0		0	1.59E+01	4.51E–04	4.51E–04	0	2.52E–03	6.23E–04	3.02E–04	1.48E–02	1.62E–02	3.02E–02
1500	1.01E+07	0		0	1.28E+01	3.29E–04	3.46E–04	0	4.31E–03	1.25E–03	2.42E–04	2.46E–02	2.28E–02	2.42E–02
2000	9.74E+06	0		0	1.02E+01	2.27E–04	3.42E–04	0	6.69E–03	1.76E–03	1.94E–04	3.73E–02	2.82E–02	1.94E–02

Year (AD)	area_obj_aqu (m^2)	area_obj_ter (m^2)	z_regoPG_aqu (m)	z_regoPG_ter (m)	z_water (m)	res_rate (m^3 m^{-2} year^{-1})	sed_rate (m^3 m^{-2} year^{-1})	Ter_growth ((m^2 year^{-1})	biom_pp_macro (kgC m^{-2})	biom_pp_micro (kgC m^{-2})	biom_pp_plank (kgC m^{-2})	NPP_macro (kgC m^{-2} year^{-1})	NPP_micro (kgC m^{-2} year^{-1})	NPP_plank (kgC m^{-2} year^{-1})
2500	8.90E+06	0		0	8.05E+00	3.08E–05	2.32E–04	0	9.69E–03	2.19E–03	1.53E–04	5.29E–02	3.27E–02	1.53E–02
3000	7.46E+06	0		0	6.41E+00	4.82E–05	1.66E–04	0	1.29E–02	2.52E–03	1.22E–04	6.92E–02	3.61E–02	1.22E–02
3500	6.05E+06	0		0	4.65E+00	1.18E–04	1.35E–04	0	1.74E–02	2.87E–03	8.84E–05	9.21E–02	3.98E–02	8.84E–03
4000	4.70E+06	0	3.74E–01	0	2.84E+00	1.80E–04	1.29E–04	5.50E+02	2.37E–02	3.23E–03	5.40E–05	1.24E–01	4.36E–02	5.40E–03
4500	1.74E+06		4.59E–01		1.45E+00	6.64E–04	1.24E–04		2.21E–02	3.80E–03	8.18E–05	8.64E–02	5.53E–02	2.43E–02
4600	1.00E+06	3.30E+05	5.06E–01	4.81E–01	2.03E+00	8.06E–05	1.23E–04	2.32E+02	2.21E–02	3.80E–03	8.12E–05	8.65E–02	5.53E–02	2.43E–02
4700	9.82E+05	3.53E+05	5.40E–01	4.84E–01	2.02E+00	2.20E–04	3.37E–04	1.92E+02	2.21E–02	3.80E–03	8.12E–05	8.65E–02	5.53E–02	2.43E–02
4800	9.63E+05	3.72E+05	5.72E–01	4.92E–01	2.00E+00	2.20E–04	3.36E–04	1.92E+02	2.21E–02	3.80E–03	8.04E–05	8.66E–02	5.54E–02	2.43E–02
4900	9.44E+05	3.92E+05	6.05E–01	4.97E–01	1.98E+00	2.19E–04	3.34E–04	1.92E+02	2.21E–02	3.81E–03	7.96E–05	8.66E–02	5.54E–02	2.43E–02
5000	9.25E+05	4.11E+05	6.38E–01	5.03E–01	1.96E+00	2.18E–04	3.33E–04	1.92E+02	2.22E–02	3.81E–03	7.88E–05	8.67E–02	5.55E–02	2.43E–02
5100	9.06E+05	4.30E+05	6.72E–01	5.08E–01	1.94E+00	2.16E–04	3.31E–04	1.92E+02	2.22E–02	3.81E–03	7.80E–05	8.68E–02	5.56E–02	2.43E–02
5200	8.86E+05	4.49E+05	7.07E–01	5.12E–01	1.92E+00	2.15E–04	3.29E–04	1.92E+02	2.22E–02	3.82E–03	7.72E–05	8.69E–02	5.56E–02	2.43E–02
5300	8.67E+05	4.68E+05	7.42E–01	5.16E–01	1.90E+00	2.14E–04	3.27E–04	1.92E+02	2.22E–02	3.82E–03	7.65E–05	8.70E–02	5.57E–02	2.43E–02
5400	8.48E+05	4.88E+05	7.79E–01	5.18E–01	1.88E+00	2.13E–04	3.26E–04	1.92E+02	2.22E–02	3.82E–03	7.57E–05	8.70E–02	5.57E–02	2.43E–02
5500	8.29E+05	5.07E+05	8.18E–01	5.17E–01	1.86E+00	2.12E–04	3.24E–04	1.92E+02	2.22E–02	3.82E–03	7.50E–05	8.70E–02	5.57E–02	2.43E–02
5600	8.10E+05	5.26E+05	8.57E–01	5.19E–01	1.84E+00	2.11E–04	3.23E–04	1.92E+02	2.22E–02	3.82E–03	7.42E–05	8.70E–02	5.57E–02	2.43E–02
5700	7.90E+05	5.45E+05	8.99E–01	5.17E–01	1.82E+00	2.10E–04	3.21E–04	1.92E+02	2.22E–02	3.82E–03	7.35E–05	8.70E–02	5.57E–02	2.43E–02
5800	7.71E+05	5.64E+05	8.81E–01	5.98E–01	1.81E+00	2.08E–04	3.19E–04	1.92E+02	2.22E–02	3.82E–03	7.28E–05	8.70E–02	5.57E–02	2.43E–02
5900	7.52E+05	5.84E+05	8.94E–01	5.92E–01	1.82E+00			1.92E+02	2.22E–02	3.82E–03	7.34E–05	8.70E–02	5.57E–02	2.43E–02
6000	7.33E+05	6.03E+05	9.34E–01	5.92E–01	1.80E+00	2.10E–04	3.20E–04	1.92E+02	2.22E–02	3.82E–03	7.24E–05	8.70E–02	5.57E–02	2.43E–02
6100	7.14E+05	6.22E+05	9.72E–01	5.96E–01	1.78E+00	2.08E–04	3.18E–04	1.92E+02	2.22E–02	3.82E–03	7.16E–05	8.70E–02	5.57E–02	2.43E–02
6200	6.94E+05	6.41E+05	1.01E+00	6.04E–01	1.75E+00	2.06E–04	3.15E–04	1.92E+02	2.22E–02	3.82E–03	7.06E–05	8.70E–02	5.57E–02	2.43E–02
6300	6.75E+05	6.60E+05	1.04E+00	6.17E–01	1.73E+00	2.04E–04	3.13E–04	1.92E+02	2.22E–02	3.82E–03	6.97E–05	8.70E–02	5.57E–02	2.43E–02
6400	6.56E+05	6.80E+05	1.07E+00	6.23E–01	1.71E+00	2.03E–04	3.10E–04	1.92E+02	2.22E–02	3.82E–03	6.88E–05	8.70E–02	5.57E–02	2.43E–02
6500	6.37E+05	6.99E+05	1.11E+00	6.29E–01	1.68E+00	2.01E–04	3.07E–04	1.92E+02	2.22E–02	3.82E–03	6.78E–05	8.70E–02	5.57E–02	2.43E–02
6600	6.18E+05	7.18E+05	1.15E+00	6.41E–01	1.66E+00	1.99E–04	3.04E–04	1.92E+02	2.22E–02	3.82E–03	6.69E–05	8.70E–02	5.57E–02	2.43E–02
6700	5.98E+05	7.37E+05	1.18E+00	6.49E–01	1.64E+00	1.97E–04	3.01E–04	1.92E+02	2.22E–02	3.82E–03	6.60E–05	8.70E–02	5.57E–02	2.43E–02
6800	5.79E+05	7.56E+05	1.21E+00	6.67E–01	1.61E+00	1.95E–04	2.98E–04	1.92E+02	2.22E–02	3.82E–03	6.50E–05	8.70E–02	5.57E–02	2.43E–02
6900	5.60E+05	7.76E+05	1.22E+00	6.90E–01	1.59E+00	1.93E–04	2.95E–04	1.92E+02	2.22E–02	3.82E–03	6.40E–05	8.70E–02	5.57E–02	2.43E–02
7000	5.41E+05	7.95E+05	1.25E+00	7.07E–01	1.56E+00	1.91E–04	2.92E–04	1.92E+02	2.22E–02	3.82E–03	6.30E–05	8.70E–02	5.57E–02	2.43E–02

Year (AD)	area_obj_aqu (m^2)	area_obj_ter (m^2)	z_regoPG_aqu (m)	z_regoPG_ter (m)	z_water (m)	res_rate (m^3 m^{-2} year^{-1})	sed_rate (m^3 m^{-2} year^{-1})	Ter_growth ((m^2 year^{-1})	biom_pp_macro (kgC m^{-2})	biom_pp_micro (kgC m^{-2})	biom_pp_plank (kgC m^{-2})	NPP_macro (kgC m^{-2} year^{-1})	NPP_micro (kgC m^{-2} year^{-1})	NPP_plank (kgC m^{-2} year^{-1})
7100	5.22E+05	8.14E+05	1.27E+00	7.23E–01	1.54E+00	1.89E–04	2.88E–04	1.92E+02	2.22E–02	3.82E–03	6.20E–05	8.70E–02	5.57E–02	2.43E–02
7200	5.02E+05	8.33E+05	1.29E+00	7.41E–01	1.51E+00	1.86E–04	2.85E–04	1.92E+02	2.22E–02	3.82E–03	6.10E–05	8.70E–02	5.57E–02	2.43E–02
7300	4.83E+05	8.52E+05	1.31E+00	7.58E–01	1.49E+00	1.84E–04	2.81E–04	1.92E+02	2.22E–02	3.82E–03	5.99E–05	8.70E–02	5.57E–02	2.43E–02
7400	4.64E+05	8.72E+05	1.33E+00	7.76E–01	1.46E+00	1.81E–04	2.78E–04	1.92E+02	2.22E–02	3.82E–03	5.88E–05	8.70E–02	5.57E–02	2.43E–02
7500	4.45E+05	8.91E+05	1.35E+00	7.93E–01	1.43E+00	1.79E–04	2.73E–04	1.92E+02	2.22E–02	3.82E–03	5.76E–05	8.70E–02	5.57E–02	2.43E–02
7600	4.26E+05	9.10E+05	1.36E+00	8.11E–01	1.40E+00	1.76E–04	2.69E–04	1.92E+02	2.22E–02	3.82E–03	5.64E–05	8.70E–02	5.57E–02	2.43E–02
7700	4.06E+05	9.29E+05	1.39E+00	8.21E–01	1.38E+00	1.73E–04	2.65E–04	1.92E+02	2.22E–02	3.82E–03	5.54E–05	8.70E–02	5.57E–02	2.43E–02
7800	3.87E+05	9.48E+05	1.42E+00	8.32E–01	1.35E+00	1.71E–04	2.61E–04	1.92E+02	2.22E–02	3.82E–03	5.43E–05	8.70E–02	5.57E–02	2.43E–02
7900	3.68E+05	9.68E+05	1.45E+00	8.43E–01	1.33E+00	1.68E–04	2.57E–04	1.92E+02	2.22E–02	3.82E–03	5.34E–05	8.70E–02	5.57E–02	2.43E–02
8000	3.49E+05	9.87E+05	1.47E+00	8.56E–01	1.30E+00	1.66E–04	2.53E–04	1.92E+02	2.22E–02	3.82E–03	5.25E–05	8.70E–02	5.57E–02	2.43E–02
8100	3.30E+05	1.01E+06	1.48E+00	8.72E–01	1.28E+00	1.63E–04	2.50E–04	1.92E+02	2.22E–02	3.82E–03	5.16E–05	8.70E–02	5.57E–02	2.43E–02
8200	3.10E+05	1.03E+06	1.49E+00	8.89E–01	1.26E+00	1.61E–04	2.47E–04	1.92E+02	2.22E–02	3.82E–03	5.07E–05	8.70E–02	5.57E–02	2.43E–02
8300	2.91E+05	1.04E+06	1.48E+00	9.09E–01	1.24E+00	1.59E–04	2.44E–04	1.92E+02	2.22E–02	3.82E–03	4.98E–05	8.70E–02	5.57E–02	2.43E–02
8400	2.72E+05	1.06E+06	1.50E+00	9.22E–01	1.22E+00	1.57E–04	2.41E–04	1.92E+02	2.22E–02	3.82E–03	4.90E–05	8.70E–02	5.57E–02	2.43E–02
8500	2.53E+05	1.08E+06	1.49E+00	9.39E–01	1.20E+00	1.55E–04	2.38E–04	1.92E+02	2.22E–02	3.82E–03	4.81E–05	8.70E–02	5.57E–02	2.43E–02
8600	2.34E+05	1.10E+06	1.50E+00	9.53E–01	1.18E+00	1.53E–04	2.34E–04	1.92E+02	2.22E–02	3.82E–03	4.74E–05	8.70E–02	5.57E–02	2.43E–02
8700	2.14E+05	1.12E+06	1.50E+00	9.65E–01	1.16E+00	1.52E–04	2.32E–04	1.92E+02	2.22E–02	3.82E–03	4.67E–05	8.70E–02	5.57E–02	2.43E–02
8800	1.95E+05	1.14E+06	1.51E+00	9.78E–01	1.14E+00	1.50E–04	2.30E–04	1.92E+02	2.22E–02	3.82E–03	4.59E–05	8.70E–02	5.57E–02	2.43E–02
8900	1.76E+05	1.16E+06	1.52E+00	9.89E–01	1.12E+00	1.49E–04	2.28E–04	1.92E+02	2.22E–02	3.82E–03	4.51E–05	8.70E–02	5.57E–02	2.43E–02
9000	1.57E+05	1.18E+06	1.53E+00	9.99E–01	1.10E+00	1.47E–04	2.25E–04	1.92E+02	2.22E–02	3.82E–03	4.45E–05	8.70E–02	5.57E–02	2.43E–02
9100	1.38E+05	1.20E+06	1.55E+00	1.01E+00	1.09E+00	1.47E–04	2.24E–04	1.92E+02	2.22E–02	3.82E–03	4.39E–05	8.70E–02	5.57E–02	2.43E–02
9200	1.18E+05	1.22E+06	1.57E+00	1.02E+00	1.07E+00	1.46E–04	2.24E–04	1.92E+02	2.22E–02	3.82E–03	4.33E–05	8.70E–02	5.57E–02	2.43E–02
9300	9.92E+04	1.24E+06	1.59E+00	1.03E+00	1.06E+00	1.46E–04	2.24E–04	1.92E+02	2.22E–02	3.82E–03	4.27E–05	8.70E–02	5.57E–02	2.43E–02
9400	8.00E+04	1.26E+06	1.58E+00	1.04E+00	1.05E+00	1.47E–04	2.25E–04	1.92E+02	2.22E–02	3.82E–03	4.21E–05	8.70E–02	5.57E–02	2.43E–02
9500	6.08E+04	1.27E+06	1.60E+00	1.05E+00	1.03E+00	1.49E–04	2.28E–04	1.92E+02	2.22E–02	3.82E–03	4.17E–05	8.70E–02	5.57E–02	2.43E–02
9600	4.16E+04	1.29E+06	1.66E+00	1.05E+00	1.03E+00	1.54E–04	2.36E–04	1.92E+02	2.22E–02	3.82E–03	4.13E–05	8.70E–02	5.57E–02	2.43E–02
9700	2.24E+04	1.31E+06	1.64E+00	1.06E+00	1.02E+00	1.68E–04	2.57E–04	1.69E+02	2.22E–02	3.82E–03	4.10E–05	8.70E–02	5.57E–02	2.43E–02
9800	5.53E+03	1.33E+06	9.23E–01	1.07E+00	3.63E–01	2.57E–04	2.57E–04	0	2.22E–02	3.82E–03	1.46E–05	8.70E–02	5.57E–02	2.43E–02

Table C-2. Time-dependent parameters for object 121_1.

Year (AD)	area_obj_aqu (m^2)	area_obj_ter (m^2)	z_regoPG_aqu (m)	z_regoPG_ter (m)	z_water (m)	res_rate (m^3 m^{-2} $year^{-1}$)	sed_rate (m^3 m^{-2} $year^{-1}$)	Ter_growth ((m^2 $year^{-1}$)	biom_pp_macro (kgC m^{-2})	biom_pp_micro (kgC m^{-2})	biom_pp_plank (kgC m^{-2})	NPP_macro (kgC m^{-2} $year^{-1}$)	NPP_micro (kgC m^{-2} $year^{-1}$)	NPP_plank (kgC m^{-2} $year^{-1}$)
–8500	4.95E+06	0		0	1.33E+02	0	1.23E–04	0	0	0	3.80E–04	0	0	3.61E–02
–8000	4.95E+06	0		0	1.06E+02	0	1.23E–04	0	0	0	3.80E–04	0	0	3.61E–02
–7500	4.95E+06	0		0	8.44E+01	3.40E–04	1.23E–04	0	0	0	3.80E–04	0	0	3.61E–02
–7000	4.95E+06	0		0	7.56E+01	1.53E–04	1.23E–04	0	0	0	3.80E–04	0	0	3.61E–02
–6500	4.95E+06	0		0	7.34E+01	1.23E–04	1.23E–04	0	0	0	3.80E–04	0	0	3.61E–02
–6000	4.95E+06	0		0	7.04E+01	1.23E–04	1.23E–04	0	0	0	3.80E–04	0	0	3.61E–02
–5500	4.95E+06	0		0	6.64E+01	1.23E–04	1.23E–04	0	0	0	3.80E–04	0	0	3.61E–02
–5000	4.95E+06	0		0	6.15E+01	1.23E–04	1.23E–04	0	0	0	3.80E–04	0	0	3.61E–02
–4500	4.95E+06	0		0	5.63E+01	1.23E–04	1.23E–04	0	0	0	3.80E–04	0	0	3.61E–02
–4000	4.95E+06	0		0	5.09E+01	1.23E–04	1.23E–04	0	0	0	3.80E–04	0	0	3.61E–02
–3500	4.95E+06	0		0	4.56E+01	1.23E–04	1.23E–04	0	0	0	3.80E–04	0	0	3.61E–02
–3000	4.95E+06	0		0	4.05E+01	1.23E–04	1.23E–04	0	0	0	3.80E–04	0	0	3.61E–02
–2500	4.95E+06	0		0	3.57E+01	1.26E–04	1.26E–04	0	0	0	3.80E–04	0	0	3.61E–02
–2000	4.95E+06	0		0	3.13E+01	1.82E–04	1.82E–04	0	0	0	3.80E–04	0	0	3.61E–02
–1500	4.95E+06	0		0	2.74E+01	3.28E–04	3.28E–04	0	0	0	3.80E–04	0	0	3.61E–02
–1000	4.95E+06	0		0	2.38E+01	4.60E–04	4.60E–04	0	0	0	3.80E–04	0	0	3.61E–02
–500	4.95E+06	0		0	1.98E+01	5.07E–04	5.07E–04	0	0	0	3.77E–04	0	0	3.77E–02
0	4.95E+06	0		0	1.62E+01	7.37E–04	7.37E–04	0	2.37E–03	5.52E–04	3.09E–04	1.39E–02	1.55E–02	3.09E–02
500	4.95E+06	0		0	1.31E+01	7.86E–04	7.86E–04	0	4.08E–03	1.18E–03	2.49E–04	2.33E–02	2.21E–02	2.49E–02
1000	4.90E+06	0		0	9.84E+00	4.37E–04	4.51E–04	0	7.13E–03	1.83E–03	1.87E–04	3.96E–02	2.89E–02	1.87E–02
1500	4.42E+06	0		0	7.37E+00	7.83E–05	3.46E–04	0	1.09E–02	2.33E–03	1.40E–04	5.92E–02	3.41E–02	1.40E–02
2000	3.47E+06	0		0	5.77E+00	6.48E–05	3.42E–04	0	1.44E–02	2.65E–03	1.10E–04	7.68E–02	3.75E–02	1.10E–02
2500	2.43E+06	0		0	4.49E+00	1.95E–04	2.32E–04	0	1.79E–02	2.90E–03	8.52E–05	9.47E–02	4.02E–02	8.52E–03
3000	1.73E+06	0		0	2.78E+00	2.93E–04	1.66E–04	0	2.40E–02	3.24E–03	5.28E–05	1.25E–01	4.38E–02	5.28E–03
3500	8.10E+05	0	5.95E–01	0	1.25E+00	7.62E–04	1.35E–04	1.95E+02	2.22E–02	3.82E–03	5.74E–05	8.70E–02	5.57E–02	2.37E–03
3900	1.55E+05	7.80E+04	6.63E–01	6.62E–01	1.42E+00	8.42E–05	1.29E–04	1.16E+02	2.22E–02	3.82E–03	5.82E–05	8.70E–02	5.57E–02	2.43E–02

Year (AD)	area_obj_aqu (m^2)	area_obj_ter (m^2)	z_regoPG_aqu (m)	z_regoPG_ter (m)	z_water (m)	res_rate (m^3 m^{-2} $year^{-1}$)	sed_rate (m^3 m^{-2} $year^{-1}$)	Ter_growth ((m^2 $year^{-1}$)	biom_pp_macro (kgC m^{-2})	biom_pp_micro (kgC m^{-2})	biom_pp_plank (kgC m^{-2})	NPP_macro (kgC m^{-2} $year^{-1}$)	NPP_micro (kgC m^{-2} $year^{-1}$)	NPP_plank (kgC m^{-2} $year^{-1}$)
4000	1.48E+05	8.96E+04	6.90E–01	6.64E–01	1.44E+00	1.81E–04	2.77E–04	6.40E+01	2.22E–02	3.82E–03	5.89E–05	8.70E–02	5.57E–02	2.43E–02
4100	1.41E+05	9.60E+04	7.19E–01	6.66E–01	1.46E+00	1.83E–04	2.81E–04	6.40E+01	2.22E–02	3.82E–03	5.91E–05	8.70E–02	5.57E–02	2.43E–02
4200	1.35E+05	1.02E+05	7.49E–01	6.68E–01	1.47E+00	1.86E–04	2.84E–04	6.40E+01	2.22E–02	3.82E–03	5.92E–05	8.70E–02	5.57E–02	2.43E–02
4300	1.28E+05	1.09E+05	7.82E–01	6.69E–01	1.47E+00	1.87E–04	2.86E–04	6.40E+01	2.22E–02	3.82E–03	5.95E–05	8.70E–02	5.57E–02	2.43E–02
4400	1.22E+05	1.15E+05	8.16E–01	6.70E–01	1.48E+00	1.88E–04	2.87E–04	6.40E+01	2.22E–02	3.82E–03	6.00E–05	8.70E–02	5.57E–02	2.43E–02
4500	1.16E+05	1.22E+05	8.52E–01	6.71E–01	1.49E+00	1.89E–04	2.89E–04	6.40E+01	2.22E–02	3.82E–03	6.05E–05	8.70E–02	5.57E–02	2.43E–02
4600	1.09E+05	1.28E+05	8.92E–01	6.72E–01	1.50E+00	1.91E–04	2.92E–04	6.40E+01	2.22E–02	3.82E–03	6.11E–05	8.70E–02	5.57E–02	2.43E–02
4700	1.03E+05	1.34E+05	9.35E–01	6.73E–01	1.52E+00	1.93E–04	2.95E–04	6.40E+01	2.22E–02	3.82E–03	6.32E–05	8.70E–02	5.57E–02	2.43E–02
4800	9.64E+04	1.41E+05	9.52E–01	6.74E–01	1.57E+00			6.40E+01	2.22E–02	3.82E–03	6.43E–05	8.70E–02	5.57E–02	2.43E–02
4900	9.00E+04	1.47E+05	1.00E+00	6.76E–01	1.60E+00	2.03E–04	3.10E–04	6.40E+01	2.22E–02	3.82E–03	6.48E–05	8.70E–02	5.57E–02	2.43E–02
5000	8.36E+04	1.54E+05	1.05E+00	6.79E–01	1.61E+00	2.07E–04	3.16E–04	6.40E+01	2.22E–02	3.82E–03	6.47E–05	8.70E–02	5.57E–02	2.43E–02
5100	7.72E+04	1.60E+05	1.10E+00	6.87E–01	1.61E+00	2.09E–04	3.20E–04	6.40E+01	2.22E–02	3.82E–03	6.47E–05	8.70E–02	5.57E–02	2.43E–02
5200	7.08E+04	1.66E+05	1.12E+00	7.10E–01	1.61E+00	2.10E–04	3.21E–04	6.40E+01	2.22E–02	3.82E–03	6.50E–05	8.70E–02	5.57E–02	2.43E–02
5300	6.44E+04	1.73E+05	1.18E+00	7.15E–01	1.61E+00	2.11E–04	3.22E–04	6.40E+01	2.22E–02	3.82E–03	6.53E–05	8.70E–02	5.57E–02	2.43E–02
5400	5.80E+04	1.79E+05	1.25E+00	7.21E–01	1.62E+00	2.13E–04	3.25E–04	6.40E+01	2.22E–02	3.82E–03	6.52E–05	8.70E–02	5.57E–02	2.43E–02
5500	5.16E+04	1.86E+05	1.30E+00	7.33E–01	1.62E+00	2.15E–04	3.29E–04	6.40E+01	2.22E–02	3.82E–03	6.55E–05	8.70E–02	5.57E–02	2.43E–02
5600	4.52E+04	1.92E+05	1.34E+00	7.51E–01	1.63E+00	2.17E–04	3.31E–04	6.40E+01	2.22E–02	3.82E–03	6.61E–05	8.70E–02	5.57E–02	2.43E–02
5700	3.88E+04	1.98E+05	1.42E+00	7.63E–01	1.64E+00	2.20E–04	3.36E–04	6.40E+01	2.22E–02	3.82E–03	6.53E–05	8.70E–02	5.57E–02	2.43E–02
5800	3.24E+04	2.05E+05	1.48E+00	7.78E–01	1.62E+00	2.25E–04	3.44E–04	6.40E+01	2.22E–02	3.82E–03	6.42E–05	8.70E–02	5.57E–02	2.43E–02
5900	2.60E+04	2.11E+05	1.51E+00	8.01E–01	1.59E+00	2.26E–04	3.46E–04	6.40E+01	2.22E–02	3.82E–03	6.32E–05	8.70E–02	5.57E–02	2.43E–02
6000	1.96E+04	2.18E+05	1.54E+00	8.23E–01	1.57E+00	2.29E–04	3.50E–04	6.40E+01	2.22E–02	3.82E–03	6.24E–05	8.70E–02	5.57E–02	2.43E–02
6100	1.32E+04	2.24E+05	1.56E+00	8.45E–01	1.55E+00	2.36E–04	3.61E–04	6.40E+01	2.22E–02	3.82E–03	6.17E–05	8.70E–02	5.57E–02	2.43E–02
6200	6.80E+03	2.30E+05	1.50E+00	8.68E–01	1.53E+00	2.58E–04	3.94E–04	5.62E+01	2.22E–02	3.82E–03	2.70E–05	8.70E–02	5.57E–02	2.43E–02
6300	1.18E+03	2.36E+05	5.16E–01	8.86E–01	6.70E–01	3.94E–04	3.94E–04	0	2.22E–02	3.82E–03	2.70E–05	8.70E–02	5.57E–02	2.43E–02

Table C-3. Time-dependent parameters for object 121_2.

Year (AD)	area_obj_aqu (m^2)	area_obj_ter (m^2)	z_regoPG_aqu (m)	z_regoPG_ter (m)	z_water (m)	res_rate (m^3 m^{-2} $year^{-1}$)	sed_rate (m^3 m^{-2} $year^{-1}$)	Ter_growth ((m^2 $year^{-1}$)	biom_pp_macro (kgC m^{-2})	biom_pp_micro (kgC m^{-2})	biom_pp_plank (kgC m^{-2})	NPP_macro (kgC m^{-2} $year^{-1}$)	NPP_micro (kgC m^{-2} $year^{-1}$)	NPP_plank (kgC m^{-2} $year^{-1}$)
–8500	4.26E+05	0.00E+00		0.00E+00	1.36E+02	0.00E+00	1.23E–04	0.00E+00	0.00E+00	0.00E+00	3.80E–04	0.00E+00	0.00E+00	3.61E–02
–8000	4.26E+05	0.00E+00		0.00E+00	1.09E+02	0.00E+00	1.23E–04	0.00E+00	0.00E+00	0.00E+00	3.80E–04	0.00E+00	0.00E+00	3.61E–02
–7500	4.26E+05	0.00E+00		0.00E+00	8.75E+01	3.69E–04	1.23E–04	0.00E+00	0.00E+00	0.00E+00	3.80E–04	0.00E+00	0.00E+00	3.61E–02
–7000	4.26E+05	0.00E+00		0.00E+00	7.86E+01	1.24E–04	1.23E–04	0.00E+00	0.00E+00	0.00E+00	3.80E–04	0.00E+00	0.00E+00	3.61E–02
–6500	4.26E+05	0.00E+00		0.00E+00	7.64E+01	1.23E–04	1.23E–04	0.00E+00	0.00E+00	0.00E+00	3.80E–04	0.00E+00	0.00E+00	3.61E–02
–6000	4.26E+05	0.00E+00		0.00E+00	7.35E+01	1.23E–04	1.23E–04	0.00E+00	0.00E+00	0.00E+00	3.80E–04	0.00E+00	0.00E+00	3.61E–02
–5500	4.26E+05	0.00E+00		0.00E+00	6.94E+01	1.23E–04	1.23E–04	0.00E+00	0.00E+00	0.00E+00	3.80E–04	0.00E+00	0.00E+00	3.61E–02
–5000	4.26E+05	0.00E+00		0.00E+00	6.46E+01	1.23E–04	1.23E–04	0.00E+00	0.00E+00	0.00E+00	3.80E–04	0.00E+00	0.00E+00	3.61E–02
–4500	4.26E+05	0.00E+00		0.00E+00	5.93E+01	1.23E–04	1.23E–04	0.00E+00	0.00E+00	0.00E+00	3.80E–04	0.00E+00	0.00E+00	3.61E–02
–4000	4.26E+05	0.00E+00		0.00E+00	5.40E+01	1.23E–04	1.23E–04	0.00E+00	0.00E+00	0.00E+00	3.80E–04	0.00E+00	0.00E+00	3.61E–02
–3500	4.26E+05	0.00E+00		0.00E+00	4.87E+01	1.23E–04	1.23E–04	0.00E+00	0.00E+00	0.00E+00	3.80E–04	0.00E+00	0.00E+00	3.61E–02
–3000	4.26E+05	0.00E+00		0.00E+00	4.35E+01	1.23E–04	1.23E–04	0.00E+00	0.00E+00	0.00E+00	3.80E–04	0.00E+00	0.00E+00	3.61E–02
–2500	4.26E+05	0.00E+00		0.00E+00	3.86E+01	1.26E–04	1.26E–04	0.00E+00	0.00E+00	0.00E+00	3.80E–04	0.00E+00	0.00E+00	3.61E–02
–2000	4.26E+05	0.00E+00		0.00E+00	3.39E+01	1.82E–04	1.82E–04	0.00E+00	0.00E+00	0.00E+00	3.80E–04	0.00E+00	0.00E+00	3.61E–02
–1500	4.26E+05	0.00E+00		0.00E+00	2.97E+01	3.28E–04	3.28E–04	0.00E+00	0.00E+00	0.00E+00	3.80E–04	0.00E+00	0.00E+00	3.61E–02
–1000	4.26E+05	0.00E+00		0.00E+00	2.63E+01	4.60E–04	4.60E–04	0.00E+00	0.00E+00	0.00E+00	3.80E–04	0.00E+00	0.00E+00	3.61E–02
–500	4.26E+05	0.00E+00		0.00E+00	2.30E+01	5.07E–04	5.07E–04	0.00E+00	0.00E+00	0.00E+00	3.80E–04	0.00E+00	0.00E+00	3.61E–02
0	4.26E+05	0.00E+00		0.00E+00	1.94E+01	7.37E–04	7.37E–04	0.00E+00	0.00E+00	0.00E+00	3.69E–04	0.00E+00	0.00E+00	3.69E–02
500	4.26E+05	0.00E+00		0.00E+00	1.60E+01	7.86E–04	7.86E–04	0.00E+00	2.49E–03	6.10E–04	3.03E–04	1.46E–02	1.61E–02	3.03E–02
1000	4.26E+05	0.00E+00		0.00E+00	1.26E+01	4.51E–04	4.51E–04	0.00E+00	4.43E–03	1.28E–03	2.39E–04	2.52E–02	2.31E–02	2.39E–02
1500	4.26E+05	0.00E+00		0.00E+00	9.29E+00	4.42E–05	3.46E–04	0.00E+00	7.83E–03	1.94E–03	1.77E–04	4.33E–02	3.01E–02	1.77E–02
2000	4.22E+05	0.00E+00		0.00E+00	6.22E+00	7.99E–06	3.42E–04	0.00E+00	1.33E–02	2.56E–03	1.18E–04	7.13E–02	3.65E–02	1.18E–02
2500	3.78E+05	0.00E+00	4.39E–01	0.00E+00	3.67E+00	6.43E–05	2.32E–04	1.95E+01	2.06E–02	3.07E–03	6.98E–05	1.08E–01	4.19E–02	6.98E–03
3000	2.38E+05	9.74E+03	5.28E–01	4.62E–01	1.88E+00	3.87E–04	1.66E–04	2.12E+02	2.22E–02	3.82E–03	7.56E–05	8.70E–02	5.57E–02	2.43E–02
3500	6.08E+04	1.16E+05	5.43E–01	5.13E–01	6.81E–01	1.30E–03	1.35E–04	3.33E+02	2.22E–02	3.82E–03	2.74E–05	8.70E–02	5.57E–02	2.43E–02
3682.7	0.00E+00	1.77E+05	0.00E+00	5.26E–01	0.00E+00	1.35E–04	1.35E–04	0.00E+00	2.22E–02	3.82E–03	2.74E–05	8.70E–02	5.57E–02	2.43E–02
4000	0.00E+00	1.77E+05	0.00E+00	5.26E–01	0.00E+00	1.35E–04	1.35E–04	0.00E+00	2.22E–02	3.82E–03	2.74E–05	8.70E–02	5.57E–02	2.43E–02

Table C-4. Time-dependent parameters for object 157_1.

Year (AD)	area_obj_aqu (m^2)	area_obj_ter (m^2)	z_regoPG_aqu (m)	z_regoPG_ter (m)	z_water (m)	res_rate (m^3 m^{-2} $year^{-1}$)	sed_rate (m^3 m^{-2} $year^{-1}$)	Ter_growth ((m^2 $year^{-1}$)	biom_pp_macro (kgC m^{-2})	biom_pp_micro (kgC m^{-2})	biom_pp_plank (kgC m^{-2})	NPP_macro (kgC m^{-2} $year^{-1}$)	NPP_micro (kgC m^{-2} $year^{-1}$)	NPP_plank (kgC m^{-2} $year^{-1}$)
–8500	6.67E+05	0		0	1.41E+02	0	1.23E–04	0	0	0	3.80E–04	0	0	3.61E–02
–8000	6.67E+05	0		0	1.13E+02	0	1.23E–04	0	0	0	3.80E–04	0	0	3.61E–02
–7500	6.67E+05	0		0	9.21E+01	1.32E–04	1.23E–04	0	0	0	3.80E–04	0	0	3.61E–02
–7000	6.67E+05	0		0	8.34E+01	3.60E–04	1.23E–04	0	0	0	3.80E–04	0	0	3.61E–02
–6500	6.67E+05	0		0	8.11E+01	1.17E–04	1.23E–04	0	0	0	3.80E–04	0	0	3.61E–02
–6000	6.67E+05	0		0	7.82E+01	1.29E–04	1.23E–04	0	0	0	3.80E–04	0	0	3.61E–02
–5500	6.67E+05	0		0	7.41E+01	1.23E–04	1.23E–04	0	0	0	3.80E–04	0	0	3.61E–02
–5000	6.67E+05	0		0	6.93E+01	1.23E–04	1.23E–04	0	0	0	3.80E–04	0	0	3.61E–02
–4500	6.67E+05	0		0	6.41E+01	1.23E–04	1.23E–04	0	0	0	3.80E–04	0	0	3.61E–02
–4000	6.67E+05	0		0	5.87E+01	1.23E–04	1.23E–04	0	0	0	3.80E–04	0	0	3.61E–02
–3500	6.67E+05	0		0	5.34E+01	1.23E–04	1.23E–04	0	0	0	3.80E–04	0	0	3.61E–02
–3000	6.67E+05	0		0	4.83E+01	1.23E–04	1.23E–04	0	0	0	3.80E–04	0	0	3.61E–02
–2500	6.67E+05	0		0	4.34E+01	1.26E–04	1.26E–04	0	0	0	3.80E–04	0	0	3.61E–02
–2000	6.67E+05	0		0	3.87E+01	1.82E–04	1.82E–04	0	0	0	3.80E–04	0	0	3.61E–02
–1500	6.67E+05	0		0	3.43E+01	3.28E–04	3.28E–04	0	0	0	3.80E–04	0	0	3.61E–02
–1000	6.67E+05	0		0	3.01E+01	4.60E–04	4.60E–04	0	0	0	3.80E–04	0	0	3.61E–02
–500	6.67E+05	0		0	2.63E+01	5.07E–04	5.07E–04	0	0	0	3.80E–04	0	0	3.61E–02
0	6.67E+05	0		0	2.29E+01	7.37E–04	7.37E–04	0	0	0	3.80E–04	0	0	3.61E–02
500	6.67E+05	0		0	2.06E+01	7.86E–04	7.86E–04	0	0	0	3.80E–04	0	0	3.61E–02
1000	6.67E+05	0		0	1.73E+01	4.51E–04	4.51E–04	0	1.98E–03	3.46E–04	3.28E–04	1.18E–02	1.33E–02	3.28E–02
1500	6.67E+05	0		0	1.41E+01	3.46E–04	3.46E–04	0	3.42E–03	9.78E–04	2.68E–04	1.97E–02	2.00E–02	2.68E–02
2000	6.66E+05	0		0	1.11E+01	1.77E–04	3.42E–04	0	5.76E–03	1.58E–03	2.10E–04	3.23E–02	2.63E–02	2.10E–02
2500	6.55E+05	0		0	8.20E+00	1.46E–05	2.32E–04	0	9.44E–03	2.16E–03	1.56E–04	5.16E–02	3.24E–02	1.56E–02
3000	6.20E+05	0		0	5.66E+00	6.05E–06	1.66E–04	0	1.46E–02	2.67E–03	1.08E–04	7.81E–02	3.77E–02	1.08E–02
3500	5.20E+05	0		0	3.61E+00	6.38E–05	1.35E–04	0	2.08E–02	3.08E–03	6.86E–05	1.09E–01	4.20E–02	6.86E–03

Year (AD)	area_obj_aqu (m^2)	area_obj_ter (m^2)	z_regoPG_aqu (m)	z_regoPG_ter (m)	z_water (m)	res_rate (m^3 m^{-2} $year^{-1}$)	sed_rate (m^3 m^{-2} $year^{-1}$)	Ter_growth ((m^2 $year^{-1}$)	biom_pp_macro (kgC m^{-2})	biom_pp_micro (kgC m^{-2})	biom_pp_plank (kgC m^{-2})	NPP_macro (kgC m^{-2} $year^{-1}$)	NPP_micro (kgC m^{-2} $year^{-1}$)	NPP_plank (kgC m^{-2} $year^{-1}$)
4000	3.23E+05	0	4.66E–01	0	2.01E+00	2.97E–04	1.29E–04	9.20E+01	2.22E–02	3.82E–03	8.10E–05	8.70E–02	5.57E–02	3.82E–03
4500	5.68E+04	4.60E+04	5.65E–01	5.61E–01	2.03E+00	8.14E–05	1.24E–04	4.80E+01	2.22E–02	3.82E–03	8.18E–05	8.70E–02	5.57E–02	2.43E–02
4600	5.20E+04	5.08E+04	6.04E–01	5.65E–01	2.05E+00	2.66E–04	4.06E–04	4.80E+01	2.22E–02	3.82E–03	8.24E–05	8.70E–02	5.57E–02	2.43E–02
4700	4.72E+04	5.56E+04	6.48E–01	5.69E–01	2.04E+00	2.69E–04	4.11E–04	4.80E+01	2.22E–02	3.82E–03	8.23E–05	8.70E–02	5.57E–02	2.43E–02
4800	4.24E+04	6.04E+04	6.92E–01	5.74E–01	2.02E+00	2.70E–04	4.13E–04	4.80E+01	2.22E–02	3.82E–03	8.14E–05	8.70E–02	5.57E–02	2.43E–02
4900	3.76E+04	6.52E+04	7.35E–01	5.83E–01	2.00E+00	2.69E–04	4.11E–04	4.80E+01	2.22E–02	3.82E–03	8.06E–05	8.70E–02	5.57E–02	2.43E–02
5000	3.28E+04	7.00E+04	7.79E–01	5.94E–01	1.97E+00	2.69E–04	4.11E–04	4.80E+01	2.22E–02	3.82E–03	7.94E–05	8.70E–02	5.57E–02	2.43E–02
5100	2.80E+04	7.48E+04	8.14E–01	6.09E–01	1.93E+00	2.67E–04	4.09E–04	4.80E+01	2.22E–02	3.82E–03	7.78E–05	8.70E–02	5.57E–02	2.43E–02
5200	2.32E+04	7.96E+04	8.32E–01	6.29E–01	1.89E+00	2.66E–04	4.06E–04	4.80E+01	2.22E–02	3.82E–03	7.63E–05	8.70E–02	5.57E–02	2.43E–02
5300	1.84E+04	8.44E+04	8.28E–01	6.52E–01	1.85E+00	2.66E–04	4.06E–04	4.80E+01	2.22E–02	3.82E–03	7.46E–05	8.70E–02	5.57E–02	2.43E–02
5400	1.36E+04	8.92E+04	7.70E–01	6.71E–01	1.83E+00			4.80E+01	2.22E–02	3.82E–03	7.37E–05	8.70E–02	5.57E–02	2.43E–02
5500	8.80E+03	9.40E+04	7.91E–01	6.79E–01	1.79E+00	2.80E–04	4.29E–04	4.80E+01	2.22E–02	3.82E–03	7.23E–05	8.70E–02	5.57E–02	2.43E–02
5600	4.00E+03	9.88E+04	6.74E–01	6.92E–01	1.66E+00	3.11E–04	4.75E–04	3.53E+01	2.22E–02	3.82E–03	6.68E–05	8.70E–02	5.57E–02	2.43E–02
5700	4.68E+02	1.02E+05	6.74E–01	6.93E–01	3.60E–01	4.75E–04	4.75E–04	0	2.22E–02	3.82E–03	1.46E–05	8.70E–02	5.57E–02	2.43E–02

Table C-5. Time-dependent parameters for object 157_2.

Year (AD)	area_obj_aqu (m^2)	area_obj_ter (m^2)	z_regoPG_aqu (m)	z_regoPG_ter (m)	z_water (m)	res_rate (m^3 m^{-2} $year^{-1}$)	sed_rate (m^3 m^{-2} $year^{-1}$)	Ter_growth ((m^2 $year^{-1}$)	biom_pp_macro (kgC m^{-2})	biom_pp_micro (kgC m^{-2})	biom_pp_plank (kgC m^{-2})	NPP_macro (kgC m^{-2} $year^{-1}$)	NPP_micro (kgC m^{-2} $year^{-1}$)	NPP_plank (kgC m^{-2} $year^{-1}$)
–8500	1.09E+06	0		0	1.35E+02	0	1.23E–04	0	0	0	3.80E–04	0	0	3.61E–02
–8000	1.09E+06	0		0	1.07E+02	0	1.23E–04	0	0	0	3.80E–04	0	0	3.61E–02
–7500	1.09E+06	0		0	8.61E+01	3.69E–04	1.23E–04	0	0	0	3.80E–04	0	0	3.61E–02
–7000	1.09E+06	0		0	7.72E+01	1.24E–04	1.23E–04	0	0	0	3.80E–04	0	0	3.61E–02
–6500	1.09E+06	0		0	7.50E+01	1.23E–04	1.23E–04	0	0	0	3.80E–04	0	0	3.61E–02
–6000	1.09E+06	0		0	7.21E+01	1.23E–04	1.23E–04	0	0	0	3.80E–04	0	0	3.61E–02
–5500	1.09E+06	0		0	6.80E+01	1.23E–04	1.23E–04	0	0	0	3.80E–04	0	0	3.61E–02
–5000	1.09E+06	0		0	6.32E+01	1.23E–04	1.23E–04	0	0	0	3.80E–04	0	0	3.61E–02
–4500	1.09E+06	0		0	5.79E+01	1.23E–04	1.23E–04	0	0	0	3.80E–04	0	0	3.61E–02
–4000	1.09E+06	0		0	5.26E+01	1.23E–04	1.23E–04	0	0	0	3.80E–04	0	0	3.61E–02
–3500	1.09E+06	0		0	4.73E+01	1.23E–04	1.23E–04	0	0	0	3.80E–04	0	0	3.61E–02
–3000	1.09E+06	0		0	4.22E+01	1.23E–04	1.23E–04	0	0	0	3.80E–04	0	0	3.61E–02
–2500	1.09E+06	0		0	3.72E+01	1.26E–04	1.26E–04	0	0	0	3.80E–04	0	0	3.61E–02
–2000	1.09E+06	0		0	3.27E+01	1.82E–04	1.82E–04	0	0	0	3.80E–04	0	0	3.61E–02
–1500	1.09E+06	0		0	2.86E+01	3.28E–04	3.28E–04	0	0	0	3.80E–04	0	0	3.61E–02
–1000	1.09E+06	0		0	2.55E+01	4.60E–04	4.60E–04	0	0	0	3.80E–04	0	0	3.61E–02
–500	1.09E+06	0		0	2.14E+01	5.07E–04	5.07E–04	0	0	0	3.80E–04	0	0	3.61E–02
0	1.09E+06	0		0	1.79E+01	7.37E–04	7.37E–04	0	1.78E–03	2.19E–04	3.40E–04	1.06E–02	1.20E–02	3.40E–02
500	1.09E+06	0		0	1.46E+01	7.86E–04	7.86E–04	0	3.13E–03	8.78E–04	2.78E–04	1.82E–02	1.89E–02	2.78E–02
1000	1.09E+06	0		0	1.13E+01	4.51E–04	4.51E–04	0	5.57E–03	1.55E–03	2.14E–04	3.13E–02	2.59E–02	2.14E–02
1500	1.08E+06	0		0	8.22E+00	3.19E–04	3.46E–04	0	9.41E–03	2.16E–03	1.56E–04	5.15E–02	3.23E–02	1.56E–02
2000	9.78E+05	0		0	5.89E+00	2.63E–04	3.42E–04	0	1.41E–02	2.62E–03	1.12E–04	7.53E–02	3.72E–02	1.12E–02
2500	7.52E+05	0	1.34E–01	0	4.06E+00	7.33E–05	2.32E–04	5.42E–01	1.92E–02	2.99E–03	7.72E–05	1.01E–01	4.11E–02	7.72E–03
3000	4.82E+05	2.71E+02	2.31E–01	1.16E–01	2.68E+00	9.51E–05	1.66E–04	5.41E+01	2.44E–02	3.26E–03	5.09E–05	1.27E–01	4.40E–02	1.32E–03
3500	1.92E+05	2.73E+04	3.10E–01	2.65E–01	1.89E+00	3.84E–04	1.35E–04	2.09E+02	2.22E–02	3.82E–03	7.61E–05	8.70E–02	5.57E–02	2.43E–02
4000	3.76E+04	1.32E+05	4.03E–01	2.88E–01	8.26E–01	8.17E–04	1.29E–04	5.45E+01	2.22E–02	3.82E–03	3.33E–05	8.70E–02	5.57E–02	2.43E–02
4275.7	0	1.47E+05	4.03E–01	3.13E–01	0	1.29E–04	1.29E–04	0	2.22E–02	3.82E–03	3.33E–05	8.70E–02	5.57E–02	2.43E–02
4500	0	1.47E+05	4.03E–01	3.13E–01	0	1.29E–04	1.29E–04	0	2.22E–02	3.82E–03	3.33E–05	8.70E–02	5.57E–02	2.43E–02

Table C-6. Time-dependent parameters for object 159.

Year (AD)	area_obj_aqu (m^2)	area_obj_ter (m^2)	z_regoPG_aqu (m)	z_regoPG_ter (m)	z_water (m)	res_rate (m^3 m^{-2} $year^{-1}$)	sed_rate (m^3 m^{-2} $year^{-1}$)	Ter_growth ((m^2 $year^{-1}$)	biom_pp_macro (kgC m^{-2})	biom_pp_micro (kgC m^{-2})	biom_pp_plank (kgC m^{-2})	NPP_macro (kgC m^{-2} $year^{-1}$)	NPP_micro (kgC m^{-2} $year^{-1}$)	NPP_plank (kgC m^{-2} $year^{-1}$)
–8500	5.06E+05	0		0	1.38E+02	0	1.23E–04	0	0	0	3.80E–04	0	0	3.61E–02
–8000	5.06E+05	0		0	1.11E+02	0	1.23E–04	0	0	0	3.80E–04	0	0	3.61E–02
–7500	5.06E+05	0		0	8.95E+01	2.46E–04	1.23E–04	0	0	0	3.80E–04	0	0	3.61E–02
–7000	5.06E+05	0		0	8.07E+01	2.47E–04	1.23E–04	0	0	0	3.80E–04	0	0	3.61E–02
–6500	5.06E+05	0		0	7.85E+01	1.23E–04	1.23E–04	0	0	0	3.80E–04	0	0	3.61E–02
–6000	5.06E+05	0		0	7.56E+01	1.23E–04	1.23E–04	0	0	0	3.80E–04	0	0	3.61E–02
–5500	5.06E+05	0		0	7.15E+01	1.23E–04	1.23E–04	0	0	0	3.80E–04	0	0	3.61E–02
–5000	5.06E+05	0		0	6.67E+01	1.23E–04	1.23E–04	0	0	0	3.80E–04	0	0	3.61E–02
–4500	5.06E+05	0		0	6.14E+01	1.23E–04	1.23E–04	0	0	0	3.80E–04	0	0	3.61E–02
–4000	5.06E+05	0		0	5.61E+01	1.23E–04	1.23E–04	0	0	0	3.80E–04	0	0	3.61E–02
–3500	5.06E+05	0		0	5.08E+01	1.23E–04	1.23E–04	0	0	0	3.80E–04	0	0	3.61E–02
–3000	5.06E+05	0		0	4.56E+01	1.23E–04	1.23E–04	0	0	0	3.80E–04	0	0	3.61E–02
–2500	5.06E+05	0		0	4.07E+01	1.26E–04	1.26E–04	0	0	0	3.80E–04	0	0	3.61E–02
–2000	5.06E+05	0		0	3.60E+01	1.82E–04	1.82E–04	0	0	0	3.80E–04	0	0	3.61E–02
–1500	5.06E+05	0		0	3.17E+01	3.28E–04	3.28E–04	0	0	0	3.80E–04	0	0	3.61E–02
–1000	5.06E+05	0		0	2.78E+01	4.60E–04	4.60E–04	0	0	0	3.80E–04	0	0	3.61E–02
–500	5.06E+05	0		0	2.43E+01	5.07E–04	5.07E–04	0	0	0	3.80E–04	0	0	3.61E–02
0	5.06E+05	0		0	2.10E+01	7.37E–04	7.37E–04	0	0	0	3.80E–04	0	0	3.61E–02
500	5.06E+05	0		0	1.82E+01	7.86E–04	7.86E–04	0	1.70E–03	1.69E–04	3.45E–04	1.02E–02	1.15E–02	3.45E–02
1000	5.06E+05	0		0	1.48E+01	4.51E–04	4.51E–04	0	3.03E–03	8.39E–04	2.81E–04	1.76E–02	1.85E–02	2.81E–02
1500	5.06E+05	0		0	1.16E+01	3.46E–04	3.46E–04	0	5.22E–03	1.47E–03	2.21E–04	2.95E–02	2.51E–02	2.21E–02
2000	4.94E+05	0		0	8.89E+00	2.59E–04	3.42E–04	0	8.39E–03	2.02E–03	1.69E–04	4.62E–02	3.09E–02	1.69E–02
2500	4.63E+05	0		0	6.42E+00	2.36E–05	2.32E–04	0	1.28E–02	2.52E–03	1.22E–04	6.91E–02	3.61E–02	1.22E–02
3000	3.75E+05	0		0	4.63E+00	2.47E–05	1.66E–04	0						
3500	2.57E+05	0	3.34E–01	0	3.01E+00	1.60E–04	1.35E–04	7.60E+01	2.22E–02	3.82E–03	1.21E–04	8.70E–02	5.57E–02	2.43E–02
4000	1.18E+05		4.30E–01		1.89E+00	4.56E–04	1.29E–04		2.22E–02	3.82E–03	7.62E–05	8.70E–02	5.57E–02	2.43E–02
4100	5.76E+04	4.56E+04	4.98E–01	3.99E–01	2.30E+00	8.42E–05	1.29E–04	4.80E+01	2.22E–02	3.82E–03	9.25E–05	8.70E–02	5.57E–02	2.43E–02
4200	5.28E+04	5.04E+04	5.46E–01	4.08E–01	2.30E+00	3.00E–04	4.58E–04	4.80E+01	2.22E–02	3.82E–03	9.27E–05	8.70E–02	5.57E–02	2.43E–02
4300	4.80E+04	5.52E+04	5.92E–01	4.22E–01	2.30E+00	3.02E–04	4.61E–04	4.80E+01	2.22E–02	3.82E–03	9.26E–05	8.70E–02	5.57E–02	2.43E–02
4400	4.32E+04	6.00E+04	6.41E–01	4.36E–01	2.29E+00	3.03E–04	4.63E–04	4.80E+01	2.22E–02	3.82E–03	9.24E–05	8.70E–02	5.57E–02	2.43E–02
4500	3.84E+04	6.48E+04	6.93E–01	4.50E–01	2.30E+00	3.05E–04	4.66E–04	4.80E+01	2.22E–02	3.82E–03	9.25E–05	8.70E–02	5.57E–02	2.43E–02

Year (AD)	area_obj_aqu (m^2)	area_obj_ter (m^2)	z_regoPG_aqu (m)	z_regoPG_ter (m)	z_water (m)	res_rate ($m^3\ m^{-2}\ year^{-1}$)	sed_rate ($m^3\ m^{-2}\ year^{-1}$)	Ter_growth (($m^2\ year^{-1}$)	biom_pp_macro (kgC m^{-2})	biom_pp_micro (kgC m^{-2})	biom_pp_plank (kgC m^{-2})	NPP_macro (kgC $m^{-2}\ year^{-1}$)	NPP_micro (kgC $m^{-2}\ year^{-1}$)	NPP_plank (kgC $m^{-2}\ year^{-1}$)
4600	3.36E+04	6.96E+04	7.49E–01	4.63E–01	2.30E+00	3.07E–04	4.70E–04	4.80E+01	2.22E–02	3.82E–03	9.27E–05	8.70E–02	5.57E–02	2.43E–02
4700	2.88E+04	7.44E+04	8.07E–01	4.79E–01	2.32E+00	3.11E–04	4.76E–04	2.40E+01	2.22E–02	3.82E–03	9.35E–05	8.70E–02	5.57E–02	2.43E–02
4800	2.64E+04	7.68E+04	8.67E–01	4.86E–01	2.32E+00	3.04E–04	4.66E–04	4.40E+01	2.22E–02	3.82E–03	9.33E–05	8.70E–02	5.57E–02	2.43E–02
4900	2.20E+04	8.12E+04	9.11E–01	5.09E–01	2.33E+00	3.18E–04	4.86E–04	8.00E+00	2.22E–02	3.82E–03	9.38E–05	8.70E–02	5.57E–02	2.43E–02
5000	2.12E+04	8.20E+04	9.56E–01	5.13E–01	2.30E+00	2.99E–04	4.56E–04	2.40E+01	2.22E–02	3.82E–03	9.25E–05	8.70E–02	5.57E–02	2.43E–02
5100	1.88E+04	8.44E+04	9.99E–01	5.27E–01	2.29E+00	3.06E–04	4.68E–04	2.00E+01	2.22E–02	3.82E–03	9.21E–05	8.70E–02	5.57E–02	2.43E–02
5200	1.68E+04	8.64E+04	1.04E+00	5.40E–01	2.28E+00	3.04E–04	4.65E–04	1.60E+01	2.22E–02	3.82E–03	9.16E–05	8.70E–02	5.57E–02	2.43E–02
5300	1.52E+04	8.80E+04	1.08E+00	5.50E–01	2.26E+00	3.01E–04	4.60E–04	2.40E+01	2.22E–02	3.82E–03	9.09E–05	8.70E–02	5.57E–02	2.43E–02
5400	1.28E+04	9.04E+04	1.12E+00	5.65E–01	2.26E+00	3.09E–04	4.72E–04	2.40E+01	2.22E–02	3.82E–03	9.09E–05	8.70E–02	5.57E–02	2.43E–02
5500	1.04E+04	9.28E+04	1.16E+00	5.82E–01	2.27E+00	3.13E–04	4.79E–04	1.20E+01	2.22E–02	3.82E–03	9.14E–05	8.70E–02	5.57E–02	2.43E–02
5600	9.20E+03	9.40E+04	1.21E+00	5.89E–01	2.26E+00	3.04E–04	4.64E–04	1.20E+01	2.22E–02	3.82E–03	9.10E–05	8.70E–02	5.57E–02	2.43E–02
5700	8.00E+03	9.52E+04	1.25E+00	5.98E–01	2.25E+00	3.05E–04	4.66E–04	4.00E+00	2.22E–02	3.82E–03	9.07E–05	8.70E–02	5.57E–02	2.43E–02
5800	7.60E+03	9.56E+04	1.29E+00	6.01E–01	2.22E+00	2.91E–04	4.45E–04	4.00E+00	2.22E–02	3.82E–03	8.94E–05	8.70E–02	5.57E–02	2.43E–02
5900	7.20E+03	9.60E+04	1.33E+00	6.04E–01	2.19E+00	2.88E–04	4.41E–04	1.60E+01	2.22E–02	3.82E–03	8.82E–05	8.70E–02	5.57E–02	2.43E–02
6000	5.60E+03	9.76E+04	1.38E+00	6.17E–01	2.20E+00	3.11E–04	4.75E–04	1.20E+01	2.22E–02	3.82E–03	8.85E–05	8.70E–02	5.57E–02	2.43E–02
6100	4.40E+03	9.88E+04	1.42E+00	6.26E–01	2.20E+00	3.10E–04	4.74E–04	0	2.22E–02	3.82E–03	8.87E–05	8.70E–02	5.57E–02	2.43E–02
6200	4.40E+03	9.88E+04	1.46E+00	6.26E–01	2.16E+00	2.78E–04	4.25E–04	8.00E+00	2.22E–02	3.82E–03	8.69E–05	8.70E–02	5.57E–02	2.43E–02
6300	3.60E+03	9.96E+04	1.50E+00	6.34E–01	2.15E+00	2.99E–04	4.58E–04	1.20E+01	2.22E–02	3.82E–03	8.65E–05	8.70E–02	5.57E–02	2.43E–02
6400	2.40E+03	1.01E+05	1.53E+00	6.45E–01	2.17E+00	3.25E–04	4.97E–04	4.00E+00	2.22E–02	3.82E–03	8.76E–05	8.70E–02	5.57E–02	2.43E–02
6500	2.00E+03	1.01E+05	1.56E+00	6.49E–01	2.16E+00	3.00E–04	4.59E–04	4.00E+00	2.22E–02	3.82E–03	8.72E–05	8.70E–02	5.57E–02	2.43E–02
6600	1.60E+03	1.02E+05	1.61E+00	6.52E–01	2.16E+00	3.02E–04	4.61E–04	4.00E+00	2.22E–02	3.82E–03	8.71E–05	8.70E–02	5.57E–02	2.43E–02
6700	1.20E+03	1.02E+05	1.63E+00	6.56E–01	2.17E+00	3.13E–04	4.79E–04	4.00E+00	2.22E–02	3.82E–03	8.73E–05	8.70E–02	5.57E–02	2.43E–02
6800	8.00E+02	1.02E+05	1.68E+00	6.60E–01	2.20E+00	3.27E–04	5.00E–04	0	2.22E–02	3.82E–03	8.85E–05	8.70E–02	5.57E–02	2.43E–02
6900	8.00E+02	1.02E+05	1.72E+00	6.60E–01	2.16E+00	2.78E–04	4.25E–04	4.00E+00	2.22E–02	3.82E–03	8.68E–05	8.70E–02	5.57E–02	2.43E–02
7000	4.00E+02	1.03E+05	1.76E+00	6.65E–01	2.24E+00	3.71E–04	5.67E–04	0	2.22E–02	3.82E–03	9.03E–05	8.70E–02	5.57E–02	2.43E–02
7100	4.00E+02	1.03E+05	1.80E+00	6.65E–01	2.20E+00	2.78E–04	4.25E–04	0	2.22E–02	3.82E–03	8.86E–05	8.70E–02	5.57E–02	2.43E–02
7200	4.00E+02	1.03E+05	1.85E+00	6.65E–01	2.16E+00	2.78E–04	4.25E–04	0	2.22E–02	3.82E–03	8.69E–05	8.70E–02	5.57E–02	2.43E–02
7300	4.00E+02	1.03E+05	1.89E+00	6.65E–01	2.12E+00	2.78E–04	4.25E–04	0	2.22E–02	3.82E–03	8.52E–05	8.70E–02	5.57E–02	2.43E–02
7400	4.00E+02	1.03E+05	1.93E+00	6.65E–01	2.08E+00	2.62E–04	4.00E–04	0	2.22E–02	3.82E–03	8.36E–05	8.70E–02	5.57E–02	2.43E–02
7500	4.00E+02	1.03E+05	1.97E+00	6.65E–01	2.04E+00	2.62E–04	4.00E–04	1.91E+00	2.22E–02	3.82E–03	8.20E–05	8.70E–02	5.57E–02	2.43E–02
7600	2.09E+02	1.03E+05	1.97E+00	6.70E–01	1.10E–01	4.00E–04	4.00E–04	0	2.22E–02	3.82E–03	4.43E–06	8.70E–02	5.57E–02	2.43E–02

Table C-7. Time-dependent parameters for object 160.

Year (AD)	area_obj_aqu (m^2)	area_obj_ter (m^2)	z_regoPG_aqu (m)	z_regoPG_ter (m)	z_water (m)	res_rate (m^3 m^{-2} $year^{-1}$)	sed_rate (m^3 m^{-2} $year^{-1}$)	Ter_growth ((m^2 $year^{-1}$)	biom_pp_macro (kgC m^{-2})	biom_pp_micro (kgC m^{-2})	biom_pp_plank (kgC m^{-2})	NPP_macro (kgC m^{-2} $year^{-1}$)	NPP_micro (kgC m^{-2} $year^{-1}$)	NPP_plank (kgC m^{-2} $year^{-1}$)
–8500	3.48E+05	0		0	1.36E+02	0	1.23E–04	0	0	0	3.80E–04	0	0	3.61E–02
–8000	3.48E+05	0		0	1.09E+02	0	1.23E–04	0	0	0	3.80E–04	0	0	3.61E–02
–7500	3.48E+05	0		0	8.74E+01	3.68E–04	1.23E–04	0	0	0	3.80E–04	0	0	3.61E–02
–7000	3.48E+05	0		0	7.86E+01	1.25E–04	1.23E–04	0	0	0	3.80E–04	0	0	3.61E–02
–6500	3.48E+05	0		0	7.63E+01	1.23E–04	1.23E–04	0	0	0	3.80E–04	0	0	3.61E–02
–6000	3.48E+05	0		0	7.34E+01	1.23E–04	1.23E–04	0	0	0	3.80E–04	0	0	3.61E–02
–5500	3.48E+05	0		0	6.93E+01	1.23E–04	1.23E–04	0	0	0	3.80E–04	0	0	3.61E–02
–5000	3.48E+05	0		0	6.45E+01	1.23E–04	1.23E–04	0	0	0	3.80E–04	0	0	3.61E–02
–4500	3.48E+05	0		0	5.93E+01	1.23E–04	1.23E–04	0	0	0	3.80E–04	0	0	3.61E–02
–4000	3.48E+05	0		0	5.39E+01	1.23E–04	1.23E–04	0	0	0	3.80E–04	0	0	3.61E–02
–3500	3.48E+05	0		0	4.86E+01	1.23E–04	1.23E–04	0	0	0	3.80E–04	0	0	3.61E–02
–3000	3.48E+05	0		0	4.35E+01	1.23E–04	1.23E–04	0	0	0	3.80E–04	0	0	3.61E–02
–2500	3.48E+05	0		0	3.86E+01	1.26E–04	1.26E–04	0	0	0	3.80E–04	0	0	3.61E–02
–2000	3.48E+05	0		0	3.40E+01	1.82E–04	1.82E–04	0	0	0	3.80E–04	0	0	3.61E–02
–1500	3.48E+05	0		0	2.98E+01	3.28E–04	3.28E–04	0	0	0	3.80E–04	0	0	3.61E–02
–1000	3.48E+05	0		0	2.61E+01	4.60E–04	4.60E–04	0	0	0	3.80E–04	0	0	3.61E–02
–500	3.48E+05	0		0	2.27E+01	5.07E–04	5.07E–04	0	0	0	3.80E–04	0	0	3.61E–02
0	3.48E+05	0		0	1.94E+01	7.37E–04	7.37E–04	0	0	0	3.69E–04	0	0	3.69E–02
500	3.48E+05	0		0	1.63E+01	7.86E–04	7.86E–04	0	2.34E–03	5.36E–04	3.10E–04	1.38E–02	1.53E–02	3.10E–02
1000	3.48E+05	0		0	1.30E+01	4.51E–04	4.51E–04	0	4.16E–03	1.21E–03	2.46E–04	2.37E–02	2.24E–02	2.46E–02
1500	3.46E+05	0		0	9.85E+00	3.03E–04	3.46E–04	0	7.12E–03	1.83E–03	1.87E–04	3.95E–02	2.89E–02	1.87E–02
2000	3.29E+05	0		0	7.27E+00	6.01E–05	3.42E–04	0	1.11E–02	2.35E–03	1.38E–04	6.01E–02	3.43E–02	1.38E–02
2500	3.06E+05	0	2.78E–01	0	4.68E+00	2.48E–05	2.32E–04	6.80E+01	2.22E–02	3.82E–03	1.88E–04	8.70E–02	5.57E–02	8.89E–03
3000	2.24E+05		3.66E–01		2.83E+00	1.63E–04	1.66E–04		2.22E–02	3.82E–03	1.14E–04	8.70E–02	5.57E–02	2.43E–02
3300	1.04E+05	5.44E+04	4.31E–01	4.30E–01	2.89E+00	8.80E–05	1.35E–04	5.60E+01	2.04E–02	3.51E–03	1.16E–04	7.99E–02	5.12E–02	2.43E–02
3400	9.84E+04	6.00E+04	4.85E–01	4.36E–01	2.92E+00	3.66E–04	5.60E–04	5.60E+01	2.05E–02	3.53E–03	1.18E–04	8.02E–02	5.14E–02	2.43E–02

Year (AD)	area_obj_aqu (m^2)	area_obj_ter (m^2)	z_regoPG_aqu (m)	z_regoPG_ter (m)	z_water (m)	res_rate (m^3 m^{-2} $year^{-1}$)	sed_rate (m^3 m^{-2} $year^{-1}$)	Ter_growth ((m^2 $year^{-1}$)	biom_pp_macro (kgC m^{-2})	biom_pp_micro (kgC m^{-2})	biom_pp_plank (kgC m^{-2})	NPP_macro (kgC m^{-2} $year^{-1}$)	NPP_micro (kgC m^{-2} $year^{-1}$)	NPP_plank (kgC m^{-2} $year^{-1}$)
3500	9.28E+04	6.56E+04	5.36E–01	4.51E–01	2.94E+00	3.71E–04	5.68E–04	5.60E+01	2.08E–02	3.57E–03	1.18E–04	8.13E–02	5.21E–02	2.43E–02
3600	8.72E+04	7.12E+04	5.96E–01	4.57E–01	2.96E+00	3.75E–04	5.73E–04	5.60E+01	2.13E–02	3.66E–03	1.19E–04	8.34E–02	5.34E–02	2.43E–02
3700	8.16E+04	7.68E+04	6.59E–01	4.63E–01	2.98E+00	3.79E–04	5.79E–04	5.60E+01	2.19E–02	3.77E–03	1.20E–04	8.57E–02	5.48E–02	2.43E–02
3800	7.60E+04	8.24E+04	7.28E–01	4.68E–01	3.01E+00	3.82E–04	5.84E–04	5.60E+01	2.20E–02	3.78E–03	1.21E–04	8.60E–02	5.51E–02	2.43E–02
3900	7.04E+04	8.80E+04	7.98E–01	4.78E–01	3.03E+00	3.87E–04	5.92E–04	5.60E+01	2.21E–02	3.80E–03	1.22E–04	8.65E–02	5.53E–02	2.43E–02
4000	6.48E+04	9.36E+04	8.75E–01	4.88E–01	3.07E+00	3.92E–04	5.99E–04	4.00E+01	2.22E–02	3.82E–03	1.24E–04	8.70E–02	5.57E–02	2.43E–02
4100	6.08E+04	9.76E+04	9.29E–01	5.09E–01	3.08E+00	3.94E–04	6.02E–04	1.60E+01	2.22E–02	3.82E–03	1.24E–04	8.70E–02	5.57E–02	2.43E–02
4200	5.92E+04	9.92E+04	9.87E–01	5.17E–01	3.05E+00	3.88E–04	5.94E–04	2.00E+01	2.22E–02	3.82E–03	1.23E–04	8.70E–02	5.57E–02	2.43E–02
4300	5.72E+04	1.01E+05	1.04E+00	5.29E–01	3.02E+00	3.86E–04	5.90E–04	3.20E+01	2.22E–02	3.82E–03	1.22E–04	8.70E–02	5.57E–02	2.43E–02
4400	5.40E+04	1.04E+05	1.09E+00	5.50E–01	3.03E+00	3.88E–04	5.93E–04	2.00E+01	2.22E–02	3.82E–03	1.22E–04	8.70E–02	5.57E–02	2.43E–02
4500	5.20E+04	1.06E+05	1.15E+00	5.62E–01	3.01E+00	3.85E–04	5.88E–04	8.00E+00	2.22E–02	3.82E–03	1.21E–04	8.70E–02	5.57E–02	2.43E–02
4600	5.12E+04	1.07E+05	1.21E+00	5.67E–01	2.96E+00	3.78E–04	5.78E–04	4.00E+00	2.22E–02	3.82E–03	1.19E–04	8.70E–02	5.57E–02	2.43E–02
4700	5.08E+04	1.08E+05	1.26E+00	5.70E–01	2.91E+00	3.71E–04	5.68E–04	1.60E+01	2.22E–02	3.82E–03	1.17E–04	8.70E–02	5.57E–02	2.43E–02
4800	4.92E+04	1.09E+05	1.32E+00	5.80E–01	2.89E+00	3.70E–04	5.65E–04	2.00E+01	2.22E–02	3.82E–03	1.16E–04	8.70E–02	5.57E–02	2.43E–02
4900	4.72E+04	1.11E+05	1.37E+00	5.95E–01	2.87E+00	3.68E–04	5.63E–04	8.00E+00	2.22E–02	3.82E–03	1.16E–04	8.70E–02	5.57E–02	2.43E–02
5000	4.64E+04	1.12E+05	1.43E+00	6.01E–01	2.83E+00	3.62E–04	5.53E–04	4.00E+00	2.22E–02	3.82E–03	1.14E–04	8.70E–02	5.57E–02	2.43E–02
5100	4.60E+04	1.12E+05	1.48E+00	6.05E–01	2.78E+00	3.55E–04	5.43E–04	1.60E+01	2.22E–02	3.82E–03	1.12E–04	8.70E–02	5.57E–02	2.43E–02
5200	4.44E+04	1.14E+05	1.53E+00	6.18E–01	2.75E+00	3.54E–04	5.41E–04	8.00E+00	2.22E–02	3.82E–03	1.11E–04	8.70E–02	5.57E–02	2.43E–02
5300	4.36E+04	1.15E+05	1.58E+00	6.25E–01	2.72E+00	3.48E–04	5.32E–04	1.60E+01	2.22E–02	3.82E–03	1.09E–04	8.70E–02	5.57E–02	2.43E–02
5400	4.20E+04	1.16E+05	1.64E+00	6.39E–01	2.69E+00	3.46E–04	5.29E–04	1.60E+01	2.22E–02	3.82E–03	1.08E–04	8.70E–02	5.57E–02	2.43E–02
5500	4.04E+04	1.18E+05	1.69E+00	6.54E–01	2.66E+00	3.43E–04	5.25E–04	4.00E+00	2.22E–02	3.82E–03	1.07E–04	8.70E–02	5.57E–02	2.43E–02
5600	4.00E+04	1.18E+05	1.74E+00	6.57E–01	2.62E+00	3.35E–04	5.13E–04	1.60E+01	2.22E–02	3.82E–03	1.06E–04	8.70E–02	5.57E–02	2.43E–02
5700	3.84E+04	1.20E+05	1.79E+00	6.73E–01	2.59E+00	3.35E–04	5.12E–04	1.20E+01	2.22E–02	3.82E–03	1.04E–04	8.70E–02	5.57E–02	2.43E–02
5800	3.72E+04	1.21E+05	1.84E+00	6.84E–01	2.56E+00	3.30E–04	5.05E–04	1.60E+01	2.22E–02	3.82E–03	1.03E–04	8.70E–02	5.57E–02	2.43E–02
5900	3.56E+04	1.23E+05	1.89E+00	7.00E–01	2.54E+00	3.28E–04	5.02E–04	1.60E+01	2.22E–02	3.82E–03	1.02E–04	8.70E–02	5.57E–02	2.43E–02
6000	3.40E+04	1.24E+05	1.93E+00	7.16E–01	2.51E+00	3.26E–04	4.98E–04	8.00E+00	2.22E–02	3.82E–03	1.01E–04	8.70E–02	5.57E–02	2.43E–02
6100	3.32E+04	1.25E+05	1.98E+00	7.24E–01	2.48E+00	3.19E–04	4.88E–04	1.60E+01	2.22E–02	3.82E–03	9.98E–05	8.70E–02	5.57E–02	2.43E–02

Year (AD)	area_obj_aqu (m^2)	area_obj_ter (m^2)	z_regoPG_aqu (m)	z_regoPG_ter (m)	z_water (m)	res_rate (m^3 m^{-2} $year^{-1}$)	sed_rate (m^3 m^{-2} $year^{-1}$)	Ter_growth ((m^2 $year^{-1}$)	biom_pp_macro (kgC m^{-2})	biom_pp_micro (kgC m^{-2})	biom_pp_plank (kgC m^{-2})	NPP_macro (kgC m^{-2} $year^{-1}$)	NPP_micro (kgC m^{-2} $year^{-1}$)	NPP_plank (kgC m^{-2} $year^{-1}$)
6200	3.16E+04	1.27E+05	2.03E+00	7.41E–01	2.45E+00	3.19E–04	4.87E–04	1.20E+01	2.22E–02	3.82E–03	9.88E–05	8.70E–02	5.57E–02	2.43E–02
6300	3.04E+04	1.28E+05	2.07E+00	7.54E–01	2.42E+00	3.14E–04	4.80E–04	2.00E+01	2.22E–02	3.82E–03	9.76E–05	8.70E–02	5.57E–02	2.43E–02
6400	2.84E+04	1.30E+05	2.12E+00	7.75E–01	2.40E+00	3.15E–04	4.81E–04	2.80E+01	2.22E–02	3.82E–03	9.68E–05	8.70E–02	5.57E–02	2.43E–02
6500	2.56E+04	1.33E+05	2.17E+00	8.04E–01	2.40E+00	3.18E–04	4.86E–04	1.60E+01	2.22E–02	3.82E–03	9.67E–05	8.70E–02	5.57E–02	2.43E–02
6600	2.40E+04	1.34E+05	2.21E+00	8.20E–01	2.38E+00	3.11E–04	4.76E–04	1.60E+01	2.22E–02	3.82E–03	9.58E–05	8.70E–02	5.57E–02	2.43E–02
6700	2.24E+04	1.36E+05	2.26E+00	8.38E–01	2.36E+00	3.09E–04	4.73E–04	1.20E+01	2.22E–02	3.82E–03	9.50E–05	8.70E–02	5.57E–02	2.43E–02
6800	2.12E+04	1.37E+05	2.30E+00	8.50E–01	2.33E+00	3.05E–04	4.66E–04	2.00E+01	2.22E–02	3.82E–03	9.39E–05	8.70E–02	5.57E–02	2.43E–02
6900	1.92E+04	1.39E+05	2.35E+00	8.72E–01	2.32E+00	3.08E–04	4.71E–04	1.60E+01	2.22E–02	3.82E–03	9.35E–05	8.70E–02	5.57E–02	2.43E–02
7000	1.76E+04	1.41E+05	2.39E+00	8.90E–01	2.30E+00	3.05E–04	4.66E–04	1.20E+01	2.22E–02	3.82E–03	9.27E–05	8.70E–02	5.57E–02	2.43E–02
7100	1.64E+04	1.42E+05	2.44E+00	9.02E–01	2.28E+00	3.00E–04	4.59E–04	1.60E+01	2.22E–02	3.82E–03	9.17E–05	8.70E–02	5.57E–02	2.43E–02
7200	1.48E+04	1.44E+05	2.48E+00	9.20E–01	2.26E+00	3.01E–04	4.61E–04	2.80E+01	2.22E–02	3.82E–03	9.11E–05	8.70E–02	5.57E–02	2.43E–02
7300	1.20E+04	1.46E+05	2.52E+00	9.51E–01	2.27E+00	3.14E–04	4.81E–04	8.00E+00	2.22E–02	3.82E–03	9.15E–05	8.70E–02	5.57E–02	2.43E–02
7400	1.12E+04	1.47E+05	2.57E+00	9.60E–01	2.25E+00	2.97E–04	4.53E–04	1.20E+01	2.22E–02	3.82E–03	9.05E–05	8.70E–02	5.57E–02	2.43E–02
7500	1.00E+04	1.48E+05	2.61E+00	9.73E–01	2.23E+00	2.99E–04	4.58E–04	4.00E+00	2.22E–02	3.82E–03	8.99E–05	8.70E–02	5.57E–02	2.43E–02
7600	9.60E+03	1.49E+05	2.65E+00	9.77E–01	2.20E+00	2.87E–04	4.39E–04	1.20E+01	2.22E–02	3.82E–03	8.85E–05	8.70E–02	5.57E–02	2.43E–02
7700	8.40E+03	1.50E+05	2.70E+00	9.91E–01	2.18E+00	2.95E–04	4.51E–04	4.00E+00	2.22E–02	3.82E–03	8.78E–05	8.70E–02	5.57E–02	2.43E–02
7800	8.00E+03	1.50E+05	2.74E+00	9.96E–01	2.15E+00	2.82E–04	4.30E–04	1.20E+01	2.22E–02	3.82E–03	8.64E–05	8.70E–02	5.57E–02	2.43E–02
7900	6.80E+03	1.52E+05	2.78E+00	1.01E+00	2.13E+00	2.93E–04	4.47E–04	8.00E+00	2.22E–02	3.82E–03	8.56E–05	8.70E–02	5.57E–02	2.43E–02
8000	6.00E+03	1.52E+05	2.82E+00	1.02E+00	2.10E+00	2.85E–04	4.36E–04	2.00E+01	2.22E–02	3.82E–03	8.46E–05	8.70E–02	5.57E–02	2.43E–02
8100	4.00E+03	1.54E+05	2.86E+00	1.04E+00	2.10E+00	3.18E–04	4.86E–04	8.00E+00	2.22E–02	3.82E–03	8.47E–05	8.70E–02	5.57E–02	2.43E–02
8200	3.20E+03	1.55E+05	2.90E+00	1.05E+00	2.08E+00	2.94E–04	4.50E–04	1.60E+01	2.22E–02	3.82E–03	8.38E–05	8.70E–02	5.57E–02	2.43E–02
8300	1.60E+03	1.57E+05	2.93E+00	1.07E+00	2.09E+00	3.52E–04	5.38E–04	4.00E+00	2.22E–02	3.82E–03	8.43E–05	8.70E–02	5.57E–02	2.43E–02
8400	1.20E+03	1.57E+05	2.98E+00	1.08E+00	2.08E+00	2.99E–04	4.57E–04	4.00E+00	2.22E–02	3.82E–03	8.38E–05	8.70E–02	5.57E–02	2.43E–02
8500	8.00E+02	1.58E+05	3.01E+00	1.08E+00	2.07E+00	3.20E–04	4.90E–04	3.71E+00	2.22E–02	3.82E–03	8.35E–05	8.70E–02	5.57E–02	2.43E–02
8600	4.29E+02	1.58E+05	2.81E+00	1.09E+00	2.07E+00	4.90E–04	4.90E–04	0	2.22E–02	3.82E–03	8.34E–05	8.70E–02	5.57E–02	2.43E–02

Appendix D

Hydrological data

Table D-1. The inter compartment water flows for the seven biosphere objects for the global warming climate case. The suffixes _iso och _end, represent the water flows at the time of isolation start and the time of isolation end, the water flow is linearly interpolated during the time period in between.

Parameter name	obj 116 ($m^3 m^{-2} year^{-1}$)	obj 121_1 ($m^3 m^{-2} year^{-1}$)	obj 121_2 ($m^3 m^{-2} year^{-1}$)	obj 157_1 ($m^3 m^{-2} year^{-1}$)	obj 157_2 ($m^3 m^{-2} year^{-1}$)	obj 159 ($m^3 m^{-2} year^{-1}$)	obj 160 ($m^3 m^{-2} year^{-1}$)
q_downstream_end	1.69E+00	1.74E+01	3.94E-01	4.26E+00	1.25E+00	1.27E+00	3.48E-01
q_downstream_iso	1.47E+00	1.62E+01	3.76E-01	3.41E+00	1.16E+00	1.12E+00	3.53E-01
q_gl_low_lake	1.69E–02	1.21E–06	1.91E–02	6.10E–04	4.20E–02	1.03E–02	1.55E–04
q_gl_low_sea	8.97E–03	2.54E–03	1.78E–02	3.64E–03	2.13E–02	2.34E–02	2.00E–02
q_gl_low_ter_end	7.86E–03	3.34E–05	2.59E–02	8.62E–04	4.83E–02	3.71E–02	5.75E–02
q_gl_low_ter_iso	8.86E–03	1.12E–04	1.91E–02	1.77E–03	4.20E–02	5.68E–02	5.96E–02
q_gl_pg_lake	2.60E–02	9.00E–02	1.04E–01	1.75E–02	2.21E–01	2.29E–01	2.83E–01
q_gl_pg_sea	3.27E–02	3.56E–02	3.06E–02	2.01E–02	2.93E–02	3.44E–02	3.21E–02
q_gl_pg_ter_end	2.98E–02	5.36E–02	9.35E–02	3.06E–02	2.44E–01	9.95E–02	3.23E–02
q_gl_pg_ter_iso	5.95E–02	6.16E–02	1.04E–01	4.33E–02	2.21E–01	1.06E–01	5.73E–02
q_low_gl_lake	1.78E–02	6.93E–02	9.82E–02	1.02E–02	1.84E–01	2.22E–01	2.11E–01
q_low_gl_sea	9.47E–03	2.34E–02	2.26E–02	3.69E–03	2.83E–02	2.74E–02	2.09E–02
q_low_gl_ter_end	1.91E–02	5.24E–02	8.95E–02	1.68E–02	2.22E–01	8.67E–02	2.63E–02
q_low_gl_ter_iso	2.77E–02	5.76E–02	9.82E–02	2.22E–02	1.84E–01	9.04E–02	5.02E–02
q_peat_pg_ter_end	1.55E–02	1.58E–03	1.44E–01	6.12E–03	2.76E–01	7.55E–02	7.74E–02
q_peat_pg_ter_iso	3.06E–02	7.21E–03	3.00E–01	1.12E–02	3.08E–01	1.07E–01	7.92E–02
q_peat_up_ter_end	1.02E–01	1.41E–01	3.10E–01	2.34E–01	6.94E–01	5.04E–01	4.52E–01
q_peat_up_ter_iso	1.04E–01	2.87E–01	3.69E–01	1.40E–01	6.56E–01	5.01E–01	1.76E–01
q_pg_gl_lake	2.62E–02	5.37E–04	1.96E–02	2.58E–03	7.20E–02	1.15E–02	3.02E–03
q_pg_gl_sea	3.21E–02	1.57E–02	2.59E–02	1.97E–02	2.23E–02	3.03E–02	3.10E–02
q_pg_gl_ter_end	1.43E–02	1.39E–03	2.63E–02	5.23E–03	6.25E–02	5.33E–02	6.46E–02
q_pg_gl_ter_iso	2.59E–02	5.10E–03	1.96E–02	8.81E–03	7.20E–02	8.18E–02	6.81E–02
q_pg_peat_ter_end	3.34E–02	5.48E–02	2.20E–01	3.33E–02	5.34E–01	1.16E–01	3.99E–02

Parameter name	obj 116 (m^3 m^{-2} $year^{-1}$)	obj 121_1 (m^3 m^{-2} $year^{-1}$)	obj 121_2 (m^3 m^{-2} $year^{-1}$)	obj 157_1 (m^3 m^{-2} $year^{-1}$)	obj 157_2 (m^3 m^{-2} $year^{-1}$)	obj 159 (m^3 m^{-2} $year^{-1}$)	obj 160 (m^3 m^{-2} $year^{-1}$)
q_pg_peat_ter_iso	6.83E–02	6.35E–02	3.96E–01	4.80E–02	4.97E–01	1.21E–01	6.65E–02
q_pg_up_lake	2.16E+00	1.05E+00	3.96E–01	1.29E+00	4.97E–01	9.85E–01	9.32E–01
q_pg_up_sea	3.77E–02	4.01E–02	3.58E–02	2.35E–02	3.09E–02	3.85E–02	3.66E–02
q_up_peat_ter_end	7.13E–02	7.88E–02	2.29E–01	2.01E–01	3.93E–01	2.15E–01	5.13E–01
q_up_peat_ter_iso	1.16E–01	2.63E–01	3.31E–01	1.56E–01	4.11E–01	2.40E–01	2.75E–01
q_up_pg_lake	2.11E+00	8.49E–01	3.00E–01	1.19E+00	3.08E–01	6.82E–01	4.10E–01
q_up_pg_sea	3.70E–02	2.03E–02	3.11E–02	2.29E–02	2.38E–02	3.44E–02	3.55E–02
q_up_wat_lake	2.16E+00	1.05E+00	3.69E–01	1.29E+00	6.56E–01	9.85E–01	9.32E–01
q_up_wat_sea	3.77E–02	4.01E–02	3.58E–02	2.35E–02	3.09E–02	3.85E–02	3.66E–02
q_up_wat_ter_end	1.27E+00	8.78E–01	3.94E–01	3.27E+00	1.25E+00	1.27E+00	3.52E–01
q_up_wat_ter_iso	9.77E–01	7.06E–01	3.76E–01	2.90E+00	1.16E+00	1.09E+00	2.93E–01
q_wat_up_lake	2.11E+00	8.49E–01	3.31E–01	1.19E+00	4.11E–01	6.82E–01	4.10E–01
q_wat_up_sea	3.70E–02	2.03E–02	3.11E–02	2.29E–02	2.38E–02	3.44E–02	3.55E–02
q_wat_up_ter_end	1.07E–03	1.56E–03	0.00E+00	2.60E–03	0.00E+00	3.37E–03	3.72E–03
q_wat_up_ter_iso	1.74E–03	–1.98E–05	0.00E+00	1.10E–03	0.00E+00	0.00E+00	0.00E+00

Table D-2. Water flow during periglacial conditions in object 114.

Parameter name	q (m^3 m^{-2} $year^{-1}$)
q_downstream_end	9.88E+01
q_gl_low_lake	1.55E–03
q_gl_pg_lake	1.15E–02
q_low_gl_lake	9.77E–03
q_pg_gl_lake	2.55E–03
q_pg_up_lake	5.91E–02
q_up_pg_lake	4.30E–02
q_up_wat_lake	5.91E–02
q_wat_up_lake	4.30E–02

Table D-3. Water flow during periglacial conditions in object 157_1.

Parameter name	q (m^3 $m^{-2}$$year^{-1}$)
q_downstream_end_perm	4.033
q_low_gl_ter_end_perm	0.031
q_gl_low_ter_end_perm	0.000
q_gl_pg_ter_end_perm	0.031
q_pg_gl_ter_end_perm	0.000
q_up_wat_ter_end_perm	3.295
q_wat_up_ter_end_perm	0.000
q_pg_peat_ter_end_perm	0.031
q_peat_pg_ter_end_perm	0.000
q_peat_up_ter_end_perm	0.396
q_up_peat_ter_end_perm	0.021
q_low_gl_lake_perm	0.000
q_gl_low_lake_perm	0.000
q_gl_pg_lake_perm	0.000
q_pg_gl_lake_perm	0.000
q_pg_up_lake_perm	0.000
q_up_pg_lake_perm	0.000
q_up_wat_lake_perm	0.284
q_wat_up_lake_perm	0.284
WF_lobj116_perm	0.000

Table D-4. The inter compartment water flows for the seven biosphere objects for the extended global warming climate case. The suffixes _iso och _end, represent the water flows at the time of isolation start and the time of isolation end, the water flow is linearly interpolated during the time period in between.

Parameter name	obj 116 (m^3 m^{-2} $year^{-1}$)	obj 121_1 (m^3 m^{-2} $year^{-1}$)	obj 121_2 (m^3 m^{-2} $year^{-1}$)	obj 157_1 (m^3 m^{-2} $year^{-1}$)	obj 1517_2 (m^3 m^{-2} $year^{-1}$)	obj 159 (m^3 m^{-2} $year^{-1}$)	obj 160 (m^3 m^{-2} $year^{-1}$)
q_downstream_end	3.59E+00	4.72E+01	1.00E+00	8.83E+00	2.89E+00	2.79E+00	1.22E+00
q_downstream_iso	3.59E+00	4.72E+01	1.00E+00	8.83E+00	2.89E+00	2.79E+00	1.22E+00
q_gl_low_lake	1.78E–02	2.85E–03	7.41E–02	7.93E–03	6.82E–02	1.50E–02	1.95E–05
q_gl_low_sea	8.97E–03	2.54E–03	1.78E–02	3.64E–03	2.13E–02	2.34E–02	2.00E–02
q_gl_low_ter_end	1.10E–02	2.58E–03	7.41E–02	8.52E–03	6.82E–02	6.41E–02	6.96E–02
q_gl_low_ter_iso	2.58E–02	3.57E–03	7.41E–02	1.12E–02	6.82E–02	6.97E–02	7.64E–02
q_gl_pg_lake	2.69E–02	5.34E–02	1.89E–01	2.96E–02	2.70E–01	2.58E–01	3.40E–01
q_gl_pg_sea	3.27E–02	3.56E–02	3.06E–02	2.01E–02	2.93E–02	3.44E–02	3.21E–02
q_gl_pg_ter_end	4.60E–02	8.30E–02	1.89E–01	6.84E–02	2.70E–01	1.41E–01	7.74E–02
q_gl_pg_ter_iso	1.08E–01	1.15E–01	1.89E–01	8.98E–02	2.70E–01	1.54E–01	8.49E–02
q_low_gl_lake	1.54E–02	4.13E–02	1.82E–01	6.77E–03	2.27E–01	2.49E–01	2.54E–01
q_low_gl_sea	9.47E–03	2.34E–02	2.26E–02	3.69E–03	2.83E–02	2.74E–02	2.09E–02
q_low_gl_ter_end	2.36E–02	6.51E–02	1.82E–01	3.18E–02	2.27E–01	1.23E–01	6.89E–02
q_low_gl_ter_iso	5.54E–02	9.00E–02	1.82E–01	4.18E–02	2.27E–01	1.34E–01	7.56E–02
q_peat_pg_ter_end	3.06E–02	1.68E–02	1.41E–01	2.93E–02	2.40E–01	1.01E–01	9.14E–02
q_peat_pg_ter_iso	7.21E–02	2.32E–02	1.41E–01	3.85E–02	2.40E–01	1.10E–01	1.00E–01
q_peat_up_ter_end	5.46E–02	1.60E–01	3.28E–01	1.43E–01	7.39E–01	6.75E–01	2.81E–01
q_peat_up_ter_iso	1.28E–01	2.21E–01	3.28E–01	1.88E–01	7.39E–01	7.35E–01	3.09E–01
q_pg_gl_lake	3.01E–02	9.26E–03	7.54E–02	1.49E–02	8.76E–02	1.66E–02	1.11E–02
q_pg_gl_sea	3.21E–02	1.57E–02	2.59E–02	1.97E–02	2.23E–02	3.03E–02	3.10E–02
q_pg_gl_ter_end	2.69E–02	1.51E–02	7.54E–02	2.57E–02	8.76E–02	8.24E–02	7.91E–02
q_pg_gl_ter_iso	6.33E–02	2.09E–02	7.54E–02	3.38E–02	8.76E–02	8.96E–02	8.68E–02
q_pg_peat_ter_end	5.11E–02	8.53E–02	3.14E–01	7.53E–02	5.96E–01	1.59E–01	8.84E–02
q_pg_peat_ter_iso	1.20E–01	1.18E–01	3.14E–01	9.89E–02	5.96E–01	1.73E–01	9.69E–02
q_pg_up_lake	2.07E+00	1.03E+00	3.14E–01	1.20E+00	5.96E–01	8.45E–01	7.87E–01
q_pg_up_sea	3.77E–02	4.01E–02	3.58E–02	2.35E–02	3.09E–02	3.85E–02	3.66E–02
q_up_peat_ter_end	5.03E–02	1.12E–01	1.49E–01	1.29E–01	3.06E–01	2.52E–01	4.02E–01
q_up_peat_ter_iso	1.18E–01	1.54E–01	1.49E–01	1.69E–01	3.06E–01	2.75E–01	4.41E–01
q_up_pg_lake	1.98E+00	9.01E–01	1.41E–01	1.09E+00	2.40E–01	4.93E–01	1.25E–01
q_up_pg_sea	3.70E–02	2.03E–02	3.11E–02	2.29E–02	2.38E–02	3.44E–02	3.55E–02
q_up_wat_lake	2.07E+00	1.03E+00	3.28E–01	1.20E+00	7.39E–01	8.45E–01	7.87E–01
q_up_wat_sea	3.77E–02	4.01E–02	3.58E–02	2.35E–02	3.09E–02	3.85E–02	3.66E–02
q_up_wat_ter_end	2.78E+00	2.15E+00	1.00E+00	7.69E+00	2.89E+00	2.76E+00	1.12E+00
q_up_wat_ter_iso	2.78E+00	2.15E+00	1.00E+00	7.69E+00	2.89E+00	2.76E+00	1.12E+00
q_wat_up_lake	1.98E+00	9.01E–01	1.49E–01	1.09E+00	3.06E–01	4.93E–01	1.25E–01
q_wat_up_sea	3.70E–02	2.03E–02	3.11E–02	2.29E–02	2.38E–02	3.44E–02	3.55E–02
q_wat_up_ter_end	9.29E–03	1.32E–03	0.00E+00	0.00E+00	0.00E+00	0.00E+00	0.00E+00
q_wat_up_ter_iso	9.29E–03	1.32E–03	0.00E+00	0.00E+00	0.00E+00	0.00E+00	0.00E+00

Table D-5. Inter-basin water flow between the seven biosphere objects during the marine stage.

Time (year)	Parameter namn	Water flow (m^3 $year^{-1}$)	Description
Biosphere object 10			
–6500	WF_lobj121_1	1.25E+11	Water flow from lobj10 to lobj121_1
–6500	WF_lobj157_2	9.69E+09	Water flow from lobj10 to lobj157_2
–6500	WF_lobj116	1.79E+11	Water flow from lobj10 to lobj116
–6500	WF_Baltic	1.67E+12	Water flow from lobj10 to Baltic
–3000	WF_lobj121_1	7.66E+10	Water flow from lobj10 to lobj121_1
–3000	WF_lobj157_2	2.73E+09	Water flow from lobj10 to lobj157_2
–3000	WF_lobj116	1.45E+11	Water flow from lobj10 to lobj116
–3000	WF_Baltic	1.34E+12	Water flow from lobj10 to Baltic
–1000	WF_lobj121_1	4.61E+10	Water flow from lobj10 to lobj121_1
–1000	WF_lobj157_2	1.42E+09	Water flow from lobj10 to lobj157_2
–1000	WF_lobj116	8.25E+10	Water flow from lobj10 to lobj116
–1000	WF_Baltic	5.43E+11	Water flow from lobj10 to Baltic
0	WF_lobj121_1	5.81E+10	Water flow from lobj10 to lobj121_1
0	WF_lobj157_2	6.08E+08	Water flow from lobj10 to lobj157_2
0	WF_lobj116	9.77E+10	Water flow from lobj10 to lobj116
0	WF_Baltic	2.04E+11	Water flow from lobj10 to Baltic
1000	WF_lobj121_1	3.43E+10	Water flow from lobj10 to lobj121_1
1000	WF_lobj157_2	8.79E+08	Water flow from lobj10 to lobj157_2
1000	WF_lobj116	6.04E+10	Water flow from lobj10 to lobj116
1000	WF_Baltic	7.19E+10	Water flow from lobj10 to Baltic
2000	WF_lobj121_1	8.19E+09	Water flow from lobj10 to lobj121_1
2000	WF_lobj157_2	0.00E+00	Water flow from lobj10 to lobj157_2
2000	WF_lobj116	3.06E+10	Water flow from lobj10 to lobj116
2000	WF_Baltic	6.33E+10	Water flow from lobj10 to Baltic
3000	WF_lobj121_1	1.02E+09	Water flow from lobj10 to lobj121_1
3000	WF_lobj116	3.26E+09	Water flow from lobj10 to lobj116
3000	WF_Baltic	4.32E+10	Water flow from lobj10 to Baltic
3818	WF_lobj121_1	0.00E+00	Water flow from lobj10 to lobj121_1
4000	WF_lobj116	2.72E+08	Water flow from lobj10 to lobj116
4000	WF_Baltic	1.94E+10	Water flow from lobj10 to Baltic
4540	WF_lobj116	0.00E+00	Water flow from lobj10 to lobj116
5000	WF_Baltic	8.43E+09	Water flow from lobj10 to Baltic
6000	WF_Baltic	4.43E+09	Water flow from lobj10 to Baltic
7000	WF_Baltic	2.48E+09	Water flow from lobj10 to Baltic
8000	WF_Baltic	1.14E+09	Water flow from lobj10 to Baltic
9000	WF_Baltic	3.08E+08	Water flow from lobj10 to Baltic
Biosphere object 116			
–6500	WF_lobj160	1.23E+10	Water flow from lobj116 to lobj160
–6500	WF_lobj121_1	2.39E+10	Water flow from lobj116 to lobj121_1
–6500	WF_lobj159	3.11E+10	Water flow from lobj116 to lobj159
–6500	WF_lobj157_2	6.87E+09	Water flow from lobj116 to lobj157_2
–6500	WF_lobj157_1	3.68E+10	Water flow from lobj116 to lobj157_1
–6500	WF_lobj10	1.88E+11	Water flow from lobj116 to lobj10
–3000	WF_lobj160	5.52E+09	Water flow from lobj116 to lobj160
–3000	WF_lobj121_1	2.43E+10	Water flow from lobj116 to lobj121_1
–3000	WF_lobj159	1.83E+10	Water flow from lobj116 to lobj159
–3000	WF_lobj157_2	9.75E+09	Water flow from lobj116 to lobj157_2
–3000	WF_lobj157_1	3.52E+10	Water flow from lobj116 to lobj157_1
–3000	WF_lobj10	1.09E+11	Water flow from lobj116 to lobj10
–1000	WF_lobj160	3.44E+09	Water flow from lobj116 to lobj160
–1000	WF_lobj121_1	1.14E+10	Water flow from lobj116 to lobj121_1
–1000	WF_lobj159	1.18E+10	Water flow from lobj116 to lobj159
–1000	WF_lobj157_2	4.95E+09	Water flow from lobj116 to lobj157_2
–1000	WF_lobj157_1	1.97E+10	Water flow from lobj116 to lobj157_1

Time (year)	Parameter namn	Water flow (m^3 year^{-1})	Description
–1000	WF_lobj10	7.14E+10	Water flow from lobj116 to lobj10
0	WF_lobj160	4.16E+09	Water flow from lobj116 to lobj160
0	WF_lobj121_1	1.13E+10	Water flow from lobj116 to lobj121_1
0	WF_lobj159	1.48E+10	Water flow from lobj116 to lobj159
0	WF_lobj157_2	5.39E+09	Water flow from lobj116 to lobj157_2
0	WF_lobj157_1	2.22E+10	Water flow from lobj116 to lobj157_1
0	WF_lobj10	8.45E+10	Water flow from lobj116 to lobj10
1000	WF_lobj160	2.31E+09	Water flow from lobj116 to lobj160
1000	WF_lobj121_1	4.66E+09	Water flow from lobj116 to lobj121_1
1000	WF_lobj159	7.41E+09	Water flow from lobj116 to lobj159
1000	WF_lobj157_2	3.86E+09	Water flow from lobj116 to lobj157_2
1000	WF_lobj157_1	1.40E+10	Water flow from lobj116 to lobj157_1
1000	WF_lobj10	5.79E+10	Water flow from lobj116 to lobj10
2000	WF_lobj160	2.81E+09	Water flow from lobj116 to lobj160
2000	WF_lobj121_1	3.42E+09	Water flow from lobj116 to lobj121_1
2000	WF_lobj159	5.60E+09	Water flow from lobj116 to lobj159
2000	WF_lobj157_2	5.11E+08	Water flow from lobj116 to lobj157_2
2000	WF_lobj157_1	5.16E+09	Water flow from lobj116 to lobj157_1
2000	WF_lobj10	2.97E+10	Water flow from lobj116 to lobj10
3000	WF_lobj160	0.00E+00	Water flow from lobj116 to lobj160
3000	WF_lobj121_1	6.84E+08	Water flow from lobj116 to lobj121_1
3000	WF_lobj159	7.34E+08	Water flow from lobj116 to lobj159
3000	WF_lobj157_2	0.00E+00	Water flow from lobj116 to lobj157_2
3000	WF_lobj157_1	2.07E+09	Water flow from lobj116 to lobj157_1
3000	WF_lobj10	3.30E+09	Water flow from lobj116 to lobj10
3500	WF_lobj121_1	0.00E+00	Water flow from lobj116 to lobj121_1
4000	WF_lobj159	0.00E+00	Water flow from lobj116 to lobj159
4000	WF_lobj157_1	1.97E+07	Water flow from lobj116 to lobj157_1
4000	WF_lobj10	2.79E+08	Water flow from lobj116 to lobj10
4493.155894	WF_lobj157_1	0.00E+00	Water flow from lobj116 to lobj157_1
4540.466926	WF_lobj10	2.19E+06	Water flow from lobj116 to lobj10
9900	WF_lobj10	2.52E+06	Water flow from lobj116 to lobj10
Biosphere object 121_1			
–6500	WF_lobj160	1.02E+10	Water flow from lobj121_1 to lobj160
–6500	WF_lobj121_2	2.75E+10	Water flow from lobj121_1 to lobj121_2
–6500	WF_lobj116	2.77E+10	Water flow from lobj121_1 to lobj116
–6500	WF_lobj10	1.16E+11	Water flow from lobj121_1 to lobj10
–3000	WF_lobj160	4.18E+09	Water flow from lobj121_1 to lobj160
–3000	WF_lobj121_2	1.43E+10	Water flow from lobj121_1 to lobj121_2
–3000	WF_lobj116	9.77E+09	Water flow from lobj121_1 to lobj116
–3000	WF_lobj10	1.11E+11	Water flow from lobj121_1 to lobj10
–1000	WF_lobj160	3.42E+09	Water flow from lobj121_1 to lobj160
–1000	WF_lobj121_2	1.02E+10	Water flow from lobj121_1 to lobj121_2
–1000	WF_lobj116	7.15E+09	Water flow from lobj121_1 to lobj116
–1000	WF_lobj10	5.74E+10	Water flow from lobj121_1 to lobj10
0	WF_lobj160	3.82E+09	Water flow from lobj121_1 to lobj160
0	WF_lobj121_2	1.07E+10	Water flow from lobj121_1 to lobj121_2
0	WF_lobj116	1.29E+10	Water flow from lobj121_1 to lobj116
0	WF_lobj10	6.90E+10	Water flow from lobj121_1 to lobj10
1000	WF_lobj160	2.25E+09	Water flow from lobj121_1 to lobj160
1000	WF_lobj121_2	7.97E+09	Water flow from lobj121_1 to lobj121_2
1000	WF_lobj116	6.91E+09	Water flow from lobj121_1 to lobj116
1000	WF_lobj10	3.62E+10	Water flow from lobj121_1 to lobj10
2000	WF_lobj160	1.26E+09	Water flow from lobj121_1 to lobj160
2000	WF_lobj121_2	2.26E+09	Water flow from lobj121_1 to lobj121_2
2000	WF_lobj116	3.80E+09	Water flow from lobj121_1 to lobj116

Time (year)	Parameter namn	Water flow (m³ year⁻¹)	Description
2000	WF_lobj10	9.07E+09	Water flow from lobj121_1 to lobj10
3000	WF_lobj160	5.16E+07	Water flow from lobj121_1 to lobj160
3000	WF_lobj121_2	3.67E+08	Water flow from lobj121_1 to lobj121_2
3000	WF_lobj116	6.89E+08	Water flow from lobj121_1 to lobj116
3000	WF_lobj10	9.58E+08	Water flow from lobj121_1 to lobj10
3210.469314	WF_lobj160	0.00E+00	Water flow from lobj121_1 to lobj160
3500	WF_lobj116	0.00E+00	Water flow from lobj121_1 to lobj116
3682.656827	WF_lobj121_2	0.00E+00	Water flow from lobj121_1 to lobj121_2
3818.450185	WF_lobj10	4.37E+06	Water flow from lobj121_1 to lobj10
6400	WF_lobj10	4.69E+06	Water flow from lobj121_1 to lobj10
Biosphere object 121_2			
–6500	WF_lobj160	7.14E+09	Water flow from lobj121_2 to lobj160
–6500	WF_lobj157_2	1.86E+10	Water flow from lobj121_2 to lobj157_2
–6500	WF_lobj121_1	2.60E+10	Water flow from lobj121_2 to lobj121_1
–3000	WF_lobj160	6.93E+09	Water flow from lobj121_2 to lobj160
–3000	WF_lobj157_2	6.13E+09	Water flow from lobj121_2 to lobj157_2
–3000	WF_lobj121_1	2.10E+10	Water flow from lobj121_2 to lobj121_1
–1000	WF_lobj160	4.15E+09	Water flow from lobj121_2 to lobj160
–1000	WF_lobj157_2	4.23E+09	Water flow from lobj121_2 to lobj157_2
–1000	WF_lobj121_1	1.22E+10	Water flow from lobj121_2 to lobj121_1
0	WF_lobj160	3.88E+09	Water flow from lobj121_2 to lobj160
0	WF_lobj157_2	2.97E+09	Water flow from lobj121_2 to lobj157_2
0	WF_lobj121_1	1.65E+10	Water flow from lobj121_2 to lobj121_1
1000	WF_lobj160	3.53E+09	Water flow from lobj121_2 to lobj160
1000	WF_lobj157_2	1.98E+09	Water flow from lobj121_2 to lobj157_2
1000	WF_lobj121_1	9.76E+09	Water flow from lobj121_2 to lobj121_1
2000	WF_lobj160	5.32E+08	Water flow from lobj121_2 to lobj160
2000	WF_lobj157_2	6.24E+08	Water flow from lobj121_2 to lobj157_2
2000	WF_lobj121_1	3.17E+09	Water flow from lobj121_2 to lobj121_1
3000	WF_lobj160	1.06E+08	Water flow from lobj121_2 to lobj160
3000	WF_lobj157_2	0.00E+00	Water flow from lobj121_2 to lobj157_2
3000	WF_lobj121_1	3.08E+08	Water flow from lobj121_2 to lobj121_1
3210.469314	WF_lobj160	0.00E+00	Water flow from lobj121_2 to lobj160
3682.656827	WF_lobj121_1	6.63E+04	Water flow from lobj121_2 to lobj121_1
4000	WF_lobj121_1	6.95E+04	Water flow from lobj121_2 to lobj121_1
Biosphere object 157_1			
–6500	WF_lobj159	7.72E+09	Water flow from lobj157_1 to lobj159
–6500	WF_lobj157_2	2.58E+10	Water flow from lobj157_1 to lobj157_2
–6500	WF_lobj116	4.27E+10	Water flow from lobj157_1 to lobj116
–3000	WF_lobj159	9.62E+09	Water flow from lobj157_1 to lobj159
–3000	WF_lobj157_2	2.17E+10	Water flow from lobj157_1 to lobj157_2
–3000	WF_lobj116	1.49E+10	Water flow from lobj157_1 to lobj116
–1000	WF_lobj159	5.26E+09	Water flow from lobj157_1 to lobj159
–1000	WF_lobj157_2	1.12E+10	Water flow from lobj157_1 to lobj157_2
–1000	WF_lobj116	1.34E+10	Water flow from lobj157_1 to lobj116
0	WF_lobj159	4.77E+09	Water flow from lobj157_1 to lobj159
0	WF_lobj157_2	1.55E+10	Water flow from lobj157_1 to lobj157_2
0	WF_lobj116	7.48E+09	Water flow from lobj157_1 to lobj116
1000	WF_lobj159	2.62E+09	Water flow from lobj157_1 to lobj159
1000	WF_lobj157_2	8.95E+09	Water flow from lobj157_1 to lobj157_2
1000	WF_lobj116	6.48E+09	Water flow from lobj157_1 to lobj116
2000	WF_lobj159	8.01E+08	Water flow from lobj157_1 to lobj159
2000	WF_lobj157_2	2.78E+09	Water flow from lobj157_1 to lobj157_2
2000	WF_lobj116	3.06E+09	Water flow from lobj157_1 to lobj116
3000	WF_lobj159	1.96E+08	Water flow from lobj157_1 to lobj159
3000	WF_lobj157_2	7.87E+08	Water flow from lobj157_1 to lobj157_2

Time (year)	Parameter namn	Water flow (m^3 year^{-1})	Description
3000	WF_lobj116	1.63E+09	Water flow from lobj157_1 to lobj116
4000	WF_lobj116	2.04E+07	Water flow from lobj157_1 to lobj116
4083	WF_lobj159	0.00E+00	Water flow from lobj157_1 to lobj159
4275	WF_lobj157_2	0.00E+00	Water flow from lobj157_1 to lobj157_2
4493	WF_lobj116	3.53E+05	Water flow from lobj157_1 to lobj116
5700	WF_lobj116	4.42E+05	Water flow from lobj157_1 to lobj116
Biosphere object 157_2			
–6500	WF_lobj160	3.01E+09	Water flow from lobj157_2 to lobj160
–6500	WF_lobj121_2	1.60E+10	Water flow from lobj157_2 to lobj121_2
–6500	WF_lobj159	1.37E+10	Water flow from lobj157_2 to lobj159
–6500	WF_lobj157_1	3.00E+10	Water flow from lobj157_2 to lobj157_1
–6500	WF_lobj116	8.03E+09	Water flow from lobj157_2 to lobj116
–6500	WF_lobj10	9.26E+09	Water flow from lobj157_2 to lobj10
–3000	WF_lobj160	5.60E+09	Water flow from lobj157_2 to lobj160
–3000	WF_lobj121_2	1.60E+10	Water flow from lobj157_2 to lobj121_2
–3000	WF_lobj159	1.05E+10	Water flow from lobj157_2 to lobj159
–3000	WF_lobj157_1	7.86E+09	Water flow from lobj157_2 to lobj157_1
–3000	WF_lobj116	5.79E+09	Water flow from lobj157_2 to lobj116
–3000	WF_lobj10	3.97E+09	Water flow from lobj157_2 to lobj10
–1000	WF_lobj160	2.70E+09	Water flow from lobj157_2 to lobj160
–1000	WF_lobj121_2	7.05E+09	Water flow from lobj157_2 to lobj121_2
–1000	WF_lobj159	6.56E+09	Water flow from lobj157_2 to lobj159
–1000	WF_lobj157_1	6.64E+09	Water flow from lobj157_2 to lobj157_1
–1000	WF_lobj116	3.95E+09	Water flow from lobj157_2 to lobj116
–1000	WF_lobj10	1.82E+09	Water flow from lobj157_2 to lobj10
0	WF_lobj160	3.70E+09	Water flow from lobj157_2 to lobj160
0	WF_lobj121_2	8.59E+09	Water flow from lobj157_2 to lobj121_2
0	WF_lobj159	1.82E+09	Water flow from lobj157_2 to lobj159
0	WF_lobj157_1	3.50E+09	Water flow from lobj157_2 to lobj157_1
0	WF_lobj116	4.97E+09	Water flow from lobj157_2 to lobj116
0	WF_lobj10	2.88E+09	Water flow from lobj157_2 to lobj10
1000	WF_lobj160	2.86E+09	Water flow from lobj157_2 to lobj160
1000	WF_lobj121_2	4.57E+09	Water flow from lobj157_2 to lobj121_2
1000	WF_lobj159	2.47E+09	Water flow from lobj157_2 to lobj159
1000	WF_lobj157_1	2.81E+09	Water flow from lobj157_2 to lobj157_1
1000	WF_lobj116	3.00E+09	Water flow from lobj157_2 to lobj116
1000	WF_lobj10	1.45E+09	Water flow from lobj157_2 to lobj10
2000	WF_lobj160	5.06E+08	Water flow from lobj157_2 to lobj160
2000	WF_lobj121_2	2.80E+08	Water flow from lobj157_2 to lobj121_2
2000	WF_lobj159	2.48E+09	Water flow from lobj157_2 to lobj159
2000	WF_lobj157_1	7.48E+08	Water flow from lobj157_2 to lobj157_1
2000	WF_lobj116	5.39E+08	Water flow from lobj157_2 to lobj116
2000	WF_lobj10	0.00E+00	Water flow from lobj157_2 to lobj10
3000	WF_lobj160	0.00E+00	Water flow from lobj157_2 to lobj160
3000	WF_lobj121_2	0.00E+00	Water flow from lobj157_2 to lobj121_2
3000	WF_lobj159	7.86E+08	Water flow from lobj157_2 to lobj159
3000	WF_lobj157_1	4.01E+08	Water flow from lobj157_2 to lobj157_1
3000	WF_lobj116	0.00E+00	Water flow from lobj157_2 to lobj116
3500	WF_lobj159	0.00E+00	Water flow from lobj157_2 to lobj159
4275	WF_lobj157_1	1.71E+05	Water flow from lobj157_2 to lobj157_1
4500	WF_lobj157_1	1.84E+05	Water flow from lobj157_2 to lobj157_1
Biosphere object 159			
–6500	WF_lobj157_1	9.61E+09	Water flow from lobj159 to lobj157_1
–6500	WF_lobj157_2	1.37E+10	Water flow from lobj159 to lobj157_2
–6500	WF_lobj116	2.95E+10	Water flow from lobj159 to lobj116

Time (year)	Parameter namn	Water flow (m^3 year^{-1})	Description
–3000	WF_lobj157_1	2.93E+09	Water flow from lobj159 to lobj157_1
–3000	WF_lobj157_2	1.11E+10	Water flow from lobj159 to lobj157_2
–3000	WF_lobj116	2.36E+10	Water flow from lobj159 to lobj116
–1000	WF_lobj157_1	3.01E+09	Water flow from lobj159 to lobj157_1
–1000	WF_lobj157_2	6.67E+09	Water flow from lobj159 to lobj157_2
–1000	WF_lobj116	1.30E+10	Water flow from lobj159 to lobj116
0	WF_lobj157_1	2.04E+09	Water flow from lobj159 to lobj157_1
0	WF_lobj157_2	2.99E+09	Water flow from lobj159 to lobj157_2
0	WF_lobj116	1.61E+10	Water flow from lobj159 to lobj116
1000	WF_lobj157_1	1.22E+09	Water flow from lobj159 to lobj157_1
1000	WF_lobj157_2	1.38E+09	Water flow from lobj159 to lobj157_2
1000	WF_lobj116	9.78E+09	Water flow from lobj159 to lobj116
2000	WF_lobj157_1	7.42E+08	Water flow from lobj159 to lobj157_1
2000	WF_lobj157_2	5.51E+08	Water flow from lobj159 to lobj157_2
2000	WF_lobj116	7.27E+09	Water flow from lobj159 to lobj116
3000	WF_lobj157_1	1.44E+08	Water flow from lobj159 to lobj157_1
3000	WF_lobj157_2	4.00E+08	Water flow from lobj159 to lobj157_2
3000	WF_lobj116	1.17E+09	Water flow from lobj159 to lobj116
3500	WF_lobj157_2	0.00E+00	Water flow from lobj159 to lobj157_2
4000	WF_lobj116	0.00E+00	Water flow from lobj159 to lobj116
4083.65019	WF_lobj157_1	1.16E+05	Water flow from lobj159 to lobj157_1
7600	WF_lobj157_1	1.31E+05	Water flow from lobj159 to lobj157_1
Biosphere object 160			
–6500	WF_lobj121_1	8.23E+09	Water flow from lobj160 to lobj121_1
–6500	WF_lobj121_2	8.26E+09	Water flow from lobj160 to lobj121_2
–6500	WF_lobj157_2	4.05E+09	Water flow from lobj160 to lobj157_2
–6500	WF_lobj116	1.20E+10	Water flow from lobj160 to lobj116
–3000	WF_lobj121_1	1.12E+10	Water flow from lobj160 to lobj121_1
–3000	WF_lobj121_2	3.62E+09	Water flow from lobj160 to lobj121_2
–3000	WF_lobj157_2	1.91E+09	Water flow from lobj160 to lobj157_2
–3000	WF_lobj116	5.53E+09	Water flow from lobj160 to lobj116
–1000	WF_lobj121_1	5.48E+09	Water flow from lobj160 to lobj121_1
–1000	WF_lobj121_2	3.16E+09	Water flow from lobj160 to lobj121_2
–1000	WF_lobj157_2	1.65E+09	Water flow from lobj160 to lobj157_2
–1000	WF_lobj116	3.57E+09	Water flow from lobj160 to lobj116
0	WF_lobj121_1	5.57E+09	Water flow from lobj160 to lobj121_1
0	WF_lobj121_2	4.01E+09	Water flow from lobj160 to lobj121_2
0	WF_lobj157_2	2.35E+09	Water flow from lobj160 to lobj157_2
0	WF_lobj116	3.29E+09	Water flow from lobj160 to lobj116
1000	WF_lobj121_1	3.15E+09	Water flow from lobj160 to lobj121_1
1000	WF_lobj121_2	2.74E+09	Water flow from lobj160 to lobj121_2
1000	WF_lobj157_2	1.57E+09	Water flow from lobj160 to lobj157_2
1000	WF_lobj116	3.54E+09	Water flow from lobj160 to lobj116
2000	WF_lobj121_1	1.22E+09	Water flow from lobj160 to lobj121_1
2000	WF_lobj121_2	1.78E+09	Water flow from lobj160 to lobj121_2
2000	WF_lobj157_2	2.12E+08	Water flow from lobj160 to lobj157_2
2000	WF_lobj116	1.60E+09	Water flow from lobj160 to lobj116
3000	WF_lobj121_1	1.09E+08	Water flow from lobj160 to lobj121_1
3000	WF_lobj121_2	4.86E+07	Water flow from lobj160 to lobj121_2
3000	WF_lobj157_2	0.00E+00	Water flow from lobj160 to lobj157_2
3000	WF_lobj116	0.00E+00	Water flow from lobj160 to lobj116
3210	WF_lobj121_1	5.59E+04	Water flow from lobj160 to lobj121_1
3210	WF_lobj121_2	0.00E+00	Water flow from lobj160 to lobj121_2
8800	WF_lobj121_1	5.51E+04	Water flow from lobj160 to lobj121_1

Appendix E

Does coefficient for non-human biota

Table E-1. DCC_ext_beta_gamma for marine organisms ((µGy h^{-1})/(Bq l^{-1})).

Radionuclides	(Wading) bird	Benthic fish	Benthic mollusc	Crustacean	European otter	Macroalgae	Mammal	Pelagic fish	Phyto-plankton	Polychaete worm	Ruddy turnstone	Vascular plant	Zooplankton
Ac-227	6.63E–08	7.32E–08	9.16E–08	6.97E–08	5.53E–08	1.10E–07	2.50E–08	7.23E–08	2.12E–07	9.69E–08	7.17E–08	8.98E–08	1.31E–07
Ag-108m	7.99E–04	8.53E–04	9.06E–04	8.20E–04	7.21E–04	9.36E–04	4.04E–04	8.37E–04	9.73E–04	9.19E–04	8.33E–04	9.03E–04	9.51E–04
Am-241	1.10E–05	1.20E–05	1.50E–05	1.10E–05	8.40E–06	1.70E–05	3.30E–06	1.20E–05	3.20E–03	1.50E–05	1.16E–05	1.50E–05	1.80E–05
Am-242m	7.86E–06	8.89E–06	1.22E–05	8.32E–06	6.37E–06	2.07E–05	2.78E–06	8.70E–06	7.72E–05	1.39E–05	8.61E–06	1.18E–05	2.47E–05
Am-243	1.06E–04	1.14E–04	1.25E–04	1.09E–04	9.11E–05	1.34E–04	4.24E–05	1.12E–04	1.89E–04	1.27E–04	1.12E–04	1.24E–04	1.39E–04
Ba-133	1.89E–04	2.04E–04	2.21E–04	1.95E–04	1.65E–04	2.28E–04	8.36E–05	2.00E–04	2.37E–04	2.24E–04	1.99E–04	2.20E–04	2.31E–04
Be-10	9.14E–07	1.14E–06	3.57E–06	1.07E–06	5.50E–07	1.62E–05	1.88E–07	1.16E–06	1.11E–04	5.50E–06	1.14E–06	3.13E–06	2.14E–05
C-14-ind	1.80E–08	1.80E–08	7.20E–08	2.10E–08	1.04E–08	1.60E–07	3.60E–09	2.30E–08	2.90E–05	7.20E–08	2.30E–08	6.20E–08	4.30E–07
C-14-inorg	1.80E–08	1.80E–08	7.20E–08	2.10E–08	1.04E–08	1.60E–07	3.60E–09	2.30E–08	2.90E–05	7.20E–08	2.30E–08	6.20E–08	4.30E–07
C-14-org	1.80E–08	1.80E–08	7.20E–08	2.10E–08	1.04E–08	1.60E–07	3.60E–09	2.30E–08	2.90E–05	7.20E–08	2.30E–08	6.20E–08	4.30E–07
Ca-41	2.04E–09	2.07E–09	8.59E–09	2.42E–09	1.16E–09	2.38E–08	4.04E–10	2.67E–09	7.94E–08	1.03E–08	2.62E–09	7.39E–09	4.18E–08
Cd-113m	5.56E–07	6.79E–07	2.16E–06	6.48E–07	3.34E–07	9.54E–06	1.14E–07	7.07E–07	7.15E–05	3.20E–06	6.94E–07	1.89E–06	1.30E–05
Cl-36	1.40E–06	1.80E–06	5.10E–06	1.60E–06	8.32E–07	2.30E–05	3.10E–07	1.70E–06	1.60E–04	8.60E–06	1.67E–06	4.60E–06	3.10E–05
Cm-242	1.60E–07	2.30E–07	4.80E–07	1.80E–07	9.15E–08	7.60E–07	3.10E–08	2.10E–07	3.50E–03	5.80E–07	2.05E–07	4.60E–07	9.10E–07
Cm-243	6.20E–05	6.60E–05	7.20E–05	6.40E–05	5.37E–05	7.70E–05	2.60E–05	6.50E–05	3.50E–03	7.40E–05	6.48E–05	7.20E–05	7.90E–05
Cm-244	1.40E–07	2.10E–07	4.40E–07	1.70E–07	8.14E–08	7.00E–07	2.80E–08	1.90E–07	3.30E–03	5.30E–07	1.86E–07	4.20E–07	8.40E–07
Cm-245	4.23E–05	4.56E–05	5.03E–05	4.38E–05	3.63E–05	5.31E–05	1.66E–05	4.50E–05	5.99E–05	5.14E–05	4.47E–05	5.00E–05	5.45E–05
Cm-246	1.27E–07	1.88E–07	3.96E–07	1.50E–07	7.34E–08	6.24E–07	2.49E–08	1.73E–07	9.92E–07	4.77E–07	1.67E–07	3.78E–07	7.53E–07
Co-60	1.30E–03	1.30E–03	1.40E–03	1.30E–03	1.16E–03	1.40E–03	7.20E–04	1.30E–03	1.50E–03	1.40E–03	1.31E–03	1.40E–03	1.40E–03
Cs-134	7.70E–04	8.20E–04	8.70E–04	7.90E–04	7.00E–04	9.00E–04	4.00E–04	8.10E–04	9.90E–04	8.80E–04	8.02E–04	8.70E–04	9.10E–04
Cs-135	4.30E–08	4.30E–08	1.70E–07	5.00E–08	2.49E–08	4.30E–07	8.60E–09	5.50E–08	3.90E–05	1.70E–07	5.36E–08	1.40E–07	9.90E–07
Cs-137	2.80E–04	3.00E–04	3.20E–04	2.90E–04	2.53E–04	3.40E–04	1.40E–04	2.90E–04	4.70E–04	3.30E–04	2.91E–04	3.20E–04	3.50E–04
Eu-152	5.70E–04	6.10E–04	6.50E–04	5.90E–04	5.22E–04	6.70E–04	3.10E–04	6.00E–04	7.30E–04	6.50E–04	5.97E–04	6.40E–04	6.70E–04
Eu-154	6.20E–04	6.60E–04	7.00E–04	6.40E–04	5.67E–04	7.30E–04	3.40E–04	6.50E–04	8.80E–04	7.10E–04	6.46E–04	7.00E–04	7.50E–04
Eu-155	2.81E–05	3.04E–05	3.34E–05	2.92E–05	2.36E–05	3.45E–05	1.02E–05	3.00E–05	3.93E–05	3.39E–05	2.99E–05	3.33E–05	3.51E–05
Fe-55	1.47E–08	1.49E–08	6.18E–08	1.74E–08	8.32E–09	1.71E–07	2.91E–09	1.92E–08	5.72E–07	7.42E–08	1.88E–08	5.32E–08	3.00E–07
Gd-152	0	0	0	0	0	0	0	0	0	0	0	0	0
H-3	3.60E–13	7.72E–13	2.90E–12	7.40E–15	1.94E–13	2.00E–11	3.30E–14	8.30E–15	3.23E–06	2.90E–12	8.11E–15	2.60E–12	1.60E–13
Ho-166m	8.62E–04	9.18E–04	9.72E–04	8.84E–04	7.79E–04	9.97E–04	4.39E–04	9.02E–04	1.03E–03	9.83E–04	8.98E–04	9.69E–04	1.01E–03
I-129	7.10E–06	9.20E–06	1.20E–05	7.90E–06	4.85E–06	1.30E–05	1.60E–06	8.50E–06	5.10E–05	1.30E–05	8.38E–06	1.20E–05	1.40E–05
In-115	3.51E–07	4.05E–07	1.36E–06	4.09E–07	2.11E–07	5.72E–06	7.11E–08	4.46E–07	5.08E–05	1.81E–06	4.38E–07	1.18E–06	8.15E–06

Radionuclides	(Wading) bird	Benthic fish	Benthic mollusc	Crustacean	European otter	Macroalgae	Mammal	Pelagic fish	Phyto-plankton	Polychaete worm	Ruddy turnstone	Vascular plant	Zooplankton
Mo-93	7.91E–07	1.19E–06	2.68E–06	9.44E–07	4.46E–07	4.36E–06	1.52E–07	1.09E–06	6.12E–06	3.27E–06	1.05E–06	2.55E–06	5.16E–06
Nb-93m	1.41E–07	2.11E–07	4.78E–07	1.69E–07	7.95E–08	7.78E–07	2.70E–08	1.96E–07	1.47E–06	5.83E–07	1.89E–07	4.54E–07	9.67E–07
Nb-94	7.80E–04	8.30E–04	8.80E–04	8.00E–04	7.12E–04	9.00E–04	4.10E–04	8.20E–04	1.00E–03	8.90E–04	8.13E–04	8.80E–04	9.10E–04
Ni-59	2.50E–08	2.50E–08	1.00E–07	2.90E–08	1.40E–08	2.90E–07	4.90E–09	3.20E–08	4.00E–06	1.20E–07	3.16E–08	8.90E–08	5.00E–07
Ni-63	1.10E–09	1.10E–09	4.70E–09	1.60E–09	6.06E–10	7.00E–09	1.70E–10	1.70E–09	9.90E–06	4.60E–09	1.71E–09	4.00E–09	3.60E–08
Np-237	1.20E–05	1.30E–05	1.60E–05	1.30E–05	9.89E–06	1.80E–05	4.30E–06	1.30E–05	2.80E–03	1.70E–05	1.30E–05	1.60E–05	1.90E–05
Pa-231	1.84E–05	2.01E–05	2.29E–05	1.91E–05	1.60E–05	2.53E–05	8.04E–06	1.97E–05	3.01E–05	2.37E–05	1.95E–05	2.27E–05	2.66E–05
Pb-210	3.90E–06	6.10E–06	1.30E–05	4.50E–06	2.47E–06	4.70E–05	8.80E–07	4.90E–06	2.50E–04	2.20E–05	4.81E–06	1.20E–05	7.20E–05
Pd-107	1.33E–10	1.27E–10	5.73E–10	3.08E–10	6.43E–11	8.18E–10	1.58E–11	3.41E–10	3.42E–08	5.62E–10	3.34E–10	4.88E–10	7.54E–09
Pm-147	4.07E–08	4.12E–08	1.53E–07	4.75E–08	2.44E–08	4.00E–07	8.57E–09	5.17E–08	7.55E–06	1.57E–07	5.08E–08	1.33E–07	9.00E–07
Po-210	4.20E–09	4.50E–09	4.70E–09	4.30E–09	3.85E–09	4.90E–09	2.20E–09	4.40E–09	3.10E–03	4.80E–09	4.39E–09	4.70E–09	4.90E–09
Pu-238	1.40E–07	2.00E–07	4.40E–07	1.60E–07	8.08E–08	7.10E–07	2.80E–08	1.90E–07	3.20E–03	5.30E–07	1.80E–07	4.10E–07	8.80E–07
Pu-239	7.70E–08	1.00E–07	1.90E–07	8.80E–08	5.27E–08	3.00E–07	2.10E–08	9.70E–08	3.00E–03	2.30E–07	9.46E–08	1.90E–07	3.60E–07
Pu-240	1.30E–07	1.90E–07	4.20E–07	1.60E–07	7.82E–08	6.80E–07	2.70E–08	1.80E–07	3.00E–03	5.10E–07	1.74E–07	4.00E–07	8.50E–07
Pu-241	8.20E–10	9.10E–10	1.10E–09	8.60E–10	6.84E–10	1.30E–09	3.10E–10	8.90E–10	3.10E–06	1.20E–09	8.80E–10	1.10E–09	1.40E–09
Pu-242	1.11E–07	1.60E–07	3.48E–07	1.31E–07	6.54E–08	5.66E–07	2.28E–08	1.50E–07	9.74E–07	4.20E–07	1.45E–07	3.30E–07	7.03E–07
Ra-226	9.00E–04	9.70E–04	1.00E–03	9.20E–04	8.20E–04	1.10E–03	5.00E–04	9.40E–04	1.50E–02	1.10E–03	9.36E–04	1.00E–03	1.20E–03
Ra-228	4.90E–04	5.20E–04	5.60E–04	5.00E–04	4.42E–04	6.00E–04	2.60E–04	5.10E–04	8.40E–04	5.70E–04	5.06E–04	5.50E–04	6.40E–04
Ru-106	1.50E–04	2.20E–04	2.80E–04	1.60E–04	1.21E–04	4.90E–04	6.10E–05	1.70E–04	9.40E–04	3.40E–04	1.65E–04	2.70E–04	7.40E–04
Sb-125	2.10E–04	2.20E–04	2.40E–04	2.10E–04	1.87E–04	2.50E–04	1.00E–04	2.20E–04	3.10E–04	2.40E–04	2.18E–04	2.40E–04	2.50E–04
Se-79	2.40E–08	2.40E–08	9.40E–08	2.80E–08	1.36E–08	2.10E–07	4.70E–09	3.10E–08	3.20E–05	9.40E–08	3.01E–08	8.10E–08	5.60E–07
Sm-147	0	0	0	0	0	0	0	0	0	0	0	0	0
Sm-151	2.62E–09	3.06E–09	9.64E–09	3.36E–09	1.49E–09	1.48E–08	4.60E–10	3.74E–09	3.94E–07	9.98E–09	3.65E–09	8.54E–09	5.39E–08
Sn-126	7.97E–04	8.60E–04	9.25E–04	8.19E–04	7.17E–04	1.01E–03	4.00E–04	8.37E–04	1.29E–03	9.53E–04	8.33E–04	9.19E–04	1.10E–03
Sr-90	2.00E–05	5.00E–05	7.70E–05	2.30E–05	1.22E–05	2.00E–04	4.20E–06	2.70E–05	6.50E–04	1.10E–04	2.61E–05	6.90E–05	3.60E–04
Tc-99	1.20E–07	1.20E–07	4.60E–07	1.40E–07	7.16E–08	1.50E–06	2.40E–08	1.50E–07	5.80E–05	5.00E–07	1.50E–07	4.00E–07	2.70E–06
Th-228	8.10E–04	8.80E–04	9.40E–04	8.30E–04	7.43E–04	1.10E–03	4.80E–04	8.50E–04	2.00E–02	9.80E–04	8.39E–04	9.30E–04	1.20E–03
Th-229	4.14E–05	4.46E–05	4.94E–05	4.29E–05	3.54E–05	5.25E–05	1.60E–05	4.41E–05	6.35E–05	5.04E–05	4.38E–05	4.91E–05	5.44E–05
Th-230	2.40E–07	2.80E–07	4.40E–07	2.60E–07	1.85E–07	6.30E–07	7.70E–08	2.80E–07	2.70E–03	4.90E–07	2.72E–07	4.20E–07	7.90E–07
Th-232	1.40E–07	1.80E–07	3.20E–07	1.60E–07	1.03E–07	5.00E–07	4.10E–08	1.70E–07	2.30E–03	3.70E–07	1.69E–07	3.00E–07	6.50E–07
U-232	2.40E–07	3.04E–07	5.59E–07	2.68E–07	1.69E–07	8.67E–07	6.76E–08	2.94E–07	1.79E–06	6.51E–07	2.87E–07	5.34E–07	1.08E–06
U-233	2.18E–07	2.59E–07	3.97E–07	2.36E–07	1.70E–07	5.58E–07	7.51E–08	2.52E–07	9.34E–07	4.45E–07	2.48E–07	3.83E–07	6.67E–07
U-234	1.50E–07	2.00E–07	4.10E–07	1.80E–07	1.02E–07	6.60E–07	3.90E–08	2.00E–07	2.80E–03	4.90E–07	1.90E–07	3.90E–07	8.30E–07
U-235	8.10E–05	8.70E–05	9.60E–05	8.40E–05	7.04E–05	1.00E–04	3.40E–05	8.60E–05	2.80E–03	9.80E–05	8.54E–05	9.50E–05	1.00E–04
U-236	1.20E–07	1.64E–07	3.54E–07	1.39E–07	7.50E–08	5.89E–07	2.73E–08	1.57E–07	1.14E–06	4.25E–07	1.52E–07	3.35E–07	7.42E–07
U-238	9.50E–08	1.30E–07	3.00E–07	1.10E–07	5.69E–08	5.10E–07	2.00E–08	1.30E–07	2.40E–03	3.60E–07	1.23E–07	2.80E–07	6.40E–07
Zr-93	1.38E–09	1.35E–09	5.87E–09	1.95E–09	7.56E–10	8.76E–09	2.16E–10	2.14E–09	3.29E–07	5.76E–09	2.10E–09	5.01E–09	4.39E–08

Tabel E-2. DCC_ext_beta_gamma for liminc organisms ((μGy h^{-1})/(Bq l^{-1})).

Radionuclides	Amphibian	Benthic fish	Bird	Bivalve mollusc	Crustacean	Gastropod	Insect larvae	Mammal	Microphyto-benthos	Pelagic fish	Phyto-plankton	Vascular plant	Zooplankton
Ac-227	8.82E–08	6.67E–08	6.63E–08	8.35E–08	1.47E–07	1.02E–07	1.46E–07	5.76E–08	6.56E–07	6.81E–08	6.56E–07	1.44E–07	1.54E–07
Ag-108m	8.99E–04	8.06E–04	7.99E–04	8.85E–04	9.60E–04	9.23E–04	9.59E–04	7.31E–04	9.74E–04	8.15E–04	9.74E–04	9.53E–04	9.65E–04
Am-241	1.40E–05	1.10E–05	1.10E–05	1.40E–05	1.80E–05	1.60E–05	1.80E–05	8.90E–06	2.27E–05	1.10E–05	3.20E–03	1.80E–05	1.90E–05
Am-242m	1.15E–05	7.89E–06	7.86E–06	1.06E–05	3.54E–05	1.43E–05	3.41E–05	6.70E–06	9.14E–05	8.07E–06	9.14E–05	3.87E–05	4.74E–05
Am-243	1.24E–04	1.07E–04	1.06E–04	1.21E–04	1.48E–04	1.29E–04	1.46E–04	9.39E–05	2.14E–04	1.08E–04	2.14E–04	1.52E–04	1.56E–04
Ba-133	2.19E–04	1.91E–04	1.89E–04	2.15E–04	2.33E–04	2.25E–04	2.32E–04	1.69E–04	2.42E–04	1.93E–04	2.42E–04	2.33E–04	2.34E–04
Be-10	2.92E–06	8.74E–07	9.14E–07	2.24E–06	3.95E–05	5.73E–06	3.73E–05	6.47E–07	1.24E–04	9.16E–07	1.24E–04	4.59E–05	6.12E–05
C-14-ind	5.90E–08	1.70E–08	1.80E–08	4.50E–08	9.00E–07	1.20E–07	8.20E–07	1.20E–08	8.90E–06	1.80E–08	2.90E–05	1.10E–06	1.30E–06
C-14-inorg	5.90E–08	1.70E–08	1.80E–08	4.50E–08	9.00E–07	1.20E–07	8.20E–07	1.20E–08	8.90E–06	1.80E–08	2.90E–05	1.10E–06	1.30E–06
C-14-org	5.90E–08	1.70E–08	1.80E–08	4.50E–08	9.00E–07	1.20E–07	8.20E–07	1.20E–08	8.90E–06	1.80E–08	2.90E–05	1.10E–06	1.30E–06
Ca-41	6.94E–09	1.94E–09	2.04E–09	5.31E–09	5.81E–08	1.42E–08	5.69E–08	1.39E–09	8.03E–08	2.04E–09	8.03E–08	5.38E–08	6.27E–08
Cd-113m	1.77E–06	5.31E–07	5.56E–07	1.36E–06	2.43E–05	3.47E–06	2.29E–05	3.93E–07	8.33E–05	5.57E–07	8.33E–05	2.91E–05	3.75E–05
Cl-36	4.20E–06	1.30E–06	1.40E–06	3.30E–06	5.40E–05	8.30E–06	5.10E–05	9.80E–07	1.40E–04	1.40E–06	1.60E–04	5.50E–05	8.10E–05
Cm-242	4.30E–07	1.60E–07	1.60E–07	3.60E–07	1.00E–06	6.20E–07	1.00E–06	1.10E–07	1.81E–06	1.70E–07	3.50E–03	9.80E–07	1.00E–06
Cm-243	7.10E–05	6.20E–05	6.20E–05	7.00E–05	8.30E–05	7.40E–05	8.20E–05	5.50E–05	1.12E–04	6.30E–05	3.50E–03	8.50E–05	8.60E–05
Cm-244	4.00E–07	1.40E–07	1.40E–07	3.30E–07	9.30E–07	5.70E–07	9.20E–07	9.60E–08	1.62E–06	1.50E–07	3.30E–03	9.00E–07	9.50E–07
Cm-245	4.97E–05	4.26E–05	4.23E–05	4.86E–05	5.57E–05	5.18E–05	5.56E–05	3.75E–05	6.48E–05	4.32E–05	6.48E–05	5.58E–05	5.64E–05
Cm-246	3.56E–07	1.28E–07	1.27E–07	2.97E–07	8.34E–07	5.11E–07	8.28E–07	8.64E–08	1.50E–06	1.38E–07	1.50E–06	8.03E–07	8.57E–07
Co-60	1.40E–03	1.30E–03	1.30E–03	1.40E–03	1.40E–03	1.40E–03	1.40E–03	1.20E–03	1.47E–03	1.30E–03	1.50E–03	1.40E–03	1.50E–03
Cs-134	8.60E–04	7.80E–04	7.70E–04	8.50E–04	9.20E–04	8.80E–04	9.20E–04	7.10E–04	9.72E–04	7.90E–04	9.90E–04	9.20E–04	9.30E–04
Cs-135	1.40E–07	4.10E–08	4.30E–08	1.00E–07	2.20E–06	2.70E–07	2.00E–06	3.00E–08	1.56E–05	4.30E–08	3.90E–05	2.70E–06	3.00E–06
Cs-137	3.20E–04	2.80E–04	2.80E–04	3.10E–04	3.70E–04	3.30E–04	3.70E–04	2.60E–04	4.45E–04	2.90E–04	4.70E–04	3.70E–04	3.90E–04
Eu-152	6.40E–04	5.80E–04	5.70E–04	6.30E–04	6.80E–04	6.60E–04	6.80E–04	5.30E–04	7.12E–04	5.80E–04	7.30E–04	6.80E–04	6.90E–04
Eu-154	6.90E–04	6.30E–04	6.20E–04	6.80E–04	7.80E–04	7.10E–04	7.70E–04	5.70E–04	8.46E–04	6.30E–04	8.80E–04	7.70E–04	7.90E–04
Eu-155	3.31E–05	2.83E–05	2.81E–05	3.25E–05	3.58E–05	3.41E–05	3.57E–05	2.45E–05	4.51E–05	2.88E–05	4.51E–05	3.60E–05	3.63E–05
Fe-55	4.99E–08	1.39E–08	1.47E–08	3.82E–08	4.18E–07	1.02E–07	4.10E–07	9.97E–09	5.78E–07	1.47E–08	5.78E–07	3.87E–07	4.51E–07
Gd-152	0	0	0	0	0	0	0	0	0	0	0	0	0
H-3	2.50E–12	3.70E–13	3.60E–13	1.50E–12	2.50E–13	4.80E–14	2.40E–13	2.80E–13	4.99E–08	3.60E–13	3.23E–06	8.64E–10	1.27E–10
Ho-166m	9.65E–04	8.70E–04	8.62E–04	9.52E–04	1.01E–03	9.87E–04	1.01E–03	7.89E–04	1.04E–03	8.80E–04	1.04E–03	1.01E–03	1.02E–03
I-129	1.20E–05	7.30E–06	7.10E–06	1.10E–05	1.50E–05	1.30E–05	1.50E–05	5.20E–06	2.36E–05	7.70E–06	5.10E–05	1.50E–05	1.50E–05
In-115	1.11E–06	3.35E–07	3.51E–07	8.55E–07	1.57E–05	2.18E–06	1.47E–05	2.48E–07	6.25E–05	3.51E–07	6.25E–05	2.03E–05	2.44E–05
Mo-93	2.38E–06	7.94E–07	7.91E–07	1.96E–06	5.63E–06	3.50E–06	5.60E–06	5.33E–07	6.26E–06	8.58E–07	6.26E–06	5.48E–06	5.76E–06
Nb-93m	4.26E–07	1.42E–07	1.41E–07	3.49E–07	1.08E–06	6.31E–07	1.07E–06	9.51E–08	3.39E–06	1.53E–07	3.39E–06	1.04E–06	1.14E–06

Radionuclides	Amphibian	Benthic fish	Bird	Bivalve mollusc	Crustacean	Gastropod	Insect larvae	Mammal	Microphyto-benthos	Pelagic fish	Phyto-plankton	Vascular plant	Zooplankton
Nb-94	8.70E–04	7.90E–04	7.80E–04	8.60E–04	9.30E–04	8.90E–04	9.20E–04	7.20E–04	9.80E–04	8.00E–04	1.00E–03	9.30E–04	9.40E–04
Ni-59	8.40E–08	2.30E–08	2.50E–08	6.40E–08	7.00E–07	1.70E–07	6.90E–07	1.70E–08	9.69E–07	2.50E–08	4.00E–06	6.50E–07	7.60E–07
Ni-63	3.80E–09	1.10E–09	1.10E–09	2.90E–09	5.70E–08	9.40E–09	5.40E–08	7.40E–10	1.38E–06	1.10E–09	9.90E–06	6.04E–08	8.70E–08
Np-237	1.60E–05	1.20E–05	1.20E–05	1.50E–05	2.00E–05	1.70E–05	2.00E–05	1.00E–05	2.84E–05	1.20E–05	2.80E–03	2.00E–05	2.00E–05
Pa-231	2.24E–05	1.86E–05	1.84E–05	2.17E–05	2.76E–05	2.41E–05	2.75E–05	1.64E–05	3.34E–05	1.89E–05	3.34E–05	2.76E–05	2.81E–05
Pb-210	1.10E–05	3.80E–06	3.90E–06	8.70E–06	3.60E–05	2.10E–05	1.10E–04	2.80E–06	2.17E–04	4.00E–06	2.50E–04	9.60E–05	1.50E–04
Pd-107	4.59E–10	1.25E–10	1.33E–10	3.53E–10	1.20E–08	1.91E–09	1.14E–08	8.16E–11	3.46E–07	1.33E–10	3.46E–07	8.06E–09	1.12E–08
Pm-147	1.25E–07	3.89E–08	4.07E–08	9.71E–08	1.94E–06	2.44E–07	1.78E–06	2.87E–08	1.41E–05	4.07E–08	1.41E–05	2.41E–06	2.75E–06
Po-210	4.70E–09	4.30E–09	4.20E–09	4.60E–09	4.90E–09	4.80E–09	4.90E–09	3.90E–09	4.95E–09	4.30E–09	3.10E–03	4.90E–09	4.90E–09
Pu-238	3.90E–07	1.40E–07	1.40E–07	3.20E–07	1.00E–06	5.70E–07	9.90E–07	9.50E–08	1.89E–06	1.50E–07	3.20E–03	9.50E–07	1.00E–06
Pu-239	1.80E–07	7.80E–08	7.70E–08	1.50E–07	4.00E–07	2.40E–07	4.00E–07	5.90E–08	8.46E–07	8.20E–08	3.00E–03	4.00E–07	4.20E–07
Pu-240	3.70E–07	1.30E–07	1.30E–07	3.10E–07	9.50E–07	5.50E–07	9.40E–07	9.20E–08	1.88E–06	1.40E–07	3.00E–03	9.20E–07	9.90E–07
Pu-241	1.10E–09	8.20E–10	8.20E–10	1.00E–09	1.50E–09	1.20E–09	1.50E–09	7.10E–10	5.70E–08	8.40E–10	3.10E–06	2.43E–09	1.80E–09
Pu-242	3.11E–07	1.11E–07	1.11E–07	2.58E–07	7.92E–07	4.56E–07	7.85E–07	7.66E–08	1.55E–06	1.19E–07	1.55E–06	7.59E–07	8.18E–07
Ra-226	1.00E–03	9.10E–04	9.00E–04	1.00E–03	1.30E–03	1.10E–03	1.30E–03	8.30E–04	1.53E–03	9.20E–04	1.50E–02	1.30E–03	1.40E–03
Ra-228	5.50E–04	4.90E–04	4.90E–04	5.40E–04	6.90E–04	5.70E–04	6.80E–04	4.50E–04	7.91E–04	5.00E–04	8.40E–04	6.60E–04	7.20E–04
Ru-106	2.50E–04	1.50E–04	1.50E–04	2.20E–04	8.30E–04	3.90E–04	8.20E–04	1.20E–04	9.33E–04	1.60E–04	9.40E–04	7.10E–04	8.70E–04
Sb-125	2.40E–04	2.10E–04	2.10E–04	2.30E–04	2.60E–04	2.40E–04	2.60E–04	1.90E–04	2.81E–04	2.10E–04	3.10E–04	2.60E–04	2.60E–04
Se-79	7.70E–08	2.30E–08	2.40E–08	5.90E–08	1.20E–06	1.50E–07	1.10E–06	1.60E–08	1.08E–05	2.40E–08	3.20E–05	1.50E–06	1.70E–06
Sm-147	0	0	0	0	0	0	0	0	0	0	0	0	0
Sm-151	8.06E–09	2.56E–09	2.62E–09	6.36E–09	8.48E–08	1.63E–08	8.06E–08	1.78E–09	1.81E–06	2.71E–09	1.81E–06	9.71E–08	1.34E–07
Sn-126	9.12E–04	8.05E–04	7.97E–04	8.93E–04	1.17E–03	9.60E–04	1.16E–03	7.27E–04	1.31E–03	8.14E–04	1.31E–03	1.12E–03	1.21E–03
Sr-90	6.30E–05	2.10E–05	2.00E–05	4.90E–05	4.50E–04	1.20E–04	4.40E–04	1.40E–05	6.24E–04	2.40E–05	6.50E–04	3.70E–04	5.10E–04
Tc-99	3.70E–07	1.10E–07	1.20E–07	2.90E–07	5.70E–06	7.30E–07	5.30E–06	8.50E–08	3.15E–05	1.20E–07	5.80E–05	7.70E–06	8.40E–06
Th-228	9.20E–04	8.20E–04	8.10E–04	9.00E–04	1.30E–03	9.90E–04	1.30E–03	7.50E–04	1.35E–03	8.30E–04	2.00E–02	1.20E–03	1.40E–03
Th-229	4.88E–05	4.17E–05	4.14E–05	4.77E–05	5.64E–05	5.10E–05	5.61E–05	3.66E–05	7.30E–05	4.23E–05	7.30E–05	5.66E–05	5.75E–05
Th-230	4.10E–07	2.40E–07	2.40E–07	3.60E–07	9.20E–07	5.30E–07	9.00E–07	2.00E–07	2.88E–06	2.50E–07	2.70E–03	9.40E–07	1.00E–06
Th-232	2.90E–07	1.40E–07	1.40E–07	2.50E–07	7.50E–07	4.00E–07	7.40E–07	1.10E–07	2.25E–06	1.50E–07	2.30E–03	7.60E–07	8.30E–07
U-232	5.08E–07	2.41E–07	2.40E–07	4.38E–07	1.23E–06	7.05E–07	1.22E–06	1.86E–07	3.28E–06	2.52E–07	3.28E–06	1.24E–06	1.34E–06
U-233	3.70E–07	2.20E–07	2.18E–07	3.32E–07	7.47E–07	4.74E–07	7.40E–07	1.80E–07	1.35E–06	2.27E–07	1.35E–06	7.29E–07	7.76E–07
U-234	3.70E–07	1.50E–07	1.50E–07	3.10E–07	9.50E–07	5.30E–07	9.40E–07	1.10E–07	2.40E–06	1.60E–07	2.80E–03	9.50E–07	1.00E–06
U-235	9.50E–05	8.20E–05	8.10E–05	9.30E–05	1.10E–04	9.90E–05	1.10E–04	7.20E–05	1.41E–04	8.30E–05	2.80E–03	1.10E–04	1.10E–04
U-236	3.16E–07	1.20E–07	1.20E–07	2.63E–07	8.47E–07	4.65E–07	8.39E–07	8.62E–08	2.00E–06	1.28E–07	2.00E–06	8.35E–07	9.08E–07
U-238	2.70E–07	9.50E–08	9.50E–08	2.20E–07	7.30E–07	4.00E–07	7.20E–07	6.60E–08	1.73E–06	1.00E–07	2.40E–03	7.20E–07	7.80E–07
Zr-93	4.71E–09	1.31E–09	1.38E–09	3.56E–09	6.98E–08	1.16E–08	6.65E–08	9.23E–10	1.69E–06	1.38E–09	1.69E–06	7.45E–08	1.09E–07

Tabel E-3. DCC_ext_low_beta for limnic organisms ((μGy h^{-1})/(Bq l^{-1})).

Radionuclides	Amphibian	Benthic fish	Bird	Bivalve mollusc	Crustacean	Gastropod	Insect larvae	Mammal	Microphyto-benthos	Pelagic fish	Phyto-plankton	Vascular plant	Zooplankton
Ac-227	1.03E–14	6.03E–16	4.22E–16	3.27E–15	8.96E–28	6.46E–28	8.89E–28	6.60E–16	1.14E–07	4.22E–16	1.14E–07	1.61E–09	3.59E–12
Ag-108m	1.09E–15	6.03E–17	4.13E–17	3.32E–16	1.16E–30	8.35E–31	1.15E–30	6.77E–17	1.50E–08	4.13E–17	1.49E–08	2.11E–10	4.17E–13
Am-241	0	0	0	0	0	0	0	0	1.20E–07	0	0	0	0
Am-242m	7.90E–15	4.38E–16	3.01E–16	2.41E–15	6.28E–29	4.53E–29	6.23E–29	4.91E–16	1.07E–07	3.01E–16	1.06E–07	1.50E–09	3.00E–12
Am-243	1.57E–14	8.72E–16	5.98E–16	4.80E–15	1.37E–28	9.91E–29	1.36E–28	9.77E–16	2.11E–07	5.98E–16	2.11E–07	2.98E–09	5.95E–12
Ba-133	3.82E–15	2.11E–16	1.44E–16	1.16E–15	0	0	0	2.37E–16	5.25E–08	1.44E–16	5.25E–08	7.40E–10	1.46E–12
Be-10	9.18E–17	5.72E–18	4.11E–18	3.05E–17	1.79E–29	1.29E–29	1.78E–29	6.09E–18	7.07E–10	4.11E–18	7.06E–10	1.01E–11	2.79E–14
C-14-ind	0	0	0	0	0	0	0	0	1.11E–08	0	0	0	0
C-14-inorg	0	0	0	0	0	0	0	0	1.11E–08	0	0	0	0
C-14-org	0	0	0	0	0	0	0	0	1.11E–08	0	0	0	0
Ca-41	1.16E–15	6.41E–17	4.38E–17	3.53E–16	0	0	0	7.19E–17	1.59E–08	4.38E–17	1.59E–08	2.25E–10	4.44E–13
Cd-113m	3.99E–16	2.47E–17	1.77E–17	1.32E–16	7.42E–29	5.35E–29	7.36E–29	2.64E–17	3.19E–09	1.77E–17	3.19E–09	4.54E–11	1.23E–13
Cl-36	0	0	0	0	0	0	0	0	1.62E–09	0	0	0	0
Cm-242	0	0	0	0	0	0	0	0	1.65E–08	0	0	0	0
Cm-243	0	0	0	0	0	0	0	0	1.70E–07	0	0	0	0
Cm-244	0	0	0	0	0	0	0	0	1.53E–08	0	0	0	0
Cm-245	7.60E–15	4.20E–16	2.87E–16	2.31E–15	0	0	0	4.71E–16	1.04E–07	2.87E–16	1.04E–07	1.47E–09	2.91E–12
Cm-246	9.91E–16	5.47E–17	3.74E–17	3.01E–16	0	0	0	6.14E–17	1.36E–08	3.74E–17	1.36E–08	1.92E–10	3.79E–13
Co-60	0	0	0	0	0	0	0	0	6.60E–09	0	0	0	0
Cs-134	0	0	0	0	0	0	0	0	9.86E–09	0	0	0	0
Cs-135	0	0	0	0	0	0	0	0	8.81E–09	0	0	0	0
Cs-137	0	0	0	0	0	0	0	0	6.57E–09	0	0	0	0
Eu-152	0	0	0	0	0	0	0	0	5.28E–08	0	0	0	0
Eu-154	0	0	0	0	0	0	0	0	3.22E–08	0	0	0	0
Eu-155	5.31E–15	3.06E–16	2.13E–16	1.66E–15	3.49E–28	2.51E–28	3.46E–28	3.37E–16	6.21E–08	2.13E–16	6.21E–08	8.78E–10	1.89E–12
Fe-55	2.96E–15	1.63E–16	1.12E–16	9.00E–16	0	0	0	1.84E–16	4.07E–08	1.12E–16	4.06E–08	5.73E–10	1.13E–12
Gd-152	0	0	0	0	0	0	0	0	0	0	0	0	0
H-3	0	0	0	0	0	0	0	0	6.51E–08	0	6.60E–08	9.36E–10	2.60E–12
Ho-166m	9.87E–15	5.72E–16	3.99E–16	3.11E–15	7.32E–28	5.28E–28	7.26E–28	6.29E–16	1.13E–07	3.99E–16	1.13E–07	1.60E–09	3.48E–12
I-129	0	0	0	0	0	0	0	0	8.27E–08	0	0	0	0
In-115	5.08E–16	3.15E–17	2.26E–17	1.68E–16	9.43E–29	6.80E–29	9.36E–29	3.36E–17	4.06E–09	2.26E–17	4.06E–09	5.78E–11	1.56E–13
Mo-93	6.63E–16	3.66E–17	2.51E–17	2.02E–16	0	0	0	4.11E–17	9.11E–09	2.51E–17	9.10E–09	1.28E–10	2.54E–13
Nb-93m	5.40E–16	2.98E–17	2.04E–17	1.64E–16	0	0	0	3.35E–17	7.41E–09	2.04E–17	7.41E–09	1.05E–10	2.07E–13

Radionuclides	Amphibian	Benthic fish	Bird	Bivalve mollusc	Crustacean	Gastropod	Insect larvae	Mammal	Microphyto-benthos	Pelagic fish	Phyto-plankton	Vascular plant	Zooplankton
Nb-94	0	0	0	0	0	0	0	0	3.56E–09	0	0	0	0
Ni-59	0	0	0	0	0	0	0	0	5.09E–08	0	0	0	0
Ni-63	0	0	0	0	0	0	0	0	3.44E–08	0	0	6.10E–10	0
Np-237	0	0	0	0	0	0	0	0	1.19E–07	0	0	0	0
Pa-231	1.08E–14	5.98E–16	4.09E–16	3.29E–15	0	0	0	6.71E–16	1.49E–07	4.09E–16	1.49E–07	2.10E–09	4.14E–12
Pb-210	0	0	0	0	0	0	0	0	8.89E–08	0	0	0	0
Pd-107	5.79E–15	3.55E–16	2.54E–16	1.90E–15	9.80E–28	7.07E–28	9.72E–28	3.81E–16	4.93E–08	2.54E–16	4.92E–08	6.99E–10	1.82E–12
Pm-147	1.35E–15	8.37E–17	5.99E–17	4.46E–16	2.49E–28	1.79E–28	2.47E–28	8.93E–17	1.09E–08	5.99E–17	1.09E–08	1.55E–10	4.17E–13
Po-210	0	0	0	0	0	0	0	0	7.09E–15	0	0	0	0
Pu-238	0	0	0	0	0	0	0	0	1.67E–08	0	0	0	0
Pu-239	0	0	0	0	0	0	0	0	2.95E–08	0	0	0	0
Pu-240	0	0	0	0	0	0	0	0	1.59E–08	0	0	0	0
Pu-241	0	0	0	0	0	0	0	0	5.51E–08	0	0	7.68E–10	0
Pu-242	9.59E–16	5.29E–17	3.62E–17	2.92E–16	0	0	0	5.94E–17	1.32E–08	3.62E–17	1.32E–08	1.86E–10	3.67E–13
Ra-226	0	0	0	0	0	0	0	0	3.25E–08	0	0	0	0
Ra-228	0	0	0	0	0	0	0	0	1.85E–07	0	0	0	0
Ru-106	0	0	0	0	0	0	0	0	4.85E–08	0	0	0	0
Sb-125	0	0	0	0	0	0	0	0	4.27E–08	0	0	0	0
Se-79	0	0	0	0	0	0	0	0	9.34E–09	0	0	0	0
Sm-147	0	0	0	0	0	0	0	0	0	0	0	0	0
Sm-151	3.79E–15	2.34E–16	1.67E–16	1.25E–15	6.68E–28	4.82E–28	6.62E–28	2.50E–16	3.14E–08	1.67E–16	3.14E–08	4.47E–10	1.18E–12
Sn-126	3.37E–15	1.91E–16	1.32E–16	1.04E–15	1.28E–28	9.24E–29	1.27E–28	2.12E–16	4.24E–08	1.32E–16	4.23E–08	5.98E–10	1.24E–12
Sr-90	0	0	0	0	0	0	0	0	3.27E–09	0	0	0	0
Tc-99	0	0	0	0	0	0	0	0	5.69E–09	0	0	0	0
Th-228	0	0	0	0	0	0	0	0	7.71E–08	0	0	0	0
Th-229	1.55E–14	8.55E–16	5.85E–16	4.71E–15	0	0	0	9.60E–16	2.13E–07	5.85E–16	2.12E–07	3.00E–09	5.92E–12
Th-230	0	0	0	0	0	0	0	0	1.12E–08	0	0	0	0
Th-232	0	0	0	0	0	0	0	0	1.12E–08	0	0	0	0
U-232	1.28E–15	7.08E–17	4.84E–17	3.90E–16	0	0	0	7.95E–17	1.76E–08	4.84E–17	1.76E–08	2.48E–10	4.90E–13
U-233	9.07E–16	5.01E–17	3.43E–17	2.76E–16	0	0	0	5.62E–17	1.25E–08	3.43E–17	1.24E–08	1.76E–10	3.47E–13
U-234	0	0	0	0	0	0	0	0	1.47E–08	0	0	0	0
U-235	0	0	0	0	0	0	0	0	2.47E–07	0	0	0	0
U-236	1.01E–15	5.58E–17	3.82E–17	3.07E–16	0	0	0	6.26E–17	1.39E–08	3.82E–17	1.39E–08	1.96E–10	3.86E–13
U-238	0	0	0	0	0	0	0	0	1.22E–08	0	0	0	0
Zr-93	3.50E–15	2.17E–16	1.55E–16	1.16E–15	6.44E–28	4.65E–28	6.39E–28	2.31E–16	2.81E–08	1.55E–16	2.81E–08	4.00E–10	1.08E–12

Tabel E-4. DCC_ext_low_beta for marine organisms ((µGy h⁻¹)/(Bq l⁻¹)).

Radionuclides	(Wading) bird	Benthic fish	Benthic mollusc	Crustacean	European otter	Macroalgae	Mammal	Pelagic fish	Phyto-plankton	Polychaete worm	Ruddy turnstone	Vascular plant	Zooplankton
Ac-227	4.22E–16	1.03E–14	9.37E–15	4.35E–28	2.94E–16	3.29E–12	6.26E–17	4.46E–28	1.57E–11	9.89E–15	4.44E–28	1.10E–14	8.20E–28
Ag-108m	4.13E–17	1.16E–15	9.76E–16	5.62E–31	2.93E–17	4.07E–13	6.35E–18	5.77E–31	1.84E–12	1.03E–15	5.74E–31	1.16E–15	1.06E–30
Am-241	0	0	0	0	2.34E–16	0	0	0	0	0	0	0	0
Am-242m	3.01E–16	8.37E–15	7.07E–15	3.05E–29	2.13E–16	2.91E–12	4.61E–17	3.13E–29	1.32E–11	7.49E–15	3.11E–29	8.38E–15	5.75E–29
Am-243	5.98E–16	1.66E–14	1.41E–14	6.67E–29	4.23E–16	5.78E–12	9.17E–17	6.85E–29	2.62E–11	1.49E–14	6.81E–29	1.67E–14	1.26E–28
Ba-133	1.44E–16	4.08E–15	3.42E–15	0	1.02E–16	1.43E–12	2.22E–17	0	6.45E–12	3.62E–15	0	4.06E–15	0
Be-10	4.11E–18	8.40E–17	8.49E–17	8.70E–30	2.82E–18	2.30E–14	5.84E–19	8.93E–30	1.20E–13	8.92E–17	8.88E–30	9.75E–17	1.64E–29
C-14-ind	0	0	0	0	4.28E–17	0	0	0	0	0	1.31E–28	0	0
C-14-inorg	0	0	0	0	4.28E–17	0	0	0	0	0	1.31E–28	0	0
C-14-org	0	0	0	0	4.28E–17	0	0	0	0	0	1.31E–28	0	0
Ca-41	4.38E–17	1.24E–15	1.04E–15	0	3.11E–17	4.33E–13	6.75E–18	0	1.96E–12	1.10E–15	0	1.23E–15	0
Cd-113m	1.77E–17	3.68E–16	3.68E–16	3.60E–29	1.22E–17	1.03E–13	2.53E–18	3.70E–29	5.28E–13	3.88E–16	3.68E–29	4.24E–16	6.79E–29
Cl-36	0	0	0	0	5.90E–18	0	0	0	0	0	1.69E–29	0	0
Cm-242	0	0	0	0	3.21E–17	0	0	0	0	0	0	0	0
Cm-243	0	0	0	0	3.31E–16	0	0	0	0	0	0	0	0
Cm-244	0	0	0	0	2.99E–17	0	0	0	0	0	0	0	0
Cm-245	2.87E–16	8.11E–15	6.80E–15	0	2.04E–16	2.84E–12	4.42E–17	0	1.28E–11	7.20E–15	0	8.07E–15	0
Cm-246	3.74E–17	1.06E–15	8.86E–16	0	2.65E–17	3.70E–13	5.76E–18	0	1.67E–12	9.39E–16	0	1.05E–15	0
Co-60	0	0	0	0	2.51E–17	0	0	0	0	0	7.54E–29	0	0
Cs-134	0	0	0	0	3.61E–17	0	0	0	0	0	1.04E–28	0	0
Cs-135	0	0	0	0	3.33E–17	0	0	0	0	0	9.96E–29	0	0
Cs-137	0	0	0	0	1.92E–17	0	0	0	0	0	3.97E–29	0	0
Eu-152	0	0	0	0	1.05E–16	0	0	0	0	0	9.84E–30	0	0
Eu-154	0	0	0	0	7.13E–17	0	0	0	0	0	5.33E–29	0	0
Eu-155	2.13E–16	5.39E–15	4.80E–15	1.69E–28	1.49E–16	1.76E–12	3.18E–17	1.74E–28	8.27E–12	5.07E–15	1.73E–28	5.63E–15	3.19E–28
Fe-55	1.12E–16	3.16E–15	2.65E–15	0	7.93E–17	1.11E–12	1.72E–17	0	4.99E–12	2.80E–15	0	3.14E–15	0
Gd-152	0	0	0	0	0	0	0	0	0	0	0	0	0
H-3	0	7.80E–15	0	0	2.02E–16	1.98E–12	0	0	6.60E–08	0	4.66E–28	0	0
Ho-166m	3.99E–16	9.97E–15	8.94E–15	3.55E–28	2.79E–16	3.23E–12	5.95E–17	3.65E–28	1.52E–11	9.45E–15	3.63E–28	1.05E–14	6.70E–28
I-129	0	0	0	0	1.83E–16	0	0	0	0	0	1.34E–28	0	0
In-115	2.26E–17	4.69E–16	4.69E–16	4.58E–29	1.55E–17	1.31E–13	3.22E–18	4.70E–29	6.72E–13	4.93E–16	4.67E–29	5.39E–16	8.64E–29
Mo-93	2.51E–17	7.07E–16	5.93E–16	0	1.78E–17	2.48E–13	3.86E–18	0	1.12E–12	6.28E–16	0	7.04E–16	0
Nb-93m	2.04E–17	5.76E–16	4.83E–16	0	1.45E–17	2.02E–13	3.14E–18	0	9.10E–13	5.11E–16	0	5.73E–16	0

Radionuclides	(Wading) bird	Benthic fish	Benthic mollusc	Crustacean	European otter	Macroalgae	Mammal	Pelagic fish	Phyto-plankton	Polychaete worm	Ruddy turnstone	Vascular plant	Zooplankton
Nb-94	0	0	0	0	1.35E–17	0	0	0	0	0	4.05E–29	0	0
Ni-59	0	0	0	0	9.92E–17	0	0	0	0	0	0	0	0
Ni-63	0	0	0	0	1.26E–16	0	0	0	0	0	3.63E–28	0	0
Np-237	0	0	0	0	2.32E–16	0	0	0	0	0	0	0	0
Pa-231	4.09E–16	1.15E–14	9.67E–15	0	2.90E–16	4.04E–12	6.29E–17	0	1.82E–11	1.02E–14	0	1.15E–14	0
Pb-210	0	0	0	0	2.19E–16	0	0	0	0	0	2.84E–28	0	0
Pd-107	2.54E–16	5.42E–15	5.33E–15	4.76E–28	1.75E–16	1.55E–12	3.64E–17	4.88E–28	7.85E–12	5.61E–15	4.86E–28	6.15E–15	8.97E–28
Pm-147	5.99E–17	1.25E–15	1.25E–15	1.21E–28	4.11E–17	3.49E–13	8.56E–18	1.24E–28	1.79E–12	1.31E–15	1.23E–28	1.43E–15	2.28E–28
Po-210	0	0	0	0	1.38E–23	0	0	0	0	0	0	0	0
Pu-238	0	0	0	0	3.26E–17	0	0	0	0	0	0	0	0
Pu-239	0	0	0	0	5.75E–17	0	0	0	0	0	0	0	0
Pu-240	0	0	0	0	3.10E–17	0	0	0	0	0	0	0	0
Pu-241	0	0	0	0	1.69E–16	0	0	0	0	0	3.82E–28	0	0
Pu-242	3.62E–17	1.02E–15	8.57E–16	0	2.57E–17	3.58E–13	5.57E–18	0	1.62E–12	9.08E–16	0	1.02E–15	0
Ra-226	0	0	0	0	7.06E–17	0	0	0	0	0	4.47E–29	0	0
Ra-228	0	0	0	0	4.40E–16	0	0	0	0	0	4.91E–28	0	0
Ru-106	0	0	0	0	1.70E–16	0	0	0	0	0	4.69E–28	0	0
Sb-125	0	0	0	0	1.05E–16	0	0	0	0	0	1.33E–28	0	0
Se-79	0	0	0	0	3.58E–17	0	0	0	0	0	1.09E–28	0	0
Sm-147	0	0	0	0	0	0	0	0	0	0	0	0	0
Sm-151	1.67E–16	3.53E–15	3.49E–15	3.24E–28	1.15E–16	9.97E–13	2.39E–17	3.33E–28	5.09E–12	3.68E–15	3.31E–28	4.02E–15	6.12E–28
Sn-126	1.32E–16	3.50E–15	3.03E–15	6.22E–29	9.29E–17	1.18E–12	2.00E–17	6.38E–29	5.44E–12	3.21E–15	6.35E–29	3.58E–15	1.17E–28
Sr-90	0	0	0	0	1.25E–17	0	0	0	0	0	3.76E–29	0	0
Tc-99	0	0	0	0	2.16E–17	0	0	0	0	0	6.52E–29	0	0
Th-228	0	0	0	0	1.65E–16	0	0	0	0	0	9.24E–29	0	0
Th-229	5.85E–16	1.65E–14	1.38E–14	0	4.15E–16	5.78E–12	9.00E–17	0	2.61E–11	1.47E–14	0	1.64E–14	0
Th-230	0	0	0	0	2.19E–17	0	0	0	0	0	0	0	0
Th-232	0	0	0	0	2.18E–17	0	0	0	0	0	0	0	0
U-232	4.84E–17	1.37E–15	1.15E–15	0	3.43E–17	4.79E–13	7.45E–18	0	2.16E–12	1.21E–15	0	1.36E–15	0
U-233	3.43E–17	9.67E–16	8.10E–16	0	2.43E–17	3.39E–13	5.27E–18	0	1.53E–12	8.59E–16	0	9.62E–16	0
U-234	0	0	0	0	2.88E–17	0	0	0	0	0	0	0	0
U-235	0	0	0	0	4.98E–16	0	0	0	0	0	1.03E–28	0	0
U-236	3.82E–17	1.08E–15	9.03E–16	0	2.71E–17	3.77E–13	5.88E–18	0	1.70E–12	9.57E–16	0	1.07E–15	0
U-238	0	0	0	0	2.38E–17	0	0	0	0	0	0	0	0
Zr-93	1.55E–16	3.23E–15	3.23E–15	3.13E–28	1.07E–16	9.02E–13	2.22E–17	3.21E–28	4.64E–12	3.40E–15	3.19E–28	3.71E–15	5.90E–28

Tabel E-5. DCC_ext_in_soil_beta_gamma for terrestrial organisms (μGy h^{-1})/(Bq $kgdw^{-1}$)).

Radionuclides	Amphibian	Bird	Bird egg	Detritivorous invertebrate	Flying insects	Gastropod	Grasses & Herbs	Lichen & bryophytes	Mammal (Deer)	Mammal (Rat)	Reptile	Shrub	Soil Invertebrate (worm)	Tree
Ac-227	4.97E–08			5.10E–08		5.08E–08				4.65E–08	4.40E–08		5.05E–08	
Ag-108m	8.48E–04			8.66E–04		8.64E–04				8.06E–04	7.73E–04		8.60E–04	
Am-241	6.00E–06			6.20E–06		6.10E–06				5.50E–06	5.20E–06		6.10E–06	
Am-242m	4.84E–06			4.96E–06		4.95E–06				4.54E–06	4.30E–06		4.92E–06	
Am-243	7.67E–05			7.82E–05		7.80E–05				7.31E–05	7.02E–05		7.77E–05	
Ba-133	1.75E–04			1.79E–04		1.78E–04				1.66E–04	1.60E–04		1.78E–04	
Be-10	0			0		0				0	0		0	
C-14-ind	0			0		0				0	0		0	
C-14-inorg	0			0		0				0	0		0	
C-14-org	0			0		0				0	0		0	
Ca-41	8.15E–09			8.70E–09		8.62E–09				6.86E–09	5.84E–09		8.50E–09	
Cd-113m	0			0		0				0	0		0	
Cl-36	7.90E–08			8.10E–08		8.10E–08				7.50E–08	7.20E–08		8.00E–08	
Cm-242	1.70E–07			1.80E–07		1.80E–07				1.40E–07	1.20E–07		1.80E–07	
Cm-243	4.90E–05			5.00E–05		5.00E–05				4.70E–05	4.50E–05		5.00E–05	
Cm-244	1.60E–07			1.70E–07		1.60E–07				1.30E–07	1.10E–07		1.60E–07	
Cm-245	2.77E–05			2.83E–05		2.82E–05				2.65E–05	2.55E–05		2.81E–05	
Cm-246	1.39E–07			1.48E–07		1.47E–07				1.18E–07	1.02E–07		1.45E–07	
Co-60	1.30E–03			1.30E–03		1.30E–03				1.20E–03	1.20E–03		1.30E–03	
Cs-134	8.20E–04			8.40E–04		8.30E–04				7.80E–04	7.50E–04		8.30E–04	
Cs-135	0			0		0				0	0		0	
Cs-137	3.00E–04			3.10E–04		3.00E–04				2.80E–04	2.70E–04		3.00E–04	
Eu-152	5.70E–04			5.80E–04		5.80E–04				5.50E–04	5.30E–04		5.80E–04	
Eu-154	6.30E–04			6.40E–04		6.40E–04				6.00E–04	5.80E–04		6.30E–04	
Eu-155	1.56E–05			1.59E–05		1.59E–05				1.49E–05	1.44E–05		1.58E–05	
Fe-55	5.86E–08			6.26E–08		6.20E–08				4.93E–08	4.20E–08		6.12E–08	
Gd-152	0			0		0				0	0		0	
H-3	0			0		0				0	0		0	
Ho-166m	8.89E–04			9.08E–04		9.05E–04				8.47E–04	8.13E–04		9.01E–04	
I-129	3.40E–06			3.60E–06		3.50E–06				3.00E–06	2.70E–06		3.50E–06	
In-115	0			0		0				0	0		0	
Mo-93	9.65E–07			1.03E–06		1.02E–06				8.16E–07	7.00E–07		1.01E–06	
Nb-93m	1.70E–07			1.81E–07		1.80E–07				1.44E–07	1.23E–07		1.77E–07	

Radionuclides	Amphibian	Bird	Bird egg	Detritivorous invertebrate	Flying insects	Gastropod	Grasses & Herbs	Lichen & bryophytes	Mammal (Deer)	Mammal (Rat)	Reptile	Shrub	Soil Invertebrate (worm)	Tree
Nb-94	8.30E–04			8.50E–04		8.40E–04				7.90E–04	7.60E–04		8.40E–04	
Ni-59	9.80E–08			1.00E–07		1.00E–07				8.20E–08	7.00E–08		1.00E–07	
Ni-63	0			0		0				0	0		0	
Np-237	7.50E–06			7.70E–06		7.70E–06				7.00E–06	6.70E–06		7.60E–06	
Pa-231	1.76E–05			1.80E–05		1.79E–05				1.66E–05	1.58E–05		1.78E–05	
Pb-210	5.80E–07			6.10E–07		6.10E–07				5.20E–07	4.70E–07		6.00E–07	
Pd-107														
Pm-147	1.27E–09			1.30E–09		1.30E–09				1.21E–09	1.17E–09		1.29E–09	
Po-210	4.50E–09			4.60E–09		4.60E–09				4.30E–09	4.10E–09		4.50E–09	
Pu-238	1.60E–07			1.70E–07		1.70E–07				1.40E–07	1.20E–07		1.70E–07	
Pu-239	8.20E–08			8.60E–08		8.60E–08				7.20E–08	6.40E–08		8.50E–08	
Pu-240	1.60E–07			1.70E–07		1.60E–07				1.30E–07	1.10E–07		1.60E–07	
Pu-241	5.50E–10			5.60E–10		5.60E–10				5.20E–10	4.90E–10		5.60E–10	
Pu-242	1.30E–07			1.39E–07		1.37E–07				1.11E–07	9.55E–08		1.36E–07	
Ra-226	8.90E–04			9.10E–04		9.00E–04				8.50E–04	8.20E–04		9.00E–04	
Ra-228	4.90E–04			5.00E–04		5.00E–04				4.70E–04	4.50E–04		5.00E–04	
Ru-106	1.10E–04			1.10E–04		1.10E–04				1.00E–04	9.80E–05		1.10E–04	
Sb-125	2.20E–04			2.20E–04		2.20E–04				2.10E–04	2.00E–04		2.20E–04	
Se-79	0			0		0				0	0		0	
Sm-147	0			0		0				0	0		0	
Sm-151	9.46E–10			1.01E–09		9.97E–10				8.06E–10	6.96E–10		9.84E–10	
Sn-126	8.26E–04			8.44E–04		8.41E–04				7.86E–04	7.54E–04		8.37E–04	
Sr-90	1.50E–10			1.60E–10		1.50E–10				1.20E–10	1.10E–10		1.50E–10	
Tc-99	0			0		0				0	0		0	
Th-228	7.80E–04			7.90E–04		7.90E–04				7.40E–04	7.20E–04		7.90E–04	
Th-229	2.74E–05			2.79E–05		2.79E–05				2.61E–05	2.51E–05		2.77E–05	
Th-230	2.00E–07			2.10E–07		2.10E–07				1.80E–07	1.70E–07		2.10E–07	
Th-232	1.40E–07			1.50E–07		1.50E–07				1.20E–07	1.10E–07		1.40E–07	
U-232	2.40E–07			2.52E–07		2.50E–07				2.11E–07	1.88E–07		2.48E–07	
U-233	2.03E–07			2.11E–07		2.10E–07				1.84E–07	1.69E–07		2.08E–07	
U-234	1.70E–07			1.80E–07		1.80E–07				1.50E–07	1.30E–07		1.70E–07	
U-235	6.60E–05			6.70E–05		6.70E–05				6.30E–05	6.00E–05		6.70E–05	
U-236	1.43E–07			1.52E–07		1.51E–07				1.23E–07	1.06E–07		1.49E–07	
U-238	1.20E–07			1.30E–07		1.30E–07				1.00E–07	8.70E–08		1.20E–07	
Zr-93	0			0		0				0	0		0	

Tabel E-6. DCC_ext_on_soil_beta_gamma for terrestrial organisms ((µGy h^{-1})/(Bq $kgdw^{-1}$).

Radio-nuclides	Amphibian	Bird	Bird egg	Detritivorous invertebrate	European otter	Flying insects	Gastropod	Grasses & Herbs	Lichen & bryophytes	Mammal (Deer)	Mammal (Rat)	Reptile	Ruddy turnstone	Shrub	Soil Invertebrate (worm)	Tree
Ac-227	2.21E–08	2.04E–08	2.21E–08	2.24E–08	1.77E–08	2.24E–08	2.24E–08	2.82E–08	1.16E–08	8.80E–09	2.16E–08	2.11E–08	2.13E–08	2.18E–08		1.65E–08
Ag-108m	3.29E–04	3.05E–04	3.28E–04	3.32E–04	2.72E–04	3.32E–04	3.31E–04	3.25E–04	1.73E–04	1.61E–04	3.22E–04	3.14E–04	3.17E–04	3.07E–04		2.59E–04
Am-241	2.60E–06	2.50E–06	2.50E–06	2.60E–06	2.04E–06	2.60E–06	2.60E–06	3.30E–06	5.90E–11	9.20E–07	2.50E–06	2.40E–06	2.46E–06	2.70E–06		1.90E–06
Am-242m	2.21E–06	2.04E–06	2.20E–06	2.23E–06	1.78E–06	2.23E–06	2.22E–06	2.85E–06	1.16E–06	8.85E–07	2.16E–06	2.10E–06	2.12E–06	2.35E–06		1.76E–06
Am-243	3.49E–05	3.21E–05	3.48E–05	3.52E–05	2.83E–05	3.52E–05	3.52E–05	3.69E–05	1.83E–05	1.52E–05	3.41E–05	3.31E–05	3.35E–05	3.44E–05		2.89E–05
Ba-133	7.29E–05	6.67E–05	7.25E–05	7.34E–05	5.91E–05	7.34E–05	7.34E–05	7.42E–05	3.82E–05	3.43E–05	7.10E–05	6.90E–05	6.96E–05	6.97E–05		5.83E–05
Be-10	0	0	0	0	0	0	0	0	0	0	0	0	0	0		0
C-14-ind	0	0	0	0	0	0	0	0	0	0	0	0	0	0		0
C-14-inorg	0	0	0	0	0	0	0	0	0	0	0	0	0	0		0
C-14-org	0	0	0	0	0	0	0	0	0	0	0	0	0	0		0
Ca-41	8.54E–41	8.23E–41	8.52E–41	8.78E–41	7.34E–41	8.77E–41	8.75E–41	1.07E–08	4.57E–41	3.25E–41	8.50E–41	8.54E–41	8.53E–41	7.70E–10		2.26E–13
Cd-113m	0	0	0	0	0	0	0	0	0	0	0	0	0	0		0
Cl-36	3.10E–08	3.10E–08	3.10E–08	3.10E–08	2.56E–08	3.10E–08	3.10E–08	3.10E–08	1.60E–12	1.50E–08	3.00E–08	3.00E–08	2.99E–08	2.90E–08		2.50E–08
Cm-242	4.60E–08	4.60E–08	4.60E–08	4.70E–08	3.56E–08	4.70E–08	4.70E–08	1.40E–07	6.90E–13	1.30E–08	4.50E–08	4.40E–08	4.46E–08	6.40E–08		1.30E–08
Cm-243	2.20E–05	2.20E–05	2.20E–05	2.20E–05	1.80E–05	2.20E–05	2.20E–05	2.30E–05	8.40E–10	9.90E–06	2.20E–05	2.10E–05	2.12E–05	2.10E–05		1.80E–05
Cm-244	4.20E–08	4.20E–08	4.20E–08	4.30E–08	3.20E–08	4.30E–08	4.20E–08	1.30E–07	5.90E–13	1.10E–08	4.10E–08	4.00E–08	4.02E–08	5.80E–08		1.10E–08
Cm-245	1.35E–05	1.24E–05	1.34E–05	1.36E–05	1.09E–05	1.36E–05	1.36E–05	1.47E–05	7.07E–06	5.63E–06	1.32E–05	1.28E–05	1.29E–05	1.35E–05		1.13E–05
Cm-246	3.74E–08	3.42E–08	3.72E–08	3.82E–08	2.86E–08	3.82E–08	3.80E–08	1.13E–07	1.96E–08	1.01E–08	3.65E–08	3.57E–08	3.60E–08	5.18E–08		9.84E–09
Co-60	4.90E–04	4.90E–04	4.90E–04	5.00E–04	4.20E–04	5.00E–04	5.00E–04	4.80E–04	3.00E–08	2.60E–04	4.80E–04	4.70E–04	4.75E–04	4.50E–04		3.90E–04
Cs-134	3.20E–04	3.10E–04	3.10E–04	3.20E–04	2.63E–04	3.20E–04	3.20E–04	3.10E–04	1.70E–08	1.60E–04	3.10E–04	3.00E–04	3.04E–04	2.90E–04		2.50E–04
Cs-135	0	0	0	0	0	0	0	0	0	0	0	0	0	0		0
Cs-137	1.10E–04	1.10E–04	1.10E–04	1.20E–04	9.51E–05	1.20E–04	1.20E–04	1.10E–04	6.10E–09	5.60E–05	1.10E–04	1.10E–04	1.10E–04	1.10E–04		9.00E–05
Eu-152	2.20E–04	2.20E–04	2.20E–04	2.30E–04	1.89E–04	2.30E–04	2.30E–04	2.20E–04	1.30E–08	1.10E–04	2.20E–04	2.10E–04	2.15E–04	2.10E–04		1.80E–04
Eu-154	2.40E–04	2.40E–04	2.40E–04	2.50E–04	2.06E–04	2.50E–04	2.50E–04	2.40E–04	1.40E–08	1.20E–04	2.40E–04	2.30E–04	2.35E–04	2.20E–04		1.90E–04
Eu-155	7.59E–06	7.04E–06	7.57E–06	7.67E–06	6.16E–06	7.66E–06	7.65E–06	8.41E–06	3.99E–06	3.07E–06	7.43E–06	7.24E–06	7.30E–06	7.84E–06		6.60E–06
Fe-55	6.15E–40	5.92E–40	6.13E–40	6.32E–40	5.28E–40	6.31E–40	6.29E–40	7.70E–08	3.29E–40	2.34E–40	6.11E–40	6.14E–40	6.14E–40	5.54E–09		1.62E–12
Gd-152	0	0	0	0	0	0	0	0	0	0	0	0	0	0		0
H-3	0	0	0	0	0	0	0	0	0	0	0	0	0	0		0
Ho-166m	3.48E–04	3.23E–04	3.47E–04	3.51E–04	2.89E–04	3.51E–04	3.50E–04	3.43E–04	1.83E–04	1.70E–04	3.40E–04	3.32E–04	3.34E–04	3.24E–04		2.75E–04
I-129	1.10E–06	1.10E–06	1.10E–06	1.20E–06	9.13E–07	1.10E–06	1.10E–06	1.90E–06	2.20E–11	4.00E–07	1.10E–06	1.10E–06	1.10E–06	1.60E–06		8.80E–07
In-115	0	0	0	0	0	0	0	0	0	0	0	0	0	0		0
Mo-93	9.99E–08	9.24E–08	9.95E–08	1.01E–07	7.90E–08	1.01E–07	1.01E–07	7.90E–07	5.39E–08	3.09E–08	9.78E–08	9.58E–08	9.65E–08	3.59E–07		5.34E–08

Radio-nuclides	Amphibian	Bird	Bird egg	Detritivorous invertebrate	European otter	Flying insects	Gastropod	Grasses & Herbs	Lichen & bryophytes	Mammal (Deer)	Mammal (Rat)	Reptile	Ruddy turnstone	Shrub	Soil Invertebrate (worm)	Tree
Nb-93m	1.76E–08	1.63E–08	1.75E–08	1.78E–08	1.39E–08	1.78E–08	1.78E–08	1.40E–07	9.49E–09	5.44E–09	1.72E–08	1.69E–08	1.70E–08	6.33E–08		9.41E–09
Nb-94	3.20E–04	3.20E–04	3.20E–04	3.20E–04	2.67E–04	3.20E–04	3.20E–04	3.10E–04	1.80E–08	1.60E–04	3.10E–04	3.00E–04	3.07E–04	2.90E–04		2.50E–04
Ni-59	1.00E–39	1.00E–39	1.00E–39	1.10E–39	8.86E–40	1.10E–39	1.10E–39	1.30E–07	1.50E–44	3.70E–40	1.00E–39	1.00E–39	1.03E–39	9.30E–09		2.70E–12
Ni-63	0	0	0	0	0	0	0	0	0	0	0	0	0	0		0
Np-237	3.60E–06	3.60E–06	3.60E–06	3.60E–06	2.86E–06	3.60E–06	3.60E–06	4.20E–06	1.00E–10	1.40E–06	3.50E–06	3.40E–06	3.43E–06	3.60E–06		2.80E–06
Pa-231	7.34E–06	6.70E–06	7.30E–06	7.40E–06	5.92E–06	7.40E–06	7.40E–06	7.91E–06	3.85E–06	3.37E–06	7.14E–06	6.94E–06	7.00E–06	6.95E–06		5.65E–06
Pb-210	2.80E–07	2.80E–07	2.80E–07	2.90E–07	2.14E–07	2.90E–07	2.90E–07	4.00E–07	4.10E–12	7.70E–08	2.80E–07	7.20E–06	2.71E–07	2.00E–07		1.30E–07
Pd-107					0								0			
Pm-147	6.07E–10	5.60E–10	6.05E–10	6.12E–10	4.92E–10	6.12E–10	6.11E–10	6.60E–10	3.19E–10	2.53E–10	5.93E–10	5.77E–10	5.83E–10	6.19E–10		5.13E–10
Po-210	1.70E–09	1.70E–09	1.70E–09	1.70E–09	1.44E–09	1.70E–09	1.70E–09	1.70E–09	9.60E–14	8.60E–10	1.70E–09	1.60E–09	1.66E–09	1.60E–09		1.40E–09
Pu-238	6.30E–08	6.30E–08	6.30E–08	6.50E–08	4.67E–08	6.50E–08	6.50E–08	1.40E–07	6.60E–13	1.40E–08	6.10E–08	6.00E–08	6.06E–08	5.80E–08		1.10E–08
Pu-239	3.30E–08	3.20E–08	3.20E–08	3.40E–08	2.48E–08	3.30E–08	3.30E–08	6.00E–08	6.10E–13	9.50E–09	3.20E–08	3.10E–08	3.13E–08	3.10E–08		1.10E–08
Pu-240	6.00E–08	6.00E–08	6.00E–08	6.20E–08	4.46E–08	6.20E–08	6.20E–08	1.30E–07	6.40E–13	1.40E–08	5.90E–08	5.70E–08	5.78E–08	5.60E–08		1.00E–08
Pu-241	2.60E–10	2.60E–10	2.60E–10	2.70E–10	2.12E–10	2.70E–10	2.70E–10	3.20E–10	7.70E–15	1.00E–10	2.60E–10	2.50E–10	2.54E–10	2.60E–10		2.00E–10
Pu-242	5.01E–08	4.55E–08	4.98E–08	5.18E–08	3.72E–08	5.17E–08	5.14E–08	1.08E–07	2.59E–08	1.17E–08	4.88E–08	4.78E–08	4.82E–08	4.63E–08		8.74E–09
Ra-226	3.40E–04	3.40E–04	3.40E–04	3.50E–04	2.91E–04	3.50E–04	3.50E–04	3.30E–04	2.00E–08	1.80E–04	3.40E–04	3.30E–04	3.32E–04	3.20E–04		2.70E–04
Ra-228	1.90E–04	1.90E–04	1.90E–04	1.90E–04	1.61E–04	1.90E–04	1.90E–04	1.90E–04	1.10E–08	9.70E–05	1.90E–04	1.80E–04	1.85E–04	1.80E–04		1.50E–04
Ru-106	4.20E–05	4.10E–05	4.10E–05	4.20E–05	3.45E–05	4.20E–05	4.20E–05	4.10E–05	2.20E–09	2.10E–05	4.10E–05	4.00E–05	4.01E–05	3.90E–05		3.30E–05
Sb-125	8.50E–05	8.50E–05	8.50E–05	8.60E–05	7.02E–05	8.60E–05	8.60E–05	8.50E–05	4.20E–09	4.10E–05	8.30E–05	8.10E–05	8.20E–05	8.00E–05		6.70E–05
Se-79	0	0	0	0	0	0	0	0	0	0	0	0	0	0		0
Sm-147	0	0	0	0	0	0	0	0	0	0	0	0	0	0		0
Sm-151	2.44E–10	2.25E–10	2.43E–10	2.48E–10	1.93E–10	2.47E–10	2.46E–10	8.20E–10	1.28E–10	7.74E–11	2.39E–10	2.33E–10	2.35E–10	3.28E–10		8.81E–11
Sn-126	3.22E–04	2.98E–04	3.21E–04	3.24E–04	2.66E–04	3.24E–04	3.24E–04	3.18E–04	1.69E–04	1.58E–04	3.14E–04	3.07E–04	3.09E–04	3.01E–04		2.54E–04
Sr-90	1.60E–11	1.60E–11	1.60E–11	1.60E–11	1.25E–11	1.60E–11	1.60E–11	1.30E–10	3.70E–16	4.60E–12	1.60E–11	1.50E–11	1.55E–11	5.10E–11		5.90E–12
Tc-99	0	0	0	0	0	0	0	0	0	0	0	0	0	0		0
Th-228	2.90E–04	2.90E–04	2.90E–04	2.90E–04	2.50E–04	2.90E–04	2.90E–04	2.80E–04	1.80E–08	1.60E–04	2.90E–04	2.80E–04	2.83E–04	2.70E–04		2.30E–04
Th-229	1.28E–05	1.19E–05	1.28E–05	1.30E–05	1.04E–05	1.29E–05	1.29E–05	1.42E–05	6.74E–06	5.38E–06	1.25E–05	1.22E–05	1.23E–05	1.29E–05		1.08E–05
Th-230	7.10E–08	7.00E–08	7.00E–08	7.20E–08	5.58E–08	7.20E–08	7.20E–08	1.40E–07	1.80E–12	2.50E–08	6.90E–08	6.70E–08	6.80E–08	7.80E–08		4.40E–08
Th-232	4.30E–08	4.30E–08	4.30E–08	4.40E–08	3.32E–08	4.40E–08	4.30E–08	1.10E–07	9.00E–13	1.30E–08	4.20E–08	4.10E–08	4.12E–08	5.00E–08		2.10E–08
U-232	9.96E–08	9.06E–08	9.91E–08	1.03E–07	7.52E–08	1.03E–07	1.02E–07	1.82E–07	5.18E–08	2.77E–08	9.71E–08	9.50E–08	9.57E–08	8.86E–08		3.54E–08
U-233	8.72E–08	7.95E–08	8.67E–08	8.91E–08	6.77E–08	8.89E–08	8.87E–08	1.30E–07	4.54E–08	3.03E–08	8.49E–08	8.29E–08	8.36E–08	7.91E–08		4.69E–08
U-234	6.90E–08	6.90E–08	6.90E–08	7.20E–08	5.14E–08	7.10E–08	7.10E–08	1.40E–07	9.10E–13	1.70E–08	6.70E–08	6.60E–08	6.65E–08	5.90E–08		1.80E–08
U-235	2.90E–05	2.90E–05	2.90E–05	3.00E–05	2.38E–05	3.00E–05	3.00E–05	3.10E–05	1.10E–09	1.30E–05	2.90E–05	2.80E–05	2.81E–05	2.80E–05		2.40E–05
U-236	5.82E–08	5.27E–08	5.79E–08	6.06E–08	4.28E–08	6.03E–08	6.00E–08	1.20E–07	3.01E–08	1.33E–08	5.67E–08	5.56E–08	5.60E–08	4.87E–08		1.10E–08
U-238	4.80E–08	4.80E–08	4.80E–08	5.00E–08	3.49E–08	5.00E–08	4.90E–08	1.00E–07	4.60E–13	1.00E–08	4.70E–08	4.60E–08	4.61E–08	4.00E–08		6.90E–09
Zr-93	0	0	0	0	0	0	0	0	0	0	0	0	0	0		0

Tabel E-7. DCC_ext_in_air_beta_gamma for terrestrial organisms ((μGy h^{-1})/(Bq $kgdw^{-1}$)).

Radio-nuclides	Amphibian	Bird	Bird egg	Detritivorous invertebrate	European otter	Flying insects	Gastropod	Grasses & Herbs	Lichen & bryophytes	Mammal (Deer)	Mammal (Rat)	Reptile	Ruddy turnstone	Shrub	Soil Invertebrate (worm)	Tree
Ac-227		2.05E–08	2.21E–08										2.13E–08			
Ag-108m		3.05E–04	3.28E–04										3.17E–04			
Am-241		2.00E–06				2.60E–06							2.47E–06			
Am-242m		2.04E–06	2.20E–06										2.12E–06			
Am-243		3.22E–05	3.48E–05										3.35E–05			
Ba-133		6.69E–05	7.25E–05										6.96E–05			
Be-10		0	0										0			
C-14-ind		0				0							0			
C-14-inorg		0				0							0			
C-14-org		0				0							0			
Ca-41		8.54E–41	8.54E–41										8.54E–41			
Cd-113m		0	0										0			
Cl-36		2.70E–08				3.10E–08							2.99E–08			
Cm-242		1.90E–08				4.70E–08							4.47E–08			
Cm-243		1.90E–05				2.20E–05							2.12E–05			
Cm-244		1.60E–08				4.30E–08							4.03E–08			
Cm-245		1.25E–05	1.34E–05										1.29E–05			
Cm-246		3.47E–08	3.73E–08										3.60E–08			
Co-60		4.30E–04				5.00E–04							4.75E–04			
Cs-134		2.80E–04				3.20E–04							3.04E–04			
Cs-135		0				0							0			
Cs-137		1.00E–04				1.20E–04							1.10E–04			
Eu-152		2.00E–04				2.30E–04							2.15E–04			
Eu-154		2.10E–04				2.50E–04							2.35E–04			
Eu-155		7.04E–06	7.57E–06										7.31E–06			
Fe-55		6.15E–40	6.15E–40										6.15E–40			
Gd-152		0	0										0			
H-3		0				0							0			
Ho-166m		3.22E–04	3.47E–04										3.34E–04			
I-129		8.80E–07				1.10E–06							1.10E–06			
In-115		0	0										0			
Mo-93		9.33E–08	9.97E–08										9.66E–08			
Nb-93m		1.64E–08	1.76E–08										1.70E–08			

Radio-nuclides	Amphibian	Bird	Bird egg	Detritivorous invertebrate	European otter	Flying insects	Gastropod	Grasses & Herbs	Lichen & bryophytes	Mammal (Deer)	Mammal (Rat)	Reptile	Ruddy turnstone	Shrub	Soil Invertebrate (worm)	Tree
Nb-94		2.80E–04				3.20E–04							3.07E–04			
Ni-59		6.60E–41				1.10E–39							1.03E–39			
Ni-63		0				0							0			
Np-237		2.90E–06				3.60E–06							3.43E–06			
Pa-231		6.73E–06	7.30E–06										7.01E–06			
Pb-210		1.40E–07				2.90E–07							2.71E–07			
Pd-107													0			
Pm-147		5.61E–10	6.05E–10										5.83E–10			
Po-210		1.50E–09				1.70E–09							1.66E–09			
Pu-238		1.80E–08				6.50E–08							6.07E–08			
Pu-239		1.50E–08				3.30E–08							3.14E–08			
Pu-240		1.80E–08				6.20E–08							5.79E–08			
Pu-241		2.10E–10				2.70E–10							2.54E–10			
Pu-242		4.65E–08	5.00E–08										4.83E–08			
Ra-226		3.00E–04				3.50E–04							3.32E–04			
Ra-228		1.70E–04				1.90E–04							1.85E–04			
Ru-106		3.60E–05				4.20E–05							4.01E–05			
Sb-125		7.40E–05				8.60E–05							8.20E–05			
Se-79		0				0							0			
Sm-147		0	0										0			
Sm-151		2.27E–10	2.43E–10										2.35E–10			
Sn-126		2.98E–04	3.21E–04										3.09E–04			
Sr-90		6.40E–12				1.60E–11							1.55E–11			
Tc-99		0				0							0			
Th-228		2.60E–04				2.90E–04							2.83E–04			
Th-229		1.19E–05	1.28E–05										1.23E–05			
Th-230		4.90E–08				7.20E–08							6.80E–08			
Th-232		2.40E–08				4.40E–08							4.12E–08			
U-232		9.23E–08	9.94E–08										9.59E–08			
U-233		8.05E–08	8.69E–08										8.36E–08			
U-234		2.50E–08				7.10E–08							6.66E–08			
U-235		2.50E–05				3.00E–05							2.81E–05			
U-236		5.40E–08	5.81E–08										5.61E–08			
U-238		1.20E–08				5.00E–08							4.62E–08			
Zr-93		0	0										0			

Tabel E-8. DCC_int_alpha for terrestrial organisms ((µGy h^{-1})/(Bq $kgfw^{-1}$)).

Radio-nuclides	Amphibian	Bird	Bird egg	Detritivorous invertebrate	European otter	Flying insects	Gastropod	Grasses & Herbs	Lichen & bryophytes	Mammal (Deer)	Mammal (Rat)	Reptile	Ruddy turnstone	Shrub	Soil Invertebrate (worm)	Tree
Ac-227	3.93E–05	3.93E–05	3.93E–05	3.93E–05	3.93E–05	3.93E–05	3.93E–05	3.93E–05	3.93E–05	3.93E–05	3.93E–05	3.93E–05	3.93E–05	3.93E–05	3.93E–05	3.93E–05
Ag-108m	0	0	0	0	0	0	0	0	0	0	0	0	0	0	0	0
Am-241	3.17E–03	3.17E–03	3.17E–03	3.17E–03	3.16E–03	3.17E–03	3.17E–03	3.17E–03	3.17E–03	3.17E–03	3.17E–03	3.17E–03	3.16E–03	3.17E–03	3.17E–03	3.17E–03
Am-242m	1.43E–05	1.43E–05	1.43E–05	1.43E–05	1.43E–05	1.43E–05	1.43E–05	1.43E–05	1.43E–05	1.43E–05	1.43E–05	1.43E–05	1.43E–05	1.43E–05	1.43E–05	1.43E–05
Am-243	3.04E–03	3.04E–03	3.04E–03	3.04E–03	3.04E–03	3.04E–03	3.04E–03	3.04E–03	3.04E–03	3.04E–03	3.04E–03	3.04E–03	3.04E–03	3.04E–03	3.04E–03	3.04E–03
Ba-133	0	0	0	0	0	0	0	0	0	0	0	0	0	0	0	0
Be-10	0	0	0	0	0	0	0	0	0	0	0	0	0	0	0	0
C-14-ind	0	0	0	0	0	0	0	0	0	0	0	0	0	0	0	0
C-14-inorg	0	0	0	0	0	0	0	0	0	0	0	0	0	0	0	0
C-14-org	0	0	0	0	0	0	0	0	0	0	0	0	0	0	0	0
Ca-41	0	0	0	0	0	0	0	0	0	0	0	0	0	0	0	0
Cd-113m	0	0	0	0	0	0	0	0	0	0	0	0	0	0	0	0
Cl-36	0	0	0	0	0	0	0	0	0	0	0	0	0	0	0	0
Cm-242	3.50E–03	3.50E–03	3.50E–03	3.50E–03	3.52E–03	3.50E–03	3.50E–03	3.50E–03	3.50E–03	3.50E–03	3.50E–03	3.50E–03	3.52E–03	3.50E–03	3.50E–03	3.50E–03
Cm-243	3.33E–03	3.30E–03	3.30E–03	3.33E–03	3.34E–03	3.33E–03	3.33E–03	3.33E–03	3.33E–03	3.36E–03	3.30E–03	3.30E–03	3.34E–03	3.33E–03	3.33E–03	3.36E–03
Cm-244	3.30E–03	3.30E–03	3.30E–03	3.30E–03	3.34E–03	3.30E–03	3.30E–03	3.30E–03	3.30E–03	3.30E–03	3.30E–03	3.30E–03	3.34E–03	3.30E–03	3.30E–03	3.30E–03
Cm-245	3.09E–03	3.09E–03	3.09E–03	3.09E–03	3.09E–03	3.09E–03	3.09E–03	3.09E–03	3.09E–03	3.09E–03	3.09E–03	3.09E–03	3.09E–03	3.09E–03	3.09E–03	3.09E–03
Cm-246	3.10E–03	3.10E–03	3.10E–03	3.10E–03	3.10E–03	3.10E–03	3.10E–03	3.10E–03	3.10E–03	3.10E–03	3.10E–03	3.10E–03	3.10E–03	3.10E–03	3.10E–03	3.10E–03
Co-60	0	0	0	0	0	0	0	0	0	0	0	0	0	0	0	0
Cs-134	0	0	0	0	0	0	0	0	0	0	0	0	0	0	0	0
Cs-135	0	0	0	0	0	0	0	0	0	0	0	0	0	0	0	0
Cs-137	0	0	0	0	0	0	0	0	0	0	0	0	0	0	0	0
Eu-152	0	0	0	0	0	0	0	0	0	0	0	0	0	0	0	0
Eu-154	0	0	0	0	0	0	0	0	0	0	0	0	0	0	0	0
Eu-155	0	0	0	0	0	0	0	0	0	0	0	0	0	0	0	0
Fe-55	0	0	0	0	0	0	0	0	0	0	0	0	0	0	0	0
Gd-152	1.24E–03	1.24E–03	1.24E–03	1.24E–03	1.24E–03	1.24E–03	1.24E–03	1.24E–03	1.24E–03	1.24E–03	1.24E–03	1.24E–03	1.24E–03	1.24E–03	1.24E–03	1.24E–03
H-3	0	0	0	0	0	0	0	0	0	0	0	0	0	0	0	0
Ho-166m	0	0	0	0	0	0	0	0	0	0	0	0	0	0	0	0
I-129	0	0	0	0	0	0	0	0	0	0	0	0	0	0	0	0
In-115	0	0	0	0	0	0	0	0	0	0	0	0	0	0	0	0
Mo-93	0	0	0	0	0	0	0	0	0	0	0	0	0	0	0	0
Nb-93m	0	0	0	0	0	0	0	0	0	0	0	0	0	0	0	0

Radio-nuclides	Amphibian	Bird	Bird egg	Detritivorous invertebrate	European otter	Flying insects	Gastropod	Grasses & Herbs	Lichen & bryophytes	Mammal (Deer)	Mammal (Rat)	Reptile	Ruddy turnstone	Shrub	Soil Invertebrate (worm)	Tree
Nb-94	0	0	0	0	0	0	0	0	0	0	0	0	0	0	0	0
Ni-59	0	0	0	0	0	0	0	0	0	0	0	0	0	0	0	0
Ni-63	0	0	0	0	0	0	0	0	0	0	0	0	0	0	0	0
Np-237	2.74E–03	2.74E–03	2.74E–03	2.77E–03	2.75E–03	2.74E–03	2.74E–03	2.74E–03	2.77E–03	2.74E–03	2.74E–03	2.74E–03	2.75E–03	2.74E–03	2.74E–03	2.74E–03
Pa-231	2.87E–03	2.87E–03	2.87E–03	2.87E–03	2.87E–03	2.87E–03	2.87E–03	2.87E–03	2.87E–03	2.87E–03	2.87E–03	2.87E–03	2.87E–03	2.87E–03	2.87E–03	2.87E–03
Pb-210	0	0	0	0	0	0	0	0	0	0	0	0	0	0	0	0
Pd-107					0								0			
Pm-147	0	0	0	0	0	0	0	0	0	0	0	0	0	0	0	0
Po-210	3.10E–03	3.10E–03	3.10E–03	3.10E–03	3.06E–03	3.10E–03	3.10E–03	3.10E–03	3.10E–03	3.10E–03	3.10E–03	3.10E–03	3.06E–03	3.10E–03	3.10E–03	3.10E–03
Pu-238	3.20E–03	3.20E–03	3.20E–03	3.20E–03	3.16E–03	3.20E–03	3.20E–03	3.20E–03	3.20E–03	3.20E–03	3.20E–03	3.20E–03	3.16E–03	3.20E–03	3.20E–03	3.20E–03
Pu-239	3.00E–03	3.00E–03	3.00E–03	3.00E–03	2.97E–03	3.00E–03	3.00E–03	3.00E–03	3.00E–03	3.00E–03	3.00E–03	3.00E–03	2.97E–03	3.00E–03	3.00E–03	3.00E–03
Pu-240	3.00E–03	3.00E–03	3.00E–03	3.00E–03	2.97E–03	3.00E–03	3.00E–03	3.00E–03	3.00E–03	3.00E–03	3.00E–03	3.00E–03	2.97E–03	3.00E–03	3.00E–03	3.00E–03
Pu-241	6.20E–08	6.20E–08	6.20E–08	6.20E–08	6.92E–08	6.20E–08	6.20E–08	6.20E–08	6.20E–08	6.20E–08	6.20E–08	6.20E–08	6.92E–08	6.20E–08	6.20E–08	6.20E–08
Pu-242	2.82E–03	2.82E–03	2.82E–03	2.82E–03	2.82E–03	2.82E–03	2.82E–03	2.82E–03	2.82E–03	2.82E–03	2.82E–03	2.82E–03	2.82E–03	2.82E–03	2.82E–03	2.82E–03
Ra-226	1.34E–02	1.43E–02	1.34E–02	1.36E–02	1.38E–02	1.36E–02	1.36E–02	1.36E–02	1.37E–02	1.38E–02	1.34E–02	1.34E–02	1.38E–02	1.36E–02	1.36E–02	1.40E–02
Ra-228	0	0	0	0	0	0	0	0	0	0	0	0	0	0	0	0
Ru-106	0	0	0	0	0	0	0	0	0	0	0	0	0	0	0	0
Sb-125	0	0	0	0	0	0	0	0	0	0	0	0	0	0	0	0
Se-79	0	0	0	0	0	0	0	0	0	0	0	0	0	0	0	0
Sm-147	1.30E–03	1.30E–03	1.30E–03	1.30E–03	1.30E–03	1.30E–03	1.30E–03	1.30E–03	1.30E–03	1.30E–03	1.30E–03	1.30E–03	1.30E–03	1.30E–03	1.30E–03	1.30E–03
Sm-151	0	0	0	0	0	0	0	0	0	0	0	0	0	0	0	0
Sn-126	0	0	0	0	0	0	0	0	0	0	0	0	0	0	0	0
Sr-90	0	0	0	0	0	0	0	0	0	0	0	0	0	0	0	0
Tc-99	0	0	0	0	0	0	0	0	0	0	0	0	0	0	0	0
Th-228	1.84E–02	1.82E–02	1.84E–02	1.86E–02	1.85E–02	1.84E–02	1.84E–02	1.84E–02	1.86E–02	1.88E–02	1.82E–02	1.82E–02	1.85E–02	1.84E–02	1.84E–02	1.90E–02
Th-229	2.81E–03	2.81E–03	2.81E–03	2.81E–03	2.81E–03	2.81E–03	2.81E–03	2.81E–03	2.81E–03	2.81E–03	2.81E–03	2.81E–03	2.81E–03	2.81E–03	2.81E–03	2.81E–03
Th-230	2.70E–03	2.70E–03	2.70E–03	2.70E–03	2.69E–03	2.70E–03	2.70E–03	2.70E–03	2.70E–03	2.70E–03	2.70E–03	2.70E–03	2.69E–03	2.70E–03	2.70E–03	2.70E–03
Th-232	2.30E–03	2.30E–03	2.30E–03	2.30E–03	2.30E–03	2.30E–03	2.30E–03	2.30E–03	2.30E–03	2.30E–03	2.30E–03	2.30E–03	2.30E–03	2.30E–03	2.30E–03	2.30E–03
U-232	3.06E–03	3.06E–03	3.06E–03	3.06E–03	3.06E–03	3.06E–03	3.06E–03	3.06E–03	3.06E–03	3.06E–03	3.06E–03	3.06E–03	3.06E–03	3.06E–03	3.06E–03	3.06E–03
U-233	2.78E–03	2.78E–03	2.78E–03	2.78E–03	2.78E–03	2.78E–03	2.78E–03	2.78E–03	2.78E–03	2.78E–03	2.78E–03	2.78E–03	2.78E–03	2.78E–03	2.78E–03	2.78E–03
U-234	2.80E–03	2.80E–03	2.80E–03	2.80E–03	2.74E–03	2.80E–03	2.80E–03	2.80E–03	2.80E–03	2.80E–03	2.80E–03	2.80E–03	2.74E–03	2.80E–03	2.80E–03	2.80E–03
U-235	2.57E–03	2.57E–03	2.57E–03	2.57E–03	2.54E–03	2.57E–03	2.57E–03	2.57E–03	2.57E–03	2.51E–03	2.57E–03	2.57E–03	2.54E–03	2.57E–03	2.57E–03	2.51E–03
U-236	2.60E–03	2.60E–03	2.60E–03	2.60E–03	2.60E–03	2.60E–03	2.60E–03	2.60E–03	2.60E–03	2.60E–03	2.60E–03	2.60E–03	2.60E–03	2.60E–03	2.60E–03	2.60E–03
U-238	2.40E–03	2.40E–03	2.40E–03	2.40E–03	2.41E–03	2.40E–03	2.40E–03	2.40E–03	2.40E–03	2.40E–03	2.40E–03	2.40E–03	2.41E–03	2.40E–03	2.40E–03	2.40E–03
Zr-93	0	0	0	0	0	0	0	0	0	0	0	0	0	0	0	0

Tabel E-9. DCC_int_alpha for limnic organism ((µGy h^{-1})/(Bq $kgfw^{-1}$)).

Radionuclides	Amphibian	Benthic fish	Bird	Bivalve mollusc	Crustacean	Gastropod	Insect larvae	Mammal	Microphyto-benthos	Pelagic fish	Phytoplank-ton	Vascular plant	Zooplankton
Ac-227	3.93E–05	3.93E–05	3.93E–05	3.93E–05	3.93E–05	3.93E–05	3.93E–05	3.93E–05	3.93E–05	3.93E–05	3.93E–05	3.93E–05	3.93E–05
Ag-108m	0	0	0	0	0	0	0	0	0	0	0	0	0
Am-241	3.17E–03	3.17E–03	3.17E–03	3.17E–03	3.17E–03	3.17E–03	3.17E–03	3.17E–03	3.16E–03	3.17E–03	3.17E–03	3.17E–03	3.17E–03
Am-242m	1.43E–05	1.43E–05	1.43E–05	1.43E–05	1.43E–05	1.43E–05	1.43E–05	1.43E–05	1.43E–05	1.43E–05	1.43E–05	1.43E–05	1.43E–05
Am-243	3.04E–03	3.04E–03	3.04E–03	3.04E–03	3.04E–03	3.04E–03	3.04E–03	3.04E–03	3.04E–03	3.04E–03	3.04E–03	3.04E–03	3.04E–03
Ba-133	0	0	0	0	0	0	0	0	0	0	0	0	0
Be-10	0	0	0	0	0	0	0	0	0	0	0	0	0
C-14-ind	0	0	0	0	0	0	0	0	0	0	0	0	0
C-14-inorg	0	0	0	0	0	0	0	0	0	0	0	0	0
C-14-org	0	0	0	0	0	0	0	0	0	0	0	0	0
Ca-41	0	0	0	0	0	0	0	0	0	0	0	0	0
Cd-113m	0	0	0	0	0	0	0	0	0	0	0	0	0
Cl-36	0	0	0	0	0	0	0	0	0	0	0	0	0
Cm-242	3.50E–03	3.50E–03	3.50E–03	3.50E–03	3.50E–03	3.50E–03	3.50E–03	3.50E–03	3.52E–03	3.50E–03	3.50E–03	3.50E–03	3.50E–03
Cm-243	3.33E–03	3.30E–03	3.30E–03	3.30E–03	3.33E–03	3.33E–03	3.33E–03	3.30E–03	3.34E–03	3.30E–03	3.33E–03	3.33E–03	3.33E–03
Cm-244	3.30E–03	3.30E–03	3.30E–03	3.30E–03	3.30E–03	3.30E–03	3.30E–03	3.30E–03	3.34E–03	3.30E–03	3.30E–03	3.30E–03	3.30E–03
Cm-245	3.09E–03	3.09E–03	3.09E–03	3.09E–03	3.09E–03	3.09E–03	3.09E–03	3.09E–03	3.09E–03	3.09E–03	3.09E–03	3.09E–03	3.09E–03
Cm-246	3.10E–03	3.10E–03	3.10E–03	3.10E–03	3.10E–03	3.10E–03	3.10E–03	3.10E–03	3.10E–03	3.10E–03	3.10E–03	3.10E–03	3.10E–03
Co-60	0	0	0	0	0	0	0	0	0	0	0	0	0
Cs-134	0	0	0	0	0	0	0	0	0	0	0	0	0
Cs-135	0	0	0	0	0	0	0	0	0	0	0	0	0
Cs-137	0	0	0	0	0	0	0	0	0	0	0	0	0
Eu-152	0	0	0	0	0	0	0	0	0	0	0	0	0
Eu-154	0	0	0	0	0	0	0	0	0	0	0	0	0
Eu-155	0	0	0	0	0	0	0	0	0	0	0	0	0
Fe-55	0	0	0	0	0	0	0	0	0	0	0	0	0
Gd-152	1.24E–03	1.24E–03	1.24E–03	1.24E–03	1.24E–03	1.24E–03	1.24E–03	1.24E–03	1.24E–03	1.24E–03	1.24E–03	1.24E–03	1.24E–03
H-3	0	0	0	0	0	0	0	0	0	0	0	0	0
Ho-166m	0	0	0	0	0	0	0	0	0	0	0	0	0
I-129	0	0	0	0	0	0	0	0	0	0	0	0	0
In-115	0	0	0	0	0	0	0	0	0	0	0	0	0
Mo-93	0	0	0	0	0	0	0	0	0	0	0	0	0
Nb-93m	0	0	0	0	0	0	0	0	0	0	0	0	0

Radionuclides	Amphibian	Benthic fish	Bird	Bivalve mollusc	Crustacean	Gastropod	Insect larvae	Mammal	Microphyto-benthos	Pelagic fish	Phytoplank-ton	Vascular plant	Zooplankton
Nb-94	0	0	0	0	0	0	0	0	0	0	0	0	0
Ni-59	0	0	0	0	0	0	0	0	0	0	0	0	0
Ni-63	0	0	0	0	0	0	0	0	0	0	0	0	0
Np-237	2.74E–03	2.74E–03	2.74E–03	2.74E–03	2.77E–03	2.74E–03	2.77E–03	2.74E–03	2.75E–03	2.74E–03	2.77E–03	2.77E–03	2.77E–03
Pa-231	2.87E–03	2.87E–03	2.87E–03	2.87E–03	2.87E–03	2.87E–03	2.87E–03	2.87E–03	2.87E–03	2.87E–03	2.87E–03	2.87E–03	2.87E–03
Pb-210	0	0	0	0	0	0	0	0	0	0	0	0	0
Pd-107	0	0	0	0	0	0	0	0	0	0	0	0	0
Pm-147	0	0	0	0	0	0	0	0	0	0	0	0	0
Po-210	3.10E–03	3.10E–03	3.10E–03	3.10E–03	3.10E–03	3.10E–03	3.10E–03	3.10E–03	3.06E–03	3.10E–03	3.10E–03	3.10E–03	3.10E–03
Pu-238	3.20E–03	3.20E–03	3.20E–03	3.20E–03	3.20E–03	3.20E–03	3.20E–03	3.20E–03	3.16E–03	3.20E–03	3.20E–03	3.20E–03	3.20E–03
Pu-239	3.00E–03	3.00E–03	3.00E–03	3.00E–03	3.00E–03	3.00E–03	3.00E–03	3.00E–03	2.97E–03	3.00E–03	3.00E–03	3.00E–03	3.00E–03
Pu-240	3.00E–03	3.00E–03	3.00E–03	3.00E–03	3.00E–03	3.00E–03	3.00E–03	3.00E–03	2.97E–03	3.00E–03	3.00E–03	3.00E–03	3.00E–03
Pu-241	6.20E–08	6.20E–08	6.20E–08	6.20E–08	6.20E–08	6.20E–08	6.20E–08	6.20E–08	6.92E–08	6.20E–08	6.20E–08	6.20E–08	6.20E–08
Pu-242	2.82E–03	2.82E–03	2.82E–03	2.82E–03	2.82E–03	2.82E–03	2.82E–03	2.82E–03	2.82E–03	2.82E–03	2.82E–03	2.82E–03	2.82E–03
Ra-226	1.34E–02	1.43E–02	1.43E–02	1.34E–02	1.37E–02	1.34E–02	1.37E–02	1.43E–02	1.38E–02	1.43E–02	1.39E–02	1.37E–02	1.37E–02
Ra-228	0	0	0	0	0	0	0	0	0	0	0	0	0
Ru-106	0	0	0	0	0	0	0	0	0	0	0	0	0
Sb-125	0	0	0	0	0	0	0	0	0	0	0	0	0
Se-79	0	0	0	0	0	0	0	0	0	0	0	0	0
Sm-147	1.30E–03	1.30E–03	1.30E–03	1.30E–03	1.30E–03	1.30E–03	1.30E–03	1.30E–03	1.30E–03	1.30E–03	1.30E–03	1.30E–03	1.30E–03
Sm-151	0	0	0	0	0	0	0	0	0	0	0	0	0
Sn-126	0	0	0	0	0	0	0	0	0	0	0	0	0
Sr-90	0	0	0	0	0	0	0	0	0	0	0	0	0
Tc-99	0	0	0	0	0	0	0	0	0	0	0	0	0
Th-228	1.84E–02	1.82E–02	1.82E–02	1.84E–02	1.88E–02	1.84E–02	1.88E–02	1.82E–02	1.85E–02	1.82E–02	1.88E–02	1.86E–02	1.88E–02
Th-229	2.81E–03	2.81E–03	2.81E–03	2.81E–03	2.81E–03	2.81E–03	2.81E–03	2.81E–03	2.81E–03	2.81E–03	2.81E–03	2.81E–03	2.81E–03
Th-230	2.70E–03	2.70E–03	2.70E–03	2.70E–03	2.70E–03	2.70E–03	2.70E–03	2.70E–03	2.69E–03	2.70E–03	2.70E–03	2.70E–03	2.70E–03
Th-232	2.30E–03	2.30E–03	2.30E–03	2.30E–03	2.30E–03	2.30E–03	2.30E–03	2.30E–03	2.30E–03	2.30E–03	2.30E–03	2.30E–03	2.30E–03
U-232	3.06E–03	3.06E–03	3.06E–03	3.06E–03	3.06E–03	3.06E–03	3.06E–03	3.06E–03	3.06E–03	3.06E–03	3.06E–03	3.06E–03	3.06E–03
U-233	2.78E–03	2.78E–03	2.78E–03	2.78E–03	2.78E–03	2.78E–03	2.78E–03	2.78E–03	2.78E–03	2.78E–03	2.78E–03	2.78E–03	2.78E–03
U-234	2.80E–03	2.80E–03	2.80E–03	2.80E–03	2.80E–03	2.80E–03	2.80E–03	2.80E–03	2.74E–03	2.80E–03	2.80E–03	2.80E–03	2.80E–03
U-235	2.57E–03	2.57E–03	2.57E–03	2.57E–03	2.59E–03	2.57E–03	2.59E–03	2.54E–03	2.54E–03	2.57E–03	2.50E–03	2.59E–03	2.59E–03
U-236	2.60E–03	2.60E–03	2.60E–03	2.60E–03	2.60E–03	2.60E–03	2.60E–03	2.60E–03	2.60E–03	2.60E–03	2.60E–03	2.60E–03	2.60E–03
U-238	2.40E–03	2.40E–03	2.40E–03	2.40E–03	2.40E–03	2.40E–03	2.40E–03	2.40E–03	2.41E–03	2.40E–03	2.40E–03	2.40E–03	2.40E–03
Zr-93	0	0	0	0	0	0	0	0	0	0	0	0	0

Tabel E-10. DCC_int_alpha for marine organisms ((µGy h^{-1})/(Bq $kgfw^{-1}$)).

Radionuclides	(Wading) bird	Benthic fish	Benthic mollusc	Crustacean	European otter	Macroalgae	Mammal	Pelagic fish	Phyto-plankton	Polychaete worm	Ruddy turnstone	Vascular plant	Zooplankton
Ac-227	3.93E–05	3.93E–05	3.93E–05	3.93E–05	3.93E–05	3.93E–05	3.93E–05	3.93E–05	3.93E–05	3.93E–05	3.93E–05	3.93E–05	3.93E–05
Ag-108m	0	0	0	0	0	0	0	0	0	0	0	0	0
Am-241	3.17E–03	3.17E–03	3.17E–03	3.17E–03	3.16E–03	3.17E–03	3.17E–03	3.17E–03	3.17E–03	3.17E–03	3.16E–03	3.17E–03	3.17E–03
Am-242m	1.43E–05	1.43E–05	1.43E–05	1.43E–05	1.43E–05	1.43E–05	1.43E–05	1.43E–05	1.43E–05	1.43E–05	1.43E–05	1.43E–05	1.43E–05
Am-243	3.04E–03	3.04E–03	3.04E–03	3.04E–03	3.04E–03	3.04E–03	3.04E–03	3.04E–03	3.04E–03	3.04E–03	3.04E–03	3.04E–03	3.04E–03
Ba-133	0	0	0	0	0	0	0	0	0	0	0	0	0
Be-10	0	0	0	0	0	0	0	0	0	0	0	0	0
C-14-ind	0	0	0	0	0	0	0	0	0	0	0	0	0
C-14-inorg	0	0	0	0	0	0	0	0	0	0	0	0	0
C-14-org	0	0	0	0	0	0	0	0	0	0	0	0	0
Ca-41	0	0	0	0	0	0	0	0	0	0	0	0	0
Cd-113m	0	0	0	0	0	0	0	0	0	0	0	0	0
Cl-36	0	0	0	0	0	0	0	0	0	0	0	0	0
Cm-242	3.50E–03	3.50E–03	3.50E–03	3.50E–03	3.52E–03	3.50E–03	3.50E–03	3.50E–03	3.50E–03	3.50E–03	3.52E–03	3.50E–03	3.50E–03
Cm-243	3.30E–03	3.30E–03	3.33E–03	3.30E–03	3.34E–03	3.33E–03	3.36E–03	3.30E–03	3.33E–03	3.33E–03	3.34E–03	3.33E–03	3.33E–03
Cm-244	3.30E–03	3.30E–03	3.30E–03	3.30E–03	3.34E–03	3.30E–03	3.30E–03	3.30E–03	3.30E–03	3.30E–03	3.34E–03	3.30E–03	3.30E–03
Cm-245	3.09E–03	3.09E–03	3.09E–03	3.09E–03	3.09E–03	3.09E–03	3.09E–03	3.09E–03	3.09E–03	3.09E–03	3.09E–03	3.09E–03	3.09E–03
Cm-246	3.10E–03	3.10E–03	3.10E–03	3.10E–03	3.10E–03	3.10E–03	3.10E–03	3.10E–03	3.10E–03	3.10E–03	3.10E–03	3.10E–03	3.10E–03
Co-60	0	0	0	0	0	0	0	0	0	0	0	0	0
Cs-134	0	0	0	0	0	0	0	0	0	0	0	0	0
Cs-135	0	0	0	0	0	0	0	0	0	0	0	0	0
Cs-137	0	0	0	0	0	0	0	0	0	0	0	0	0
Eu-152	0	0	0	0	0	0	0	0	0	0	0	0	0
Eu-154	0	0	0	0	0	0	0	0	0	0	0	0	0
Eu-155	0	0	0	0	0	0	0	0	0	0	0	0	0
Fe-55	0	0	0	0	0	0	0	0	0	0	0	0	0
Gd-152	1.24E–03	1.24E–03	1.24E–03	1.24E–03	1.24E–03	1.24E–03	1.24E–03	1.24E–03	1.24E–03	1.24E–03	1.24E–03	1.24E–03	1.24E–03
H-3	0	0	0	0	0	0	0	0	0	0	0	0	0
Ho-166m	0	0	0	0	0	0	0	0	0	0	0	0	0
I-129	0	0	0	0	0	0	0	0	0	0	0	0	0
In-115	0	0	0	0	0	0	0	0	0	0	0	0	0
Mo-93	0	0	0	0	0	0	0	0	0	0	0	0	0
Nb-93m	0	0	0	0	0	0	0	0	0	0	0	0	0

Radionuclides	(Wading) bird	Benthic fish	Benthic mollusc	Crustacean	European otter	Macroalgae	Mammal	Pelagic fish	Phyto-plankton	Polychaete worm	Ruddy turnstone	Vascular plant	Zooplankton
Nb-94	0	0	0	0	0	0	0	0	0	0	0	0	0
Ni-59	0	0	0	0	0	0	0	0	0	0	0	0	0
Ni-63	0	0	0	0	0	0	0	0	0	0	0	0	0
Np-237	2.74E–03	2.74E–03	2.74E–03	2.74E–03	2.75E–03	2.74E–03	2.74E–03	2.74E–03	2.77E–03	2.74E–03	2.75E–03	2.74E–03	2.77E–03
Pa-231	2.87E–03	2.87E–03	2.87E–03	2.87E–03	2.87E–03	2.87E–03	2.87E–03	2.87E–03	2.87E–03	2.87E–03	2.87E–03	2.87E–03	2.87E–03
Pb-210	0	0	0	0	0	0	0	0	0	0	0	0	0
Pd-107	0	0	0	0	0	0	0	0	0	0	0	0	0
Pm-147	0	0	0	0	0	0	0	0	0	0	0	0	0
Po-210	3.10E–03	3.10E–03	3.10E–03	3.10E–03	3.06E–03	3.10E–03	3.10E–03	3.10E–03	3.10E–03	3.10E–03	3.06E–03	3.10E–03	3.10E–03
Pu-238	3.20E–03	3.20E–03	3.20E–03	3.20E–03	3.16E–03	3.20E–03	3.20E–03	3.20E–03	3.20E–03	3.20E–03	3.16E–03	3.20E–03	3.20E–03
Pu-239	3.00E–03	3.00E–03	3.00E–03	3.00E–03	2.97E–03	3.00E–03	3.00E–03	3.00E–03	3.00E–03	3.00E–03	2.97E–03	3.00E–03	3.00E–03
Pu-240	3.00E–03	3.00E–03	3.00E–03	3.00E–03	2.97E–03	3.00E–03	3.00E–03	3.00E–03	3.00E–03	3.00E–03	2.97E–03	3.00E–03	3.00E–03
Pu-241	6.20E–08	6.20E–08	6.20E–08	6.20E–08	6.92E–08	6.20E–08	6.20E–08	6.20E–08	6.20E–08	6.20E–08	6.92E–08	6.20E–08	6.20E–08
Pu-242	2.82E–03	2.82E–03	2.82E–03	2.82E–03	2.82E–03	2.82E–03	2.82E–03	2.82E–03	2.82E–03	2.82E–03	2.82E–03	2.82E–03	2.82E–03
Ra-226	1.43E–02	1.34E–02	1.34E–02	1.43E–02	1.38E–02	1.36E–02	1.40E–02	1.33E–02	1.39E–02	1.34E–02	1.38E–02	1.34E–02	1.36E–02
Ra-228	0	0	0	0	0	0	0	0	0	0	0	0	0
Ru-106	0	0	0	0	0	0	0	0	0	0	0	0	0
Sb-125	0	0	0	0	0	0	0	0	0	0	0	0	0
Se-79	0	0	0	0	0	0	0	0	0	0	0	0	0
Sm-147	1.30E–03	1.30E–03	1.30E–03	1.30E–03	1.30E–03	1.30E–03	1.30E–03	1.30E–03	1.30E–03	1.30E–03	1.30E–03	1.30E–03	1.30E–03
Sm-151	0	0	0	0	0	0	0	0	0	0	0	0	0
Sn-126	0	0	0	0	0	0	0	0	0	0	0	0	0
Sr-90	0	0	0	0	0	0	0	0	0	0	0	0	0
Tc-99	0	0	0	0	0	0	0	0	0	0	0	0	0
Th-228	1.82E–02	1.82E–02	1.84E–02	1.82E–02	1.85E–02	1.84E–02	1.88E–02	1.82E–02	1.88E–02	1.84E–02	1.85E–02	1.84E–02	1.86E–02
Th-229	2.81E–03	2.81E–03	2.81E–03	2.81E–03	2.81E–03	2.81E–03	2.81E–03	2.81E–03	2.81E–03	2.81E–03	2.81E–03	2.81E–03	2.81E–03
Th-230	2.70E–03	2.70E–03	2.70E–03	2.70E–03	2.69E–03	2.70E–03	2.70E–03	2.70E–03	2.70E–03	2.70E–03	2.69E–03	2.70E–03	2.70E–03
Th-232	2.30E–03	2.30E–03	2.30E–03	2.30E–03	2.30E–03	2.30E–03	2.30E–03	2.30E–03	2.30E–03	2.30E–03	2.30E–03	2.30E–03	2.30E–03
U-232	3.06E–03	3.06E–03	3.06E–03	3.06E–03	3.06E–03	3.06E–03	3.06E–03	3.06E–03	3.06E–03	3.06E–03	3.06E–03	3.06E–03	3.06E–03
U-233	2.78E–03	2.78E–03	2.78E–03	2.78E–03	2.78E–03	2.78E–03	2.78E–03	2.78E–03	2.78E–03	2.78E–03	2.78E–03	2.78E–03	2.78E–03
U-234	2.80E–03	2.80E–03	2.80E–03	2.80E–03	2.74E–03	2.80E–03	2.80E–03	2.80E–03	2.80E–03	2.80E–03	2.74E–03	2.80E–03	2.80E–03
U-235	2.57E–03	2.57E–03	2.57E–03	2.57E–03	2.54E–03	2.57E–03	2.51E–03	2.57E–03	2.59E–03	2.57E–03	2.54E–03	2.57E–03	2.57E–03
U-236	2.60E–03	2.60E–03	2.60E–03	2.60E–03	2.60E–03	2.60E–03	2.60E–03	2.60E–03	2.60E–03	2.60E–03	2.60E–03	2.60E–03	2.60E–03
U-238	2.40E–03	2.40E–03	2.40E–03	2.40E–03	2.41E–03	2.40E–03	2.40E–03	2.40E–03	2.40E–03	2.40E–03	2.41E–03	2.40E–03	2.40E–03
Zr-93	0	0	0	0	0	0	0	0	0	0	0	0	0

Tabel E-11. DCC_int_beta_gamma for marine organisms ((µGy h^{-1})/(Bq kgfw^{-1})).

Radionuclides	(Wading) bird	Benthic fish	Benthic mollusc	Crustacean	European otter	Macroalgae	Mammal	Pelagic fish	Phyto-plankton	Polychaete worm	Ruddy turnstone	Vascular plant	Zooplankton
Ac-227	4.74E–06	4.73E–06	4.71E–06	4.73E–06	4.75E–06	4.69E–06	4.78E–06	4.73E–06	4.58E–06	4.70E–06	4.73E–06	4.71E–06	4.67E–06
Ag-108m	1.79E–04	1.25E–04	7.19E–05	1.58E–04	2.56E–04	4.20E–05	5.73E–04	1.41E–04	4.86E–06	5.94E–05	1.45E–04	7.51E–05	2.74E–05
Am-241	3.20E–05	3.20E–05	3.20E–05	3.20E–05	3.47E–05	3.20E–05	3.20E–05	3.20E–05	2.10E–09	3.20E–05	3.15E–05	3.20E–05	3.20E–05
Am-242m	1.29E–04	1.28E–04	1.24E–04	1.29E–04	1.30E–04	1.16E–04	1.34E–04	1.28E–04	5.95E–05	1.23E–04	1.28E–04	1.25E–04	1.12E–04
Am-243	1.80E–04	1.71E–04	1.60E–04	1.76E–04	1.94E–04	1.51E–04	2.43E–04	1.73E–04	9.63E–05	1.58E–04	1.74E–04	1.61E–04	1.47E–04
Ba-133	7.01E–05	5.46E–05	3.78E–05	6.39E–05	9.36E–05	3.03E–05	1.75E–04	5.88E–05	2.13E–05	3.45E–05	6.00E–05	3.88E–05	2.78E–05
Be-10	1.44E–04	1.44E–04	1.42E–04	1.44E–04	1.45E–04	1.29E–04	1.45E–04	1.44E–04	3.41E–05	1.40E–04	1.44E–04	1.42E–04	1.24E–04
C-14-ind	2.87E–05	2.87E–05	2.77E–05	2.87E–05	2.81E–05	2.77E–05	2.87E–05	2.87E–05	1.78E–09	2.77E–05	2.81E–05	2.77E–05	2.77E–05
C-14-inorg	2.87E–05	2.87E–05	2.77E–05	2.87E–05	2.81E–05	2.77E–05	2.87E–05	2.87E–05	1.78E–09	2.77E–05	2.81E–05	2.77E–05	2.77E–05
C-14-org	2.87E–05	2.87E–05	2.77E–05	2.87E–05	2.81E–05	2.77E–05	2.87E–05	2.87E–05	1.78E–09	2.77E–05	2.81E–05	2.77E–05	2.77E–05
Ca-41	2.39E–07	2.39E–07	2.33E–07	2.39E–07	2.40E–07	2.18E–07	2.41E–07	2.39E–07	1.62E–07	2.31E–07	2.39E–07	2.34E–07	2.00E–07
Cd-113m	1.06E–04	1.06E–04	1.05E–04	1.06E–04	1.07E–04	9.73E–05	1.07E–04	1.06E–04	3.53E–05	1.04E–04	1.06E–04	1.05E–04	9.39E–05
Cl-36	1.60E–04	1.60E–04	1.60E–04	1.60E–04	1.57E–04	1.40E–04	1.60E–04	1.60E–04	4.30E–09	1.50E–04	1.56E–04	1.60E–04	1.30E–04
Cm-242	0	0	0	0	5.68E–06	0	0	0	0	0	5.57E–06	0	0
Cm-243	1.02E–04	6.80E–05	6.80E–05	6.80E–05	9.55E–05	6.80E–05	1.40E–04	6.80E–05	4.40E–09	6.80E–05	8.44E–05	6.80E–05	6.80E–05
Cm-244	0	0	0	0	5.09E–06	0	0	0	0	0	4.99E–06	0	0
Cm-245	4.55E–05	4.22E–05	3.73E–05	4.40E–05	5.15E–05	3.44E–05	7.12E–05	4.29E–05	2.79E–05	3.61E–05	4.31E–05	3.76E–05	3.31E–05
Cm-246	4.69E–06	4.62E–06	4.39E–06	4.66E–06	4.74E–06	4.14E–06	4.79E–06	4.64E–06	3.82E–06	4.29E–06	4.65E–06	4.41E–06	4.04E–06
Co-60	2.40E–04	1.70E–04	9.80E–05	2.10E–04	3.37E–04	6.80E–05	7.80E–04	1.90E–04	3.00E–09	8.50E–05	1.92E–04	1.00E–04	5.60E–05
Cs-134	2.20E–04	1.70E–04	1.20E–04	2.00E–04	2.92E–04	9.50E–05	5.90E–04	1.90E–04	3.27E–09	1.10E–04	1.89E–04	1.30E–04	8.40E–05
Cs-135	3.86E–05	3.86E–05	3.86E–05	3.86E–05	3.86E–05	3.76E–05	3.86E–05	3.86E–05	2.28E–09	3.86E–05	3.85E–05	3.86E–05	3.76E–05
Cs-137	1.90E–04	1.70E–04	1.50E–04	1.80E–04	2.16E–04	1.30E–04	3.30E–04	1.80E–04	4.26E–09	1.40E–04	1.77E–04	1.50E–04	1.20E–04
Eu-152	1.57E–04	1.16E–04	8.35E–05	1.37E–04	2.08E–04	6.46E–05	4.16E–04	1.26E–04	2.28E–09	7.68E–05	1.33E–04	8.64E–05	5.55E–05
Eu-154	2.57E–04	2.18E–04	1.78E–04	2.48E–04	3.16E–04	1.49E–04	5.50E–04	2.38E–04	5.19E–09	1.68E–04	2.37E–04	1.88E–04	1.29E–04
Eu-155	4.07E–05	3.84E–05	3.54E–05	3.96E–05	4.52E–05	3.43E–05	5.86E–05	3.88E–05	2.95E–05	3.49E–05	3.89E–05	3.55E–05	3.37E–05
Fe-55	9.58E–07	9.58E–07	9.11E–07	9.56E–07	9.65E–07	8.02E–07	9.70E–07	9.54E–07	4.01E–07	8.99E–07	9.54E–07	9.20E–07	6.73E–07
Gd-152	0	0	0	0	0	0	0	0	0	0	0	0	0
H-3	8.25E–07	8.25E–07	8.25E–07	8.25E–07	8.10E–07	8.25E–07	8.25E–07	8.25E–07	5.25E–11	8.25E–07	8.10E–07	8.25E–07	8.25E–07
Ho-166m	2.16E–04	1.60E–04	1.06E–04	1.94E–04	2.99E–04	8.13E–05	6.39E–04	1.76E–04	5.15E–05	9.49E–05	1.80E–04	1.09E–04	7.19E–05
I-129	3.92E–05	3.70E–05	3.39E–05	3.83E–05	4.12E–05	3.31E–05	4.41E–05	3.70E–05	1.98E–09	3.31E–05	3.77E–05	3.39E–05	3.22E–05
In-115	8.73E–05	8.72E–05	8.63E–05	8.72E–05	8.74E–05	8.19E–05	8.75E–05	8.72E–05	3.68E–05	8.58E–05	8.72E–05	8.64E–05	7.95E–05
Mo-93	7.19E–06	6.75E–06	5.10E–06	7.04E–06	7.53E–06	3.27E–06	7.80E–06	6.88E–06	1.81E–06	4.32E–06	6.92E–06	5.21E–06	2.60E–06
Nb-93m	1.62E–05	1.61E–05	1.58E–05	1.62E–05	1.63E–05	1.55E–05	1.63E–05	1.62E–05	1.49E–05	1.57E–05	1.62E–05	1.59E–05	1.54E–05

Radionuclides	(Wading) bird	Benthic fish	Benthic mollusc	Crustacean	European otter	Macroalgae	Mammal	Pelagic fish	Phyto-plankton	Polychaete worm	Ruddy turnstone	Vascular plant	Zooplankton
Nb-94	2.20E–04	1.70E–04	1.30E–04	2.00E–04	2.93E–04	1.00E–04	5.90E–04	1.90E–04	4.00E–09	1.20E–04	1.92E–04	1.30E–04	9.10E–05
Ni-59	1.36E–06	1.36E–06	1.29E–06	1.36E–06	1.37E–06	1.11E–06	1.40E–06	1.36E–06	3.78E–11	1.25E–06	1.36E–06	1.29E–06	8.75E–07
Ni-63	8.71E–06	8.71E–06	8.71E–06	8.71E–06	8.68E–06	8.71E–06	8.71E–06	8.71E–06	5.63E–10	8.71E–06	8.68E–06	8.71E–06	8.71E–06
Np-237	5.60E–05	2.80E–05	2.80E–05	5.60E–05	4.51E–05	2.80E–05	5.60E–05	2.80E–05	1.80E–09	2.80E–05	4.20E–05	2.80E–05	2.80E–05
Pa-231	3.92E–05	3.75E–05	3.45E–05	3.85E–05	4.16E–05	3.18E–05	4.95E–05	3.79E–05	2.74E–05	3.34E–05	3.81E–05	3.47E–05	3.07E–05
Pb-210	2.45E–04	2.35E–04	2.35E–04	2.35E–04	2.43E–04	1.96E–04	2.45E–04	2.35E–04	5.23E–09	2.25E–04	2.40E–04	2.35E–04	1.76E–04
Pd-107	3.55E–06	3.55E–06	3.55E–06	3.55E–06	3.55E–06	3.55E–06	3.55E–06	3.55E–06	3.51E–06	3.55E–06	3.55E–06	3.55E–06	3.55E–06
Pm-147	3.54E–05	3.54E–05	3.53E–05	3.54E–05	3.54E–05	3.50E–05	3.54E–05	3.54E–05	2.79E–05	3.53E–05	3.54E–05	3.53E–05	3.45E–05
Po-210	0	0	0	0	1.11E–09	0	0	0	0	0	5.61E–10	0	0
Pu-238	0	0	0	0	6.24E–06	0	0	0	0	0	6.14E–06	0	0
Pu-239	0	0	0	0	3.12E–06	0	0	0	0	0	3.08E–06	0	0
Pu-240	0	0	0	0	6.21E–06	0	0	0	0	0	6.11E–06	0	0
Pu-241	8.37E–07	8.37E–07	8.37E–07	8.37E–07	8.37E–07	8.37E–07	8.37E–07	8.37E–07	5.40E–11	8.37E–07	8.37E–07	8.37E–07	8.37E–07
Pu-242	5.07E–06	5.01E–06	4.80E–06	5.05E–06	5.11E–06	4.56E–06	5.15E–06	5.03E–06	4.21E–06	4.71E–06	5.04E–06	4.82E–06	4.45E–06
Ra-226	7.50E–04	5.60E–04	5.60E–04	7.50E–04	7.48E–04	4.20E–04	1.05E–03	7.00E–04	9.10E–09	5.60E–04	6.33E–04	5.60E–04	4.20E–04
Ra-228	3.49E–04	3.20E–04	2.81E–04	3.40E–04	3.93E–04	2.30E–04	5.68E–04	3.30E–04	6.62E–09	2.62E–04	3.30E–04	2.81E–04	1.90E–04
Ru-106	7.90E–04	7.30E–04	6.60E–04	7.80E–04	8.18E–04	4.50E–04	8.80E–04	7.70E–04	3.49E–09	6.00E–04	7.74E–04	6.80E–04	1.98E–04
Sb-125	9.51E–05	7.97E–05	6.43E–05	8.92E–05	1.17E–04	5.51E–05	1.98E–04	8.44E–05	2.60E–09	6.08E–05	8.53E–05	6.53E–05	5.23E–05
Se-79	3.17E–05	3.17E–05	3.17E–05	3.17E–05	3.19E–05	3.17E–05	3.17E–05	3.17E–05	1.98E–09	3.17E–05	3.18E–05	3.17E–05	3.17E–05
Sm-147	0	0	0	0	0	0	0	0	0	0	0	0	0
Sm-151	1.03E–05	1.03E–05	1.03E–05	1.03E–05	1.03E–05	1.03E–05	1.03E–05	1.03E–05	9.92E–06	1.03E–05	1.03E–05	1.03E–05	1.03E–05
Sn-126	5.66E–04	5.03E–04	4.38E–04	5.45E–04	6.47E–04	3.50E–04	9.64E–04	5.26E–04	7.60E–05	4.11E–04	5.31E–04	4.45E–04	2.63E–04
Sr-90	6.30E–04	6.00E–04	5.80E–04	6.30E–04	6.39E–04	4.50E–04	6.50E–04	6.20E–04	7.60E–09	5.40E–04	6.25E–04	5.80E–04	2.90E–04
Tc-99	5.80E–05	5.80E–05	5.80E–05	5.80E–05	5.81E–05	5.70E–05	5.80E–05	5.80E–05	3.10E–09	5.80E–05	5.80E–05	5.80E–05	5.60E–05
Th-228	7.60E–04	7.60E–04	5.70E–04	7.60E–04	6.72E–04	5.70E–04	1.20E–03	7.60E–04	1.20E–08	5.70E–04	5.76E–04	5.70E–04	3.80E–04
Th-229	7.11E–05	6.78E–05	6.28E–05	6.96E–05	7.71E–05	5.95E–05	9.64E–05	6.84E–05	4.89E–05	6.15E–05	6.87E–05	6.31E–05	5.77E–05
Th-230	0	0	0	0	8.48E–06	0	0	0	0	0	8.40E–06	0	0
Th-232	0	0	0	0	7.22E–06	0	0	0	0	0	7.15E–06	0	0
U-232	1.01E–05	1.00E–05	9.74E–06	1.01E–05	1.02E–05	9.40E–06	1.03E–05	1.01E–05	8.55E–06	9.61E–06	1.01E–05	9.77E–06	9.21E–06
U-233	3.60E–06	3.56E–06	3.40E–06	3.58E–06	3.65E–06	3.22E–06	3.74E–06	3.57E–06	2.88E–06	3.33E–06	3.57E–06	3.41E–06	3.13E–06
U-234	0	0	0	0	7.74E–06	0	0	0	0	0	7.65E–06	0	0
U-235	1.35E–04	1.35E–04	1.08E–04	1.35E–04	1.46E–04	1.08E–04	1.89E–04	1.35E–04	6.80E–09	1.08E–04	1.31E–04	1.35E–04	1.08E–04
U-236	6.61E–06	6.55E–06	6.34E–06	6.59E–06	6.65E–06	6.07E–06	6.69E–06	6.57E–06	5.58E–06	6.23E–06	6.57E–06	6.35E–06	5.94E–06
U-238	0	0	0	0	5.83E–06	0	0	0	0	0	5.77E–06	0	0
Zr-93	1.03E–05	1.03E–05	1.03E–05	1.03E–05	1.03E–05	1.03E–05	1.03E–05	1.03E–05	1.00E–05	1.03E–05	1.03E–05	1.03E–05	1.03E–05

Tabel E-12. DCC_int_beta_gamma for limnic organisms ((μGy h^{-1})/(Bq $kgfw^{-1}$)).

Radionuclides	Amphibian	Benthic fish	Bird	Bivalve mollusc	Crustacean	Gastropod	Insect larvae	Mammal	Microphyto-benthos	Pelagic fish	Phyto-plankton	Vascular plant	Zooplankton
Ac-227	4.71E–06	4.74E–06	4.74E–06	4.72E–06	4.66E–06	4.70E–06	4.66E–06	4.74E–06	4.14E–06	4.73E–06	4.14E–06	4.66E–06	4.64E–06
Ag-108m	7.94E–05	1.72E–04	1.79E–04	9.31E–05	1.80E–05	5.55E–05	1.88E–05	2.47E–04	3.84E–06	1.62E–04	3.84E–06	2.49E–05	1.25E–05
Am-241	3.20E–05	3.20E–05	3.20E–05	3.20E–05	3.20E–05	3.20E–05	3.20E–05	3.20E–05	2.03E–05	3.20E–05	6.50E–11	3.20E–05	3.20E–05
Am-242m	1.25E–04	1.29E–04	1.29E–04	1.26E–04	1.01E–04	1.22E–04	1.03E–04	1.30E–04	4.53E–05	1.29E–04	4.53E–05	9.81E–05	8.92E–05
Am-243	1.62E–04	1.79E–04	1.80E–04	1.64E–04	1.38E–04	1.56E–04	1.39E–04	1.91E–04	7.17E–05	1.77E–04	7.17E–05	1.33E–04	1.29E–04
Ba-133	4.00E–05	6.82E–05	7.01E–05	4.41E–05	2.62E–05	3.33E–05	2.63E–05	9.00E–05	1.72E–05	6.55E–05	1.72E–05	2.61E–05	2.49E–05
Be-10	1.42E–04	1.44E–04	1.44E–04	1.43E–04	1.06E–04	1.40E–04	1.08E–04	1.45E–04	2.13E–05	1.44E–04	2.13E–05	9.96E–05	8.38E–05
C-14-ind	2.77E–05	2.87E–05	2.87E–05	2.77E–05	2.77E–05	2.77E–05	2.77E–05	2.87E–05	1.93E–05	2.87E–05	5.35E–11	2.67E–05	2.67E–05
C-14-inorg	2.77E–05	2.87E–05	2.87E–05	2.77E–05	2.77E–05	2.77E–05	2.77E–05	2.87E–05	1.93E–05	2.87E–05	5.35E–11	2.67E–05	2.67E–05
C-14-org	2.77E–05	2.87E–05	2.87E–05	2.77E–05	2.77E–05	2.77E–05	2.77E–05	2.87E–05	1.93E–05	2.87E–05	5.35E–11	2.67E–05	2.67E–05
Ca-41	2.34E–07	2.39E–07	2.39E–07	2.36E–07	1.83E–07	2.27E–07	1.84E–07	2.40E–07	1.61E–07	2.39E–07	1.61E–07	1.88E–07	1.79E–07
Cd-113m	1.05E–04	1.06E–04	1.06E–04	1.06E–04	8.27E–05	1.03E–04	8.41E–05	1.06E–04	2.35E–05	1.06E–04	2.35E–05	7.78E–05	6.92E–05
Cl-36	1.60E–04	1.60E–04	1.60E–04	1.60E–04	1.10E–04	1.50E–04	1.10E–04	1.60E–04	1.79E–05	1.60E–04	1.20E–10	1.10E–04	8.00E–05
Cm-242	0	0	0	0	0	0	0	0	3.96E–06	0	0	0	0
Cm-243	6.80E–05	1.02E–04	1.02E–04	6.80E–05	6.80E–05	6.80E–05	6.80E–05	1.02E–04	3.71E–05	1.02E–04	1.40E–10	6.80E–05	6.80E–05
Cm-244	0	0	0	0	0	0	0	0	3.55E–06	0	0	0	0
Cm-245	3.80E–05	4.52E–05	4.55E–05	3.91E–05	3.19E–05	3.57E–05	3.21E–05	5.03E–05	2.30E–05	4.46E–05	2.30E–05	3.19E–05	3.13E–05
Cm-246	4.44E–06	4.69E–06	4.69E–06	4.50E–06	3.98E–06	4.27E–06	3.98E–06	4.73E–06	3.31E–06	4.68E–06	3.31E–06	3.99E–06	3.94E–06
Co-60	1.10E–04	2.30E–04	2.40E–04	1.20E–04	5.10E–05	7.90E–05	5.20E–05	3.30E–04	2.56E–05	2.10E–04	8.81E–11	5.20E–05	4.80E–05
Cs-134	1.30E–04	2.10E–04	2.20E–04	1.40E–04	7.03E–05	1.10E–04	7.20E–05	2.80E–04	1.88E–05	2.10E–04	9.31E–11	6.93E–05	5.64E–05
Cs-135	3.86E–05	3.86E–05	3.86E–05	3.86E–05	3.66E–05	3.86E–05	3.66E–05	3.86E–05	2.30E–05	3.86E–05	6.83E–11	3.56E–05	3.56E–05
Cs-137	1.50E–04	1.90E–04	1.90E–04	1.60E–04	9.60E–05	1.40E–04	9.80E–05	2.10E–04	2.36E–05	1.80E–04	1.19E–10	9.80E–05	7.60E–05
Eu-152	8.83E–05	1.47E–04	1.57E–04	9.70E–05	4.65E–05	7.39E–05	4.74E–05	1.96E–04	1.71E–05	1.47E–04	6.83E–11	4.84E–05	3.96E–05
Eu-154	1.88E–04	2.57E–04	2.57E–04	1.98E–04	1.08E–04	1.68E–04	1.08E–04	3.07E–04	3.64E–05	2.48E–04	1.47E–10	1.18E–04	8.82E–05
Eu-155	3.57E–05	4.05E–05	4.07E–05	3.63E–05	3.30E–05	3.47E–05	3.31E–05	4.43E–05	2.37E–05	4.00E–05	2.37E–05	3.28E–05	3.25E–05
Fe-55	9.23E–07	9.59E–07	9.58E–07	9.35E–07	5.55E–07	8.71E–07	5.64E–07	9.63E–07	3.95E–07	9.58E–07	3.95E–07	5.86E–07	5.22E–07
Gd-152	0	0	0	0	0	0	0	0	0	0	0	0	0
H-3	8.25E–07	8.25E–07	8.25E–07	8.25E–07	8.25E–07	8.25E–07	8.25E–07	8.25E–07	7.57E–07	8.25E–07	1.68E–12	8.25E–07	8.25E–07
Ho-166m	1.13E–04	2.08E–04	2.16E–04	1.27E–04	6.64E–05	9.09E–05	6.70E–05	2.89E–04	3.97E–05	1.99E–04	3.97E–05	6.76E–05	6.29E–05
I-129	3.39E–05	3.92E–05	3.92E–05	3.52E–05	3.10E–05	3.31E–05	3.10E–05	4.09E–05	2.24E–05	3.83E–05	6.11E–11	3.10E–05	3.10E–05
In-115	8.65E–05	8.73E–05	8.73E–05	8.68E–05	7.20E–05	8.54E–05	7.29E–05	8.74E–05	2.51E–05	8.73E–05	2.51E–05	6.73E–05	6.32E–05
Mo-93	5.42E–06	7.21E–06	7.19E–06	5.91E–06	2.21E–06	4.20E–06	2.23E–06	7.43E–06	1.68E–06	7.14E–06	1.68E–06	2.35E–06	2.10E–06
Nb-93m	1.59E–05	1.62E–05	1.62E–05	1.60E–05	1.53E–05	1.57E–05	1.53E–05	1.63E–05	1.30E–05	1.62E–05	1.30E–05	1.53E–05	1.52E–05

Radionuclides	Amphibian	Benthic fish	Bird	Bivalve mollusc	Crustacean	Gastropod	Insect larvae	Mammal	Microphyto-benthos	Pelagic fish	Phyto-plankton	Vascular plant	Zooplankton
Nb-94	1.30E–04	2.20E–04	2.20E–04	1.40E–04	7.90E–05	1.10E–04	8.10E–05	2.90E–04	2.49E–05	2.10E–04	1.20E–10	7.60E–05	6.80E–05
Ni-59	1.29E–06	1.36E–06	1.36E–06	1.33E–06	6.93E–07	1.22E–06	6.93E–07	1.36E–06	4.19E–07	1.36E–06	1.11E–12	7.48E–07	6.27E–07
Ni-63	8.71E–06	8.71E–06	8.71E–06	8.71E–06	8.62E–06	8.71E–06	8.62E–06	8.71E–06	7.30E–06	8.71E–06	1.76E–11	8.62E–06	8.62E–06
Np-237	2.80E–05	5.60E–05	5.60E–05	2.80E–05	2.80E–05	2.80E–05	2.80E–05	5.60E–05	2.66E–05	5.60E–05	5.70E–11	2.80E–05	2.80E–05
Pa-231	3.50E–05	3.90E–05	3.92E–05	3.58E–05	2.98E–05	3.32E–05	2.99E–05	4.12E–05	2.41E–05	3.87E–05	2.41E–05	2.98E–05	2.93E–05
Pb-210	2.35E–04	2.45E–04	2.45E–04	2.35E–04	1.36E–04	2.25E–04	1.36E–04	2.45E–04	2.83E–05	2.45E–04	1.50E–10	1.46E–04	9.60E–05
Pd-107	3.55E–06	3.55E–06	3.55E–06	3.55E–06	3.54E–06	3.55E–06	3.54E–06	3.55E–06	3.20E–06	3.55E–06	3.20E–06	3.54E–06	3.54E–06
Pm-147	3.53E–05	3.54E–05	3.54E–05	3.53E–05	3.35E–05	3.52E–05	3.37E–05	3.54E–05	2.13E–05	3.54E–05	2.13E–05	3.30E–05	3.27E–05
Po-210	0	0	0	0	0	0	0	0	2.93E–13	0	0	0	0
Pu-238	0	0	0	0	0	0	0	0	4.42E–06	0	0	0	0
Pu-239	0	0	0	0	0	0	0	0	2.32E–06	0	0	0	0
Pu-240	0	0	0	0	0	0	0	0	4.40E–06	0	0	0	0
Pu-241	8.37E–07	8.37E–07	8.37E–07	8.37E–07	8.37E–07	8.37E–07	8.37E–07	8.37E–07	7.78E–07	8.37E–07	1.70E–12	8.37E–07	8.37E–07
Pu-242	4.85E–06	5.07E–06	5.07E–06	4.91E–06	4.38E–06	4.69E–06	4.39E–06	5.10E–06	3.62E–06	5.06E–06	3.62E–06	4.40E–06	4.35E–06
Ra-226	5.60E–04	7.50E–04	7.50E–04	5.60E–04	2.80E–04	5.60E–04	2.80E–04	7.50E–04	4.29E–05	7.50E–04	2.90E–10	2.80E–04	2.80E–04
Ra-228	2.91E–04	3.40E–04	3.49E–04	3.01E–04	1.50E–04	2.62E–04	1.50E–04	3.92E–04	4.45E–05	3.40E–04	1.91E–10	1.71E–04	1.12E–04
Ru-106	6.90E–04	7.90E–04	7.90E–04	7.20E–04	1.08E–04	5.50E–04	1.19E–04	8.20E–04	5.86E–06	7.80E–04	9.12E–11	2.28E–04	7.06E–05
Sb-125	6.72E–05	9.31E–05	9.51E–05	7.01E–05	4.70E–05	5.99E–05	4.79E–05	1.16E–04	2.25E–05	9.02E–05	7.81E–11	4.61E–05	4.32E–05
Se-79	3.17E–05	3.17E–05	3.17E–05	3.17E–05	3.07E–05	3.17E–05	3.07E–05	3.17E–05	2.10E–05	3.17E–05	5.94E–11	3.07E–05	2.97E–05
Sm-147	0	0	0	0	0	0	0	0	0	0	0	0	0
Sm-151	1.03E–05	1.03E–05	1.03E–05	1.03E–05	1.02E–05	1.03E–05	1.02E–05	1.03E–05	8.51E–06	1.03E–05	8.51E–06	1.02E–05	1.02E–05
Sn-126	4.51E–04	5.59E–04	5.66E–04	4.70E–04	1.94E–04	4.04E–04	2.00E–04	6.37E–04	5.62E–05	5.49E–04	5.62E–05	2.46E–04	1.50E–04
Sr-90	5.90E–04	6.30E–04	6.30E–04	6.00E–04	2.00E–04	5.30E–04	2.10E–04	6.40E–04	2.77E–05	6.30E–04	2.10E–10	2.80E–04	1.40E–04
Tc-99	5.80E–05	5.80E–05	5.80E–05	5.80E–05	5.30E–05	5.80E–05	5.30E–05	5.80E–05	2.66E–05	5.80E–05	9.30E–11	5.10E–05	5.00E–05
Th-228	5.70E–04	7.60E–04	7.60E–04	5.70E–04	1.90E–04	5.70E–04	1.90E–04	7.60E–04	6.26E–05	7.60E–04	3.80E–10	3.80E–04	1.90E–04
Th-229	6.35E–05	7.08E–05	7.11E–05	6.47E–05	5.60E–05	6.11E–05	5.62E–05	7.59E–05	3.94E–05	7.02E–05	3.94E–05	5.56E–05	5.48E–05
Th-230	0	0	0	0	0	0	0	0	5.78E–06	0	0	0	0
Th-232	0	0	0	0	0	0	0	0	5.06E–06	0	0	0	0
U-232	9.80E–06	1.01E–05	1.01E–05	9.89E–06	9.08E–06	9.58E–06	9.09E–06	1.02E–05	7.06E–06	1.01E–05	7.06E–06	9.08E–06	8.97E–06
U-233	3.43E–06	3.60E–06	3.60E–06	3.48E–06	3.07E–06	3.31E–06	3.07E–06	3.64E–06	2.47E–06	3.60E–06	2.47E–06	3.07E–06	3.03E–06
U-234	0	0	0	0	0	0	0	0	5.44E–06	0	0	0	0
U-235	1.35E–04	1.35E–04	1.35E–04	1.35E–04	1.08E–04	1.08E–04	1.08E–04	1.35E–04	7.47E–05	1.35E–04	2.16E–10	1.08E–04	1.08E–04
U-236	6.38E–06	6.61E–06	6.61E–06	6.44E–06	5.85E–06	6.21E–06	5.86E–06	6.64E–06	4.72E–06	6.60E–06	4.72E–06	5.86E–06	5.79E–06
U-238	0	0	0	0	0	0	0	0	4.15E–06	0	0	0	0
Zr-93	1.03E–05	1.03E–05	1.03E–05	1.03E–05	1.03E–05	1.03E–05	1.03E–05	1.03E–05	8.65E–06	1.03E–05	8.65E–06	1.03E–05	1.02E–05

Tabel E-13. DCC_int_beta_gamma for terrestrial organisms ((μGy h^{-1})/(Bq $kgfw^{-1}$)).

Radio-nuclides	Amphibian	Bird	Bird egg	Detritivorous invertebrate	European otter	Flying insects	Gastropod	Grasses & Herbs	Lichen & bryophytes	Mammal (Deer)	Mammal (Rat)	Reptile	Ruddy turnstone	Shrub	Soil Invertebrate (worm)	Tree
Ac-227	4.71E–06	4.74E–06	4.72E–06	4.68E–06	4.75E–06	4.68E–06	4.69E–06	4.69E–06	4.67E–06	4.78E–06	4.73E–06	4.72E–06	4.73E–06	4.69E–06	4.69E–06	4.78E–06
Ag-108m	7.94E–05	1.79E–04	8.99E–05	3.22E–05	2.56E–04	4.15E–05	4.80E–05	5.05E–05	2.68E–05	6.17E–04	1.27E–04	1.15E–04	1.45E–04	5.05E–05	5.28E–05	5.73E–04
Am-241	3.20E–05	3.20E–05	3.20E–05	3.20E–05	3.47E–05	3.20E–05	3.20E–05	3.20E–05	3.20E–05	3.20E–05	3.20E–05	3.20E–05	3.15E–05	3.20E–05	3.20E–05	3.20E–05
Am-242m	1.25E–04	1.29E–04	1.26E–04	1.15E–04	1.30E–04	1.19E–04	1.21E–04	1.21E–04	1.09E–04	1.34E–04	1.28E–04	1.27E–04	1.28E–04	1.21E–04	1.22E–04	1.34E–04
Am-243	1.62E–04	1.80E–04	1.64E–04	1.48E–04	1.94E–04	1.52E–04	1.54E–04	1.55E–04	1.44E–04	2.47E–04	1.70E–04	1.69E–04	1.74E–04	1.55E–04	1.56E–04	2.48E–04
Ba-133	4.00E–05	7.01E–05	4.32E–05	2.84E–05	9.36E–05	3.01E–05	3.15E–05	3.20E–05	2.74E–05	1.83E–04	5.44E–05	5.14E–05	6.00E–05	3.20E–05	3.26E–05	1.81E–04
Be-10	1.42E–04	1.44E–04	1.43E–04	1.28E–04	1.45E–04	1.35E–04	1.37E–04	1.38E–04	1.20E–04	1.45E–04	1.44E–04	1.44E–04	1.44E–04	1.38E–04	1.39E–04	1.45E–04
C-14-ind	2.77E–05	2.87E–05	2.77E–05	2.77E–05	2.81E–05	2.77E–05	2.77E–05	2.77E–05	2.77E–05	2.87E–05	2.87E–05	2.87E–05	2.81E–05	2.77E–05	2.77E–05	2.87E–05
C-14-inorg	2.77E–05	2.87E–05	2.77E–05	2.77E–05	2.81E–05	2.77E–05	2.77E–05	2.77E–05	2.77E–05	2.87E–05	2.87E–05	2.87E–05	2.81E–05	2.77E–05	2.77E–05	2.87E–05
C-14-org	2.77E–05	2.87E–05	2.77E–05	2.77E–05	2.81E–05	2.77E–05	2.77E–05	2.77E–05	2.77E–05	2.87E–05	2.87E–05	2.87E–05	2.81E–05	2.77E–05	2.77E–05	2.87E–05
Ca-41	2.34E–07	2.39E–07	2.35E–07	2.03E–07	2.40E–07	2.16E–07	2.22E–07	2.24E–07	1.93E–07	2.41E–07	2.38E–07	2.39E–07	2.39E–07	2.24E–07	2.26E–07	2.41E–07
Cd-113m	1.05E–04	1.06E–04	1.05E–04	9.64E–05	1.07E–04	1.00E–04	1.02E–04	1.03E–04	9.09E–05	1.07E–04	1.06E–04	1.06E–04	1.06E–04	1.03E–04	1.03E–04	1.07E–04
Cl-36	1.60E–04	1.60E–04	1.60E–04	1.40E–04	1.57E–04	1.40E–04	1.50E–04	1.50E–04	1.30E–04	1.60E–04	1.60E–04	1.60E–04	1.56E–04	1.50E–04	1.50E–04	1.60E–04
Cm-242	0	0	0	0	5.68E–06	0	0	0	0	0	0	0	5.57E–06	0	0	0
Cm-243	6.80E–05	1.02E–04	6.80E–05	6.80E–05	9.55E–05	6.80E–05	6.80E–05	6.80E–05	6.80E–05	1.40E–04	6.80E–05	6.80E–05	8.44E–05	6.80E–05	6.80E–05	1.40E–04
Cm-244	0	0	0	0	5.09E–06	0	0	0	0	0	0	0	4.99E–06	0	0	0
Cm-245	3.80E–05	4.55E–05	3.89E–05	3.35E–05	5.15E–05	3.43E–05	3.50E–05	3.52E–05	3.28E–05	7.27E–05	4.17E–05	4.12E–05	4.31E–05	3.52E–05	3.54E–05	7.36E–05
Cm-246	4.44E–06	4.69E–06	4.49E–06	4.07E–06	4.74E–06	4.15E–06	4.20E–06	4.22E–06	4.03E–06	4.79E–06	4.61E–06	4.58E–06	4.65E–06	4.22E–06	4.24E–06	4.79E–06
Co-60	1.10E–04	2.40E–04	1.20E–04	5.90E–05	3.37E–04	6.40E–05	7.10E–05	7.40E–05	5.50E–05	8.50E–04	1.70E–04	1.50E–04	1.92E–04	7.40E–05	7.70E–05	7.30E–04
Cs-134	1.30E–04	2.20E–04	1.40E–04	8.80E–05	2.92E–04	9.70E–05	1.00E–04	1.00E–04	8.20E–05	6.30E–04	1.70E–04	1.60E–04	1.89E–04	1.00E–04	1.10E–04	5.80E–04
Cs-135	3.86E–05	3.86E–05	3.86E–05	3.76E–05	3.86E–05	3.76E–05	3.86E–05	3.86E–05	3.76E–05	3.86E–05	3.86E–05	3.86E–05	3.85E–05	3.86E–05	3.86E–05	3.86E–05
Cs-137	1.50E–04	1.90E–04	1.60E–04	1.20E–04	2.16E–04	1.40E–04	1.40E–04	1.40E–04	1.10E–04	3.40E–04	1.70E–04	1.70E–04	1.77E–04	1.40E–04	1.40E–04	3.20E–04
Eu-152	8.83E–05	1.57E–04	9.60E–05	5.89E–05	2.08E–04	6.46E–05	6.84E–05	7.03E–05	5.45E–05	4.55E–04	1.16E–04	1.16E–04	1.33E–04	7.03E–05	7.13E–05	4.06E–04
Eu-154	1.88E–04	2.57E–04	1.98E–04	1.39E–04	3.16E–04	1.49E–04	1.58E–04	1.68E–04	1.29E–04	5.80E–04	2.28E–04	2.18E–04	2.37E–04	1.68E–04	1.68E–04	5.30E–04
Eu-155	3.57E–05	4.07E–05	3.61E–05	3.39E–05	4.52E–05	3.42E–05	3.44E–05	3.45E–05	3.36E–05	5.95E–05	3.80E–05	3.77E–05	3.89E–05	3.45E–05	3.46E–05	6.03E–05
Fe-55	9.23E–07	9.58E–07	9.30E–07	7.00E–07	9.65E–07	7.92E–07	8.37E–07	8.50E–07	6.25E–07	9.70E–07	9.50E–07	9.55E–07	9.54E–07	8.50E–07	8.64E–07	9.71E–07
Gd-152	0	0	0	0	0	0	0	0	0	0	0	0	0	0	0	0
H-3	8.25E–07	8.25E–07	8.25E–07	8.25E–07	8.10E–07	1.09E–06	8.25E–07	8.25E–07	8.25E–07	8.25E–07	8.25E–07	8.25E–07	8.10E–07	8.25E–07	8.25E–07	8.25E–07
Ho-166m	1.13E–04	2.16E–04	1.23E–04	7.42E–05	2.99E–04	7.99E–05	8.47E–05	8.66E–05	7.08E–05	6.86E–04	1.61E–04	1.50E–04	1.80E–04	8.66E–05	8.88E–05	6.37E–04
I-129	3.39E–05	3.92E–05	3.52E–05	3.22E–05	4.12E–05	3.22E–05	3.31E–05	3.31E–05	3.22E–05	4.50E–05	3.70E–05	3.61E–05	3.77E–05	3.31E–05	3.31E–05	4.50E–05
In-115	8.65E–05	8.73E–05	8.67E–05	8.10E–05	8.74E–05	8.36E–05	8.47E–05	8.51E–05	7.72E–05	8.76E–05	8.71E–05	8.72E–05	8.72E–05	8.51E–05	8.53E–05	8.76E–05
Mo-93	5.42E–06	7.19E–06	5.82E–06	2.77E–06	7.53E–06	3.30E–06	3.73E–06	3.84E–06	2.48E–06	7.81E–06	6.66E–06	6.48E–06	6.92E–06	3.84E–06	3.95E–06	7.84E–06
Nb-93m	1.59E–05	1.62E–05	1.60E–05	1.54E–05	1.63E–05	1.55E–05	1.56E–05	1.56E–05	1.54E–05	1.63E–05	1.61E–05	1.61E–05	1.62E–05	1.56E–05	1.56E–05	1.63E–05

Radio-nuclides	Amphibian	Bird	Bird egg	Detritivorous invertebrate	European otter	Flying insects	Gastropod	Grasses & Herbs	Lichen & bryophytes	Mammal (Deer)	Mammal (Rat)	Reptile	Ruddy turnstone	Shrub	Soil Invertebrate (worm)	Tree
Nb-94	1.30E–04	2.20E–04	1.40E–04	9.40E–05	2.93E–04	1.00E–04	1.10E–04	1.10E–04	8.80E–05	6.40E–04	1.80E–04	1.70E–04	1.92E–04	1.10E–04	1.10E–04	5.80E–04
Ni-59	1.29E–06	1.36E–06	1.29E–06	9.36E–07	1.37E–06	1.07E–06	1.18E–06	1.18E–06	7.82E–07	1.40E–06	1.36E–06	1.36E–06	1.36E–06	1.18E–06	1.18E–06	1.40E–06
Ni-63	8.71E–06	8.71E–06	8.71E–06	8.71E–06	8.68E–06	8.91E–06	8.71E–06	8.71E–06	8.71E–06	8.71E–06	8.71E–06	8.71E–06	8.68E–06	8.71E–06	8.71E–06	8.71E–06
Np-237	2.80E–05	5.60E–05	2.80E–05	2.80E–05	4.51E–05	2.80E–05	2.80E–05	2.80E–05	2.80E–05	5.60E–05	2.80E–05	2.80E–05	4.20E–05	2.80E–05	2.80E–05	5.60E–05
Pa-231	3.50E–05	3.92E–05	3.56E–05	3.10E–05	4.16E–05	3.19E–05	3.25E–05	3.27E–05	3.04E–05	5.03E–05	3.73E–05	3.69E–05	3.81E–05	3.27E–05	3.29E–05	5.01E–05
Pb-210	2.35E–04	2.45E–04	2.35E–04	1.86E–04	2.43E–04	2.06E–04	2.16E–04	2.16E–04	1.67E–04	2.45E–04	2.35E–04	2.35E–04	2.40E–04	2.16E–04	2.25E–04	2.45E–04
Pd-107	3.55E–06	3.55E–06	3.55E–06	3.55E–06	3.55E–06	3.55E–06	3.55E–06	3.55E–06	3.55E–06	3.55E–06	3.55E–06	3.55E–06	3.55E–06	3.55E–06	3.55E–06	3.55E–06
Pm-147	3.53E–05	3.54E–05	3.53E–05	3.47E–05	3.54E–05	3.50E–05	3.51E–05	3.52E–05	3.42E–05	3.54E–05	3.54E–05	3.54E–05	3.54E–05	3.52E–05	3.52E–05	3.54E–05
Po-210	0	0	0	0	1.11E–09	0	0	0	0	0	0	0	5.61E–10	0	0	0
Pu-238	0	0	0	0	6.24E–06	0	0	0	0	0	0	0	6.14E–06	0	0	0
Pu-239	0	0	0	0	3.12E–06	0	0	0	0	0	0	0	3.08E–06	0	0	0
Pu-240	0	0	0	0	6.21E–06	0	0	0	0	0	0	0	6.11E–06	0	0	0
Pu-241	8.37E–07	8.37E–07	8.37E–07	8.37E–07	8.37E–07	1.05E–06	8.37E–07	8.37E–07	8.37E–07	8.37E–07	8.37E–07	8.37E–07	8.37E–07	8.37E–07	8.37E–07	8.37E–07
Pu-242	4.85E–06	5.07E–06	4.90E–06	4.48E–06	5.11E–06	4.56E–06	4.62E–06	4.64E–06	4.44E–06	5.16E–06	5.00E–06	4.98E–06	5.04E–06	4.64E–06	4.66E–06	5.16E–06
Ra-226	5.60E–04	7.50E–04	5.60E–04	4.20E–04	7.48E–04	4.20E–04	4.20E–04	5.60E–04	4.20E–04	1.20E–03	7.00E–04	5.60E–04	6.33E–04	5.60E–04	5.60E–04	1.05E–03
Ra-228	2.91E–04	3.49E–04	2.91E–04	2.11E–04	3.93E–04	2.30E–04	2.50E–04	2.52E–04	1.90E–04	6.04E–04	3.20E–04	3.10E–04	3.30E–04	2.52E–04	2.62E–04	5.59E–04
Ru-106	6.90E–04	7.90E–04	7.10E–04	2.57E–04	8.18E–04	3.60E–04	4.70E–04	5.10E–04	1.98E–04	8.80E–04	7.60E–04	7.20E–04	7.74E–04	5.10E–04	5.40E–04	8.80E–04
Sb-125	6.72E–05	9.51E–05	7.01E–05	5.32E–05	1.17E–04	5.61E–05	5.80E–05	5.80E–05	5.13E–05	2.18E–04	7.97E–05	7.68E–05	8.53E–05	5.80E–05	5.89E–05	2.08E–04
Se-79	3.17E–05	3.17E–05	3.17E–05	3.17E–05	3.19E–05	3.17E–05	3.17E–05	3.17E–05	3.17E–05	3.17E–05	3.17E–05	3.17E–05	3.18E–05	3.17E–05	3.17E–05	3.17E–05
Sm-147	0	0	0	0	0	0	0	0	0	0	0	0	0	0	0	0
Sm-151	1.03E–05	1.03E–05	1.03E–05	1.03E–05	1.03E–05	1.03E–05	1.03E–05	1.03E–05	1.03E–05	1.03E–05	1.03E–05	1.03E–05	1.03E–05	1.03E–05	1.03E–05	1.03E–05
Sn-126	4.51E–04	5.66E–04	4.65E–04	2.99E–04	6.47E–04	3.51E–04	3.79E–04	3.90E–04	2.61E–04	1.01E–03	5.10E–04	4.92E–04	5.31E–04	3.90E–04	3.97E–04	9.64E–04
Sr-90	5.90E–04	6.30E–04	6.00E–04	3.50E–04	6.39E–04	4.20E–04	4.90E–04	5.10E–04	2.90E–04	6.50E–04	6.20E–04	6.00E–04	6.25E–04	5.10E–04	5.20E–04	6.50E–04
Tc-99	5.80E–05	5.80E–05	5.80E–05	5.60E–05	5.81E–05	5.70E–05	5.70E–05	5.80E–05	5.40E–05	5.80E–05	5.80E–05	5.80E–05	5.80E–05	5.80E–05	5.80E–05	5.80E–05
Th-228	5.70E–04	7.60E–04	5.70E–04	3.80E–04	6.72E–04	5.70E–04	5.70E–04	5.70E–04	3.80E–04	1.20E–03	7.60E–04	7.60E–04	5.76E–04	5.70E–04	5.70E–04	1.00E–03
Th-229	6.35E–05	7.11E–05	6.44E–05	5.82E–05	7.71E–05	5.94E–05	6.02E–05	6.05E–05	5.73E–05	9.79E–05	6.73E–05	6.69E–05	6.87E–05	6.05E–05	6.08E–05	9.88E–05
Th-230	0	0	0	0	8.48E–06	0	0	0	0	0	0	0	8.40E–06	0	0	0
Th-232	0	0	0	0	7.22E–06	0	0	0	0	0	0	0	7.15E–06	0	0	0
U-232	9.80E–06	1.01E–05	9.87E–06	9.26E–06	1.02E–05	9.39E–06	9.48E–06	9.51E–06	9.19E–06	1.03E–05	1.00E–05	9.99E–06	1.01E–05	9.51E–06	9.53E–06	1.03E–05
U-233	3.43E–06	3.60E–06	3.47E–06	3.15E–06	3.65E–06	3.22E–06	3.26E–06	3.28E–06	3.11E–06	3.75E–06	3.55E–06	3.53E–06	3.57E–06	3.28E–06	3.29E–06	3.75E–06
U-234	0	0	0	0	7.74E–06	0	0	0	0	0	0	0	7.65E–06	0	0	0
U-235	1.35E–04	1.35E–04	1.35E–04	1.08E–04	1.46E–04	1.08E–04	1.08E–04	1.08E–04	1.08E–04	1.89E–04	1.35E–04	1.35E–04	1.31E–04	1.08E–04	1.08E–04	1.89E–04
U-236	6.38E–06	6.61E–06	6.43E–06	5.97E–06	6.65E–06	6.07E–06	6.14E–06	6.16E–06	5.92E–06	6.70E–06	6.54E–06	6.52E–06	6.57E–06	6.16E–06	6.17E–06	6.70E–06
U-238	0	0	0	0	5.83E–06	0	0	0	0	0	0	0	5.77E–06	0	0	0
Zr-93	1.03E–05	1.03E–05	1.03E–05	1.03E–05	1.03E–05	1.03E–05	1.03E–05	1.03E–05	1.03E–05	1.03E–05	1.03E–05	1.03E–05	1.03E–05	1.03E–05	1.03E–05	1.03E–05

Table E-14. DCC_int_low_beta for terrestrial organisms.

Radio-nuclides	Amphibian	Bird	Bird egg	Detritivorous invertebrate	European otter	Flying insects	Gastropod	Grasses & Herbs	Lichen & bryophytes	Mammal (Deer)	Mammal (Rat)	Reptile	Ruddy turnstone	Shrub	Soil Invertebrate (worm)	Tree
Ac-227	4.45E–06	4.45E–06	4.45E–06	4.45E–06	4.45E–06	4.45E–06	4.45E–06	4.45E–06	4.45E–06	4.45E–06	4.45E–06	4.45E–06	4.45E–06	4.45E–06	4.45E–06	4.45E–06
Ag-108m	1.81E–06	1.81E–06	1.81E–06	1.81E–06	1.81E–06	1.81E–06	1.81E–06	1.81E–06	1.81E–06	1.81E–06	1.81E–06	1.81E–06	1.81E–06	1.81E–06	1.81E–06	1.81E–06
Am-241	0	0	0	0	5.73E–06	0	0	0	0	0	0	0	5.73E–06	0	0	0
Am-242m	5.26E–06	5.26E–06	5.26E–06	5.26E–06	5.26E–06	5.26E–06	5.26E–06	5.26E–06	5.26E–06	5.26E–06	5.26E–06	5.26E–06	5.26E–06	5.26E–06	5.26E–06	5.26E–06
Am-243	9.72E–06	9.72E–06	9.72E–06	9.72E–06	9.72E–06	9.72E–06	9.72E–06	9.72E–06	9.72E–06	9.72E–06	9.72E–06	9.72E–06	9.72E–06	9.72E–06	9.72E–06	9.72E–06
Ba-133	4.42E–06	4.42E–06	4.42E–06	4.42E–06	4.42E–06	4.42E–06	4.42E–06	4.42E–06	4.42E–06	4.42E–06	4.42E–06	4.42E–06	4.42E–06	4.42E–06	4.42E–06	4.42E–06
Be-10	2.33E–08	2.33E–08	2.33E–08	2.33E–08	2.33E–08	2.33E–08	2.33E–08	2.33E–08	2.33E–08	2.33E–08	2.33E–08	2.33E–08	2.33E–08	2.33E–08	2.33E–08	2.33E–08
C-14-ind	2.80E–07	2.90E–07	2.80E–07	2.80E–07	3.73E–07	2.80E–07	2.80E–07	2.80E–07	2.80E–07	2.90E–07	2.90E–07	2.90E–07	3.73E–07	2.80E–07	2.80E–07	2.90E–07
C-14-inorg	2.80E–07	2.90E–07	2.80E–07	2.80E–07	3.73E–07	2.80E–07	2.80E–07	2.80E–07	2.80E–07	2.90E–07	2.90E–07	2.90E–07	3.73E–07	2.80E–07	2.80E–07	2.90E–07
C-14-org	2.80E–07	2.90E–07	2.80E–07	2.80E–07	3.73E–07	2.80E–07	2.80E–07	2.80E–07	2.80E–07	2.90E–07	2.90E–07	2.90E–07	3.73E–07	2.80E–07	2.80E–07	2.90E–07
Ca-41	1.35E–06	1.35E–06	1.35E–06	1.35E–06	1.35E–06	1.35E–06	1.35E–06	1.35E–06	1.35E–06	1.35E–06	1.35E–06	1.35E–06	1.35E–06	1.35E–06	1.35E–06	1.35E–06
Cd-113m	1.09E–07	1.09E–07	1.09E–07	1.09E–07	1.09E–07	1.09E–07	1.09E–07	1.09E–07	1.09E–07	1.09E–07	1.09E–07	1.09E–07	1.09E–07	1.09E–07	1.09E–07	1.09E–07
Cl-36	0	0	0	0	6.91E–08	0	0	0	0	0	0	0	6.91E–08	0	0	0
Cm-242	0	0	0	0	8.19E–07	0	0	0	0	0	0	0	8.19E–07	0	0	0
Cm-243	0	0	0	0	7.95E–06	0	0	0	0	0	0	0	7.95E–06	0	0	0
Cm-244	0	0	0	0	7.62E–07	0	0	0	0	0	0	0	7.62E–07	0	0	0
Cm-245	4.93E–06	4.93E–06	4.93E–06	4.93E–06	4.93E–06	4.93E–06	4.93E–06	4.93E–06	4.93E–06	4.93E–06	4.93E–06	4.93E–06	4.93E–06	4.93E–06	4.93E–06	4.93E–06
Cm-246	6.77E–07	6.77E–07	6.77E–07	6.77E–07	6.77E–07	6.77E–07	6.77E–07	6.77E–07	6.77E–07	6.77E–07	6.77E–07	6.77E–07	6.77E–07	6.77E–07	6.77E–07	6.77E–07
Co-60	0	0	0	0	2.26E–07	0	0	0	0	0	0	0	2.26E–07	0	0	0
Cs-134	0	0	0	0	3.59E–07	0	0	0	0	0	0	0	3.59E–07	0	0	0
Cs-135	3.90E–07	3.90E–07	3.90E–07	3.80E–07	3.05E–07	3.80E–07	3.90E–07	3.90E–07	3.80E–07	3.90E–07	3.90E–07	3.90E–07	3.05E–07	3.90E–07	3.90E–07	3.90E–07
Cs-137	0	0	0	0	3.71E–07	0	0	0	0	0	0	0	3.71E–07	0	0	0
Eu-152	3.68E–06	3.20E–06	2.97E–06	3.10E–06	3.42E–06	3.40E–06	3.60E–06	3.70E–06	3.48E–06	4.60E–06	3.60E–06	3.60E–06	3.42E–06	3.70E–06	3.75E–06	4.10E–06
Eu-154	1.90E–06	2.60E–06	2.00E–06	1.40E–06	1.83E–06	1.50E–06	1.60E–06	1.70E–06	1.30E–06	0	2.30E–06	2.20E–06	1.83E–06	1.70E–06	1.70E–06	0
Eu-155	2.72E–06	2.72E–06	2.72E–06	2.72E–06	2.72E–06	2.72E–06	2.72E–06	2.72E–06	2.72E–06	2.72E–06	2.72E–06	2.72E–06	2.72E–06	2.72E–06	2.72E–06	2.72E–06
Fe-55	2.43E–06	2.43E–06	2.43E–06	2.43E–06	2.43E–06	2.43E–06	2.43E–06	2.43E–06	2.43E–06	2.43E–06	2.43E–06	2.43E–06	2.43E–06	2.43E–06	2.43E–06	2.43E–06
Gd-152	0	0	0	0	0	0	0	0	0	0	0	0	0	0	0	0
H-3	2.48E–06	2.48E–06	2.48E–06	2.48E–06	2.47E–06	2.21E–06	2.48E–06	2.48E–06	2.48E–06	2.48E–06	2.48E–06	2.48E–06	2.47E–06	2.48E–06	2.48E–06	2.48E–06
Ho-166m	5.42E–06	5.42E–06	5.42E–06	5.42E–06	5.42E–06	5.42E–06	5.42E–06	5.42E–06	5.42E–06	5.42E–06	5.42E–06	5.42E–06	5.42E–06	5.42E–06	5.42E–06	5.42E–06
I-129	5.07E–06	4.84E–06	4.80E–06	4.81E–06	4.94E–06	4.81E–06	4.94E–06	4.94E–06	4.81E–06	5.00E–06	5.04E–06	4.92E–06	4.94E–06	4.94E–06	4.94E–06	5.00E–06
In-115	1.39E–07	1.39E–07	1.39E–07	1.39E–07	1.39E–07	1.39E–07	1.39E–07	1.39E–07	1.39E–07	1.39E–07	1.39E–07	1.39E–07	1.39E–07	1.39E–07	1.39E–07	1.39E–07
Mo-93	1.41E–06	1.41E–06	1.41E–06	1.41E–06	1.41E–06	1.41E–06	1.41E–06	1.41E–06	1.41E–06	1.41E–06	1.41E–06	1.41E–06	1.41E–06	1.41E–06	1.41E–06	1.41E–06
Nb-93m	1.16E–06	1.16E–06	1.16E–06	1.16E–06	1.16E–06	1.16E–06	1.16E–06	1.16E–06	1.16E–06	1.16E–06	1.16E–06	1.16E–06	1.16E–06	1.16E–06	1.16E–06	1.16E–06

Radio-nuclides	Amphibian	Bird	Bird egg	Detritivorous invertebrate	European otter	Flying insects	Gastropod	Grasses & Herbs	Lichen & bryophytes	Mammal (Deer)	Mammal (Rat)	Reptile	Ruddy turnstone	Shrub	Soil Invertebrate (worm)	Tree
Nb-94	0	0	0	0	1.25E–07	0	0	0	0	0	0	0	1.25E–07	0	0	0
Ni-59	2.61E–06	2.64E–06	2.61E–06	2.66E–06	2.63E–06	2.63E–06	2.62E–06	2.62E–06	2.62E–06	2.60E–06	2.64E–06	2.64E–06	2.63E–06	2.62E–06	2.62E–06	2.60E–06
Ni-63	1.19E–06	1.19E–06	1.19E–06	1.19E–06	1.21E–06	9.90E–07	1.19E–06	1.19E–06	1.19E–06	1.19E–06	1.19E–06	1.19E–06	1.21E–06	1.19E–06	1.19E–06	1.19E–06
Np-237	0	0	0	0	5.49E–06	0	0	0	0	0	0	0	5.49E–06	0	0	0
Pa-231	7.58E–06	7.58E–06	7.58E–06	7.58E–06	7.58E–06	7.58E–06	7.58E–06	7.58E–06	7.58E–06	7.58E–06	7.58E–06	7.58E–06	7.58E–06	7.58E–06	7.58E–06	7.58E–06
Pb-210	4.80E–06	5.00E–06	4.80E–06	3.80E–06	4.23E–06	4.20E–06	4.40E–06	4.40E–06	3.40E–06	5.00E–06	4.80E–06	4.80E–06	4.23E–06	4.40E–06	4.60E–06	5.00E–06
Pd-107	1.79E–06	1.79E–06	1.79E–06	1.79E–06	1.79E–06	1.79E–06	1.79E–06	1.79E–06	1.79E–06	1.79E–06	1.79E–06	1.79E–06	1.79E–06	1.79E–06	1.79E–06	1.79E–06
Pm-147	3.74E–07	3.74E–07	3.74E–07	3.74E–07	3.74E–07	3.74E–07	3.74E–07	3.74E–07	3.74E–07	3.74E–07	3.74E–07	3.74E–07	3.74E–07	3.74E–07	3.74E–07	3.74E–07
Po-210	0	0	0	0	3.66E–13	0	0	0	0	0	0	0	3.66E–13	0	0	0
Pu-238	0	0	0	0	8.70E–07	0	0	0	0	0	0	0	8.70E–07	0	0	0
Pu-239	0	0	0	0	1.18E–06	0	0	0	0	0	0	0	1.18E–06	0	0	0
Pu-240	0	0	0	0	8.28E–07	0	0	0	0	0	0	0	8.28E–07	0	0	0
Pu-241	2.20E–06	2.20E–06	2.20E–06	2.20E–06	2.19E–06	1.98E–06	2.20E–06	2.20E–06	2.20E–06	2.20E–06	2.20E–06	2.20E–06	2.19E–06	2.20E–06	2.20E–06	2.20E–06
Pu-242	6.87E–07	6.87E–07	6.87E–07	6.87E–07	6.87E–07	6.87E–07	6.87E–07	6.87E–07	6.87E–07	6.87E–07	6.87E–07	6.87E–07	6.87E–07	6.87E–07	6.87E–07	6.87E–07
Ra-226	0	0	0	0	1.63E–06	0	0	0	0	0	0	0	1.63E–06	0	0	0
Ra-228	9.00E–06	1.08E–05	9.00E–06	8.80E–06	9.14E–06	9.60E–06	1.04E–05	7.80E–06	1.00E–05	6.10E–06	9.90E–06	9.60E–06	9.14E–06	7.80E–06	8.10E–06	1.14E–05
Ru-106	0	0	0	2.60E–06	1.76E–06	0	0	0	2.00E–06	0	0	0	1.76E–06	0	0	0
Sb-125	2.80E–06	2.94E–06	2.92E–06	2.80E–06	2.93E–06	2.95E–06	3.05E–06	3.05E–06	2.70E–06	2.20E–06	3.32E–06	3.20E–06	2.93E–06	3.05E–06	3.10E–06	2.10E–06
Se-79	3.20E–07	3.20E–07	3.20E–07	3.20E–07	3.19E–07	3.20E–07	3.20E–07	3.20E–07	3.20E–07	3.20E–07	3.20E–07	3.20E–07	3.19E–07	3.20E–07	3.20E–07	3.20E–07
Sm-147	0	0	0	0	0	0	0	0	0	0	0	0	0	0	0	0
Sm-151	1.11E–06	1.11E–06	1.11E–06	1.11E–06	1.11E–06	1.11E–06	1.11E–06	1.11E–06	1.11E–06	1.11E–06	1.11E–06	1.11E–06	1.11E–06	1.11E–06	1.11E–06	1.11E–06
Sn-126	3.70E–06	3.70E–06	3.70E–06	3.70E–06	3.70E–06	3.70E–06	3.70E–06	3.70E–06	3.70E–06	3.70E–06	3.70E–06	3.70E–06	3.70E–06	3.70E–06	3.70E–06	3.70E–06
Sr-90	0	0	0	0	1.12E–07	0	0	0	0	0	0	0	1.12E–07	0	0	0
Tc-99	0	0	0	0	1.95E–07	0	0	0	0	0	0	0	1.95E–07	0	0	0
Th-228	0	0	0	0	3.73E–06	0	0	0	0	0	0	0	3.73E–06	0	0	0
Th-229	9.75E–06	9.75E–06	9.75E–06	9.75E–06	9.75E–06	9.75E–06	9.75E–06	9.75E–06	9.75E–06	9.75E–06	9.75E–06	9.75E–06	9.75E–06	9.75E–06	9.75E–06	9.75E–06
Th-230	0	0	0	0	6.49E–07	0	0	0	0	0	0	0	6.49E–07	0	0	0
Th-232	0	0	0	0	6.44E–07	0	0	0	0	0	0	0	6.44E–07	0	0	0
U-232	9.65E–07	9.65E–07	9.65E–07	9.65E–07	9.65E–07	9.65E–07	9.65E–07	9.65E–07	9.65E–07	9.65E–07	9.65E–07	9.65E–07	9.65E–07	9.65E–07	9.65E–07	9.65E–07
U-233	5.93E–07	5.93E–07	5.93E–07	5.93E–07	5.93E–07	5.93E–07	5.93E–07	5.93E–07	5.93E–07	5.93E–07	5.93E–07	5.93E–07	5.93E–07	5.93E–07	5.93E–07	5.93E–07
U-234	0	0	0	0	8.07E–07	0	0	0	0	0	0	0	8.07E–07	0	0	0
U-235	0	0	0	0	1.23E–05	0	0	0	0	0	0	0	1.23E–05	0	0	0
U-236	7.59E–07	7.59E–07	7.59E–07	7.59E–07	7.59E–07	7.59E–07	7.59E–07	7.59E–07	7.59E–07	7.59E–07	7.59E–07	7.59E–07	7.59E–07	7.59E–07	7.59E–07	7.59E–07
U-238	0	0	0	0	6.68E–07	0	0	0	0	0	0	0	6.68E–07	0	0	0
Zr-93	9.76E–07	9.76E–07	9.76E–07	9.76E–07	9.76E–07	9.76E–07	9.76E–07	9.76E–07	9.76E–07	9.76E–07	9.76E–07	9.76E–07	9.76E–07	9.76E–07	9.76E–07	9.76E–07

E-15. DCC_int_low_beta for limnic organisms ((µGy h^{-1})/(Bq kgfw^{-1})).

Radionuclides	Amphibian	Benthic fish	Bird	Bivalve mollusc	Crustacean	Gastropod	Insect larvae	Mammal	Microphyto-benthos	Pelagic fish	Phyto-plankton	Vascular plant	Zooplankton
Ac-227	4.45E–06	4.45E–06	4.45E–06	4.45E–06	4.45E–06	4.45E–06	4.45E–06	4.45E–06	4.33E–06	4.45E–06	4.33E–06	4.45E–06	4.45E–06
Ag-108m	1.81E–06	1.81E–06	1.81E–06	1.81E–06	1.81E–06	1.81E–06	1.81E–06	1.81E–06	1.79E–06	1.81E–06	1.79E–06	1.81E–06	1.81E–06
Am-241	0	0	0	0	0	0	0	0	5.61E–06	0	0	0	0
Am-242m	5.26E–06	5.26E–06	5.26E–06	5.26E–06	5.26E–06	5.26E–06	5.26E–06	5.26E–06	5.15E–06	5.26E–06	5.15E–06	5.26E–06	5.26E–06
Am-243	9.72E–06	9.72E–06	9.72E–06	9.72E–06	9.72E–06	9.72E–06	9.72E–06	9.72E–06	9.51E–06	9.72E–06	9.51E–06	9.72E–06	9.72E–06
Ba-133	4.42E–06	4.42E–06	4.42E–06	4.42E–06	4.42E–06	4.42E–06	4.42E–06	4.42E–06	4.37E–06	4.42E–06	4.37E–06	4.42E–06	4.42E–06
Be-10	2.33E–08	2.33E–08	2.33E–08	2.33E–08	2.33E–08	2.33E–08	2.33E–08	2.33E–08	2.26E–08	2.33E–08	2.26E–08	2.33E–08	2.33E–08
C-14-ind	2.80E–07	2.90E–07	2.90E–07	2.80E–07	2.80E–07	2.80E–07	2.80E–07	2.90E–07	3.62E–07	2.90E–07	5.40E–13	2.70E–07	2.70E–07
C-14-inorg	2.80E–07	2.90E–07	2.90E–07	2.80E–07	2.80E–07	2.80E–07	2.80E–07	2.90E–07	3.62E–07	2.90E–07	5.40E–13	2.70E–07	2.70E–07
C-14-org	2.80E–07	2.90E–07	2.90E–07	2.80E–07	2.80E–07	2.80E–07	2.80E–07	2.90E–07	3.62E–07	2.90E–07	5.40E–13	2.70E–07	2.70E–07
Ca-41	1.35E–06	1.35E–06	1.35E–06	1.35E–06	1.35E–06	1.35E–06	1.35E–06	1.35E–06	1.33E–06	1.35E–06	1.33E–06	1.35E–06	1.35E–06
Cd-113m	1.09E–07	1.09E–07	1.09E–07	1.09E–07	1.09E–07	1.09E–07	1.09E–07	1.09E–07	1.06E–07	1.09E–07	1.06E–07	1.09E–07	1.09E–07
Cl-36	0	0	0	0	0	0	0	0	6.74E–08	0	0	0	0
Cm-242	0	0	0	0	0	0	0	0	8.03E–07	0	0	0	0
Cm-243	0	0	0	0	0	0	0	0	7.78E–06	0	0	0	0
Cm-244	0	0	0	0	0	0	0	0	7.47E–07	0	0	0	0
Cm-245	4.93E–06	4.93E–06	4.93E–06	4.93E–06	4.93E–06	4.93E–06	4.93E–06	4.93E–06	4.83E–06	4.93E–06	4.83E–06	4.93E–06	4.93E–06
Cm-246	6.77E–07	6.77E–07	6.77E–07	6.77E–07	6.77E–07	6.77E–07	6.77E–07	6.77E–07	6.63E–07	6.77E–07	6.63E–07	6.77E–07	6.77E–07
Co-60	0	0	0	0	0	0	0	0	2.20E–07	0	8.90E–13	0	0
Cs-134	0	0	0	0	7.10E–07	0	0	0	3.49E–07	0	9.40E–13	7.00E–07	5.70E–07
Cs-135	3.90E–07	3.90E–07	3.90E–07	3.90E–07	3.70E–07	3.90E–07	3.70E–07	3.90E–07	2.96E–07	3.90E–07	6.90E–13	3.60E–07	3.60E–07
Cs-137	0	0	0	0	0	0	0	0	3.64E–07	0	1.20E–12	0	0
Eu-152	3.68E–06	3.00E–06	3.20E–06	3.00E–06	3.50E–06	3.08E–06	3.57E–06	4.00E–06	3.36E–06	3.00E–06	6.75E–12	3.64E–06	3.44E–06
Eu-154	1.90E–06	2.60E–06	2.60E–06	2.00E–06	2.20E–06	1.70E–06	2.20E–06	3.10E–06	1.80E–06	2.50E–06	3.00E–12	2.40E–06	1.80E–06
Eu-155	2.72E–06	2.72E–06	2.72E–06	2.72E–06	2.72E–06	2.72E–06	2.72E–06	2.72E–06	2.65E–06	2.72E–06	2.65E–06	2.71E–06	2.72E–06
Fe-55	2.43E–06	2.43E–06	2.43E–06	2.43E–06	2.43E–06	2.43E–06	2.43E–06	2.43E–06	2.38E–06	2.43E–06	2.38E–06	2.42E–06	2.43E–06
Gd-152	0	0	0	0	0	0	0	0	0	0	0	0	0
H-3	2.48E–06	2.48E–06	2.48E–06	2.48E–06	2.48E–06	2.48E–06	2.48E–06	2.48E–06	2.41E–06	2.48E–06	5.03E–12	2.48E–06	2.48E–06
Ho-166m	5.42E–06	5.42E–06	5.42E–06	5.42E–06	5.42E–06	5.42E–06	5.42E–06	5.42E–06	5.30E–06	5.42E–06	5.30E–06	5.41E–06	5.42E–06
I-129	5.07E–06	4.84E–06	4.84E–06	4.80E–06	5.04E–06	4.94E–06	5.04E–06	5.06E–06	4.86E–06	4.73E–06	9.94E–12	5.04E–06	5.04E–06
In-115	1.39E–07	1.39E–07	1.39E–07	1.39E–07	1.39E–07	1.39E–07	1.39E–07	1.39E–07	1.35E–07	1.39E–07	1.35E–07	1.39E–07	1.39E–07
Mo-93	1.41E–06	1.41E–06	1.41E–06	1.41E–06	1.41E–06	1.41E–06	1.41E–06	1.41E–06	1.40E–06	1.41E–06	1.40E–06	1.41E–06	1.41E–06
Nb-93m	1.16E–06	1.16E–06	1.16E–06	1.16E–06	1.16E–06	1.16E–06	1.16E–06	1.16E–06	1.15E–06	1.16E–06	1.15E–06	1.16E–06	1.16E–06

Radionuclides	Amphibian	Benthic fish	Bird	Bivalve mollusc	Crustacean	Gastropod	Insect larvae	Mammal	Microphyto-benthos	Pelagic fish	Phyto-plankton	Vascular plant	Zooplankton
Nb-94	0	0	0	0	0	0	0	0	1.22E–07	0	0	0	0
Ni-59	2.61E–06	2.64E–06	2.64E–06	2.57E–06	2.61E–06	2.58E–06	2.61E–06	2.64E–06	2.57E–06	2.64E–06	5.40E–12	2.65E–06	2.67E–06
Ni-63	1.19E–06	1.19E–06	1.19E–06	1.19E–06	1.18E–06	1.19E–06	1.18E–06	1.19E–06	1.17E–06	1.19E–06	2.40E–12	1.18E–06	1.18E–06
Np-237	0	0	0	0	0	0	0	0	5.37E–06	0	0	0	0
Pa-231	7.58E–06	7.58E–06	7.58E–06	7.58E–06	7.58E–06	7.58E–06	7.58E–06	7.58E–06	7.43E–06	7.58E–06	7.43E–06	7.58E–06	7.58E–06
Pb-210	4.80E–06	5.00E–06	5.00E–06	4.80E–06	4.20E–06	4.60E–06	4.20E–06	5.00E–06	4.14E–06	5.00E–06	9.60E–12	4.50E–06	4.00E–06
Pd-107	1.79E–06	1.79E–06	1.79E–06	1.79E–06	1.79E–06	1.79E–06	1.79E–06	1.79E–06	1.74E–06	1.79E–06	1.74E–06	1.79E–06	1.79E–06
Pm-147	3.74E–07	3.74E–07	3.74E–07	3.74E–07	3.74E–07	3.74E–07	3.74E–07	3.74E–07	3.63E–07	3.74E–07	3.63E–07	3.74E–07	3.74E–07
Po-210	0	0	0	0	0	0	0	0	3.59E–13	0	0	0	0
Pu-238	0	0	0	0	0	0	0	0	8.54E–07	0	0	0	0
Pu-239	0	0	0	0	0	0	0	0	1.15E–06	0	0	0	0
Pu-240	0	0	0	0	0	0	0	0	8.12E–07	0	0	0	0
Pu-241	2.20E–06	2.20E–06	2.20E–06	2.20E–06	2.20E–06	2.20E–06	2.20E–06	2.20E–06	2.14E–06	2.20E–06	4.47E–12	2.20E–06	2.20E–06
Pu-242	6.87E–07	6.87E–07	6.87E–07	6.87E–07	6.87E–07	6.87E–07	6.87E–07	6.87E–07	6.74E–07	6.87E–07	6.74E–07	6.87E–07	6.87E–07
Ra-226	0	0	0	0	0	0	0	0	1.60E–06	0	0	0	0
Ra-228	9.00E–06	1.05E–05	1.08E–05	9.30E–06	9.60E–06	8.10E–06	9.60E–06	8.00E–06	8.96E–06	1.05E–05	1.89E–11	9.00E–06	8.40E–06
Ru-106	0	0	0	0	2.20E–06	0	1.20E–06	0	1.71E–06	0	3.80E–12	2.30E–06	1.44E–06
Sb-125	2.80E–06	2.88E–06	2.94E–06	2.92E–06	3.00E–06	3.15E–06	3.06E–06	3.60E–06	2.88E–06	2.79E–06	5.88E–12	2.94E–06	2.76E–06
Se-79	3.20E–07	3.20E–07	3.20E–07	3.20E–07	3.10E–07	3.20E–07	3.10E–07	3.20E–07	3.10E–07	3.20E–07	6.00E–13	3.10E–07	3.00E–07
Sm-147	0	0	0	0	0	0	0	0	0	0	0	0	0
Sm-151	1.11E–06	1.11E–06	1.11E–06	1.11E–06	1.11E–06	1.11E–06	1.11E–06	1.11E–06	1.08E–06	1.11E–06	1.08E–06	1.11E–06	1.11E–06
Sn-126	3.70E–06	3.70E–06	3.70E–06	3.70E–06	3.70E–06	3.70E–06	3.70E–06	3.70E–06	3.66E–06	3.70E–06	3.66E–06	3.70E–06	3.70E–06
Sr-90	0	0	0	0	0	0	0	0	1.09E–07	0	0	0	0
Tc-99	0	0	0	0	0	0	0	0	1.90E–07	0	0	0	0
Th-228	0	0	0	0	0	0	0	0	3.65E–06	0	0	0	0
Th-229	9.75E–06	9.75E–06	9.75E–06	9.75E–06	9.75E–06	9.75E–06	9.75E–06	9.75E–06	9.54E–06	9.75E–06	9.54E–06	9.75E–06	9.75E–06
Th-230	0	0	0	0	0	0	0	0	6.37E–07	0	0	0	0
Th-232	0	0	0	0	0	0	0	0	6.33E–07	0	0	0	0
U-232	9.65E–07	9.65E–07	9.65E–07	9.65E–07	9.65E–07	9.65E–07	9.65E–07	9.65E–07	9.48E–07	9.65E–07	9.48E–07	9.65E–07	9.65E–07
U-233	5.93E–07	5.93E–07	5.93E–07	5.93E–07	5.93E–07	5.93E–07	5.93E–07	5.93E–07	5.81E–07	5.93E–07	5.81E–07	5.93E–07	5.93E–07
U-234	0	0	0	0	0	0	0	0	7.93E–07	0	0	0	0
U-235	0	0	0	0	0	0	0	0	1.20E–05	0	0	0	0
U-236	7.59E–07	7.59E–07	7.59E–07	7.59E–07	7.59E–07	7.59E–07	7.59E–07	7.59E–07	7.45E–07	7.59E–07	7.45E–07	7.59E–07	7.59E–07
U-238	0	0	0	0	0	0	0	0	6.56E–07	0	0	0	0
Zr-93	9.76E–07	9.76E–07	9.76E–07	9.76E–07	9.76E–07	9.76E–07	9.76E–07	9.76E–07	9.47E–07	9.76E–07	9.47E–07	9.75E–07	9.76E–07

Tabel E-16. DCC_int_low_beta for marine organisms ((µGy h^{-1})/(Bq $kgfw^{-1}$)).

Radionuclides	(Wading) bird	Benthic fish	Benthic mollusc	Crustacean	European otter	Macroalgae	Mammal	Pelagic fish	Phyto-plankton	Polychaete worm	Ruddy turnstone	Vascular plant	Zooplankton
Ac-227	4.45E-06	4.45E-06	4.45E-06	4.45E-06	4.45E-06	4.45E-06	4.45E-06	4.45E-06	4.45E-06	4.45E-06	4.45E-06	4.45E-06	4.45E-06
Ag-108m	1.81E-06	1.81E-06	1.81E-06	1.81E-06	1.81E-06	1.81E-06	1.81E-06	1.81E-06	1.81E-06	1.81E-06	1.81E-06	1.81E-06	1.81E-06
Am-241	0	0	0	0	5.73E-06	0	0	0	0	0	5.73E-06	0	0
Am-242m	5.26E-06	5.26E-06	5.26E-06	5.26E-06	5.26E-06	5.26E-06	5.26E-06	5.26E-06	5.26E-06	5.26E-06	5.26E-06	5.26E-06	5.26E-06
Am-243	9.72E-06	9.72E-06	9.72E-06	9.72E-06	9.72E-06	9.72E-06	9.72E-06	9.72E-06	9.72E-06	9.72E-06	9.72E-06	9.72E-06	9.72E-06
Ba-133	4.42E-06	4.42E-06	4.42E-06	4.42E-06	4.42E-06	4.42E-06	4.42E-06	4.42E-06	4.42E-06	4.42E-06	4.42E-06	4.42E-06	4.42E-06
Be-10	2.33E-08	2.33E-08	2.33E-08	2.33E-08	2.33E-08	2.33E-08	2.33E-08	2.33E-08	2.33E-08	2.33E-08	2.33E-08	2.33E-08	2.33E-08
C-14-ind	2.90E-07	2.90E-07	2.80E-07	2.90E-07	3.73E-07	2.80E-07	2.90E-07	2.90E-07	1.80E-11	2.80E-07	3.73E-07	2.80E-07	2.80E-07
C-14-inorg	2.90E-07	2.90E-07	2.80E-07	2.90E-07	3.73E-07	2.80E-07	2.90E-07	2.90E-07	1.80E-11	2.80E-07	3.73E-07	2.80E-07	2.80E-07
C-14-org	2.90E-07	2.90E-07	2.80E-07	2.90E-07	3.73E-07	2.80E-07	2.90E-07	2.90E-07	1.80E-11	2.80E-07	3.73E-07	2.80E-07	2.80E-07
Ca-41	1.35E-06	1.35E-06	1.35E-06	1.35E-06	1.35E-06	1.35E-06	1.35E-06	1.35E-06	1.35E-06	1.35E-06	1.35E-06	1.35E-06	1.35E-06
Cd-113m	1.09E-07	1.09E-07	1.09E-07	1.09E-07	1.09E-07	1.09E-07	1.09E-07	1.09E-07	1.09E-07	1.09E-07	1.09E-07	1.09E-07	1.09E-07
Cl-36	0	0	0	0	6.91E-08	0	0	0	0	0	6.91E-08	0	0
Cm-242	0	0	0	0	8.19E-07	0	0	0	0	0	8.19E-07	0	0
Cm-243	0	0	0	0	7.95E-06	0	0	0	0	0	7.95E-06	0	0
Cm-244	0	0	0	0	7.62E-07	0	0	0	0	0	7.62E-07	0	0
Cm-245	4.93E-06	4.93E-06	4.93E-06	4.93E-06	4.93E-06	4.93E-06	4.93E-06	4.93E-06	4.93E-06	4.93E-06	4.93E-06	4.93E-06	4.93E-06
Cm-246	6.77E-07	6.77E-07	6.77E-07	6.77E-07	6.77E-07	6.77E-07	6.77E-07	6.77E-07	6.77E-07	6.77E-07	6.77E-07	6.77E-07	6.77E-07
Co-60	0	0	0	0	2.26E-07	0	0	0	0	0	2.26E-07	0	0
Cs-134	0	0	0	0	3.59E-07	0	0	0	3.30E-11	0	3.59E-07	0	0
Cs-135	3.90E-07	3.90E-07	3.90E-07	3.90E-07	3.05E-07	3.80E-07	3.90E-07	3.90E-07	2.30E-11	3.90E-07	3.05E-07	3.90E-07	3.80E-07
Cs-137	0	0	0	0	3.71E-07	0	0	0	4.30E-11	0	3.71E-07	0	0
Eu-152	3.20E-06	3.60E-06	3.48E-06	2.80E-06	3.42E-06	3.40E-06	4.20E-06	3.90E-06	2.25E-10	3.20E-06	3.42E-06	3.60E-06	3.54E-06
Eu-154	2.60E-06	2.20E-06	1.80E-06	2.50E-06	1.83E-06	1.50E-06	0	2.40E-06	1.06E-10	1.70E-06	1.83E-06	1.90E-06	1.30E-06
Eu-155	2.72E-06	2.72E-06	2.72E-06	2.72E-06	2.72E-06	2.72E-06	2.72E-06	2.72E-06	2.72E-06	2.72E-06	2.72E-06	2.72E-06	2.72E-06
Fe-55	2.43E-06	2.43E-06	2.43E-06	2.43E-06	2.43E-06	2.43E-06	2.43E-06	2.43E-06	2.43E-06	2.43E-06	2.43E-06	2.43E-06	2.43E-06
Gd-152	0	0	0	0	0	0	0	0	0	0	0	0	0
H-3	2.48E-06	2.48E-06	2.48E-06	2.48E-06	2.47E-06	2.48E-06	2.48E-06	2.48E-06	1.58E-10	2.48E-06	2.47E-06	2.48E-06	2.48E-06
Ho-166m	5.42E-06	5.42E-06	5.42E-06	5.42E-06	5.42E-06	5.42E-06	5.42E-06	5.42E-06	5.42E-06	5.42E-06	5.42E-06	5.42E-06	5.42E-06
I-129	4.84E-06	5.04E-06	5.07E-06	4.73E-06	4.94E-06	4.94E-06	4.90E-06	5.04E-06	3.22E-10	4.94E-06	4.94E-06	5.07E-06	4.81E-06
In-115	1.39E-07	1.39E-07	1.39E-07	1.39E-07	1.39E-07	1.39E-07	1.39E-07	1.39E-07	1.39E-07	1.39E-07	1.39E-07	1.39E-07	1.39E-07
Mo-93	1.41E-06	1.41E-06	1.41E-06	1.41E-06	1.41E-06	1.41E-06	1.41E-06	1.41E-06	1.41E-06	1.41E-06	1.41E-06	1.41E-06	1.41E-06
Nb-93m	1.16E-06	1.16E-06	1.16E-06	1.16E-06	1.16E-06	1.16E-06	1.16E-06	1.16E-06	1.16E-06	1.16E-06	1.16E-06	1.16E-06	1.16E-06

Radionuclides	(Wading) bird	Benthic fish	Benthic mollusc	Crustacean	European otter	Macroalgae	Mammal	Pelagic fish	Phyto-plankton	Polychaete worm	Ruddy turnstone	Vascular plant	Zooplankton
Nb-94	0	0	0	0	1.25E-07	0	0	0	0	0	1.25E-07	0	0
Ni-59	2.64E-06	2.64E-06	2.61E-06	2.64E-06	2.63E-06	2.59E-06	2.60E-06	2.64E-06	1.72E-10	2.65E-06	2.63E-06	2.61E-06	2.63E-06
Ni-63	1.19E-06	1.19E-06	1.19E-06	1.19E-06	1.21E-06	1.19E-06	1.19E-06	1.19E-06	7.68E-11	1.19E-06	1.21E-06	1.19E-06	1.19E-06
Np-237	0	0	0	0	5.49E-06	0	0	0	0	0	5.49E-06	0	0
Pa-231	7.58E-06	7.58E-06	7.58E-06	7.58E-06	7.58E-06	7.58E-06	7.58E-06	7.58E-06	7.58E-06	7.58E-06	7.58E-06	7.58E-06	7.58E-06
Pb-210	5.00E-06	4.80E-06	4.80E-06	4.80E-06	4.23E-06	4.00E-06	5.00E-06	4.80E-06	2.75E-10	4.60E-06	4.23E-06	4.80E-06	3.60E-06
Pd-107	1.79E-06	1.79E-06	1.79E-06	1.79E-06	1.79E-06	1.79E-06	1.79E-06	1.79E-06	1.79E-06	1.79E-06	1.79E-06	1.79E-06	1.79E-06
Pm-147	3.74E-07	3.74E-07	3.74E-07	3.74E-07	3.74E-07	3.74E-07	3.74E-07	3.74E-07	3.74E-07	3.74E-07	3.74E-07	3.74E-07	3.74E-07
Po-210	0	0	0	0	3.66E-13	0	0	0	0	0	3.66E-13	0	0
Pu-238	0	0	0	0	8.70E-07	0	0	0	0	0	8.70E-07	0	0
Pu-239	0	0	0	0	1.18E-06	0	0	0	0	0	1.18E-06	0	0
Pu-240	0	0	0	0	8.28E-07	0	0	0	0	0	8.28E-07	0	0
Pu-241	2.20E-06	2.20E-06	2.20E-06	2.20E-06	2.19E-06	2.20E-06	2.20E-06	2.20E-06	1.42E-10	2.20E-06	2.19E-06	2.20E-06	2.20E-06
Pu-242	6.87E-07	6.87E-07	6.87E-07	6.87E-07	6.87E-07	6.87E-07	6.87E-07	6.87E-07	6.87E-07	6.87E-07	6.87E-07	6.87E-07	6.87E-07
Ra-226	0	0	0	0	1.63E-06	0	0	0	0	0	1.63E-06	0	0
Ra-228	1.08E-05	9.90E-06	8.70E-06	1.05E-05	9.14E-06	9.60E-06	1.16E-05	1.02E-05	5.76E-10	8.10E-06	9.14E-06	8.70E-06	1.00E-05
Ru-106	0	0	0	0	1.76E-06	0	0	0	1.08E-10	0	1.76E-06	0	2.00E-06
Sb-125	2.94E-06	3.32E-06	2.68E-06	2.76E-06	2.93E-06	2.90E-06	2.00E-06	2.61E-06	1.96E-10	3.20E-06	2.93E-06	2.72E-06	2.75E-06
Se-79	3.20E-07	3.20E-07	3.20E-07	3.20E-07	3.19E-07	3.20E-07	3.20E-07	3.20E-07	2.00E-11	3.20E-07	3.19E-07	3.20E-07	3.20E-07
Sm-147	0	0	0	0	0	0	0	0	0	0	0	0	0
Sm-151	1.11E-06	1.11E-06	1.11E-06	1.11E-06	1.11E-06	1.11E-06	1.11E-06	1.11E-06	1.11E-06	1.11E-06	1.11E-06	1.11E-06	1.11E-06
Sn-126	3.70E-06	3.70E-06	3.70E-06	3.70E-06	3.70E-06	3.70E-06	3.70E-06	3.70E-06	3.70E-06	3.70E-06	3.70E-06	3.70E-06	3.70E-06
Sr-90	0	0	0	0	1.12E-07	0	0	0	0	0	1.12E-07	0	0
Tc-99	0	0	0	0	1.95E-07	0	0	0	0	0	1.95E-07	0	0
Th-228	0	0	0	0	3.73E-06	0	0	0	0	0	3.73E-06	0	0
Th-229	9.75E-06	9.75E-06	9.75E-06	9.75E-06	9.75E-06	9.75E-06	9.75E-06	9.75E-06	9.75E-06	9.75E-06	9.75E-06	9.75E-06	9.75E-06
Th-230	0	0	0	0	6.49E-07	0	0	0	0	0	6.49E-07	0	0
Th-232	0	0	0	0	6.44E-07	0	0	0	0	0	6.44E-07	0	0
U-232	9.65E-07	9.65E-07	9.65E-07	9.65E-07	9.65E-07	9.65E-07	9.65E-07	9.65E-07	9.65E-07	9.65E-07	9.65E-07	9.65E-07	9.65E-07
U-233	5.93E-07	5.93E-07	5.93E-07	5.93E-07	5.93E-07	5.93E-07	5.93E-07	5.93E-07	5.93E-07	5.93E-07	5.93E-07	5.93E-07	5.93E-07
U-234	0	0	0	0	8.07E-07	0	0	0	0	0	8.07E-07	0	0
U-235	0	0	0	0	1.23E-05	0	0	0	0	0	1.23E-05	0	0
U-236	7.59E-07	7.59E-07	7.59E-07	7.59E-07	7.59E-07	7.59E-07	7.59E-07	7.59E-07	7.59E-07	7.59E-07	7.59E-07	7.59E-07	7.59E-07
U-238	0	0	0	0	6.68E-07	0	0	0	0	0	6.68E-07	0	0
Zr-93	9.76E-07	9.76E-07	9.76E-07	9.76E-07	9.76E-07	9.76E-07	9.76E-07	9.76E-07	9.76E-07	9.76E-07	9.76E-07	9.76E-07	9.76E-07

Appendix F

Probabilistic parameters

In Table F-1 the parameters that were varied probabilistic are listed (in total 141 parameters). In addition to these parameters, the element-specific Kd, CR and TC values were varied probabilistic (in total 2139 parameters). For each parameter 1000 values were drawn out of the PDF using Latin Hypercube stratified sampling.

For the early periglacial climate calculation case the parameters biom_pp_ter_perm, conc_C_atmos, NPP_ter piston_vel_ter, solubilityCoef_ter och minRate_regoUp_ter were varied in addition to these listed in Table F-1.

Table F-1. In this table the parameters that were varied in the probailistic simulations are listed.

Parameter name	Parameter name	Parameter name	Parameter name
biom_pp_ter	f_rootUptake	prod_edib_fish_sea	washoffCoef
conc_C_atmos	height_CA_cereal	prod_edib_game	z_regoUp
conc_C_meat	height_CA_fodder	prod_edib_mush	**Inland-outfield**
conc_C_milk	height_CA_ter	solubilityCoef_lake	biom_cereal
conc_Cl_PP_ter	height_CA_tuber	solubilityCoef_sea	conc_DIC_regoUp
conc_Cl_regoUp_ter_D	ingRate_water_cattle	solubilityCoef_ter	conc_Dust
conc_DIC_lake	LAI_cereal	vel_wind_height_ref_aqu	D_CO2_soil
conc_DIC_regoUp_ter	LAI_fodder	vel_wind_height_ref_ter	dens_regoUp
conc_DIC_sea	LAI_ter	z_min_prod_edib_fish_sea	minRate
conc_Dust_ter	LAI_tuber	z_regoUp_lake	NPP_cereal
conc_PM_lake	leaf_width_cereal	z_regoUp_sea	percolation_agri
conc_PM_sea	leaf_width_fodder	z_regoUp_ter	poro_regoUp
dens_regoGL	leaf_width_ter	z0_aqu	S_w_regoUp
dens_regoLow	leaf_width_tuber	**Garden plot**	z_regoUp
dens_regoPeat	minRate_regoPG_lake	amount_irrig	**Drained mire**
dens_regoPG	minRate_regoPG_sea	area_support_wood	biom_cereal
dens_regoUp_lake	minRate_regoPG_ter	biom_tuber	biom_fodder
dens_regoUp_sea	minRate_regoUp_lake	biom_veg	biom_tuber
dens_regoUp_ter	minRate_regoUp_sea	conc_DIC_regoUp	compact_gyttja
df_decomp_aqu[Cl]	minRate_regoUp_ter	conc_Dust	compact_peat
df_decomp_ter[Cl]	minRate_water_PM_lake	D_CO2_soil	conc_DIC_regoUp
f_C_fish	minRate_water_PM_sea	dens_regoUp	conc_Dust
f_C_peat	NPP_ter	f_combust[C]	D_CO2_soil_clay
f_DW_FW_fish_lake	piston_vel_lake	height_CA_veg	D_CO2_soil_peat
f_DW_FW_fish_sea	piston_vel_sea	LAI_veg	dens_regoUp_clay
f_H2CO3_lake	piston_vel_ter	leaf_width_veg	dens_regoUp_peat
f_H2CO3_sea	poro_regoGL	LeafStoreCapacy_veg	Flux_water_satSoil_agri
f_H2CO3_ter	poro_regoLow	minRate	minRate
f_mush_herbiv	poro_regoPeat	N_irrig	NPP_cereal
f_refrac_macro_lake	poro_regoPG	NPP_ag_veg	NPP_fodder
f_refrac_macro_sea	poro_regoUp_lake	NPP_tuber	NPP_tuber
f_refrac_micro_lake	poro_regoUp_sea	NPP_veg	percolation_agri
f_refrac_micro_sea	poro_regoUp_ter	percolation_agri	poro_regoUp_clay
f_refrac_plank_lake	prod_edib_berry	poro_regoUp	poro_regoUp_peat
f_refrac_plank_sea	prod_edib_cray_lake	S_w_regoUp	S_w_regoUp_clay
f_refrac_ter	prod_edib_fish_lake	time_vegPeriod	S_w_regoUp_peat